SEISMIC RESISTANT DESIGN OF BASE ISOLATED MULTISTOREY STRUCTURES

A Thesis
submitted in partial fulfilment
of the requirements for the degree of
Doctor of Philosophy in Civil Engineering
at the
University of Canterbury
Christchurch
New Zealand

by T. ANDRIONO
supervised by A.J. Carr

October 1989

ABSTRACT

The Base Isolation technique and its benefits in reducing the transmitted earthquake energy into a structure has gained increasing recognition during the last two decades. This recognition is indicated by the application of Base Isolation systems to a large number of bridges, several multistorey buildings and some power plants in countries which have high seismic risk. Unfortunately, the currently available design procedures, especially for multistorey structures, seem inadequate and too restrictive and as a result present practice still relies upon a series of deterministic time history analyses which are not only impractical for design purposes but appear unable to give the designer a clear insight into the seismic behaviour of the multistorey structure.

This research is carried out to investigate in more detail the effects of various structural parameters and ground motion characteristics on the seismic response of Base Isolated multistorey structures. It also reviews the shortcomings of the current design methods. The results are then used to develop two simplified analysis methods for practical design.

The first method which is called the Code-Type approach can be used to accurately estimate the inertia forces, not only at the level of the isolation devices but throughout the height of the multistorey structure. It is recommended for use as a preliminary design tool or even a final design tool for simple Base Isolated multistorey structures. The second procedure which is based on the Component Mode Synthesis method is suggested for final design purposes of more complex Base Isolated multistorey structures. This method enables the designer to evaluate the effects of the isolation devices on the contribution of each mode of vibration to the total response of the structure.

ACKNOWLEDGEMENTS

The research described in this thesis was carried out in the Department of Civil Engineering, University of Canterbury, under the overall guidance of its Head, Professor R. Park and the supervision of Dr A.J. Carr.

I wish to sincerely thank Dr A.J. Carr for his invaluable advice and encouragement. His enthusiasm, patience and cheerful heart are greatly appreciated. I would like to express my gratitude to Professor R. Park for his personal attention and to Professor M.J.N. Priestley for his priceless ideas and suggestions at the initial stage of this work. Dr P.J. Moss is thanked for his assistance during Dr Carr's study leave.

The financial support provided by the Ministry of Works and Development, New Zealand is gratefully acknowledged. I wish also to deeply thank Petra Christian University in Indonesia for granting invaluable opportunity and support which enabled me to pursue my further study in New Zealand.

I am also grateful and would like to extend my special thanks to:

- Mr A.W. Charleson for his moral support and effort in proof reading the manuscript of this thesis.

- Friends and fellow students, especially Drs D.L. Hutchison, H.J. Pam, Messrs D.H. Turkington, L.S. Wijanto, G.A. MacRae, L.L. Dodd, H. Anggawijaya, for their assistance, encouragement, contructive comments and fruitful discussions.

- Mrs V.J. Grey for her draughting assistance.

- Mr B. Hutchison for his assistance in computer facilities.

Finally, I wish to express my deep gratitude to my parents, my sister and my fiancée for their prayers, love, understanding and encouragement.

TABLE OF CONTENTS

NOTATION

Add. λ	= Additional hysteretic damping
App.	= Results obtained from the Code-Type Approach
B	= Bulge Parameter (Lee's method)
B_D	= Bulge Parameter independent from number of storeys
BI	= Base Isolation or Base Isolated
b (subscript)	= beam
	or bearing or BI system
C	= Damping matrix
	or Basic seismic coefficient (NZS4203)
	or Linear interpolation factor (Lee's method)
C^*	= Generalized damping matrix
C_d	= Seismic coefficient (NZS4203)
c (subscript)	= column
D	= Peak displacement (SEAONC)
d	= Peak displacement (Kelly's method)
d_b	= Maximum base displacement (Lee's method)
E	= Young's modulus
E_h	= Additional hysteretic damping
e (subscript)	= Elastic condition
eff (subscript)	= effective
F	= Force or Lateral inertia force
F_y	= Yield strength or yield force
F_i	= Equivalent static lateral force at ith floor
F_s	= Shear force
G	= Shear modulus
g	= Acceleration of gravity
h_i	= Height of floor i
I	= moment of inertia
	or Identity matrix
	or Importance factor (NZS4203:1976)
I_b	= Beam moment of inertia
I_c	= Column moment of inertia
K	= Stiffness matrix
K^*	= Generalized stiffness matrix
K_s	= Effective stiffness (Turkington's method)
k	= stiffness (in general)
k_{EA}	= Effective stiffness (Kelly's method)

k_d = post-yield stiffness (Blakeley's and Turkington's methods)

k_{eff} = Effective stiffness of BI system

k_{es} = Effective stiffness (Blakeley's method)

k_u = Elastic stiffness (Blakeley's and Turkington's methods)

k_o = Initial or elastic stiffness

L = length

M = Mass
or Mass matrix
or Earthquake magnitude (local or Richter magnitude)
or Material factor (NZS4203)
or Overturning moment

M^* = Generalized mass matrix

m = nodal mass or floor mass

P (t) = Loading as function of time

P_i = Participation factor of mode i (Kelly's method)

$P_1, P_2, ...$ = Earthquake parameters (Lee's method)
e.g. 10% damped spectral velocity at 1st and 2nd mode periods

p = exponent used in the Code-Type approach formula for predicting the equivalent lateral force distribution

PF_i = Participation factor of mode i

$PF_{i(UI)}$ = PF_i at unisolated condition

$PF_{i(IUY)}$ = PF_i at isolated unyielded condition

$PF_{i(IY)}$ = PF_i at isolated yielded condition

Q_d = Characteristic dissipator shear strength (Blakeley's method)

R = The ratio of the hysteresis loop area to the area of its enclosing rectangle

r = Displacement of a degree-of-freedom due to a unit ground displacement
or A constant which controls abruptness of loss of stiffness in the Ramberg-Osgood hysteresis loop model
or linear correlation coefficient

S = Structural type factor (NZS4203)

s (subscript) = superstructure

S_a = Spectral acceleration

S_d = Spectral displacement

SA = "Sum of Absolutes" mode combination technique

SRSS = "Square root of the Sum Squakers

T_i = ith mode period

$T_{i(UI)}$ = T_i at unisolated condition

$T_{i(IUY)}$ = Ti at isolated unyielded condition

$T_{i(IY)}$	=	Ti at isolated yielded condition
T_r	=	Rubber thickness (DIS manual)
$T_{1\ eff}$	=	Effective fundamental period
THA	=	Results obtained from inelastic Time history Analyses
t	=	time
u	=	Relative displacement
$\dot{u}$	=	Relative velocity
$\ddot{u}$	=	Relative acceleration
$\ddot{u}_g$	=	Ground acceleration
V	=	Base shear
v	=	Total-motion displacement
$\dot{v}$	=	Total-motion velocity
$\ddot{v}$	=	Total-motion acceleration
W	=	Total weight of the structure (incl. the base mass)
	or	Total weight of the superstructure (Lee's method)
W_d	=	Work done in hysteresis
W_i	=	Total weight of ith floor
W_s	=	Elastic stiffness or strain energy
W_t	=	Total weight of the structure (NZS4203)
	or	Area of the circumscribed rectangle of the bilinear hysteresis loop
x_{max}	=	peak displacement
x_y	=	yield displacement
Y_i	=	ith mode amplitude
	or	ith mode generalized coordinate
α	=	A constant related to the mass matrix in Rayleigh's damping model
β	=	A constant related to the stiffness matrix in Rayleigh's damping model
Δ_s	=	Displacement of the superstructure (Blakeley's method)
Δ_{max}	=	Peak displacement (SEAONC)
δ	=	displacement
δ_y	=	yield displacement
ϕ_c	=	Constraint modes (Component Mode Synthesis method)
ϕ_i	=	Eigen vector of mode i (mode shape)
$\phi_{i(UI)}$	=	ϕ_i at unisolated condition
$\phi_{i(IUY)}$	=	ϕ_i at isolated unyielded condition
$\phi_{i(IY)}$	=	ϕ_i at isolated yielded condition
$\phi_{i\ eff}$	=	Effective eigen vector of mode i (Kelly's method)
ϕ_n	=	Normal modes

λ	=	Fraction of critical damping
λ_i	=	Equivalent viscous damping of mode i
$\lambda_{i\ eff}$	=	Effective equivalent viscous damping of mode i
μ	=	The ratio of maximum displacement to the yield displacement of BI system
π	=	3.1415926
θ	=	Load distribution defining angle (Lee's method) or Normalized mode shape matrix
Σ	=	Total
ω	=	Circular frequency
Ψ	=	Matrix of preselected component modes

CHAPTER 1

INTRODUCTION

1.1 GENERAL

The risk of being damaged by strong earthquakes may be high for most structures constructed in seismically active areas, since for economic reasons, these structures generally are not designed to resist the effects of large ground excitations entirely by elastic behaviour. Current seismic resistant design practices allow the structure to develop localized plastic deformations in order to give increased flexibility and dissipate a considerable amount of energy. It has been realized, that such plastic deformations not only can cause progressive deterioration of the structural components but also lead to severe and expensive non-structural damage which may even occur during moderate earthquakes.

A Base Isolation system offers an attractive alternative means for protecting structures against earthquake by restricting all plastic deformations to relatively cheap and replaceable devices so allowing the rest of the structure, as far as possible, to remain elastic with significant attenuation of transmitted ground motion energy. Since a Base Isolation system apparently increases the degree of protection, it is very suitable for installation in a wide range of structures especially for vital and sensitive buildings such as telephone exchanges, television and radio stations, power plants, hospitals, police and army headquarters, computer and information centres which are expected to remain functional after a severe earthquake attack. Furthermore this system is also useful for preservation purposes, such as protecting monumental and historical buildings from seismic risk.

The ability of this system to significantly reduce the ductility demand in the superstructure makes possible the simplification of the structural detailing and other seismic design considerations required by the more conventional approach. Therefore, a wider choice of architectural forms and structural materials would be available to the designer.

Since the early part of this century, many ingenious schemes have been suggested in order to fulfill the so-called "supporting the superstructure and letting the ground move underneath" idea. Unfortunately most of the proposed systems are unacceptably complicated and in fact they inherit some major weaknesses such as excessive permanent offset due to lack of restoring forces. Lee[1.1] and Kelly[1.2] reviewed, to a large extent, the historical development of these systems.

It is noted that not until the 1970's did several practical Base Isolation devices, which provide both flexibility and energy dissipating capacity, emerge as the result of considerable research in this field conducted in New Zealand. Recognition of this work has been indicated

by the application of this system to a number of highway bridges, railway bridges, multistorey buildings and some power plants in this last decade.

As well as the experimental work on the devices, there were also several research projects carried out to investigate the seismic response of Base Isolated structures through theoretical analyses and shake table tests. A comprehensive selection of papers and research reports on this topic published during 1900-1984 were listed by Kelly [1.2].

Only a few of these research projects were designed to study the seismic behaviour of Base Isolated multistorey structures. However three prominent research projects provided some contributions towards the provision of guidelines for design purposes. Priestley, Crosbie and Carr[1.3] studied the seismic performance of Base Isolated brick masonry shear wall structures. Although this research was more directed to solve a problem for a specific type of structure, it also presented some useful design considerations and recommendations for further research in the general field of Base Isolation systems. Experimental work followed by analytical studies was carried out by Kelly, Eidinger and Derham[1.4]. This was based on shake table tests of a 20 ton three-storey single-bay moment-resistant steel frame structure. From this work, a simple design procedure based upon elastic response spectra was suggested. Lee and Medland[1.5] conducted a detailed investigation of the seismic performance of Base Isolated multistorey shear structures. To a large extent this study discussed the effect of the Base Isolation parameters on the likely variation of the shape of storey-shear envelopes. It also produced some design charts which are based mainly upon the parameters of five selected types of Base Isolation system. The results of these three investigations were used as a starting point of this study, together with several other research results as described in more detail in Chapter 3.

1.2 OBJECTIVES OF RESEARCH

Many practical Base Isolation schemes have been developed in recent years and it is believed that interest in the application of this technique will continue to grow. However, there is still no simple and reliable design procedure which is able to give the designer a clear insight to the seismic behaviour of Base Isolated multistorey structures. Some currently available design procedures[1.4,1.5,1.6,1.7,1.8,1.9] seem inadequate and too restrictive and therefore present practice still relies upon a series of deterministic dynamic inelastic time history analyses[1.10,1.11].

The first objective of this study is to review the current design methods and to investigate in more detail the seismic behaviour of a wide variety of Base Isolated multistorey structures.

Then based on the results obtained, this research will attempt to accomplish its second objective which is to develop simple design procedures for this type of structure.

1.3 SCOPE AND OUTLINE OF THE THESIS

The following outline describes the scope of the study. First, the principles of dynamic analysis and structure modelling are discussed in Chapter 2. The current design methods and the existing design guide-lines are reviewed in Chapter 3. Chapter 4 presents the seismic response of Base Isolated multistorey structures, with elastic superstructures, subjected to the North-South component of El Centro 1940 earthquake which is commonly considered as the "standard" and on which many codes have been historically based. The effects of a wide range variation of Base Isolation system parameters on the seismic behaviour of a series of two dimensional multistorey building models are investigated. Some discussions of design aspects of simple Base Isolated multistorey structures are also presented in Chapter 4.

A reliable method of analysis for general Base Isolated multistorey structures based on the Component Mode Synthesis method has been developed as part of this research. This method, as discussed in Chapter 5, enables the evaluation of the modal contributions of the structure irrespective of the inelastic behaviour of the Base Isolation devices during a strong earthquake and therefore gives clear insight into the seismic response of Base Isolated multistorey structures.

Effects of the ground motion characteristics on the structuctural behaviour of Base Isolated multistorey buildings are studied in order to be able to select the right system for a particular type of ground motion so that the Base Isolation system will provide the guaranteed benefit. A range of earthquake records other than the N-S component of El Centro 1940 are used as the basis of the analyses in this section. The results of this investigation are reported in Chapter 6.

Chapter 7 presents two simplified analysis methods which are proposed for design purposes of Base Isolated multistorey structures. In this chapter the seismic response of Base Isolated multistorey structures with superstructure components permitted to deform inelastically is also investigated. This results in a better understanding of the likely performance of this type of structures under the most credible ground excitation.

Finally, some conclusions and recommendations for future research are presented in Chapter 8.

1.4 REFERENCES

1.1 LEE, D.M. and MEDLAND, I.C., Base Isolation - An Historical Development and the Influence of High Mode Responses, Bulletin of the New Zealand National Society for Earthquake Engineering, Vol.11, No.4, 1978, pp. 219-233.

1.2 KELLY, J.M., Aseismic base isolation: review and bibliography, Soil Dynamics and Earthquake Engineering, Vol.5, No.3, 1986, pp.202-216.

1.3 PRIESTLEY, M.J.N., CROSBIE, R.L., and CARR, A.J., Seismic Forces in Base Isolated Masonry Structures, Bulletin of the New Zealand National Society for Earthquake Engineering, Vol.10, No.2, 1977, pp.55-68.

1.4 KELLY, J.M., EIDINGER, J.M., and DERHAM, C.J., A Practical Soft Story Earthquake Isolation System, Report No.UCB/EERC-77/27, Earthquake Engineering Research Center, Univ. of California, Berkeley, 1977.

1.5 LEE, D.M., The Effect of Base Isolation on Multi Storey Shear Structures, Ph.D. Thesis, Dept. of Theoritical and Applied Mechanics, Univ. of Auckland, New Zealand 1978.

1.6 BLAKELEY, R.W.G., et al, Recommendations for the Design and Construction of Base Isolated Structures, Bulletin of the New Zealand National Society for Earthquake Eng., Vol.12, No.2, 1979, pp.136-157.

1.7 Base Isolation Subcmt. of the Seimology Committee, Structural Engineers Association of Northern California, Tentative Seismic Isolation Design Requirements, California, 1983.

1.8 Dynamic Isolation Systems Inc., Seismic Base Isolation Using Lead-Rubber Bearings, Design Procedures for Buildings, Berkeley, 1984.

1.9 MAYES, R.L. et al, Design Guidelines for Base Isolated Buildings with Energy Dissipators, Earthquake Spectra, Vol.1, No.1, 1984.

1.10 BROADMAN, P.R., WOOD, B.J., and CARR, A.J., Union House - A Cross Braced Structure with Energy Dissipators, Bulletin of the New Zealand National Society of Earthquake Engineering, Vol.16, No.2, 1983, pp. 83-97.

1.11 CHARLESON, A.W., WRIGHT, P.D., and SKINNER, R.I., Wellington Central Police Station Base Isolation of An Essential Facility, Proc. Pacific Conference on Earthquake Engineering, Vol.2, 1987, pp. 377-388.

CHAPTER 2

PRINCIPLES OF DYNAMIC ANALYSIS AND STRUCTURE MODELLING

2.1 INTRODUCTION

Structural dynamic problems differ from their static loading counterpart in two important respects. First, as the most fundamental distinction is the role played by acceleration in a structural dynamic load case. This acceleration creates inertia forces which in turn may significantly contribute to the structural response as described elsewhere[2.1,2.2]. Second, because of its time-varying nature, there is no single solution for a dynamic problem as there is for a static problem.

Dynamic analyses are required in order to be able to predict the response of structures subjected to dynamic loading. In these analysis methods, the real structures are represented by appropriate analytical models which can be described mathematically. The complexity of an analytical model is determined by the real structural properties and behaviour it must represent. For example, the mass distribution of some structures are required to be represented by interconnected finite element models with cubic hermitian polynomials while others can be represented accurately enough by simple discrete-parameter models. These discrete-parameter models are also known as the lumped-mass models because the mass of the system is assumed to be represented by a finite number of point masses. It should be noted that although the structure modelling may be made as simple as possible in order to reduce the computing effort, it must not omit any characteristics of the prototype that significantly affect its dynamic behaviour.

Once the analytical model has been created, the mathematical equations of motion can be formulated accordingly. If the dynamic loading is a known function of time then a deterministic method for solving these equations can be applied. For a multi-degree of freedom system, the equations of motion can be expressed in the matrix form as shown in Eq. 2.1. The left hand side terms of this second order differential equation represent the resulting forces from the motion, whereas the right hand side term is the externally applied dynamic load.

$$[M]\{\ddot{v}\} + [C]\{\dot{v}\} + [K]\{v\} = \{P(t)\} \qquad (2.1)$$

where [M] $\{\ddot{v}\}$, [C] $\{\dot{v}\}$, [K] {v} are the inertia, damping, and elastic forces respectively and {P(t)} is the vector of the applied loads.

For multistorey buildings, it is reasonable to lump the mass of the structure at certain nodes at which the translational and rotational degrees of freedom are defined. In this case, the lumped-mass matrix has a simple diagonal form. The off-diagonal terms of this matrix vanish since an

acceleration of any mass point produces an inertia force at that point only[2.1]. It is also commonly assumed that in most civil engineering structures, the mass remains constant with time.

During the dynamic analysis, the likely change of the structural stiffness due to inelastic or non-linear actions within the structural components should be taken into account. The stiffness matrix of individual members can be assembled into the global stiffness matrix [K] using the Direct Stiffness Method[2.3].

Damping is present in all dynamically responding structures. It may take form in many different mechanisms, such as internal friction, fluid resistance, sliding friction etc. However, the assumption of linear viscous damping which provides the simplest mathematical model of damping, namely a force directly proportional to the velocity[2.2], appears to be physically justifiable for most civil engineering cases[2.4]. If a deterministic non-linear time history analysis is used, the most common model is to form the damping matrix by making it proportional to the mass and stiffness matrices, thus

$$[C] = \alpha [M] + \beta [K] \tag{2.2}$$

where α and β are constants. Based on this concept, there are several types of damping model which have been developed as discussed in more detail in Chapter 4. It is also essential to be able to relate this damping matrix to the modal damping ratios which can be estimated from the known physical properties of the structure[2.5,2.6].

Earthquake loading is a special case of the dynamic problem in the sense its excitation is applied in the form of support motion rather than by any external load. As illustrated in Fig. 2.1 the total motion of the structure, v, can be considered as the sum of the ground motion, $u_{g(t)}$, and the motion of the structure itself, u, relative to the ground.

$$\{v\} = \{u\} + \{r\} u_g(t) \tag{2.3}$$

where {r} is the displacements of all degrees of freedom due to a unit ground displacement.

Substituting Eq. 2.3 into Eq. 2.1 leads to

$$[M]\{\ddot{u}\} + [C]\{\dot{u}\} + [K]\{u\} = \{P(t)\} - [M]\{r\}\ddot{u}_g(t) - [C]\{r\}\dot{u}_g(t) - [K]\{r\}u_g(t) \tag{2.4}$$

The velocity of the ground motion, $\dot{u}_g$ (t) and its displacement, u_g (t), can be found by integration of the given ground acceleration, $\ddot{u}_g$ (t).

If the ground motion is considered to be uniform over the site, i.e. travelling wave effects are not considered, the structure undergoes a "rigid-base" translation and Eq. 2.4 can be considerably simplified. No forces are generated within the structure due to a "rigid-base" displacement, thus

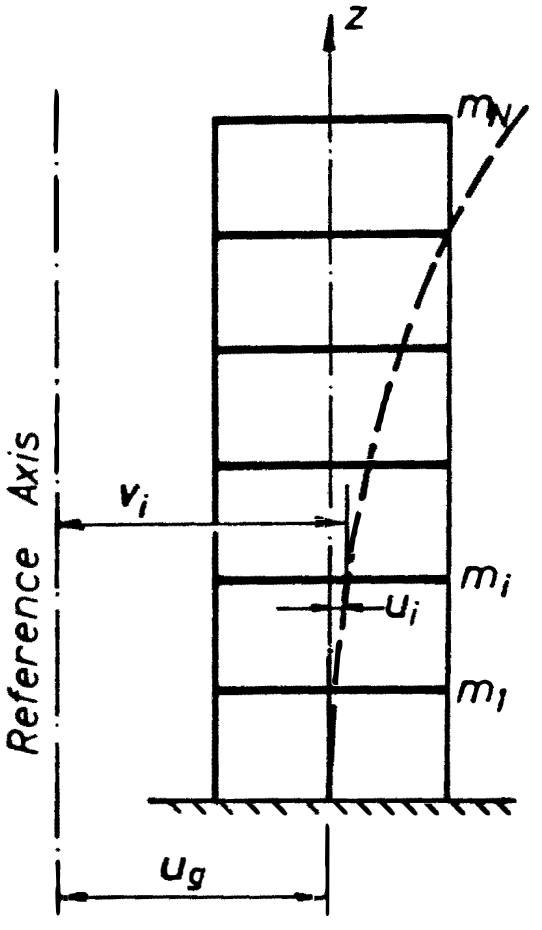

Fig. 2.1 Relative and Total Motion of a Multistorey Structure with Rigid Translation

$$[K]\{r\} = \{0\} \tag{2.5}$$

and also if the damping forces are considered to be only due to differential velocities

$$[C]\{r\} = \{0\} \tag{2.6}$$

Eq. 2.4 then becomes

$$[M]\{\ddot{u}\} + [C]\{\dot{u}\} + [K]\{u\} = \{P(t)\} - [M]\{r\}\,\ddot{u}_g(t) \tag{2.7}$$

If $\{P(t)\} = \{0\}$, the term $-[M]\{r\}\,\ddot{u}_g(t)$ can be treated as the effective "earthquake load".

2.2 METHODS OF DYNAMIC ANALYSIS

The deterministic analysis methods commonly used for predicting the dynamic response of structures can be catagorized into two groups, namely: (1) the rigorous procedure of dynamic analysis; and (2) the approximate procedures which are suitable for design purposes since they require much less computational effort.

2.2.1 THE RIGOROUS PROCEDURE

Earthquake excitation may force the structural components well beyond the post-yield range of their material behaviour. To deal with this non-linearity, a step-by-step integration procedure of solving the equations of motion is required for the dynamic analysis. In this method, an actual or simulated time dependent earthquake accelerogram is applied to the base and the corresponding response-history of the structure during the applied motion can be computed step-by-step by taking into account any changes of the structural properties at each prescribed time interval. Fuller description of this procedure is given elsewhere[2.1,2.2].

2.2.2 THE APPROXIMATE PROCEDURES

For linear-elastic systems, it is possible to use a mode-superposition procedure within the above step-by-step technique. This mode-superposition analysis basically involves several steps[2.1]: (1) Computing the normal modes and frequencies of the structure's free-vibration based on its mass and stiffness, (2) Formulating the generalized mass, damping and stiffness matrices, and the generalized "applied load" vector by taking advantage of the orthogonality of these properties, (3) Solving the uncoupled equations of motion in the modal coordinates for each individual mode, so that the structure can be treated as several single degree of freedom systems, (4) Transforming back the modal responses into the structural coordinate terms, (5) Combining the responses from each normal mode.

This mode-superposition procedure can save considerable computation time by using only the first few modes, which generally gives a good approximation to the overall structural response.

Using ground motion response spectra is an attractive alternative means of analysis by following the steps of the mode superposition technique. In this response spectrum analysis, the maximum displacement and force responses for each mode of the structure can be found directly, by reference to appropriate earthquake response spectra as a function of the modal natural periods and damping ratios, instead of evaluating them at each time step during the earthquake history, hence saving considerably computing effort.

However, in order to determine the total maximum responses, it is unreasonable to merely add these maximum modal responses since these maxima may not occur at the same time. In most cases, this ordinary summation may usually, but not necessarily, lead to overestimation of the actual total maximum response. To overcome this problem, various combination methods have been proposed. The simplest and most popular among these schemes is the SRSS combination method which determines the total maximum responses as the Square Root of the Sum of the Squares of the modal responses considered.

Besides the response spectrum analysis, the equivalent static lateral force analysis provides another type of approximate procedure which is still adopted by many loading codes[2.7] and is widely used in current design practice for non-isolated structures. This approach is based on the same principles as the response spectrum procedure. The main differences between these two methods, as discussed below, make the latter procedure much simpler and requiring less computational effort.

(1) Computation of the normal mode shapes and natural periods.

Except for the fundamental natural period, the mode shapes and periods of the other higher natural modes are not required in the equivalent static lateral force method. The fundamental natural period is usually estimated by simple empirical formulas given in the loading codes[2.7,2.8] and not calculated from the structural mass and stiffness. This is only suitable for preliminary design purposes where the structural properties have not yet been determined with any degree of certainty.

(2) Calculation of the lateral forces.

The magnitude of the base shear is obtained from the code spectra acceleration for the fundamental natural period and the appropriate amount of damping. The lateral force distribution over the entire height of the structure is based on one of the simple empirical formulae [2.7,2.8], which primarily consider only the first mode contribution although they can be modified to approximately account for the effects of the higher modes.

The simplicity of these approximate procedures make them suitable for design purposes. Many attempts have been made to apply these procedures for inelastic structures. Some use the so-called inelastic response spectra[2.6,2.9] considering the likely ductility factor. Others find an equivalent stiffness and increase in the damping ratio from the hysteresis loop of the yielded structural system. Based on the effective first mode period and the total equivalent viscous damping ratio, the maximum responses can be predicted using the response spectra for the linear system. This is usually known as the Equivalent Linear Method[2.10,2.11].

2.3 STRUCTURE MODELLING

In this section, the analytical models used in the study to represent a wide variety of Base Isolated multistorey structures are presented. The description includes the idealization of the Base Isolation system as well as that of the superstructure.

2.3.1 BASE ISOLATION SYSTEM

A desireable Base Isolation (BI) system should embody several essential characteristics :

(1) Horizontal flexibility which is able to lengthen the fundamental natural period of the structure. Under earthquakes with acceleration response spectra that diminish at longer natural periods, this action may significantly reduce the inertia forces induced in the superstructure. The isolation system should also provide sufficient vertical stiffness to transfer the vertical loads without differential settlement or unexpected rocking mechanisms.

(2) The capability of dissipating earthquake energy so as to resist excessive horizontal displacements at the base of the building. This additional hysteretic damping will reduce further the inertia forces.

(3) A so-called mechanical fuse which will guarantee sufficient stiffness of the structure at working lateral load level such as occurs with wind and micro-tremors but softens on detecting high seismic accelerations.

(4) Sufficient restoring force to relocate the structure to its original position after an earthquake attack.

(5) Is cheap, easily constructed and replaced, not susceptible to fatigue effects under ambient loadings and requires minimal maintenance during its effective life.

The design strategy will determine which characteristics should be emphasised so that the most appropriate selection of a BI system can be made for the particular situation. There are

many practical Base Isolation devices available at present. They have been installed in a variety of structures ranging from bridges to power plants and multistorey buildings in many countries. The majority of these installation are in bridges.

It is informative to conduct a broad parametric study which covers the likely variation of parameters of the commonly used Base Isolation systems, such as :

(1) Lead-rubber bearings
(2) Lead extrusion devices
(3) Mild steel energy dissipators :
    a. Torsional beams
    b. Tapered plate cantilevers
    c. Bent round bars
    d. Flexural beams
(4) PTFE sliding bearings
(5) Combinations of sleeved piles and mild steel energy dissipators or lead extrusion devices.

All of these systems can be categorized as displacement amplitude dependent devices. Their hysteretic behaviour is a function of the deformation imposed on the system, as described elsewhere[2.12,2.13,2.14,2.15,2.16]. The general form of these hysteresis loops are summarized in Fig. 2.2 and are used as a basis to determine the range of parameters which should be incorporated in this investigation. Bilinear hysteresis loop models are adapted to represent the general behaviour of these systems. Table 2.1 lists the parameters of the bilinear model considered in the analyses.

A limited number of analyses are carried out using the Ramberg-Osgood model[2.17], as shown in Fig. 2.3, in order to investigate the sensitivity of the hysteresis loop model on the seismic response of Base Isolated multistorey structures.

Another model of BI system which has an elastic spring and a velocity-dependent dashpot is also considered in this study. Since the linear stiffness of the elastic spring and the viscous damping supplied by the dashpot can be corresponded to the effective secant stiffness of a displacement-dependent device and its hysteretic damping respectively, it is informative to compare their effects on the structural behaviour. The results are presented in Chapter 5.

Some implementation of BI systems which consist of viscous dampers and elastomeric bearings have taken place in Japan[2.18]. The viscous dampers do not lengthen the fundamental period of the building. Force reduction relies mainly upon the amount of damping which is dependent on velocity. For a certain type of ground motions with peak spectral accelerations in longer periods, these velocity-dependent devices may be more suitable than the displacement-dependent devices. Some analyses are carried out using these dampers as reported in Chapter 6.

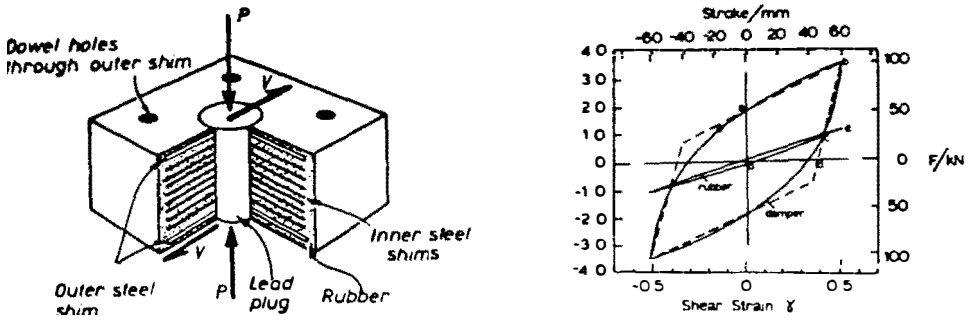

LEAD-RUBBER BEARING

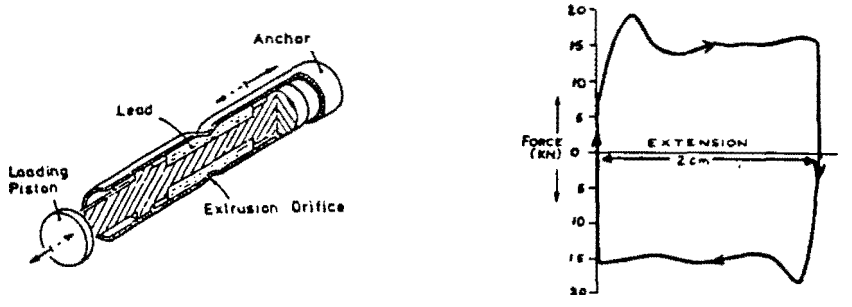

LEAD EXTRUSION DEVICE

TORSIONAL STEEL BEAM

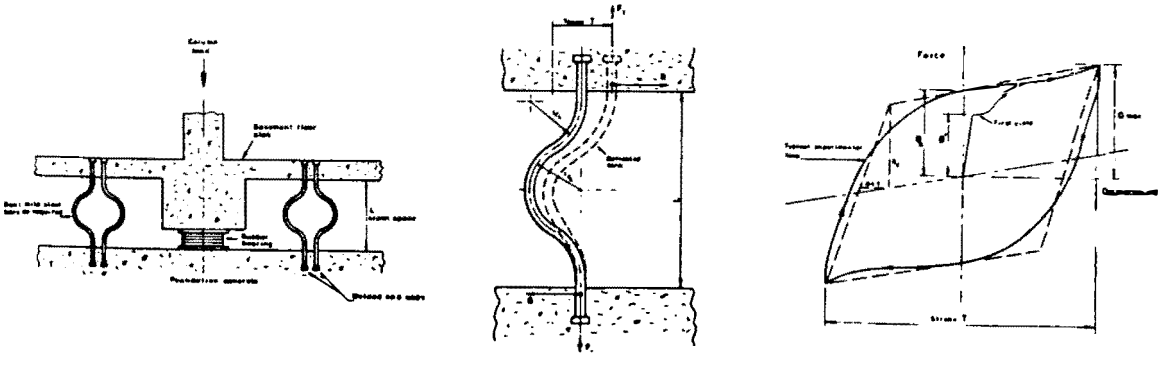

BENT ROUND BAR

Fig. 2.2 Base Isolation Devices and Their Hysteresis Loops

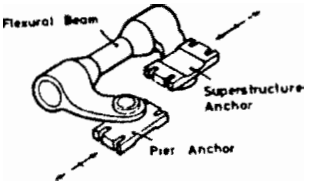

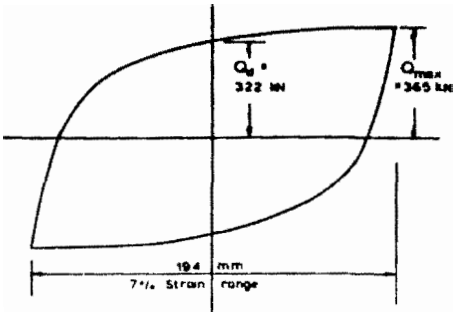

FLEXURAL BEAM DISSIPATOR

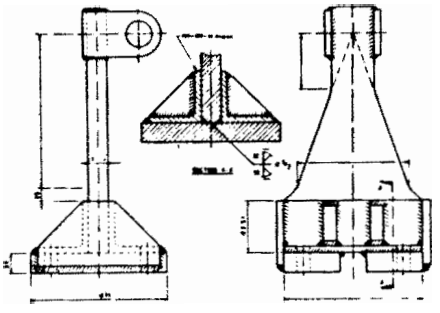

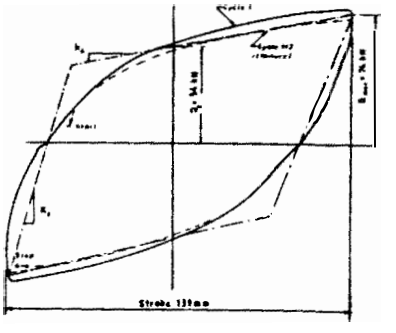

TAPERED CANTILEVER PLATE

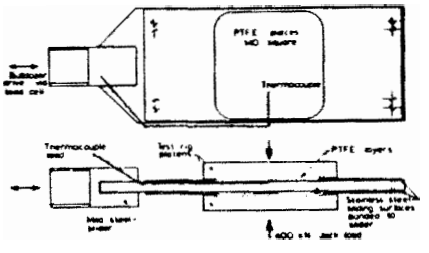

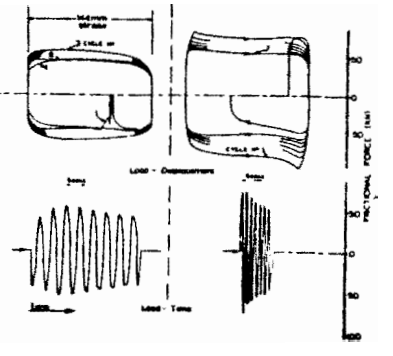

PTFE SLIDING LAYERS

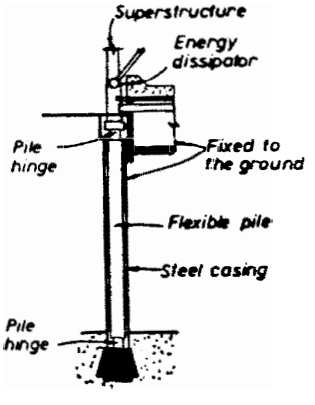

COMBINATION OF SLEEVED PILES AND ENERGY DISSIPATORS

Fig. 2.2 Base Isolation Devices . . . (continued)

Table 2.1 Parameters of Bilinear Hysteresis Loop Model

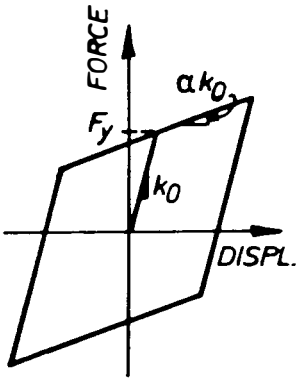

Note:

W = total weight of the structure

m = metre

k_o (W/m)	αk_o (W/m)	α	F_y/W (%)
2.50	0.750	0.300	
	1.250	0.500	For most cases:
			3.0 5.0 7.0
5.00	0.750	0.150	
	1.250	0.250	For certain cases:
			1.0 3.0 5.0 7.0
10.00	0.500	0.050	10.0 15.0 25.0
	0.750	0.075	
	1.250	0.125	
	1.500	0.150	
	2.500	0.250	
25.00	0.750	0.030	
	1.250	0.050	
	3.750	0.150	

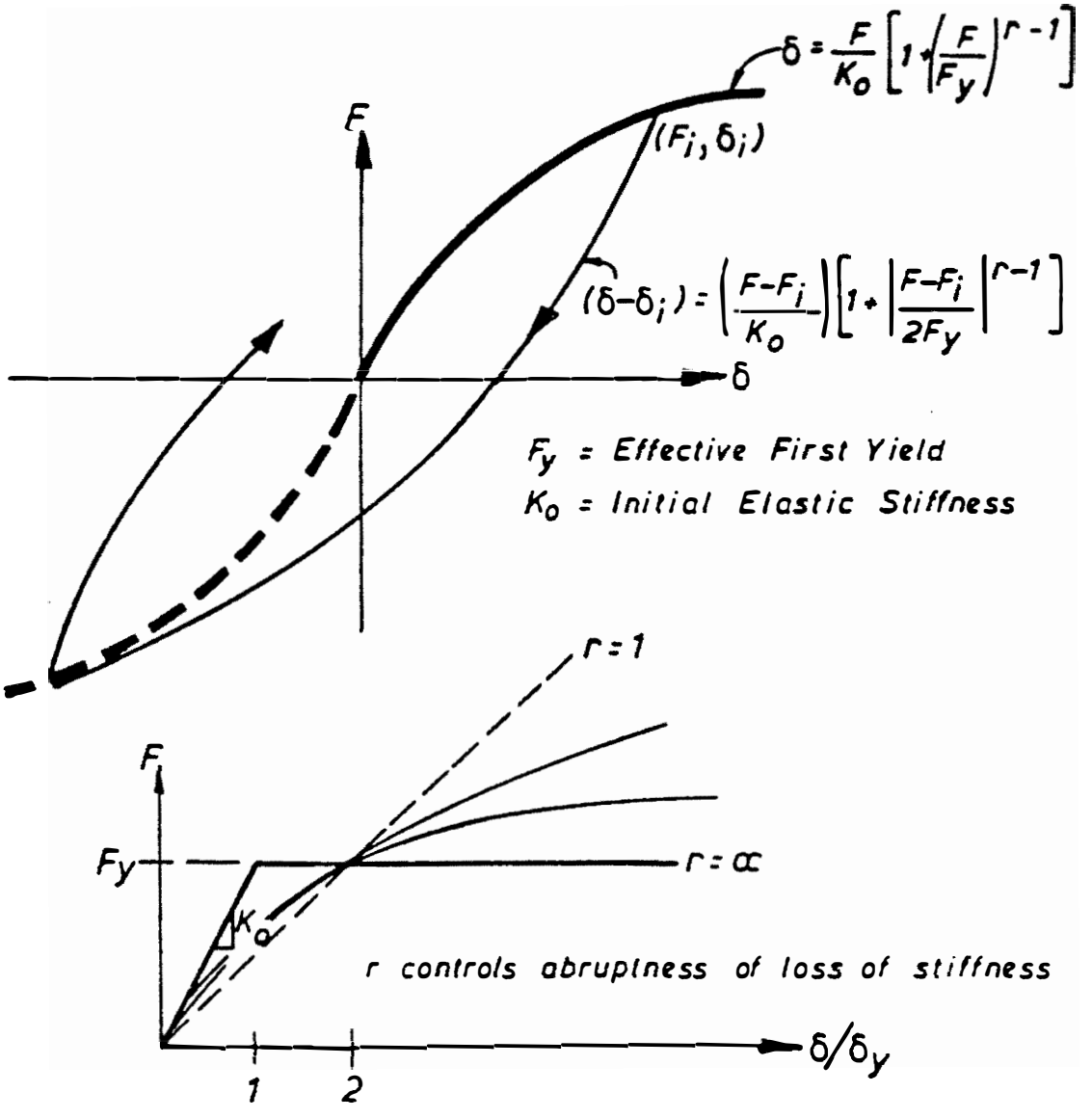

Fig. 2.3 Ramberg-Osgood Hysteresis Loop Model

2.3.2 SUPERSTRUCTURE

Many analyses, especially at the preliminary stages, normally still use the very simple "shear-beam" model to represent the actual multistorey structure. In this model, it is assumed that the floor slabs and beams act as infinitely stiff members, so that the lateral deflections result only from the column flexure without rotation at the joints. This study starts by investigating the seismic response of BI multistorey structures with "shear-beam" superstructure models, as was done earlier by Lee and Medland[2.19,2.20]. However, the other superstructure models, which have more than just one degree of freedom per floor, are also considered in the later investigations.

Cruz and Chopra[2.21] indicated that for a fixed fundamental natural period of a multistorey structure, the response contributions of the higher vibration modes increase with decreasing beam-to-column stiffness ratio. This ratio was originally defined by Blume[2.22] as a joint rotation index, and is based on the properties of beams and columns in the storey closest to the mid-height of the frame :

$$\rho = \frac{\sum_{\text{beams}} E I_b / L_b}{\sum_{\text{columns}} E I_c / L_c} \qquad (2.8)$$

where E is the elastic modulus of the structural material, I_b and I_c are the beam and column moments of inertia, L_b and L_c are the length of the beam and column respectively. A complete range of frame behaviour can be covered simply by varying this stiffness ratio, from $\rho = 0.0$ for flexural "cantilever-beam" structures, in which the beams impose no restraint on joint rotation, to the "shear-beam" structures, where the joint rotations are completely restrained ($\rho = \infty$).

Fig. 2.4 illustrates the superstructure models considered in this study. For simplicity a one dimensional flexural member with lumped mass at each floor was adopted to model the "shear-beam" and the "cantilever-beam" structures. Only one horizontal displacement per floor is allowed for the "shear-beam" structures, whereas for the "cantilever-beam" structures, one horizontal and one rotational degree of freedom are allowed at each node, except at the base where only one degree of freedom is allowed by assuming the base floor as perfectly rigid. A single bay building frame with constant storey height = h, bay width = 2h and beam-to-columns stiffness ratio $\rho = 0.125$ was also selected for studying the behaviour of Base Isolated moment resistant frames. A value of $\rho = 0.125$ was chosen as it is considered to be a representative of many existing buildings. All joints have three degrees of freedom with a lumped- mass representation. The horizontal degrees of freedom of the nodes at the same floor are coupled to each other and the base floor is considered as infinitely stiff so that only a horizontal displacement is allowed.

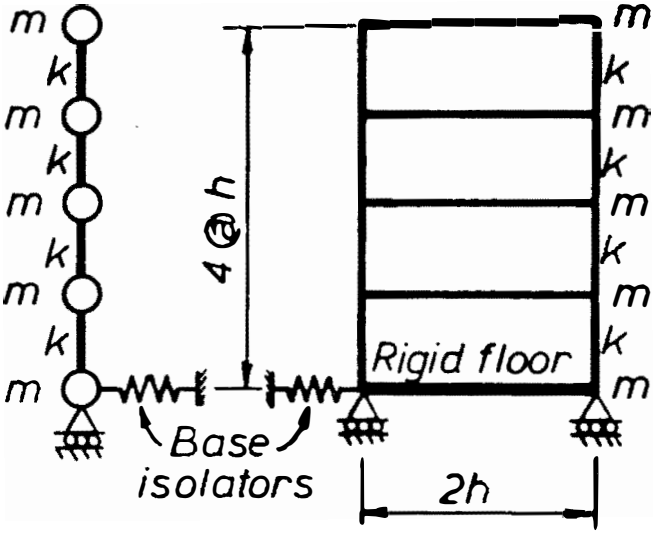

Fig. 2.4 Uniform Four-Storey Superstructure Models

All members are considered as prismatic with constant cross-section and the height of all storeys is uniform. In all of the analyses, only flexural deformations are considered, except in some analyses with a refined model of the superstructure, as described in Section 7.4 of Chapter 7 wheremore rigorous assumptions are made.

As standard models, a series of four-storey superstructures with uniform mass and stiffness over their height were adopted. The structural mass and stiffness was arranged, so that a range of fundamental natural periods, $T_{1(UI)}$ from 0.2 secs to 2.0 secs was obtained for the equivalent unisolated fixed-base structure.

To study the effects of non-uniformity of the structural mass and stiffness over the superstructure's height, the standard models were then modified to obtain various superstructure models as listed in Table 2.2. Eight and twelve storey uniform structure models were also considered for studying the effect of number of storeys on the lateral inertia force distribution.

In these analyses a constant percentage of damping[2.22] was adopted for all natural modes of free vibration. Many researchers have found that this damping model is an appropriate represention of the damping mechanism of real structures[2.22,2.23,2.24].

For most models, the damping ratios of all modes were assumed to be 5% of critical damping. However, this assumption is not always valid since the superstructure and the Base Isolation system were made from different materials and therefore they may have different damping values. To study the effect of this damping value variation on the overall structural response, it is considered necessary to be able to vary independently the superstructure's modal damping value and the Base Isolation's damping value. For this purpose the computer program ISODYN described in Chapter 5 was employed.

Plastic deformation in the superstructure may occur if an earthquake of magnitude greater than the design level earthquake occurs. The effects of these plastic hinges on the seismic performance of a Base Isolated multistorey building were also studied using refined models as discussed in Chapter 7.

Table 2.2 Floor Mass and Storey Stiffness of the Superstructure Models

Floor i	Case 1		Case 2		Case 3		Case 4		Case 5		Case 6		Case 7	
	mass	stiff.	mass	stiff.	mass	stiff.	mass	stiff.	mass	stiff.	mass	stiff.	mass	stiff.
4	m	I	m	I	m	I	m	I	m	0.75 I	0.50 m	I	0.50 m	0.75 I
3	m	I	m	I	m	I	m	I	m	1.00 I	0.75 m	I	0.75 m	1.00 I
2	m	I	m	I	m	I	m	I	m	1.25 I	1.00 m	I	1.00 m	1.25 I
1	m	I	m	I	m	I	m	I	m	1.50 I	1.25 m	I	1.25 m	1.50 I
Ground	m		0.44 m		1.71 m		2.67 m		m		1.50 m		1.50 m	

Note m = floor mass

I = moment of inertia

The elastic Young's modulus and the storey height are the same for all structures

Case 1 Base Mass m = $0.2 \Sigma m_i$ (tot. mass of the struct. incl. base mass)

Case 2 " $0.44\,m = 0.1 \Sigma m_i$

Case 3 " $1.71\,m = 0.3 \Sigma m_i$

Case 4 " $2.67\,m = 0.4 \Sigma m_i$

2.4 REFERENCES

2.1 CLOUGH, R.W. and PENZIEN, J., Dynamics of Structures, McGraw-Hill Inc., 1975, 634pp.

2.2 CRAIG, R.R., Jr., Structural Dynamics - An Introduction to Computer Methods, John Wiley & Sons Inc., 1981, 527pp.

2.3 RUBINSTEIN, M.F., Matrix Computer Analysis of Structures, Prentice-Hall Inc., 1966, p.224.

2.4 BOUWKAMP, J.G. and REA, D., Chapter 8: Dynamic Testing and the Formulation of Mathematical Models, Earthquake Engineering by Wiegel, R.L. as coord. editor, Prentice-Hall, Inc., 1970, pp.151-165.

2.5 DOWRICK, D.J., Earthquake Resistant Design: A Manual for Engineers and Architects, John Wiley & Sons Ltd., 1977, 374pp.

2.6 CHOPRA, A.K. and NEWMARK, N.M., Chapter 2 : Analysis, Design of Earthquake Resistant Structures edited by Rosenblueth, E., Pentech Press Ltd., 1980, pp.27-53.

2.7 International Association of Earthq. Engineering, Earthquake Resistant Regulations - A World List, Ga-kujutsu Bunken Fukyu-Kai, Tokyo, 1973.

2.8 Applied Technology Council, An Investigation of the Correlation between Earthquake Ground Motion and Building Performance, ATC-10, California, 1982.

2.9 Code of Practice for General Structural Design Loadings for Buildings, Draft for Comment DZ4203:1986, Standard Association of New Zealand.

2.10 IWAN, W.D. and GATES, N.C., Estimating Earthquake Response of Simple Hysteretic Structures, Journal of the Eng. Mech. Division, ASCE, Vol.105, No.EM3, 1979, pp.391-405.

2.11 TURKINGTON, D.H., Seismic Design of Bridges on Lead Rubber Bearings, Research Report 87/2, University of Canterbury, New Zealand, 1987.

2.12 TYLER, R.G., Development and Testing of Mechanical Energy Dissipating Devices and Bearings, Seismic Design of Bridges by Park, R and Blakeley, R.W.G., Part 2: Design of Bridges Incorporating Mechanical Energy Dissipating Devices, RRU Bulletin 43, National Roads Board, New Zealand, 1979, pp.75-100.

2.13 BLAKELEY, R.W.G., Parameter Studies for Design, Seismic Design of Bridges by Park, R. and Blakeley, R.W.G., Part 2: Design of Bridges Incorporating Mechanical Energy Dissipating Devices, RRU Bulletin 43, National Roads Board, New Zealand, 1979, pp.117-142.

2.14 BUCKLE, I.G., Factors Affecting the Performance of Lead-Rubber Energy Dissipators, RRU Bulletin 73, National Roads Board, New Zealand, 1984, pp.157-170.

2.15 Ministry of Works and Development New Zealand, Design of Lead-Rubber Bridge Bearings, Civil Division Publication 818/A, 1983.

2.16 SKINNER, R.I., TYLER, R.G., HEINE, A.J., and ROBINSON, W.H., Hysteretic Dampers for the Protection of Structures from Earthquakes, Bulletin of the New Zealand National Society for Earthquake Engineering, Vol.13, No.1, March 1980.

2.17 OTANI, S., Hysteresis Models of Reinforced Concrete for Earthquake Response Analysis, Journal of the Faculty of Engineering, the University of Tokyo (B), Vol.XXXVI, No.2, 1981, pp.125-159.

2.18 MAKIGUCHI, Y., Present Status of Base Isolated Building in Japan, Japan - New Zealand Workshop on Base Isolation of Highway Bridges, Welington, Nov.1987.

2.19 LEE, D.M., The Effect of Base Isolation on MultiStorey Shear Structures, Ph.D. Thesis, Dept.of Theoretical and Applied Mechanics, Univ. of Auckland, New Zealand, 1978.

2.20 LEE, D.M. and MEDLAND, I.C., Base Isolation Systems for Earthquake Protection of Multi-Storey Shear Structures, Earthquake Engineering and Structural Dynamics, Vol.7, 1979, pp.555-569.

2.21 CRUZ, E.F. and CHOPRA, A.K., Simplified Methods of Analysis for Earthquake Resistant Design of Buildings, Report No. UCB/EERC-85/01, University of California, Berkeley, 1985.

2.22 BLUME, J.A., Dynamic Characteristics of Multi-story Buildings, Journal of the Structural Division, ASCE, Vol.94, No.ST2, 1968, pp.337-402.

2.23 O'ROURKE, M., Discussion on "Response to Stochastic Wind of N-Degree Tall Buildings" by Saul,W.E., et al, Journal of the Structural Division, ASCE, Vol., No.ST12, 1976, pp.2401-2403.

2.24 JENNINGS, P., MATHIESEN, R. and HOENER, J., Forced Vibrations of a Tall Steel Frame Building, Earthquake Engineering and Structural Dynamics., Vol.1, 1972, pp.107-132.

CHAPTER 3

REVIEW OF CURRENT DESIGN METHODS AND EXISTING DESIGN GUIDE LINES

3.1 INTRODUCTION

The development of many practical Base Isolation devices since the 1970s was accompanied by proposed design methods for Base Isolated structures. The objective of these methods was to enable the designers to design this new type of structure without relying on a series of deterministic inelastic time history analyses. An equivalent linear analysis was used by most of these proposed design methods for approximating the inelastic behaviour of the isolation system as it affects the response of the elastic superstructure.

Seven present design methods are reviewed below. Six of them are presented in the following section, whereas the other approximate design method suggested by the Structural Engineers Association of Northern California (SEAONC) is presented in Section 3.3. Some optimal design procedures are briefly summarized, for interest. Two existing design guide-lines given by New Zealand National Society for Earthquake Engineering and SEAONC are also reviewed.

3.2 CURRENT DESIGN METHODS

3.2.1 PRIESTLEY, CROSBIE AND CARR (1977)[3.1,3.2]

The main aim of their study was to examine an alternative proposal of limiting inertia force in masonry buildings by seismic Base Isolation. The seismic performance of four, eight and twelve storey masonry shear walls supported on Base Isolation systems were investigated using a series of deterministic time history analyses with a limited number of earthquake records, namely the North-South component of El Centro 1940, N69W component of Taft 1952, and two artificially generated accelerograms by Jennings, namely Artificial A1 and Artificial B1[3.3]. On a fixed-base, these 4, 8 and 12 storey walls have fundamental natural periods of 0.22, 0.95 and 2.22 seconds respectively. The Base Isolation systems considered in this study were those known at that time.

Besides its above mentioned main objective, this research has given a significant contribution towards any later attempt made to investigate the seismic response of Base Isolated multistorey structures.

This study showed that an "equal-acceleration" approximation for floor masses as suggested earlier by Skinner and McVerry[3.4] using a single degree of freedom model is inadequate. Due to the influence of higher mode effects, the distribution of the maximum base shear in proportion to floor mass results in a severe under-estimation of the required moment capacity of the 4 and 8-storey masonry walls, and produces an envelope for the 12-storey which is conservative near the base of the wall but non-conservative higher up. In regard to this lateral inertia force distribution, Priestley et al[3.1,3.2] the study proposed a tentative design recommendation as follows:

1. The design lateral force should be found by distributing the base shear force V in accordance with NZS4203:1976[3.5], as expressed in Eq. 3.1, with an additional 0.2V applied at the roof level to cover inertia force distribution resulting from higher modes.

$$F_i = V \frac{W_i \, h_i}{\Sigma W_i \, h_i} \qquad (3.1)$$

where F_i is the equivalent static lateral force at ith floor, Wi and hi are the total gravity load and the height of ith floor, respectively. Note, that adding 0.2 V to the top storey effectively increasing the shear envelope at all levels by 20% of the base shear[3.2].

2. From Ref. [3.5] Base Shear $V = C_d \, Wt$ (3.2.a)

where $C_d = CISMR$ (3.2.b)

The structural type factor S and the material factor M may both be set equal to unity, since structural yield is avoided. The importance factor I and the risk factor R may also be put at unity, or at least substantially lower than their current values. In general this would then imply C_d equal to the basic seismic coefficient C.

3. Based on the results obtained from the series of time history analyses mentioned above, Crosbie[3.2] proposed some reduced values of C, for each type of BI system considered, which should be used for determining the design forces of BI masonry structures. For example, to design a squat masonry shear walls mounted on BI systems with lead energy dissipators and located in the seismic Zone A[3.5], the recommendation would be a reduction of the basic seismic coefficient C from 0.288g to 0.160g.

Designing to this requirement was found to provide an adequate flexural and shear capacity for short to intermediate period masonry shear walls (fundamental period less than 1.0 secs). However, it should be emphasized that the above recommendation was based on a limited case study for certain types of structure and BI systems. Furthermore, it did not explicitly show the correlation between the "capacity" of the BI system (in providing lateral flexibility and additional hysteretic damping) and the structural response. Such correlation is essential to give

the designer a clear understanding of how the BI system reduces the seismic forces within the structure.

3.2.2 KELLY, EIDINGER AND DERHAM (1977)[3.6]

In this study, experimental investigation was carried out using a twenty ton three-storey single bay moment resistant steel frame structure on a shaking table. The BI system used in this experiment was composed of elastic natural rubber bearings and energy absorbing devices which act as highly efficient dampers. Three earthquake records were used in the testing program, namely: the N-S component of El Centro 1940, the N65E component of Parkfield 1966 and the S16E component of Pacoima Dam 1971. Different amplitudes of these accelerograms were considered.

The experimental results showed that for "small" earthquakes, the model structure behaved as if it had a fixed-base foundation. A "large" earthquake caused the BI system to yield, the first mode period of the structure increases from 0.6 to 1.0 seconds and the equivalent first mode damping was found to be 30 to 35% of critical damping. Thus, the application of BI system reduces the structure's response under a strong ground motion by over 50% compared with that of a conventional fixed-base structure. For typical Californian earthquakes which have acceleration response spectra that diminish at longer periods, this first mode period shift will be beneficial in reducing the inertia forces within the BI structure. From the test results, a post-yield stiffness of near 5% of the elastic stiffness together with yield capacity of between 5-10% of the structure's weight was found to give an optimal BI system.

The non-linear time history analyses conducted in this research were shown to give reasonable prediction for the behaviour of the structure model.

Based upon the elastic analysis, an approximate mode-superposition design method was suggested utilising the effective periods and damping factors with a simple elastic SDOF response spectra. The proposed design procedure can be briefly outlined as follows:

1. Under the code requirements for the vertical and wind loads the structure should be completely elastic.

2. Design the rubber bearings based on the required vertical strength for the gravity loads with an appropriate safety factor; the minimum vertical stiffness to avoid rocking motion; and the most desirable lateral stiffness so that in combination with the energy-absorbing devices a suitable post-yield base stiffness can be obtained.

3. Design the energy-absorbing devices by setting the yield level greater than the maximum base shear at working load level (due to the maximum wind load and small earthquakes).

4. Obtain the natural modes and frequencies of free vibration for both the elastic (e) and post yielded (y) base conditions.

5. Assume a peak displacement of the BI system and calculate the effective natural periods, the effective mode shapes and the effective mode participation factors. In this study the effective first mode period ($T_{1\,eff}$) was found from the experimental results as a linear function of the system's peak displacement, d. The linear regression equation was as follows:

$$T_{1\,eff} = 0.271\,d + 0.582 \quad \text{(d is in inch)} \tag{3.3}$$

with a coefficient of correlation, r = 0.969 (1.0 implies a perfectly linear correlation). Note, although the above equation looks convenient for use in design, it should be realized that the derivation of this emperical equation was based on the properties of a specific superstructure model and limited types of BI system. Therefore, this equation would not be applicable for other types of BI structures.

It was assumed that ϕ_{1e} changes to ϕ_{1y} and P_{1e} changes to P_{1y} in a "linear fashion" depending upon $T_{1\,eff}$. Thus the effective first mode mode shapes ($\phi_{1\,eff}$) and participation factor ($P_{1\,eff}$) were obtained from:

$$\phi_{1\,eff} = \phi_{1e} + C\,(\phi_{1y} - \phi_{1e}) \tag{3.4}$$

and

$$P_{1\,eff} = P_{1e} + C\,(P_{1y} - P_{1e}) \tag{3.5}$$

where

$$C = \frac{T_{1\,eff} - T_{1e}}{T_{1y} - T_{1e}} \tag{3.6}$$

The experimental tests showed that the second mode shape ($\phi_{2\,eff}$) is much closer to ϕ_{2y} than ϕ_{2e}. Since C is directly proportional to the amount of yielding in the base, then

$$\phi_{2\,eff} = \phi_{2e} + C(\phi_{2y} - \phi_{2e}) \tag{3.7}$$

and

$$T_{2\,eff} = T_{2e} + C\,(T_{2y} - T_{2e}) \tag{3.8}$$

This study suggested that to account for the second mode participation by the elastic and yield base transitions, P_{2e} should be used in the analysis which may be conservative as $P_{2\,eff}$ is typically very small.

The equivalent first mode damping value can be estimated using the following formula:

$$\lambda_{1\,eff} = \frac{W_d}{4\pi\,W_s} \tag{3.9}$$

where

$$W_d = 4\gamma d\, F_{EA} + 2\lambda_R\, \pi\, k_R\, d^2 \qquad (3.10)$$

$$W_s = \frac{k_{EA}\, d^2}{2} + \frac{k_R\, d^2}{2} \qquad (3.11)$$

d = one-half of maximum peak to peak displacement of the energy absorber
F_{EA} = one-half of maximum peak to peak force of the energy absorber
k_{EA} = F_{EA}/d
γ = shape factor of energy absorber
λ_R = % critical damping of structure on rubber beaming alone
k_R = horizontal shear stiffness of rubber bearings

The higher mode effective damping should be assumed to be similar to the higher mode damping for normal structures.

6. Evaluate the structure's response using the appropriate design spectra to get maximum modal displacements, $u_{j\,max}$ and maximum modal accelarations, $u_{j\,max}$

$$u_{j\,max} = \phi_{j\,eff}\, P_{j\,eff}\, S_d\,(T_{j\,eff}, \lambda_{j\,eff}) \qquad (3.12.a)$$

$$\ddot{u}_{j\,max} = \phi_{j\,eff}\, P_{j\,eff}\, S_a\,(T_{j\,eff}, \lambda_{j\,eff}) \qquad (3.12.b)$$

where S_d and S_a are the spectral displacements and spectral accelerations derived as a function of the effective period and the effective damping of that particular mode.

The base shear and the overturning moment of each mode can then be evaluated as follows

$$V_j = \sum_{i=1}^{n} m_i\, \ddot{u}_{ji\,max} \qquad (3.13)$$

$$M_j = \sum_{i=1}^{n} m_i\, \ddot{u}_{ji\,max}\, h_i \qquad (3.14)$$

where m_i is the i th floor mass and h_i is the height of floor mass i above the base. The total responses can be found by combining the modal responses using a certain mode-superposition technique.

7. If the computed base displacement is not close to the assumed displacement, new values for $\lambda_{n\ eff}$ and $T_{n\ eff}$ should be reassessed and step 6 should be repeated.

This mode-superposition design method gave reasonably good results for the actual earthquake tests performed. Further discussion on this technique is presented in Chapter 4.

3.2.3 LEE AND MEDLAND (1978)[3.7,3.8,3.9]

The result of this research was published shortly after the publication of the two investigations mentioned earlier. In this research, a more extensive analytical study was conducted to investigate the dynamic response of Base Isolated multistorey structures. The structure models used were a set of elastic "shear-beam" structures mounted on a bilinear hysteretic Base Isolation system. Eleven actual and eight simulated earthquake records were considered in the analyses.

A series of linear regression analyses were also carried out to obtain the correlation between the maximum structural response and some selected earthquake parameters which were derived from the values of the 5, 10 and 20% damped velocity and acceleration response spectra corresponding to the fundamental and second mode periods of the structure. In brief, the earthquake parameters derived at the fundamental period were called P_1 while the parameters derived at the second mode period were called P_2. Two sets of natural periods were considered for these isolated structures. The first set was determined based on the stiffness of the BI system at initial or unyielded state whereas the second set was calculated based on the post-yield stiffness of the BI system.

The structural response of five types of Base Isolation system were considered in the above regression analyses. Table 3.1 lists the properties and the natural periods of these so-called "improved" BI systems. They were called isolation system Types Standard, A, B, C and D.

Based on the results of this investigation a design procedure was proposed as outlined in the following:

1. Select an appropriate design earthquake.

2. Choose one of the 'improved' Base Isolation systems which is considered to be the most suitable for the selected design earthquake (further guidance can be found in Ref. 3.9).

3. Estimate the isolated-yielded pseudo fundamental period of the structure ($T_{1\,(IY)}$) from Table 3.1.

4. Estimate the normalised maximum shear, S from the best fit correlations between S and the earthquake parameters. For the all five "improved" BI systems, the maximum normalised shear are determined from:

$$Sstd = 0.236\ P_1 + 0.011 \quad (\pm 0.041) \qquad (3.15.a)$$

Table 3.1 Parameters of the "Improved" Isolation Systems (after Lee)[3.7]

Isol. Sys. Type	Isol. Sys. Pars. k_1/W (Nm^{-1})	k_2/W	Q/W (N)	T_1 (UI) secs	Isolated-Unyielded $T_{1(IUY)}$ secs	$T_{2(IUY)}$ secs	Isolated-Yielded $T_{1(IY)}$ secs	$T_{2(IY)}$ secs
Std.	0.5	1.0	0.05	0.3	1.004 (1.00)	0.158 (0.15)	2.183 (2.20)	0.162 (0.15)
				0.6	1.110 (1.10)	0.295 (0.30)	2.230 (2.25)	0.318 (0.30)
				0.9	1.278 (1.30)	0.405 (0.40)	2.309 (2.30)	0.466 (0.45)
A	2.5	1.0	0.05	0.3	1.395 (1.40)	0.160 (0.15)	2.183 (2.20)	0.162 (0.15)
				0.6	1.470 (1.45)	0.309 (0.30)	2.230 (2.25)	0.318 (0.30)
				0.9	1.594 (1.60)	0.438 (0.45)	2.309 (2.30)	0.466 (0.45)
B	2.5	0.5	0.05	0.3	1.395 (1.40)	0.160 (0.15)	3.076 (3.10)	0.162 (0.15)
				0.6	1.470 (1.45)	0.309 (0.30)	3.109 (3.10)	0.322 (0.30)
				0.9	1.594 (1.60)	0.438 (0.45)	3.165 (3.15)	0.476 (0.45)
C	2.5	0.05	0.05	0.3	1.395 (1.40)	0.160 (0.15)	9.695 (9.70)	0.162 (0.15)
				0.6	1.470 (1.45)	0.309 (0.30)	9.706 (9.70)	0.325 (0.30)
				0.9	1.594 (1.60)	0.438 (0.45)	9.723 (9.70)	0.486 (0.45)
D	2.5	0.05	0.025	0.3	1.395 (1.40)	0.160 (0.15)	9.695 (9.70)	0.162 (0.15)
				0.6	1.470 (1.45)	0.309 (0.30)	9.706 (9.70)	0.325 (0.30)
				0.9	1.594 (1.60)	0.438 (0.45)	9.723 (9.70)	0.486 (0.45)

Note: k_1 = initial elastic stiffness
k_2 = post-yield stiffness
W = total weight of the superstructure above the base (excl. the base mass)
The "approximate" periods given in brackets are the oscillator periods at which the response spectra are evaluated for use as parameters in describing each structure's response.

$$S_A = 0.245\ P_1 + 0.000\ (\pm 0.040) \quad (3.15.b)$$

$$S_B = 0.151\ P_1 + 0.021\ (\pm 0.038) \quad (3.15.c)$$

$$S_C = 0.050\ P_2 + 0.047\ (\pm 0.020) \quad (3.15.d)$$

$$S_D = 0.034\ P_2 + 0.030\ (\pm 0.019) \quad (3.15.e)$$

where P_1 and P_2 represent the 10% damped spectral velocity derived at $T_{1(IY)}$ and $T_{2(IY)}$, respectively. The values in brackets are the standard deviations. Note, to find the maximum shear the value obtained in Eq. 3.15 should be multiplied by the total weight of the structure above the base level (excluding the base mass).

If the maximum shear is in fact greater than was expected, Step 2 - 4 should be repeated.

5. Design the Base Isolation system by considering the actual components which have the closest parameter values of the assumed isolated system. It is suggested that the vertical stiffness of the Base Isolation system should be sufficiently large to prevent rocking effects from being significant.

6. Recalculate the structural response based on the parameters of the actual isolation system. The normalized maximum shear S can be obtained from Eqs. 3.15.a to 3.15.e with an interpolation if necessary.

7. Likewise, the maximum base displacement, d_b can be predicted based on the associated least-squares regression line for the isolated system and it was also found to be closely correlated with the normalised maximum shear S. For structures with BI system of Type Standard, d_b can be estimated from the following correlation:

$$d_b = -3.41 + 27.07\ P_1 \ (cm) \quad (3.16)$$

where P_1 represents the 10% damped spectral velocity derived at $T_{1(IY)}$. The correlations for the other types of BI system can be found in Ref. 3.9.

8. In a similar way the inertia force distribution can also be approximated. However, it was found that the prediction of shear force distribution is much more difficult. A single descriptor, called Bulge Parameter, B was used to describe the distribution. As shown in Figs. 3.1.(a) and (b) an angle defines the position of the swinging arm OC. The static horizontal load F_i, to be applied above column i, is the "distance" at level i from the ordinate AC to the swinging arm OC. Only contributions above the higher of points C or D are considered. Fig. 3.2 shows the relationships of the angle θ and parameter B which vary with the number of storeys N. To make a single relationship between θ and B which is completely independent from N, a sinusoidal curve between θ and a new parameter B_D was defined. This relationship has the form:

$$\theta = \cos^{-1}(1 - |B_D|) \quad (3.17)$$

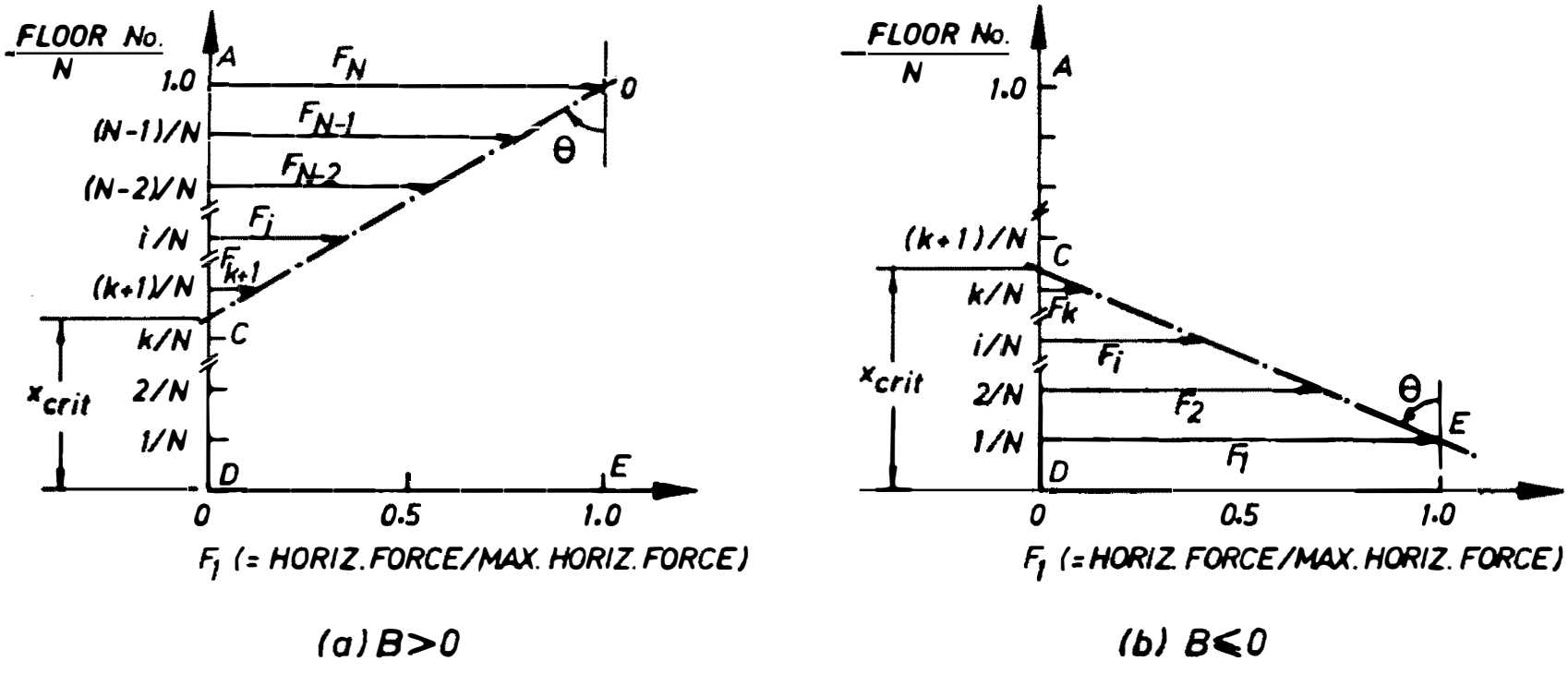

Fig. 3.1 The Equivalent Static Lateral Force Distribution Suggested by Lee and Medland[3.7,3.9]

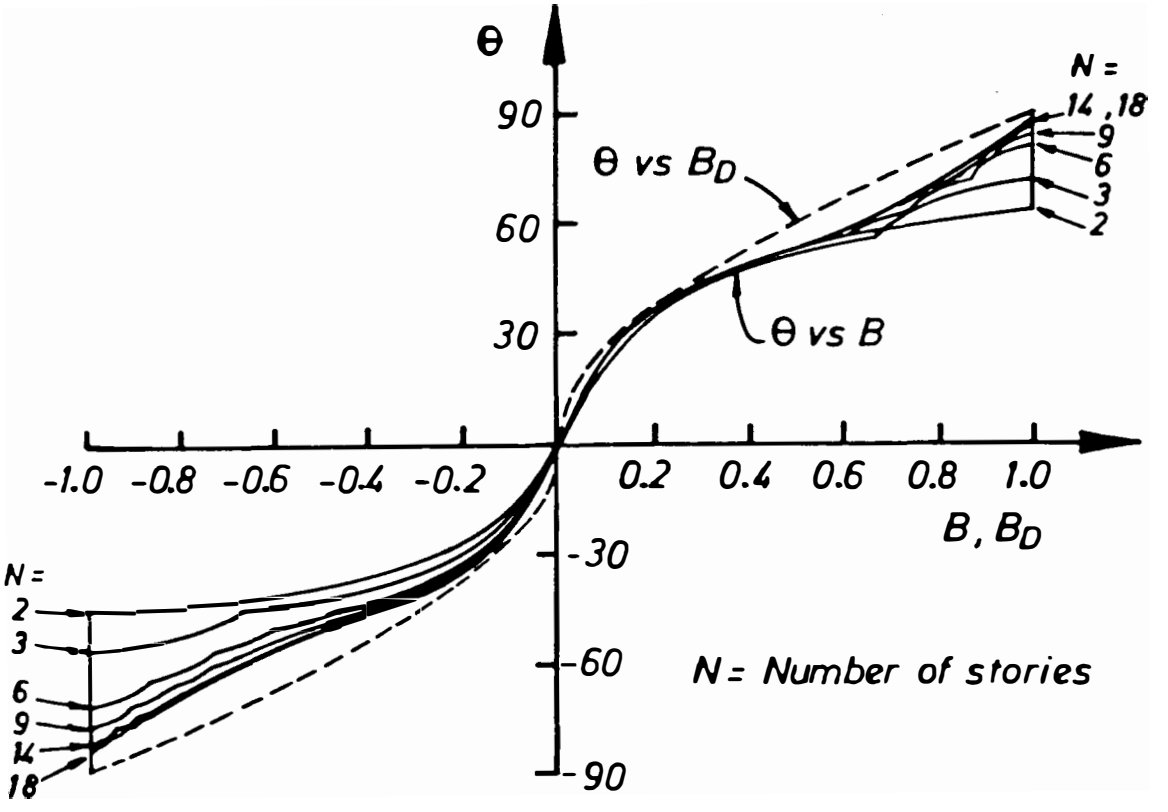

Fig. 3.2 Load Distribution Defining Angle (θ) versus the Bulge Parameters of the Design Shear Envelope (B, B_D) [3.7,3.9]

and is plotted as a dashed line on Fig. 3.2. Note, further detail about the derivation of this parameter can be found in Appendix 2 of Ref. 3.9.

For isolated structures there was a great improvement in the correlation between B_D and earthquake parameters when the structure's periods were taken into account. The ratio of the value of the 20% damped acceleration response spectrum at T_2 (IY) to the value of the same spectrum at T_1 (IY) (P_2/P_1) together with parameter P_1 gave the best description of B_D out of all parameters investigated. Thus B_D can be obtained from the following regression fits:

For $T_{1\,(UI)} = 0.3$ secs ;

$$B_D = 0.0368 + 0.0171\ (P_2/P_1) - 0.0329\ P_1 \qquad (3.18.a)$$

$$(r^2 = 0.6625)$$

For $T_{1(UI)} = 0.6$ secs ;

$$B_D = 0.2403 + 0.0251\ (P_2/P_1) - 0.0862\ P_1 \qquad (3.18.b)$$

$$(r^2 = 0.6743)$$

For $T_{1(UI)} = 0.9$ secs ;

$$B_D = 0.2574 + 0.0382\ (P_2/P_1) - 0.0541\ P_1 \qquad (3.18.c)$$

$$(r^2 = 0.7422)$$

where $T_{1(UI)}$ denotes the fundamental period of the superstructure on an unisolated fixed-base and r shows the closeness of the linear correlation between B_D and the parameters (r =1.0 implies a perfect correlation).

9. Estimate the residual plastic offset of the isolation system. The study found, however, that this offset displayed no correlation with any of the earthquake parameters considered. For the entire set of structures and earthquake considered, the residual offset had an approximate mean value of 6 mm, and an extreme maximum value of 40 mm.

The above design procedure seems attractive for use in an equivalent static force analysis. Unfortunately its use became restrictive since it was attributed to the properties of only five selected BI systems tabulated in Table 3.1 and a series of "shear-beam" superstructure models. Furthermore, the proposed formulas were derived from statistic analysis results, namely the linear correlations between the maximum structural response, e.g. base shear, base displacement, etc., and some earthquake parameters, e.g. 10% damped spectral velocity. It did not, therefore, give the designer a clear insight of the structural behaviour.

3.2.4 BLAKELEY (1978)[3.10]

This research work was carried out to study the behaviour of bridges whose decks are mounted on elastomeric bearings, with and without energy dissipating devices, under earthquake loading. The sensitivity of the bridge seismic response to the principal parameters of the Base Isolation system was investigated under three different earthquake records, namely the North-South component of El Centro 1940, Parkfield 1966 and the Artificial B1[3.3]. The aim of the study was to prepare simple design charts which could be used in lieu of a dynamic analysis, for design of bridge structures incorporating energy dissipating devices where the structural form does not present any unusual features.

Two design approaches based on the same principle were suggested. The first one estimates the structure response using the provided design response spectra such as shown in Fig. 3.3 for El Centro 1940 N-S earthquake.

For the case of a bridge with rigid abutments on which the energy dissipators are located, the first approach can be outlined as follows:

1. Calculate hysteresis loop parameters for abutment dissipators plus elastomeric bearings at abument in terms of the weight of the superstructure, W. The parameters considered are the elastic stiffness, k_{ub}, the post-yield stiffness, k_{db}, and the characteristic dissipator shear strength, Q_d as shown in Fig. 3.4.(a).

2. Calculate stiffness of pier plus elastomeric bearings, k_{pb} as illustrated in Fig. 3.4.(b).

3. Calculate hysteresis loop parameters for the whole structure by combining the parameters obtained from Step 1 and Step 2.

4. Estimate the displacement of the superstructure, Δ_s and as illustrated in Fig. 3.5 calculate the effective stiffness of the structure, k_{es} where :

$$k_{es} = \frac{F_s}{\Delta_s} = \frac{Q_{ds}}{\Delta_s} + k_{ds} \qquad (3.19)$$

5. Calculate the effective period, T_{eff} of the structure and determine the shear force, F_s from the design spectra such as shown in Fig. 3.3 for $Q_d = Q_{ds}$, where :

$$T_{eff} = 2\pi\sqrt{\frac{m}{k_{es}}} \qquad \text{and} \qquad F_s = m\ddot{u} \qquad (3.20)$$

where m is the mass of the structure and u is the response spectrum acceleration.

6. Calculate Δ_s from

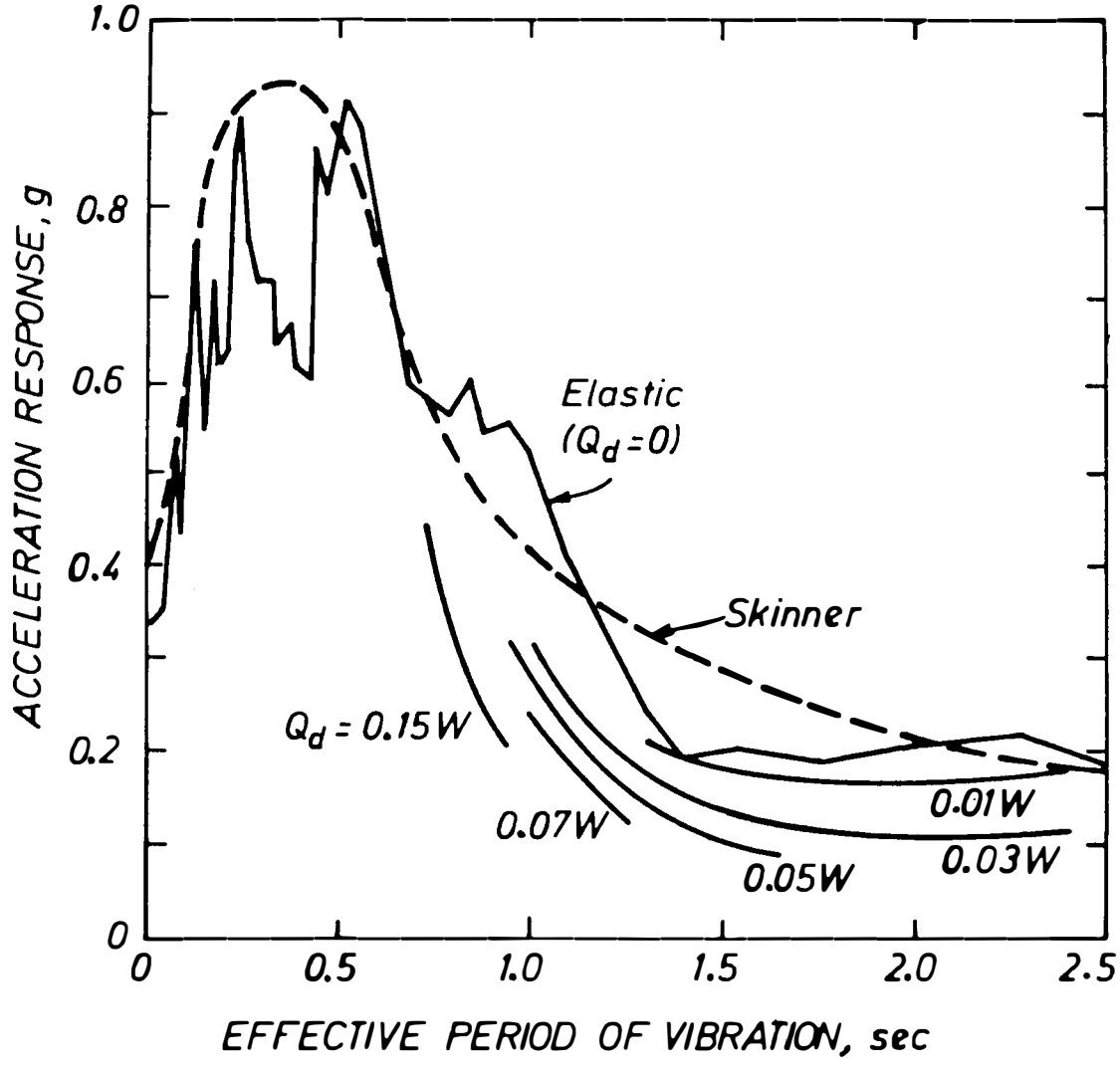

Fig. 3.3 Acceleration Response with Energy Dissipators of Varying Yield Strength[3.10]
(El Centro 1940 N-S earthquake, λ = 5% of critical damping)

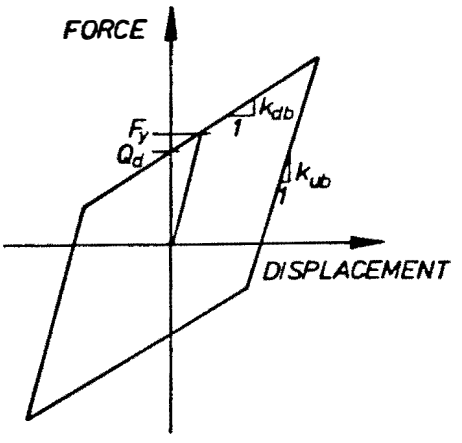

(a) Hysteresis Parameters for Energy Dissipators plus Elastomeric Bearings at the Rigid Abutments

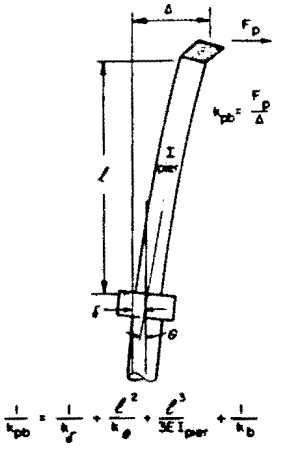

Note : k_δ = foundation translational stiffness

k_ϕ = foundation rotational stiffness

k_b = stiffness of elastomeric bearings

(b) Stiffness of Pier plus Elastomeric Bearings

Fig. 3.4 Stiffness Parameters of Isolation Systems and Bridge Substructures

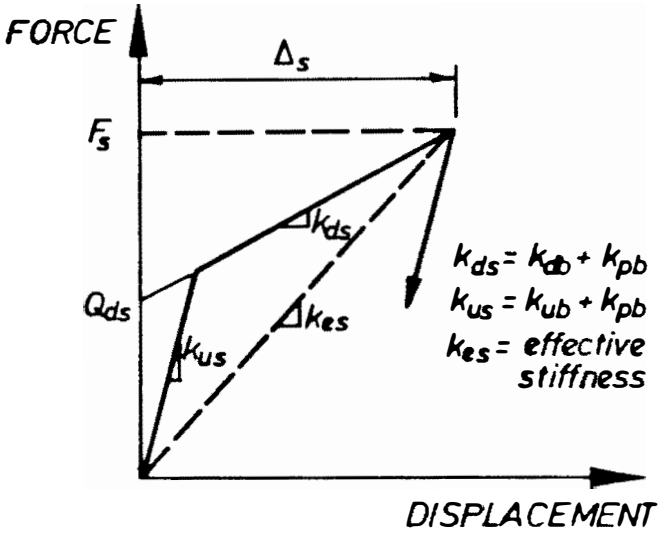

Fig. 3.5 Hysteresis Loop Parameters of the Whole Structure

$$\Delta_s = \frac{F_s - Q_{ds}}{k_{ds}} \qquad (3.21)$$

If Δ_s is not equal or close to the estimated value in Step 3, reestimate Δ_s and repeat Steps 3-5 until the two values are satisfactorily close.

7. Calculate the distributed loads to abutments and piers based on their stiffnesses.

The second approach estimates the bridge response directly from a set of design charts which were prepared using the same principles as used for the first approach described earlier. Fig. 3.6 shows an example of a typical design chart. These design methods were adopted by NZ Ministry of Works and Development for Design of Lead-Rubber Bridge Bearings[3.11].

This study also noted that energy dissipators are most effective when located on a rigid substructure which remains elastic at the design earthquake intensity. Energy dissipators are least effective when located on a very flexible or yielding substructure.

Although this study was aimed for bridge structures, the results obtained from this investigation and the design methods proposed are worthy of note.

3.2.5 DIS, INC.'S DESIGN PROCEDURES FOR BUILDINGS MOUNTED ON LEAD-RUBBER BEARINGS (1984)[3.12,3.13]

A California based consultant firm, Dynamic Isolation Systems (DIS), Inc. has developed design procedures for buildings and bridges mounted on lead-rubber bearings. The design procedures are based on the same "inelatic response spectra" approach proposed by Blakeley [3.10].

Both procedures are based on a single-degree-of-freedom (SDOF) representation. It was stated in Ref. 3.12 that provided the period of the non-isolated building is less than 1.5 seconds and the building is reasonably symmetric, this SDOF representation is a good approximation for design purposes. Thus, the inelastic response of a multistorey structure is approximately predicted in this design procedure by the pseudo elastic response of its fundamental mode. No specific guidance was given for the lateral force distribution up the height of the superstructure. It was simply recommended, that for buildings incorporating the lead-rubber bearings could be designed using the current requirements of the Uniform Building Code[3.14].

Some modification had been conducted to transform these "inelastic response spectra" approaches into a number of design charts in a format considered by DIS as suitable for design use. Fig. 3.7 shows the steps to be followed in this design procedure. Example charts of each series can be seen in Fig. 3.8 .

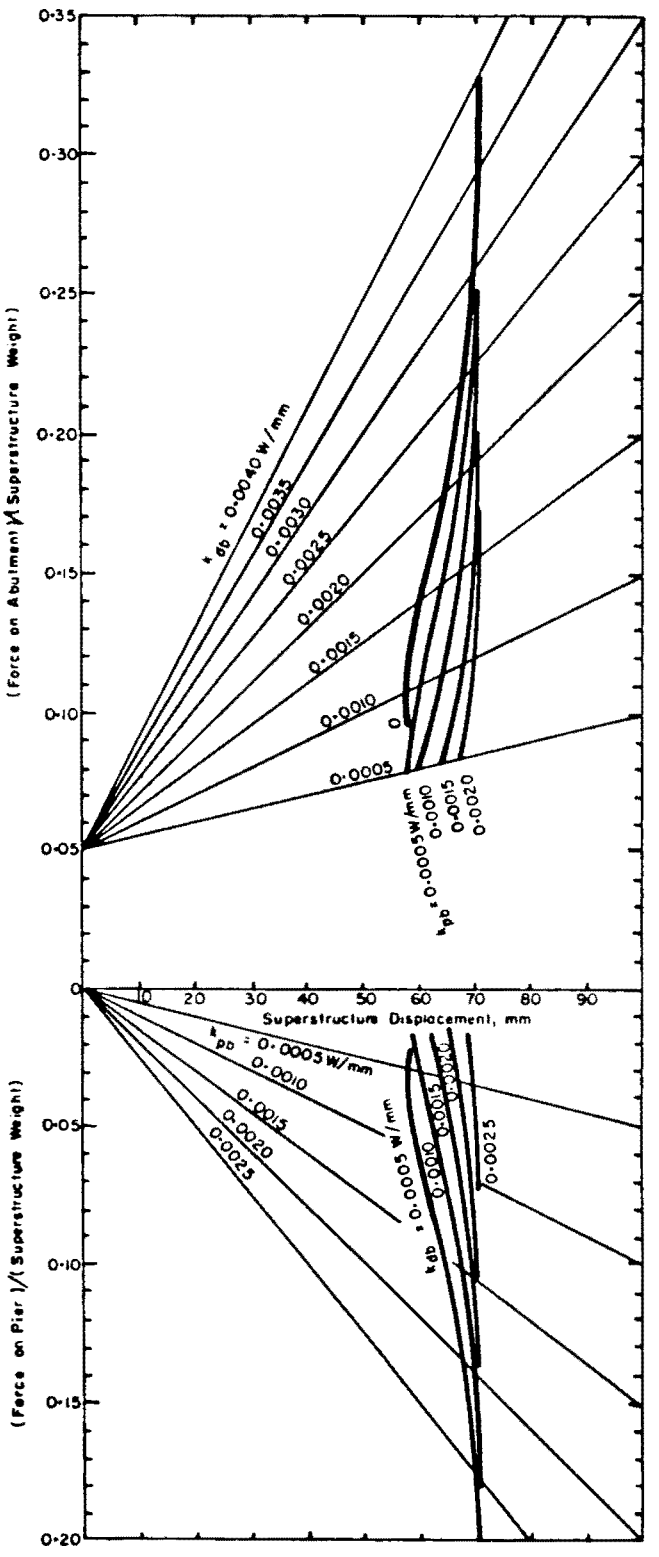

Energy Dissipator on Rigid Abutment,
Q_d = 0.05W, El Centro 1940 N-S

Fig. 3.6 An Example of Design Charts Used in the Second Approach proposed by Blakeley[3.10]

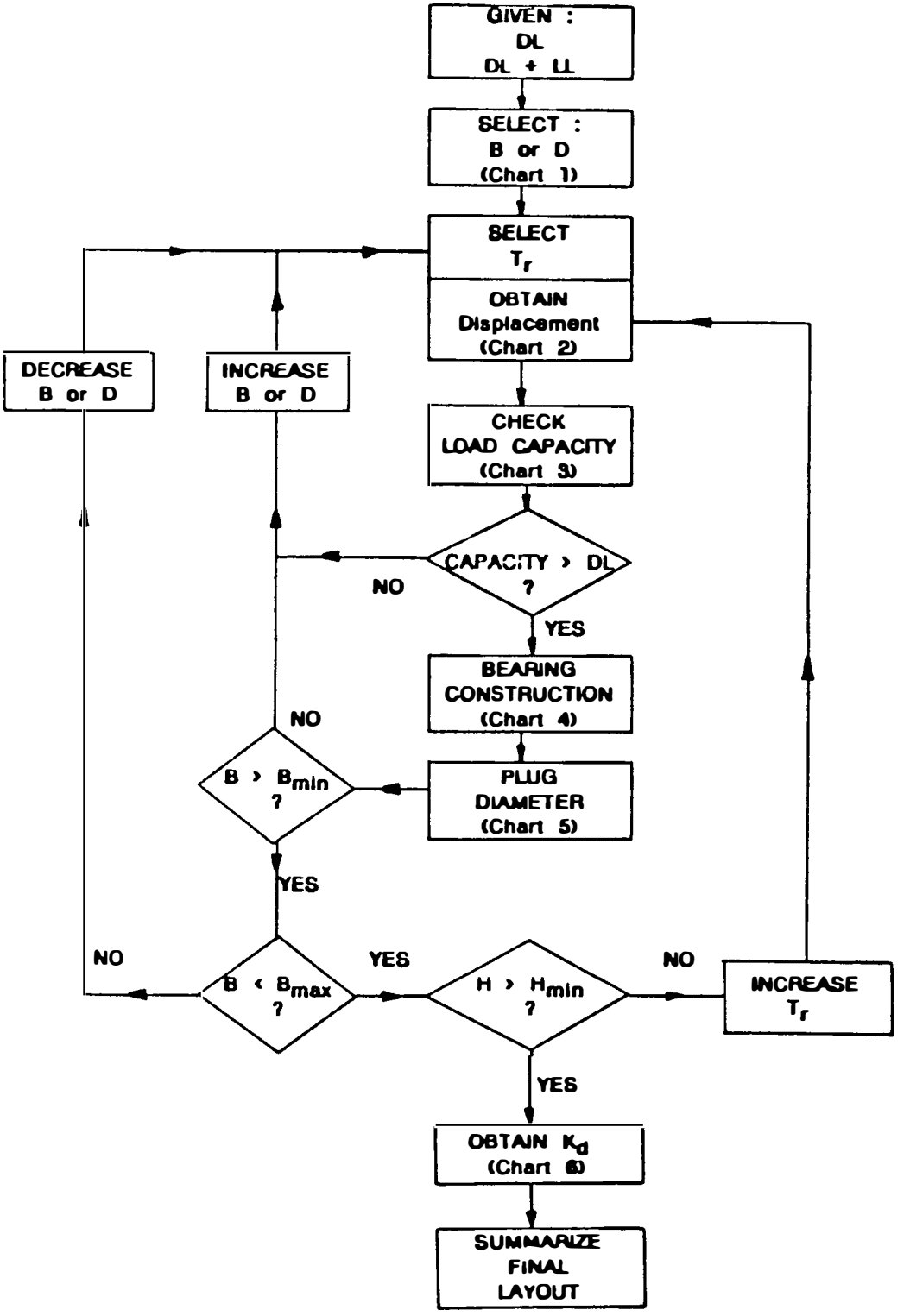

Fig. 3.7 DIS Lead Rubber Bearing Design Procedure[3.12]

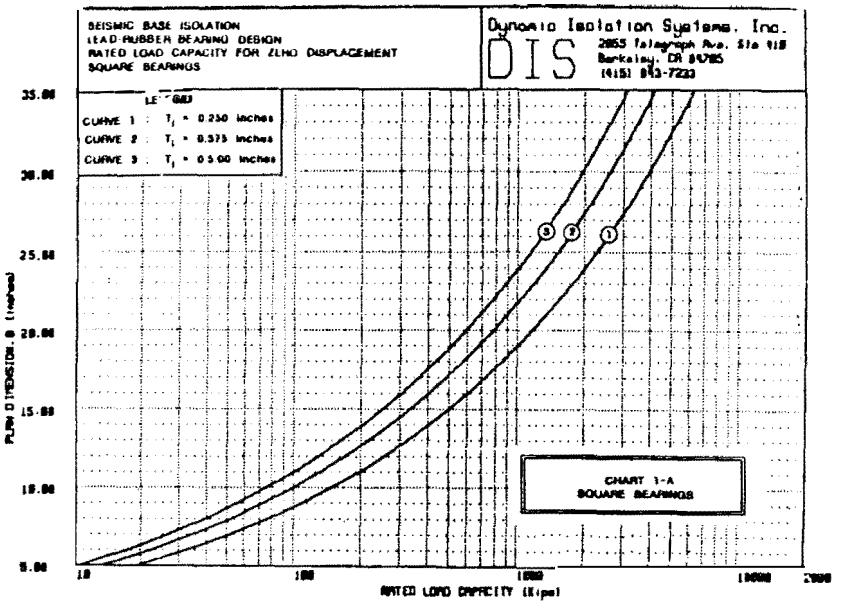

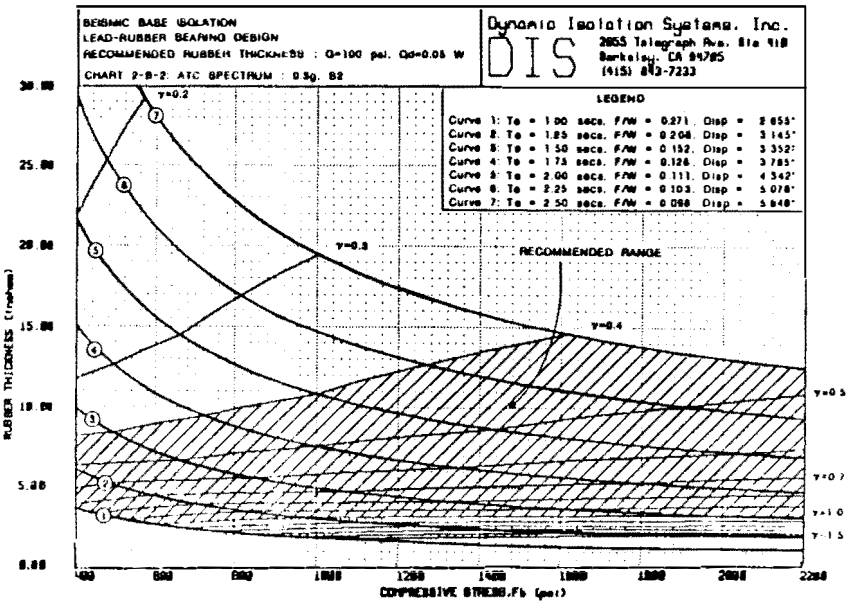

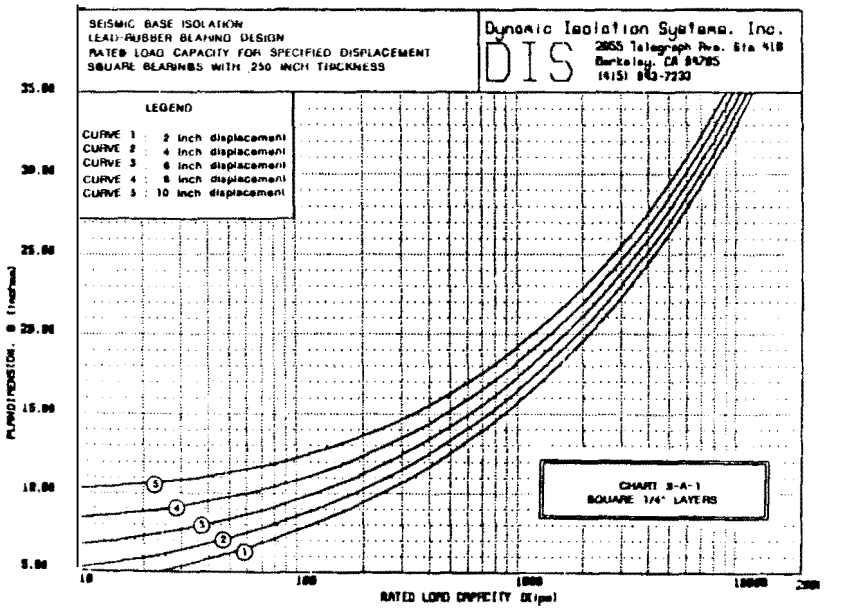

Fig. 3.8 The Series of DIS Design Charts[3.12,3.13]

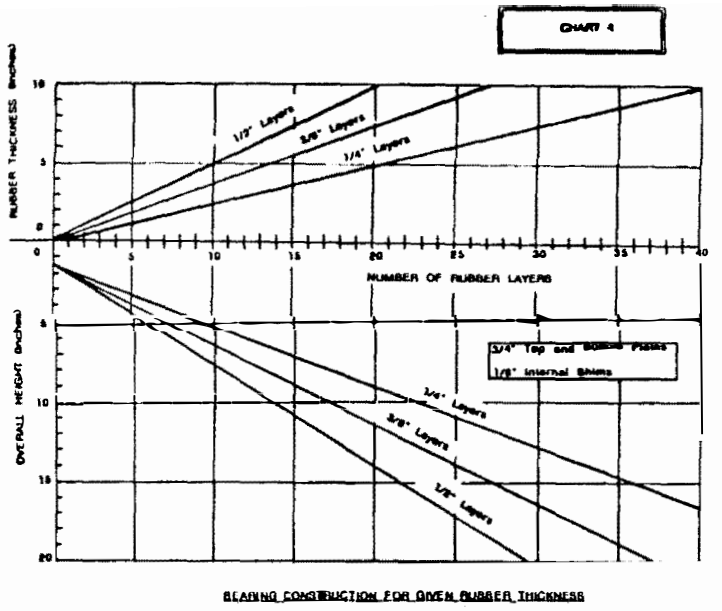

BEARING CONSTRUCTION FOR GIVEN RUBBER THICKNESS

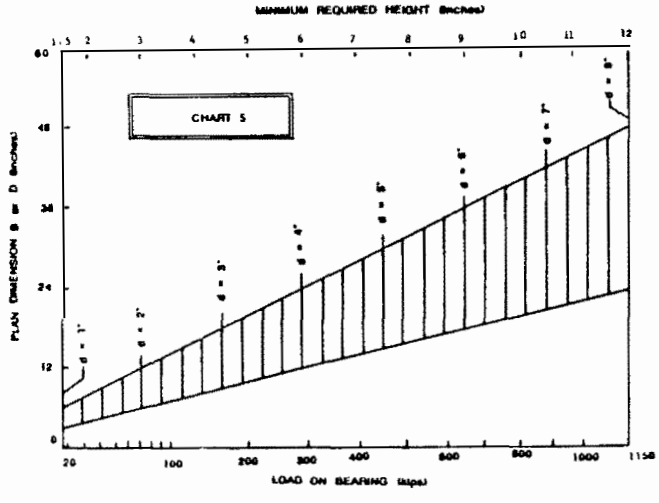

LEAD PLUG DIAMETER

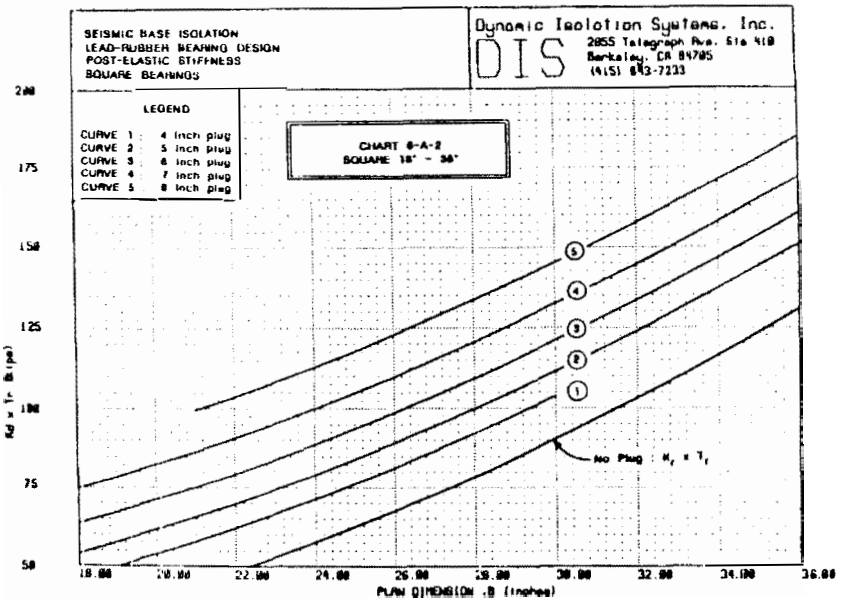

Fig. 3.8 ... (continued)

It appears that this design procedure is aimed more for designing the lead-rubber bearings and their placements on site rather than for designing the whole structure. Hence it was presented more as a design manual rather than providing the designer with a clear insight of the seismic behaviour of the structure or giving him a good feel of the sensitivity of the various BI parameters associated with the seismic response, as was noted by Turkington et al[3.15,3.16].

3.2.6 TURKINGTON, CARR, COOKE AND MOSS (1987)[3.15 , 3.16]

The purpose of this research was to supplement and extend the previous studies into seismic behaviour of bridges supported on lead-rubber bearings. This study took a fresh look at the previous work[3.11] and examined some of the underlaying concepts. It was aimed to provide a better seismic resistant design procedure for bridge structures mounted on lead-rubber bearings. For this purpose, a series of time history dynamic analysis were carried out using three earthquake records, namely El Centro 1940 N-S, Parkfield 1966, and an artifial generated record to match the New Zealand Zone A Bridge Design Spectra[3.17].

This study showed that the inelastic behaviour of the most typical bridges supported on lead-rubber bearings can be reasonably represented by an elastic SDOF structure model with an "effective period" and "effective damping". It was found that the period shift from the initial elastic period to the effective period and the increased damping due to the hysteretic behaviour of the dissipator can be estimated from the periods calculated for the initial and post elastic bearing stiffnesses and the lead dissipator yield strength. Hence the response can be predicted directly from an elastic response spectra rather than from a so-called inelastic response spectra with the iterative procedure as proposed by Blakeley[3.10,3.11]. Figs. 3.9 and 3. 10 show an example of the relationships of the initial period versus the period shift and the normalised additional damping respectively, obtained for El Centro 1940 N-S earthquake.

In this relationship, the additional damping which can be estimated using Eqs. 3.22 and 3.23 was found necessary to be normalised by dividing it by the post elastic period because the damping varied with both bearing stiffness and bridge pier flexibility.

$$C_{eff} = \frac{W_d}{\pi \omega_{eff} [x_{max}]^2} \tag{3.22}$$

$$\lambda_{eff} = \frac{C_{eff}}{2 \omega_{eff} M} \tag{3.23}$$

where $\omega_{eff} = 2\pi / T_{eff}$ and W_d is the work done in Fig 3.11 at the peak displacement X_{max}.

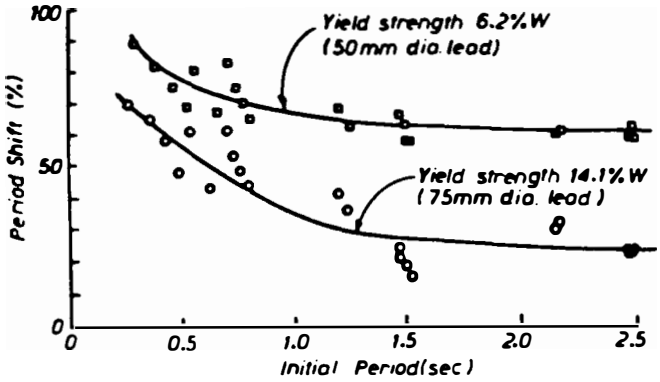

Fig. 3.9 Percentage Period Shift for El Centro 1940 (N-S)[3.15,3.16]

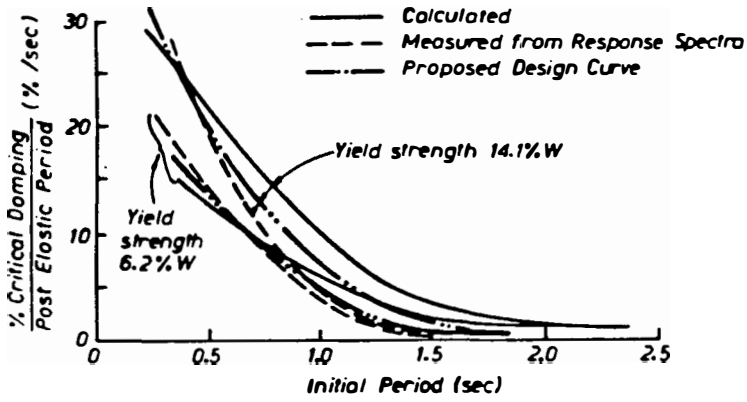

Fig. 3.10 Normalized Additional Damping for El Centro 1940 (N-S)[3.15,3.16]

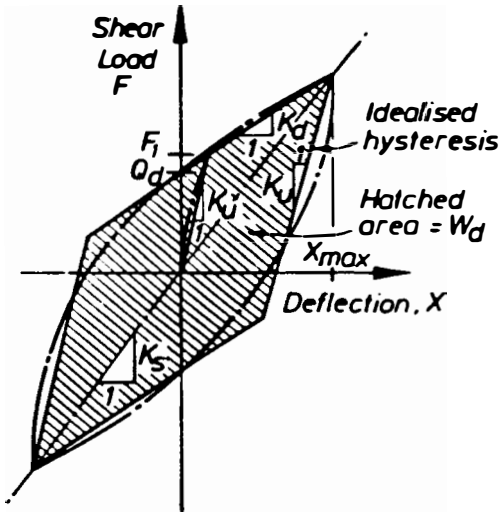

Fig. 3.11 Properties of Lead Rubber Bearings[3.15,3.16]

The steps of the proposed design procedure are as follows:

1. Make a trial selection of lead-rubber bearings by considering the gravity loads, service lateral loads, geometric constraints etc.

2. Calculate the fundamental period of the bridge with the bearings' initial and post elastic stiffness.

3. Estimate the effective dissipator yield strength by assuming the effectiveness of the dissipators in term of how many bearings at the piers and abutments actually yield, i.e. are effective.

4. Determine the "effective period" and "effective damping" from the provided design charts such as shown in Figs. 3.9 and 3.10.

5. Determine the overall seismic deck response from the design elastic response spectra for the associated "effective period" and "effective damping".

6. Calculate the deck response forces at the piers and abutments based on spectral displacement and/or the spectral acceleration. Note, a difference of about 10% between the two approaches may usually be expected and the response can be determined by taking the average.

7. Assess the seismic response of the bridge. If the distribution or level of response is not acceptable then select new bearings and repeat Steps 1-7.

8. Calculate the maximum displacement of individual bearings and check bearing failure modes at maximum dispalcement.

9. Check assumption of the effective dissipator yield level made in Step 3. If the assumption was significantly incorrect then adjust the assumed yield level and repeat Steps 3-9.

10. Determine the maximum pier base shear and bending moment.

Besides suggesting a more straight forward and conceptually clearer design method, this study also found that the vibratory earthquake records generally result in greater amount of additional damping than impulsive earthquakes, such as Parkfield 1966 and the larger magnitude earthquakes generally result in greater period shift. It also confirmed the result of the previous study[3.10] that the effectiveness of a BI system is significantly reduced as the stiffness of the substructure decreases.

3.2.7 OPTIMAL DESIGN

Some research projects have also been conducted to answer the question : "What is the 'best' choice of these energy absorbing devices for a particular structure?", in terms of degree of protection as well as cost-benefit analysis. Several optimal design approaches have been suggested as the result of these studies.

Bhatti et al[3.18] carried out an optimization study by formulating a class of optimal design problems for multistorey frames with a BI system. The optimization process required a deterministic time-history analysis of structural response at each design iteration.

Later Constantinou and Tadjbakhsh[3.19] suggested a different and perhaps a more efficient procedure than that of Bhatti et al, for designing the optimal linear Base Isolation system of multistorey shear type buildings. They used a stationary white noise random process to model the ground acceleration rather than a deterministic approach. They also conducted random vibration analyses of the BI structures with non-linear hysteretic dampers[3.20]. The hysteretic restoring force was modelled by a non-linear differential equation proposed by Wen[3.21].

Although these optimal design methods might be useful to help the designer to find the most suitable BI system for a particular structure, it would not be beneficial unless the computer program was supplied with reliable assumptions based on the structure response characterictics and a clear conceptual design philosophy. Constantinou and Tadjbakhsh[3.19], for instance, assumed that the superstructure vibrated only in the first mode and therefore neglected the contribution of the higher modes which other researchers have found to be significant.

Furthermore, the effectiveness of the algorithm depends, on a number of parameters which control the convergence and other numerical aspects. As stated by Bhatti et al[3.18] in their concluding remarks, some experience with these parameters is needed before arriving at the most suitable set of parameters for a particular problem. For these reasons, this type of investigation will not be discussed further in this thesis.

3.3 EXISTING DESIGN GUIDE LINES

3.3.1 NEW ZEALAND NATIONAL SOCIETY FOR EARTHQUAKE ENGINEERING RECOMMENDATION (1979)[3.22]

This recommendation was prepared for the design and construction of BI structures by a working group set up by the New Zealand National Society for Earthquake Engineering (NZNSEE). The philosophy of Base Isolation was reviewed, the applications of the approach, tentative code provisions and design rules were recommended and the requirements for construction of BI

structures and for maintenance of the devices were given. The recommendation was meant to be a guidance for designers and approving authorities as well as for future research.

The recommended code provisions to NZ Loadings Code[3.5] for buildings incorporating mechanical dissipating devices were as follows:

1. The following criteria shall be satisfied for the design of buildings incorporating flexible mountings and mechanical energy dissipating devices and where foundation rocking is not permitted.

2. The performance of the devices used is to be substantiated by tests.

3. Proper studies are to be made towards the selection of suitable design earthquake(s) for the building with due respect to site seismicity and geology.

4. The proposed Base Isolated structure shall be analysed using a dynamic inelastic time history analysis.

5. The structural type factor S for Base Isolated structures shall be 0.7 corresponding to the period of the total system when the mechanical energy dissipators are yielding. The shear force carried by dissipators and bearings, V, so calculated, shall be used to determine the initial level of yielding of the mechanical energy dissipators.

6. Structural members protected by Base Isolation shall be sized using the results of the inelastic dynamic analysis at the design earthquake intensity.

7. The centre of the stiffness of the isolators shall be as close as possible to the centre of mass of the building so as to reduce the response resulting from torsional motion. The horizontal force at the level considered shall be applied at a design eccentricity, e_b = 0.1 b, measured perpendicular to the loading where b is the maximum horizontal dimension of the building at that level, measured perpendicular to the loading.

8. The Seismic Force Factor, C , for parts and portions of base isolated buildings may be reduced compared to the values for non-isolated buildings and design forces are obtainable from the results of the dynamic analysis.

9. The inter-storey deflections of the Base Isolated structure shall be obtained from the "design earthquake" dynamic analysis and shall be used to detail partition, cladding and glazing separations.

10. The minimum building separation (to its neigbour's boundary) shall include the maximum allowable lateral movement of the isolators together with 1.5 times the dynamic analysis maximum interstorey drift or 0.002 times the building's height, whichever is larger.

In regard to structural detailing, it was recommended that structures incorporating energy dissipators be detailed to deform in a controlled manner under an earthquake loading greater than that designed for. This may generally be achieved by provision of suitable margins of strength between ductile and non-ductile members and by attention to detailing, but without full capacity design procedures. Where the forces in the structure are obtained from a dynamic analysis, and where the superstructure is to remain elastic up to the "design earthquake" intensity, suitable design provisions were suggested as follows[3.22] :

a. Beams of frames capable of ductile flexural yielding are to be designed for a probable flexural strength (based on a capacity reduction factor ϕ = 1.0 and probable yield strength of reinforcing steel of say, 1.15 times the minimum specified) equal to the analysis "design earthquake" moment. Curvature ductilities required in yielding members should be checked at the maximum likely earthquake intensity and critical member sizes should be increased if ductilities are excessive.

b. Columns in frames (or member shear strength) are to be designed for a dependable strength (based on the appropriate value of ϕ and minimum specified material strengths) of at least 1.10 times the force or moment calculated in that member at the "design earthquake".

c. The separation details between the isolated structure and the surrounding substructure are to allow for a deflection of at least 1.5 times the values estimated at the "design earthquake" intensity.

d. Good practice should be followed in the detailing of the transverse reinforcement to enhance ductility in the potential plastic hinge zones (incl. top and bottom regions of columns).

3.3.2 STRUCTURAL ENGINEERS ASSOCIATION OF NORTHERN CALIFORNIA'S SEISMIC ISOLATION DESIGN REQUIREMENTS (1986)[3.23]

These design requirements were developed specifically for seismically-isolated buildings and to supplement the Structural Engineers Association of California's (SEAOC) "Tentative Lateral Force Requirements, October 1985"[3.24]. The design requirements permit the use of either one of two different procedures mentioned below for determining the design-basis seismic loads. The first procedure uses a simple formula (similar to the seismic coefficient formula currently used in conventional building design) to determine peak lateral displacement and force as a function of seismic zone, soil profile, proximity to active faults, and isolated-building period and damping. The second approach, which would be required for geometrically complex or especially flexible buildings, relies on dynamic analysis procedures.

The Base Isolation system, including all connections and supporting structural elements, is required to be designed for the effects of full response at the level of approximately a 500-year return period ground motion. The superstructure, however, is not necessarily required to be designed for the full effects of the 500-year return period event, but may be designed for reduced loads, i.e. up to 2.7 times lower, provided the structural system has sufficient ductility to respond inelastically without sustaining significant damage.

a. Utilising the simple formula

Minimum earthquake displacements and forces on seismic-isolated structures shall be based on the true deformational characteristics of the isolation system. Fig. 3.12 shows an example force-deflection test curves used to determine maximum and minimum effective stiffness.

The isolation system shall be designed and constructed to withstand minimum lateral seismic displacements, D, which act in the direction of each of the main horizontal axes of the structure in accordance with the formula:

$$D = \frac{10\,ZNST}{B} \qquad (3.24)$$

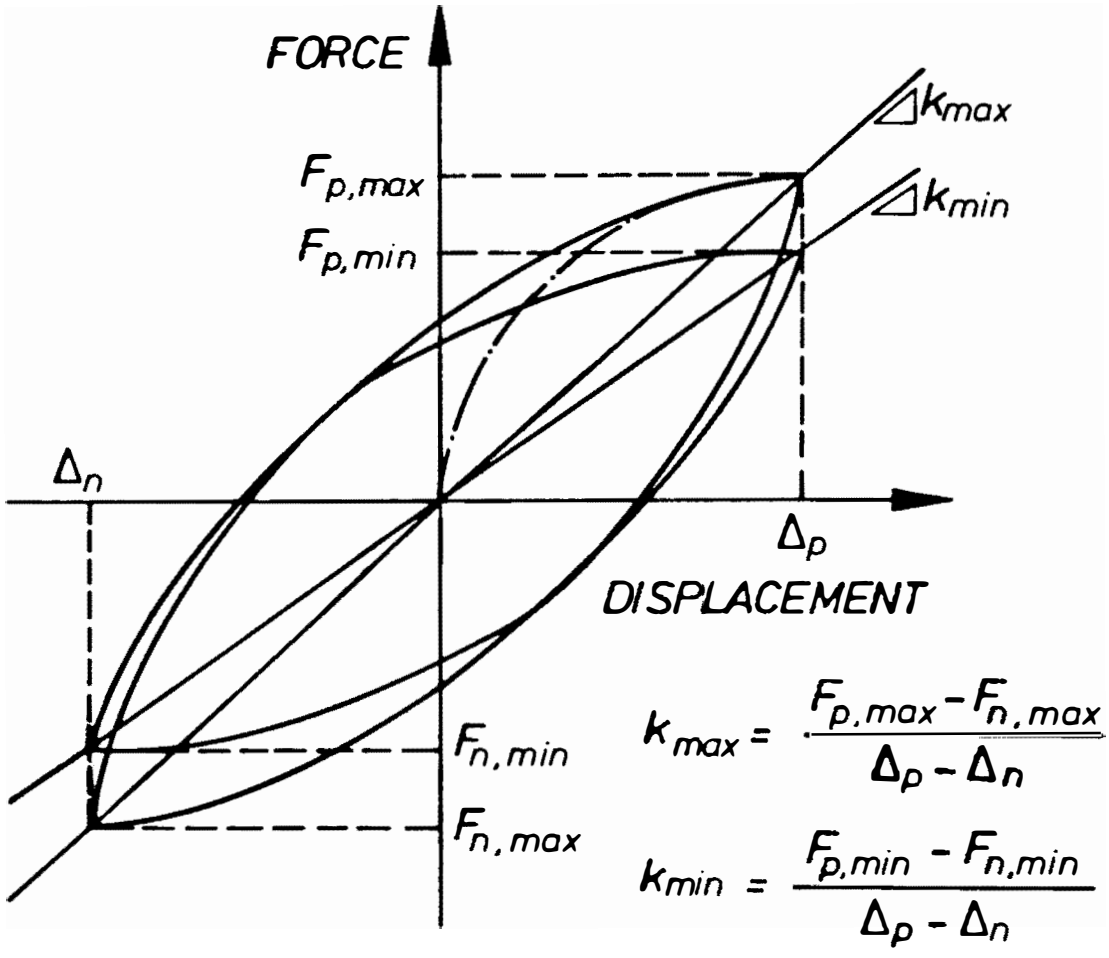

Fig. 3.12 Example of Force-Deflection Test Curves used to Determine Maximum and Minimum Effective Stiffness[3.22]

where Z is the seismic zone factor, N is the near-field coefficient (proximity to active faults), S is the site coefficient based on the soil profile, T is the isolated-structure natural period as found from Eq. 3.25 and B is the damping coefficient which corresponds to the damping value in percentage of critical damping.

$$T = 2\pi \sqrt{\frac{W}{k_{min}\, g}} \tag{3.25}$$

The total design displacement for the isolation system shall include additional displacement due to actual and accidental torsion calculated using the minimum effective stiffness of the isolation system.

All structural components at or below the isolation interface shall be designed and constructed to withstand a minimum lateral seismic force,

$$V_b = \frac{k_{max}\, D}{1.5} \tag{3.26}$$

This equation gives peak seismic shear on those mentioned structural components without reduction for ductile response. A 1.5 factor is included to reduce the peak shear level compatible with the allowable working-stress specified in Ref. 3.24.

The elements of the superstructure above the isolation system shall be designed and constructed to withstand a minimum shear force, V_S, using all the appropriate provisions corresponding to the R_W value for an unisolated structure, where

$$V_s = \frac{2\, k_{max}\, D}{R_w} \tag{3.27}$$

and R_W is the numerical coefficient related to type of structural system[3.22, 3.23].

For structures which have appreciable inelastic deformation capability, Eq. 3.27 includes an effective reduction factor of up to four ($R_W = 8$) for response beyond the working stress level. In all cases, the value of V_S shall not be less than the following:

1. the lateral seismic force required by governing building codes for a fixed-base structure with an empirical period equal to the isolated period.

2. the base shear corresponding to the design wind load.

3. the yield level of the Base Isolation system.

All non-structural components above the isolation interface shall be designed and constructed to withstand a minimum lateral seismic force, V_S. Non-structural components which cross the

isolation interface shall be designed and constructed to withstand a minimum lateral displacement as determined in Eq. 3.24. A reduction on this displacement, up to that calculated using one-half of the design basis Z coefficient, is only permitted if the failure of the non-structural component would not threaten life-safety.

This "simple formula" approach may only be fully relied upon if the elastic, fixed-base period of the building does not exceed 20% of its isolated period as determined from Eq. 3.25, otherwise more rigorous analysis shall also be performed. Under the same requirement, the superstructure shall not have significant physical discontinuities in configuration or in the lateral force resisting system. Provided these requirements are satisfied the lateral inertia force distribution over the height of the structure is given by:

$$F_i = V \frac{W_i}{\Sigma W_i} \qquad (3.28)$$

where W_i is a portion of the total weight W located at level i. This equation describes the vertical distribution of lateral force based on an assumed uniform distribution of seismic acceleration over the height of the superstructure. A similar assumption had been proposed by Skinner and McVerry[3.4] as discussed in Section 3.2.1. The only difference lies on the specific limitation set for the two approaches. Skinner and McVerry applied the assumption for isolated structures with a fundamental period (on fixed-base) not greater than 0.5 secs, whereas SEAONC required that the fixed- base fundamental period should not be greater than 20% of the "effective period". It shoul be noted, however, that the same effective fundamental period can be obtained for short period structures mounted on a BI system with either thin or fat hysteresis loops. As will be shown later in Chapter 4, structures on a BI system with thin history analized loops have a uniform shear force distribution as predicted by Eq. 3.28. However if the structure has a fat loop BI system, this equation may lead to severely underestimated storey shears, especially in the upper storeys.

b. Dynamic Analysis Procedures

The analytical model shall be three-dimensional and shall include both the deformational characteristics of the isolation system and the deformational characteristics of the superstructure. An analysis of lateral response shall be performed in both orthogonal directions of the building.

If a response spectrum analysis is conducted, two separate analyses shall be performed, one using the maximum effective stiffness, k_{max}, and the other using the minimum effective stiffness, k_{min}, of the isolation system at the design displacement, unless the difference between the minimum and maximum effective stiffness is not more than 10%. In both cases the minimum effective damping value λ at the design displacement as estimated from Eq. 3.29 shall be used.

$$\lambda = \frac{1}{2\pi} \frac{\text{Area of hysteresis loop}}{k_{eff} \Delta_{max}^2} \quad (3.29)$$

The results of these two analyses shall be considered acceptable if the calculated peak displacement of the isolation system is within 10% of the design displacement used to determine the isolation properties.

If a time history analysis is performed, at least 3 appropriate seismic inputs shall be used. The input time histories shall be selected from different recorded events and scaled such that their 5%-damped response spectrum essentially envelopes the design spectrum with a margin not more than 10% lower at any period. Each analysis shall incorporate the minimum and maximum deformational characteristics of the isolation system, as mentioned earlier for the response spectrum analysis. The maximum response of these three analyses shall be used for design.

As will be shown later in Chapters 4 and 5, however, the effect of inelastic BI systems on the seismic response of multistorey structures in general cannot simply be represented by an effective secant stiffness and effective damping as suggested above. Any response spectrum analysis or time history analysis which is based on this type of equivalent linear approach may underestimate the storey shears especially in the upper storeys of the superstructure.

3.4 SUMMARY

Comparison of the reviewed design methods is presented in a tabulated form shown in Table 3.2. From the seven design methods reviewed, five design methods are for multistorey structures while the other two methods were developed for bridge structures.

Most of the suggested approaches were based on equivalent static force analysis as commonly adopted by many loadings codes. Some have taken into account the effects of higher modes. One design method utilised a mode superposition method with an equivalent linear approximation technique in a form of response spectrum analysis[3.6].

The form of the design-aids vary from one method to another. Some methods required only a code spectral acceleration, or earthquake elastic response spectra with a wide range of damping ratios, or inelastic response spectra, whereas others required the use of some design-charts as well. One method utilised a series of charts only[3.12,3.13].

Different key parameters have been considered for design purposes. Following the basic principles of Base Isolation there should be two important parameters. Most of the methods used the first parameter, namely the effective fundamental period as a measure of the fundamental period shift due to the effect of the yielded BI system. Many means were proposed

to estimate this effective fundamental period. The second key parameter, namely the effective damping which shows the increase in damping obtained as the result of the hysteretic behaviour of the BI device was utilised directly by some methods[3.6,3.15,3.16] and indirectly by others. The method proposed by Lee and Medland[3.7,3.8,3.9] is the only one which was based on the linear regression relationships between the structure response and the earthquake parameters. For this purpose, 19 earthquake records were considered.

Among all the design methods which were based on equivalent static force analysis, there were only three which offered a method for lateral force distribution up the height of the structure. Table 3.3 lists the comparison between those three proposals. As discussed earlier, each of these methods has its shortcomings and has a different way of determining the base shear or the maximum shear response. Specific limitations were implied for two of the methods[3.1,3.2,3.23].

Finally, two existing tentative design guide-lines have been reviewed in this chapter. NZNSEE requires the use of inelastic time history analysis as the only reliable design tool, whereas SEAONC permits the use of equivalent static force analyses with a specific limitations. For more complex structures, however, SEAONC requires three dimensional response spectrum or time history analyses based on the pseudo-elastic deformational characteristics of the Base Isolation system. To a limited extend, some ductility requirements for the superstructure are also be found in these two design guide lines.

Some relevant information in regard to the shortcomings and principles of the above design methods and design guide-lines are discussed and evaluated further in the following chapters.

Table 3.2 The Current Approximate Design Methods for Base Isolated Structures

Proposed by	Aimed for	Type of Approach	Design Aid	Key Parameters	Final Results	Ground Motions Considered
1977 Priestley, Crosbie, and Carr [3.1,3.2]	Multistorey Structures (Masonry Cantilever Walls)	Equiv. Static Force Anlys with modified Basic Seismic Coeff. (higher mode effects considered)	Code Spectral Acceleration	Fund. Period of Struct. on equiv. fixed-base	- Base Shear - Lateral Forces - Overturning Moments	- El Centro 1940 N-S - Taft 1952 N69W - Artificial A1 - Artificial B1
1977 Kelly, Eidinger, and Derham [3.7]	Multistorey Moment Resistant Frames	Response Spect. Anlys with a mode-superpos. technique for equiv. linear systems	Displ. and Accel. Response Spectra (0-40% crit. dmp.)	Eff. Period, Dmp., & Parcipation Factor of the first few modes	- Storey Displ. - Storey Shears - Storey Moments	- El Centro 1940 N-S - Parkfield 1966 N65E - Pacoima Dam 1971 S16E
1978 Lee and Medland [3.8,3.9,3.10]	Multistorey "Shear-Beam" Structures	Equiv. Static Force Analysis (higher mode effects considered)	Velocity and Accl. Response Spectra Tables, Charts & Formulas	Post-yield Period, Linear Regr. Relationships betw. Str. + EQ parameters	- Max. Lat. Force - Base Displ. - Lateral Force Distribution	11 real + 8 artificial earthq. records
1978 Blakeley [3.11]	Bridge Structures	Equiv. Static Force Analysis (no higher mode effects)	Inelastic Response Spectral Accel. or Charts	Eff. Stiffness of Str. Charc. Dissipator Strength	- Superstr. Displ. - Forces on piers and abutments	- El Centro 1940 N-S - Parkfield 1966 N65E - Artificial B1
1987 Turkington, Carr, Cooke, and Moss [3.13,3.14]	Bridge Structures on Lead-Rubber Bearings	Equiv. Static Force Analysis (no higher mode effects)	Accel. and/or Displ. Response Spectra (0-40% crit. dmp.) + 2 charts to find $T_{1\,eff}$ and $\lambda_{1\,eff}$	Initial, Post-yield, Eff. Periods and Eff. Damping	- Displ. & Force of BI system, - Forces on piers & abutments	- El Centro 1940 N-S - Parkfield 1966 N65E - NZ Bridge Spectra Zone A
1984 Dynamic Isolation Systems, Inc. [3.20,3.21]	Multistorey Structures on Lead-Rubber Bearings	Equiv. Static Force Analysis (SDOF model)	a series of charts	Effective Period (Indirectly)	- Bearing Constr. Details	- ATC and - Caltrans Spectra
1986 SEAONC [3.23]	Multistorey Structures	Equiv. Static Force Analysis with uniform floor accelerations and/or 3-D Dynamic Analy. (equiv. linear system)	Code Spectral Acceleration	Eff. Min. Stiffness of BI system	- Base Displ. - Base Shear - Lat. Force Distr. or Complete Resp. from Dyn. Analy.	500-year return period level E/Q in California

Table 3.3 The Current Proposals for Equivalent Lateral Force Distribution

Description \ Proposed by	Priestley, Crosbie, & Carr[3.1,3.2]	Lee and Medland[3.8,3.9,3.10]	SEAONC[3.1,3.2]
Equivalent lateral load distribution pattern over the height of the struct.	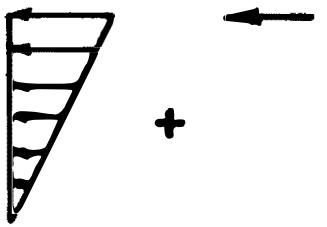 0.2 V at top	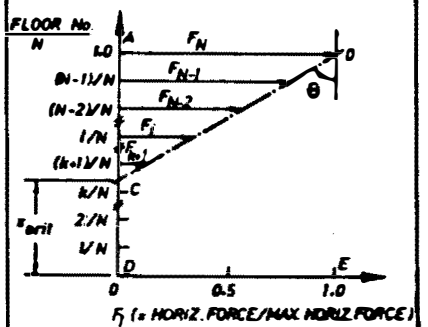	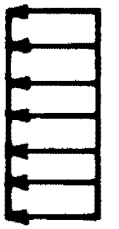
Storey Shear Force	$F_i = V \frac{W_i h_i}{\Sigma W_i h_i}$ plus 0.2 V at top	$F_i = \begin{cases} (1/N - x_{crit}) \tan\theta & ; 1/N > \max(x_{crit}, 0.0) \\ 0.0 & ; 1/N \le \max(x_{crit}, 0.0) \end{cases}$ where : $x_{crit} = 1 - \cot\theta$, $\theta = \cos^{-1}(1 - \lvert R_D \rvert)$	$F_i = V \frac{W_i}{\Sigma W_i}$ (uniformly distributed)
Specific Limitation	Short to intermediate period struc. T_1 (on fixed base) ≤ 1.0 secs	none	T_1 (on fixed base) ≤ 20% T_{1eff}
Related Code	NZS 4203 : 1976[3.5]	not specifically mentioned	SEAOC's Tentative Lateral Force Requirements, 1985[3.24]

3.5 REFERENCES

3.1 PRIESTLEY, M.J.N., CROSBIE, R.L., and CARR, A.J., Seismic Forces in Base Isolated Masonry Structures, Bulletin of the New Zealand National Society for Earthquake Engineering, Vol.11, No.4, 1978, pp.219-233.

3.2 CROSBIE, R.L., Base Isolation for Brick Masonry Shear Wall Structures, Research Report 77-2, University of Canterbury, New Zealand, 1977.

3.3 JENNINGS, P.C., (Ed.), Engineering Features of the San Fernando Earthquake, 9 Feb. 1971, Earthquake Engineering Research Laboratory, 71-02, Pasadena, California, 1971.

3.4 SKINNER, R.I., and McVERRY, G.H., Base Isolation for Increased Earthquake Resistance of Buildings, Bulletin of New Zealand Society for Earthquake Engineering, Vol.8, No.2, 1975, pp.93-101.

3.5 Code of Practice for General Structural Design and Design Loadings for Buildings, NZS 4203:1976, Standards Association of New Zealand.

3.6 KELLY, J.M., EIDINGER, J.M., and DERHAM, C.J., A Practical Soft Storey Earthquake Isolation System, Report No. UCB/EERC-77/27, Earthquake Engineering Research Centre, University of California, Berkeley, 1977.

3.7 LEE, D.M., and MEDLAND, I.C., Base Isolation - An Historical Development, and the Influence of Higher Mode Responses, Bulletin of New Zealand National Society for Earthquake Engineering, Vol.11, No. 4, 1978, pp. 219-233.

3.8 LEE, D.M., and MEDLAND, I.C., Estimation of Base Isolated Structure Responses, Bulletin of New Zealand National Society for Earthquake Engineering, Vol.11, No.4, 1978, pp.234 - 244.

3.9 LEE, D.M., The Effect of Base Isolation on Multistorey Shear Structures, Ph.D. Thesis, Dept. of Theoretical and Applied Mechanics, University of Auckland, New Zealand, 1978.

3.10 BLAKELEY, R.W.G., Parameter Studies for Design, Seismic Design of Bridges edited by Park, R. and Blakeley, R.W.G., Part 2 : Seismic Design of Bridges Incorporating Mechanical Energy Dissipating Devices, RRU Bulletin 43, National Roads Board, New Zealand, 1979, pp.117-142.

3.11 Ministry of Works and Development New Zealand, Design of Lead Rubber Bridge Bearings, Civil Division Publication 818/A, 1983.

3.12 Dynamic Isolation Systems, Inc., Seismic Base Isolation Using Lead - Rubber Bearings - Design Procedures for Buildings, 1984.

3.13 MAYES, R.L., JONES, L.R., KELLY, T.E., and BUTTON, M.R., Design Guidelines for Base Isolated Building with Energy Dissipators, Earthquake Spectra, Vol.1, No.1, 1984.

3.14 Uniform Building Code, International Conf. of Building Officials, Section 2312, 1985, pp.114-136.

3.15 TURKINGTON, D.H., CARR, A.J., COOKE, N., and MOSS, P.J., Seismic Design of Bridges on Lead-Rubber Bearings, Proc. Pacific Conference on Earthquake Engineering - New Zealand, Vol.2, 1987, pp.389-400.

3.16 TURKINGTON, D.H., Seismic Design of Bridges on Lead Rubber Bearings, Research Report 87/2, University of Canterbury, New Zealand, 1987.

3.17 BERRILL, J.B., PRIESTLEY, M.J.N., and PEEK, R., Further Comments on Seismic Design Loads for Bridges, Bulletin of the New Zealand National Society for Earthquake Engineering, Vol.14, No.1, 1981, pp.3-11.

3.18 BHATTI, M.A., PISTER, K.S., and POLAK, E., Optimal Design of an Earthquake Isolation System, Report No. UCB/EERC- 78/22, University of California, Berkeley, 1978.

3.19 CONSTANTINOU, M.C., and TADJBAKSH, I.G., Probabilistic Optimum Base Isolation of Structures, Journal of Structural Engineering, ASCE, Vol. 109/3, March 1983, pp. 676-689.

3.20 CONSTANTINOU, M.C., and TADJBAKSH, I.G., Hysteretic Dampers in Base Isolation: Random Approach, Journal of Structural Engineering, ASCE, Vol. 111/4, April 1985, pp. 705-721.

3.21 WEN, Y.K., Equivalent Linearization for Hysteretic Systems under Random Excitation, Journal of Applied Mechanics, ASME, Vol.47, March 1980, pp. 150-154.

3.22 BLAKELEY, R.W.G., et al, Recommendations for the Design and Construction of Base Isolated Structures, Bulletin of the New Zealand National Society for Earthquake Engineering, Vol. 12, No. 2, 1979, pp. 136-157.

3.23 Base Isolation Subcmt. of the Seismology Committee, Structural Engineers Assoc. of Northern Calif., Tentative Seismic Isolation Design Requirements, California, 1983.

3.24 Structural Engineers Association Of California, Tentative Lateral Force Requirements, 1985.

CHAPTER 4

THE SEISMIC RESPONSE OF BASE ISOLATED STRUCTURES WITH ELASTIC SUPERSTRUCTURES

4.1 INTRODUCTION

It has been alluded to earlier that the implementation of the BI system is meant to protect a structure from seismic risk, by concentrating the inelastic deformations to relatively cheap and replaceable devices and ensuring that, as far as possible, the rest of the structure remains elastic. In this chapter, the response of BI multistorey structures with elastic superstructures subjected to the N-S component of El Centro 1940 is discussed. Results obtained by previous researchers, such as Lee[4.1] and Kelly et al[4.2] are re-examined with a fresh viewpoint.

In order to be able to investigate the seismic behaviour of these BI multistorey structures, a reliable computer program is required as a tool for conducting the inelastic time history analyses. For this purpose, the computer program RUAUMOKO is utilised; a description of which is given in Section 4.2.

Some response history plots are displayed in Section 4.3 to describe the typical perfomance of BI multistorey structures. In Sections 4.4 and 4.5 the effect of the superstructure's fundamental period and the BI system's parameter variations are presented. The superstructure models used in this first part of investigation are "shear-beam" structures. In Section 4.6 the effect of using different types of superstructure models, namely "cantilever-beam" and "moment resistant frame" is discussed. Discussions on some design aspects are given at the end of Sections 4.4, 4.5 and 4.6 in order to develop a simple and reliable approximate design method.

Investigation on the effects of base mass, superstructure's vertical irregularities and number of storeys are also conducted as presented in Section 4.7. The analysis results are discussed to develop further the design requirements for BI multistorey structures.

For simplicity of analysis and design, the hysteresis loop of a BI system is usually modelled as a bilinear force-displacement relationship. A limited investigation of the effect of using a different hysteresis loop idealization, i.e. the Ramberg-Osgood model, is also carried out. The results are presented in Section 4.8.

4.2 DESCRIPTION OF THE COMPUTER PROGRAM RUAUMOKO USED IN THE ANALYSES

The computer program RUAUMOKO was written initially by Sharpe[4.3] and extensively developed further by Carr[4.4] over the past two decades. It was designed to produce a step-by-step time-history response of a non-linear two-dimensional general frame structure subjected to an horizontal and/or a vertical earthquake accelerogram. If required, the program carries out a static analysis for the structure, then the program performs a free-vibration modal analysis to calculate the natural periods and mode shapes of free vibration of the structure before conducting the inelastic dynamic time-history analysis. For solving the equations of motion of the structure, an algorithm based on Newmark's Constant Average Acceleration method[4.5] is used . The time step for the numerical integration in all analyses was taken equal to 0.01 seconds.

RUAUMOKO allows coupling of degrees of freedom to be done by slaving a degree of freedom at one node (or joint) to the corresponding degree of freedom of any other node. This ability is found to be useful for eliminating very high natural frequencies which might arise from the relative movement in an axial direction of the nodes at either end of a beam member. The presence of these high natural frequencies may affect the accuracy of the piece-wise time integration scheme.

The structural mass can be represented in the form of either lumped or distributed mass matrices. For a lumped mass model as is considered in this study, the included horizontal, vertical and rotational mass inertias can be defined in the input loading data.

In order to be able to model the structure components accurately, a number of member types are provided, such as a beam member with or without beam-column yield interaction, a truss member with no flexural stiffness, a shear member, and a shear wall element etc. To simulate their inelastic behaviour, there are seventeen different hysteresis models available, including models for degrading stiffness, degrading strength and slackness. At each specified time-step, the member stiffness is updated following the selected hysteretic rule. The Direct Stiffness method[4.6] is used to assemble the individual member stiffness matrices into the global stiffness matrix. With these features, the computer program provides sufficient options to allow the structural models incorporated in this study to be analysed with high reliability.

Originally the program[4.3] incorporated only the damping model based on Rayleigh's damping concept[4.7], where the damping matrix is given by a linear combination of the mass and stiffness matrices:

$$[C] = \alpha [M] + \beta [K] \qquad (4.1)$$

and $$\alpha = \frac{2\,\omega_1\,\omega_2\,(\omega_1\,\lambda_2 - \omega_2\,\lambda_1)}{\omega_1^2 - \omega_2^2} \tag{4.2}$$

$$\beta = \frac{2\,(\omega_1\,\lambda_1 - \omega_2\,\lambda_2)}{\omega_1^2 - \omega_2^2} \tag{4.3}$$

in which ω_1 , ω_2 are any two natural circular frequencies and λ_1 , λ_2 are their respective fractions of critical damping. By specifying the damping ratios of any two selected modes, all other modes with natural frequency ω_n subsequently have their fractions of critical damping given by:

$$\lambda_n = \frac{1}{2}\left(\frac{\alpha}{\omega_n} + \beta\,\omega_n\right) \tag{4.4}$$

as illustrated in Fig. 4.1. In this program , it is possible to form the Rayleigh damping matrix based on either the initial structural stiffness or the tangent stiffness.

It has been realized, that in employing this damping model care must be taken to avoid supercritically damped high modes which may lead to underestimation of the structure response, especially if the contribution of these modes are significant. Generally, the two selected frequencies should be of the lowest and the highest modes which are expected to contribute significantly to the response[4.8].

A direct approach to form an orthogonal damping matrix was suggested by Wilson and Penzien[4.9]. Principally, the contribution to the damping matrix [C] from each mode is proportional to the modal damping ratio as demonstrated in the following:

$$[C] = [\theta]\,[\beta]\,[\theta]^T \tag{4.5}$$

where $[\theta]$ is the normalized mode shape matrix defined by:

$$[\theta]^T\,[\theta] = [I] \tag{4.6}$$

and $[\beta]$ is a diagonal matrix with terms:

$$\beta_n = 2\,\lambda_n\,\omega_n\,M_n \tag{4.7}$$

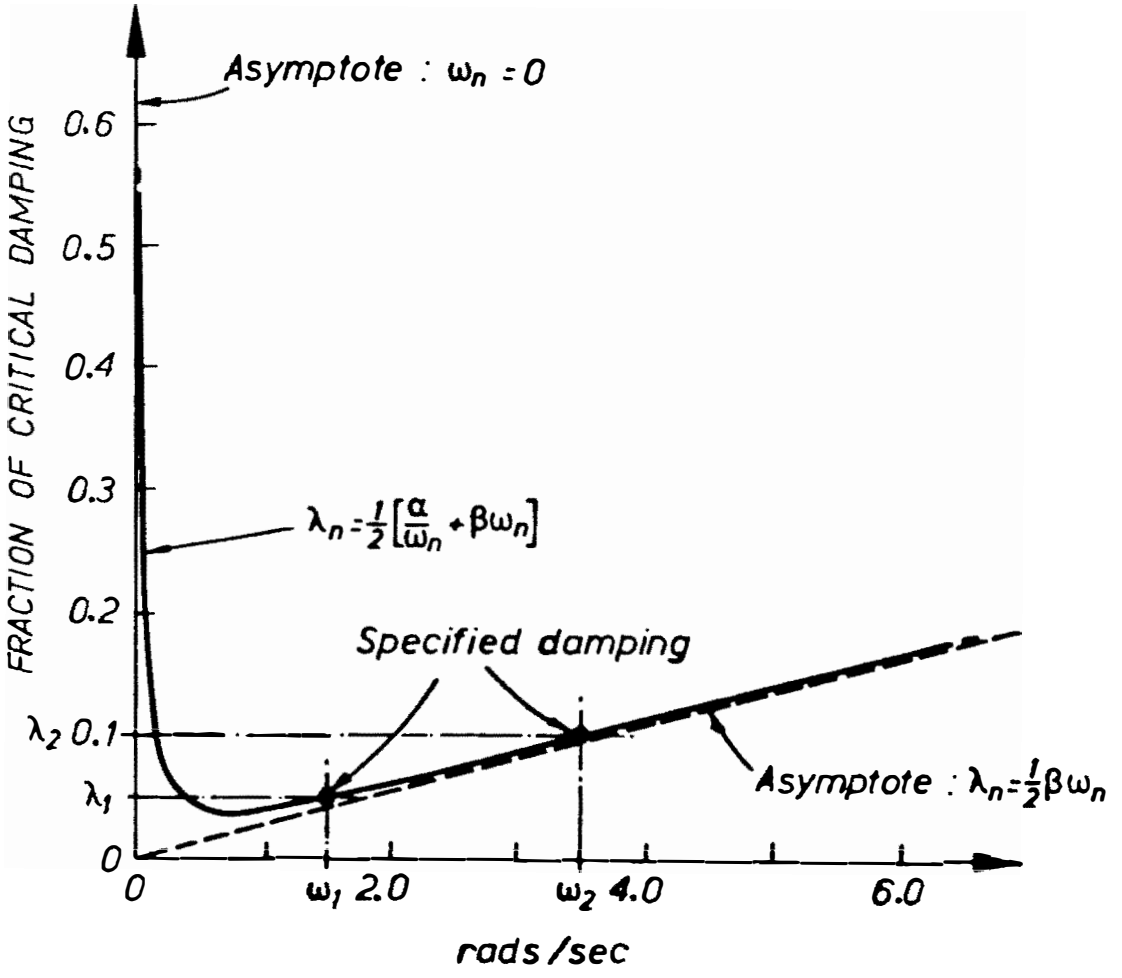

Fig. 4.1 Typical Rayleigh Damping Model

where ω_n is the circular frequency of the mode n, λ_n is the fraction of critical damping in mode n and M_n is term corresponding to the n th mode of the generalized mass matrix. As an alternative, Eq. 4.5 can also be expressed in the form of a summation of modal damping matrices $[C_n]$, i.e.:

$$[C] = \sum [C_n] \tag{4.8}$$

where $[C_n]$ may be calculated using the relation:

$$[C_n] = \beta_n \{\theta_n\} \{\theta_n\}^T \tag{4.9}$$

Based on this approach, two further models, namely linear and trilinear damping models[4.8] were developed and added to the computer program RUAUMOKO. These new models, as illustrated in Fig. 4.2, allow more control over the modal damping ratios than the Rayleigh's model since specification of the damping ratios can be associated with any mode rather than just two modes. From this linear damping model, it is possible to obtain the constant modal damping as used in this study. As reported by Chrisp[4.8], several researchers have suggested that constant modal damping is most appropriate for the dynamic analyses of structures.

It should be noted, however, that using either linear or trilinear damping model means the structural damping matrix is formed by the contribution of all modal dampings and therefore a complete modal analyses should be carried out before hand. No such analysis is required for the Rayleigh's damping model. The other disadvantage of this approach is that it produces a fully populated damping matrix. For inelastic analyses, where mode separation is not possible this causes a considerable increase in computing cost compared to the analyses using a banded damping matrix. To overcome this problem, an iterative scheme was formulated and included in the program by Carr[4.4] to compensate for the off-band terms. Fuller description of this routine can be found in Ref. 4.8.

It is worth noting some other capabilities of this computer program. It is able to include the P-Δ or even large displacement effects in the analyses. A new feature has also been added for evaluating the total energy input by the earthquake and the energy absorption capacity of the structure in the forms of elastic vibrational or kinetic energy, cumulative elastic and plastic strain energy, as well as the energy dissipated by the damping forces as suggested by Akiyama[4.10].

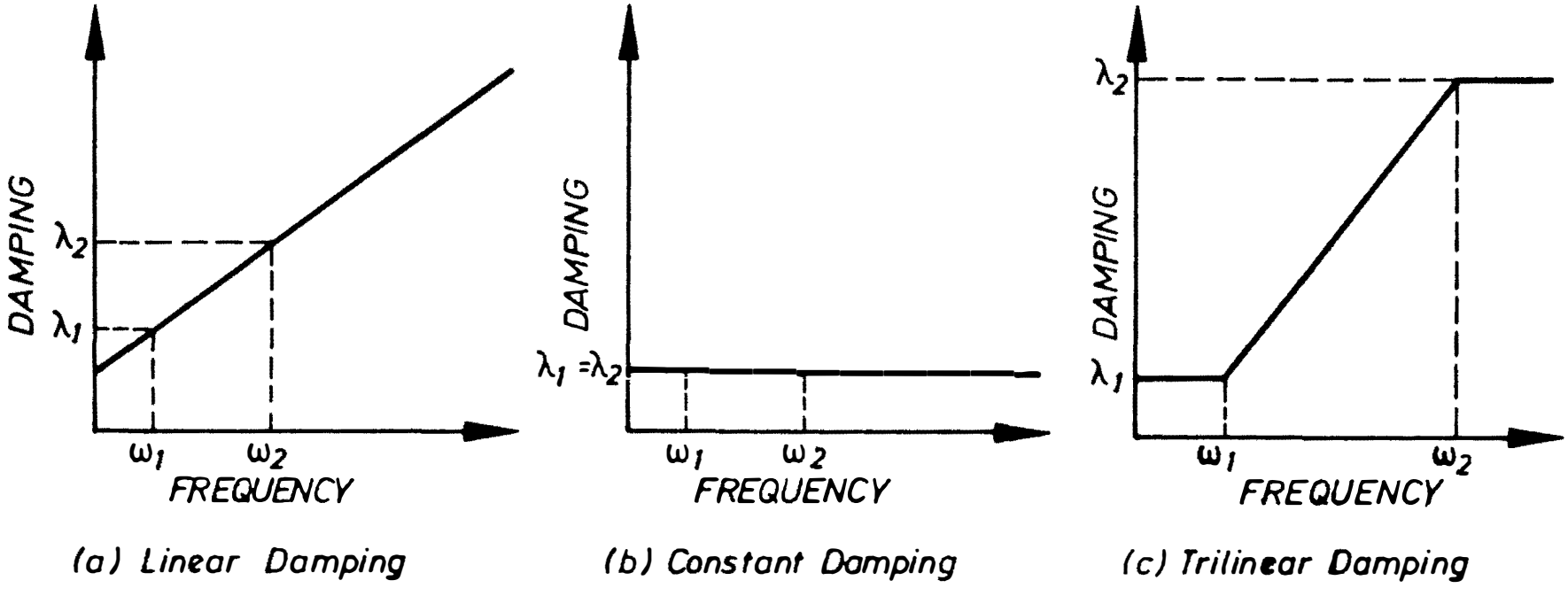

Fig. 4.2 Linear, Constant and Trilinear Damping Models

4.3 TYPICAL PERFORMANCE OF BI MULTISTOREY STRUCTURES

4.3.1 INTRODUCTION

The seismic responses of a four-storey uniform "shear-beam" structure, with and without a BI system are contrasted in order to demonstrate the typical performance of BI multistorey structures. The two structural models considered in the analyses are shown in Fig. 4.3. The ground input motion for the two deterministic time history analyses was the N-S component of El Centro 1940 N-S earthquake.

Both models have the same superstructure with fundamental period of 0.4 seconds. The unisolated model is on a fixed base, whereas the Base Isolated model is mounted on a BI system which has a bilinear force-displacement relationship. The initial stiffness, k_o , of the BI system is ten times the total weight of the structure per metre (10.0 W/m) whereas the post-yield stiffness, αk_o, and the yield strength, F_y are 1.5 W/m and 5%W respectively.

The values of various response parameters, such as lateral storey displacements, interstorey drifts, base shear, lateral storey shears, and overturning moments obtained from the analyses, are presented in order to demonstrate the typical performance of a BI multistorey structure. To describe the likely lateral inertia force distributions more clearly, another BI system which has a lower post-yield stiffness, i.e. αk_o = 0.5 W/m is also considered.

4.3.2 LATERAL STOREY DISPLACEMENT AND INTERSTOREY DRIFT

The horizontal flexibility provided by a BI system causes the BI structure to have larger lateral storey displacements compared to its fixed-base counterpart. As shown in Fig. 4.4 the maximum lateral top floor displacement of the BI structure is twice as large as the top floor displacement of the unisolated structure.

To avoid contact with adjacent buildings during earthquakes, a sufficient gap must be provided to accomodate this larger lateral displacement. Also, flexible connections should be provided for services, such as water supply, drainage system, etc., into the building.

It is worth noting , however, that the base of a BI structure moves in the horizontal direction almost as much as the top floor. Thus, there is a significant reduction in the interstorey drift as demonstrated in Fig. 4.5. The maximum drift between the first floor and the ground floor of the BI structure is less than a quarter of the maximum drift between the same stories of the unisolated structure.

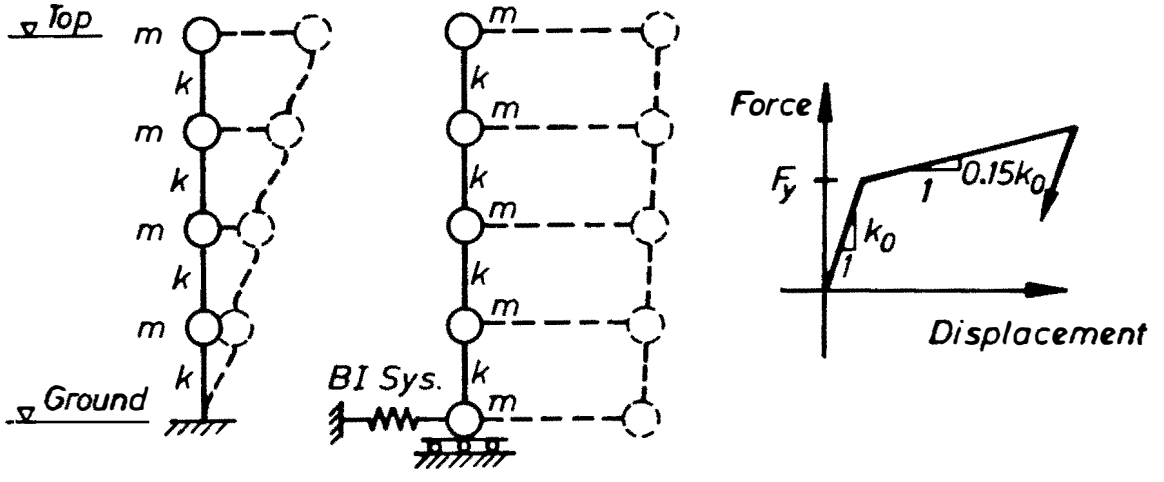

(a) Fixed-Base (b) Base Isolated (c) Hysteresis Model of the BI System

Fig. 4.3 Structural Models used in the Analyses

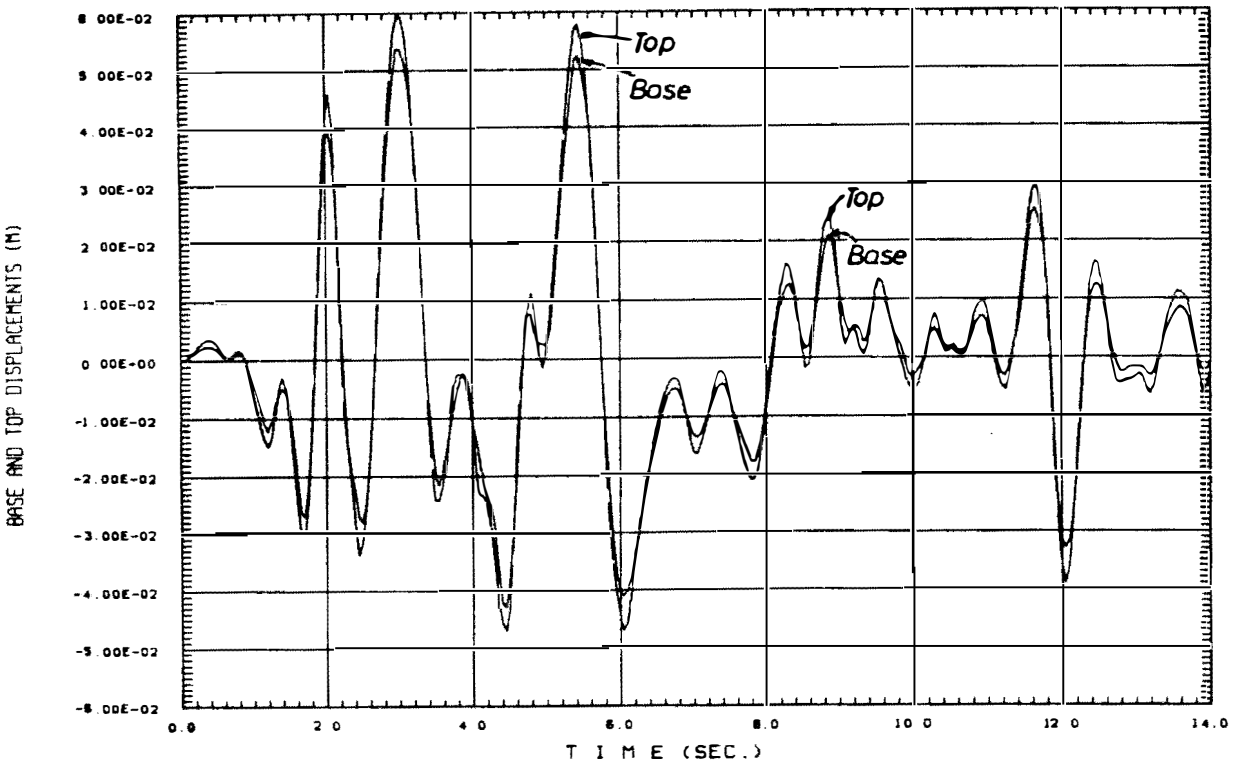

(a) Base Isolated

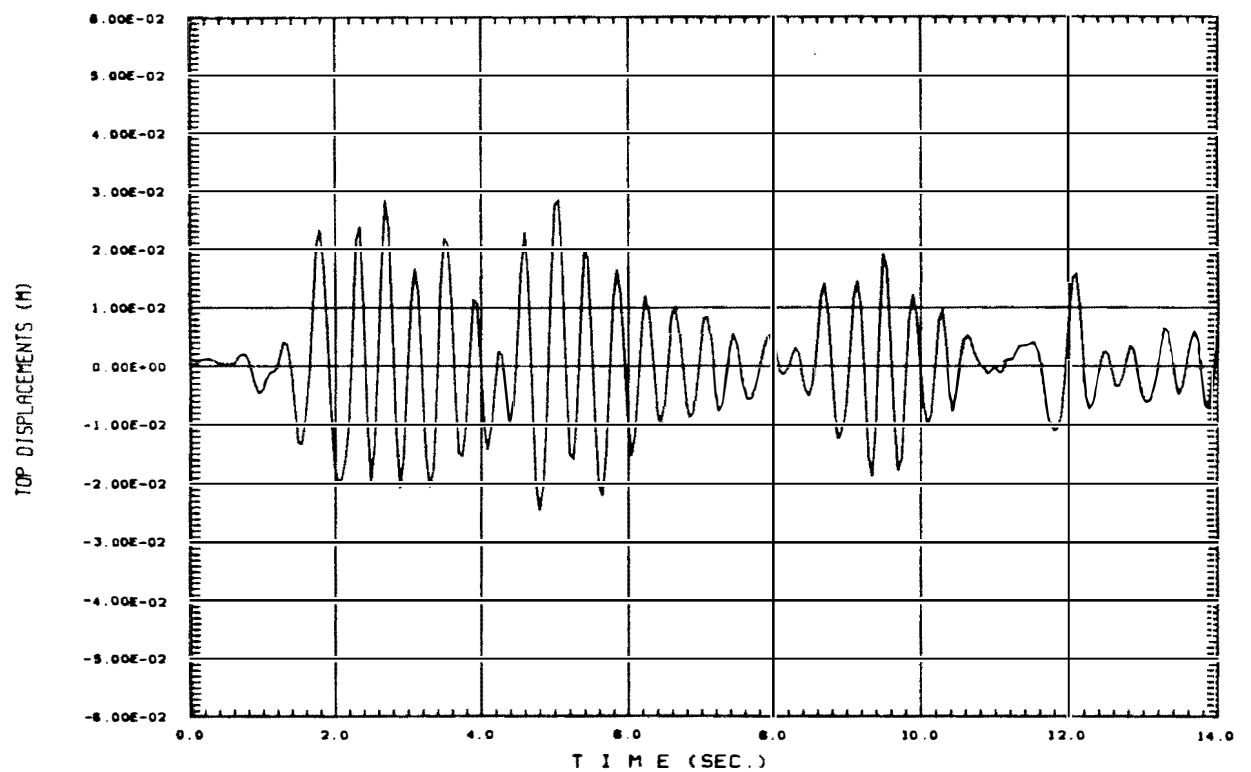

(b) Unisolated (Fixed-Base)

Fig. 4.4 The Response History of Base and Top Floor Displacements

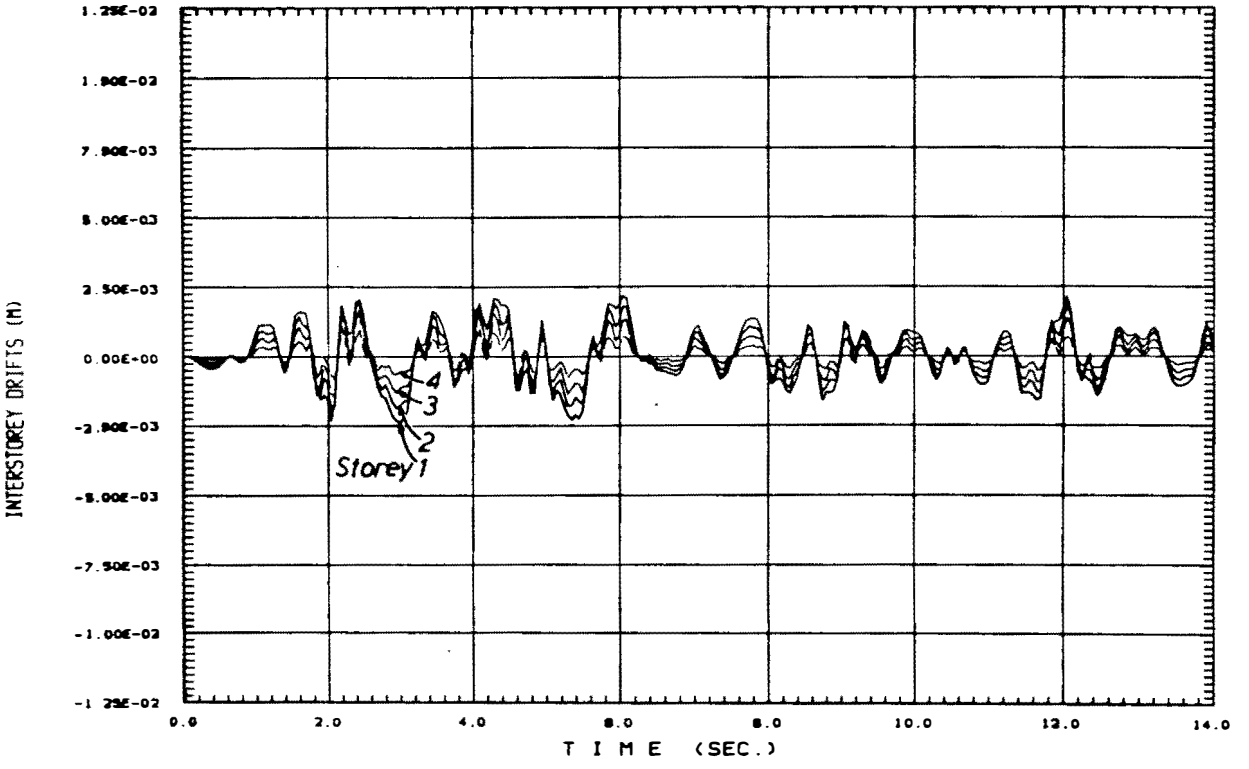

(a) Base Isolated

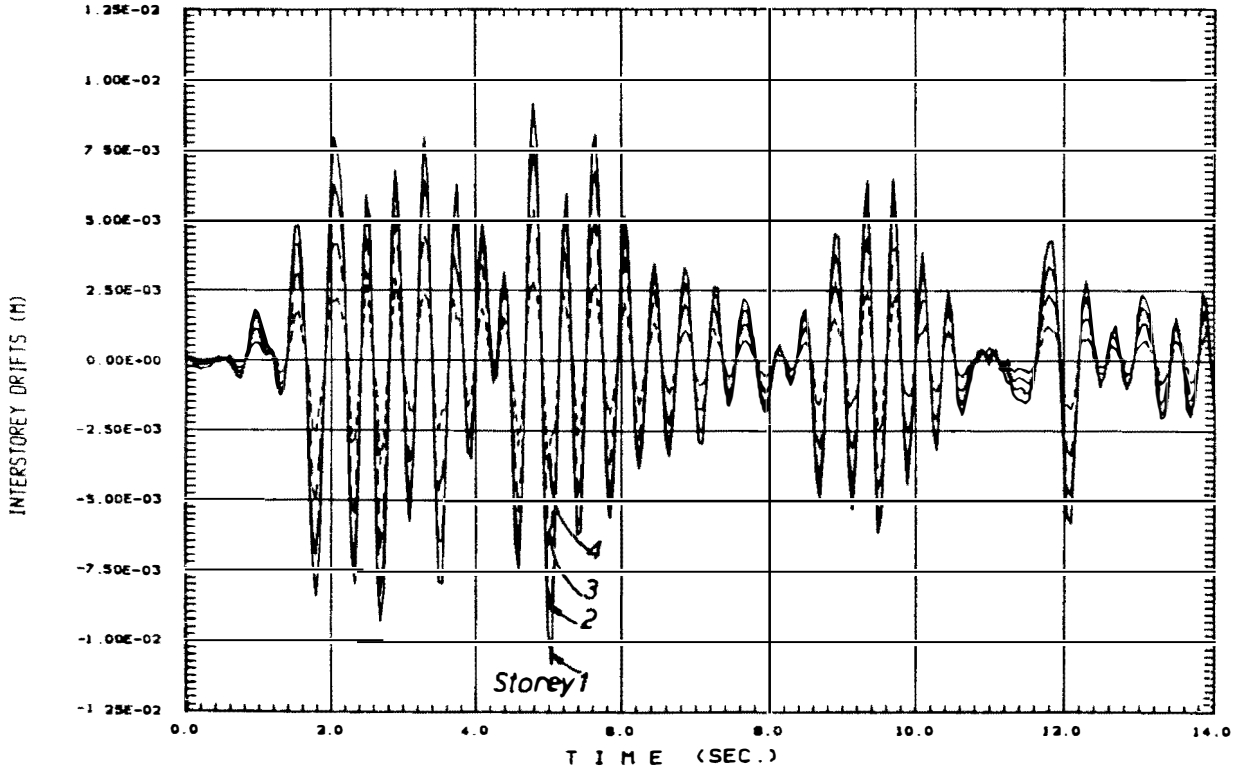

(b) Unisolated (Fixed-Base)

Fig. 4.5 The Response History of Interstorey Drifts

These small interstorey drifts during the earthquake limit the damage to non-structural elements, such as partitions, plastering, veneers, windows, and equipment installed within the building and also imply reduced force response in the members of the frame.

The benefits obtained from this significant drift reduction will offset the disadvantages caused by the larger total lateral movement.

4.3.3 BASE SHEAR, LATERAL SHEAR ENVELOPE, AND OVERTURNING MOMENT

As demonstrated in Fig. 4.4, the isolated structure has a much "gentler" response than that observed in a rigid base unisolated structure. It can be seen that the inclusion of a BI system increases significantly the fundamental period of this low-rise structure, from 0.4 seconds to approximately 1.3 seconds. As illustrated in Fig. 4.6, this fundamental period lengthening shifts the structure out from the peak spectral acceleration region of El Centro 1940 N-S earthquake and causes a reduction of the inertia forces induced into the superstructure. Further reduction is obtained from the additional hysteretic damping of the BI system.

The response history plots in Fig. 4.7 show that the base shear of the BI structure is less than a quarter of the maximum base shear of the unisolated structure. This agrees with the maximum drift between the first and the ground floor of the BI structure being only a quarter of that of the fixed-base unisolated structure. Such a reduction can completely eliminate the ductility demand of the seismic resisting elements at the ground level.

Besides the base shear the other important response parameter of a multistorey structure is its lateral storey shear envelope. For design purposes, most of the loadings codes[4.11,4.12] relate this parameter to the equivalent-static lateral force distribution over the height of the building. Fig. 4.8 depicts the lateral force distributions and the shear envelopes of the unisolated and the BI structures.

From the shear diagrams, it can be seen that there are also reductions of the storey shears over the height of the structure. In this example, the upper storey shears have a smaller reduction than the storey shear at the ground floor. Hence, the equivalent static lateral force distribution recommended by NZS 4203:1984[4.11], which gives a reasonable safety margin for the storey shears of unisolated structures, may underestimate the shears at the upper-storeys of a BI structure. This underestimation becomes more significant for a structure mounted on a BI system which has a low post-yield stiffness. Figs. 4.8.b and 4.8.c demonstrate this phenomenon.

Overturning moments have an important role for the design of columns and foundations. They have also to be taken into account to avoid any risk of structural uplift.

For the uniform "shear-beam" model used in this first stage investigation, overturning moments are merely a function of the storey shears. Thus any prediction which can be made for the storey

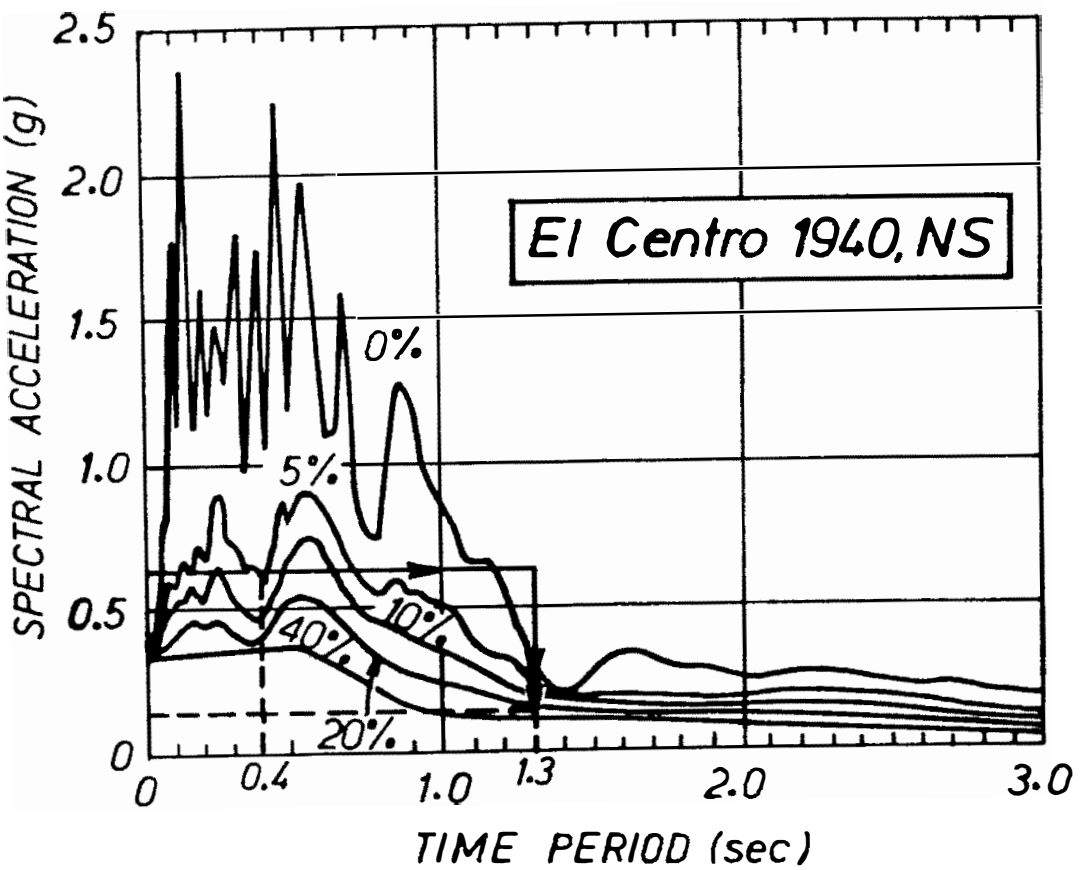

Fig. 4.6 Reduction of Spectral Acceleration due to Period Shift and Additional Damping

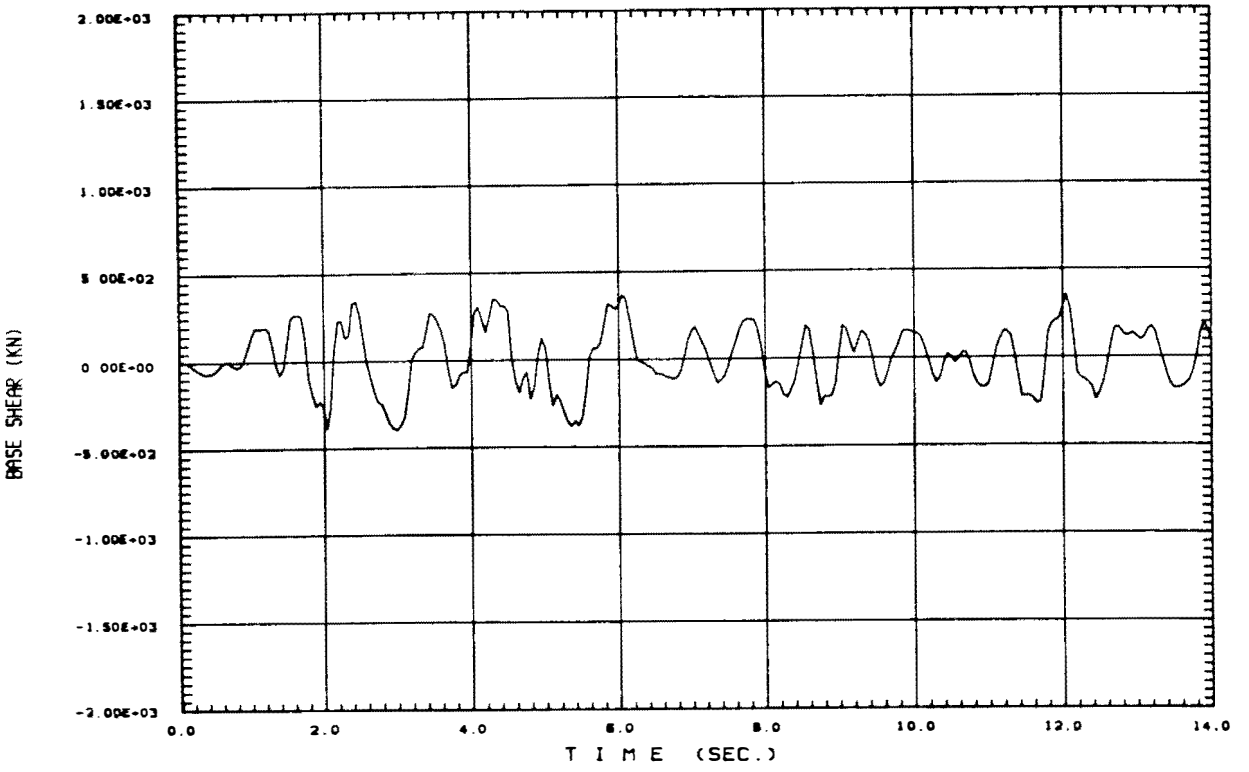

(a) Base Isolated

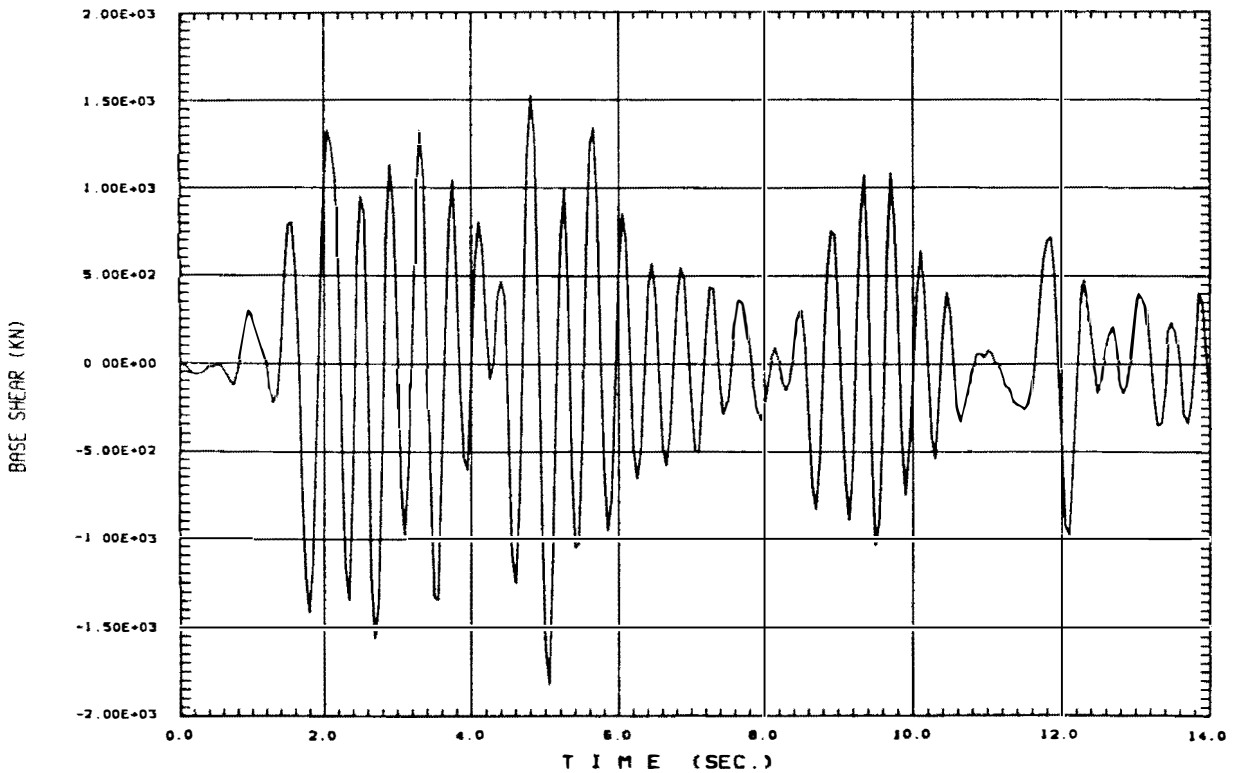

(b) Unisolated (Fixed-Base)

Fig. 4.7 The Response History of Base Shears

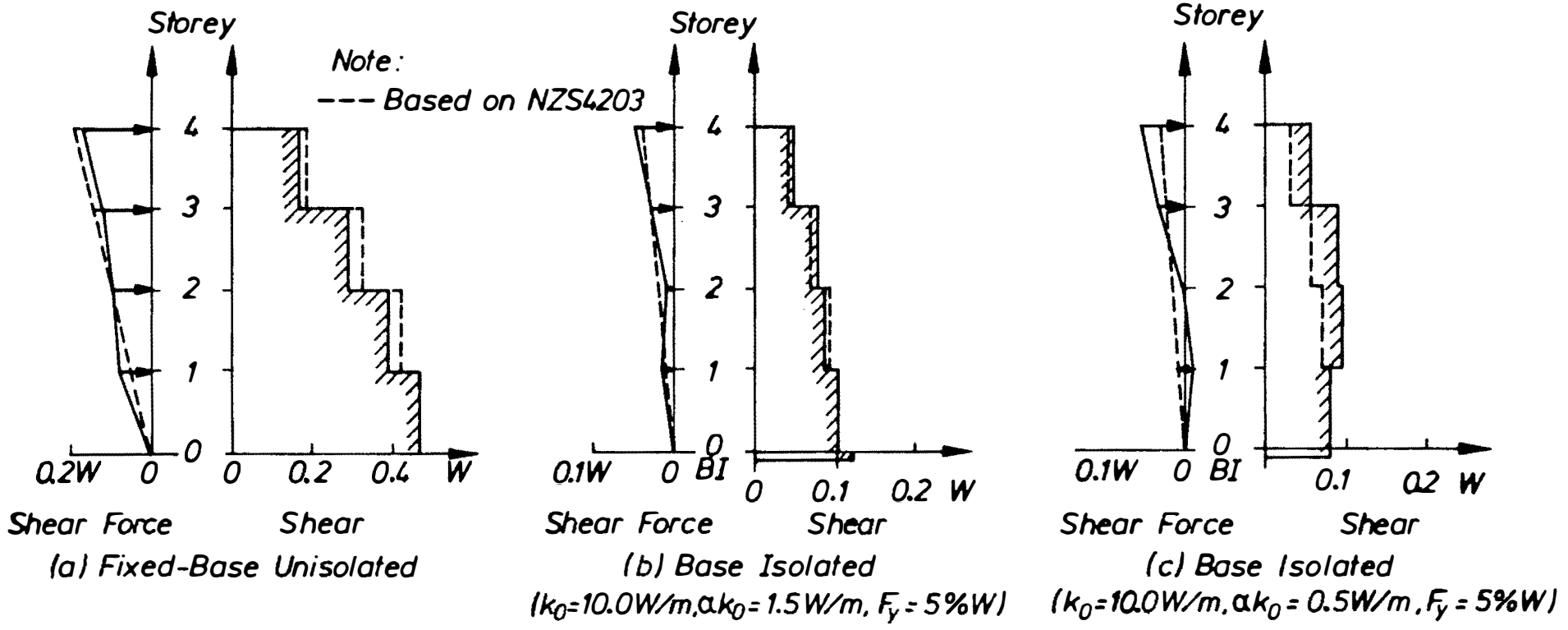

Fig. 4.8 Equivalent Static Lateral Force Distributions and Shear Envelopes of Unisolated and Base Isolated Structures

shears will provide the overturning moments as well. Fig. 4.9 compares the moment envelope of the fixed-base unisolated structure and the moment envelope of the structure mounted on a BI system with an initial stiffness, k_o of 10.0 W/m, a post-yield stiffness, αk_o of 1.5 W/m, and a yield strength, F_y of 5%W. Reduction factors which are as high as 4.5 and 3.5 are found at the ground and top storeys respectively.

4.3.4 SUMMARY

The typical performance of BI structures under an earthquake has been described. There are significant reductions in the storey shears, overturning moments, and the interstorey drifts. Larger total lateral displacements should be expected however from the extra horizontal flexibility. Evaluation of the lateral shear envelope suggests that the equivalent-static lateral force distribution may underestimate the shears in the upper storeys of BI structures.

4.4 THE EFFECT OF THE SUPERSTRUCTURE'S FUNDAMENTAL PERIOD

4.4.1 INTRODUCTION

In the case of fixed-based multistorey structures, the higher mode contributions increase as the the superstructure becomes more flexible. It is worthwhile to compare the effect of the superstructure's stiffness on the seismic response of unisolated and BI multistorey structures. For this purpose a series of four-storey uniform "shear-beam" structures are considered. The fundamental period of these structures on an unisolated fixed-based, $T_{1(UI)}$, varies from 0.1 to 2.0 seconds. The BI system on which the structure is mounted has an initial stiffness, k_o of 10.0 W/m, a post-yield stiffness, αk_o of 1.5W/m, and F_y = 5%W.

The likely period shift and the change of the modal contribution due to the variation of $T_{1(UI)}$ are presented in the following section. The evaluation is then extended to investigate this effect on base displacement, base shear, storey displacements, interstorey drifts and lateral storey shear envelope. At the end of the section a discussion on design aspects is also presented.

4.4.2 PERIOD SHIFTS AND CHANGE OF MODAL CONTRIBUTIONS

The use of Base Isolation creates a special case for the analysis of multistorey structures. It is a non-linear problem, but the inelatic deformations are designed to occur only at the base, allowing the superstructure to remain elastic. This opens an opportunity of using an equivalent linear approach to obtain some insight of the seismic behaviour of BI structures.

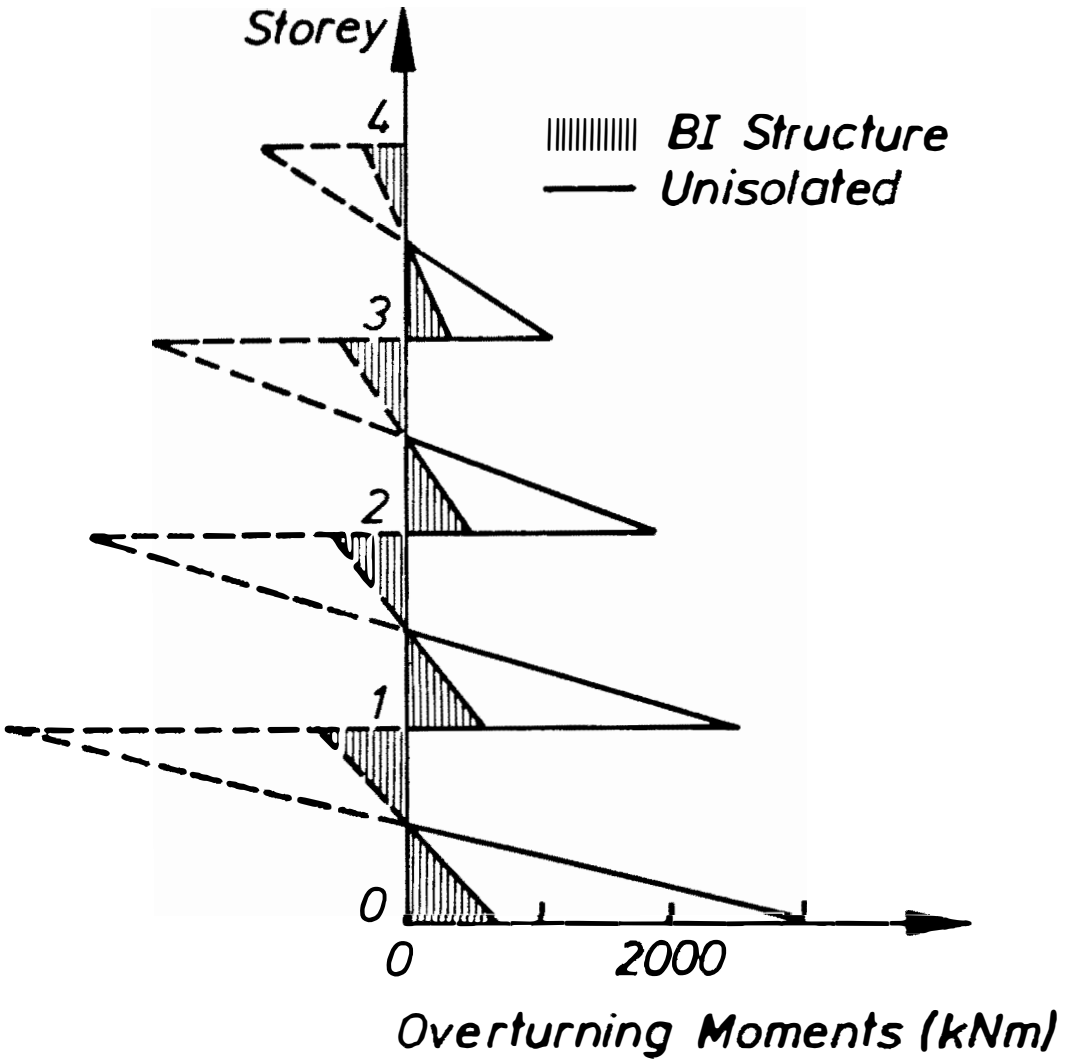

Fig. 4.9 Overturning Moments of Unisolated and Base Isolated Multistorey Structures

The most efficient way to analyse the seismic response of a linear structure is generally to transform it into a system of modal coordinates[4.7]. In this section, the equivalent linear modal properties of BI structures are evaluated at three basic conditions. Adopting the terms used by Lee[4.1], those conditions are:

1. On an unisolated fixed-base (UI).

2. Isolated with the BI system at its initial or unyielded condition (IUY).

3. Isolated with the BI system at its yielded condition (IY), i.e. : a post-yield condition which will be the case if the BI system has a "zero" yield strength.

Fig. 4.10 illustrates the shifts of the first two natural periods as the results from conducting a series of free-vibration analyses using the computer program RUAUMOKO. As shown by Lee[4.1], the horizontal flexibility of a BI system causes a great fundamental period shift, especially for a structure with a stiff superstructure or a short $T_1(UI)$. At the pseudo post-yield condition, the first mode period shifts even further. The second mode periods, however only change slightly from the period of the fixed-base structure. During an earthquake the stiffness of the BI system is cyclically changing from elastic to yield and yield to elastic conditions. Therefore as will be shown later, the effective periods of the structure lie between $T_i(IUY)$ and $T_i(IY)$.

The increase of the fundamental period shifts BI structures from the peak energy region of earthquakes which have spectral accelerations that diminish at longer periods, such as El Centro 1940 N-S ground motion. As a result the seismic generated forces in the structure are lowered. However, the slight increase of the second mode period may shift that mode to the region of dominant earthquake energy, especially in the case of flexible superstructures or structures with long $T_1(UI)$ and this may increase the contributions of the second and other higher modes.

It is important to evaluate the contribution of each mode on the structural response. In a linear structure, the modal contribution can be estimated by evaluating its modal participation factor, PF, which can be obtained from the uncoupled equation for that particular mode, as follows,

$$\ddot{Y}_i + 2 \lambda_i \omega_i \dot{Y}_i + \omega_i Y_i = - PF_i \ddot{u}_g(t) \qquad (4.10)$$

where

$$PF_i = \frac{\{\phi_i\}^T [M] \{r\}}{\{\phi_i\}^T [M] \{\phi_i\}} \qquad (4.11)$$

and Y_i is the i^{th} mode amplitude, λ_i and ω_i are the corresponding equivalent viscous damping and circular frequency, respectively. $\{\phi_i\}$ is the corresponding mode shape, $\{r\}$ is the

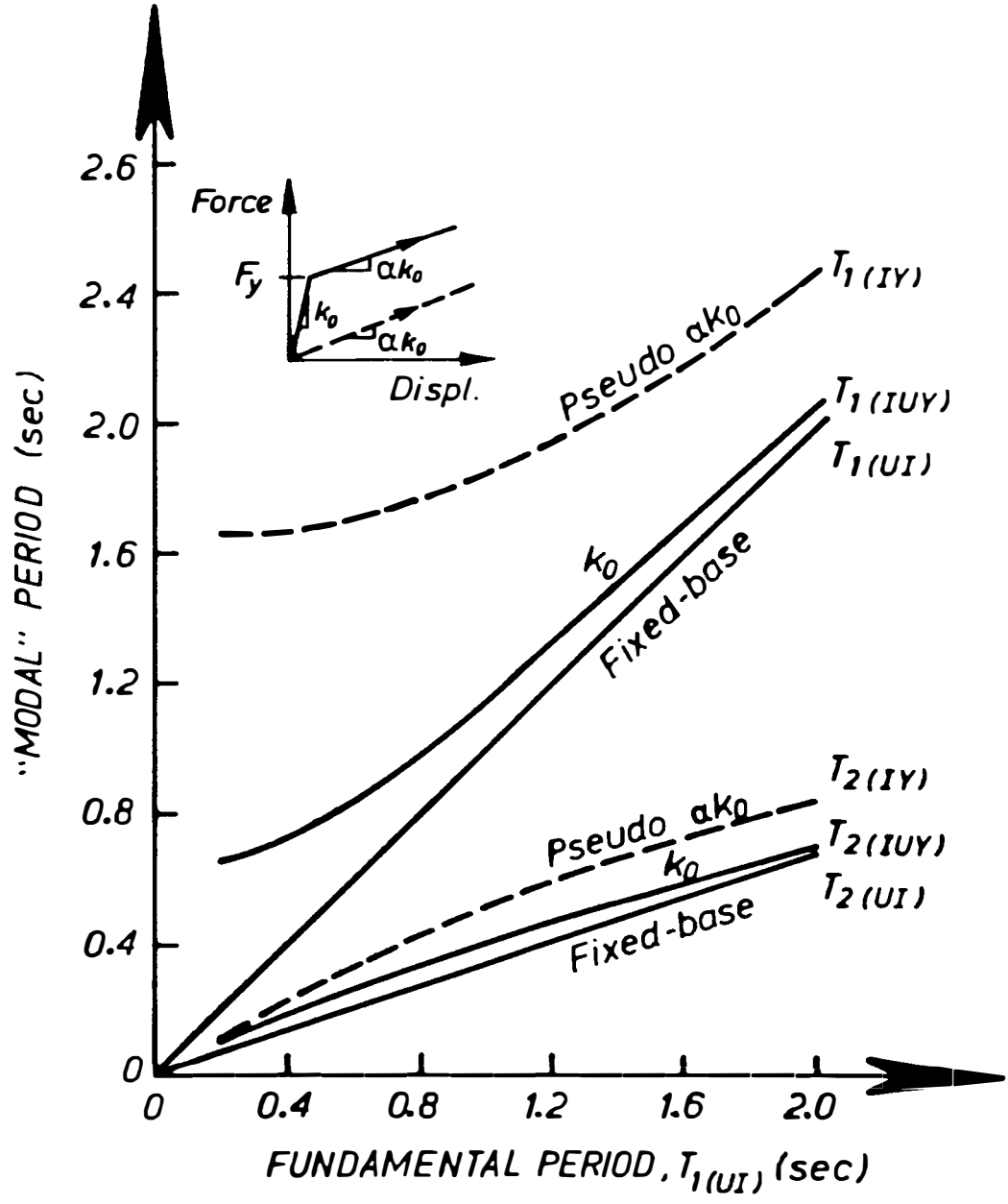

Fig. 4.10 The Effect of $T_{1(UI)}$ on the Period Shift

displacements of all degress of freedom due to a unit ground displacement, and [M] is the mass matrix.

Using a similar approach as for investigating the modal period shifts, the change of the first and the second mode participation factors are investigated. As shown in Fig. 4.11 the modal participation factors for the uniform unisolated structure are constant, since its mode shapes remain the same irrespective of the change of its fundamental periods. However, it is not so for BI structures. The ratio of the "superstructure stiffness" to the stiffness of the BI system varies as the fundamental period $T_{1(UI)}$ changes and therefore the mode shapes of BI structures also change with respect to the change of the fundamental period $T_{1(UI)}$ as shown in Table 4.1.

It can be seen from Fig. 4.11 that in general the modal participation factors at the pseudo post-yield conditions, $PF_{i(IY)}$, can be much smaller than the modal participation factors at the unyielded condition, $PF_{i(IUY)}$. The difference seems more significant for the second mode PF than the first mode PF.

From Table 4.1, it is also important to note that BI structures with short $T_{1(UI)}$ or having stiff superstructures will move as a "rigid body" on the top of the BI system, since the behaviour of these type of stiff structures normally are dominated by their first mode which has an almost uniform shape from top to bottom. As the structure becomes more flexible, the mode shapes become more and more similar to the mode shapes of an unisolated structure. Since the stiffness of the BI system cyclically changes from elastic to yield and yield to elastic one should expect that the actual modal participation factors and mode shapes lie in between "k_o" and "αk_o" conditions.

4.4.3 BASE DISPLACEMENTS

From the results of the time history analyses shown in Fig. 4.12, it can be seen that irrespective of the fundamental period, $T_{1(UI)}$, the base displacements of BI structures do not vary significantly. This fact confirms the results obtained earlier by Lee[4.1].

To be able to understand this behaviour the response history of the base displacements are presented. Fig. 4.13 shows two examples for structures with $T_{1(UI)}$ equal to 0.2 and 1.2 seconds. It is obvious that the relatively "smooth" movements experienced by the base are dominated by the first mode with its period lengthened by the BI system. This first mode dominance is still apparent even for the structure with flexible superstructure ($T_{1(UI)}$ = 1.2 seconds).

Following the approach suggested by Turkington et al[4.14], the effective fundamental period of the structures is evaluated. The period is measured from the time history plots by two methods: first it is measured on the half cycle immediately before and after the peak response, and

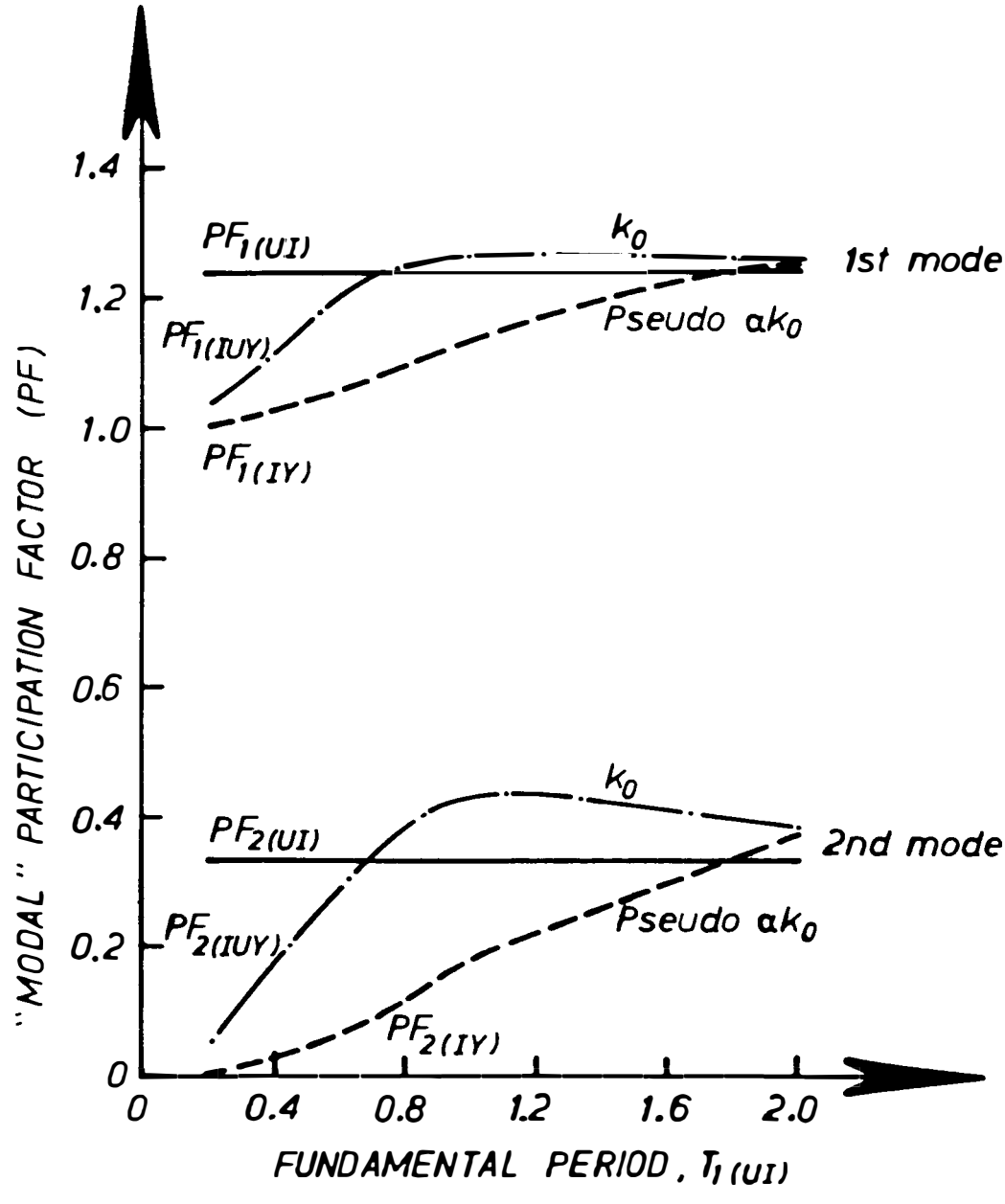

Fig. 4.11 The Change of Modal Participation Factor (PF) in respect to the Fundamental Period, $T_{1(UI)}$

Table 4.1 First and Second Mode Shapes of BI and Fixed-Base Structures

	T_1(UI)	At k_o		At αk_o	
	secs	Mode 1	Mode 2	Mode 1	Mode 2
Base Isolated	0.2	1.0000	-0.9743	1.0000	-0.9956
		0.9889	-0.5809	0.9982	-0.6121
		0.9668	0.0469	0.9947	0.0072
		0.9340	0.6559	0.9894	0.6237
		0.8908	1.0000	0.9824	1.0000
	0.4	1.0000	-0.9395	1.0000	-0.9836
		0.9636	-0.4984	0.9931	-0.5951
		0.8922	0.1767	0.9795	0.0285
		0.7884	0.7689	0.9591	0.6408
		0.6559	1.0000	0.9322	1.0000
	0.8	1.0000	-0.9236	1.0000	-0.9508
		0.9204	-0.2952	0.9758	-0.5377
		0.7675	0.5341	0.9279	0.1091
		0.5534	1.0000	0.8576	0.7085
		0.2953	0.7855	0.7665	1.0000
	1.2	1.0000	-0.9301	1.0000	-0.9933
		0.8922	-0.0870	0.9368	-0.4173
		0.6883	0.8350	0.8144	0.4007
		0.4102	1.0000	0.6405	0.9863
		0.0879	0.2585	0.4262	1.0000
	2.0	1.0000	-0.9511	1.0000	-0.9308
		0.8877	-0.0556	0.9223	-0.3098
		0.6758	0.8923	0.7729	0.5178
		0.3880	1.0000	0.5635	1.0000
		0.0567	0.1662	0.3102	0.8151
Fixed-Base		1.0000	-1.0000		
		0.8794	0.0000		
		0.6527	1.0000		
		0.3473	1.0000		
		0.0000	0.0000		

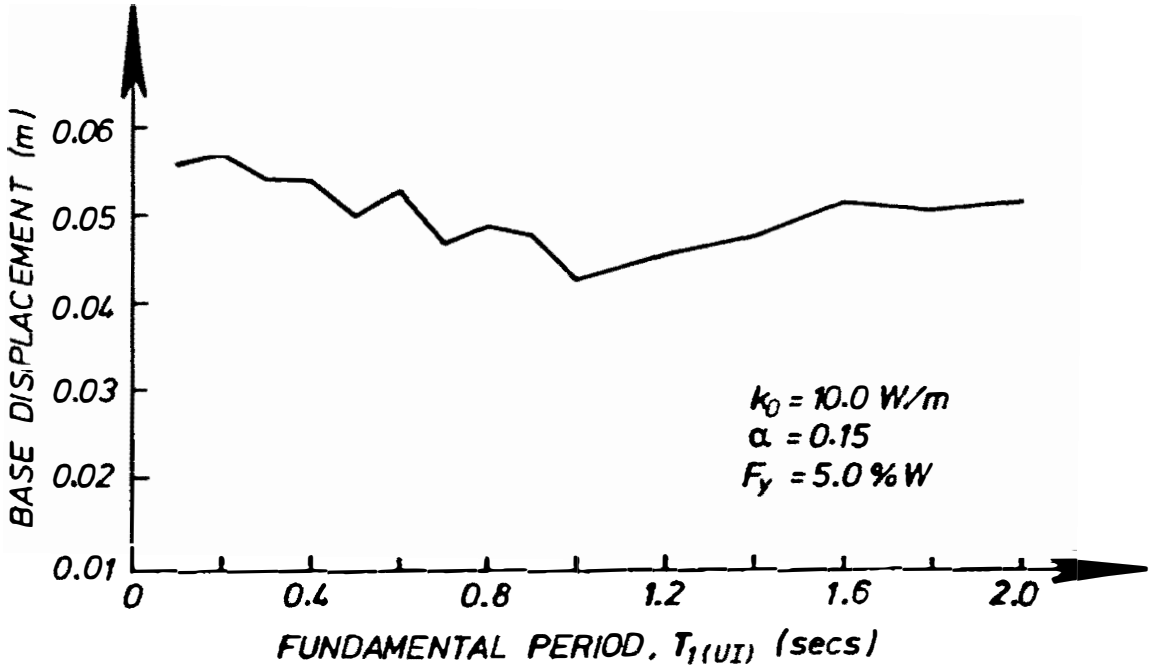

Fig. 4.12 The Effect of $T_{1(UI)}$ on Base Displacement

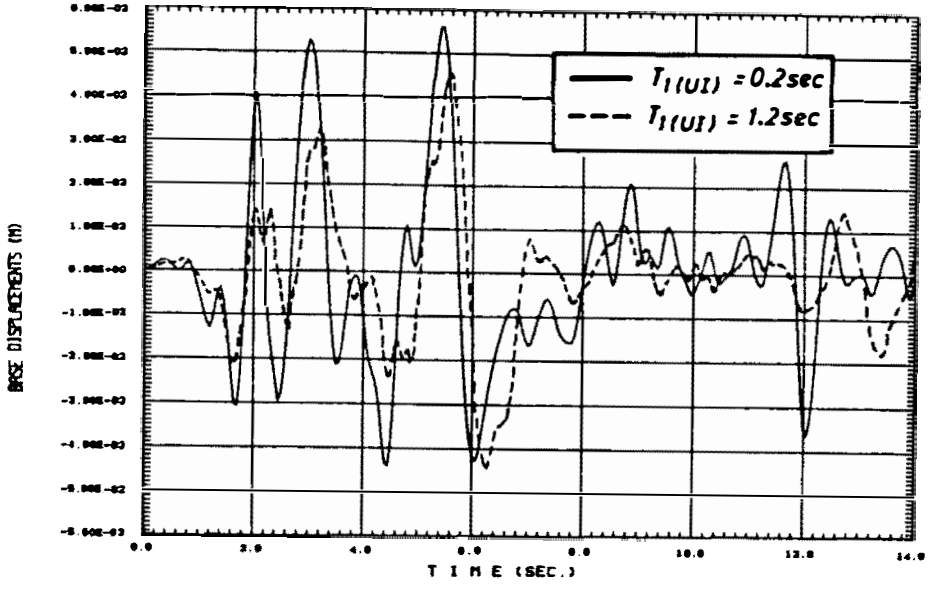

Fig. 4.13 The Response History of Base Displacements of BI Multistorey Structures with $T_{1(UI)}$ = 0.2 and 1.2 seconds

secondly it is taken as double the period of the half cycle immediately before the peak response. The average values are listed in Table 4.2.

The above measured periods are compared with the results obtained from the free-vibration modal analyses based on the effective secant stiffness of the BI system at the peak response. In this approach, first the effective fundamental period, T_{1eff}, is calculated by taking into account the mass and stiffness of the whole structure. Secondly T_{1eff} is calculated by assuming the superstructure moves as a rigid body on top of the BI system. It can be seen that the calculated T_{1eff} obtained from the first method are in good agreement with the measured values, whereas the second method underestimates the T_{1eff} of long-period structures.

Further, the expected additional damping due to the hysteretic behaviour of the BI system was also evaluated using Eqs. 3.21 and 3.22 discussed in Chapter 3. The values of the increase in the equivalent viscous damping are listed in Table 4. 2 .

Refering to the spectral displacement of the El Centro 1940 N-S earthquake, as shown in Fig. 4.14, it can now be explained why the base displacements vary only slightly as $T_{1(UI)}$ changes. Since the effective fundamental periods, T_{1eff}, range from 1.33 to 1.67 seconds accompanied by an increase of damping by more than 20% of critical value, the net results is the base displacements vary very little as $T_{1(UI)}$ ranges from 0.2 to 1.2 seconds.

4.4.4 BASE SHEAR

For design purposes, base shear is normally regarded as a major response quantity by many loadings codes[4.11,4.12,4.13]. Thus in this study base shear is used to describe the seismic performance of BI structures. It should be noted, however, that the maximum storey shears of a BI multistorey structure may not always occur at the base (see Fig. 4.8 (b) and (c)).

It has been demonstrated in Section 4.3.3, that a BI system may considerably reduce the base shear of a relatively stiff multistorey structure ($T_{1(UI)}$ = 0.4 seconds). However, as can be seen in Fig. 4.15 the reduction is less significant as the superstructure becomes more flexible. The degree of protection given by the BI system diminishes for structures with $T_{1(UI)}$ greater than 1.2 seconds.

From Fig. 4.15, it is observed that the base shear of an unisolated structure changes dramatically with the change in its fundamental period and it follows the pattern of the earthquake spectral acceleration depicted in Fig. 4.16 . However for BI structures, the change of $T_{1(UI)}$ hardly has any effect on the value of the base shear. Using an approach similar to that for the base displacement, this phenomenon can be explained as follows. The base shear is dominated by the first mode because it is strongly influenced by the characteristic of the BI system shear force. Fig. 4.17 demonstrates this phenomenon through two examples of response history of BI structures with $T_{1(UI)}$ of 0.2 and 1.2 seconds. As can be seen from these plots, the BI system

Table 4.2 Evaluation of Effective Fundamental Periods and Additional Dampings

T_1(UI) secs	Effective Fundamental Period (secs)			Additional Damping (% critical)
	Calculated		Measured fror Displ. Response History	
	1*	2*		
0.2	1.32	1.31	1.33	20.3
0.4	1.35	1.30	1.36	20.7
0.6	1.40	1.30	1.40	20.9
0.8	1.47	1.29	1.50	21.2
1.0	1.56	1.26	1.60	22.4
1.2	1.68	1.28	1.67	21.5

* NOTE : 1. Based on Free-Vibration Modal Analysis of the whole structure.

2. Based on $T_{eff} = 2\pi \sqrt{\frac{\text{Total Mass}}{k_{eff \text{ of the BI system}}}}$

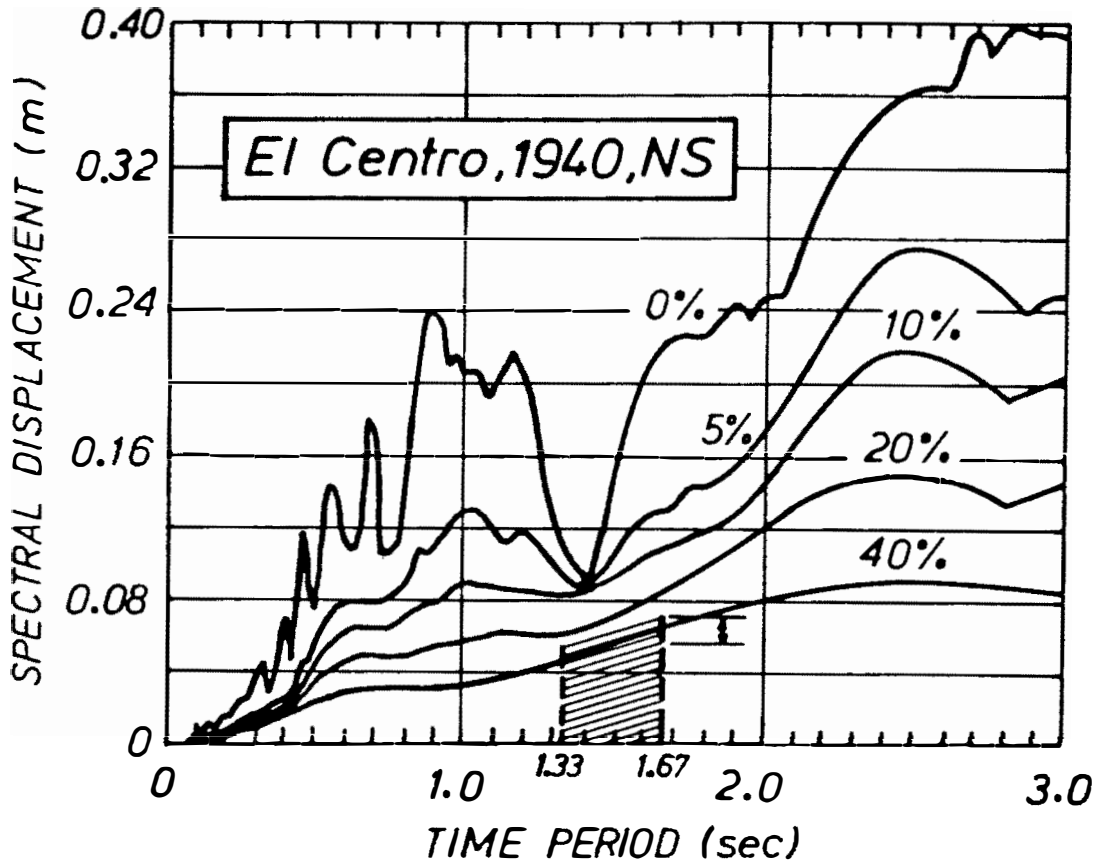

Fig. 4.14 Approximate Range of Base Displacements of BI Structures with $T_{1(UI)}$ = 0.2 to 1.2 seconds and $T_{1\,eff}$ = 1.33 to 1.67 seconds

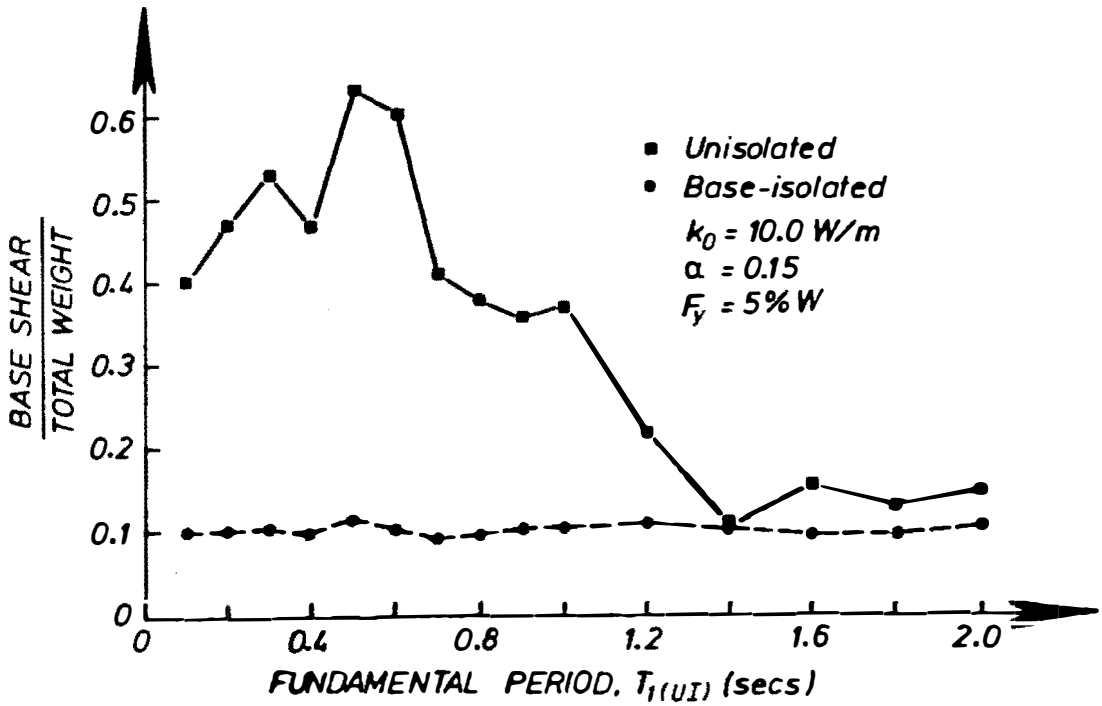

Fig. 4.15 The Effect of $T_{1(UI)}$ on Maximum Base Shears

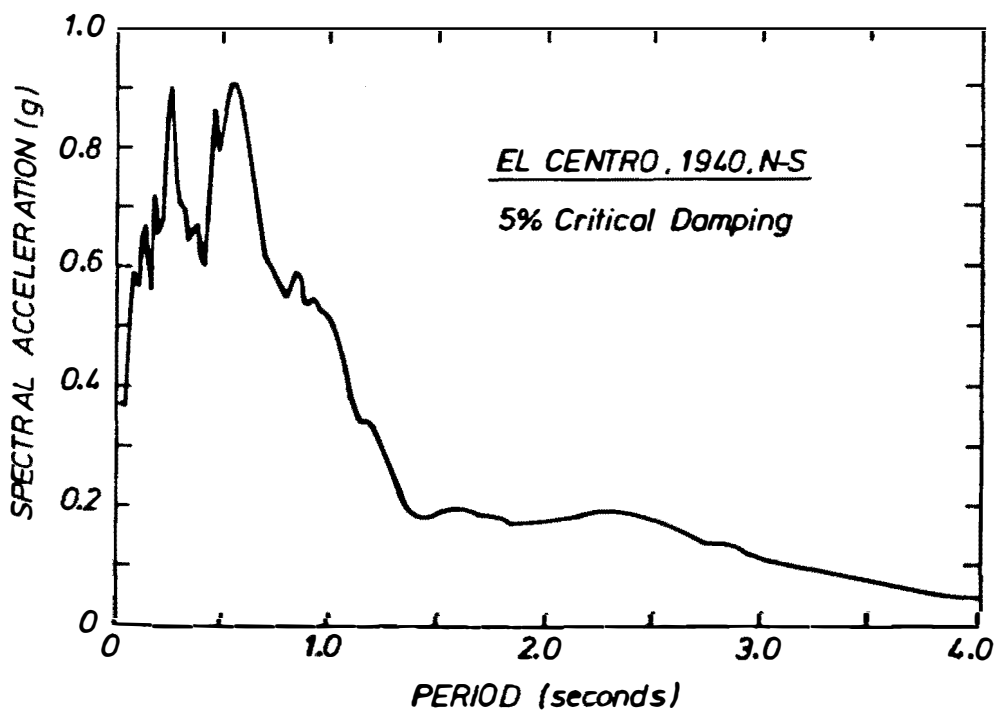

Fig. 4.16 Spectral Acceleration of El Centro 1940 N-S Earthquake

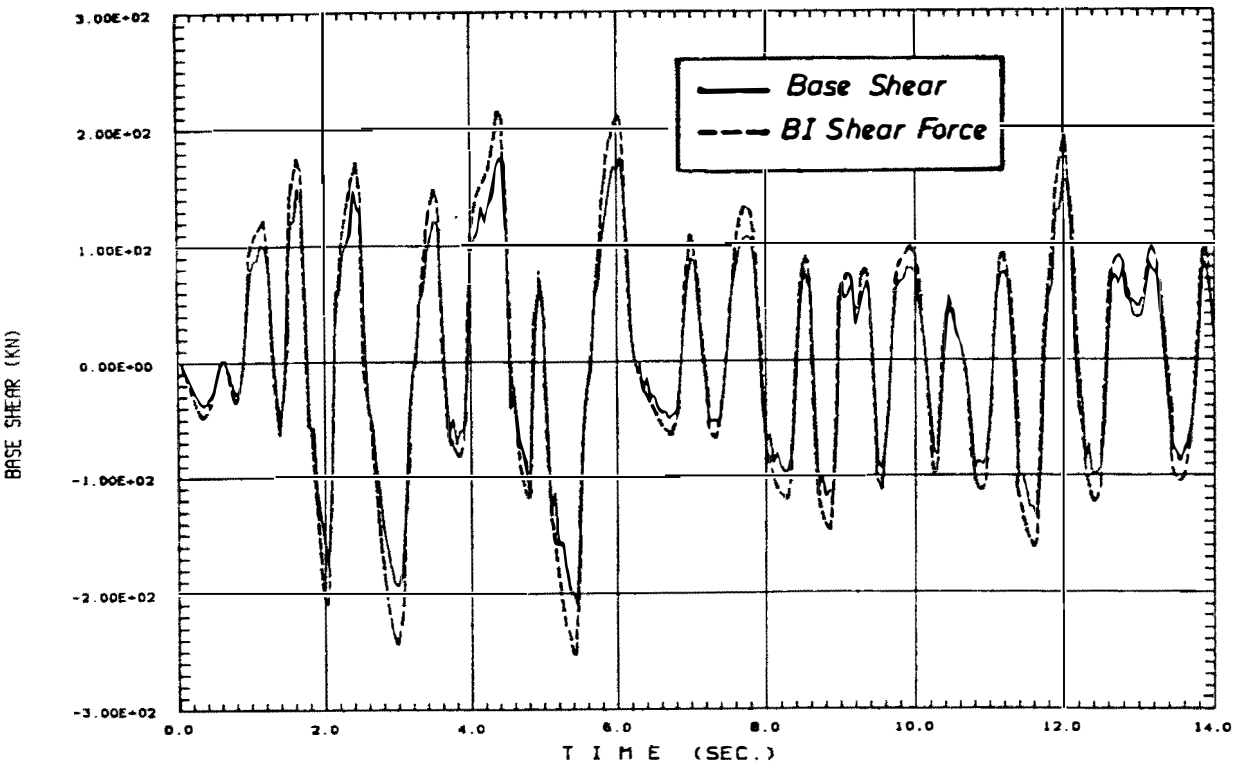

(a) $T_{1(UI)}$ = 0.2 secs

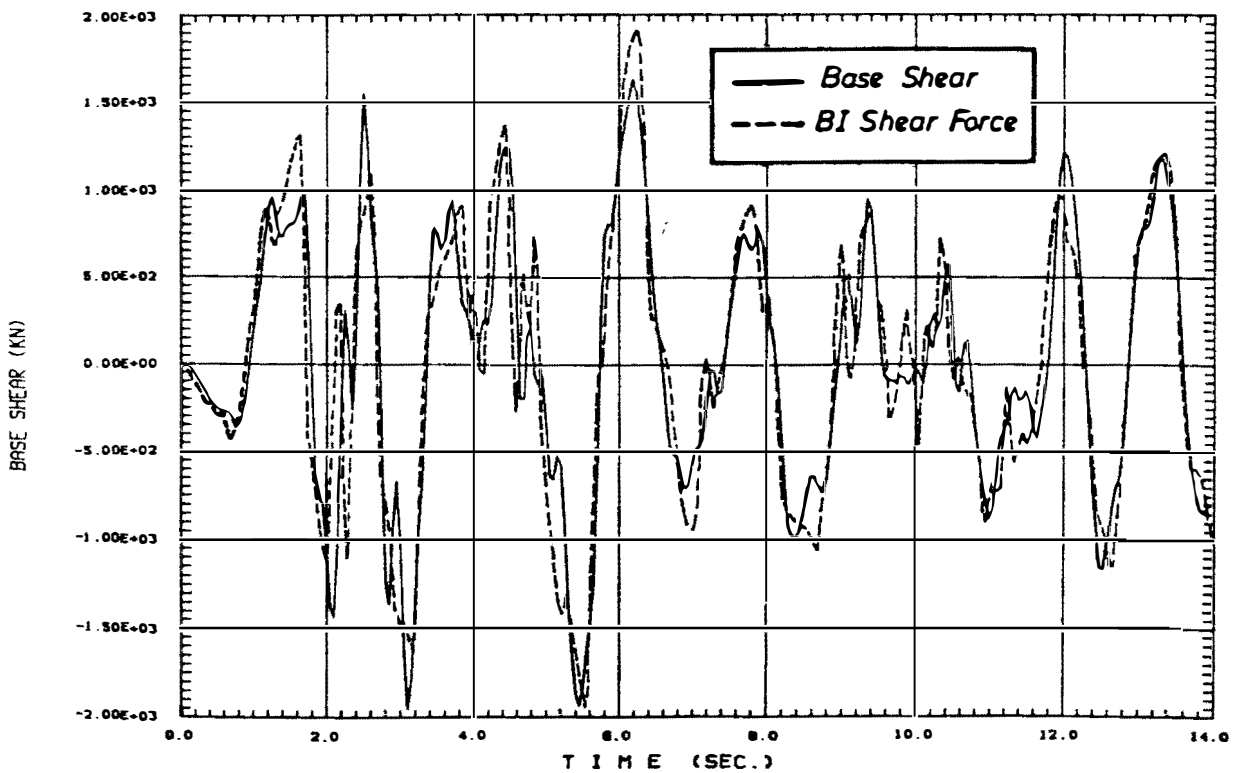

(b) $T_{1(UI)}$ = 1.2 secs

Fig. 4.17 The Response History of Base Shear and BI System's Shear Force of BI Structures

shifts the fundamental period of the structure from 0.2 and 1.2 seconds to 1.33 and 1.67 seconds, respectively. The structure is shifted out from the peak earthquake energy region to the plateau area of the earthquake spectral acceleration. Furthermore, the increased damping due to the structures with $T_{1(UI)}$ of 0.2 and 1.2 seconds. As can be seen from these plots, the BI system shifts the fundamental period of the structure from 0.2 and 1.2 seconds to 1.33 and 1.67 seconds, respectively. The structure is shifted out from the peak earthquake energy region to the plateau area of the earthquake spectral acceleration. Furthermore, the increased damping due to the hysteretic behaviour of the BI system reduces the generated seismic forces even further and makes the base shear insensitive to the change of $T_{1(UI)}$.

4.4.5 LATERAL STOREY DISPLACEMENTS AND INTERSTOREY DRIFTS

Normally the more flexible the structure is the greater the storey displacements . As shown in Fig. 4.18 flexible unisolated structures have greater storey displacements than the stiffer ones. Similar performance is also shown by BI structures with respect to their base displacements. However, the storey displacements of a BI structure relative to the base movement are much smaller when compared with the storey displacements of unisolated structures.

It is also important to point out from Fig. 4.18, that the total top displacement of BI structures with short $T_{1(UI)}$ is greater than the top displacement of their unisolated counterparts. However, the maximum top displacement of BI structures with $T_{1(UI)}$ greater than 0.4 seconds can be less than the top displacement of the corresponding unisolated structures.

Figs. 4.19 and 4.20 show the response history plots of interstorey drifts of BI structures with $T_{1(UI)}$ of 0.2 and 1.2 respectively. The interstorey drifts of the BI structure with a stiff superstructure, in this case $T_{1(UI)}$ = 0.2 seconds, are always in phase with each other revealing the dominance of the first mode. The interstorey drifts at the first storey are always the maximum and followed in sequence by the drifts of the higher storeys in an almost constant ratio. This characteristic is often observed in elastic unisolated structures, even when the superstructure is relatively flexible (see Fig. 4.21). For a BI structure with a flexible superstructure, however, the interstorey drifts are no longer in phase due to the effect of the higher modes. Because of this, the maximum drifts between the individual storeys of BI structures may not occur at the same time.

4.4.6 LATERAL STOREY SHEAR ENVELOPE

For elastic structures the storey shears are in a direct linear proportion to the interstorey drifts and the storey stiffness. Since the interstorey drifts of BI structures with stiff superstructures are governed by the characteristic of their first mode, their storey shears are also dominated by the first mode. Fig. 4.22 shows the top-storey shear of a BI structure with $T_{1(UI)}$ of 0.2 seconds.

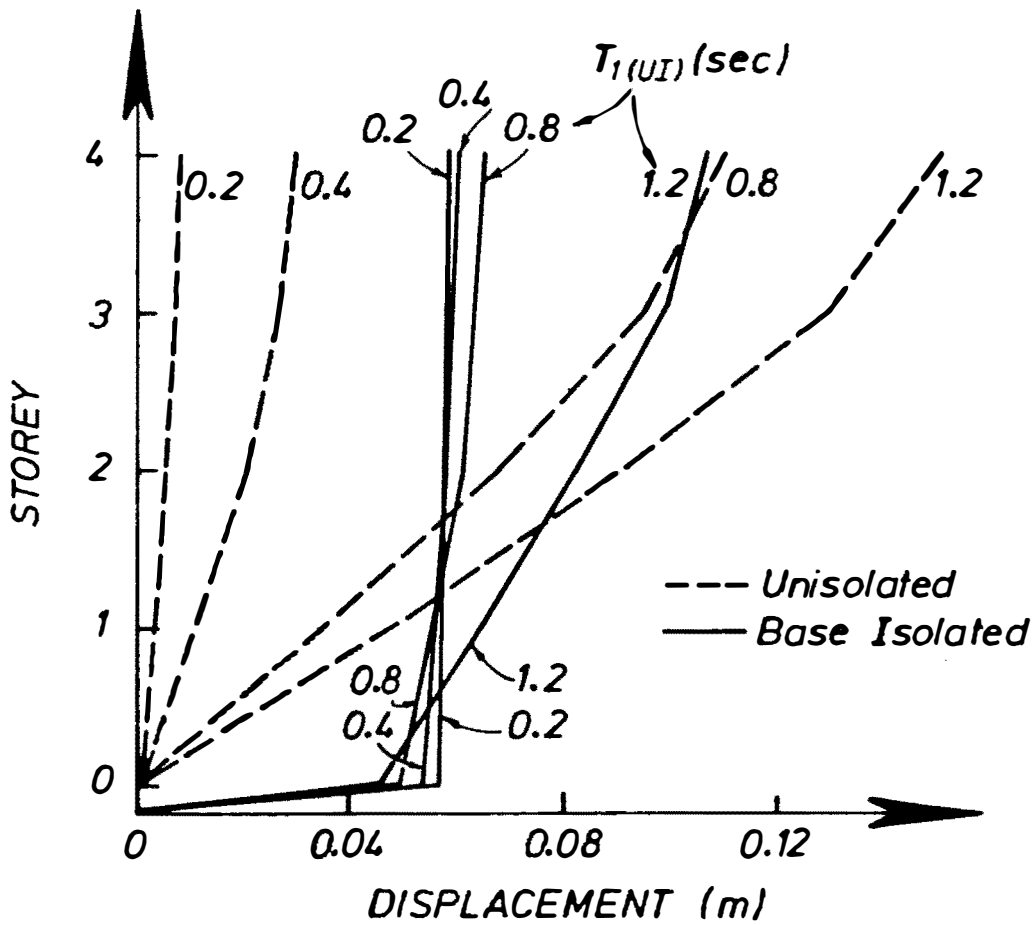

Fig. 4.18 Maximum Storey Displacements of Unisolated and BI Multistorey Structures with Various $T_{1(UI)}$

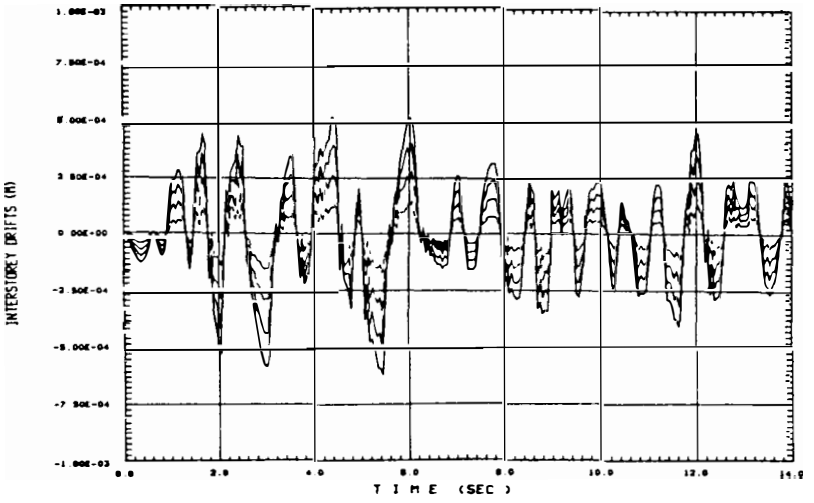

Fig. 4.19 The Response History of Interstorey Drifts of a BI Multistorey Structure with $T_{1(UI)}$ = 0.2 secs

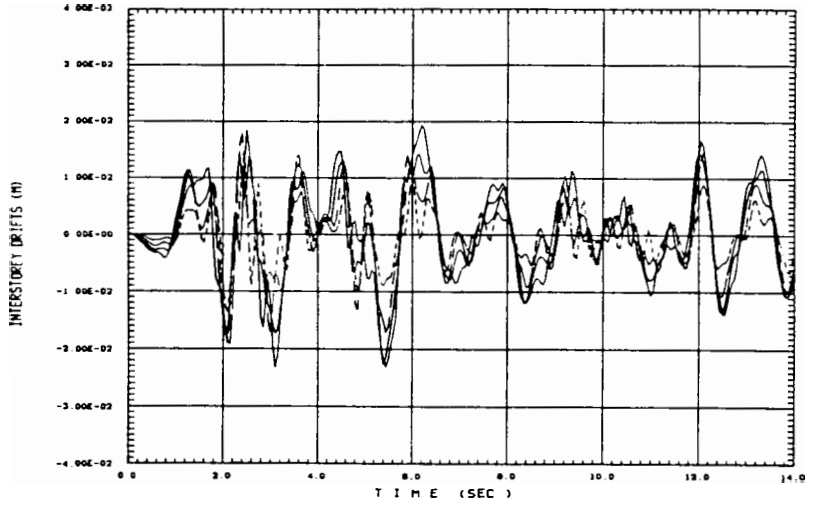

Fig. 4.20 The Response History of Interstorey Drifts of a BI Multistorey Structure with $T_{1(UI)}$ = 1.2 secs

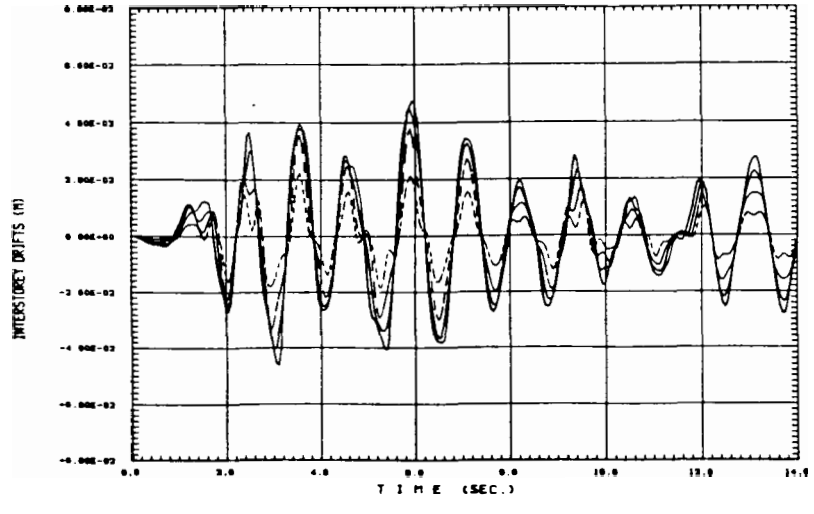

Fig. 4.21 The Response History of Interstorey Drifts of an Unisolated Multistorey Structure with $T_{1(UI)}$ = 1.2 secs

The stiffness of the superstructure causes the top floor to follow the motion induced by the base. It can be seen that the effect of the higher modes do not significantly affect the contribution of the first mode whose period is lengthened due to the implementation of BI system. For BI structures with more flexible superstructures, such as when $T_{1(UI)}$ is 1.2 seconds, the top-storey shear is obviously no longer governed only by the first mode. From the response history plot displayed in Fig. 4.23, it is evident that in the top storey the second mode with an effective period of around 0.6 seconds becomes more dominant. This indicates that the upper-storeys seem "reluctant" to follow the base movement and there is a "whip" effect in the structure.

The contribution of each mode towards the total response depends on how strong these modes are excited by the ground motion. As has been discussed earlier, the implementation of a BI system may shift the fundamental period of the structure out from the peak earthquake energy region, and may simultaneously shift the higher mode periods into the more dominant energy region of the forcing earthquake excitation.

As indicated before by Lee[4.1], the more significant the higher mode contributions compared to the contribution of the first mode, the more bulged is the lateral shear envelope. Fig. 4.24 illustrates the rapid change of lateral shear envelope of BI structures with respect to the change of $T_{1(UI)}$. The lateral shear envelope of unisolated structures on the other hand does not change so dramatically. The lateral inertia force distribution usually used in the equivalent static force analysis[4.11] was found to be non-conservative for BI structures with $T_{1(UI)} \geq 0.4$ seconds, while it does give a reasonable estimation for the shear envelope of unisolated structures. Note for convinience of presentation the storey shear envelope are represented by a series of continuous lines connecting the points of maximum shear at each floor.

4.4.7 DISCUSSION OF DESIGN ASPECTS

It has been shown that the structure response at the base is strongly governed by the first mode whose period is lengthened by the BI system when the system yields. The response in the middle to top floors, however, may have significant influence from the higher modes. As the system is, in general, non-linear the question is how to measure these modal contributions. In spite of its complexity, such quantitatively approximate measurements are very useful in gaining some insight into the structural behaviour and are beneficial for design .

Lee[4.1], to a limited extend, tried to discuss these modal contributions qualitatively. He did not, however make any attempt to employ the so-called mode-superposition concept as a basis for his design procedure. Instead, as discussed in Chapter 3, he developed some design charts for five selected BI systems based on the time history analysis results.

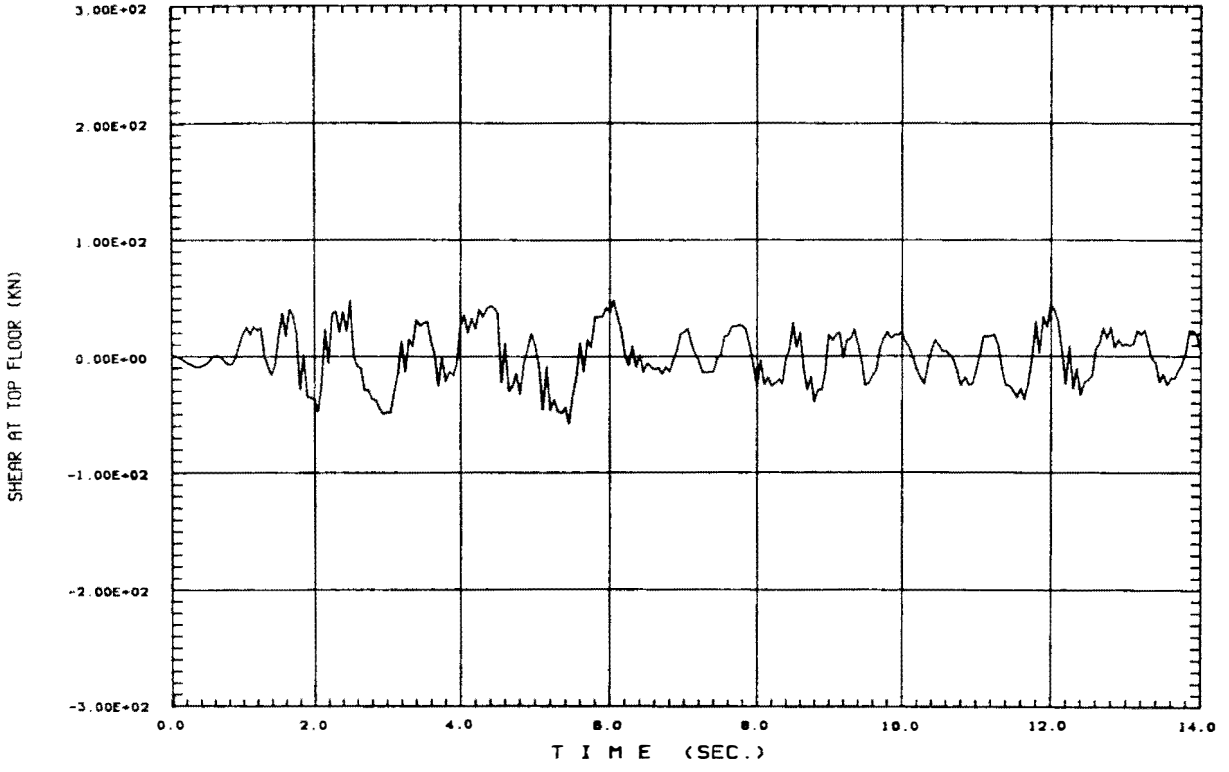

Fig. 4.22 The Response History of Top-Storey Shear of a BI Multistorey Structure with $T_{1(UI)}$ = 0.2 secs

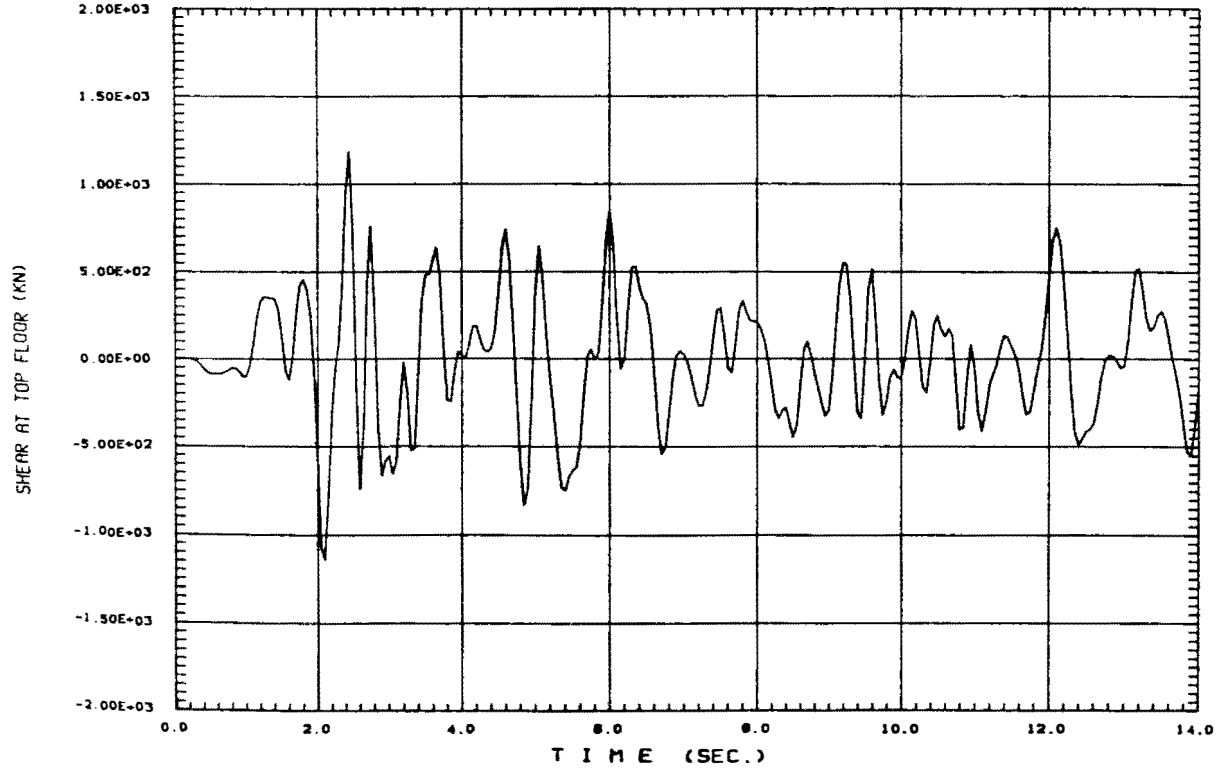

Fig. 4.23 The Response History of Top-Storey Shear of a BI Multistorey Structure with $T_{1(UI)}$ = 1.2 secs

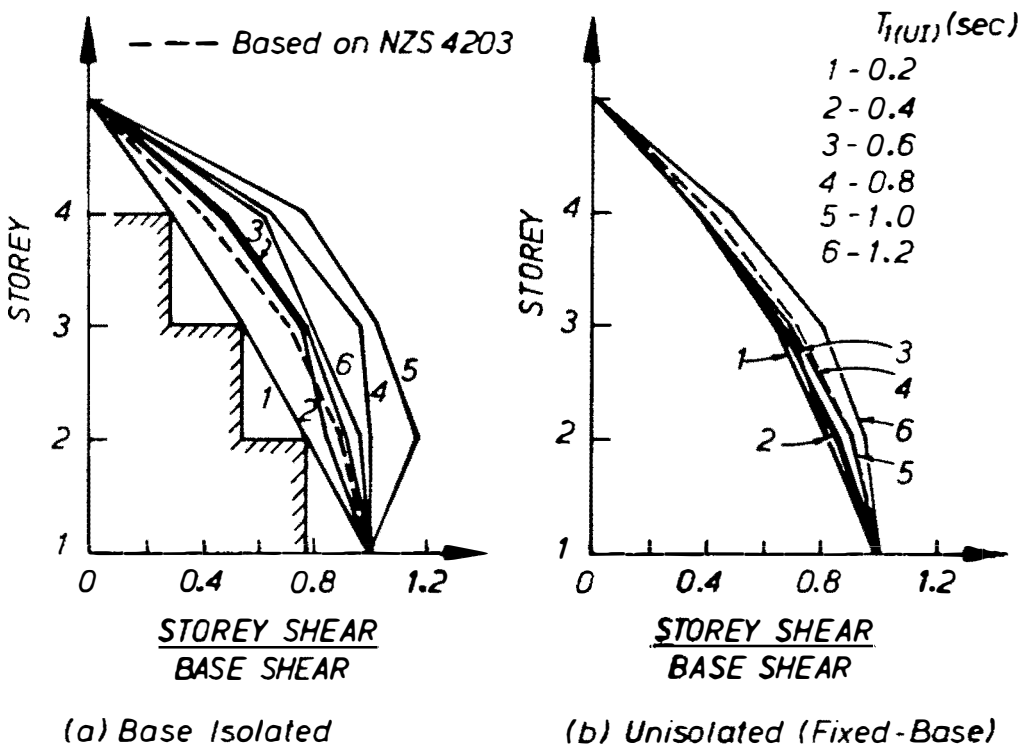

Fig. 4.24 Normalized Lateral Shear Envelopes of Unisolated and BI Structures with $T_{1(UI)}$ = 0.2 to 1.2 secs

Based on some experimental results, Kelly et al[4.2] proposed an equivalent linear mode-superposition method for BI multistorey structures. The details of the method are presented in Chapter 3. In this section Kelly's method will be reexamined.

Before evaluating the contribution of the higher modes in the middle to top storeys, the dominance of the first mode on the base displacement, base shear, and the BI system's shear force is discussed first. It has been shown from the response history plots in Section 4.4.3 and 4.4.4, that base displacement, base shear, and the BI system's shear force are strongly affected by the characteristics of the BI system which have a great influence on the structure's first mode. Table 4.2 lists the effective fundamental period and the additional equivalent viscous damping due to the hysteretic behaviour of the BI system. Using the same approximate technique as suggested by Turkington et al[4.14], these responses are calculated from the spectral displacement and spectral acceleration of El Centro 1940 N-S earthquake.

Unlike the effective fundamental period, the additional damping is more difficult to measure. Since the total equivalent viscous damping of all structures, with $T_{1(UI)}$ from 0.2 to 1.2 seconds discussed above, is estimated to be around 25% critical damping, values obtained from spectral displacement and spectral acceleration of 20% and 30% critical damping are used as an upper and lower bound, respectively. Fig. 4.25 and 4.26 demonstrate that the actual values of base displacement and shear force of BI system obtained from the time history analyses are in between these upper and lower limits.

For the base shear of BI structures with relatively low $T_{1(UI)}$, however both limits give conservative estimates. Therefore, any estimation of the base shear of stiff superstructures relative to the shear force of the BI system is conservative with a margin of 10% to 20% as shown in Fig. 4.27. As the ratio of the first floor stiffness to the effective stiffness of the BI system decreases the base shear of the structure may be greater than the shear force of the BI system.

Although further evidence is still required, the analysis results obtained so far show that the contributions of higher modes to the structure response at the base is insignificant and can be neglected for design purposes.

As alluded to earlier the higher mode contributions on the structure response in the middle to top storeys may be significant. To evaluate this phenomenon, the storey displacements and shears obtained from the time history analyses for BI structures with $T_{1(UI)}$ of 0.2, 0.4, 0.8 and 1.2 seconds are listed in Table 4.3.

It can be seen from the above table, that the response of a BI structure with a very stiff superstructure ($T_{1(UI)}$ = 0.2 sec.) is strongly dominated by its effective first mode. The maximum storey displacements and storey shears occur at the same time, i.e. 5.43 seconds. Kelly's approximate method, as tabulated in Table 4.4, demonstrates that for this stiff superstructure

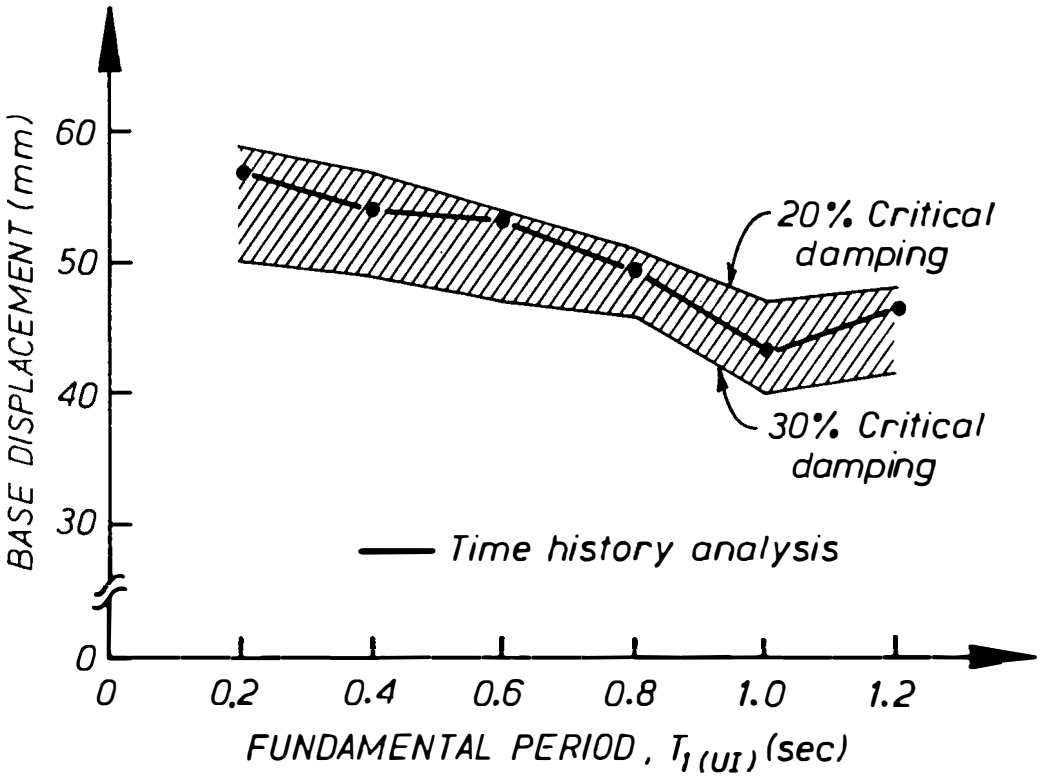

Fig. 4.25 Upper and Lower Limits of Base Displacement shown by the Approximate Method

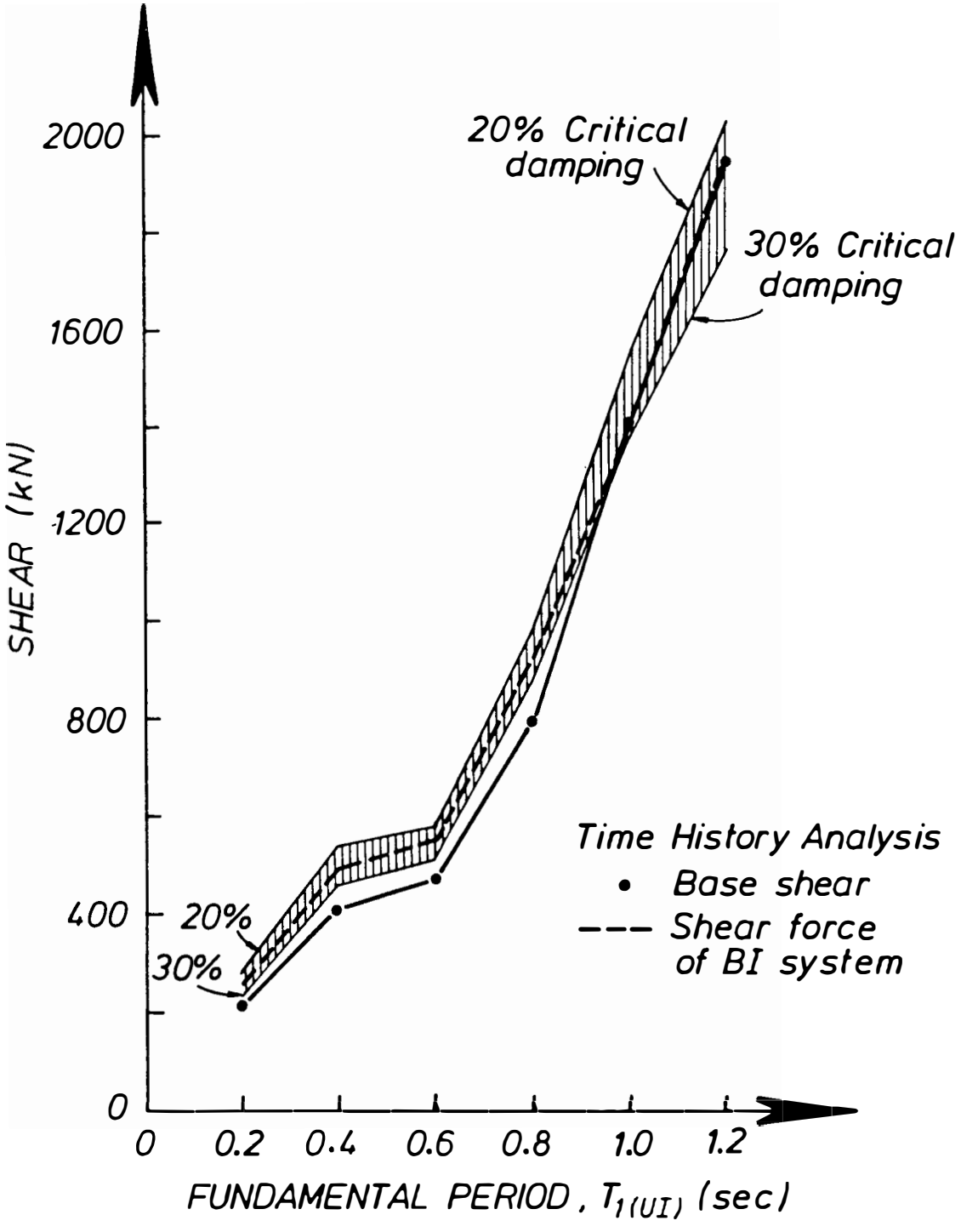

Fig. 4.26 Upper and Lower Limits of Shears shown by the Approximate Method.

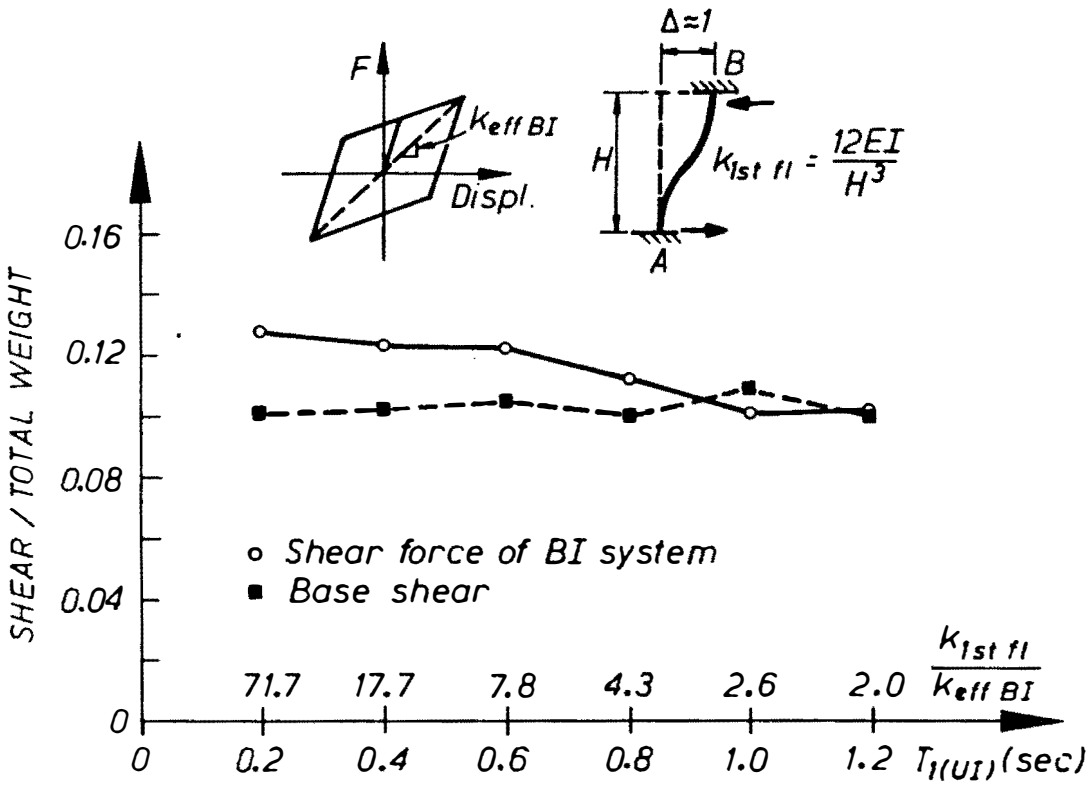

Fig. 4.27 The Difference between Base Shear and BI System's Shear Force

Table 4.3 The Time of Occurence of Maximum Storey Displacements and Storey Shears

T1(UI) secs	Sto-rey	Displacement (mm)				Shear (kN)			
		+	time	-	time	+	time	-	time
	4	58.3	5.43	45.6	4.43	61.0	5.44	49.2	2.38
	3	58.1	5.43	45.5	4.43	116.6	5.44	94.9	4.38
0.2	2	57.8	5.43	45.2	4.43	165.5	5.44	136.2	6.04
	1	57.3	5.43	44.8	4.43	211.1	5.43	175.3	4.44
	0	56.7	5.43	44.3	4.43	255.0	5.43	218.0	4.43
	4	59.8	3.01	47.2	6.06	175.3	4.62	190.9	2.21
	3	59.2	3.01	46.8	4.44	268.4	2.08	308.1	2.21
0.4	2	58.1	3.02	46.2	4.44	347.5	2.07	348.1	2.43
	1	56.4	3.02	45.1	4.43	410.3	2.98	372.2	6.07
	0	54.1	3.02	43.3	4.43	494.4	3.02	429.8	4.43
	4	65.1	2.02	65.0	4.47	503.9	1.97	410.3	2.36
	3	63.4	3.10	62.8	4.47	767.3	1.96	602.5	12.01
0.8	2	60.9	3.08	58.3	4.46	793.3	1.96	654.2	4.52
	1	56.4	3.07	52.5	4.44	791.8	2.02	673.7	4.49
	0	49.1	3.07	44.6	4.44	929.1	3.07	875.5	4.44
	4	107.0	5.47	84.2	6.29	1174.0	2.08	1188.0	2.44
	3	99.3	5.47	80.8	6.20	1485.0	2.07	1525.0	2.39
1.2	2	82.6	5.50	75.0	6.20	1898.0	5.40	1407.0	12.06
	1	65.2	5.55	63.2	6.23	1959.0	3.11	1630.0	6.21
	0	46.5	5.57	44.4	6.26	1963.0	5.57	1910.0	6.26

Table 4.4 Results of Kelly's Method compared with Results of Time History Analyses

T_1(UI) secs	Sto-rey	Displacement (mm)				Shear (kN)			
		Kelly's Method			THA	Kelly's Method			THA
		mode1	mode2	total		mode1	mode2	total	
0.2	4	56.0	-0.1	56.0	58.3	50.3	-12.9	63.2	61.0
	3	55.8	-0.1	55.8	58.1	100.3	-20.8	121.1	116.6
	2	55.2	0.0	55.2	57.8	149.9	-20.5	170.4	165.5
	1	54.5	0.1	53.4	56.8	246.7	0.8	247.5	255.0
	0	54.4	0.1	53.4	56.8	246.7	0.8	247.5	255.0
0.4	4	60.4	-1.3	60.4	59.8	103.6	-95.0	140.6*	190.9
	3	59.4	-0.8	59.4	59.2	205.6	-150.4	254.7*	308.1
	2	57.4	0.1	57.4	58.1	304.2	-142.9	336.1	348.7
	1	54.6	0.9	54.6	56.4	398.0	-76.1	405.2	410.3
	0	50.9	1.4	51.0	54.1	485.4	21.9	485.9	494.4
0.8	4	74.9	-8.8	75.5	65.1	217.7	-375.1	433.7*	503.9
	3	71.7	-4.2	71.8	63.4	426.1	-554.4	699.2	767.3
	2	65.2	2.5	65.2	60.9	615.4	-449.5	762.1	793.3
	1	56.0	7.7	56.5	56.4	778.1	-124.9	788.1	791.8
	0	44.6	8.7	45.5	49.1	907.8	242.7	939.7	929.1
1.2	4	96.5	-25.0	99.7	106.9	475.8	-1253.2	1340.5	1188.3
	3	90.1	-9.3	90.6	99.3	920.3	-1720.5	1951.2	1525.3
	2	77.8	11.5	78.6	82.5	1304.3	-1142.5	1733.9	1898.2
	1	60.7	24.0	65.3	65.2	1603.6	62.4	1604.8*	1959.2
	0	39.9	21.0	45.1	46.4	1800.2	1114.9	2117.5	1963.3

Note : * 10 - 30 % underestimate

THA = inelastic Time History Analysis

the higher mode contribution is insignificant. Based on the Sum of Absolute modal combination rule[4.7], the approximate values give a reasonably conservative estimate for both storey displacements and storey shears (see Table 4.4). An example of the detailed calculation can be found in Appendix A.

As the superstructure becomes more flexible, the maximum storey displacements and shears no longer occur at the same time. The SRSS procedure[4.7] is used in this case to combine the maximum modal responses. Kelly's approximate method, as shown in Table 4.4, does not always give a conservative shear envelope for BI structures with $T_{1(UI)} \geq 0.4$ seconds. At times, it underestimates the storey shears by more than 20%.

In order to explain the cause of these errors, two different hysteresis loops of BI systems for structures with $T_{1(UI)}$ equal to 0.4 and 0.8 seconds were plotted in Figs. 4.28 and 4.29 respectively. It is found that the shears of the upper-storeys tend to reach their maxima before the BI system has actually reached the peak displacement. For BI structures with $T_{1(UI)}$ of 0.4 and 0.8 seconds, the maxima of the shears at the fourth and third storeys occur at 2.21 seconds and at around 1.96 seconds respectively. At these times the BI systems have not yet attained their peak displacements which occur at around 3.0 and 4.4 seconds. Hence to estimate these upper-storey shears, a greater value of BI system's effective stiffness should be considered rather than those based on the values obtained at maximum base displacements which are used to predict the maximum response at the base of the structure.

However it should also be kept in mind, that the maxima of these upper-storey shears are not only affected by the higher modes, but also by the first mode at a condition when the base displacement has not yet reached its maximum value. As shown earlier, the fundamental period as well as the first mode shape may vary over a large range dependent on the effective stiffness of the BI system at that time. Shorter fundamental periods than that usually estimated at maximum base displacement together with the corresponding mode shapes may cause a significant increase of the first mode contribution to the upper-storey shears.

Kelly et al[4.2] suggested that the second mode participation factor at the elastic state should be used instead of that at the "effective state", which is typically very small, to give a conservative estimate of the second mode contribution. This may be considered as a substitute for the underestimate of the BI system effective stiffness, for structures with relatively flexible upper-storeys, at the time where the higher modes are strongly excited. The effect of the first mode at the above time, however, has not been taken into account.

Further investigation, as will be discussed in Section 4.5, is needed to study this complex phenomenon by incorporating various types of BI systems.

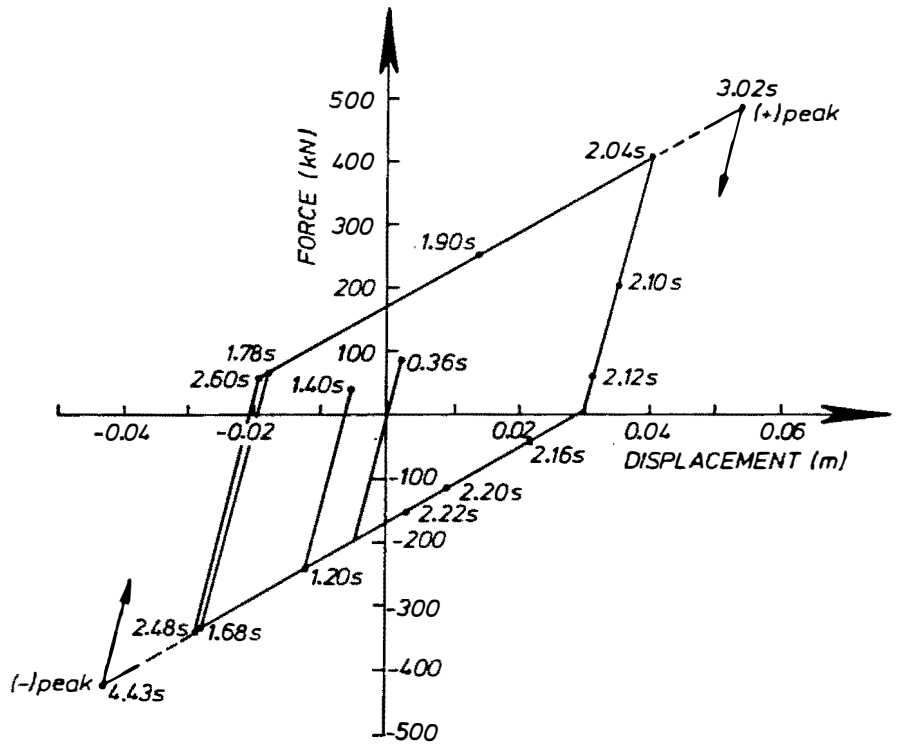

Fig. 4.28 Bilinear Hysteresis Behaviour of a BI System installed in a Multistorey Structure with $T_{1(UI)}$ = 0.4 secs

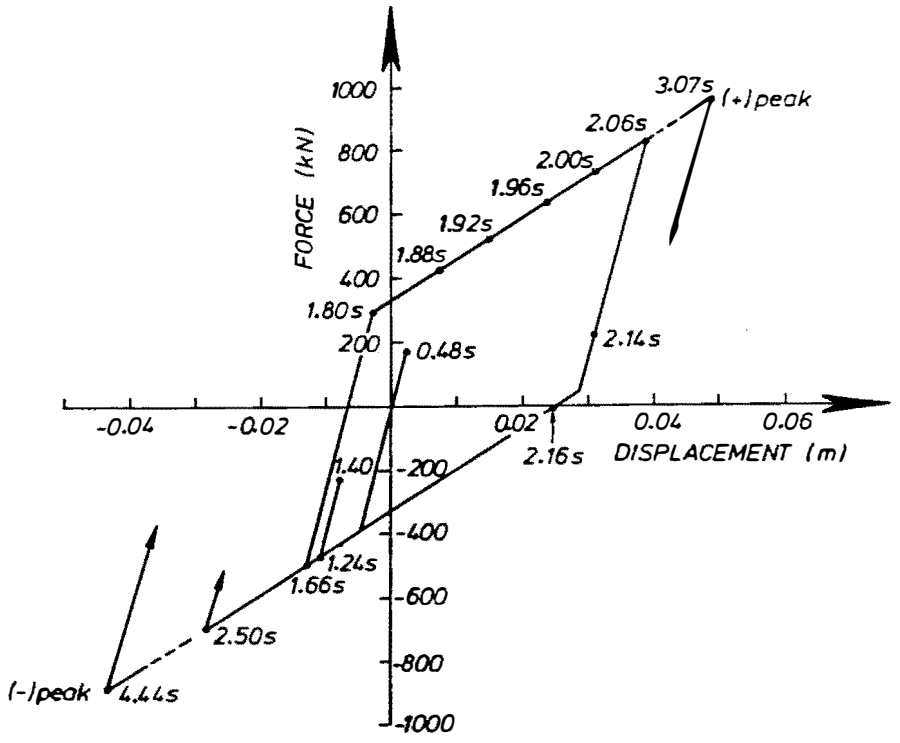

Fig. 4.29 Bilinear Hysteresis Behaviour of a BI System installed in a Multistorey Structure with $T_{1(UI)}$ = 0.8 secs

4.5 THE EFFECT OF PARAMETER VARIATION ON A BI SYSTEM

4.5.1 INTRODUCTION

In the previous section the effect of the superstructure's fundamental period, $T_{1(UI)}$, on the behaviour of BI multistorey structures has been described. The structures were mounted on one type of BI system. As there are many types of practical BI system available as mentioned earlier in Chapter 2, it is important to investigate the effect of varying BI system parameters on the structural response. For this purpose a series of bilinear hysteresis loop models were considered.

The same uniform "shear-beam" type structure with $T_{1(UI)}$ of 0.4 secs., as considered in the previous section, was used as the superstructure model for the analyses. The ground motion input is the El Centro 1940 N-S record with a 14 second duration.

First, methods to estimate the fundamental period shift and additional damping based on the characteristics of BI system hysteresis loop are discussed. The effect of parameter variation of BI system on the base displacements, base shear and lateral storey shear envelope is then described.

At the end of the section, a discussion regarding the possibility of developing an approximate equivalent linear analysis method is presented. As has been indicated earlier, an approximate analysis for inelastic systems based on linearization techniques provides a useful insight into the nature of the structural response that cannot be readily obtained from a numerical analysis. Furthermore, since the ground excitation is usually not defined explicitly, but specified in a form of design-code response spectra, approximate linearization methods used for design purposes are more practical and economical than a series of deterministic inelastic time history analyses.

4.5.2 THE PERIOD SHIFT AND THE ADDITIONAL DAMPING

The ability of a BI system to shift the structure's fundamental period away from the region of peak spectral acceleration and to provide additional damping depends on its hysteretic behaviour and the amplitude of the ground motion.

A typical idealized bilinear force-displacement relationship during an earthquake is shown in Fig. 4.30. The total response history comprises cycles of purely elastic behaviour as well as cycles during which yielding occurs. The yielding in one direction is not necessarily followed immediately by yielding in the opposite direction. Furthermore, these yielding cycles may not be centred about the origin of the force-displacement diagram. This causes further complication in developing a simple and reliable linearization technique to estimate the effective period and increase in the effective damping. Note, the apparent trilinear parts at the corners of the plot shown in Fig. 4.30 are due to the plotting program connecting lines from one response point or one step of integration to the next.

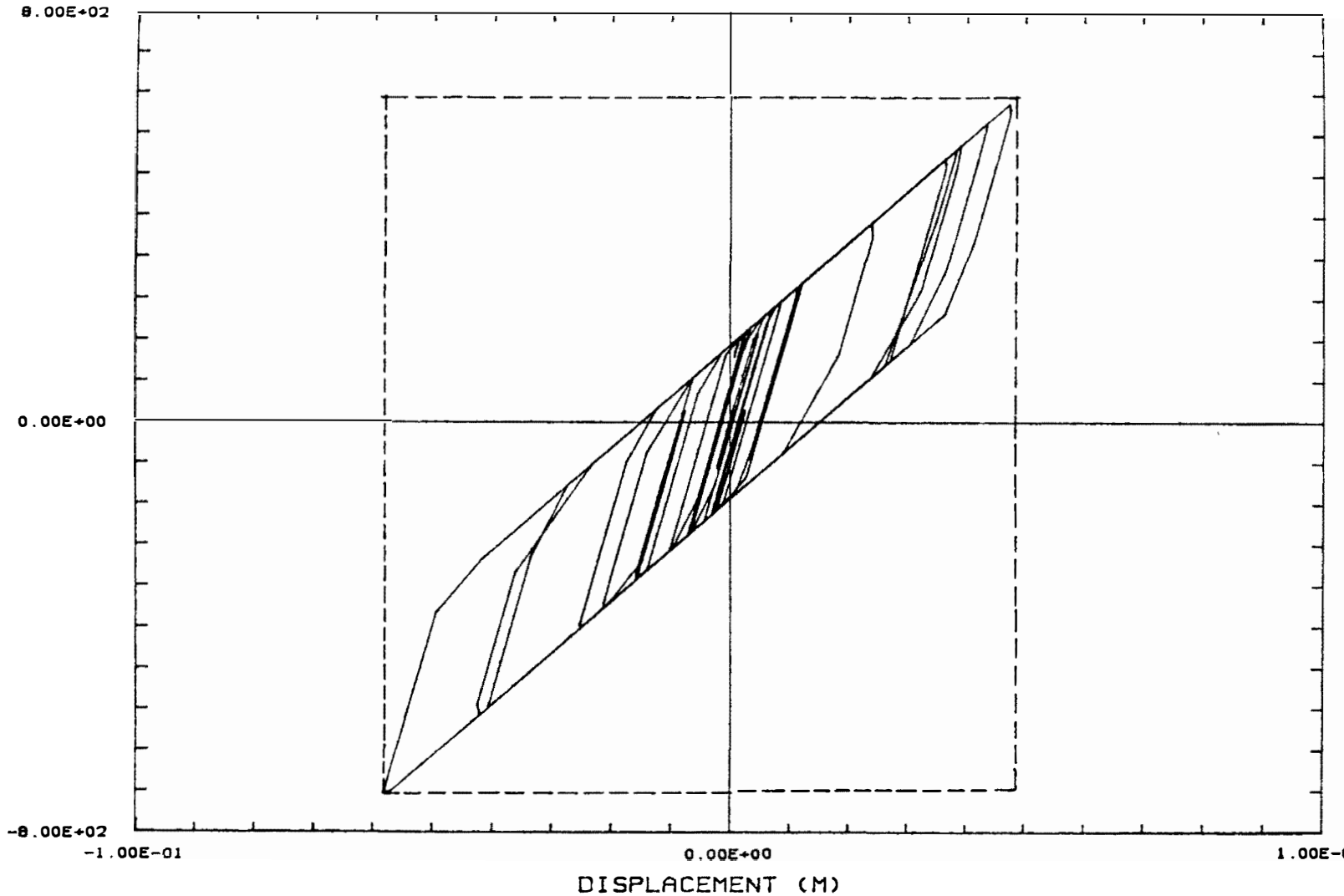

Fig. 4.30 A Typical Idealized Bilinear Force-Displacement Relationship of a BI System during an Earthquake

Many research projects have been carried out with the major aim to develop equivalent linear analysis techniques[4.15, 4.16, 4.17, 4.18]. Some of them are simple, but encounter difficulty in predicting the structure response when moderate to large non-linearities occur (see Ref. 4.17). More accurate techniques, unfortunately are rather complicated in application and usually involve some statistical predictions. For these reasons, this study which is more directed towards design application, adapts the simple techniques used for predicting the seismic performance of BI structures.

The current methods basically suggest that the effective stiffness of a BI system can be assumed simply as the secant stiffness at the maximum displacement and the effective additional damping may be estimated based on the area circumscribed by the hysteresis loop as described in Chapter 3.

For a bilinear hysteresis loop, the effective stiffness, k_{eff}, and the additional damping, E_h, can be expressed, as a function of the initial stiffness, k_o, the ratio of the post-yield stiffness to the total initial stiffness, α, and the ratio of the maximum displacement to the yield displacement of the BI system, μ, in the following equations,

$$k_{eff} = k_o \left[\frac{1-\alpha}{\mu} + \alpha\right] \tag{4.12}$$

$$E_h = \frac{2}{\pi}(1-\alpha)\left(\frac{\mu-1}{\mu^2}\right)\frac{k_o}{k_{eff}} \tag{4.13}$$

Since the amount of additional damping can be estimated from the fatness of the hysteresis loop, it is useful to introduce a factor R, which is the ratio of the loop area to the area of its enclosing rectangle. This factor may vary from zero for a linear BI system to almost one for a very fat hysteresis loop. It can be expressed in terms of α and μ as follows,

$$0.0 \le R = \frac{(1-\alpha)(\mu-1)}{\mu[1+\alpha(\mu-1)]} \le 1.0 \tag{4.14}$$

Figs 4.31 and 4.32 show the values of these effective stiffness, additional damping and R factor, respectively, in the form of charts.

As discussed in Section 4.5.7, the above simple linearization technique will be examined for a wide range of BI systems to ensure its accuracy in predicting the response of BI structures.

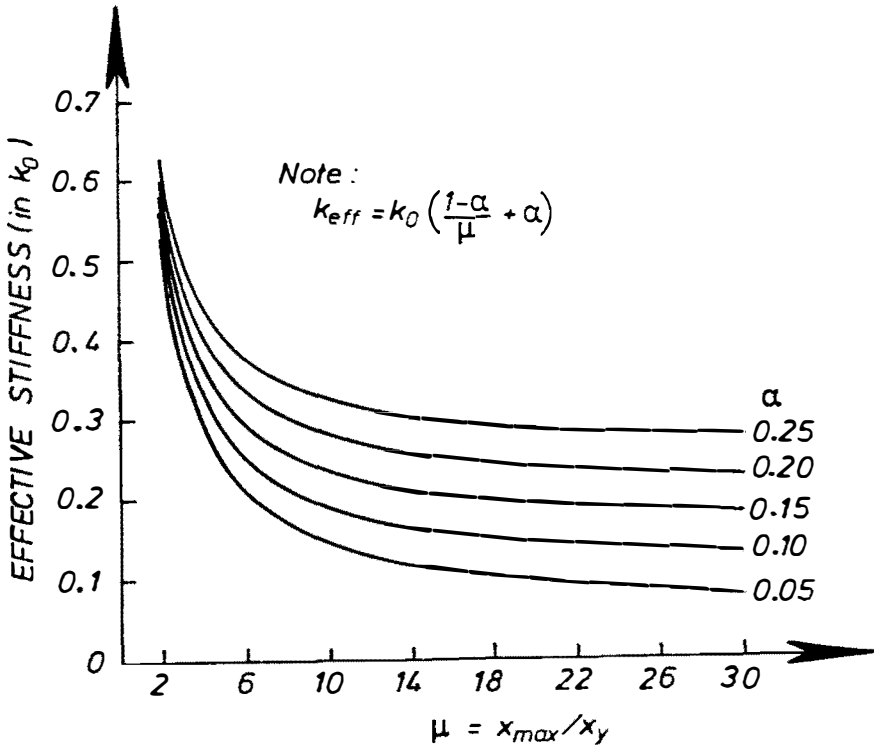

Fig. 4.31 Effective Stiffness of BI Systems with Bilinear Hysteresis Loop Model

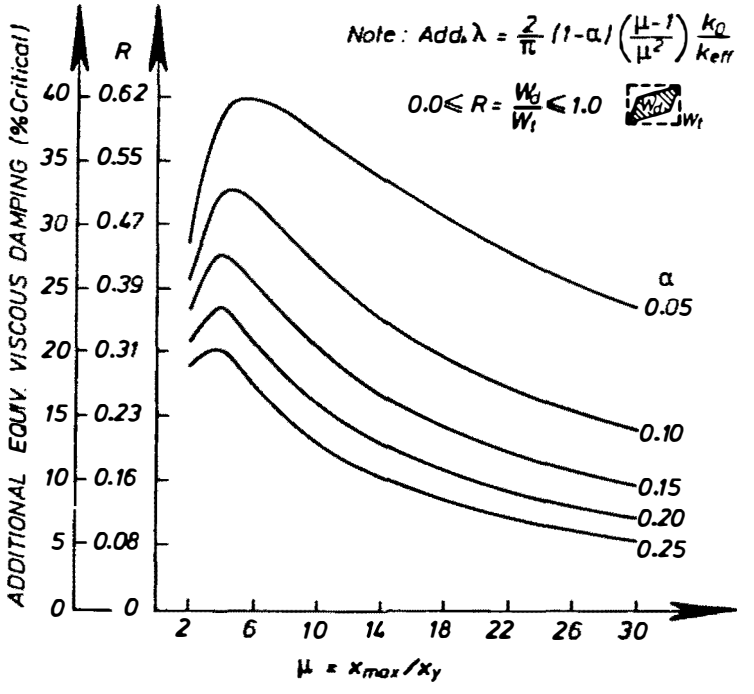

Fig. 4.32 Additional Damping of BI systems with Bilinear Hysteresis Loop Model

4.5.3 BASE DISPLACEMENT

It is demonstrated in this sub-section how the parameters of the BI systems, i.e. the initial stiffness, k_o, the post-yield stiffness, αk_o, and the yield strength, F_y, affect the base displacement of the structure.

First, k_o and F_y are varied from 2.5 W/m to 25.0 W/m and 1%W to 25%W, respectively, while αk_o is kept constant at 1.25 W/m. The effect of these parameter variations on the base displacement is displayed in Fig. 4.33. It can be seen that a BI system with a stiffer k_o tends to minimize the base displacement. This is because to increase k_o means widening the hysteresis loop which causes more increase in the effective damping and it also causes a stiffer system especially at high level of F_y. Hence it reduces the base displacement. It is also demonstrated in Fig. 4.33, that a linear BI system without energy dissipation capacity ($\alpha k_o = k_o = 1.25$ W/m) induces a very large displacement.

Likewise, selecting too low a yield strength causes a large base displacement. In this case the effect of the initial stiffness becomes insignificant, since during the entire ground shaking the system is on the post-yield condition most of the time with a narrow-band hysteresis loop having only a small amount of additional damping. On the other hand, choosing a higher yield strength to, say around 5%W, leads to a significantly smaller base displacement as it basically increases the additional damping and decreases the fundamental period shift. For a BI system with low k_o, the base displacement increases again as the yield strength becomes greater than the "optimum" point, i.e. around 5%W. This type of BI system naturally has a small capacity for energy dissipation. Thus refering to the El Centro 1940 N-S spectral displacement (see Fig. 4.14) for small damping ratios a decrease in the effective fundamental period may cause an increase in the base displacement.

If αk_o and F_y are now varied while k_o is kept constant at 10.0 W/m, the maximum base displacement response is such as presented in Fig. 4.34. In general the smaller the post-yield stiffness is the larger the base displacement. However, the effect is not so dramatic as if k_o is varied while αk_o is kept constant. At yield strength levels below 5%W, the base displacement increases rapidly as F_y decreases especially for BI systems with a small αk_o. At this condition the effective stiffness becomes smaller as αk_o decreases. Whereas at high levels of yield strength the effect of F_y becomes insignificant, since at these levels the initial stiffness is more dominant.

The maximum base displacement of a linear BI system with lateral stiffness of 10.0 W/m is also shown in Fig. 4.34. As expected, a relatively stiff linear BI system without energy dissipation capacity is able to keep the base displacement small (c.f. a much more flexible linear BI system shown in Fig. 4.33), but at the expense of higher induced inertia forces as will be shown in the following section.

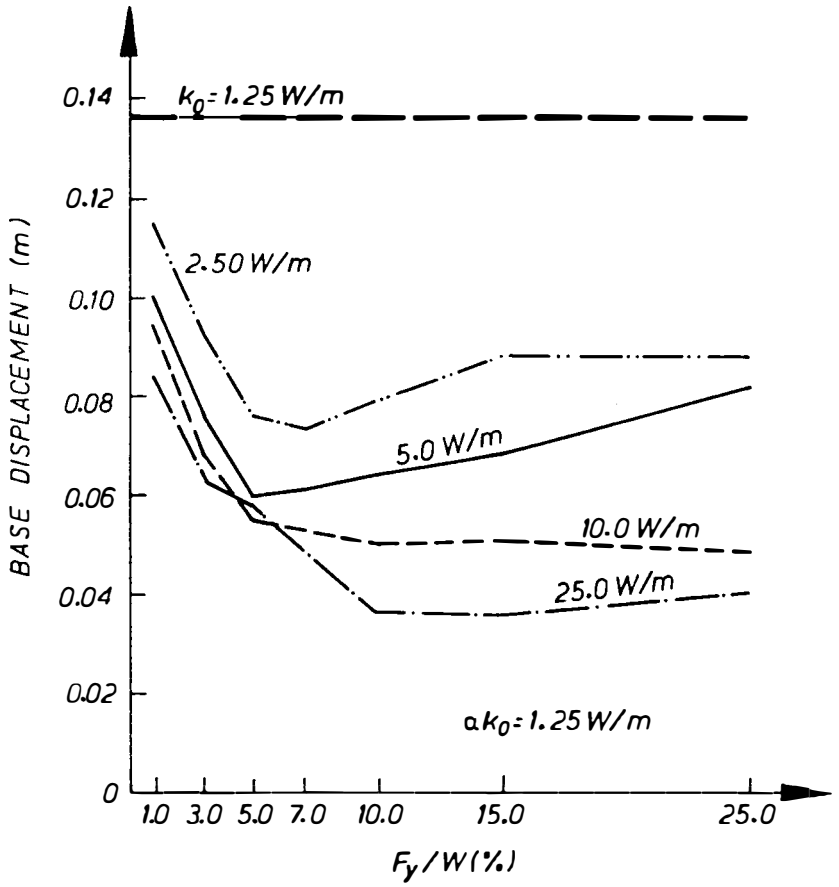

Fig. 4.33 The Effect of Varying Initial Stiffness and Yield Strength on Maximum Base Displacement

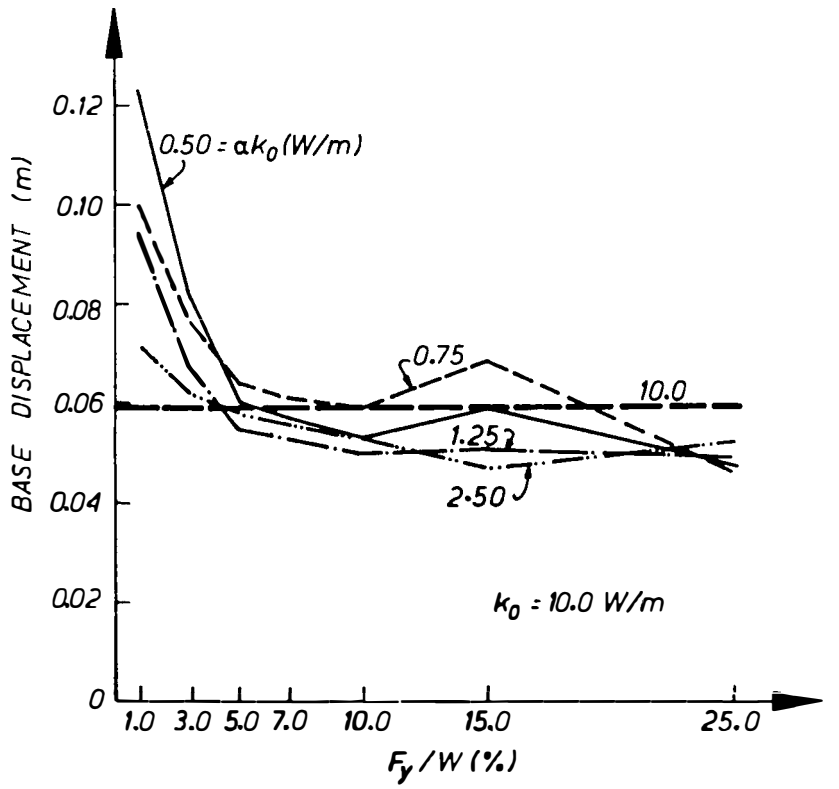

Fig. 4.34 The Effect of Varying Post-Yield Stiffness and Yield Strength on Maximum Base Displacement

4.5.4 BASE SHEAR

The effect of BI system parameter variation on the base shear of a multistorey BI structure is shown in Figs. 4.35 and 4. 36. First, the post-yield stiffness is kept constant while varying the initial elastic stiffness, k_o. It can be seen from Fig. 4.35 that in general the base shear reaches its minimum value when the yield strength is around 3.0 to 7.0%W. In this range the BI systems reach their optimum performance in reducing not only the base shear, but also the base displacement as discussed in Section 4.5.3. The BI system provides the maximum energy dissipation capacity to balance the effect of the effective secant stiffness, so that when the effective stiffness increases the base shear is kept low and even reduced.

If the yield strength is outside the above range (3.0 to 7.0%W) the energy dissipation capacity decreases, and therefore the base shear increases. For a BI system with low yield strength, the performance is significantly governed by the post-yield stiffness as the system is in the yielded region most of the time. The extreme condition will be reached when finally the BI system becomes a linear system with lateral stiffness of 1.25 W/m as shown in Fig. 4.35. On the other hand, for a BI system with high level of yield strength, the initial stiffness governs its performance. The stiffer the initial stiffness the greater the base shear will be, hence a small k_o is prefered in this case to keep the base shear moderate.

Secondly, the initial stiffness is now kept constant at 10.0 W/m while the post-yield stiffness is varied from 0.5 to 2.5 W/m. From Fig. 4.36, it can be seen that smaller shears are induced as a lower post-yield stiffness is introduced. In this case both the effective fundamental period and the additional hysteretic damping increase. The hysteresis loop widens as the post-yield stiffness decreases. However, no apparent difference is encountered as the yield strength is increased above 15%W.

Again in the range of 3.0 to 7.0%W of yield strength, the BI systems show their optimum performance. The energy dissipation capacity becomes smaller outside this range. Without energy dissipation capacity, a relatively stiff linear BI system may even shift the structure into a more dominant earthquake energy region, and therefore may induce greater base shear than if the structure is on a rigid base, as demonstrated in Fig. 4.36.

It is interesting to note that the shear force of BI systems with narrow-band or thin hysteresis loops is usually 10 to 25% greater than the base shear of the superstructure, giving a reasonable safety margin for any prediction of base shear based on the hysteresis characterestics of the BI system. An example of this trend is shown in Fig. 4.37.

As the hysteresis loop becomes fatter, either due to the increase of the initial stiffness and the yield strength or the decrease of the post-yield stiffness, the difference between the BI system shear force and the base shear decreases. The base shear may even exceed the BI system shear force, as shown in Fig. 4.38. Hence, any estimation of base shear based on the BI system shear

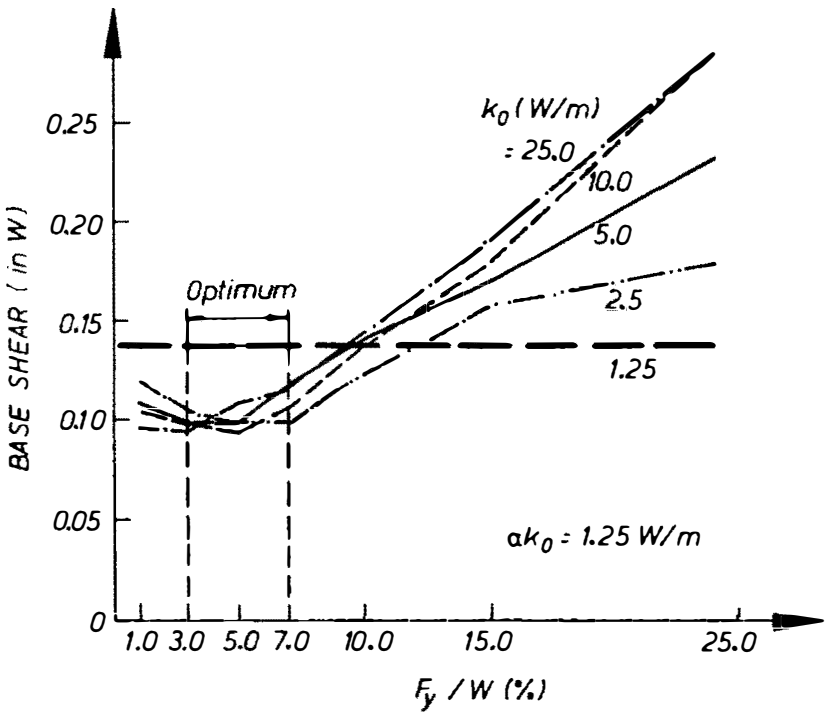

Fig. 4.35 The Effect of Varying Initial Stiffness and Yield Strength on Maximum Base Shear

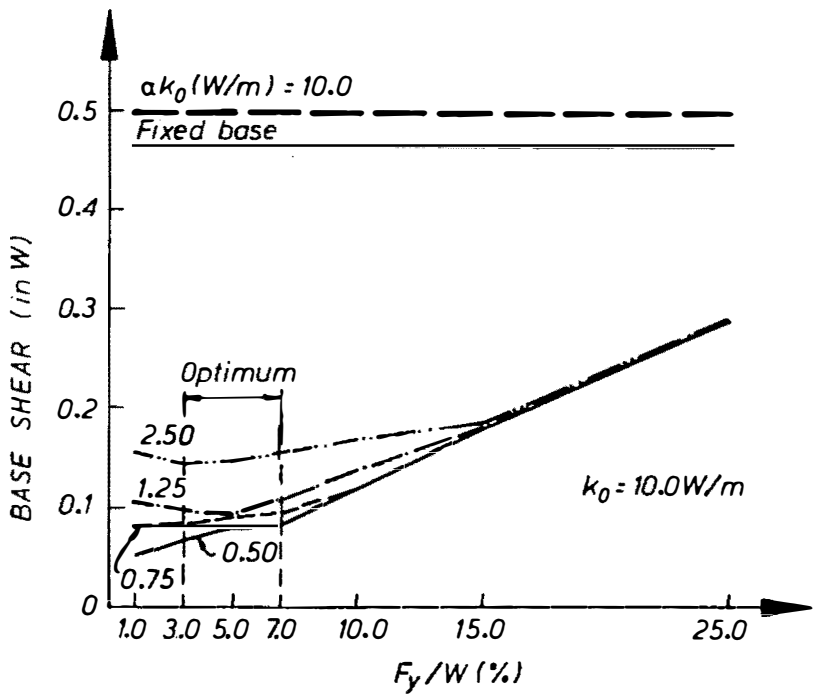

Fig. 4.36 The Effect of Varying Post-Yield Stiffness and Yield Strength on Maximum Base Shear

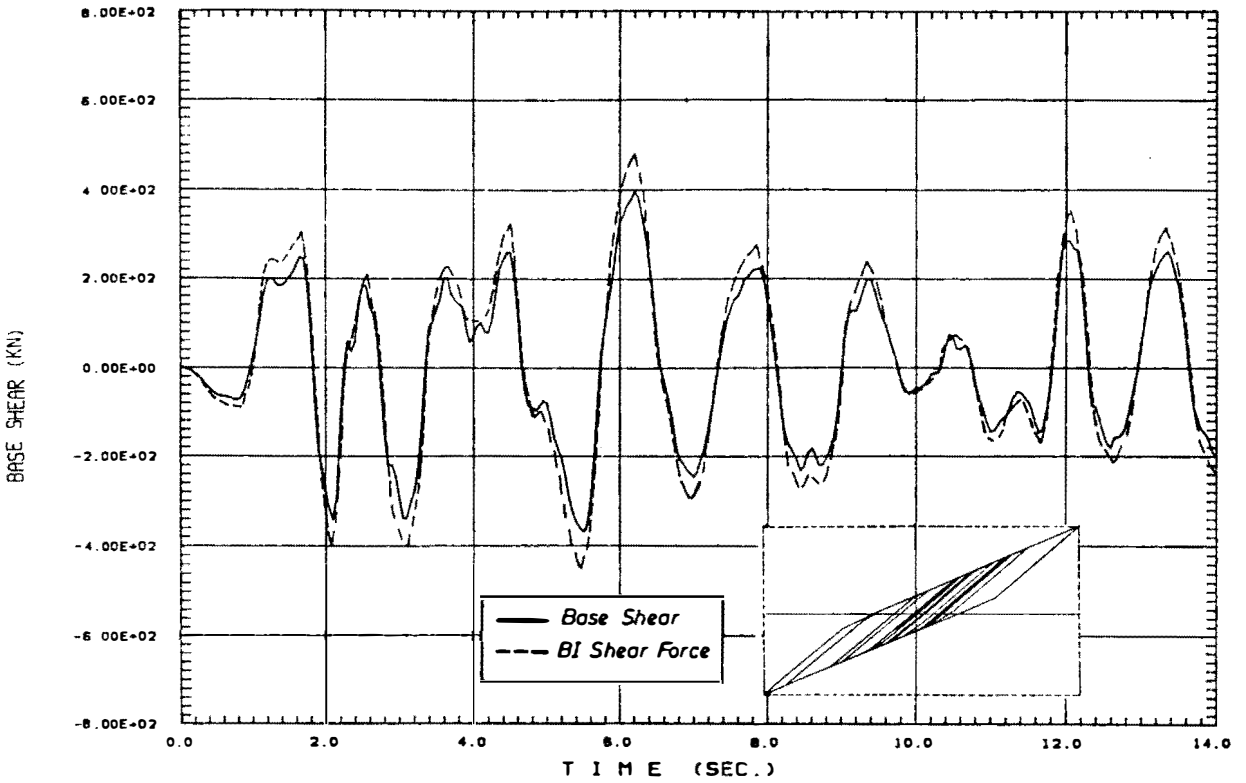

Fig. 4.37 Base Shear and Shear Force of a BI System with Thin Hysteresis Loops

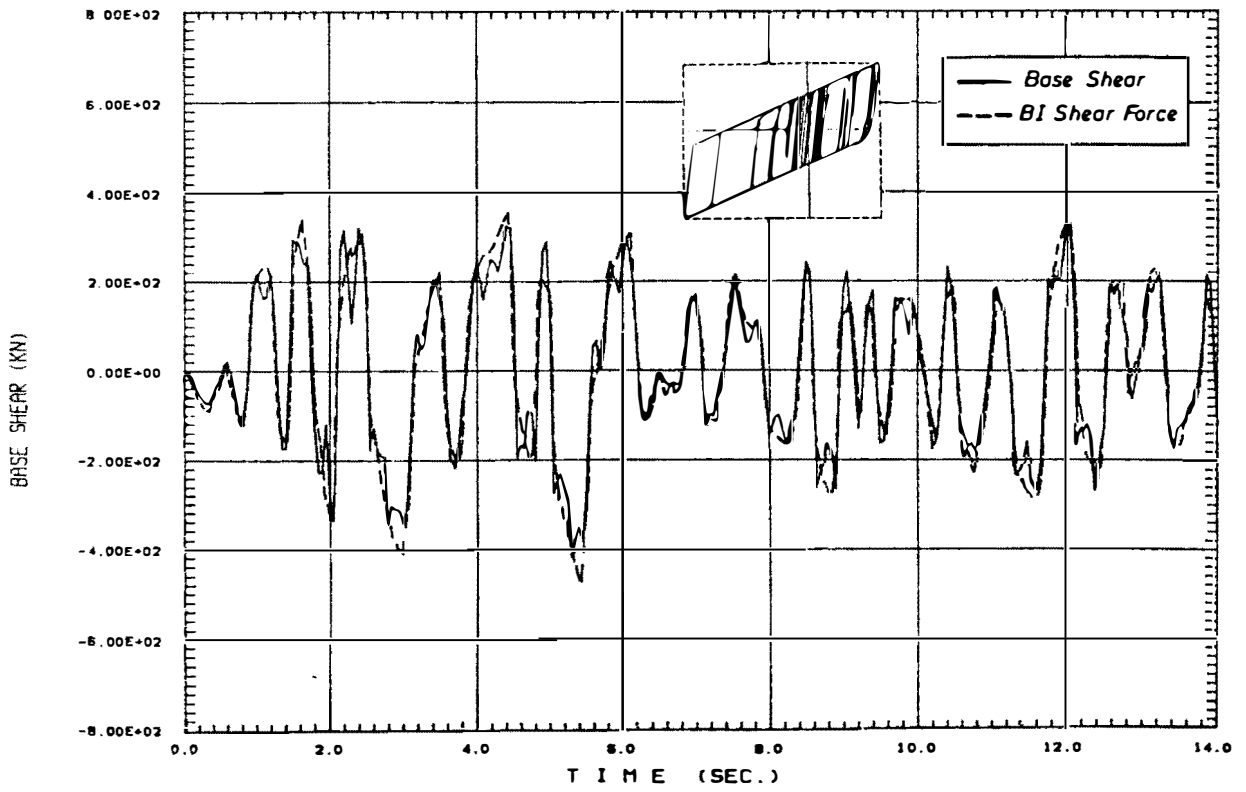

Fig. 4.38 Base Shear and Shear Force of a BI System with Fat Hysteresis Loops

force may not always be conservative. Further discussion on this matter is presented in Section 4.5.6.

4.5.5 LATERAL STOREY SHEAR ENVELOPE

The lateral shear envelopes of BI multistorey structures have become one of the major areas of attention from researchers since the late 1970s. Various types of BI system may be used to obtain the same level of reduction of base shear with reasonable base displacement, but different types of system induce different lateral shear forces at the upper levels of the superstructure.

Fig. 4.39 illustrates the effect of varying the initial stiffness while keeping the post-yield stiffness and the yield strength level constant at 1.25 W/m and 5% W, respectively. It can be seen that the difference between the base shears of a multistorey structure mounted on two different BI systems, with initial stiffness of 2.5 and 25.0 W/m is only around 10%, while at the upper levels the shears may differ as much as 94%.

Low initial stiffness causes the hysteresis loop to narrow and the effect becomes similar to the one caused by a linear BI system, which deflects the input earthquake energy rather than absorbs it. As was pointed out by Kelly[4.19], in a linear vibrating system all modes tend to be mutually orthogonal. In this case, it means all higher modes will be orthogonal to the input motion so that the transmission of high energies of input ground motion at certain frequencies, which tend to excite the higher modes, will be minimized. Therefore, the structure response becomes first mode dominant and the lateral shear envelope may even show a tendency of rigid body motion with equally distributed acceleration over the height of the superstructure. An almost straight line lateral shear envelope is depicted in Fig. 4.39 as the effect of this type of BI system.

An increase of initial stiffness, on the contrary, enhances the energy absorption capacity of the BI system. The contributions of the higher modes become significant in the upper levels of the superstructure. Hence, a more bulged lateral shear envelope is encountered. A similar effect is also found as the post-yield stiffness is decreased (Fig. 4.40) and as the yield strength level is increased (Fig. 4.41).

4.5.6 DISCUSSION OF DESIGN ASPECTS

4.5.6.1 Estimation of Base Displacement and BI System's Shear Force

From the response history plots of base displacement and shear force of the BI systems shown earlier, it can be seen that the response of the BI system is strongly dominated by a single mode. Based on this, it seems possible to estimate the maximum shear force of the BI systems using an

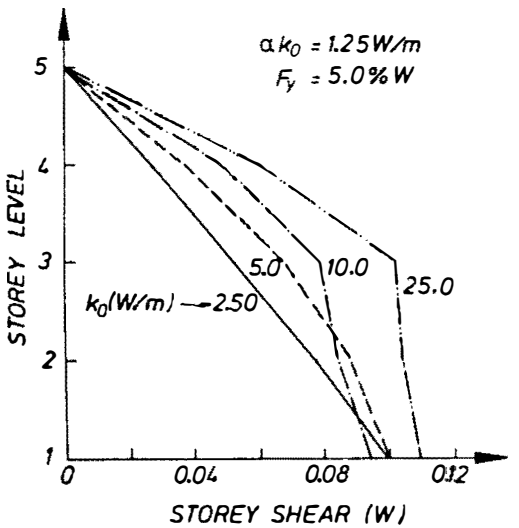

Fig. 4.39 The Effect of Varying Initial Stiffness on Lateral Storey Shears

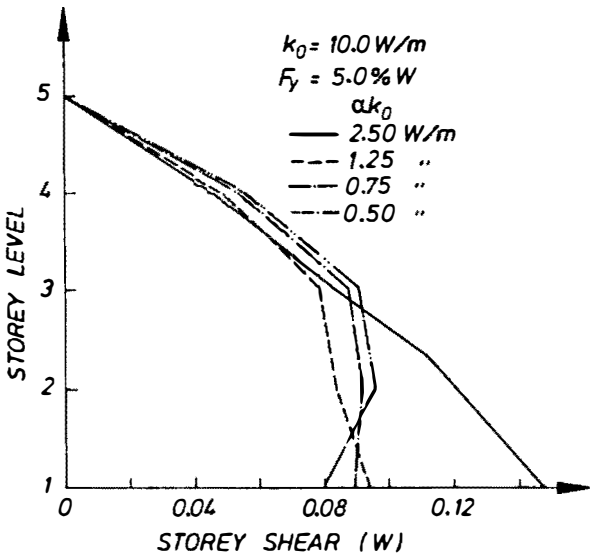

Fig. 4.40 The Effect of Varying Post-Yield Stiffness on Lateral Storey Shears

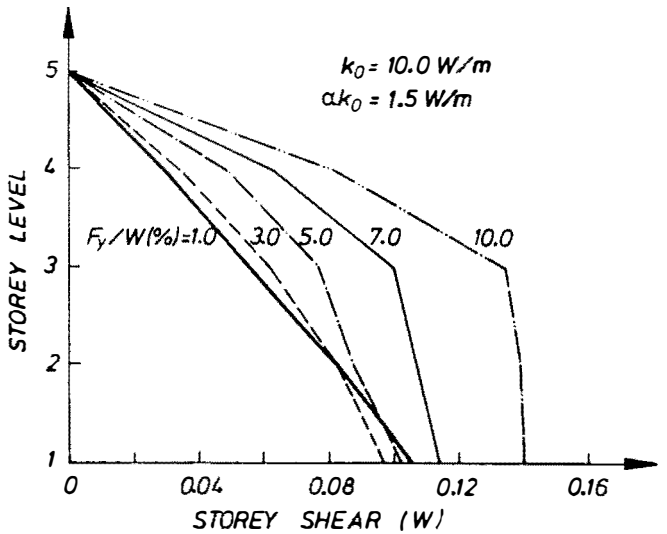

Fig. 4.41 The Effect of Varying Yield Strength on Lateral Storey Shears

equivalent linear approximation method for a SDOF system. The effective stiffness and the additional damping can be calculated using Eqs. 4.12 and 4.13, respectively. As discussed in Section 4.4, the effective fundamental period of a BI multistorey structure with $T_{1(UI)}$ less or equal to 0.4 seconds can also be estimated by assuming the superstructure to be a rigid body. This assumption saves some computational effort, especially in the preliminary design stage, since a free-vibration modal analysis for the whole structure is not required.

The accuracy of the above approximate method in predicting the base displacement and shear force of a wide variety of BI system was examined. In this method, the initial estimation of μ is based on the maximum base displacement obtained from the time history analysis shown in Figs. 4.33 and 4.34 . Similar charts can be produced for different earthquakes to give guidance in predicting the base displacement. However, in the absence of such a guide, a simple rapidly converging trial-and-error procedure can be used (see Chapter 7). For future reference this approximate method is named the code-type approach in conjunction with the name of the approach used to to predict the equivalent static lateral force distribution described in Section 4.5.6.2.

In general, the hysteresis loops are not symmetrical about the origin, whereas this code-type approach assumes that they are. However, this approach does predict the response at the base of the structure accurately . The comparisons with the time history analysis results as tabulated in Table 4.5 show that this method gives a reasonably conservative estimate for the base displacements and the BI system's shear forces for the ten cases considered. The underestimates found in three cases are less than 8% for the base displacements and less than 5% for the BI system shear forces.

4.5.6.2 Estimation of Lateral Storey Shears and Displacements.

It was found that there is a strong correlation between the factor R, which represents the fatness of the loop and the exponent p, which is used to described the equivalent static lateral force distribution over the height of the superstructure, as expressed in the following,

$$F_i = V \frac{W_i \, h_i^p}{\sum W_i \, h_i^p} \qquad (4.15)$$

where V is the base shear, W_i and h_i are the storey weight and storey height, respectively.

By considering BI systems which are most likely utilised in practice ($0.0 < R \leq 0.6$), the correlation coefficient, r, obtained from the linear regression analysis[4.20] is 0.85 and the corresponding conditional standard deviation $s_{y|x}$ is 0.4, as illustrated in Fig. 4.42. It should be noted, that this correlation is for uniform "shear-beam" BI multistorey structures with $T_{1(UI)}$ of

Table 4.5 Results of the Code-Type Approach compared to Results of Inelastic Time History Analysis

Case	k_o (W/m)	αk_o (W/m)	α	F_y (%W)	μ	k_{eff} (W/m)	$T_{1\,eff}$ (secs)	E_h (% crit)	R	Base Displacement (mm)			BI Sys. Sh.Force (kN)		
										App.	THA	% dif.	App.	THA	% dif.
1	2.50	1.25	0.50	5.0	3.80	1.58	1.60	9.8	0.15	84.8	75.9	11.7	533.6	479.4	11.3
2	5.00		0.25		6.03	1.87	1.47	17.6	0.28	65.8	60.3	9.1	490.8	451.8	8.6
3	10.00		0.125		10.92	2.05	1.44	22.6	0.35	57.3	54.6	4.9	470.8	447.8	5.1
4	25.00		0.05		29.25	2.06	1.40	24.2	0.38	56.3	58.5	-3.8	462.4	482.6	-4.2
5	10.00	0.50	0.05	5.0	12.80	1.24	1.80	35.0	0.55	71.6	64.0	11.9	356.0	318.1	11.9
6		2.50	0.25		11.70	3.14	1.13	16.9	0.26	67.8	58.0	16.9	856.0	735.4	16.4
7	10.00	1.50	0.15	3.0	20.53	1.91	1.45	13.1	0.20	69.8	61.6	13.3	534.4	471.8	13.3
8				5.0	10.82	2.28	1.33	19.8	0.31	55.0	54.1	1.7	501.6	494.6	1.4
9				7.0	7.48	2.63	1.23	23.8	0.37	50.5	54.6	-7.5	536.4	552.2	-2.9
10				10.0	4.95	3.27	1.10	26.7	0.42	46.1	49.5	-6.9	613.2	637.2	-3.8

Note : W = Total weight of the structure (incl. base mass)

x_{max} = Maximum base displacement obtained from Figs. 4.33 and 4.34

THA = Inelastic time history analysis

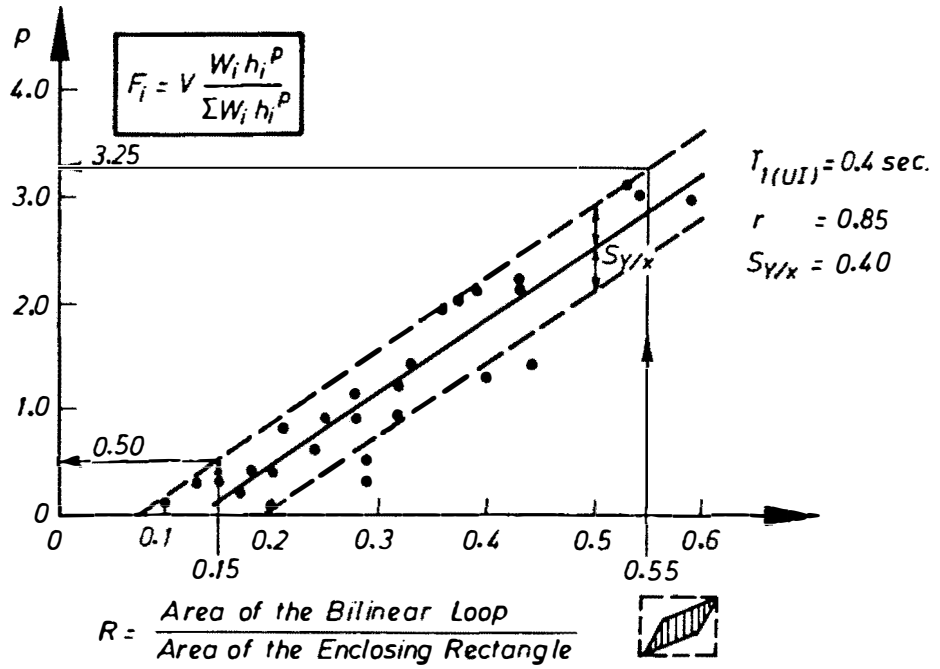

Fig. 4.42 Correlation between the Hysteresis Loop Ratio, R and the Exponent p for BI Multistorey Structures with $T_{1(UI)} = 0.4$ secs

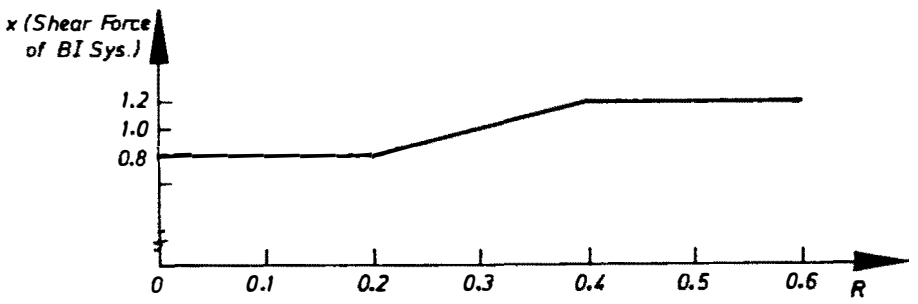

Fig. 4.43 Modification Factor Used for Predicting Base Shear from BI System's Shear Force

0.4 seconds. Correlations between R and p for BI structures with different superstructure models will be shown later in Section 4.6.

For preliminary design purposes, this relatively strong correlation can be used as a code-type approach to estimate the likely lateral shear envelope which will be obtained as a consequence of selecting a particular type of BI system.

It should be noted that for a multistorey structure with a fat loop BI system, the maximum shear may not occur at the base as is usual for structures on a thin loop BI system (see Figs. 4.39 - 4.41). For this reason, the estimation of the base shear, V, which is based on the maximum BI system shear force, should be multiplied by a factor shown in Fig. 4.43 in order to give a reasonably conservative estimate for the storey shears.

Two examples of calculating the lateral storey shears using Eq. 4.15 are shown in Table 4.6. In the first example, the BI system has a narrow hysteresis loop (R=0.15) whereas in the second one the BI system has a fat loop (R=0.55). For each case the storey shears are calculated based on the values of p with and without incorporating the conditional standard deviation, $s_{y|x}$. This code type approach estimates satisfactorily the storey shears.

For the later design stages and for more general cases, an appropriate response spectrum analysis based on a mode superposition method is usually required. This method will give the designer a clear insight of the modal contributions on the response of a BI multistorey structure. So far a method proposed by Kelly et al[4.2], described in Chapter 3, is the only known method meeting the above criterion. It is useful to examine this method by applying it to analyse the response of a multistorey structure, with $T_{1(UI)}$ of 0.4 seconds, mounted on various BI systems. The results were then compared to the ones obtained from the time history analysis, as tabulated in Table 4.7. Further details of calculation are given in Appendix A.

Refering to Table 4.7, it is found, that in general the above method is always able to predict the storey displacements and storey shears of a multistorey structure on BI system with a relatively thin hysteresis loop ($R \leq 0.26$). As the hysteresis loop widens, however, the method underestimates the structure response. The maximum underestimate for the storey displacements in Case 10 was approximately 20%. Discrepancies of storey shear which reach almost 50% were also detected at the top storey of the BI multistorey structure in Case 5 and Case 10. The effect of the underestimation for the storey displacements may not be as critical as for the storey shears, since in design considerations the former is less important than the latter.

Fig. 4.44 may be used to explain the cause of the differences in the storey shears. Essentially, Kelly's method predicts the structure's effective fundamental period, T_{1eff}, based on the condition at t_2, i.e. when the BI system reaches its peak displacement.

Table 4.6 Examples of Calculating Storey Shears Using the Code-Type Approach

(a). k_o = 2.5 W/m α = 0.50 F_y = 5%W R = 0.15

Storey i	W_i (kN)	h_i (m)	CODE-TYPE APPROACH p = 0.1 + $s_{y\|x}$ = 0.5 $W_i h_i^p$	F_i (kN)	Shear (kN)	CODE-TYPE APPROACH p = 0.1 $W_i h_i^p$	Fi (kN)	Shear (kN)	THA Shear (kN)
4	800	13.00	2884.4	138.9	138.9	1033.9	113.1	113.1	106.9
3	800	9.75	2498.0	120.3	295.2	1004.6	109.9	223.0	209.5
2	800	6.50	2034.6	98.2	357.4	964.7	105.5	328.5	308.4
1	800	3.25	1442.2	69.4	426.9*	900.1	98.4	426.9*	396.7
0	800	0.00	-		(533.6)			(533.6)	(479.4)
			Σ 8864.2		*0.8 x 533.6	3093.3		*0.8 x 533.6	

(b). k_o = 10.0 W/m α = 0.05 F_y = 5%W R = 0.55

Storey i	W_i (kN)	h_i (m)	CODE-TYPE APPROACH p = 2.85 + $s_{y\|x}$ = 3.25 $W_i h_i^p$ (10^3)	F_i (kN)	Shear (kN)	CODE-TYPE APPROACH p = 2.85 $W_i h_i^p$ (10^3)	Fi (kN)	Shear (kN)	THA Shear (kN)
4	800	13.00	3337.4	283.1	283.1	1196.3	267.3	267.3	223.6
3	800	9.75	1310.2	111.1	394.2	526.9	117.7	117.7	364.5
2	800	6.50	350.8	29.8	424.0	165.9	37.1	422.1	383.9
1	800	3.25	36.9	3.2	427.2**	23.0	5.1	427.2**	318.9
0	800	0.00	-		(356.0)			(356.0)	(318.1)
			Σ 5035.3		**1.2 x 356.0	1912.1		**1.2 x 356.0	

Note : ( ) denotes the BI system's Shear Force

Table 4.7 Results of Kelly's Method compared to Results obtained from Inelastic time history analysis

Case & R	mode 1	mode 2	SRSS	THA	mode 1	mode 2	SRSS	THA
	87.5	-0.4	87.5	81.9	110.2	-28.2	113.7	106.9
1	86.8	-0.2	86.8	81.2	219.4	-45.2	224.0	209.5
R = 0.15	85.4	0.0	85.4	80.0	326.9	-44.2	329.9	308.4
	83.3	0.3	83.3	78.2	431.8	-25.2	432.5	396.7
	80.5	0.4	80.5	75.9	533.1	3.2	533.1	479.4
	68.9	-0.7	68.9	64.7	102.8	-53.4	115.8	149.5
2	68.1	-0.4	68.1	64.3	204.3	-85.2	221.4	274.0
R = 0.28	66.4	0.0	66.4	63.6	303.4	-82.3	314.4	351.7
	64.0	0.5	64.0	62.3	398.9	-46.1	401.6	398.0
	60.9	0.8	60.9	60.3	489.7	8.8	489.8	451.8
	61.0	-1.3	61.0	59.5	100.2	-95.1	138.1	195.6
3	60.0	-0.8	60.0	59.1	198.7	-150.3	249.1	317.3
R = 0.35	58.0	0.1	58.0	58.1	294.0	-142.6	326.8	335.8
	55.1	0.9	55.1	56.0	384.4	-75.6	391.8	375.2
	51.3	1.3	51.3	54.6	468.7	22.4	469.3	447.8
	61.3	-2.2	61.3	63.6	100.8	-159.2	188.4	244.6
4	69.8	-1.2	59.8	63.2	199.0	-245.4	316.0	407.0
R = 0.38	56.8	0.3	56.8	62.4	292.2	-220.4	366.0	414.9
	52.4	1.7	52.4	60.8	378.3	-98.5	390.9	434.8
	47.0	2.2	47.0	58.5	455.5	62.0	459.7	482.6
	76.9	-1.3	76.9	69.4	76.4	-94.8	121.8*	223.6
5	75.4	-0.7	75.4	68.7	151.4	-149.2	212.5*	364.5
R = 0.55	72.5	0.1	72.5	67.5	223.5	-140.1	263.8	383.9
	68.2	0.9	68.2	65.9	291.3	-71.8	300.1	318.9
	62.8	1.3	62.8	64.0	353.8	26.2	354.8	318.1
	72.8	-1.3	72.8	67.2	183.8	-94.5	206.6	185.3
6	71.4	-0.7	71.4	66.3	364.1	-148.9	393.3	332.6
R = 0.26	68.7	0.1	68.7	64.6	537.5	-140.3	555.5	447.9
	64.7	0.9	64.7	62.0	700.8	-72.6	704.6	587.9
	59.5	1.3	59.5	58.5	851.2	25.4	851.5	735.4
	73.5	-1.3	73.5	66.9	112.6	-95.4	147.6	138.2
7	72.5	-0.8	72.5	66.3	223.6	-151.5	270.1	247.6
R = 0.2	70.5	0.1	70.5	65.3	331.5	-145.3	362.0	329.2
	67.6	0.9	67.6	63.8	435.0	-79.6	442.2	384.3
	63.8	1.3	63.8	61.6	532.7	18.5	533.0	471.8
	60.4	-1.3	60.4	59.8	103.6	-95.0	140.6	190.9
8	59.4	-0.8	59.4	59.2	205.6	-150.4	254.7	308.1
R = 0.31	57.4	0.1	57.4	58.1	304.2	-142.9	336.1	348.7
	54.6	0.9	54.6	56.4	398.0	-76.1	405.2	410.3
	50.9	1.4	51.0	54.1	485.4	21.9	485.9	494.4
	54.5	-1.3	54.5	59.0	115.8	-94.4	149.4	252.7
9	53.4	-0.8	53.4	58.3	229.2	-148.3	273.0	401.9
R = 0.37	51.2	0.1	51.2	57.1	327.9	-138.7	365.3	428.8
	47.9	0.9	47.9	55.1	439.7	-70.0	445.2	457.4
	43.8	1.4	43.8	52.4	532.7	28.0	533.4	552.2
	50.5	-1.3	50.5	57.7	134.3	-93.8	163.8*	325.1
10	49.2	-0.7	49.2	56.8	265.2	-146.4	303.0*	534.6
R = 0.42	46.8	0.2	46.8	55.0	389.7	-134.8	412.3	556.4
	43.2	1.0	43.2	52.6	504.5	-64.4	508.6	561.0
	38.6	1.3	38.6	49.5	607.2	33.7	608.2	637.2

Note : * Almost 50% underestimate.

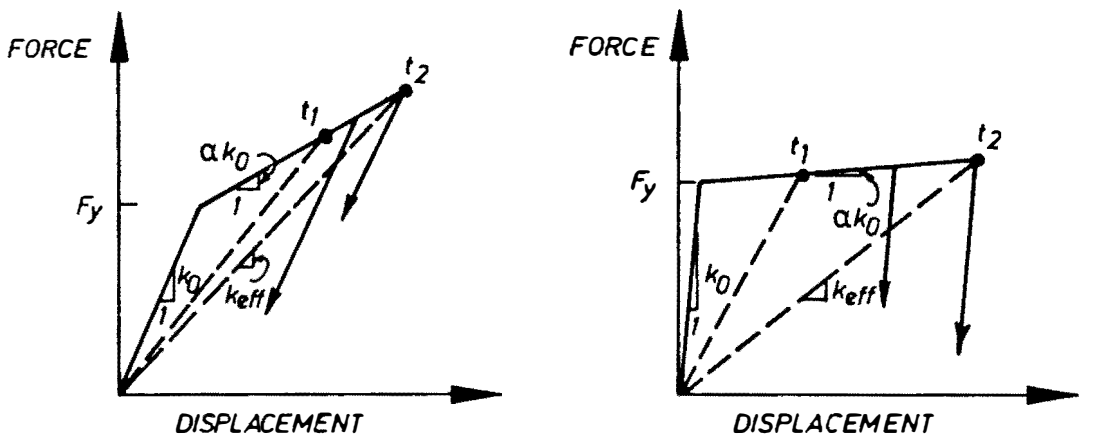

NOTE : t_1 = Time at which the upper level shears reach their peaks
t_2 = Time at which the response at base reaches its peak.

(a) "Thin" Loop with Small R *(b) "Fat" Loop with Large R*

Fig. 4.44 Two Types of Idealized Bilinear Hysteresis Loop with Different Effects on the Lateral Storey Shear Envelope

An assumption is then made that the structure changes from the elastic or Isolated Un-Yielded state to the Isolated Yielded state in a linear fashion depending upon the effective fundamental period, T_{1eff}. The transition is expressed by an interpolation factor C[4.2] as follows,

$$C = \frac{T_{1\,eff} - T_{1\,(IUY)}}{T_{1\,(IY)} - T_{1\,(IUY)}} \tag{4.16}$$

$$\phi_{1\,eff} = \phi_{1\,(IUY)} + C\,(\phi_{1\,(IY)} - \phi_{1\,(IUY)}) \tag{4.17}$$

$$PF_{1\,eff} = PF_{1\,(IUY)} + C\,(PF_{1(IY)} - PF_{1(IUY)}) \tag{4.18}$$

and

$$T_{2\,eff} = T_{2\,(IUY)} + C\,(T_{2\,(IY)} - T_{2\,(IUY)}) \tag{4.19}$$

$$\phi_{2\,eff} = \phi_{2\,(IUY)} + C\,(\phi_{2\,(IY)} - \phi_{2\,(IUY)}) \tag{4.20}$$

The effective second mode participation factor, $PF_{2\,eff}$ is taken equal to $PF_{2\,(IUY)}$ to give a conservative estimate. The second mode damping is also assumed unchanged. More complete description of this method can be found in Section 3.3.2.

As discussed in Section 4.4.7, there is a tendency for the upper-level shears to reach their peaks at a time when the BI system has not reached its peak displacement. For BI systems with thin hysteresis loops (small R), the difference between the conditions at t_1 and t_2 shown in Fig. 4.44.a is naturally small and therefore any estimation made based on the condition at t_2 is acceptable. However, this is not the case for BI system with fat loops (large R value) as illustrated in Fig. 4.44.b.

During ground shaking, the higher modes may already be excited to their maximum at t_1. For this reason, the adoption of the second mode participation factor at the elastic state is justified. However, an aspect which should not be overlooked, especially for a BI system with very fat loops, is the fact that at around t_1 the structure has a different first mode response than when it is at t_2, since the effective stiffness at t_1 can be much higher than the effective stiffness at t_2. The first mode at t_1 may not be excited to its peak, but a much shorter effective fundamental period together with a different mode shape may cause much higher shears at the upper levels of the superstructure. Due to the combination of these first mode and the higher mode responses, a more bulged lateral shear envelope is therefore encountered for multistorey structures mounted on a BI system with a higher value of R.

The time at which the upper-level shears reach their peak depends on many factors, such as the characteristics of the hysteresis loop and the nature of the ground shaking. Unless predicted in a probabilistic sense, it is impossible to estimate the exact effective fundamental period and its

corresponding mode shape, which may cause maximum response at the upper storeys when combined with the higher mode contribution.

Furthermore the response at the base of the structure is strongly governed by the single mode behaviour of the BI system and it is hardly affected by the higher mode effects of the superstructure. This behaviour seems too complex to be predicted by a response spectrum analysis using a mode superposition technique, except when the BI system has thin hysteresis loops. Further investigation to clarify this phenomenon is carried out by considering different types of superstructure model as discussed in the following section.

4.6 THE EFFECT OF SUPERSTRUCTURE'S FRAME ACTION

4.6.1 INTRODUCTION

The analysis results presented in the previous sections of this chapter are based on the response of four-storey uniform "shear-beam" superstructures in which the floor slabs and beams are assumed to be infinitely stiff so that the beam-to-column stiffness ratio, $\rho = \infty$. In this section the other superstructure models mentioned in Chapter 2 are included to investigate the effect of superstructure's frame behaviour on the seismic response of BI multistorey structures. The other models are "cantilever-beam" type structures with $\rho = 0.0$ and "moment-resistant frames" with $\rho = 0.125$.

First, the period shifts and the change of the modal properties due to these degrees of frame action are compared. Second, under the 14-second duration of El Centro 1940 N-S record the major response quantities, such as base displacements, base shears, lateral storey displacements and lateral storey shear envelopes are evaluated.

Then, based on these analysis results, a discussion of design aspects with regard to the superstructure's frame action is also presented.

4.6.2 PERIOD SHIFTS AND CHANGE OF MODAL PROPERTIES

For unisolated fixed-base multistorey structures, it has been discussed elsewhere[4.21,4.22,4.23] that as the beam-to-column stiffness ratio, ρ decreases, the natural periods spread over a wider portion of the ground motion response spectrum as illustrated in Fig. 4.45. The effect of the the spectrum shape then becomes more significant especially if the fundamental period, T_1 is large. A similar phenomenon is found for BI structures as shown in Tables 4.8.a and 4.8.b. However, there are also a number of differences which are noteworthy.

It is known that the horizontal flexibility provided by a BI system causes the natural periods of the structure to shift. As has been discussed earlier, the fundamental period of a "shear-beam" BI structure is lengthened quite considerably compared to the other higher mode periods. Refering to Tables 4.8.a and 4.8.b. for structures with $T_{1(UI)}$ of 0.2 and 1.2 respectively, it can be seen that as ρ decreases the increase of the higher mode periods become more significant both at the initial (k_0) and pseudo post-yield (αk_0) conditions. For the short period structure, the increase of the second mode period of the "cantilever-beam" BI structure ($\rho = 0.0$) is five times larger than the same increase found for the "shear-beam" BI structure ($\rho = \infty$). A similar trend is observed in the increase of the higher mode periods of structures with $T_{1(UI)} = 1.2$ seconds.

To investigate further the above trends, the ratios of the second mode period to the fundamental period of unisolated and isolated structures are tabulated in Table 4.9. A range of "linear

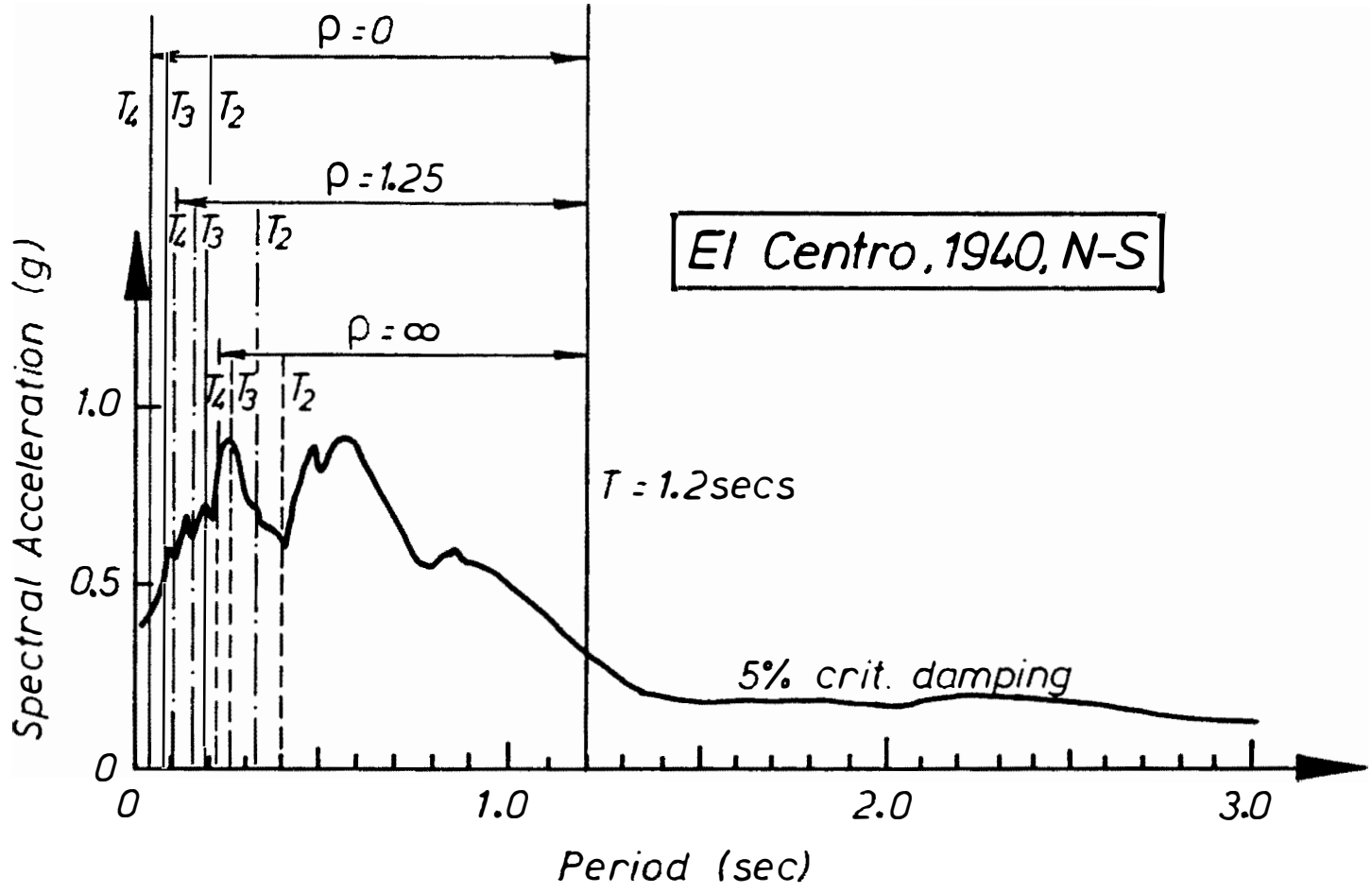

Fig. 4.45 The Spread of the First Four Natural Periods of Fixed-Base Structures with Different Beam-to-Column Stiffness Ratio

Table 4.8 The First Four Natural Periods of Unisolated and BI Structures with Different Beam-to-Column Stiffness Ratios

(a) $T1(UI) \approx 0.2$ seconds

Condition at base	Mode i	T_i	% increase	T_i	% increase	T_i	% increase
Fixed-Base Unisolated (UI)	1	0.212	-	0.202	-	0.199	-
	2	0.033	-	0.057	-	0.069	-
	3	0.012	-	0.027	-	0.045	-
	4	0.006	-	0.017	-	0.037	-
BI at k_o=10.0W/m (IUY)	1	0.655	209.0	0.656	224.7	0.657	230.1
	2	0.137	315.1	0.121	112.3	0.109	58.0
	3	0.026	116.7	0.047	74.1	0.058	28.9
	4	0.010	66.7	0.024	41.2	0.043	16.2
BI at αk_o=1.25W/m (IY)	1	1.801	749.5	1.802	792.1	1.802	805.5
	2	0.141	327.3	0.124	117.5	0.112	62.3
	3	0.026	116.7	0.047	74.1	0.059	31.1
	4	0.010	66.7	0.024	41.2	0.043	16.2

(b) $T1(UI) \approx 1.2$ seconds

Condition at base	Mode i	T_i	% increase	T_i	% increase	T_i	% increase
Fixed-Base Unisolated (UI)	1	1.190	-	1.192	-	1.180	-
	2	0.185	-	0.335	-	0.410	-
	3	0.065	-	0.159	-	0.267	-
	4	0.036	-	0.101	-	0.218	-
BI at k_o=10.0W/m (IUY)	1	1.291	8.5	1.305	9.5	1.304	10.5
	2	0.408	120.5	0.424	26.6	0.449	9.5
	3	0.141	116.9	0.244	53.4	0.288	7.9
	4	0.058	61.1	0.141	39.6	0.229	5.0
BI at αk_o=1.25W/m (IY)	1	2.037	71.2	2.064	73.1	2.079	76.2
	2	0.705	281.1	0.650	94.0	0.593	44.6
	3	0.145	123.1	0.276	73.6	0.339	27.0
	4	0.058	61.1	0.144	42.6	0.229	5.0

Table 4.9 The Ratios of the Second Mode Periods to the Fundamental Mode Periods of Unisolated and Base Isolated Structures

$T_{1(UI)}$ secs	Base Condition		Beam-to-Column Stiff. Ratio		
			$\rho = 0.0$	$\rho = 0.125$	$\rho = \infty$
0.0 - ∞	Fixed-Base		0.155	0.280	0.347
0.2	BI	10.00 W/m	0.209	0.184	0.166
		2.50	0.110	0.097	0.087
		1.25	0.078	0.069	0.062
		0.50	0.050	0.044	0.039
0.4	BI	10.00 W/m	0.339	0.305	0.278
		2.50	0.202	0.182	0.166
		1.25	0.147	0.132	0.121
		0.50	0.094	0.085	0.078
0.6	BI	10.00 W/m	0.386	0.354	0.328
		2.50	0.279	0.256	0.230
		1.25	0.210	0.194	0.175
		0.50	0.138	0.128	0.115
0.8	BI	10.00 W/m	0.378	0.355	0.342
		2.50	0.334	0.308	0.278
		1.25	0.264	0.245	0.221
		0.50	0.178	0.167	0.150
1.0	BI	10.00 W/m	0.343	0.339	0.344
		2.50	0.374	0.339	0.312
		1.25	0.317	0.286	0.262
		0.50	0.223	0.203	0.185
1.2	BI	10.00 W/m	0.316	0.324	0.344
		2.50	0.386	0.354	0.327
		1.25	0.346	0.315	0.285
		0.50	0.254	0.232	0.209

horizontal flexibility" is considered at the base of Bl structures. These flexibilities represent the likely range of conditions prior to and after the BI system yields.

For unisolated structures, Cruz and Chopra[4.23] showed that the ratio of $T_{2(UI)}/T_{1(UI)}$ does not change as $T_{1(UI)}$ varies. However, it increases as ρ inreases. For BI structures, the above ratio varies with $T_{1(UI)}$ as well as with the degree of horizontal flexibility at their base. Furthermore in general the ratio decreases as ρ increases. This indicates that BI structures with smaller ρ tends to have larger second mode periods.

Another important modal property which should also be taken into account in evaluating the likely modal contributions are the mode shapes. Fig. 4.46 shows the first two mode shapes of unisolated and isolated structures. Note that the mode shapes of the former structure do not vary with $T_{1(UI)}$ whereas the mode shapes of the latter structure are dependent on $T_{1(UI)}$ and on its degree of base flexibility.

Fig. 4.46.a shows that the mode shapes of the unisolated structures for the two extreme cases, ρ = 0.0 and ρ = ∞, are quite different and as it is expected the mode shapes of structures with ρ = 0.125 lie between those two extremes. For BI structures with short $T_{1(UI)}$, the difference in the first mode shapes as shown in Fig. 4.46.b becomes insignificant especially as the base flexibility increases. Fig. 4.46.c depicts the difference enlarging for longer period BI structures although it can be kept low by introducing larger base flexibility. The differences in the second mode shapes between the two extreme cases, however, vary in a much smaller amount compared to the change of the differences found in the first mode shapes, due to the base flexibility.

For a multistorey linear structure, in which a response spectrum analysis is applicable, the maximum modal displacements, $\{u_i\}_{max}$ and the maximum modal accelerations, $\{\ddot{u}_i\}_{max}$ can be evaluated as shown in the following :

$$\{u_i\}_{max} = \{\phi_i\}\ PF_i\ S_d\ (T_i, \lambda_i) \qquad (4.21)$$

$$\{\ddot{u}_i\}_{max} = \{\phi_i\}\ PF_i\ S_a\ (T_i, \lambda_i) \qquad (4.22)$$

where :

$\{\phi_i\}$ = mode shape vector of mode i

PF_i = modal participation factor of mode i

$$= \frac{\{\phi_i\}^T [M]\ \{r\}}{\{\phi_i\}^T [M]\ \{\phi_i\}}$$

[M] = mass matrix

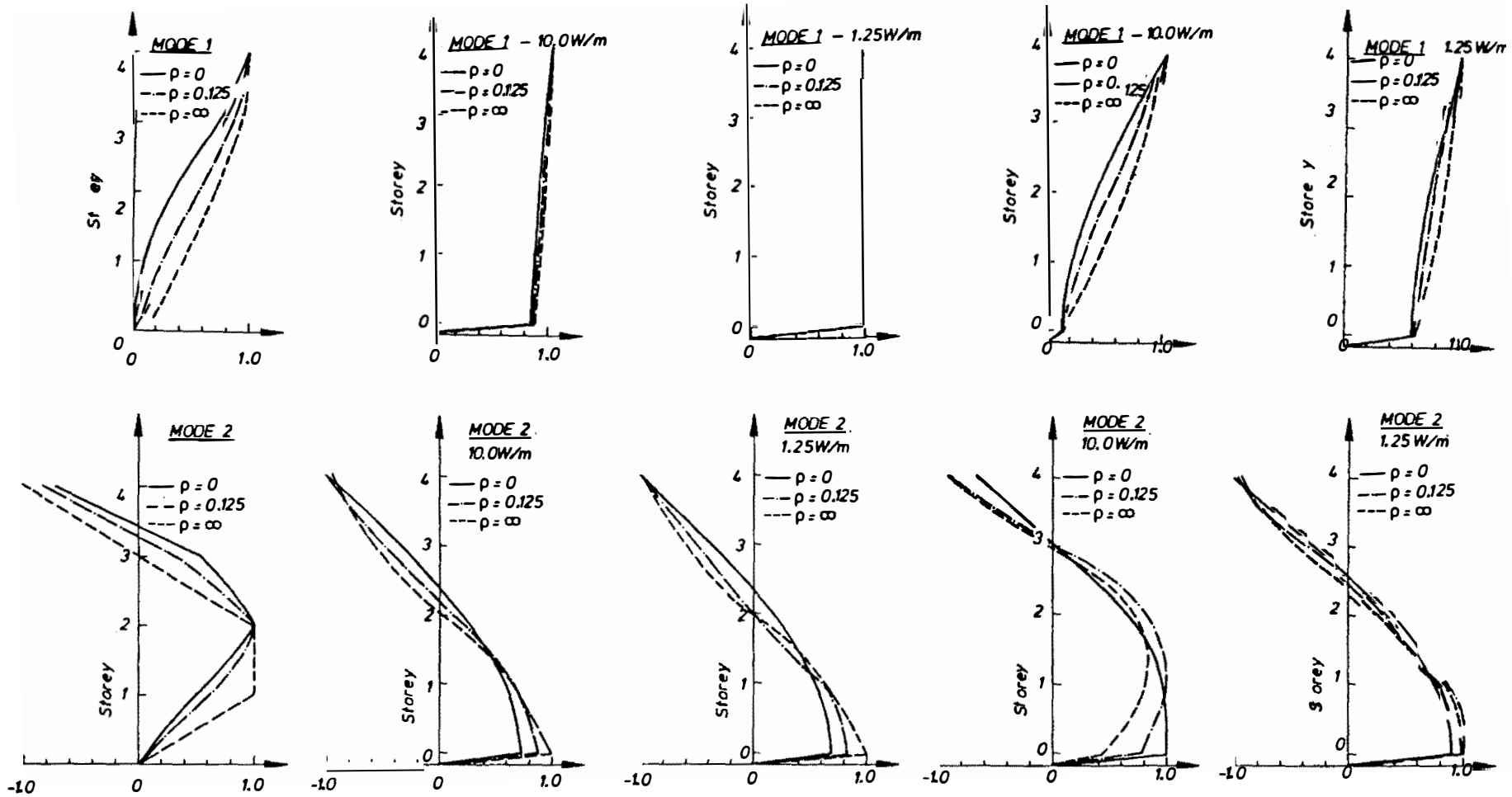

(a) Unisolated (Fixed-Base) (b) Base Isolated ($T_{1(UI)}$ = 0.2 secs) (c) Base Isolated ($T_{1(UI)}$ = 1.2 secs)

Fig. 4.46 The Mode Shapes of Unisolated and BI Four-Storey Structures with Different Beam-to-Column Stiffness Ratios

$\{r\}$ = vector of displacements due to a unit ground displacement

$S_d(T_i, \lambda_i)$ = spectral displacement as a function of the modal period and the modal damping.

$S_a(T_i, \lambda_i)$ = the corresponding spectral acceleration.

Various approximate formula for superposition of these modal responses can then be employed. The most common mode-superposition technique is the SRSS procedure which determines the total maximum responses as the Square Root of the Sum Squares of the modal responses considered.

Refering to the above equations it is also important to evaluate the likely changes of the modal participation factors caused by the frame action, in order to be able to estimate the modal contributions. Table 4.10 tabulates the modal participation factors of unisolated and BI structures with different ρ. The values of PF of unisolated structures, which are independent of $T_{1(UI)}$, decreases as ρ increases. Similar trends are followed by the PF of isolated structures. However, they vary with $T_{1(UI)}$ as well as with the degree of base flexibility.

4.6.3 EVALUATION OF THE MAJOR RESPONSE QUANTITIES

Using the 14-second duration of El Centro 1940 N-S earthquake record a series of inelastic time history analyses have been carried out to investigate the differences in the seismic response of BI structures due to the effect of the beam-to-column stiffness ratio. Some major response quantities, such as base displacement, base shear, lateral storey displacement and lateral storey shear envelope of BI structures with different types of superstructure models are compared.

4.6.3.1 Base Displacement and Base Shear

It has been shown earlier that the base displacement of BI structures with "shear-beam" type superstructures does not vary significantly with $T_{1(UI)}$. A similar trend is also found for base displacements of BI structures with different types of superstructure as can be seen in Fig. 4.47.a. In this evaluation all structures are mounted on BI systems which have an initial stiffness, k_o = 10.0W/m, a post-yield stiffness, αk_o = 1.5 W/m, and a yield strength, F_y = 5%W.

Differences in base displacement as affected by frame action is not especially evident for BI structures with $T_{1(UI)}$ less than 0.8 seconds. Fig. 4.47.b shows that within this range the base displacements of BI structures with ρ = 0.0 and ρ = 0.125 differ less than 12% when compared to the base displacements of BI structures with $\rho = \infty$. For the whole considered range of $T_{1(UI)}$, i.e. up to 2.0 seconds, the differences are less than 21%.

Table 4.10 Modal Participation Factors of Unisolated and BI Structures with Different Beam-to-Column Stiffness Ratios

T1(UI) secs	Base Condition		Beam-to-Column Stiffness Ratio					
			ρ = 0.0		ρ = 0.125		ρ = ∞	
			mode 1	mode 2	mode 1	mode 2	mode 1	mode 2
0.0 - ∞	Fixed- Base		1.347	0.636	1.296	0.488	1.241	0.333
0.2	BI	10.00 W/m	1.082	0.084	1.059	0.065	1.044	0.054
		2.50	1.021	0.022	1.016	0.017	1.012	0.014
		1.25	1.011	0.011	1.008	0.008	1.006	0.007
		0.50	1.004	0.004	1.003	0.003	1.002	0.003
0.4	BI	10.00 W/m	1.249	0.256	1.184	0.207	1.139	0.184
		2.50	1.075	0.077	1.057	0.062	1.044	0.054
		1.25	1.039	0.039	1.029	0.032	1.023	0.028
		0.50	1.016	0.016	1.012	0.013	1.009	0.011
0.6	BI	10.00 W/m	1.384	0.440	1.291	0.387	1.214	0.292
		2.50	1.154	0.157	1.121	0.134	1.090	0.115
		1.25	1.082	0.084	1.065	0.072	1.049	0.061
		0.50	1.034	0.035	1.027	0.003	1.021	0.025
0.8	BI	10.00 W/m	1.433	0.604	1.333	0.484	1.250	0.387
		2.50	1.240	0.246	1.188	0.214	1.139	0.184
		1.25	1.136	0.139	1.109	0.121	1.081	0.103
		0.50	1.058	0.059	1.047	0.052	1.036	0.044
1.0	BI	10.00 W/m	1.434	0.712	1.341	0.547	1.262	0.433
		2.50	1.333	0.343	1.248	0.306	1.185	0.253
		1.25	1.209	0.214	1.157	0.176	1.120	0.157
		0.50	1.094	0.096	1.072	0.079	1.056	0.069
1.2	BI	10.00 W/m	1.424	0.747	1.338	0.565	1.263	0.434
		2.50	1.382	0.436	1.287	0.380	1.212	0.289
		1.25	1.263	0.270	1.199	0.230	1.147	0.197
		0.50	1.125	0.128	1.097	0.107	1.073	0.092

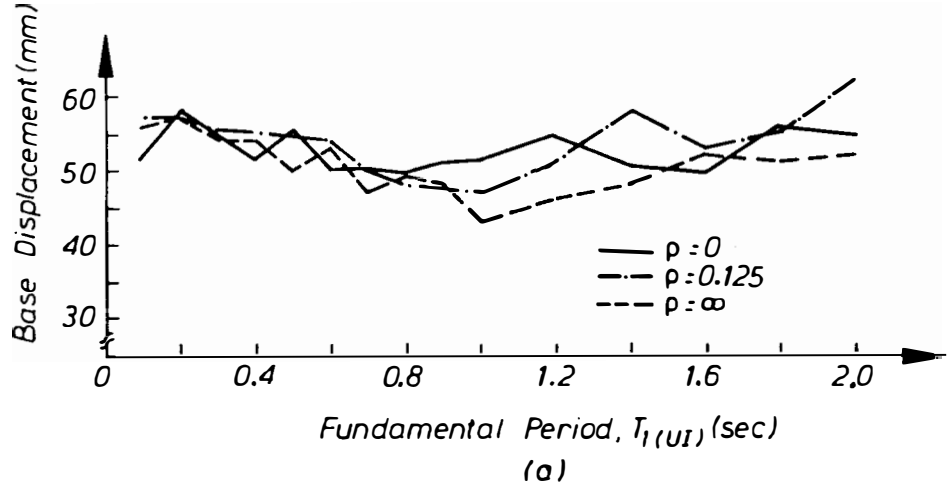

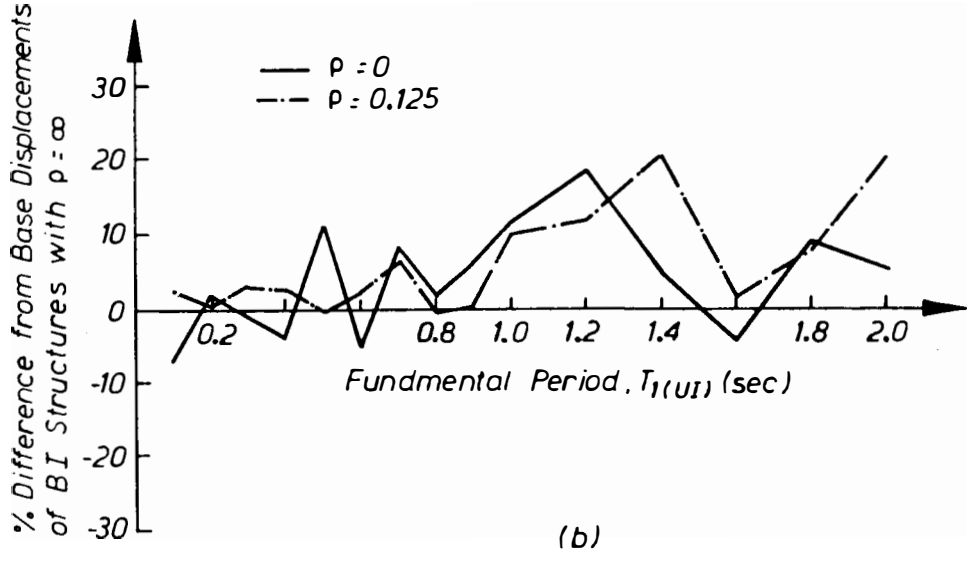

Fig. 4.47 Maximum Base Displacements of BI Structures with Different $T_{1(UI)}$ and ρ

From the response history plots shown in Figs. 4.48.a and 4.48.b of BI structures with $T_{1(UI)}$ = 0.2 and 1.2 seconds respectively, it can be seen that irrespective of the degree of frame action the base displacements are strongly dominated by almost the same effective fundamental mode, though the longer period structure reveals slightly larger differences compared to the shorter period structure.

The base shears of BI structures have similar insignificant differences. As shown in Fig. 4.49.b, for this entire range the base shears of BI structures with ρ = 0.0 and ρ = 0.125 differ less than 17% when compared to the base shear of BI structures which have $\rho = \infty$.

The normalised base shear response history plots are shown in Figs. 4.50.a and 4.50.b for BI structures with $T_{1(UI)}$ of 0.2 and 2.0 seconds respectively. Strong dominance by nearly the same effective first mode is obvious especially for the short period structure.

4.6.3.2 Lateral Storey Shear Envelope

To investigate the effect of frame action on the lateral storey shear envelope, a range of BI structures with $T_{1(UI)}$ of 0.2, 0.4, 0.8, and 1.2 seconds are considered. The structures are mounted on two different types of BI system. The first isolation system has k_0 = 2.5 W/m, αk_0 = 1.25 W/m, and F_y = 5%W. Thus it has a thin hysteresis loop or a small value for the ratio of its hysteresis loop area to the area of its enclosing rectangle, i.e. R ≈ 0.15. The second type of isolation system has a fat hysteresis loop (R ≈ 0.56), with k_0 =10.0 W/m, αk_0 = 0.5 W/m, and F_y = 5%W.

It has been shown in Section 4.5 that a "shear-beam" type multistorey structure with a fat-loop BI system has a more bulged shear envelope than the one mounted on a thin-loop BI system.

It is found in this evaluation that the lateral shear envelope of relatively short period structures on thin-loop BI systems is hardly affected by the degree of frame action. However, where the value of R is large the differences between the lateral shear envelopes become more significant. This phenomenon is shown in Figs. 4.51.a and 4.51.b. for BI structure with $T_{1(UI)}$ = 0.2 and 0.4 seconds, respectively.

For longer period structures with $T_{1(UI)}$ = 0.8 and 1.2 seconds as shown in Figs. 4.51.c and 4.51.d respectively, it is observed that the differences between the lateral shear envelopes due to the frame action are significant regardless the fatness of the BI system's hysteresis loops.

Further explanation in regard to the above phenomenon is presented in the following sub-section of this chapter as well as in Chapter 5.

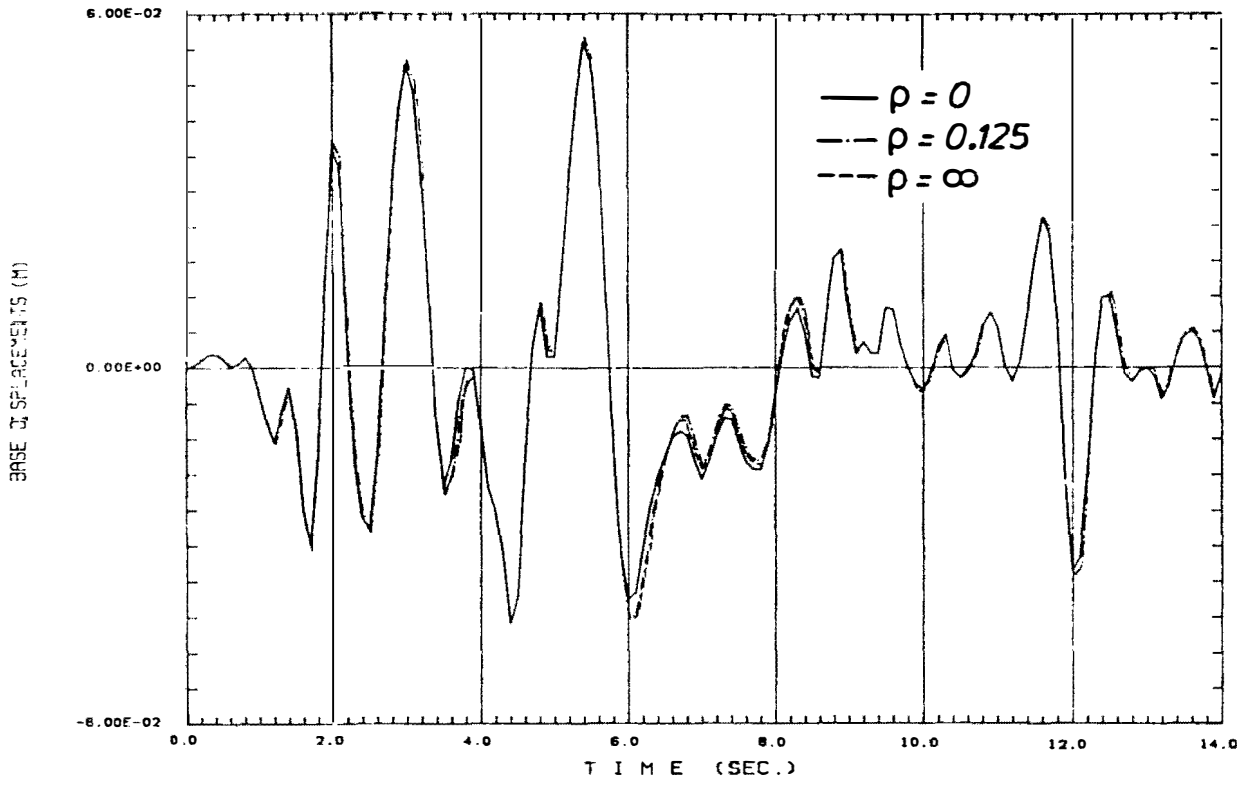

(a) $T_{1(UI)}$ = 0.2 seconds

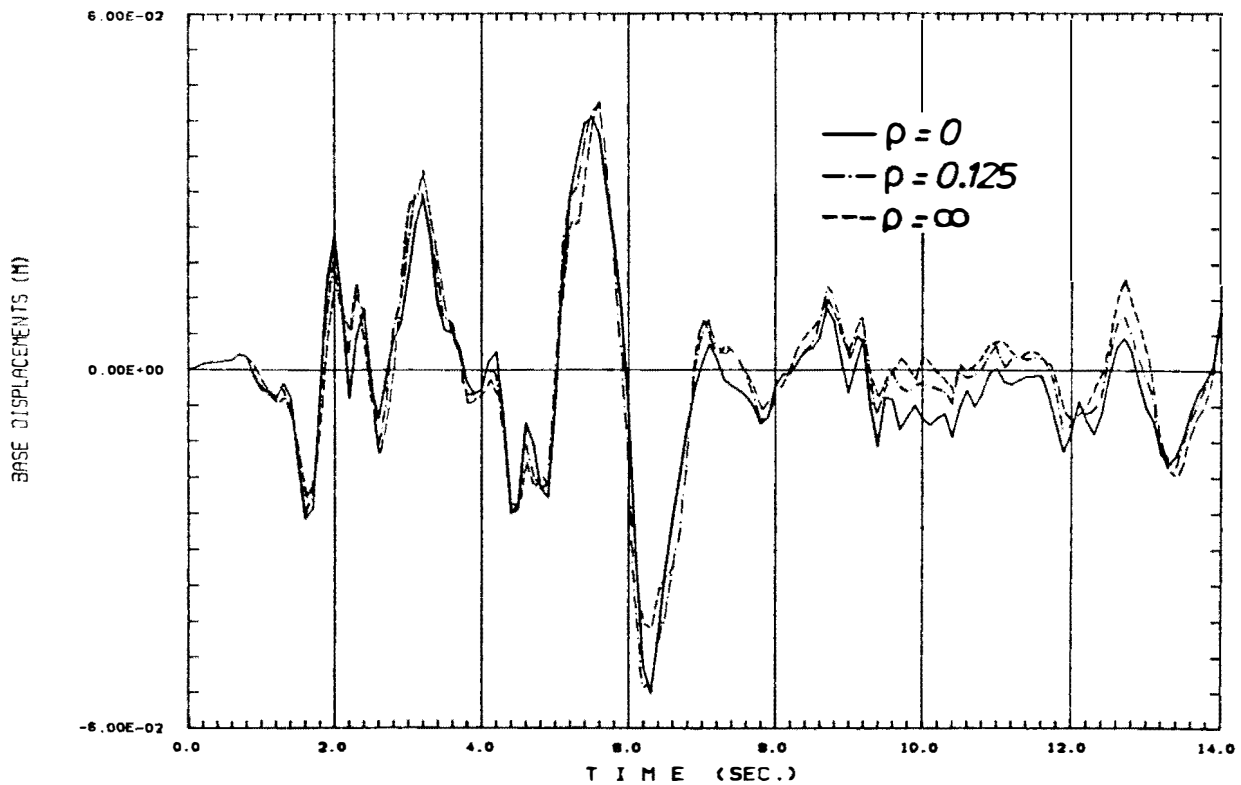

(b) $T_{1(UI)}$ = 1.2 seconds

Fig. 4.48 The Base Displacement History of BI Structures with Different ρ

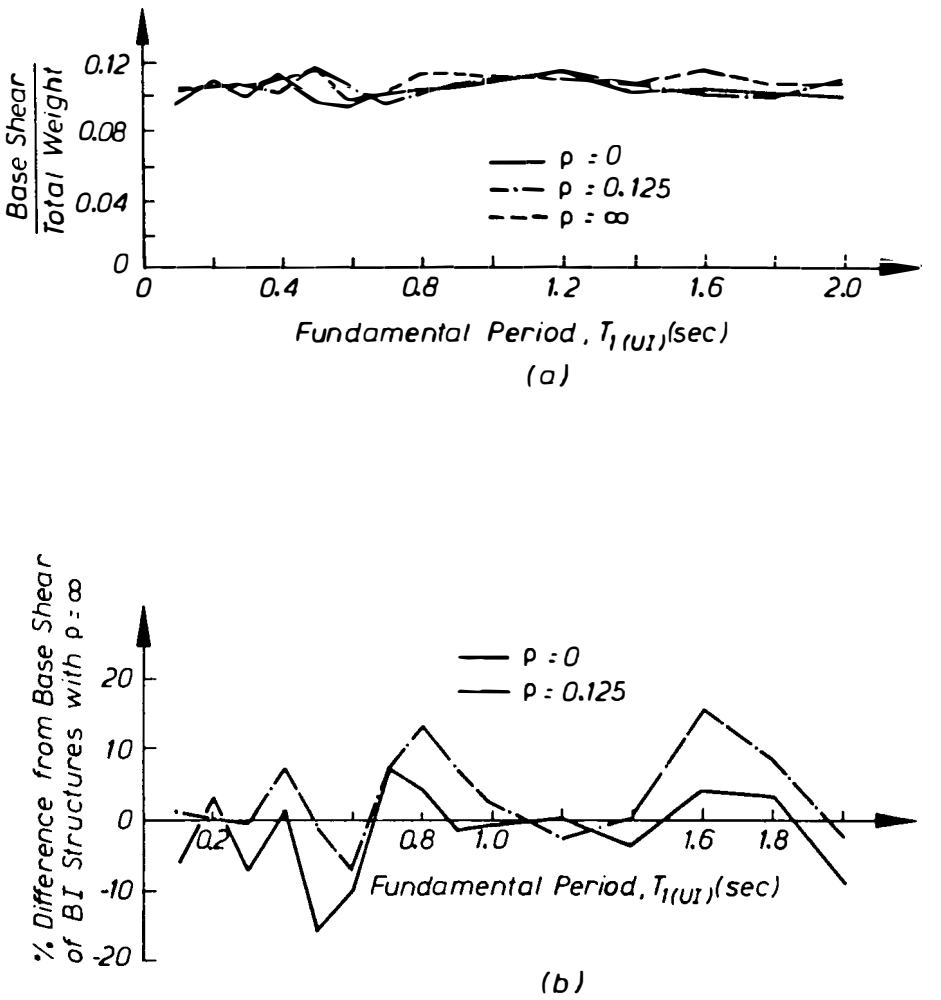

Fig. 4.49 Maximum Base Shears of BI Structures with Different $T_{1(UI)}$ and ρ

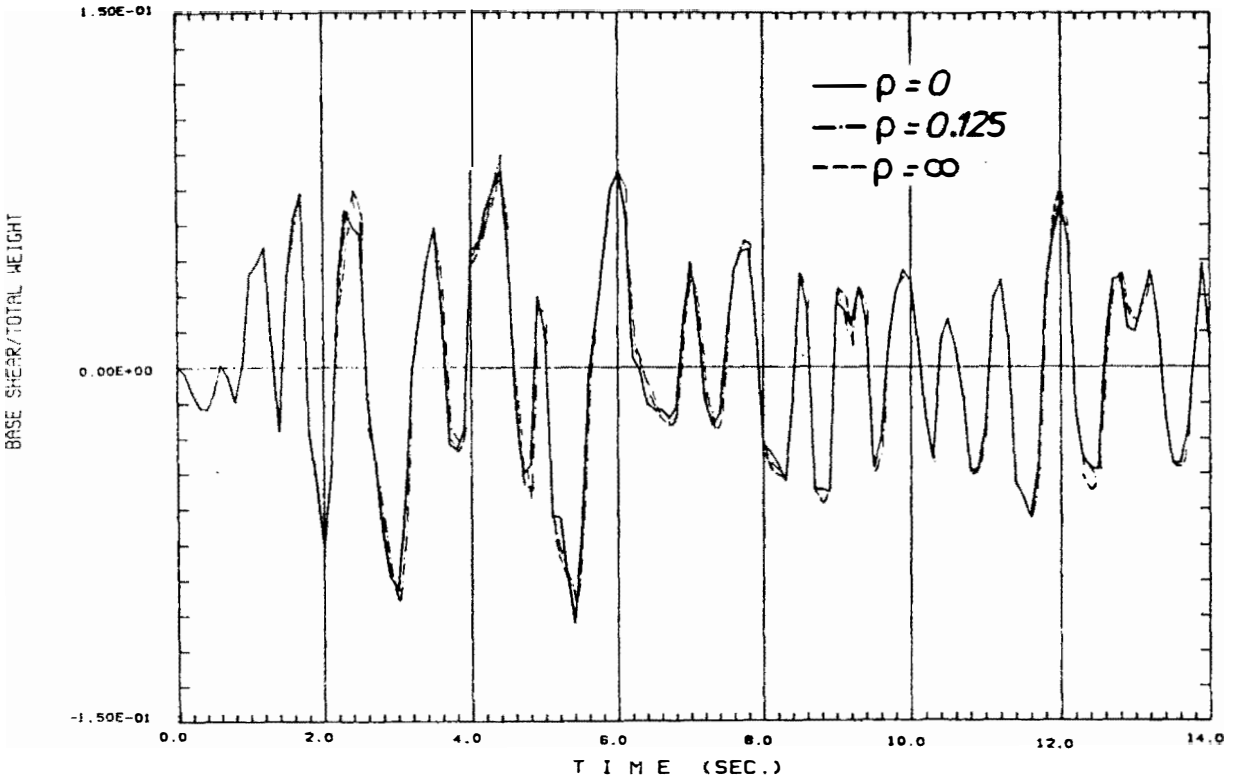

(a) $T_{1(UI)}$ = 0.2 seconds

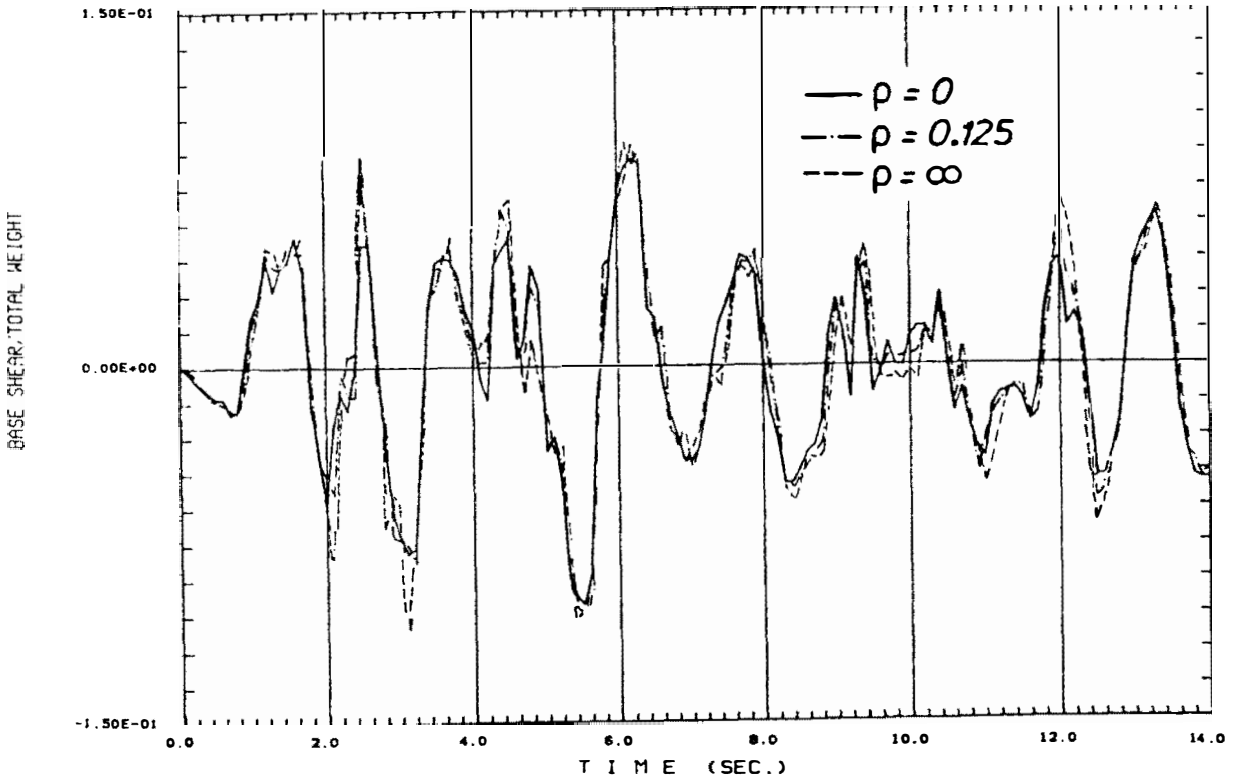

(b) $T_{1(UI)}$ = 1.2 seconds

Fig. 4.50 The Base Shear History of BI Structures with Different ρ

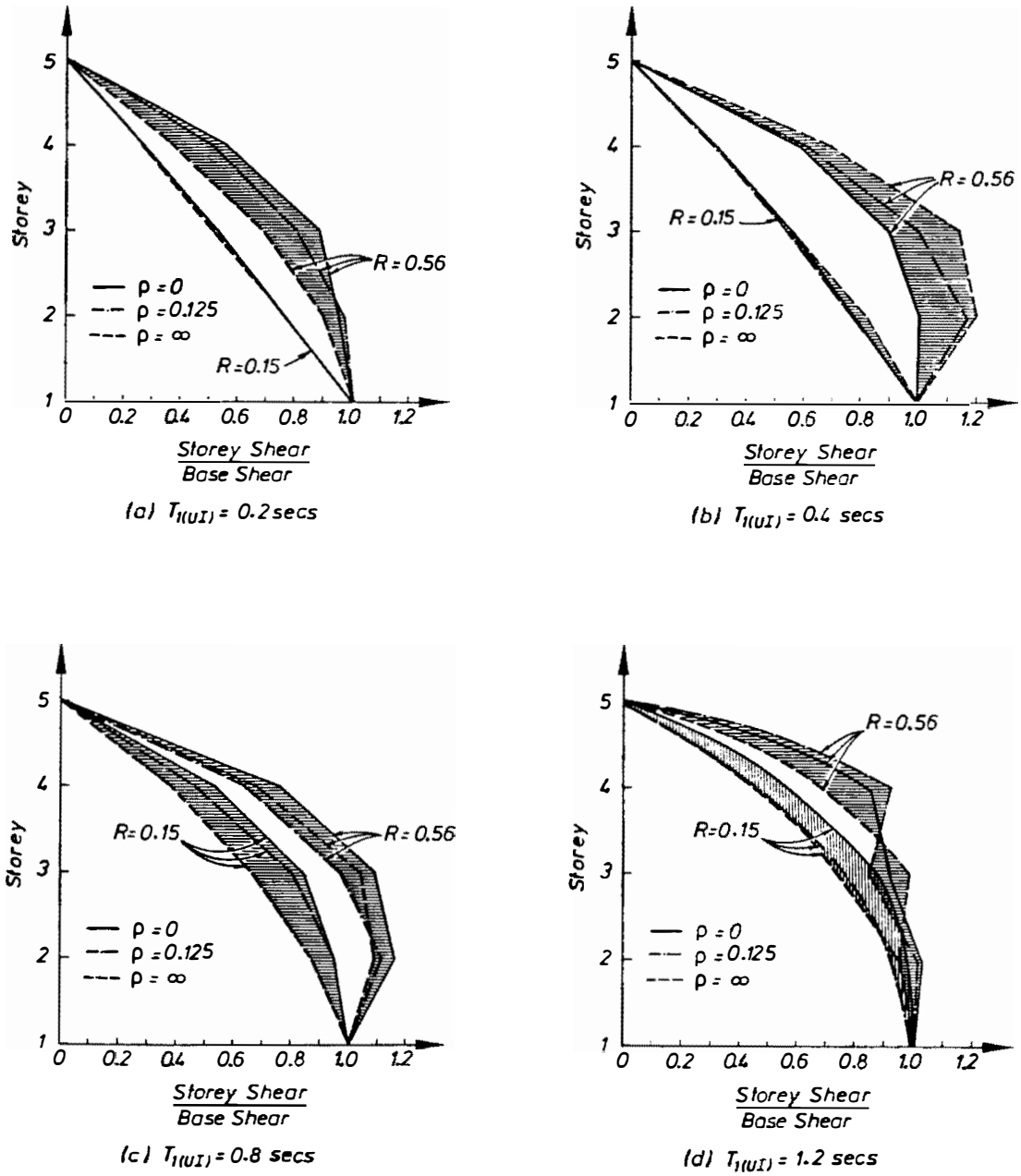

Fig. 4.51 Lateral Storey Shear Envelopes of BI Structures with Different ρ

4.6.4 DISCUSSION OF DESIGN ASPECTS

A. EVALUATION OF THE CODE-TYPE APPROACH

It has been demonstrated in the previous sections that the effective fundamental period, T_{1eff} and the effective first-mode damping, λ_{1eff} are the two key parameters which can be used for predicting the base displacement and the BI system shear force. It is informative to evaluate the effect of superstructure's frame action on these response quantities. Using Eqs. 4.12 to 4.14 the BI system's effective secant stiffness, k_{eff}, hysteresis loop ratio, R, and additional hysteretic damping, E_h, can be estimated. Three different types of BI system with thin, moderate and fat hysteresis loop are considered in this evaluation as Cases A, B, and C respectively.

As can be seen in Table 4.11 neither the effect of $T_{1(UI)}$ nor the effect of the superstructure's beam-to-column stiffness ratio, ρ is significant. This is due to the fact that the base displacements for each case are found almost the same. The approximate method used in estimating the base displacement and the BI system shear force discussed in Sections 4.4 and 4.5, therefore, can be applied irrespective of ρ.

It has been indicated in Section 4.5 that there is a strong correlation between the hysteresis loop ratio, R and the exponent p of the following code-type approach formula used to predict the equivalent static lateral force distribution,

$$F_i = V \frac{W_i \, h_i^p}{\Sigma W_i \, h_i^p} \qquad (4.15)$$

where V is the base shear, W_i and h_i are the weight and height of ith floor, respectively.

In this section the correlations between these two factors for a wider range of BI structures, i.e. with $T_{1(UI)}$ = 0.2, 0.4, 0.8 seconds and ρ = 0.0, 0.125, ∞, are listed in Table 4.12 and plotted in Fig. 4.52. These correlations are based on the linear regression analyses[4.20] of data for the two variables, i.e. R and p. The range of the most likely used BI systems is covered by incorporating isolation systems with R from 0.1 (thin loop) to 0.6 (fat loop). BI structures which have $T_{1(UI)}$ equal to 0.8 secs but with R $\geq$ 0.4 or larger than 0.8 secs are not included since their shear envelopes become difficult to approximate using this approach.

As shown in Table 4.12, the lowest correlation coefficient, r is found to be 0.70 while the average value of r is 0.84. The corresponding conditional standard deviations, $s_{y|x}$ are also listed in Table 4.12. The total samples considered in this observation are 36, 34 and 24 cases for BI structures with $T_{1(UI)}$ = 0.2, 0.4 and 0.8 seconds, respectively. The range of the BI systems' yield strengths is 3.0 to 7.0%W.

Table 4.11 The Effects of $T_{1(UI)}$ and ρ on the BI System's Effective Stiffness and Hysteretic Damping

$T_{1(UI)}$ secs	Case	$\mu = x_{max}/x_y$			k_{eff} of BI sys. (W/m)			Hyst. Loop Ratio R			Add. Damping (% crit)		
		ρ=0.0	ρ=0.125	ρ=∞	ρ=0.0	ρ=0.125	ρ=∞	ρ=0.0	ρ=0.125	ρ=∞	ρ=0.0	ρ=0.125	ρ=∞
0.2	A	3.5	3.8	3.8	1.60	1.57	1.58	0.16	0.15	0.15	10.0	9.7	9.8
	B	11.2	11.4	11.4	2.26	2.24	2.24	0.30	0.30	0.30	19.5	19.3	19.3
	C	11.7	12.6	12.4	1.31	1.26	1.26	0.56	0.55	0.55	36.1	35.2	35.5
0.4	A	3.7	3.8	3.8	1.59	1.58	1.58	0.15	0.15	0.15	9.9	9.75	9.8
	B	10.3	11.1	10.8	2.32	2.27	2.28	0.30	0.29	0.31	20.4	20.6	19.9
	C	11.9	12.6	12.8	1.30	1.25	1.24	0.56	0.55	0.55	35.7	35.3	35.1
0.8	A	3.7	3.8	3.6	1.58	1.58	1.59	0.15	0.15	0.16	9.9	9.8	10.0
	B	9.9	9.7	9.8	2.35	2.38	2.36	0.33	0.33	0.33	20.8	21.0	21.0
	C	11.5	11.2	12.0	1.33	1.35	1.29	0.57	0.57	0.56	36.1	36.4	35.9
1.2	A	4.3	4.1	3.8	1.54	1.55	1.58	0.14	0.15	0.15	9.3	9.4	9.7
	B	11.0	11.0	9.3	2.27	2.27	2.41	0.31	0.31	0.34	19.8	19.6	19.6
	C	11.1	13.3	14.1	1.35	1.21	1.17	0.57	0.54	0.53	36.7	36.0	34.1

Note in Case A : k_o = 2.5 W/m αk_o = 1.25 W/m α = 0.50 F_y = 5%W

B : k_o = 10.0 W/m αk_o = 1.50 W/m α = 0.15 F_y = 5%W

C : k_o = 10.0 W/m αk_o = 0.50 W/m α = 0.05 F_y = 5%W

Table 4.12 Correlations between the Hysteresis Loop Ratio R and the Exponent p

T1(UI) secs	Linear Regression Analysis				
	ρ	A	B	r	$s_{y\|x}$
0.2	0.000	-0.7339	4.7912	0.87	0.39
	0.125	-0.7902	4.6367	0.80	0.50
	∞	-0.4352	2.8246	0.71	0.41
0.4	0.000	-0.5517	6.0054	0.93	0.31
	0.125	-1.0670	8.1152	0.89	0.49
	∞	-0.8483	6.7600	0.85	0.40
0.8	0.000	-0.2475	9.3684	0.91	0.37
	0.125	0.0081	7.1251	0.70	0.62
	∞	-0.4347	8.5817	0.88	0.42

Note: Exponent $p = A + B\,r$

R = Hysteresis Loop Ratio

r = Correlation Coefficient (≈ 1.0 implies a perfectly linear correlation)

$s_{y|x}$ = conditional standard deviation

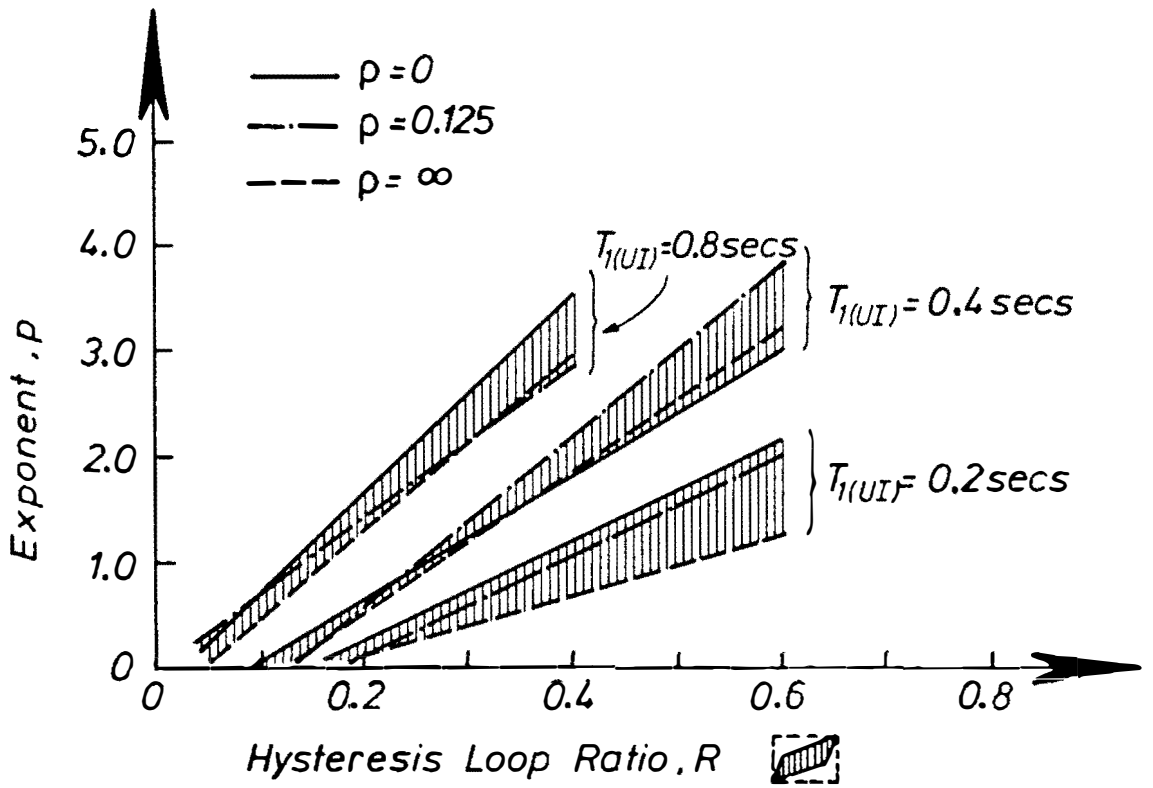

Fig. 4.52 Correlations between the Hysteresis Loop Ratio, R and the Exponent p

Fig. 4.52 shows the values of the exponent p for different ρ diverge as R increases. It is also can be seen that the slope of the correlation lines becomes steeper for BI structures with longer $T_{1(UI)}$.

As the value of exponent p increases, the lateral shear envelope becomes more bulged which indicates that the higher mode contributions to the upper storey shears have become more significant. At $T_{1(UI)}$ = 0.2 and 0.8 seconds, BI structures with ρ = 0.0 tend to have larger p and therefore more bulged shear envelopes than their counterparts with ρ = 0.125 and ρ = ∞. This trend, however is not found for BI structures with $T_{1(UI)}$ = 0.4 secs. Since the modal contributions to the storey shears are also dependent on the likely irregular shape of the earthquake spectra acceleration as well as being affected by the inelastic behaviour of the BI system, the above phenomenon cannot be approximately evaluated using only their initial and pseudo post-yield linear modal properties as discussed in Section 4.6.1.

In spite of this, the strong correlation between R and p is very useful in providing the designer with a"quick" guidance in order to be able to predict the likely equivalent static lateral force distribution for a particular BI structure.

To demonstrate the use of this Code-Type formula, some calculations for BI structures of Cases B and C are carried out. First, the trial-and-error procedure described in Section 4.5 is applied to estimate the effective fundamental period, the effective first-mode damping, the BI system's shear force and the base displacement by utilising the acceleration spectra of El Centro 1940 N-S earthquake. An example of the detailed calculation is given in Chapter 7.

The results are tabulated in Tables 4.13.a and 4.13.b for structures mounted on BI systems with moderate and fat hysteresis loops, respectively. Note that slightly different results for BI structures with ρ = ∞ are found when they are compared to the values obtained previously in Section 4.5 which are based on the time history analysis results rather than using the trial-and-error procedure to determine the base displacement and/or the BI system shear force.

The estimated values for maximum base displacements (expressed in μ) of BI structures with moderately fat hysteresis loops (Case B) are found to be close to the results obtained from the inelastic time history analyses. In Case C, however, more conservative estimated values of maximum base displacements are observed.

Like the base displacements, the maximum shear force of the BI system in Case B are predicted within a small range difference, i.e. -3.6% to +2.6% from the inelastic time history analysis results. For Case C, the BI system's maximum shear force are slightly overestimated but not by more than 15% in the most extreme case.

Using the modification factor shown in Fig. 4.43 the base shear can then be determined. For BI structures of Case B, the modification factor is 1.0 whereas for Case C is 1.2. These factors should be applied to take into account the higher mode effects which normally become dominant for BI

Table 4.13 The Storey Shears of BI Structures with Different ρ Predicted by the Code-Type Approach

(a) CASE B

$T_{1(UI)}$ secs	ρ	μ	k_{eff} (W/m)	T_{1eff} secs	λ_{1eff} (% crit)	R	p	Storey Shear (kN) App.	Storey Shear (kN) THA
								88.8	70.6
								162.9	128.7
	0.0	11.0	2.27	1.34	24.70	0.31	0.75	214.7	176.0
								246.8	216.3
								(246.8)	(252.9)
								32.4	24.4
								59.2	45.2
0.2	0.125	11.0	2.27	1.34	24.7	0.31	0.65	79.5	64.0
								92.5	78.4
								(92.5)	(96.0)
								79.0	61.0
								145.6	116.6
	∞	11.0	2.27	1.34	14.7	0.31	0.44	204.8	165.5
								246.8	211.1
								(246.8)	(255.0)
								215.5	194.1
								367.3	328.7
	0.0	10.8	2.29	1.36	24.9	0.31	1.31	455.4	408.0
								489.7	449.0
								(489.7)	(480.1)
								134.9	109.4
								225.8	186.8
0.4	0.125	10.8	2.29	1.30	24.9	0.31	1.45	275.7	235.4
								293.3	262.0
								(293.3)	(301.0)
								214.5	190.9
								360.8	308.1
	∞	10.8	2.29	1.37	24.9	0.31	1.25	418.6	348.7
								487.6	410.3
								(487.6)	(494.4)
								331.8	298.2
								476.3	440.7
	0.0	10.2	2.33	1.46	25.5	0.32	2.75	529.8	484.1
								535.2	464.2
								(535.2)	(527.0)
								215.6	183.6
								326.2	298.2
0.8	0.125	10.0	2.35	1.48	25.7	0.32	2.29	370.6	371.4
								378.2	358.2
								(378.2)	(368.5)
								539.1	503.9
								813.4	767.3
	∞	10.2	2.32	1.49	25.5	0.32	2.31	926.9	793.3
								945.8	791.8
								(945.8)	(929.1)

(b) CASE C

$T_{1(UI)}$ secs	ρ	μ	k_{eff} (W/m)	T_{1eff} secs	λ_{1eff} (% crit)	R	p	Storey Shear (kN) App.	Storey Shear (kN) THA
								88.2	72.4
								141.2	115.8
	0.0	16.2	1.09	1.93	37.2	0.51	1.71	167.7	125.6
								176.5	131.4
								(176.5)	(153.6)
								31.7	26.0
								51.5	41.8
0.2	0.125	16.1	1.09	1.93	37.3	0.51	1.57	62.8	50.6
								66.1	52.0
								(66.1)	(59.2)
								70.5	58.6
								123.3	99.0
	∞	16.1	1.09	1.93	37.3	0.51	1.00	158.6	130.9
								176.2	145.9
								(176.2)	(157.2)
								247.0	183.0
								368.4	268.3
	0.0	16.0	1.09	1.95	37.4	0.51	2.51	410.2	297.1
								418.6	297.4
								(348.8)	(309.3)
								163.6	115.6
								229.1	190.8
0.4	0.125	15.8	1.10	1.94	37.5	0.51	3.07	249.2	220.4
								251.8	189.0
								(209.8)	(189.7)
								251.2	223.6
								368.4	364.5
	∞	16.0	1.09	1.95	37.4	0.51	2.60	410.2	383.9
								418.6	318.9
								(348.8)	(318.1)
								353.8	282.8
								445.7	403.1
	0.0	15.1	1.13	1.98	38.1	0.52	4.62	459.5	429.4
								459.5	369.9
								(382.9)	(343.4)
								229.1	186.0
								303.3	283.4
0.8	0.125	14.6	1.15	1.99	38.5	0.53	3.77	322.7	329.2
								322.7	295.2
								(268.9)	(241.3)
								588.7	479.7
								766.1	727.3
	∞	15.0	1.13	2.01	38.2	0.52	4.03	806.4	766.9
								806.4	701.3
								(672.0)	(619.3)

Note : ( ) denotes the BI system's shear force
THA = inelastic Time History Analysis

structures with fat loops and cause the maximum shear to occur above the ground floor level of the structure.

The hysteresis loop ratio, R can be calculated using Eq. 4.14 and the corresponding values of exponent p can then be found by utilising the correlations of R and p tabulated in Table 4.12 or plotted in Fig. 4.52. The code-type approach formula (Eq. 4.15) should be used to obtain the equivalent static lateral forces. The lateral storey shears can then be calculated. As shown in Tables 4.13.a and 4.13.b, this approach, in general, predicts the storey shears with a reasonable accuracy when compared to the inelastic time history analysis results.

B. EVALUATION OF KELLY'S METHOD

In this section, the evaluation of Kelly's method as discussed earlier in Sections 4.4.7 and 4.5.6 is extended by considering the effect of superstructure's frame action. Essentially this method is a "modified" response spectrum analysis with a mode-superposition technique. The detailed procedure has been reviewed in Chapter 3 and some of its shortcomings have also been pointed out in Section 4.5.6.

For this purpose, four-storey structures with $T_{1(UI)}$ = 0.2, 0.4, 0.8, and 1.2 seconds mounted on BI systems with moderate (R ≈ 0.31) and fat (R ≈ 0.55) hysteresis loops are considered. The effective fundamental period, T_{1eff} and the effective first-mode damping, λ_{1eff} are determined using the same trial-and-error procedure mentioned earlier. In all cases the first two significant modes are included but for BI structures with $T_{1(UI)}$ = 1.2 seconds the third mode contribution is also taken into account. The Sum of Absolute procedure is applied for the superposition of modal contributions in Case B of BI structures with a short $T_{1(UI)}$, i.e. 0.2 seconds, whereas for the other cases the Square Root of the Sum Squares is used.

As shown in Tables 4.14.a, 4.14.b, 4.14.c the storey displacements and shears of the BI structures in Case B with $T_{1(UI)}$ = 0.2, 0.4 and 0.8 seconds respectively can be predicted reasonably well by Kelly's method irrespective of ρ.

However, as observed earlier this method may underestimate the upper storey shears of the BI structures with fat hysteresis loops. In spite of the conservative prediction for the base displacements and/or the BI system's shear forces, underestimates in the ranges of 10% to more than 30% when compared to the time hysteresis results are found for the storey shears of BI structures in Case C with $T_{1(UI)}$ = 0.2, 0.4, and 0.8 seconds, as shown in Tables 4.14.a, 4.14.b, and 4.14.c, respectively.

It is also worth noting that this method considerably overestimates the storey shears of BI structures with longer $T_{1(UI)}$. Table 4.14.d shows that overestimates of more than 50% when

Table 4.14 Results of Kelly's Method Compared With Results of Time History Analyses for BI Structures with Different $T_{1(UI)}$, ρ, and R

(a) $T_{1(UI)}$ = 0.2 seconds

Case	ρ	Sto-rey	Displacement (mm)				Shear (kN)			
			mode 1	mode2	total	THA	mode 1	mode 2	total	THA
		4	56.9	-0.3	56.9	58.0	51.1	-23.3	74.4	70.6
		3	55.8	-0.1	55.8	57.3	101.1	-32.1	133.2	128.7
	0.000	2	54.8	0.1	54.8	56.6	150.3	-27.9	178.2	176.0
		1	54.0	0.2	54.0	56.1	198.7	-14.8	213.5	216.3
		0	53.6	0.2	53.6	55.9	246.8	1.7	248.5	252.9
		4	56.3	-0.1	56.3	58.5	19.0	-6.2	25.2	24.4
B		3	55.8	-0.1	55.8	58.2	37.7	-9.4	47.1	45.2
	0.125	2	55.0	0.0	55.0	57.2	56.3	-9.1	65.4	64.0
R = 0.31		1	54.1	0.1	54.1	57.3	74.5	-5.2	79.7	78.4
		0	53.5	0.1	53.5	57.0	92.5	0.2	92.7	96.0
		4	56.0	-0.1	56.0	58.3	50.3	-12.9	63.2	61.0
		3	55.8	-0.1	55.8	58.1	100.3	-20.8	121.1	116.6
	∞	2	55.2	0.0	55.2	57.8	149.9	-20.5	170.4	165.5
		1	54.5	0.1	54.5	57.3	198.8	-12.3	211.1	211.1
		0	53.4	0.1	53.4	56.8	246.7	0.8	247.5	255.0
		4	84.5	-0.3	84.5	59.9	36.5	-23.0	43.3*	72.4
		3	82.7	-0.1	82.7	59.5	72.2	-32.1	79.0*	115.8
	0.000	2	81.1	0.1	81.1	59.0	107.2	-27.9	110.8^	125.6
		1	79.9	0.2	79.9	58.7	141.7	-14.7	142.5	131.4
		0	79.4	0.2	79.4	58.6	176.0	1.8	176.0	153.6
		4	83.5	-0.1	83.5	63.8	13.5	-6.2	14.9*	26.0
C		3	82.6	-0.1	82.6	63.6	26.9	-9.4	28.5*	41.8
	0.125	2	81.4	0.0	81.4	63.3	40.1	-8.8	41.1^	50.6
R = 0.55		1	80.0	0.1	80.0	63.0	53.1	-4.9	53.3	52.0
		0	79.1	0.1	79.1	62.8	65.9	0.4	65.9	59.2
		4	83.0	-0.1	83.0	63.1	35.9	-14.2	38.6^	53.6
		3	82.6	-0.1	82.6	63.0	71.6	-22.9	75.2^	99.0
	∞	2	81.8	0.0	81.8	62.8	106.9	-22.6	109.3^	130.9
		1	80.5	0.1	80.5	62.5	141.8	-13.5	142.4	145.9
		0	78.5	0.1	78.9	62.2	175.9	1.0	175.9	157.2

Note : ^ 10 - 30% underestimate
* above 30% underestimate

Table 4.14 (continued)

(b) $T_{1(UI)}$ = 0.4 seconds

Case	ρ	Sto-rey	Displacement (mm)				Shear (kN)			
			mode 1	mode 2	total	THA	mode 1	mode 2	total	THA
		4	62.5	-3.9	62.6	60.9	100.8	-185.3	214.9	194.1
		3	58.6	-1.3	58.7	57.4	211.0	-249.5	326.8	328.7
	0.000	2	55.1	0.9	55.1	54.4	307.1	-207.6	370.6	408.0
		1	52.5	2.4	52.5	52.2	398.5	-91.9	408.9	449.0
		0	51.4	3.0	51.4	51.7	487.9	50.4	490.9	480.1
		4	60.8	-2.1	60.8	60.8	63.6	-76.6	99.5	109.4
B		3	58.9	-1.0	58.9	59.8	125.1	-113.7	169.1	186.8
	0.125	2	56.1	0.3	56.1	58.3	183.8	-102.5	210.4	235.4
R = 0.31		1	52.8	1.5	52.8	56.5	239.0	-49.9	244.1	262.0
		0	50.8	1.9	50.9	55.3	292.1	19.7	292.7	301.0
		4	60.4	-1.3	60.4	59.8	103.6	-95.0	140.6^	190.9
		3	59.4	-0.8	59.4	59.2	205.6	-150.4	254.7^	308.1
	∞	2	57.4	0.1	57.4	58.1	304.2	-142.9	336.1	348.7
		1	54.6	0.9	54.6	56.4	398.0	-76.1	405.2	410.3
		0	50.9	1.4	51.0	54.1	485.4	21.9	485.9	494.4
		4	91.8	-3.9	91.0	61.0	77.7	-185.3	200.9	183.0
		3	86.1	-1.3	86.1	60.5	150.6	-249.1	291.1	268.3
	0.000	2	80.9	0.9	80.9	60.1	219.1	-206.3	301.0	297.1
		1	77.0	2.4	77.0	59.8	284.3	-89.6	298.1	297.4
		0	75.4	3.0	75.4	59.6	348.1	53.6	352.2	309.3
		4	88.8	-2.1	88.8	67.8	45.5	-76.6	89.1^	115.6
C		3	85.9	-1.0	86.0	66.9	89.6	-113.5	144.7^	190.8
	0.125	2	86.8	0.3	81.8	65.4	131.5	-101.9	166.4^	220.4
R = 0.55		1	76.9	1.5	76.9	63.9	171.0	-48.9	177.9	189.0
		0	74.0	1.9	74.0	63.1	208.9	20.8	210.0	189.7
		4	87.7	-1.3	87.7	69.4	74.3	-95.2	120.7*	223.6
		3	86.2	-0.8	86.2	68.7	147.3	-150.3	210.4*	364.5
	∞	2	83.3	0.1	83.3	67.5	217.8	-142.4	260.2*	383.9
		1	79.1	0.9	79.1	65.9	284.8	-75.0	294.5	318.9
		0	73.6	1.3	73.7	64.0	347.1	23.0	347.9	318.1

Note : ^ 10 - 30% underestimate
* above 30% underestimate

Table 4.14 (continued)

(c) $T_{1(UI)}$ = 0.8 seconds

Case	ρ	Sto-rey	Displacement (mm)				Shear (kN)			
			mode 1	mode 2	total	THA	mode 1	mode 2	total	THA
		4	79.3	-19.3	81.6	79.3	134.7	-361.1	385.4	298.2
		3	67.3	-5.0	67.5	68.8	249.0	-454.0	517.8	440.7
	0.000	2	56.5	7.4	56.9	59.4	344.9	-315.7	467.6	484.1
		1	48.3	15.6	50.7	52.5	426.9	-23.4	427.5	464.2
		0	45.0	18.4	48.6	49.7	503.2	321.2	597.0	527.0
		4	77.3	-12.2	78.3	70.0	91.0	-177.5	199.5	183.6
B		3	70.9	-4.6	71.0	65.9	174.4	-244.6	300.4	298.2
	0.125	2	61.4	4.1	61.6	60.2	246.6	-184.8	308.2^	371.4
R = 0.31		1	50.7	10.4	51.7	53.0	306.2	-32.8	308.0^	358.2
		0	44.3	12.3	46.0	48.4	358.2	146.5	387.1	368.5
		4	74.9	-8.8	75.5	65.1	217.7	-375.1	433.7^	503.9
		3	71.7	-4.2	71.8	63.4	426.1	-554.4	699.2	767.3
	∞	2	65.2	2.5	65.2	60.9	615.4	-449.5	762.1	793.3
		1	56.0	7.7	56.5	56.4	778.1	-124.9	788.1	791.8
		0	44.6	8.7	45.5	49.1	907.8	242.7	939.7	929.1
		4	102.3	-18.7	104.0	75.4	94.6	-350.7	363.2	282.8
		3	87.8	-4.7	88.0	69.1	175.8	-438.5	472.8	403.1
	0.000	2	74.7	7.4	75.1	63.5	245.0	-300.7	387.8	429.4
		1	64.9	15.3	66.7	59.3	305.0	-13.5	305.3^	369.9
		0	60.9	18.0	63.6	57.6	361.4	323.6	485.1	343.4
		4	97.9	-12.0	98.6	67.8	63.6	-175.1	186.3	186.0
C		3	90.1	-4.4	90.2	66.9	122.2	-239.5	268.9	283.4
	0.125	2	78.9	4.2	99.0	65.4	173.5	-178.5	248.9^	329.2
R = 0.55		1	66.2	10.3	67.0	63.9	216.5	-29.1	218.5^	295.2
		0	58.8	11.9	60.0	63.1	284.7	144.7	293.0	241.3
		4	94.2	-9.0	94.6	67.5	153.2	-379.6	409.3^	479.7
		3	90.1	-4.2	90.2	67.5	299.9	-558.1	633.5^	727.3
	∞	2	82.3	2.6	82.4	66.5	433.8	-448.2	623.8^	766.9
		1	71.4	7.7	71.8	64.1	550.0	-122.5	563.4^	701.3
		0	58.0	8.4	58.6	59.8	644.3	235.1	685.9	619.3

Note: ^ 10 - 30% underestimate

Table 4.14 (continued)

(d) $T_{1(UI)}$ = 1.2 seconds

Case	ρ	Sto-rey	Displacement (mm)					Shear (kN)				
			mode 1	mode 2	mode 3	total	THA	mode 1	mode 2	mode 3	total	THA
		4	108.0	-47.8	0.2	118.1	132.9	187.2	-687.1	50.8	714.0**	461.5
		3	84.4	-7.2	-0.2	84.7	100.9	333.6	-790.2	-0.1	857.8**	509.5
	0.000	2	63.0	26.7	-0.3	68.4	72.2	443.0	-407.1	-63.1	604.9	638.2
		1	47.0	47.5	0.0	66.8	58.4	524.5	275.3	-53.0	594.7^	669.9
		0	40.6	53.6	0.2	67.2	54.8	594.9	1045.6	7.5	1203.0**	748.3
		4	104.8	-36.0	3.6	110.8	127.1	131.3	-430.5	191.4	489.1	366.8
B		3	92.5	-10.0	-2.7	93.1	108.5	247.3	-549.7	45.0	604.4	413.0
	0.125	2	74.5	18.6	-4.1	76.9	83.9	340.7	-327.5	-177.1	504.7	473.4
R = 0.31		1	54.3	34.0	0.7	64.1	64.4	408.8	79.7	-139.0	439.0^	504.4
		0	42.5	35.4	4.2	55.5	55.2	462.0	503.5	86.2	688.0	563.8
		4	96.5	-25.0	3.2	99.7	106.9	475.8	-1253.2	427.3	1410.0	1188.3
		3	90.1	-9.3	-2.3	90.6	99.3	920.3	-1720.5	124.3	1955.1	1525.3
	∞	2	77.8	11.5	-3.6	78.8	82.5	1304.3	-1142.5	-370.1	1773.0	1898.2
		1	60.7	24.0	1.1	65.3	65.2	1603.6	62.4	-213.2	1618.9	1959.1
		0	39.9	21.0	3.4	45.2	46.4	1800.2	1114.9	254.3	2132.7	1968.3
		4	106.5	-43.4	0.2	115.0	118.1	123.7	-645.4	50.5	659.0**	397.0
		3	84.9	-5.5	-0.2	85.0	95.2	222.2	-727.5	-0.3	760.7**	422.0
	0.000	2	65.2	25.5	-0.3	70.0	75.2	297.8	-348.6	62.8	462.8	481.9
		1	50.5	43.7	0.0	66.8	61.1	356.4	301.8	-52.0	469.9	465.8
		0	44.6	48.6	0.2	66.0	55.6	408.2	1025.1	9.1	1103.4**	451.9
		4	102.4	-36.2	3.4	108.6	116.1	87.4	-433.5	181.8	478.1	365.8
C		3	90.8	-9.0	-2.7	91.3	103.1	164.8	-541.3	37.2	567.1**	337.0
	0.125	2	74.0	20.1	-3.9	76.8	88.6	228.0	-300.3	-171.0	414.0	406.4
R = 0.55		1	55.4	33.3	0.9	64.6	74.6	275.3	98.4	-120.3	316.1^	397.6
		0	44.5	32.4	4.2	55.3	66.4	313.3	486.6	106.0	588.3**	363.1
		4	97.7	-25.1	3.1	100.9	99.5	320.8	-1204.2	453.7	1326.2	1112.8
		3	91.9	-9.0	-2.4	92.0	98.2	621.4	-1636.4	103.2	1753.5	1492.5
	∞	2	79.8	11.8	-3.4	80.7	89.7	883.5	-1070.2	-390.1	1441.6	1551.9
		1	63.5	23.2	1.5	67.6	80.8	1092.1	43.2	-169.0	1106.0^	1632.7
		0	44.1	18.7	3.1	48.0	70.4	1237.0	941.1	285.0	1580.2	1447.4

Note : ** above 50% overestimate
^ 10 - 30% underestimate

compared to the time history analysis results are encountered in Case B and Case C of BI structures with $T_{1(UI)}$ = 1.2 seconds. The overestimates become more significant as ρ decreases.

Fig. 4.53 displays the change of the modal contributions for the storey shears of BI structures in Case C as predicted by Kelly's method. The modal storey shears are normalized to the so-called BI system's "first mode" shear force. The normalized storey shears obtained from the time history analyses are also shown in Fig. 4.53. Based on the "linear" modal properties presented in Section 4.6.1 and the spectral acceleration of El Centro 1940 N-S earthquake as well as the assumptions followed in Kelly's method, it can be understood that in general the second mode contribution shown by this method become more significant as ρ decreases and as $T_{1(UI)}$ increases. The first mode contributions, however, are shown to be almost the same even when they are compared to their counterparts in Case B.

As has been pointed out earlier in Sections 4.4.7 and 4.5.6, this nearly unchanging first mode contribution is the major cause of underestimating the upper storey shears, especially for BI structures with a short $T_{1(UI)}$ and a fat hysteresis loop. As $T_{1(UI)}$ increases the conservatively predicted second mode contribution, due mainly to the adoption of the initial participation factor, becomes much more significant and may compensate for the underpredicted first mode contribution in the upper storey shears. For BI structures with small ρ, the significance of this second mode contribution is much more obvious than for BI structures with larger ρ. However, for BI structures with $T_{1(UI)}$ = 1.2 seconds and small ρ, the conservatively predicted second mode causes a considerable overestimate of the storey shears. The large second mode contribution at the base definitely does not represent the actual behaviour of the BI system which is very strongly governed by the fundamental mode.

It is obvious that a response spectrum analysis with a mode superposition technique such as Kelly's method cannot satisfactorily approximate the behaviour of a wide range of inelastic systems. It seems that the modal properties of the superstructure should be analysed separately from the unimodal behaviour of the isolation system and yet without neglecting the effect of interaction between these two systems as one structure.

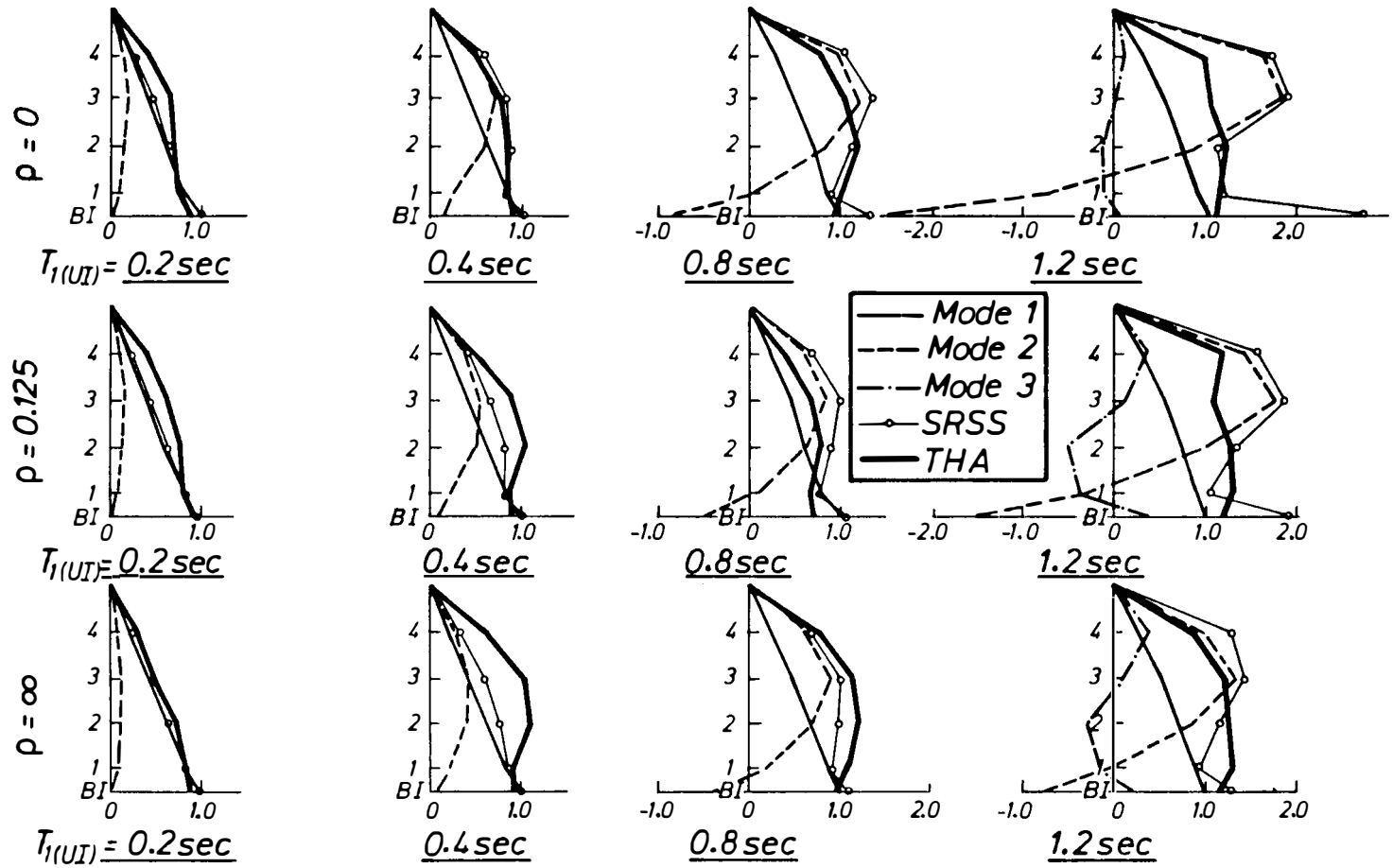

Fig. 4.53 Modal Contributions to the Storey Shears of BI Structures (Case C) Predicted Using Kelly et al's Method

4.7 THE EFFECTS OF BASE MASS, SUPERSTRUCTURE'S VERTICAL IRREGULARITIES, AND NUMBER OF STOREYS.

4.7.1 INTRODUCTION

In the following section, the effects of base mass, superstructure's vertical irregularities and number of storeys on the seismic response of BI multistorey structures under El Centro 1940 N-S are discussed. For the purpose of investigating the first two topics, a series of four-storey "shear-beam" type superstructures with $T_{1(UI)}$ of 0.4 seconds were used as the analytical models. Two other "shear-beam" superstructures, i.e. eight and twelve storey structure with $T_{1(UI)}$ = 0.8 and 1.2 seconds respectively were also incorporated in order to investigate the effect of number of storeys.

All of these structures are mounted on BI systems with thin, moderate, and fat hysteresis loops, as illustrated in Fig. 4.54. These three kinds of BI systems are assumed to represent the whole range of the likely available amplitude dependent isolation devices.

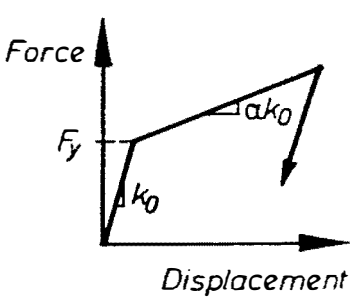

Hysteresis Loops

	k_0	α	F_y
• *Thin*	*2.5W/m*	*0.5*	*5%W*
• *Moderate*	*10.0W/m*	*0.15*	*5%W*
• *Fat*	*10.0W/m*	*0.05*	*5%W*

Fig. 4.54 Idealized Bilinear Hysteresis Loop Parameters of BI systems

4.7.2 BASE MASS

In an unisolated multistorey structure, where its base is assumed to be rigidly attached to the ground, the mass located at the base is not usually considered as part of the structure for normal seismic resistant design purposes. In a BI multistorey structure, however the base mass is attached above the BI system and it can move along with the part of the supertructure. Therefore

the effect of this base mass on the dynamic response of a BI multistorey structure must be taken into account.

It is also informative to note that $T_{1(UI)}$ which is used as one of the important design parameters for BI multistorey structures, is actually based on an equivalent fixed-base condition without incorporating the effect of the base mass. Hence, it is worthwhile to study not only the effect of the base mass on the structure response but also to evaluate the validity of the code-type approach discussed earlier in predicting the equivalent static lateral force distribution up the height of the structure.

For the above purpose, the base mass of the considered BI structure is varied from 0.1 to 0.4 of the total mass of the structure. For a four-storey structure, it means that the base mass of the structure may now differ within the likely range of 50% smaller to 100% larger when compared with the base mass of the uniform structures considered in the previous sections. As shown in Table 2.2 of Chapter 2, the uniform superstructure model has a base mass equal to 0.2 of the total structural mass and is designated as Case 1. The designation of Cases 2, 3, and 4 are for BI structures with base masses of 0.1, 0.3, and 0.4 of the total structural mass, respectively.

Figs. 4.55.a, 4.55..b, and 4.55.c show the effect of vaying the base mass on the storey displacements of BI structures mounted on BI systems with thin, moderate, and fat hysteresis loops respectively. In these all three cases, BI structures with a base weight of 0.1 W have the smallest storey dispacements. It seems that these storey displacements reach their peak values for the uniform structures (W_{base} = 0.2 W). Then as the base weight increases the storey displacements tend to decrease again. However, the differences between these values are insignificant.

The effect of base mass on the lateral storey shear envelopes is shown in Figs. 4.56.a, 4.56.b, and 4.56.c. These storey shears are normalized by their corresponding base shear to emphasize the bulging of the lateral shear envelopes. It can be seen that for BI structures with thin hysteresis loop (small R) the shear envelopes hardly change. However, as R increases the differences between the shear envelopes become more obvious. In Fig. 4.56.c where $R \approx 0.55$, it can be observed that the uniform BI structure (W_{base} = 0.2 W) has the most bulged shear envelope. Further investigation is still required to clarify this phenomenon.

As has been discussed earlier, the Code-Type approach determines the base shear from the BI system's shear force. Therefore, it is also important to note that the margin between the BI system's shear force and its corresponding base shear varies with W_{base}. As more clearly shown in Fig. 4.57, when W_{base} = 0.1 W the base shear of BI structures with thin and moderately fat loops is only slightly smaller than its corresponding BI system's shear force. For BI structures with fat hysteresis loops, the base shear is almost 30% larger than the BI system's shear force. As the ratio between W_{base} and W increases the margin between the base shear and BI system's shear force widens. The largest margin is found for BI structures with thin hysteresis loops.

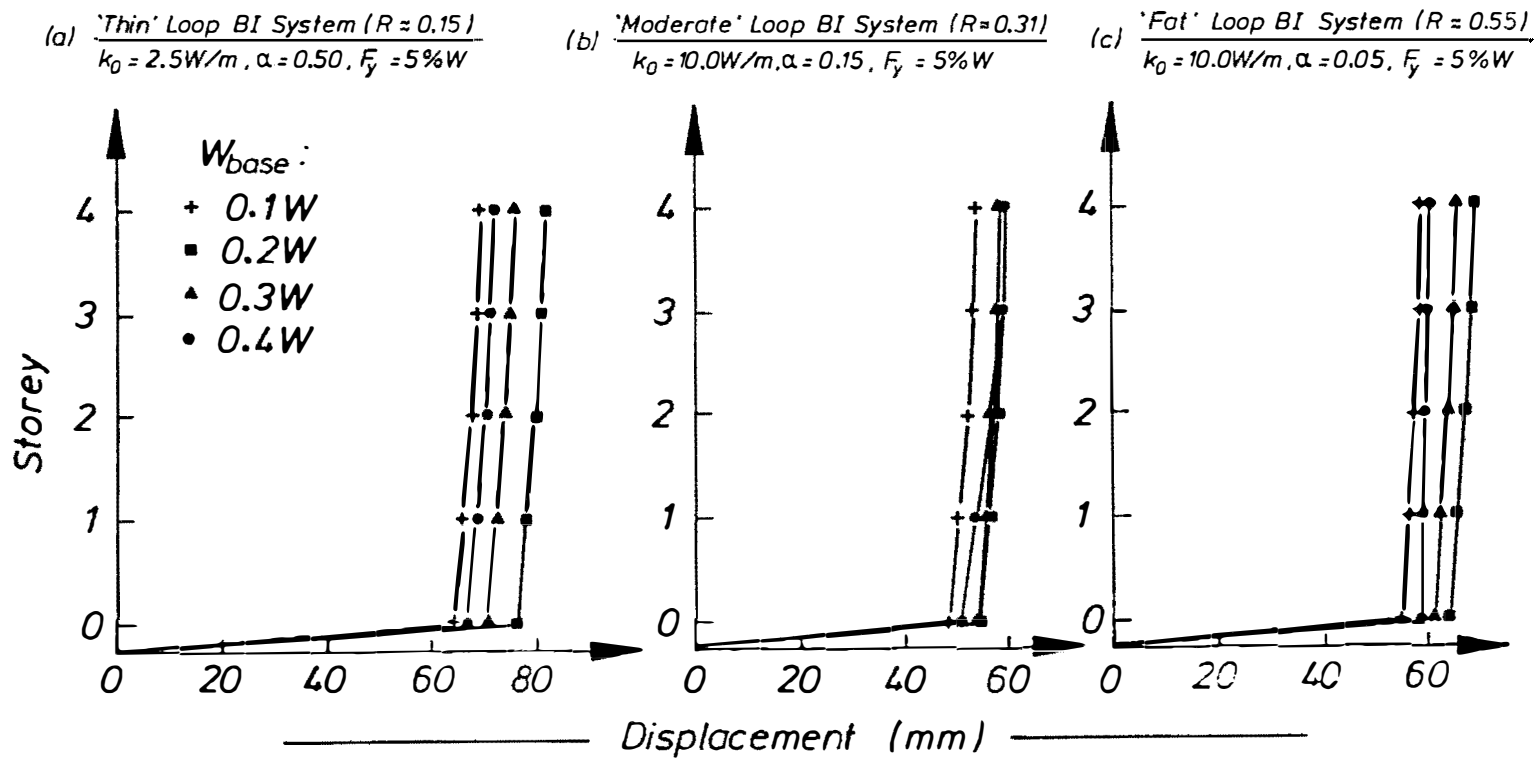

Fig. 4.55 The Effect of Base Mass on the Storey Displacements of BI Structures

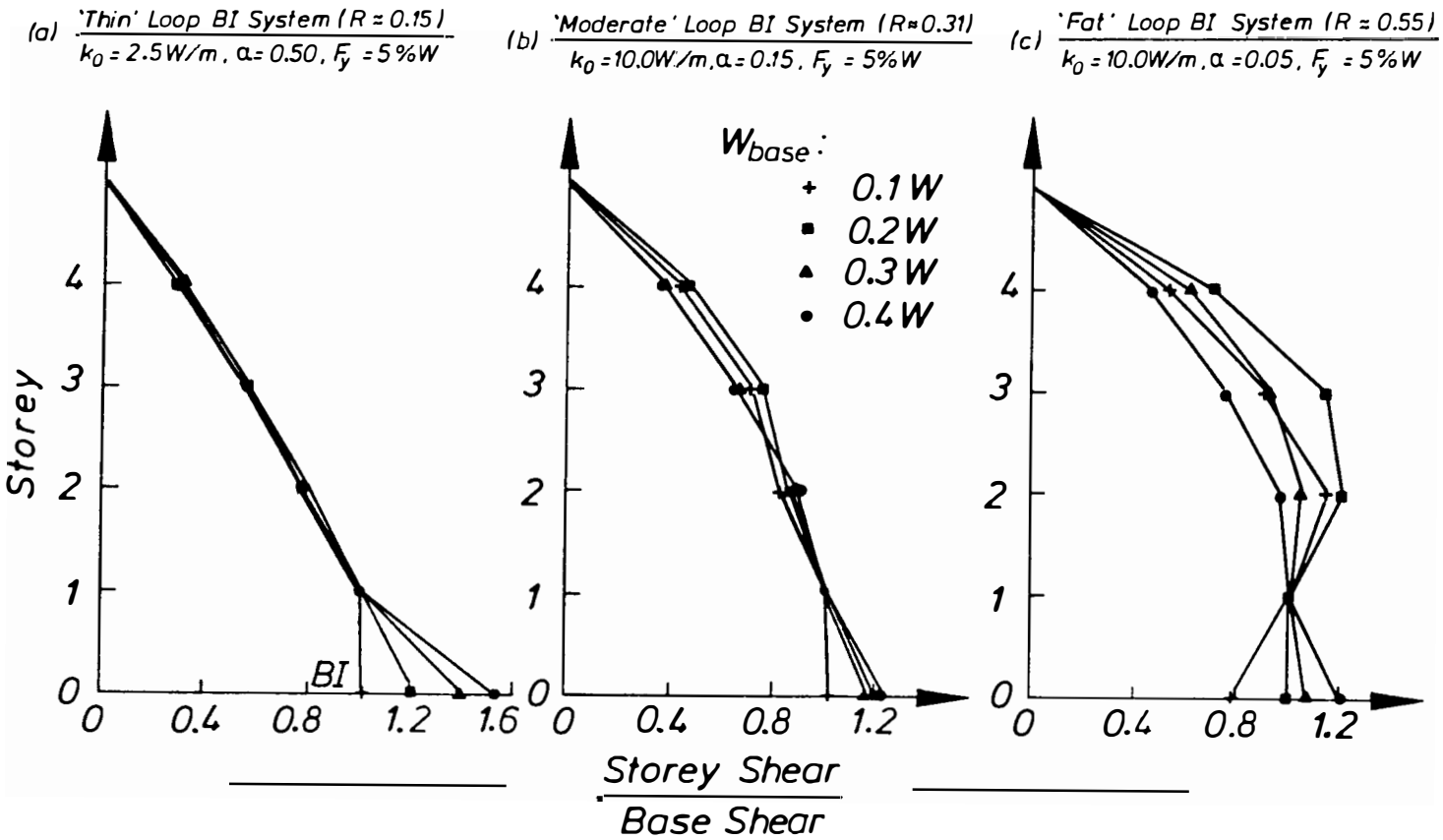

Fig. 4.56 The Effect of Base Mass on the Storey Shears of BI Structures

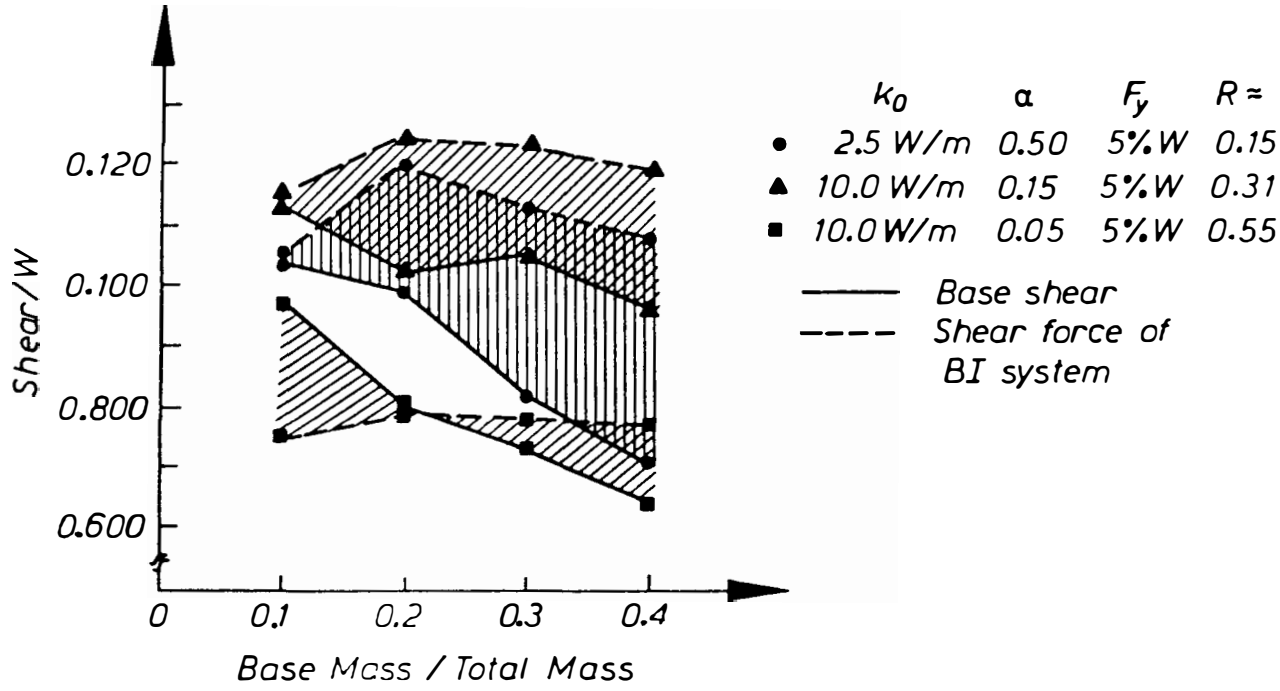

Fig. 4.57 The Effect of Base Mass on the Difference between the Base Shear and the BI System's Shear Force

The application of the Code-Type approach to predict the shear envelopes of BI structures with moderately fat hysteresis loop and W_{base} = 0.1, 0.2, 0.3 and 0.4 W is demonstrated in Table 4.15. The approximate results are still found to be reasonably in a good agreement with the time history analysis results, even for BI structures with W_{base} = 0.4 W. More investigation in this area, however is required in order to be able to propose the likely magnification or reduction factor used for estimating the base shear from the BI system's shear force and to evaluate further the limitations of this Code-Type approach.

4.7.3 SUPERSTRUCTURE'S VERTICAL IRREGULARITIES

A limited study was carried out to compare the seismic performance of BI structures with different vertical configuration of their superstructures as shown in Fig. 4.58. As has been described in Table 2.2 of Chapter 2, these four types of BI structures are designated as Cases 1, 5, 6 and 7. The structures are mounted on three types of BI system which have thin, moderate and fat hysteresis loops. Their storey displacements and storey shears are displayed in Fig. 4.59.

It can be seen that the storey displacements of BI structures in Cases 6 and 7 are less than the storey displacements found in Cases 1 and 5. The effect of varying the storey stiffness seems not so significant compared to the effect of varying the floor mass.

A Similar response is also found in the storey shears. The storey shear envelope of BI structures in Cases 6 and 7 are less bulged than the storey shear envelopes of BI structures in the other two cases, especially when they are mounted on a BI system with fat hysteresis loops. The differences found among the BI system's shear forces and the base shears are not so large when compared to the differences found in the storey shears above the base level.

The applicability of the code-type approach in predicting the storey shear envelope is also investigated. As shown in Table 4.16, the approximate values for the storey shears of the non-uniform BI structures (Cases 5, 6, and 7) mounted on BI systems with moderate and fat hysteresis loops are compared to the results obtained from the time history analyses. The code-type approach can predict satisfactorily the storey shears of BI structures in Cases 1 and 5. However, the approach significantly overestimates the storey shears of BI structures in Cases 6 and 7 although it can satisfactorily estimate the BI system shear forces.

Loadings Codes[4.11,4.12,4.24] normally specify the conditions in which the equivalent static lateral force method can be used for estimating the storey shears of unisolated multistorey structures. Shape and mass regularity and limited differences in lateral resistance or stiffness between storeys are usually found among the above conditions. For BI multistorey structures, however, further investigation is required in order to be able to specify when this code-type approach is still reliable and when the more rigorous dynamic analysis should be used.

Table 4.15 The Storey Shears of BI Structures with Different Base Masses

W_b/W	μ	k_{eff} (W/m)	T_{1eff} secs	λ_{1eff} (% crit)	R	p	Storey Shear (kN) App.	Storey Shear (kN) THA
0.1	10.5	2.31	1.37	25.0	0.32	1.31	190.7 325.0 403.1 433.4[1] (433.4)	172.1 279.9 329.0 368.8 (373.1)
0.2	10.8	2.29	1.37	24.9	0.31	1.25	214.5 360.8 418.6 487.6[1] (487.6)	190.9 308.1 348.7 410.3 (494.4)
0.3	10.5	2.31	1.36	25.0	0.32	1.31	221.2 337.0 467.5 502.7[2] (558.6)	177.5 311.6 420.8 479.8 (564.6)
0.4	10.5	2.31	1.35	25.0	0.32	1.31	229.8 391.6 485.6 522.2[3] (652.8)	187.5 335.5 446.5 515.1 (635.9)

Note : 1) 1.0× the BI system's shear force
2) 0.9 x "
3) 0.8 x "
( ) denotes the BI system's shear force

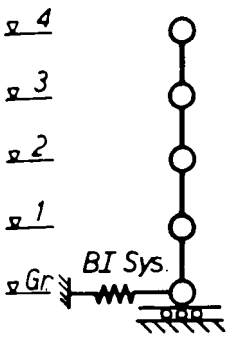

CASE 1 Uniform	CASE 5 Uniform Mass Varied Stiffness	CASE 6 Varied Mass Uniform Stiffness	CASE 7 Varied Mass Varied Stiffness
m	m	0.50m	0.5m
I	0.75I	I	0.75I
m	m	0.75m	0.75m
I	1.00I	I	1.00I
m	m	1.00m	1.00m
I	1.25I	I	1.25I
m	m	1.25m	1.25m
I	1.50I	I	1.50I
m	m	1.50m	1.50m

Note : $T_{1(UI)}$ = 0.4 secs
m = floor mass
I = moment of inertia
The Young's modulus and the storey heights are the same for all cases.
(see also Table 2.2 of Chapter 2)

Fig. 4.58 Mass and Stiffness Configurations of the Considered BI Structures

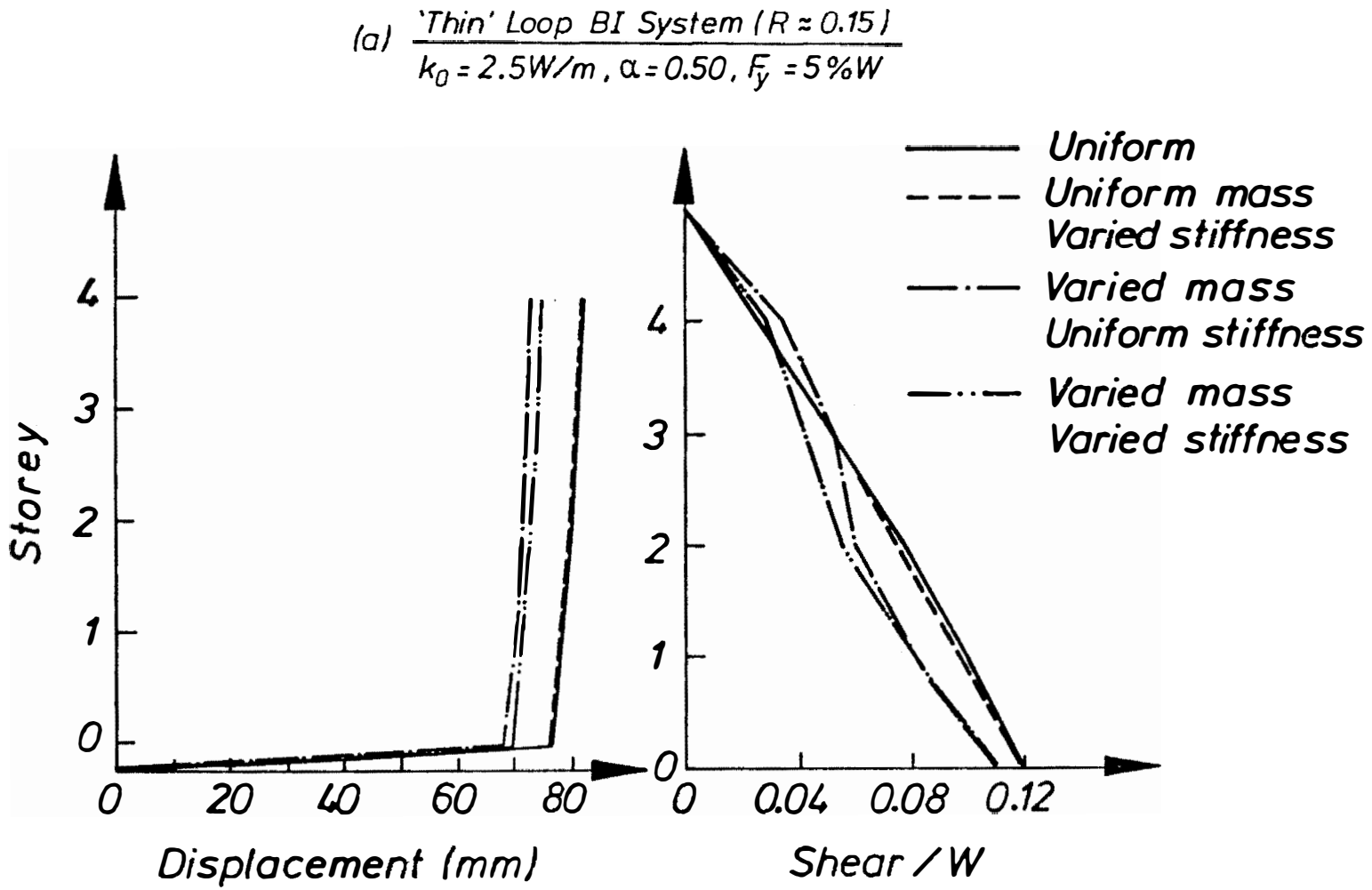

Fig. 4.59 The Effect of Superstructure Vertical Irregularities on the Storey Displacements and the Storey Shears

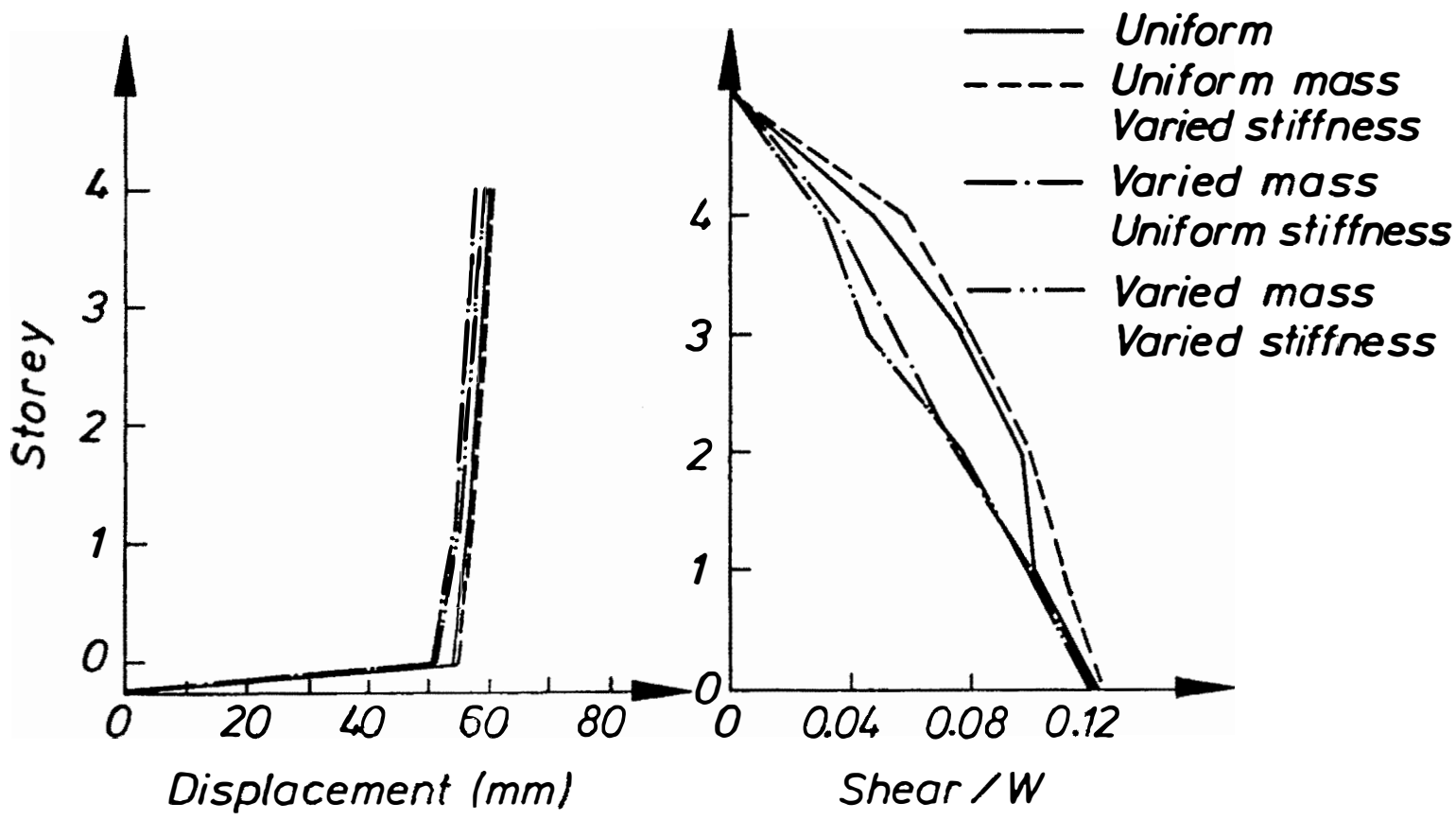

Fig. 4.59 ... (continued)

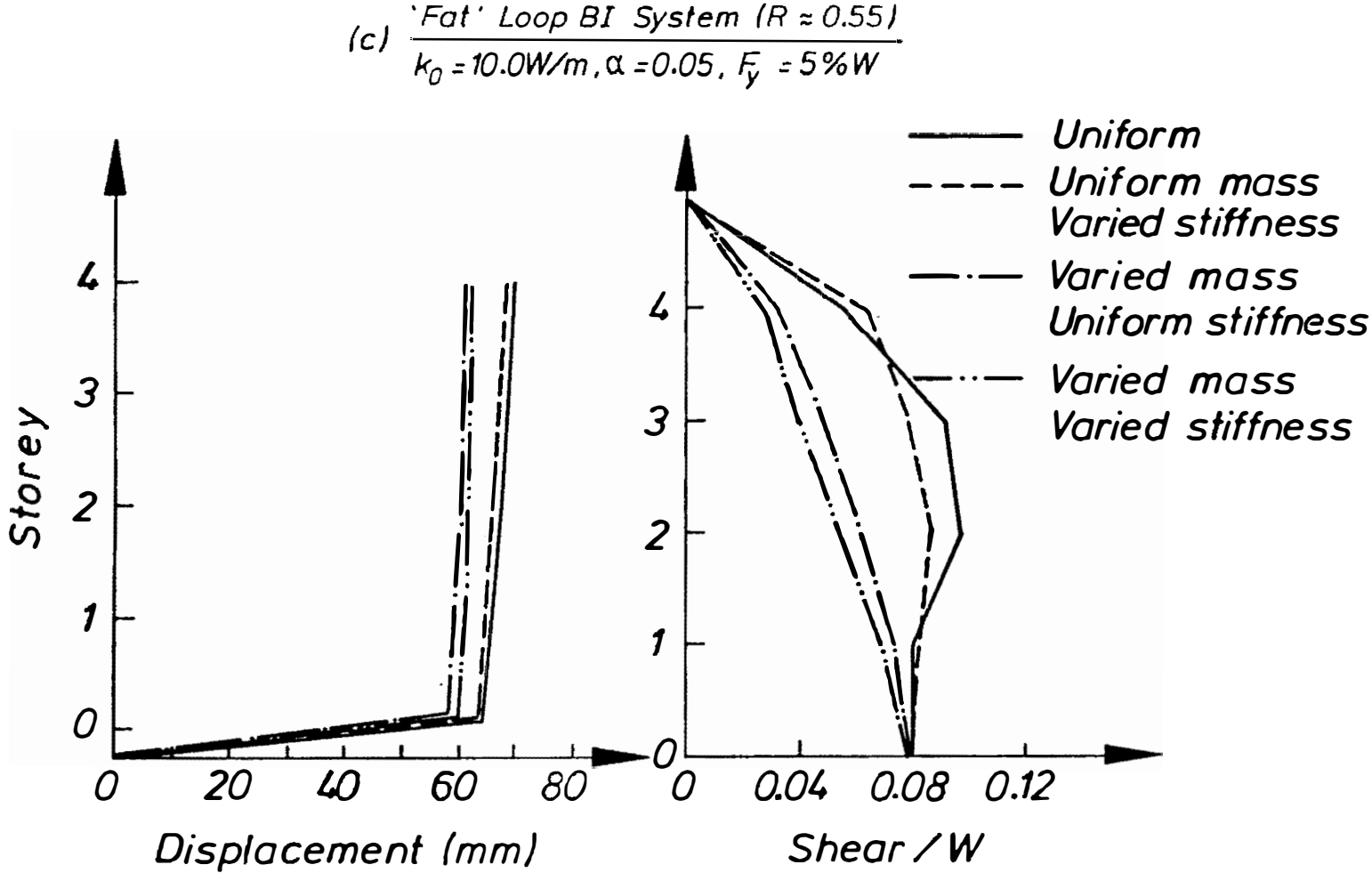

Fig. 4.59 ... (continued)

Table 4.16 The Storey Shears of BI Structures with Superstructure's Vertical Irregularities

(a) BI System : $k_o = 10.0\,W/m$ $\alpha = 0.15$ $F_y = 5\%W$

Super-structure	μ	k_{eff} (W/m)	T_{1eff} secs	λ_{1eff} (% crit)	R	p	Storey Shear (kN) App.	THA
Uniform CASE 1	10.8	2.29	1.37	24.9	0.31	1.25	214.5 360.8 418.6 487.6 (487.6)	190.9 308.1 348.7 410.3 (494.4)
Uniform Mass and Varied Stiff. CASE 5	10.5	2.31	1.36	25.0	0.32	1.31	268.8 458.2 568.2 611.0 (611.0)	291.5 384.8 514.3 559.4 (624.4)
Varied Mass and Uniform Stiffness CASE 6	10.6	2.30	1.36	25.0	0.32	1.31	207.3 420.6 587.8 672.1 (672.1)	203.6 295.7 413.9 582.3 (658.5)
Varied Mass and Varied Stiff. CASE 7	10.5	2.31	1.36	25.0	0.32	1.31	271.3 550.5 769.4 879.8 (879.8)	224.3 333.5 555.6 749.0 (863.6)

Note : Eq. 4.15 and charts in Figs. 4.42 and 4.43 are used to calculate the storey shears based on the Code-Type Approach.

Table 4.16 (continued)

(b) BI System : $k_o = 10.0\,W/m$ $\alpha = 0.05$ $F_y = 5\%W$

Super-structure	μ	k_{eff} (W/m)	T_{1eff} secs	λ_{1eff} (% crit)	R	p	Storey Shear (kN) App.	THA
Uniform CASE 1	16.0	1.09	1.95	37.4	0.51	2.60	251.2 368.4 410.2 418.6 (348.8)	223.6 364.5 383.9 318.9 (318.1)
Uniform Mass and Varied Stiff. CASE 5	16.0	1.09	1.95	37.4	0.51	2.60	313.9 460.4 512.7 523.2 (436.0)	315.7 390.3 429.3 409.4 (395.8)
Varied Mass and Uniform Stiffness CASE 6	16.0	1.09	1.95	37.4	0.51	2.60	274.8 469.9 560.6 579.2 (672.1)	179.1 262.9 336.8 396.7 (658.5)
Varied Mass and Varied Stiff. CASE 7	16.0	1.09	1.95	37.4	0.51	2.60	359.0 613.9 732.3 756.3 (630.7)	193.0 284.2 389.6 487.1 (556.4)

Note : Eq. 4.15 and charts in Figs. 4.42 and 4.43 are used to calculate the storey shears based on the Code-Type Approach.

4.7.4 NUMBER OF STOREYS

In the previous sections the seismic responses of a range of BI structures with different $T_{1(UI)}$ have been discussed. However, four-storey superstructure models were used in all of the analyses reported earlier and it is important to investigate the effect of number of storeys on the seismic performance of these structures. For this purpose, the maximum seismic responses of eight and twelve storey BI structures with $T_{1(UI)}$ of 0.8 and 1.2 seconds are compared with the maximum responses of their four-storey counterparts.

As can be seen in Fig. 4.60.a, the storey displacements of eight and four-storey structures on BI systems with moderate and fat hysteresis loops differ much less than when the structures are mounted on a BI system with thin hysteresis loops. The differences, however, are still insignificant from a design point of view. Similar results are also found when the storey displacements of the twelve storey structure and its four-storey counterpart are compared, as shown in Fig. 4.61.a.

The storey shear envelopes of the eight and four-storey BI structures are displayed in Fig. 4.60.b. These storey shears are normalized to their corresponding base shears. The normalized shears of the four-storey structures on BI systems with thin and moderately fat hysteresis loops are larger than the normalized shears of the eight-storey structures, especially at the upper levels. Similar trends are also found in comparing the shear envelopes of the twelve-storey structure and its four-storey counterpart, as shown in Fig. 4.61.b. This phenomenon will be discussed further in Chapter 5.

In Table 4.17 the use of the code-type approach to predict the storey shears of the eight-storey structure on a BI system with moderately fat hysteresis loops ($R \approx 0.32$) is demonstrated. In general the approximate storey shears are only slightly more conservative when compared with the results obtained from the time history analysis. The maximum overestimate is only found around 20% for the first few storey shears above the base level. This shows that up to this limit the code-type approach is still reliable. It should be noted, that for some reasons mentioned in Section 4.6.4 the use of this Code-Type approach is not recommended for structures with $T_{1(UI)} >$ 0.8 seconds.

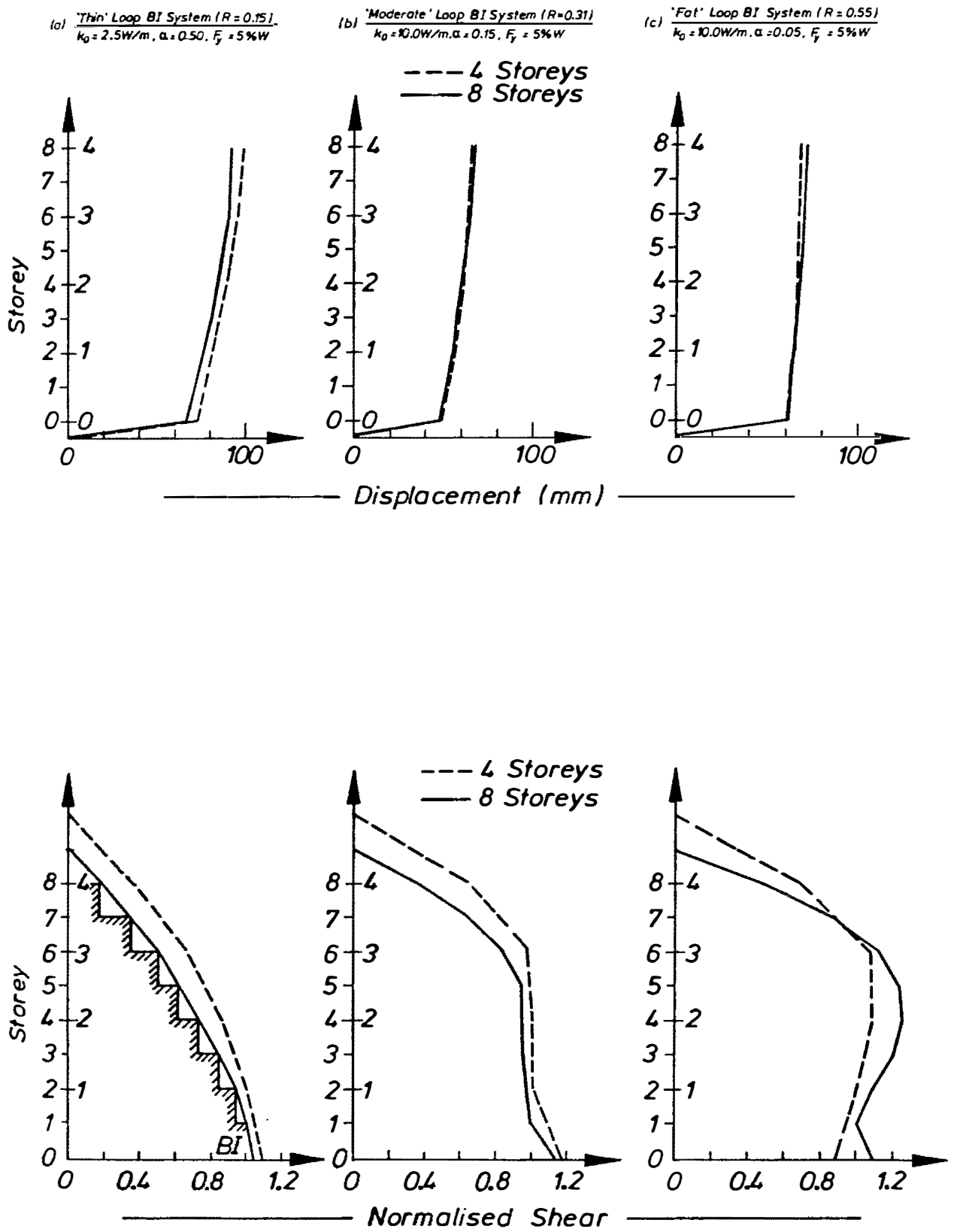

Fig. 4.60 The Effect of the Number of Storeys on the Storey Displacements and the Storey Shears of BI Structures with $T_{1(UI)}$ = 0.8 secs

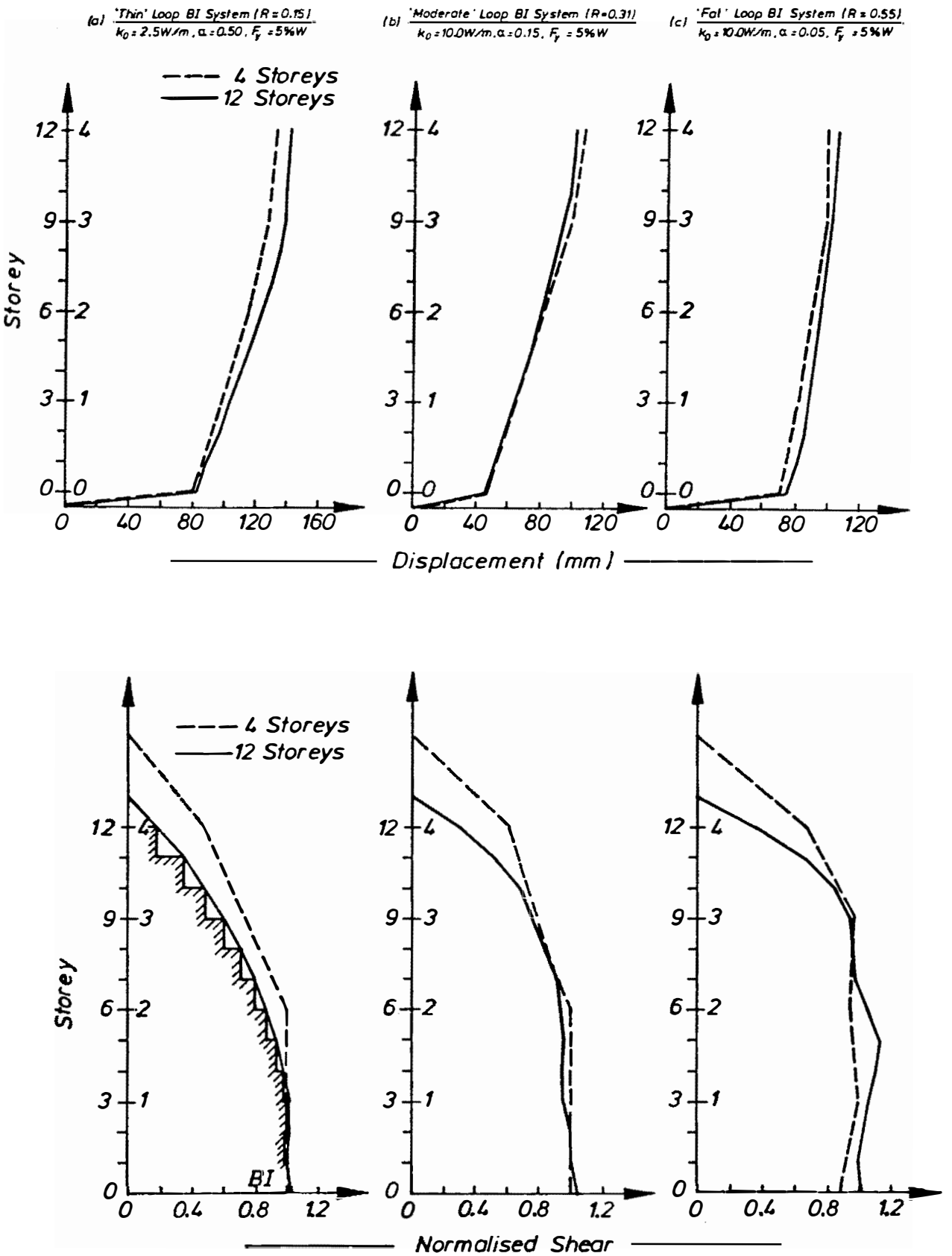

Fig. 4.61 The Effect of the Number of Storeys on the Storey Displacements and the Storey Shears of BI Structures with $T_{1(UI)}$ = 1.2 secs

Table 4.17 The Storey Shears of Eight-Storey BI Structure

μ	k_{eff} (W/m)	T_{1eff} secs	λ_{1eff} (% crit)	R	p	Storey Shear (kN)	
						App.	THA
10.0	2.35	1.49	25.7	0.32	2.31	325.0 563.9 726.4 841.1 908.0 936.7 955.8 (955.8)	284.6 517.1 682.2 764.9 769.3 771.2 788.1 (816.2)

THA = Inelastic time history analysis

4.8 THE EFFECT OF THE HYSTERESIS LOOP MODEL

As discussed earlier in Chapter 2, a bilinear hysteresis loop model is normally adopted to represent the actual cyclic load displacement relationship of the various BI systems. The properties of these BI systems are usually listed in tables or expressed in a mathematical relationship based on their idealized bilinear hysteresis loop parameters[4.25,4.26]. The use of this simple idealization enables the effect of the hysteresic behaviour of BI system on the structure response to be explained as presented in the previous sections. Furthermore, this model is very suitable for use in design. Based on its simple geometrical shape, the effective stiffness and the additional hysteretic damping can be estimated easily from the required maximum base displacement.

For several BI systems, however, the true cyclic load-displacement relationship seems more accurately represented by the Ramberg-Osgood model[4.27], which has a much more complex load-displacement relationship (Fig. 4.62) than the simpler bilinear hysteresis loop model.

The initial loading curve of the model as modified by Jennings[4.28] is expressed by

$$D = \frac{F}{k_o} \left(1 + \eta \left| \frac{F}{F_y} \right|^{r-1} \right) \tag{4.23}$$

in which r is the exponent of the Ramberg-Osgood model and η is a parameter introduced by Jennings. The unloading, load reversal and reloading path follows the relationship given by

$$D - D_0 = \frac{F - F_0}{k_0} \left(1 + \eta \left| \frac{F - F_0}{2F_y} \right|^{r-1} \right) \tag{4.24}$$

As demonstrated in Fig. 4.63 the shape of the primary curve can be controlled by the exponent from linearly elastic (r =1.0) to elasto-plastic (r = ∞). The hysteretic energy dissipation capacity of this model is expressed as[4. 29]

$$E_h = \frac{2}{\pi} \left(1 - \frac{2\eta}{r+1} \right) \left(1 - \frac{k_{eff}}{k_o} \right) \tag{4.18}$$

It is worth comparing the effect of using the Ramberg-Osgood model, against the simple bilinear model, on the response of BI multistorey structure. For this purpose, two types of Ramberg-Osgood model were selected. The first model has a thin loop (r = 2.0), whereas the second one has a fat hysteresis loop (r = 8.0). In both models, the parameter η is set to 1.0. The initial stiffness and the yield strength were determined as 10.0 W/m and 3%W, respectively. Under El Centro 1940 N-S, two inelastic time history analyses were then carried out using these two Ramberg-

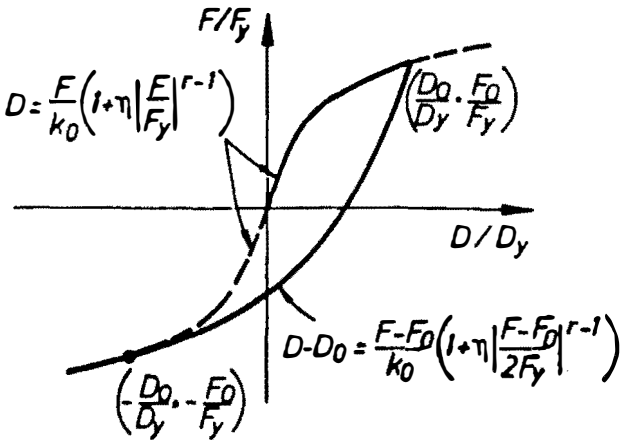

Fig. 4.62 Hysteretic Relation of the Ramberg-Osgood Model

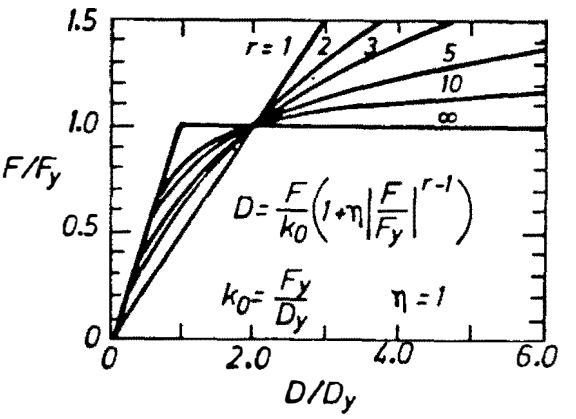

Fig. 4.63 Ramberg-Osgood Function

Table 4.18 Parameters of the Ramberg-Osgood and the Bilinear Hysteresis Loop Model

Case	Hysteresis Loop Model	k_0 (W/m)	F_y/W (%)	r	α	k_{eff} (W/m)	E_h (% cr.)	R
1	R - O	10.0	3.00	2.0	-	2.00	11.7	0.18
	Bilinear	4.6	5.00	-	0.35	2.14	12.8	0.20
2	R - O	10.0	3.00	8.0	-	0.64	46.4	0.73
	Bilinear	9.75	3.75	-	0.012	0.70	47.9	0.75

Osgood idealized hysteresis loop models. A four-storey "shear-beam" superstructure model was considered in this evaluation.

The calculated effective stiffness and the additional hysteretic damping were found as tabulated in Table 4.18. Based on these two essential parameters and the shape of the hysteresis loops, the corresponding bilinear models were then developed. The inelastic time history analyses were repeated using the bilinear idealized models with the parameters as shown in Table 4.18.

As revealed in Figs. 4.64 and 4.65, the base displacement and the base shear history plots of both cases show that the difference between the responses due to the use of the simple bilinear and the Ramberg-Osgood model is insignificant. In general the bilinear model tends to give a slightly larger maximum response when compared to the Ramberg-Osgood model, except for the base displacement in Case 2. The maximum displacement obtained using the bilinear model in Case 2 is 3.7% less than the one predicted based on the Ramberg Osgood model. For both cases, the bilinear model seems always to give larger estimates for the lateral shear envelopes as demonstrated in Fig. 4.66.

This limited investigation shows that the approximate methods based on the simple bilinear hysteresis models can be applied to give conservative estimates for practical BI systems which exhibit load-displacement relationship closer to the Ramberg-Osgood model.

4.9 SUMMARY AND CONCLUDING REMARKS

A series of deterministic inelastic time history analyses have been carried out to investigate in detail the seismic response of a wide range of BI multistorey structures with elastic superstructures, under the N-S component of El Centro 1940 earthquake. Some discussion of design aspects were also presented.

In Section 4.3, the benefits of implementing the BI system were demonstrated by contrasting the performance of isolated and non-isolated multistorey structures. With the inclusion of the BI system, the inertia forces and the interstorey drifts can be significantly reduced. This enables the superstructure to be designed with much lower ductility requirements or even with an elastic design criteria. The much smaller interstorey drifts avoid the early occurence of non-structural damage during moderate earthquakes.

It was shown in Section 4.4, that under earthquakes which have spectral accelerations that diminish with longer periods, such as El Centro 1940 earthquake, a BI system reduces the base shear most significantly for multistorey structures with short $T_{1(UI)}$. Stiff superstructures tend to move like rigid bodies on top of the BI systems and therefore undergo considerably less transmission of the earthquake energy from the base. The structure will be strongly dominated

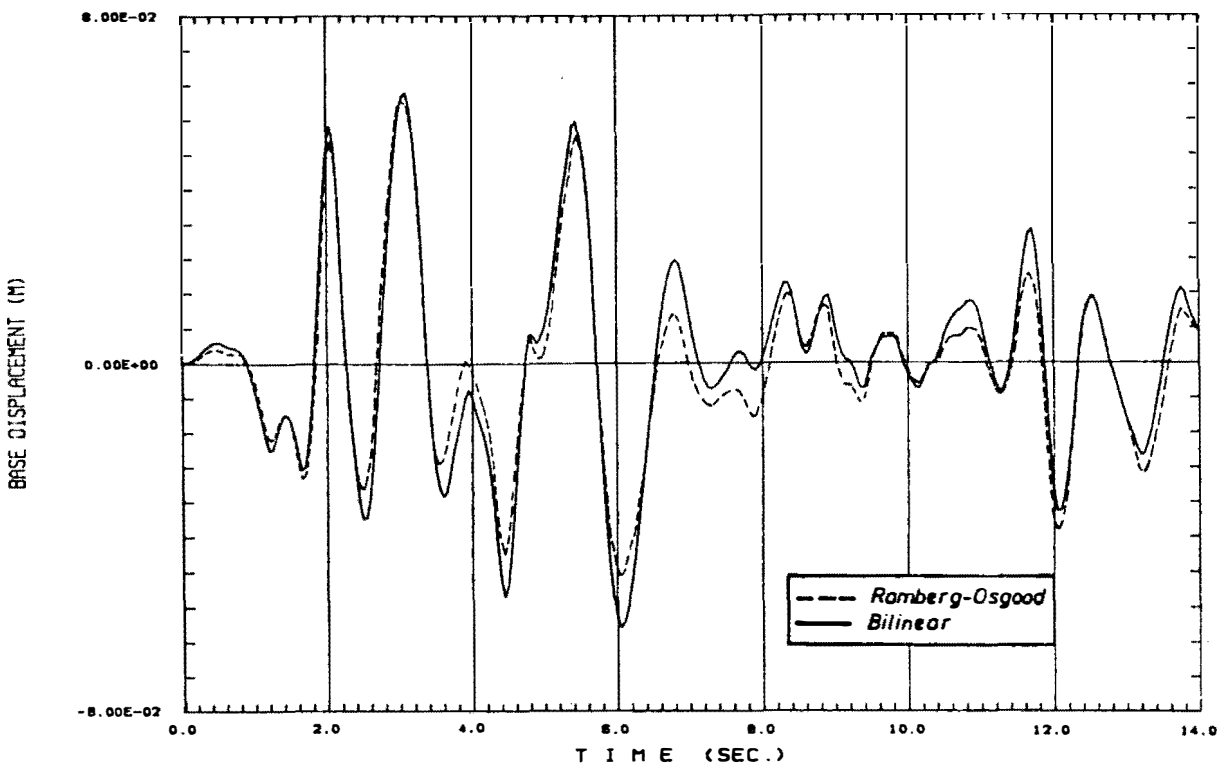

(a) "THIN" Hysteresis Loop (R ≈ 0.20)

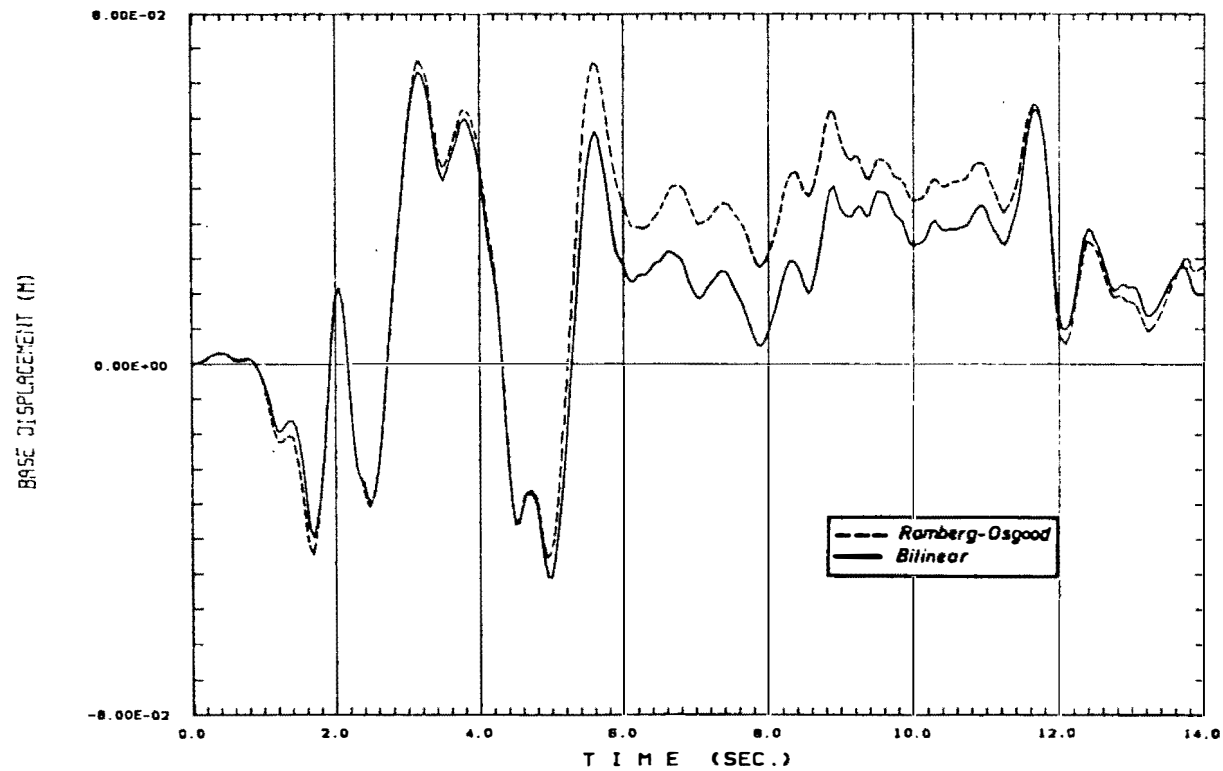

(b) "F A T" Hysteresis Loop (R ≈ 0.75)

Fig. 4.64 The Base Displacement History of BI Structures with Ramberg-Osgood and Bilinear Hysteresis Loop Models

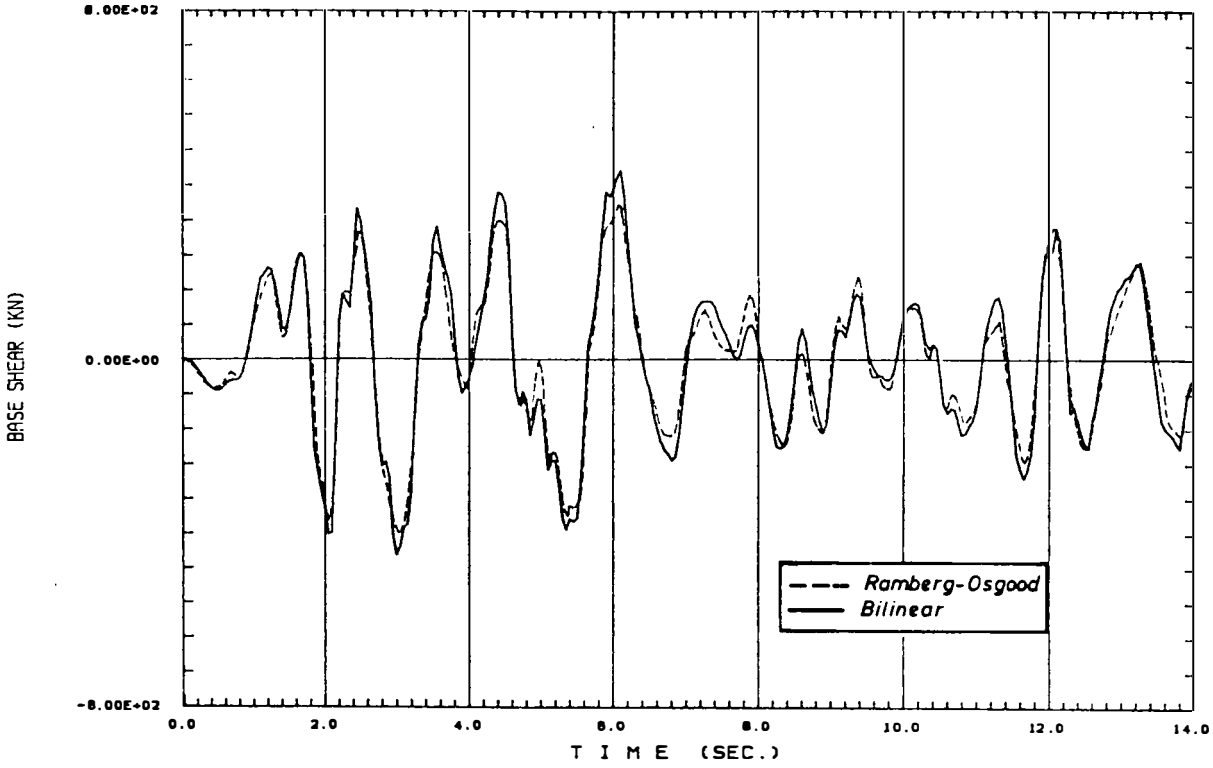

(a) "THIN" Hysteresis Loop (R ≈ 0.20)

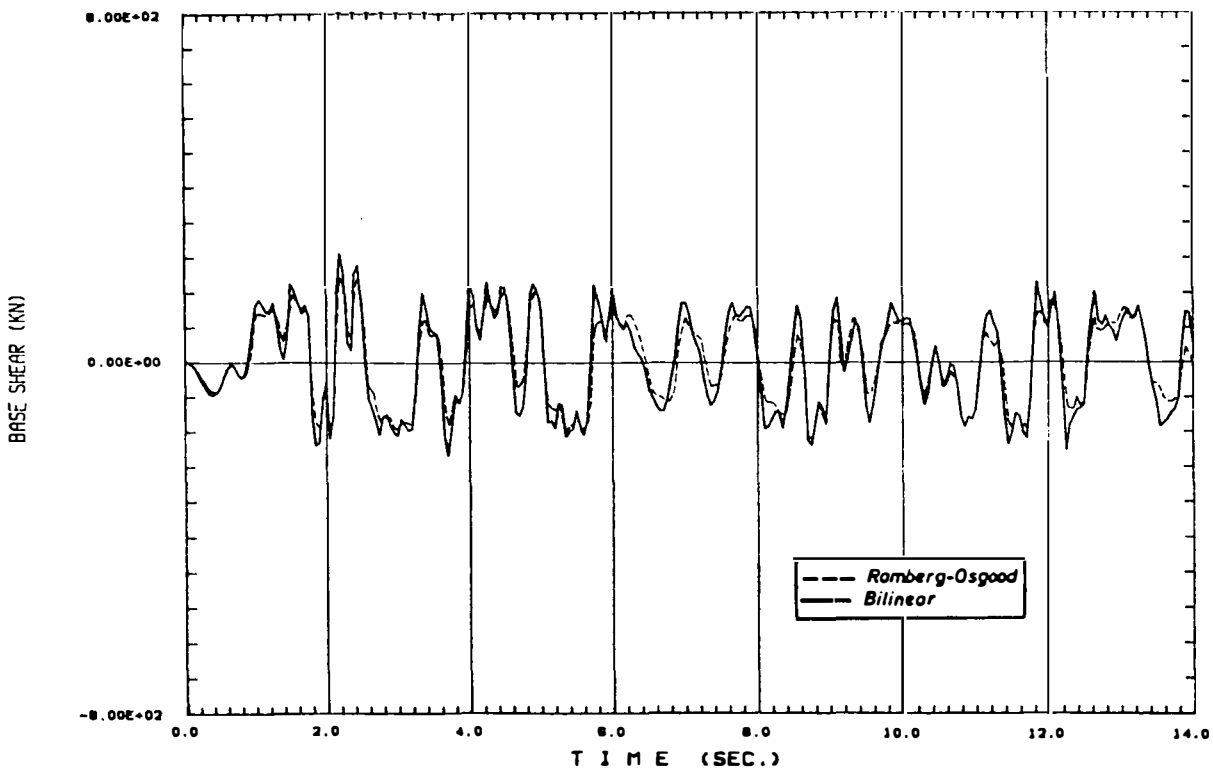

(b) "F A T" Hysteresis Loop (R ≈ 0.75)

Fig. 4.65 The Base Shear History of BI Structures with Ramberg-Osgood and Bilinear Hysteresis Loop Models

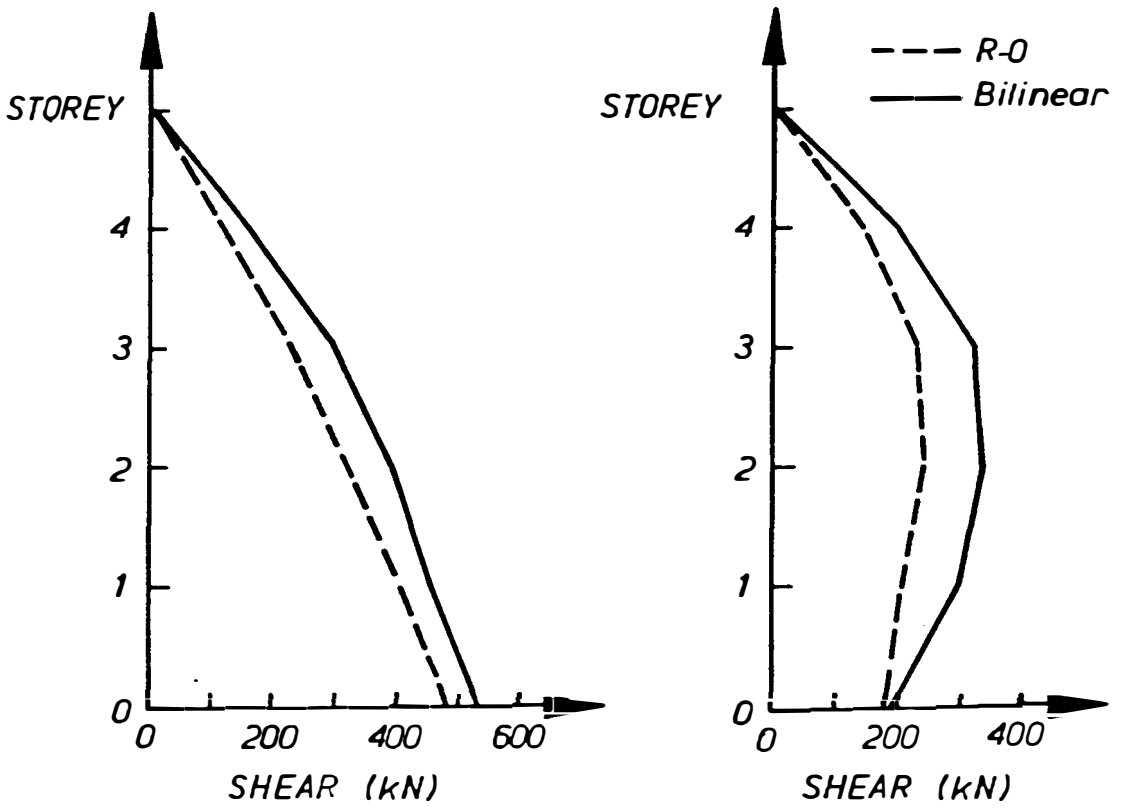

(a) Case 1 (R ≈ 0.20)

(b) Case 2 (R ≈ 0.75)

Fig. 4.66 The Effect of Hysteresis Loop Models on the Lateral Shear Envelope

by the first mode. As the superstructure becomes more flexible, however, the upper storeys no longer move in phase with the BI system and hence the higher modes make more significant contributions especially in the upper parts of the building.

The effect of parameter variation on a BI system was discussed in Section 4.5. The three key parameters of a BI system, namely: the initial stiffness, the yield strength and the post-yield stiffness have an important role in determining the effective stiffness and the energy dissipation capacity of the BI system, which in turn governs the structural response. By keeping the balance between two of the parameters, i.e. the effective stiffness and the energy dissipating capacity, an optimum BI system may be obtained.

In design practice, the initial or elastic stiffness and the yield strength are generally determined so that there are no prematurely large base movements under the lateral working load conditions, such as wind load and/or minor ground shaking. A BI system with low initial stiffness accompanied with low yield strength tends to induce small inertia forces, but it may cause excessive base displacements. To avoid this, more additional hysteretic damping should be introduced. It can be done by increasing the initial stiffness and the yield strength to a certain extent, or decreasing the post-yield stiffness.

It was also shown in Section 4.5, that a BI system with a small energy dissipation capacity tends to behave like a linear isolation system, which deflects the earthquake energy rather than absorbing it. The characteristic of structures with this type of BI system is strongly first mode dominated with almost equally distributed lateral forces over the entire height of their superstructure. Whereas if the BI system has a great energy dissipation capacity, which can be indicated by the high ratio of its loop area to the area of the enclosing rectangle (large R), the lateral shear envelope tends to be more bulged. A relatively strong correlation was found between R and the shape of the lateral shear envelope. With a large value of R the maximum inertia forces in the upper part of the building usually occur before the BI system reaches its peak displacement. The combination of the first mode and the higher modes at this time cause high forces at the upper level of the superstructure.

All of the above analyses were carried out using "shear-beam" superstructure models, in which the beam-to-column ratio, $\rho = \infty$. The effect of using other supertructure models, i.e. "cantilever-beams" with $\rho = 0.0$ and "moment resistant frames" with $\rho = 0.125$ was discussed in Section 4.6. No significant differences were found for the base displacements and base shears due to this effect. For the lateral storey shear envelope, however, this superstructure frame action may cause considerable differences especially if the BI system has relatively fat hysteresis loops.

In the discussion of design aspects presented in Section 4.4.7, 4.5.6, and 4.6.4, it was verified that the base displacement and the base shear are strongly influenced by the characteristics of the BI system and therefore their maximum values can be predicted from the effective stiffness and the additional hysteretic damping of the BI system. Based on the bilinear hysteresis loop model,

the values of the effective stiffness and the additional damping can be easily estimated. Then by utilising the strong correlation between the hysteresis loop ratio, R and the exponent p of the code-type approach formula expressed in Eq. 4.15, the storey shears can be satisfactorily predicted.

The mode-superposition method by Kelly et al. based on a response spectrum analysis for an equivalent linear system was also evaluated. It was found that the effect of the actual inelastic behaviour of a BI system on the structural response is too complex to be predicted by this method, especially if the BI system is highly non-linear and/or the superstructure has a long $T_1(UI)$.

In Section 4.8, the consequence of the use of the simple bilinear hysteresis model was compared, with that based on the more complex Ramberg-Osgood model which more accurately represents the hysteresis behaviour of some BI systems. It was found from this investigation that a bilinear hysteresis model tends to give a slightly larger estimate of the structural response than the Ramberg-Osgood model. Therefore, for practical purposes the bilinear model can be used as a reliable idealization of the cyclic load-displacement relationship of various BI systems. Further investigation is, however, still needed to clarify this phenomenon.

4.10 REFERENCES

4.1 LEE, D.M., The Effect of Base Isolation on Multistorey Shear Structure, Ph.D. Thesis, Dept. of Theoritical and Applied Mechanics, Univ, of Auckland, New Zealand, 1978.

4.2 KELLY, J.M., EIDINGER, J.M., and DERHAM, C.J., A Practical Soft Storey Earthquake Isolation System, Report No. UCB/ EERC-77/27, Earthquake Engineering Research Centre, University of California, Berkeley, 1977.

4.3 SHARPE, R.D., The Seismic Response of Inelastic Structures, Research Report 74-13, Dept. Of Civil Engineering, University of Canterbury, 1974.

4.4 CARR, A. J., Ruaumoko, Computer Program Library, Dept. of Civil Engineering, University of Canterbury, 1986.

4.5 BATHE, K.J. and WILSON, E.L., Numerical Method in Finite Element Analysis, Prentice Hall Inc., 1976.

4.6 RUBINSTEIN, M.F., Matrix Computer Analysis of Structures, Prentice Hall Inc., 1966, p.224.

4.7 CLOUGH, R.W. and PENZIEN, J., Dynamics of Structures, McGraw-Hill Inc. , 1975, 634pp.

4.8 CHRISP, D.J., Damping Models for Inelastic Structures, ME Project Report, Dept. of Civil Engineering University of Canterbury, 1980.

4.9 WILSON, E.L . and PENZIEN, J., Evaluation of Orthogonal Damping Matrices, Int. Journal for Numerical Methods in Engineering, Vol. 4, 1972, pp.5-10.

4.10 AKIYAMA, H., Earthquake-Resistant Limit-State Design for Buildings, University of Tokyo Press, 1985.

4.11 Standard Association of New Zealand. , Code of Practice for General Structural Design and Design Loadings for Buildings, NZS 4203:1984.

4.12 Applied Technology Council, An Investigation of The Correlation between Earthquake Ground Motion and Building Perfomance, 1982.

4.13 Base Isolation Subcmt. of the Seismology Committee, Structural Engineers Assc. of Northern Calif., Tentative Sismic Isolation Design Requirements, California, 1986.

4.14 TURKINGTON, D.H. , CARR, A.J. , COOKE, N. , MOSS, P.J., Seismic Design of Bridges on Lead-Rubber Bearings, Proc. Pacific Conference on Earthquake Engineering - New Zealand, Vol. 2, 1987, pp. 389-400.

4.15 IWAN, W.D., Application of Nonlinear Analysis Techniques, Applied Mech. in Earthq. Eng. , AMD-Vol.8, ASME, 1974, pp.135-161.

4.16 WEN, Y.K., Methods for Random Vibration of Hysteretic Systems, Journal of the Eng. Mech. Div. , ASCE, Vol.102, No. EM2, April 1976, pp.249-263.

4.17 IWAN, W.D. and GATES, N.C., Estimating Earthquake Response of Simple Hysteretic Structures, Journal of the Eng Mech. Div., ASCE, Vol.105, No. EM3, June 1979, pp. 391-405.

4.18 GROSSMAYER, R.L. and IWAN, W.D., A Linearization Scheme for Hysteretic Systems Subjected to Random Excitation, EESD, Vol.9, 1981, pp.171-185.

4.19 KELLY, J.M., Aseismic Base Isolation : Review and Bibliography, Soil Dynamics and Earthquake Engineering, Vol.5, No.3, 1986, pp.202-216.

4.20 Ang, A.H.S. and TANG, W.H. , Probability Concepts in Engineering Planning and Design, Volume 1 - Basic Principles, John Wiley & Sons, Inc., 1975, 409 pp.

4.21 HURTY, W.C. and RUBINSTEIN, M.F., Dynamics of Structures, Prentice Hall, 1964, pp.194-196.

4.22 PAZ, M., Structural Dynamics, Van Nostrand, 1980, pp.372-373.

4.23 CRUZ, E.F. and CHOPRA, A.K., Simplified Methods of Analysis for Earthquake Resistant Design of Buildings, Report No UBC/EERC-85/01, Univ. of California, Berkeley, Feb.1985.

4.24 Uniform Building Code, International Conf. of Building Officials, Section 2312, 1985, pp.114-136.

4.25 NZ Ministry of Works and Development, Design of Lead-Rubber Bridge Bearings, CDP 818/A, 1983.

4.26 TYLER, R.G., Development and Testing of Mechanical Energy Dissipating Devices and Barings RRU Bulletin 43, Seismic Design of Bridges by R.Park and R.W.G. Blakeley, 1979.

4.27 RAMBERG, W. and OSGOOD, W.R., Description of Stress-Strain Curves by Three Parameters, Nat. Advisory Comm. on Aeronautics, Technical Note 902, 1943.

4.28 JENNINGS, P.C., Response of Simple Yielding Structures to Earthquake Excitation, Ph.D. Thesis, California Institute of Technology, Pasadena, 1963.

4.29 OTANI, S., Hysteresis Models of Reinforced Concrete for Earthquake Response Analysis, Journal of the Faculty of Engineering, the University of Tokyo (B), Vol XXXVI, No.2, 1981.

CHAPTER 5

COMPONENT MODE SYNTHESIS METHOD FOR BASE ISOLATED MULTISTOREY STRUCTURES WITH ELASTIC SUPERSTRUCTURES

5.1 INTRODUCTION

The inclusion of Base Isolation enables the superstructure to be designed for limited ductility or even elastic behaviour, since the design forces have been considerably reduced. A BI multistorey structure may, therefore, have an elastic superstructure with some energy dissipators at its base which may undergo large plastic deformations. This phenomenon creates a unique nonlinear case, in which the plastic deformations can be concentrated in a certain part of the structure. For this reason, equivalent linear approximation methods seem feasible and attractive for use in practical design methods as well as for analysing the modal contributions of BI multistorey structures.

Most codes of design practice specify the seismic loadings in term of spectral accelerations. It is therefore necessary to provide a means of using the modal properties of the structure if the design is to proceed in a direct manner. The indirect alternative is to generate accelerograms and carry out time history analyses.

In the previous chapter, an equivalent linear approximation method with the mode superposition technique suggested by Kelly et al for BI multistorey structures was evaluated. Some analyses of modal contributions have been carried out using this method. It was found, however, that the assumptions of this method do not satisfactorily represent the actual basic characteristic response of BI multistorey structures.

In the absence of other alternatives, a series of inelastic time history analyses is normally employed to accurately predict the structural behaviour. Even with a high speed computer and computer programs that are now available, conducting a series of inelastic analyses are generally too costly and not practical for design purposes, especially since only the BI system behaves inelastically, and the superstructure is usually considered to remain elastic. Furthermore, an inelastic time history analysis does not give the designer a clear insight on the structural behaviour unless a large number of these analyses are carried out.

In this chapter, the use of the Component Mode Synthesis method for the response history analysis of a BI multistorey structure is introduced. Although in this preliminary attempt the method is still based on the step-by-step integration, it offers a much better visualization of the structural behaviour and leads to a less computational effort than the normal inelastic time history analysis.

The background of the concept, the analytical and the mathematical models used in the Component Mode Synthesis method are described in Section 5.2. Some examples of analysis results are also presented and compared with the results obtained from the inelastic time history analyses.

As reported in Section 5.3, some analyses using the above method are conducted to evaluate the change of the modal contributions to the storey shears due to the variation of the superstructure's fundamental period, BI system parameters, frame action of the superstructure, base mass, superstructure's vertical irregularities and the number of storeys. The total responses are also compared with the results obtained from the inelastic time history analyses. It is hoped that after gaining some more understanding from these modal analyses the Component Mode Synthesis method can be developed further in the future for use in the response spectrum analyses.

5.2 BASIC PRINCIPLES OF COMPONENT MODE SYNTHESIS METHOD

5.2.1 BACKGROUND OF THE CONCEPT

In the last three decades, several techniques have been developed for the dynamic analysis of large and complex structures that involve division into substructures or components. As alluded to by Hurty et al[5.1], the basic idea of these techniques is to treat the structure as an assembly of connected components, or substructures, each of which is isolated and analysed separately to derive a set of modes or displacement shapes from which a set of generalized coordinates applicable to the complete structure is synthesized.

The development of this concept, at early stages, seems to be directed more towards the need of the aircraft and aerospace industries, in which complete structures are frequently very complex and major components are often designed and produced by different organizations[5.2].

Later, soil structure interaction problems[5.3,5.4] also invited the idea of dynamic substructuring. The combined dynamic system of the soil and building often possesses a complex collection of numerous modes and therefore it is desireable to separate them into two distinct and simpler systems. This concept also allows one subsystem to be designed repetitively for optimization or for different conditions without necessarily involving the other subsystem which may only need to be designed once. Thus, a considerable reduction of computational effort may be achieved.

Another application of this concept can be found in the dynamic analysis of off-shore gravity platforms[5.5]. The dynamic substructuring enables the deck degrees-of-freedom to be reduced significantly while still retaining at the same time a high accuracy in its dynamic response.

In the case of BI multistorey structures, it is desirable to separate the BI system, which may undergo large plastic deformations, from the superstructure, which is usually designed to remain elastic. The elastic superstructure subsystem is now treated separately as a linear Multi-Degree-of-Freedom (MDOF) system. The mode superposition can then be employed by only incorporating the first few significant modes of vibration of the superstructure. A computer program called ISODYN is developed on this concept and which is especially meant to give the user a much better insight of the structural behaviour. Further description of the analytical and the mathematical models used in the computer program is presented in the following section.

5.2.2 ANALYTICAL AND MATHEMATICAL MODEL

Following the Component Mode Synthesis method proposed by Hurty et al[5.1], a BI multistorey structure is considered to be formed by two subsystems, namely: the superstructure subsystem on an assumed fixed-interface and the BI subsystem, as illustrated by a simplified model in Fig. 5.1.

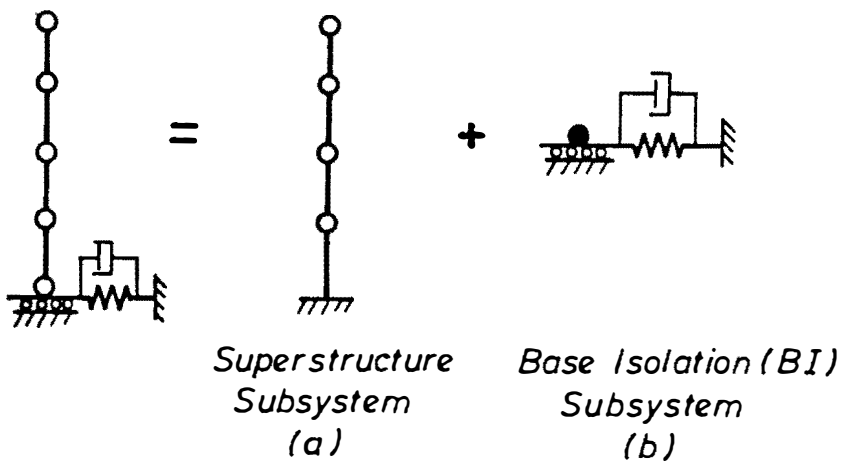

Fig. 5.1 A Simplified Model for BI Multistorey Structures

The equations of motions expressed in Eq. 5.1 can be written in a partitioned form as shown in Eq. 5.2.

$$[M]\{\ddot{u}\} + [C]\{\dot{u}\} + [K]\{u\} = -[M]\{r\}\ddot{u}_g(t) \tag{5.1}$$

$$\begin{bmatrix} m_{ss} & m_{sb} \\ m_{bs} & m_{bb} \end{bmatrix}\begin{Bmatrix} \ddot{u}_s \\ \ddot{u}_b \end{Bmatrix} + \begin{bmatrix} c_{ss} & c_{sb} \\ c_{bs} & c_{bb} \end{bmatrix}\begin{Bmatrix} \dot{u}_s \\ \dot{u}_b \end{Bmatrix} + \begin{bmatrix} k_{ss} & k_{sb} \\ k_{bs} & k_{bb} \end{bmatrix}\begin{Bmatrix} u_s \\ u_b \end{Bmatrix} = -\begin{bmatrix} m_{ss} & m_{sb} \\ m_{bs} & m_{bb} \end{bmatrix}\{r\}\ddot{u}_g(t) \tag{5.2}$$

where the subindices s and b are associated with parts of the structure, above and below the interface respectively. For a lumped mass model, the off-diagonal terms m_{sb} and m_{bs} are zero.

The above coupled equations can then be reduced, as will be shown later, in terms of component generalized coordinates, y, by the coordinate transformation

$$\{u\} = [\psi]\{y\} \tag{5.3}$$

where $[\psi]$ is a matrix of preselected component modes. These modes are actually the assumed-modes or Ritz approximation of the geometric displacement vector $\{u\}$[5.2,5.6]. In this case, they consist of the fixed-interface normal modes of the superstructure, ϕ_n, the constraint modes, ϕ_c and the unit diagonal matrix. The displacement vector, $\{u\}$ can now be expressed in term of the component generalized coordinates, y, as follows

$$\begin{Bmatrix} u_s \\ u_b \end{Bmatrix} = [\psi] \begin{Bmatrix} y_s \\ y_b \end{Bmatrix} \tag{5.4}$$

$$[\psi] = \begin{bmatrix} \phi_n & \phi_c \\ 0 & I \end{bmatrix} \tag{5.5}$$

The normal modes and their corresponding frequencies are obtained from the equations of free-vibration of the superstructure subsystem on the assumed fixed-interface,

$$(k_{ss} - \omega_i^2 m_{ss})\ \phi_i = 0 \tag{5.6}$$

The response of the superstructure relative to its base can be approximated by incorporating only a limited number of the significant lowest normal modes. This implies that the normal modes, ϕ_n consists of the n normal mode shapes of the superstructure associated with the n lowest natural frequencies of free vibration, $\omega_1, \omega_2, \ldots, \omega_n$, as expressed in the following

$$[\phi_n] = [\phi_{s1}, \phi_{s2}, \ldots, \phi_{sn}] \tag{5.7}$$

The constraint modes can be obtained by statically imposing sucessive unit displacement on the physical or geometric coordinates of the BI system(s) while all other remaining coordinates being totally constrained. Thus, the set of constraint modes is defined by the equation

$$\begin{bmatrix} k_{ss} & k_{sb} \\ k_{bs} & k_{bb} \end{bmatrix} \begin{bmatrix} \phi_n \\ I \end{bmatrix} = \begin{bmatrix} 0 \\ R_b \end{bmatrix} \tag{5.8}$$

where R_b is the set of "reactions" at the boundary points or at the BI system physical coordinates, and I is a unit diagonal matrix. From the top row partition of Eq. 5.8, the constraint modes is

$$[\phi_c] = -[k_{ss}]^{-1}[k_{sb}] \tag{5.9}$$

By substituting Eq. 5.4 to Eq. 5.2, the equations of motion for a lumped mass BI multistorey structure model can be expressed in term of the generalized coordinates as follows

$$\begin{bmatrix} m_{ss} & 0 \\ 0 & m_{bb} \end{bmatrix}[\psi]\begin{Bmatrix} \ddot{y}_s \\ \ddot{y}_b \end{Bmatrix} + \begin{bmatrix} c_{ss} & c_{sb} \\ c_{bs} & c_{bb} \end{bmatrix}[\psi]\begin{Bmatrix} \dot{y}_s \\ \dot{y}_b \end{Bmatrix} + \begin{bmatrix} k_{ss} & k_{sb} \\ k_{bs} & k_{bb} \end{bmatrix}[\psi]\begin{Bmatrix} y_s \\ y_b \end{Bmatrix} = -\begin{bmatrix} m_{ss} & 0 \\ 0 & m_{bb} \end{bmatrix}\{r\}\ddot{u}_g(t) \tag{5.10}$$

Finally, the equations of motion can be reduced in a much simpler form, as shown in Eq. 5.11 below, by multiplying Eq. 5.10 with $[\psi]^T$.

$$\begin{bmatrix} M^* & \bar{m}_{sb} \\ \bar{m}_{bs} & \bar{m}_{bb} \end{bmatrix}\begin{Bmatrix} \ddot{y}_s \\ \ddot{y}_b \end{Bmatrix} + \begin{bmatrix} C^* & 0 \\ 0 & \bar{c}_{bb} \end{bmatrix}\begin{Bmatrix} \dot{y}_s \\ \dot{y}_b \end{Bmatrix} + \begin{bmatrix} K^* & 0 \\ 0 & \bar{k}_{bb} \end{bmatrix}\begin{Bmatrix} y_s \\ y_b \end{Bmatrix} = -[\psi]^T \begin{bmatrix} m_{ss} & 0 \\ 0 & m_{bb} \end{bmatrix}\{r\}\ddot{u}_g(t) \tag{5.11}$$

where :

$$[M^*] = [\phi_n]^T [m_{ss}] [\phi_n] \tag{5.12}$$

$$[\bar{m}_{sb}] = [\bar{m}_{bs}]^T = [\phi_n]^T [m_{ss}] [\phi_c] \tag{5.13}$$

$$[\bar{m}_{bb}] = [\phi_c]^T [m_{ss}] [\phi_c] + [m_{bb}] \tag{5.14}$$

$$[C^*] = [2\lambda_i \omega_i M_i^*] \tag{5.15}$$

$$[\bar{c}_{bb}] = \text{damping coefficient of BI system, } [c_{bb}]_{BI} \tag{5.16}$$

$$[K^*] = [\phi_n]T [k_{ss}] [\phi_n] = [\omega_i^2 M_i^*] \tag{5.17}$$

$$[\bar{k}_{bb}] = [k_{bb}]_{\text{superstruct.}} + [k_{bs} \phi_c] + [k_{bb}]_{BI} \tag{5.18}$$

As the result of this mode synthesis reduction process, the global matrices of the mass, $[\bar{M}]$, damping, $[\bar{C}]$, and stiffness, $[\bar{K}]$ on the left-hand side of the equation take general forms as displayed in Fig. 5.2. For the global stiffness matrix, $[\bar{K}]$, in particular this new form is much simpler and thus needs much less storage compared to the original global stiffness matrix. As pointed out by Bell[5.5], Eq. 5.18 can even be more simplified if the superstructure is statically determinate supported, i.e.: by a single base point (maximum 6 d.o.f. in 3-dimensional case), since

the following equation

$$[k_{bb}]_{superstruct.} + [k_{bs}\,\phi_c] = [k_{bb}]_{superstruct.} - [k_{sb}]^T [k_{ss}]^{-1} [k_{sb}] \qquad (5.19)$$

which is the stiffness matrix associated with the "rigid-body" motion of the superstructure must be equal to a null matrix. Hence in this case Eq. 5.18 can be rewritten as

$$[k_{bb}] = [k_{bb}]_{BI} \qquad (5.20)$$

For a nonlinear BI system, the value of the above term may change during the ground shaking and therefore it should be updated based on the cyclic load-displacement relationship of the BI system, whereas the remaining terms of the global stiffness matrix, [K] are unaltered.

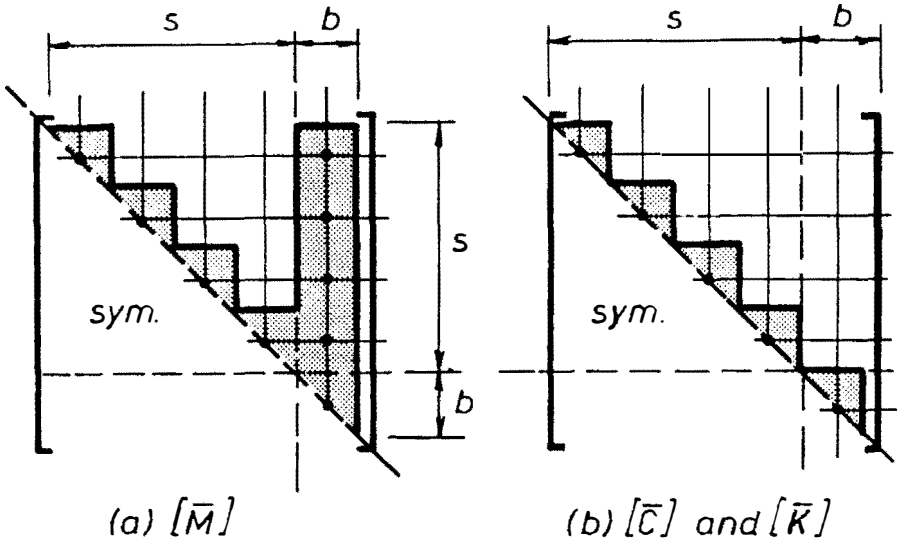

Fig. 5.2 General Form of [M̄], [C̄], and [K̄] after the Mode Synthesis Reduction Process.

The global damping matrix shown in Eq. 5.11 has a very simple form after it is generated following the relation suggested by Penzien[5.5, 5.7]. The original reduced damping matrix is

$$[\bar{C}] = [\psi]^T [C] [\psi] = \begin{bmatrix} \bar{c}_{ss} & \bar{c}_{sb} \\ \bar{c}_{bs} & \bar{c}_{bb} \end{bmatrix} \qquad (5.21)$$

where :

$$[\bar{c}_{ss}] = [C^*] \qquad (5.22.a)$$

$$[\bar{c}_{sb}] = [\phi_n]^T [c_{ss}] [\phi_c] + [\phi_n]^T [c_{sb}] \qquad (5.22.b)$$

$$[\bar{c}_{bb}] = [\phi_c]^T [c_{ss}] [\phi_c] + [c_{sb}]^T [\phi_c] + [\phi_c]^T [c_{sb}] + [c_{bb}] \qquad (5.22.c)$$

and

$$[\bar{c}_{bb}] = [c_{bb}]_{superstruct.} + [c_{bb}]_{BI} \tag{5.22.d}$$

It was assumed that the damping of the superstructure can be adequately characterized by its fixed-base damping, c_{ss}, thus it was suggested that

$$[c_{sb}] = -[c_{ss}]\,[\phi_c] \tag{5.23}$$

and

$$[c_{bb}]_{superstruct.} = [\phi_c]^T\,[c_{ss}]\,[\phi_c] \tag{5.24}$$

Substituting Eqs. 5.23 and 5.24 into Eq. 5.22 leads to the simple form of the global damping matrix as shown in Eq. 5.11.

It is worth noting, that the damping term, c_{bb}, which now only consists of the damping coefficient of the BI system, may represent the damping provided by any type of energy dissipator. An appropriate value of viscous damping can be directly supplied if the dissipator is a velocity-dependent device. In the case where a displacement-dependent device being used, the equivalent viscous damping value should be estimated. Pending further research in this area, the equivalent viscous damping can be approximated by

$$[c_{bb}]_{BI} = [2\lambda_{BI}\,\omega_{BI}\,M_{total}] \tag{5.25}$$

in which λ_{BI} is the value of the equivalent viscous damping of the BI system in term of percentage critical damping; M total is the total mass of the structure affecting the inertia force; and ω_{BI} is the circular frequency obtained from:

$$\omega_{BI} = \sqrt{\frac{k_{BI}}{M_{total}}} \tag{5.26}$$

where k_{BI} is the stiffness of the amplitude-dependent BI system, a term of the stiffness matrix $[k_{bb}]$.

All of the above features are incorporated in the computer program ISODYN developed as part of this study. The computer program can be used for analysing the seismic response of simple to complex multistorey structures subjected to an earthquake record.

5.2.3 EXAMPLES OF ANALYSIS RESULTS

The computer program ISODYN uses Newmark's constant-acceleration method[5.8,5.9] for its numerical integration scheme to solve Eq. 5.11 at each specified time step. The generalized coordinates, y, can then be transformed back to the geometric or physical coordinates, u, through Eqs. 5.4 and 5.5.

The modal contributions of the structural response can be found from the modal properties of the superstructure on an fixed-interface. At each time step the total storey displacements are obtained as the sum of these modal displacements plus the base displacement. For the storey shears and overturning moments, which are basically functions of the member deformations relative to the base displacement, their total responses are obtained as the sum of the modal contributions only and not affected directly by the base displacement.

Tables 5.1 and 5.2 list the absolute maximum values of storey displacements, storey shears and overturning moments of BI four-storey "shear-beam" structures with $T_{1(UI)}$ = 0.2 and 1.2 seconds, respectively, under 14-second duration of the North-South component of El Centro 1940 record. The structures are mounted on BI systems which have an initial stiffness of 10.0 W/m, a post-yield stiffness of 1.5 W/m and a yield strength of 5 %W. Only the contributions of the first three modes of the superstructure are considered.

The response history plots for the total base displacements, total base shears and total top-storey shears of the two BI structures mentioned above are shown in Figs. 5.3 and 5.4. In order to evaluate the accuracy of the Component Mode Synthesis method used in the computer program ISODYN, these plots are compared with the plots obtained from the inelastic time history analyses conducted earlier using the computer program RUAUMOKO. As can be seen in Figs. 5.3 and 5.4, the results obtained by using the Component Mode Synthesis method which incorporates the first three modes of the superstructure are almost identical to the results of the inelastic time history analysis.

Two other examples are presented in Tables 5.3 and 5.4 which tabulates the structural responses of BI four-storey "cantilever-beam" structures with $T_{1(UI)}$ = 0.2 and 1.2 seconds, respectively. Both structures are mounted on BI systems which have a flat hysteresis loop (R=0.55) with an initial stiffness of 10.0 W/m, a post-yield stiffness of 0.5 W/m and a yield strength of 5 %W. The modal contributions of the first three modes are considered. The total responses are compared with the results obtained from RUAUMOKO. From these comparison, it can be seen that the Component Mode Synthesis method can predict the structural response as accurately as the inelastic time history analysis. Note, that these examples are two of the extreme cases found in Section 4.6.4 (see Tables 4.14.a and 4.14.d) where the total responses were unable to be predicted by the equivalent linear approximation method.

Table 5.1 Maximum Storey Displacements, Shears, and Overturning Moments of a BI Four-Storey "Shear-Beam" Structure with $T_{1(UI)}$ = 0.2 secs

Storey	Maximum Displacement (mm)				
	mode 1	mode 2	mode 3	Base	Total
4	1.65	0.08	0.01	56.99	58.57
3	1.45	0.00	0.02	56.99	58.40
2	1.08	0.08	0.08	56.99	58.08
1	0.57	0.08	0.02	56.99	57.61
0	-	-	-	56.99	56.99
Storey	**Maximum Shear (kN)**				
	mode 1	mode 2	mode 3	Base	Total
4	66.9	26.6	10.7	-	55.8
3	125.7	26.6	3.7	-	109.1
2	169.4	0.0	9.4	-	162.8
1	192.6	26.6	7.0	-	213.8
0	-	-	-	256.0	256.0
Storey	**Maximum Overturning Moment (kN/m)**				
	mode 1	mode 2	mode 3	Base	Total
4	108.7	43.2	18.0	-	92.4
3	204.2	43.2	6.3	-	173.8
2	275.1	0.0	15.9	-	267.8
1	312.9	43.2	11.8	-	345.9
0	-	-	-	-	-

Note : The BI system has k_o = 10.0 W/m, αk_o = 1.5 W/m, and F_y = 5%W ($R \approx 0.31$)

Table 5.2 Maximum Storey Displacements, Shears, and Overturning Moments of a BI Four-Storey "Shear-Beam" Structure with $T_{1(UI)}$ = 1.2 secs

Sto-rey	Maximum Displacement (mm)				
	mode 1	mode 2	mode 3	Base	Total
4	65.70	8.12	2.35	46.23	101.62
3	57.78	0.00	2.92	46.23	95.40
2	42.88	8.12	1.15	46.23	82.03
1	22.82	8.12	3.60	46.23	64.91
0	-	-	-	46.23	46.23
Sto-rey	Maximum Shear (kN)				
	mode 1	mode 2	mode 3	Base	Total
4	664.8	681.3	462.6	-	1114.1
3	1249.5	681.3	148.5	-	1551.6
2	1683.4	0.0	406.8	-	1745.9
1	1914.3	681.3	301.9	-	1940.9
0	-	-	-	1957.2	1957.2
Sto-rey	Maximum Overturning Moment (kN/m)				
	mode 1	mode 2	mode 3	Base	Total
4	1080.4	1107.1	751.7	-	1810.4
3	2030.4	1107.1	261.1	-	2521.3
2	2735.6	0.0	661.0	-	2837.0
1	3110.8	1107.1	490.6	-	3154.0
0	-	-	-	-	-

Note : The BI system has k_0 = 10.0 W/m, αk_0 = 1.5 W/m, and F_y = 5%W ($R \approx 0.31$)

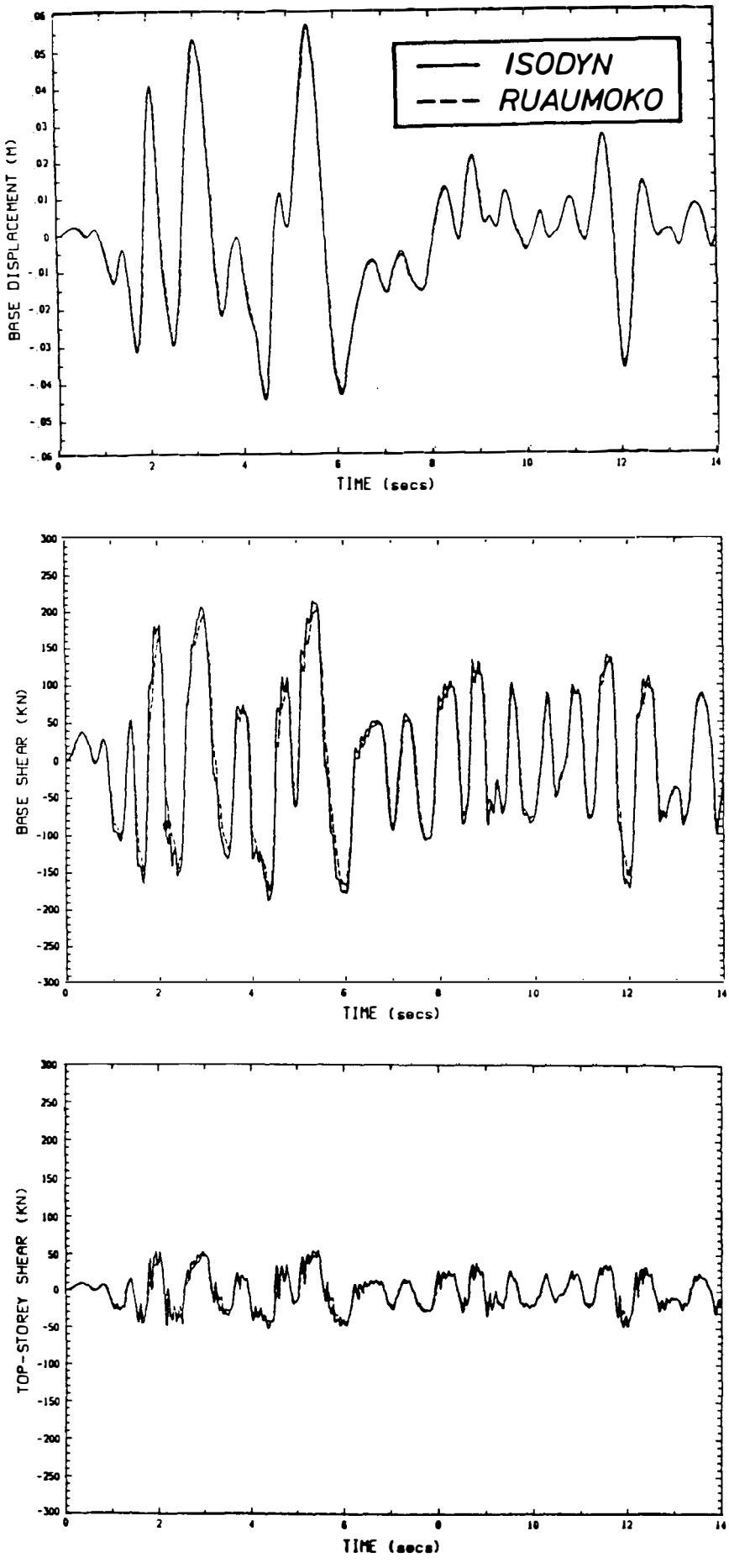

Fig. 5.3 Response History of a BI "Cantilever-Beam" Structure with $T_{1(UI)}$ = 0.2 secs

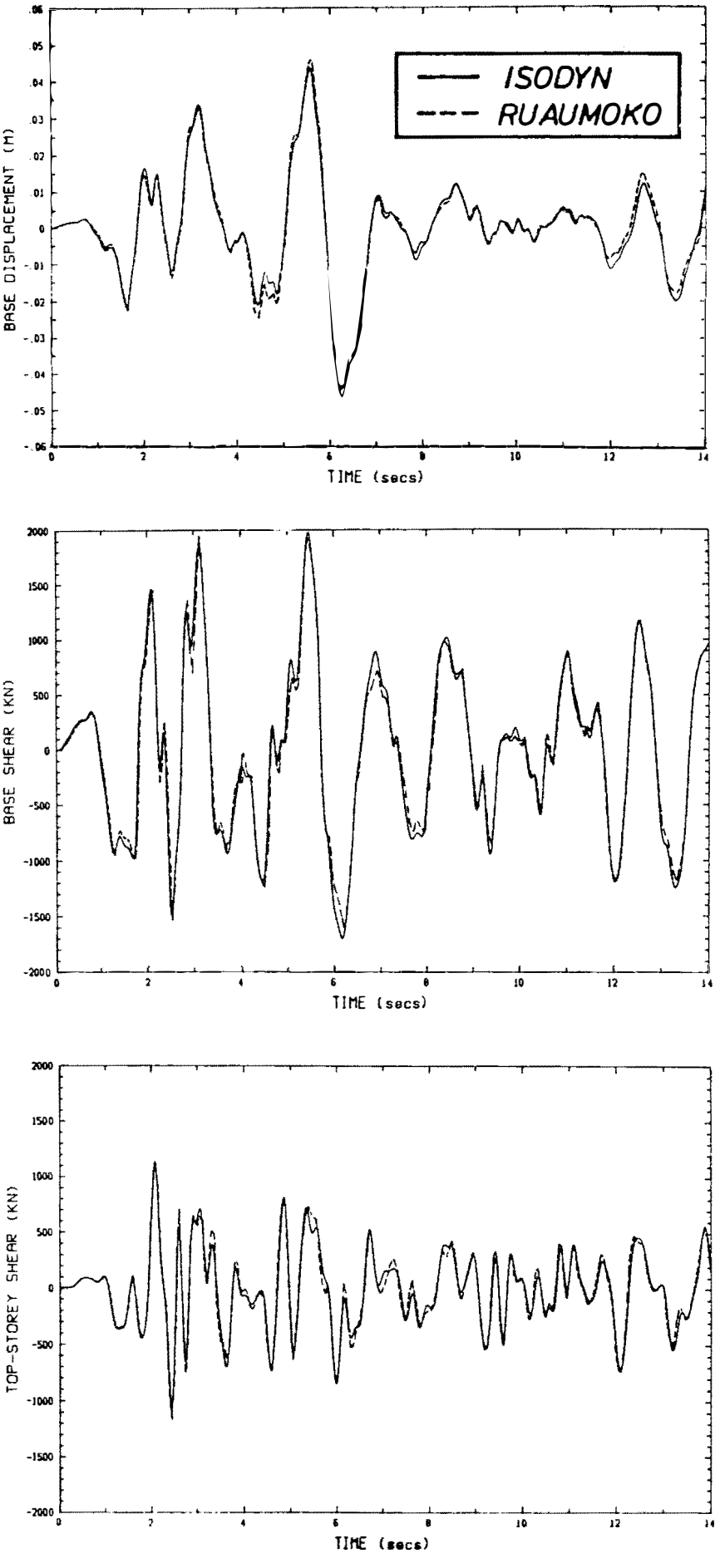

Fig. 5.4 Response History of a BI "Cantilever-Beam" Structure with $T_{1(UI)}$ = 1.2 secs

Table 5.3 Maximum Storey Displacements, Shears, and Overturning Moments of a BI Four-Storey "Cantilever-Beam" Structure with $T_{1(UI)}$ = 0.2 secs

Storey	Displacements (mm) obtained from ISODYN					RUAUMOKO
	mode 1	mode 2	mode 3	Base	Total	Total
4	2.09	0.01	0.00	62.72	64.00	59.9
3	1.07	0.01	0.00	62.72	63.56	59.5
2	0.69	0.02	0.00	62.72	63.16	59.0
1	0.19	0.01	0.00	62.72	62.85	58.7
0	-	-	-	62.72	62.72	58.6
Storey	Shears (kN) obtained from ISODYN					RUAUMOKO
	mode 1	mode 2	mode 3	Base	Total	Total
4	75.2	25.3	8.3	-	74.9	72.4
3	123.9	6.3	10.7	-	123.8	115.8
2	148.6	28.5	4.1	-	150.1	125.6
1	155.5	46.1	15.5	-	157.2	131.4
0	-	-	-	157.70	157.7	153.6
Storey	Overt. Moment (kNm) from ISODYN					RUAUMOKO
	mode 1	mode 2	mode 3	Base	Total	Total
4	244.6	82.4	27.2	-	243.5	230.0
3	647.4	89.6	7.5	-	642.6	596.1
2	1130.4	10.5	21.0	-	1130.6	993.1
1	1636.0	139.4	29.2	-	1641.7	1362.0
0	-	-	-	-	-	-

Note : The BI system has k_0 = 10.0 W/m, αk_0 = 0.5 W/m, and F_y = 5%W (R ≈ 0.55)

Table 5.4 Maximum Storey Displacements, Shears, and Overturning Moments of a BI Four-Storey "Cantilever-Beam" Structure with $T_{1(UI)}$ = 1.2 secs

Storey	Displacements (mm) obtained from ISODYN					RUAUMOKO
	mode 1	mode 2	mode 3	Base	Total	Total
4	73.93	1.55	0.05	59.20	121.1	118.1
3	47.83	1.16	0.11	59.20	98.4	95.2
2	24.25	2.14	0.37	59.20	78.6	75.2
1	6.84	1.08	0.11	59.20	64.6	61.1
0	-	-	-	59.20	59.2	55.6
Storey	Shears (kN) obtained from ISODYN					RUAUMOKO
	mode 1	mode2	mode 3	Base	Total	Total
4	252.3	219.9	53.6	-	374.4	397.0
3	415.6	55.1	68.8	-	453.3	422.0
2	498.4	247.7	26.5	-	488.7	481.9
1	521.7	400.7	99.4	-	485.4	465.8
0	-	-	-	462.6	462.6	451.9
Storey	Overt. Moment (kNm) from ISODYN					RUAUMOKO
	mode 1	mode 2	mode 3	Base	Total	Total
4	820.4	716.1	175.1	-	1217.7	1294.0
3	2171.4	896.2	48.5	-	2595.1	2469.0
2	3823.6	90.9	135.2	-	3823.5	3751.0
1	5487.1	1211.9	188.1	-	5380.7	5187.0
0	-	-	-	-	-	-

Note : The BI system has k_o = 10.0 W/m, αk_o = 0.5 W/m, and F_y = 5%W ($R \approx 0.55$)

5.3 MODAL CONTRIBUTIONS OF THE STOREY SHEARS

5.3.1 INTRODUCTION

As discussed earlier in Chapter 3, predicting the storey shears of BI multistorey structures has become the major aim of many research projects which were carried out in order to develop an approximate design method of analysis. Some attempts have also been made to evaluate the effects of the BI system on the modal contributions of the storey shears. Lee[5.10] based his qualitative explanation on the structure's linear modal properties at the initial and post-yield conditions, while Kelly et al[5.11] developed an equivalent linear approximation method as discussed in the previous chapter. It is clearly understood, however, that the effect of the inelastic behaviour of BI system cannot be completely described by an elastic analysis.

The Component Mode Synthesis method discussed in Section 5.2 enables the evaluation of these modal contributions to be conducted quantitatively with high reliability and accuracy. Using this method a series of analyses have been carried out to evaluate the modal contributions of the storey shears of BI multistorey structures subjected to El Centro 1940 N-S earthquake.

The effects of various structural properties on these modal contributions are discussed in the following subsections. It is hoped that the results of this evaluation will lead to greater understanding of the seismic behaviour of BI multistorey structures.

5.3.2 THE EFFECT OF THE SUPERSTRUCTURE'S FUNDAMENTAL PERIOD

To study the effect of the superstructure's fundamental period, $T_{1(UI)}$, on the modal contributions of storey shears, a series of four-storey "shear-beam" structures with $T_{1(UI)}$ of 0.2, 0.4, 0.8 and 1.2 seconds are considered. The first three modal storey shears of these unisolated and BI structures are incorporated in this evaluation as listed in Tables 5.5 and 5.6, respectively. The BI structures are mounted on a moderately fat loop BI system with an initial stiffness, k_o=10.0 W/m, a post-yield stiffness, αk_o= 1.5 W/m and a yield strength, F_y = 5%W. The total responses are also compared with inelastic time history analysis results. The values from these two different methods of analysis seem to be consistently in good agreement.

By contrasting the modal storey shears tabulated in Tables 5.5 and 5.6, it can be seen that the implementation of the BI system causes significant reduction of the first mode storey shears. The higher mode storey shears, however, are not so drastically reduced, except if, as will be shown later, the BI system has thin hysteresis loops. In this example, the first mode storey shears of a BI structure with $T_{1(UI)}$ of 0.4 secs are 4.6 times smaller whereas the second mode storey shears are only 2.5 times smaller when compared with the corresponding storey shears of the unisolated structure. This phenomenon explains the reason why the inclusion of a BI system may increase

Table 5.5 Modal Constributions to the Storey Shears of Fixed-Base Unisolated "Shear-Beam" Structures with Different $T_{1(UI)}$

$T_{1(UI)}$ secs	Storey	Max. Storey Shears (kN) obtained from ISODYN				RUAUMOKO
		Mode 1	Mode 2	Mode 3	Total	Total
0.2	4	323.9	58.6	20.3	344.1	341.4
	3	608.8	58.6	70.6	609.3	612.5
	2	820.2	0.0	17.6	807.4	803.6
	1	932.7	58.6	13.3	940.6	939.8
0.4	4	611.4	179.8	48.7	678.1	677.8
	3	1149.1	179.8	16.9	1173.8	1173.4
	2	1548.2	0.0	42.8	1550.5	1543.2
	1	1760.5	179.8	31.8	1863.0	1864.4
0.8	4	1088.9	408.7	135.9	1284.1	1291.2
	3	2046.5	408.7	47.2	2262.6	2242.2
	2	2757.2	0.0	119.5	2807.1	2822.7
	1	3135.4	408.7	88.7	3032.6	3034.5
1.2	4	1479.2	686.6	353.7	1897.5	1910.5
	3	2779.9	686.6	109.2	3192.6	3197.7
	2	3745.4	0.0	311.0	3793.7	3787.7
	1	4259.1	686.6	230.9	3983.2	3987.5

Note: $T_{1(UI)}$ = 0.2 secs Total Weight W = 2000 kN (incl. base mass)

0.4 secs 4000 kN

0.8 secs 8000 kN

1.2 secs 17500 kN

Table 5.6 Modal Constributions to the Storey Shears of Base Isolated "Shear-Beam" Structures with Different $T_{1(UI)}$

$T_{1(UI)}$ secs	Storey	Max. Storey Shears (kN) obtained from ISODYN				RUAUMOKO
		Mode 1	Mode 2	Mode 3	Total	Total
0.2	4	66.9	26.6	10.7	55.8	61.0
	3	125.7	26.6	3.7	109.1	116.6
	2	169.4	0.0	9.4	162.8	165.5
	1	192.6	26.6	7.0	213.8	211.1
	BI	-	-	-	256.0	255.0
0.4	4	132.1	70.2	28.1	188.7	190.9
	3	248.4	70.2	9.7	304.2	308.1
	2	334.6	0.0	24.7	324.8	348.7
	1	380.5	70.2	18.3	423.0	410.3
	BI	-	-	-	495.1	494.4
0.8	4	335.4	231.4	101.3	477.1	503.9
	3	630.4	231.4	35.2	745.0	767.3
	2	849.3	0.0	89.1	832.1	793.3
	1	965.8	231.4	66.1	897.4	791.8
	BI	-	-	-	933.2	929.1
1.2	4	669.8	681.3	462.6	1114.1	1188.3
	3	1249.5	681.3	160.7	1551.6	1525.3
	2	1685.4	0.0	406.8	1745.9	1898.2
	1	1914.3	681.3	594.3	1940.9	1959.4
	BI	-	-	-	1957.2	1963.3

Note : Properties of BI system : k_o = 10.0 W/m, αk_o = 1.5 W/m, F_y = 5%W.
W is as specified in Table 5.5.

the significance of the higher mode contributions to the storey shears especially in the upper storeys.

Fig. 5.5 visualizes the effect of the BI system in reducing the first and second mode top storey shears of short to long period structures (0.2 secs ≤ $T1(UI)$ ≤ 1.2 secs). It can be clearly seen that the first mode storey shears are reduced more significantly when compared with the shears of the second mode.

Besides evaluating the changes of the modal responses, it is also important to observe the contribution of these maximum modal responses to the maximum total storey shears. For this purpose, the modal contributions are expressed in terms of percentages of the total responses. Note, the occurences of these maximum values are not necessarily at the same time and therefore it is possible to encounter some modal contributions which are greater than 100% of the total response since the combinations are not simply a summation of all modal contributions.

From Figs. 5.6.a and 5.6.b, it can be seen that the first mode contributions for the base shear are always dominant (above 90% of the total response) irrespective of $T_{1(UI)}$ and whether the structure is isolated or unisolated. The BI system, however, causes the second mode contributions to increase from 6 to 12% and from 17 to 34% for the structures with $T_{1(UI)}$ of 0.2 and 1.2 seconds, respectively.

For fixed-base and BI structures with $T_{1(UI)}$ = 0.2 seconds, the first mode contributions of the top-storey shears are still large, i.e. 94% and 120% respectively, although they are accompanied with larger second mode contributions, i.e.: 17% and 48% respectively. For the longer period structures ($T_{1(UI)}$ = 1.2 seconds), the first mode contributions to its top-storey shears become less and the second mode contributions become much more significant. The decrease of the first mode contribution and the increase of the second mode contribution are more enhanced due to the inclusion of a BI system. The fixed-base structure has 78% first mode and 36% second mode contributions to its top-storey shears whereas the BI structure has 59% and 61% for its first and second mode contributions, respectively. The trends of changes of these modal contributions due to the effect of $T_{1(UI)}$ are displayed more clearly in Fig. 5.7 for fixed-base structures and in Fig. 5.8 for BI structures.

5.3.3 THE EFFECT OF PARAMETER VARIATIONS ON A BI SYSTEM

For this purpose of evaluation, the "shear-beam" superstructure model with $T_{1(UI)}$ of 0.4 seconds is considered. The parameters of the BI system, on which this superstructure is mounted, are varied. First, the initial stiffness, k_o is varied from 2.5W/m to 25.0W/m while the post-yield stiffness, αk_o and the yield strength, F_y are kept constant at 1.25W/m and 5%W, respectively. As the value of k_o becomes larger the hysteresis loop widens and therefore the hysteresis loop

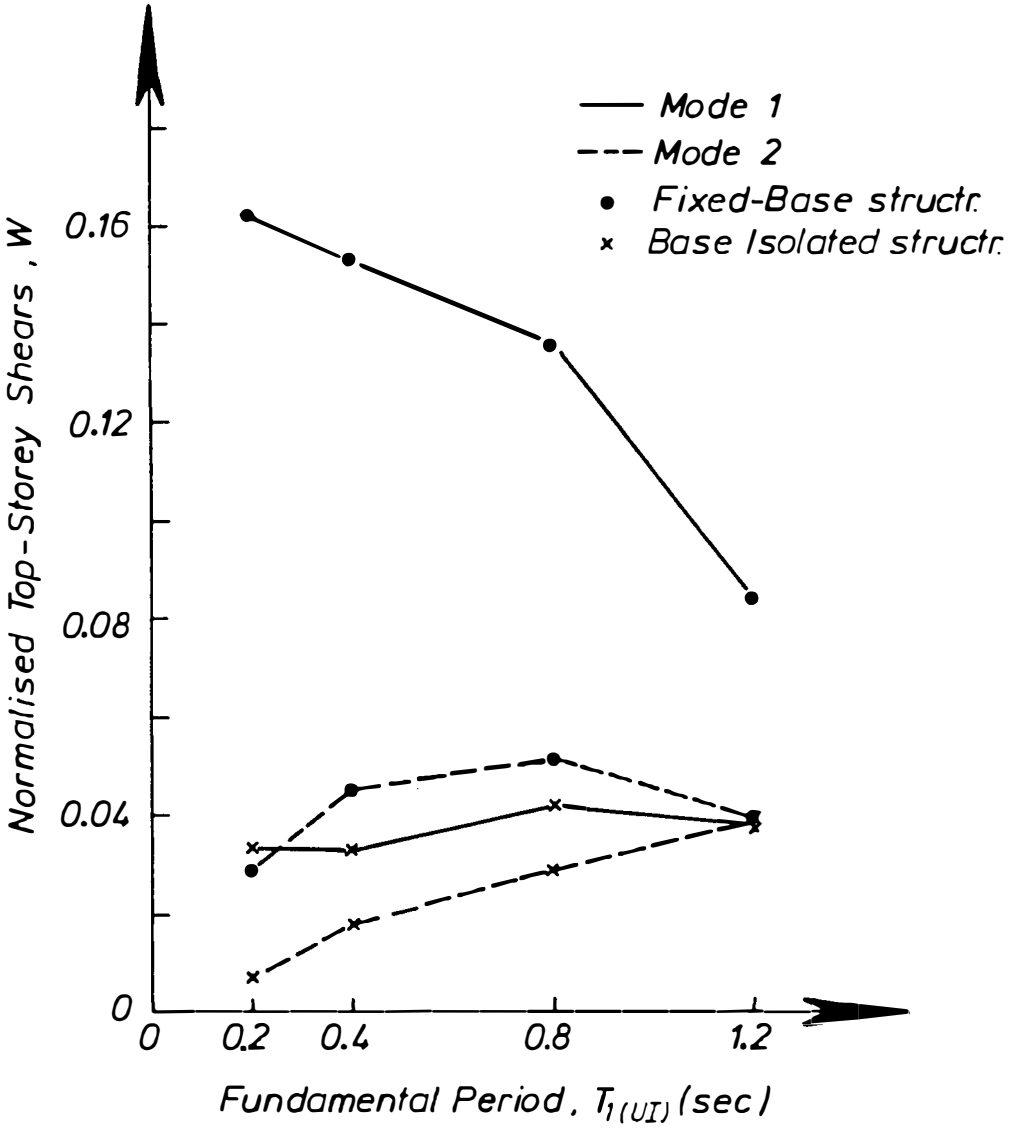

Fig. 5.5 The Effect of BI System in Reducing the Top-Storey Shears of the First and Second Modes

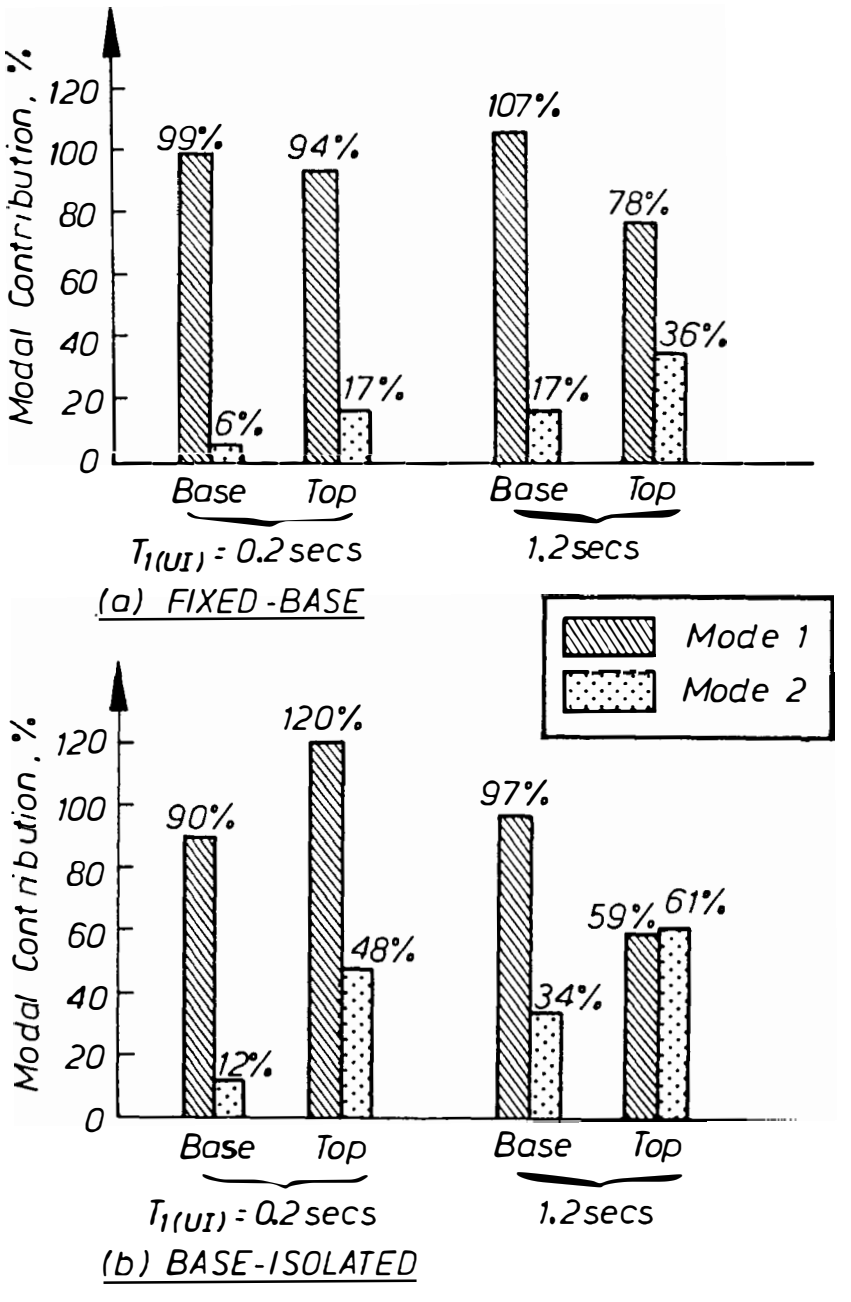

Fig. 5.6 Modal Contributions to Base and Top-Storey Shears of Fixed Base and BI Structures with $T_{1(UI)}$ = 0.2 and 1.2 secs

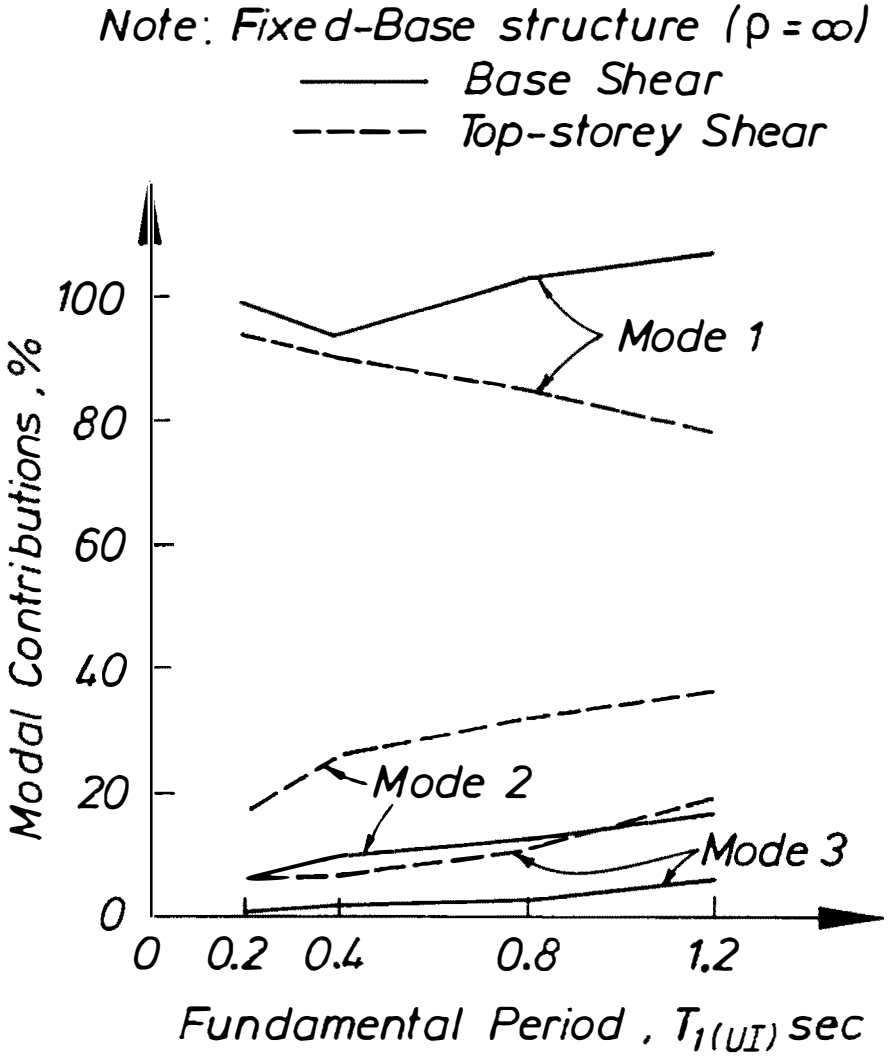

Fig. 5.7 Trends of Changes of Modal Contributions to Base and Top Storey Shears of Fixed-Base 'Shear-Beam' Structures with Different $T_{1(UI)}$

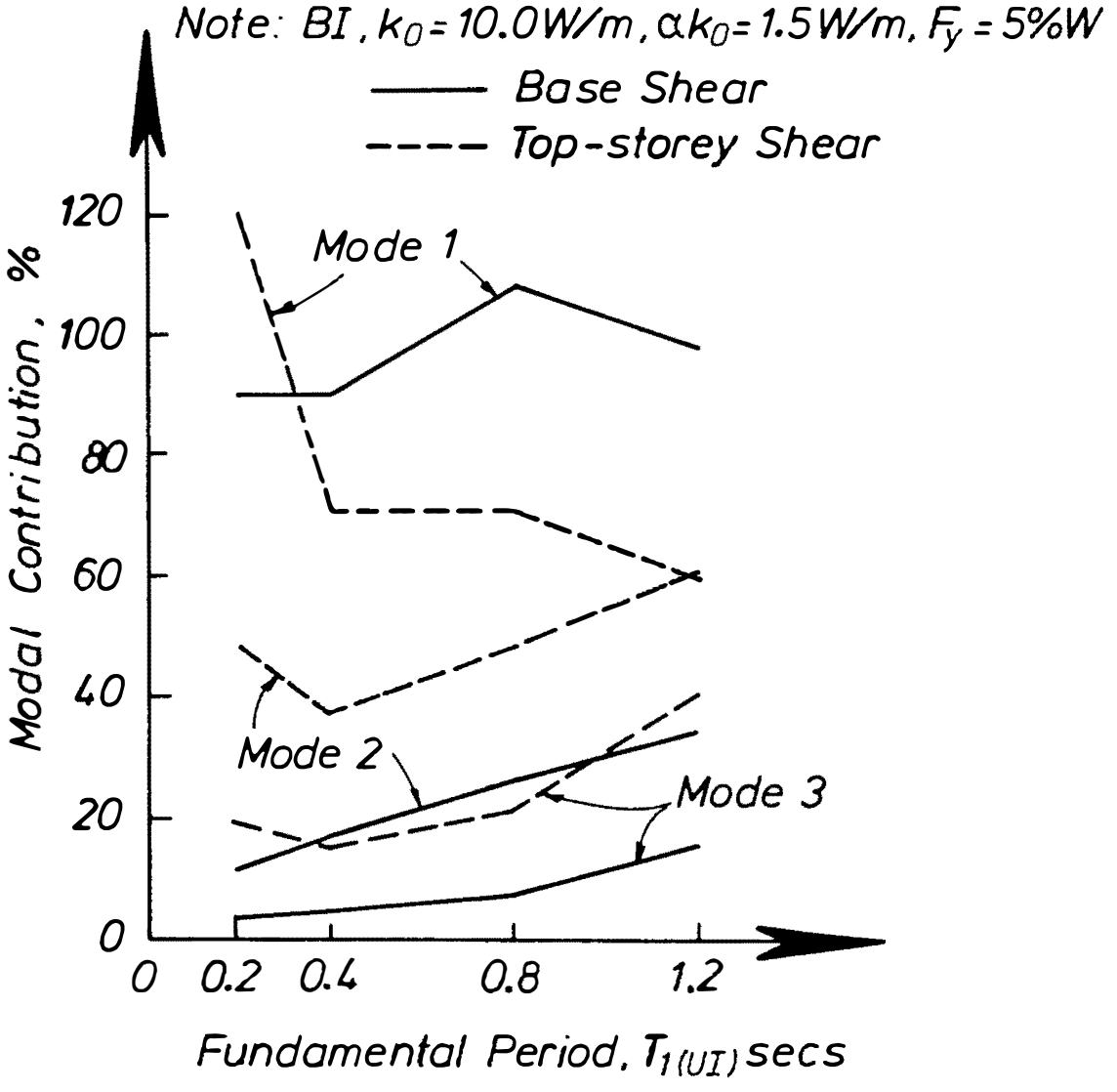

Fig. 5.8 Trends of Changes of Modal Contributions to Base and Top Storey Shears of BI 'Shear-Beam' Structures with Different $T_{1(UI)}$

ratio, R increases. As was discussed in Section 4.5, a BI structure with a large value of R has a more bulged storey shear envelope than one with a small R or thin hysteresis loops.

The effect of varying k_o on the modal storey shears is shown in Table 5.7. The first modal storey shears increase only 31% as k_o is varied from 2.5 to 25.0 W/m, whereas the second and third modal storey shears increase 147% and 205%, respectively. By contrasting these modal storey shears with the corresponding values of the fixed-base structure ($T_{1(UI)}$ = 0.4 secs) listed in Table 5.5, it can be observed that for a BI structure with thin hysteresis loops (k_o = 2.5 W/m and R = 0.15) all modal storey shears are reduced almost equally, i.e. 4.9, 4.6, and 3.6 times for the first, second, and third modes, respectively. For BI structures with fatter hysteresis loops (ko = 25.0 W/m or R = 0.38), the first modal storey shears are reduced 3.75 times whereas the second and third modal storey shears are only reduced 1.9 and 1.2 times, respectively.

The trends of changes of their modal contributions to the total response are displayed in Fig. 5.9. Each value is obtained as the percentage of the modal response from its corresponding total value tabulated in Table 5.7. For the base shears, it is obvious that the first mode contributions are very dominant since they vary around 90 to 103% accompanied by the second and third mode contributions which are only 9.6 to 21% and 2.2 to 6% of the total response, respectively. For top storey shears, however, the first mode contribution considerably decreases from 120 to 66% as k_o increases from 2.5 W/m to 10.0 W/m. As a contrast, the second and third mode contributions to the total top storey shears, i.e. 40% and 15% respectively, are hardly affected by the variation of the initial stiffness, k_o.

In the second step of this evaluation, αk_0 is varied from 0.5 to 2.5W/m while k_o and F_y are kept constant at 10.0W/m and 5%W, respectively. It has been realised that as αk_0 decreases the hysteresis loop becomes fatter and the value of R increases and the storey shear envelope tends to be more bulged.

From Table 5.8 it can be observed that the first modal storey shear becomes 7% less and 32% larger as αk_o varies from 0.5W/m to 1.5 and 2.5W/m, respectively. It is also important to note that, unlike the case when k_o is varied, the storey shears of the higher modes do not vary significantly. The second mode storey shears differ by less than 17% as αk_o varies from 0.5 to 2.5W/m.

The other aspect which should also be evaluated is how these modal storey shears contribute to the corresponding total responses. Fig. 5.10 shows the trends of changes of the modal contributions to base and top-storey shears. Similar effect as discussed earlier is also found in this case. The first mode contribution to the top-storey shears increases from 68% to 103% as the hysteresis loop becomes thinner or as αk_o increases from 0.5 to 2.5 W/m, whereas the second and third mode contributions are found almost at 40% and around 15% respectively. The base shears are strongly dominated by the first mode.

Table 5.7 The Effect of Varying k_o on the Modal Contributions to Storey Shears

k_o	R	Storey	Max. Storey Shears (kN) obtained from ISODYN				RUAUMOKO
			Mode 1	Mode 2	Mode 3	Total	Total
2.5	0.15	4	124.6	38.0	13.4	103.5	106.9
		3	234.1	38.0	46.5	205.6	209.5
		2	315.4	0.0	11.8	303.0	308.4
		1	358.7	38.0	8.7	396.0	396.7
		BI	-	-	-	486.2	479.4
5.0	0.28	4	134.6	62.5	22.0	138.2	149.5
		3	253.1	62.5	76.3	245.2	274.0
		2	340.9	0.0	19.3	333.0	351.7
		1	387.7	62.5	14.3	401.8	398.0
		BI	-	-	-	453.6	451.8
10.0	0.35	4	131.3	76.8	31.0	198.9	195.6
		3	246.7	76.8	10.8	324.6	317.3
		2	332.4	0.0	27.3	341.3	335.8
		1	378.0	76.8	20.2	393.8	375.2
		BI	-	-	-	448.7	447.8
25.0	0.38	4	162.8	94.0	40.7	243.1	244.6
		3	306.0	94.0	14.1	387.9	407.0
		2	412.2	0.0	35.8	402.1	414.9
		1	468.8	94.0	26.6	452.9	434.8
		BI	-	-	-	471.5	482.6

Note: $T_{1(UI)}$ = 0.4 secs.

ρ = ∞

αk_o = 1.25 W/m

W = 4000 kN

Fy = 5%W

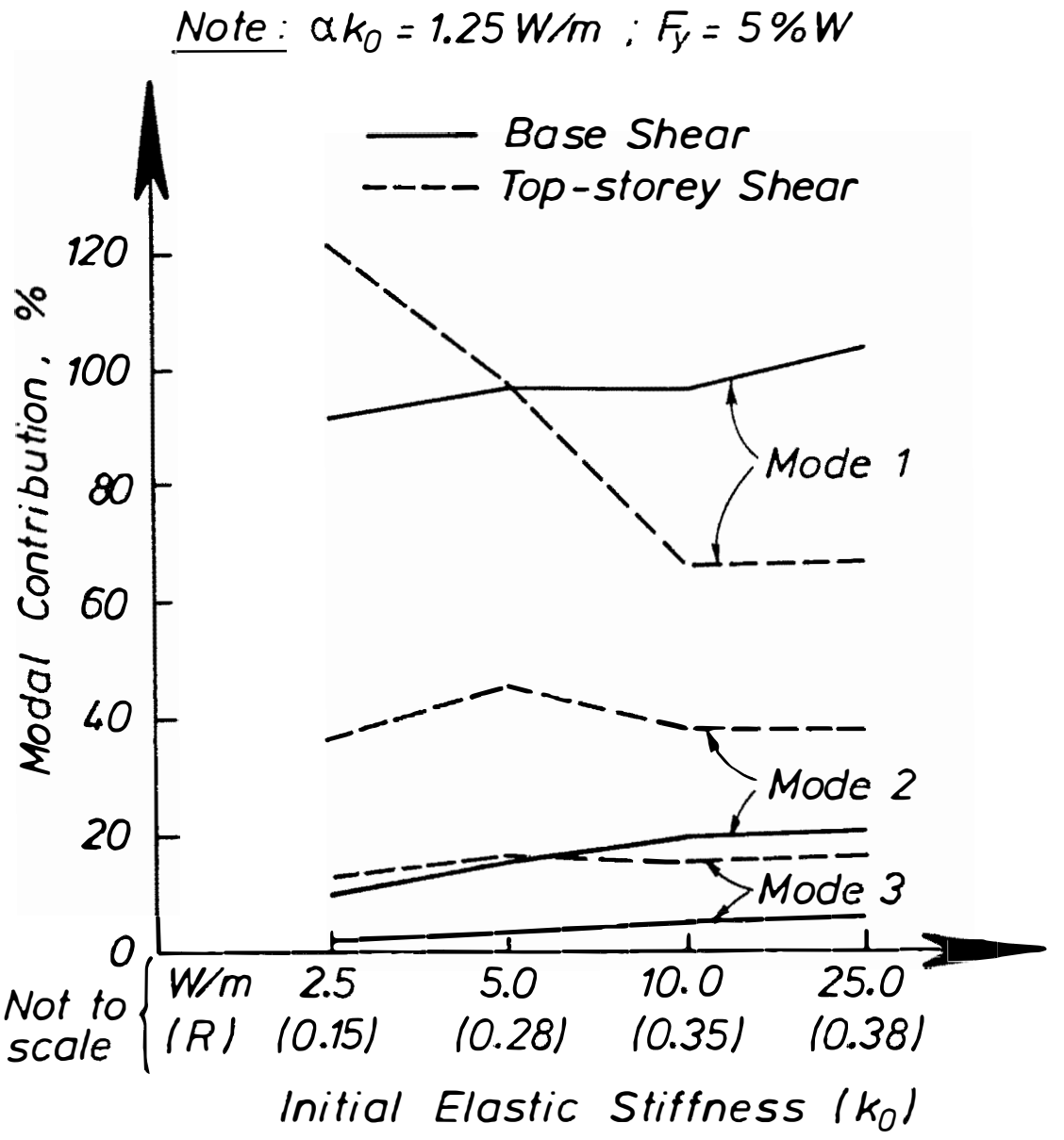

Fig. 5.9 The Effect of Varying k_0 on the Modal Contributions to Base and Top-Storey Shears

Table 5.8 The Effect of Varying αk_o on the Modal Contributions to Storey Shears

αk_o	R	Storey	Max. Storey Shears (kN) obtained from ISODYN				RUAUMOKO
			Mode 1	Mode 2	Mode 3	Total	Total
0.5	0.55	4	142.3	77.9	29.8	210.0	223.6
		3	267.5	77.9	10.3	345.8	364.5
		2	360.4	0.0	26.2	373.2	383.9
		1	409.8	77.9	19.4	342.3	318.9
		BI	-	-	-	318.1	318.1
1.5	0.31	4	132.1	70.2	28.1	188.7	190.9
		3	248.4	70.2	9.7	304.2	308.1
		2	334.6	0.0	24.7	324.8	348.7
		1	380.5	70.2	18.3	423.0	410.3
		BI	-	-	-	495.1	494.4
2.5	0.26	4	188.3	64.8	30.1	176.0	185.3
		3	353.9	64.8	10.5	316.1	332.6
		2	476.8	0.0	26.5	458.6	447.9
		1	542.2	64.8	19.7	609.2	587.9
		BI	-	-	-	744.0	735.4

Note: $T_{1(UI)}$ = 0.4 secs.

ρ = ∞

k_o = 10.0W/m

W = 4000 kN

Fy = 5%W

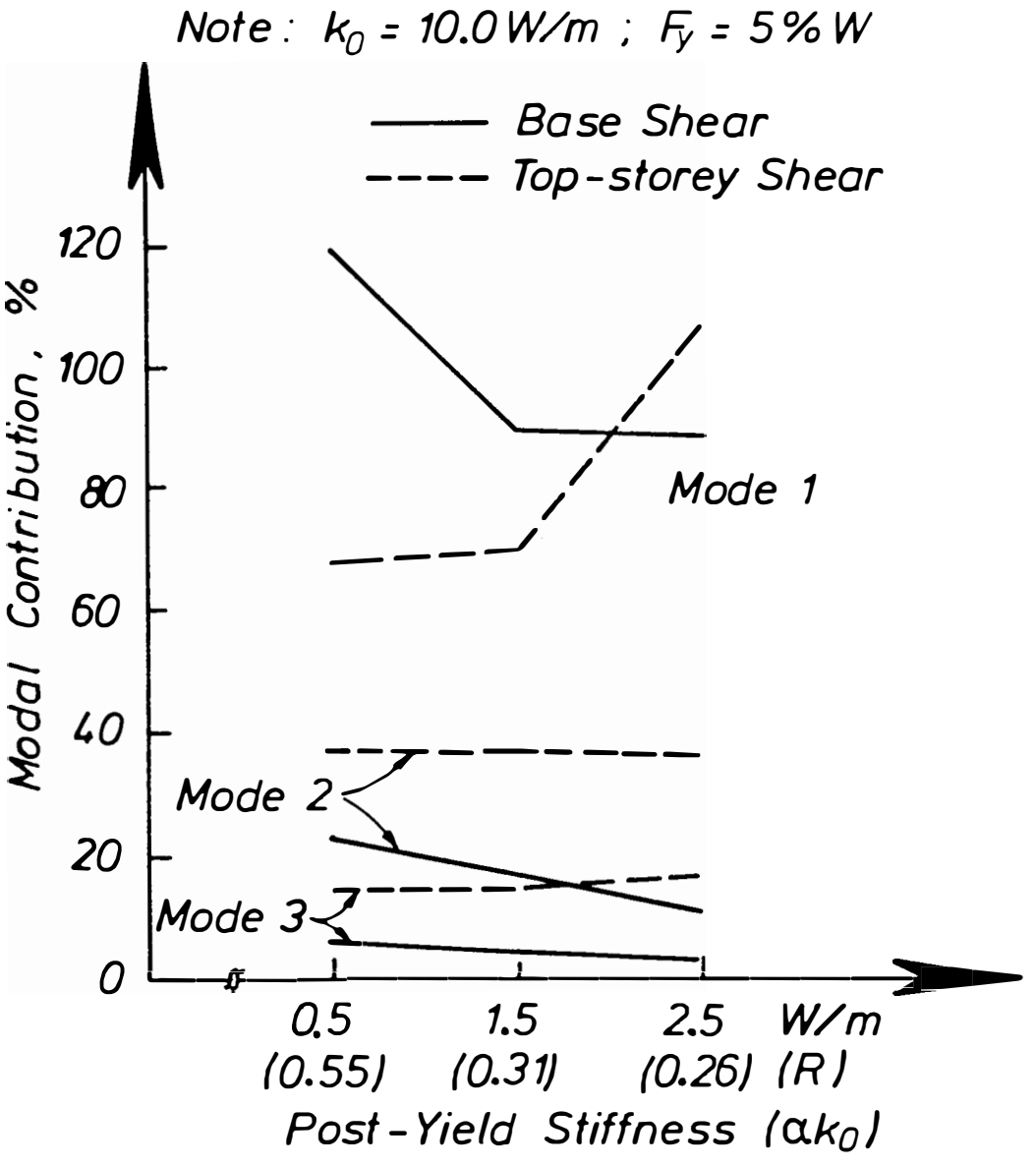

Fig. 5.10 The Effect of Varying αk_0 on the Modal Contributions to Base and Top-Storey Shears

It is also informative to study the effect of varying the yield strength on the modal storey shears. For this purpose, a BI system with k_o of 10.0W/m and αk_o of 1.5W/m is chosen. Its yield strength, F_y is varied from 3% to 10%W. Their modal and total responses are listed in Table 5.9. As has been indicated in Section 4.5, BI systems with larger F_y have fatter hysteresis loops and cause more bulged storey shear envelopes than BI systems with smaller F_y.

From Table 5.9 it is observed that the first, second, and third modal storey shears increase 73%, 117%, and 106% respectively as F_y increases from 3 to 10%W, whereas, as shown in Fig. 5.11, the first mode contribution to the top storey shears are found constant at around 40% and 15% respectively irrespective of F_y. In all cases, the base shears are strongly governed by the first mode.

Note that the total responses tabulated in Tables 5.7, 5.8 and 5.9 are consistently in a good agreement with the inelastic time history analysis results obtained from the computer program RUAUMOKO.

5.3.4 THE EFFECT OF VISCOUS DAMPING OF THE BI SYSTEM

It has been mentioned in Section 5.2.2, that the use of the Component Mode Synthesis method enables the computer program ISODYN to analyse the modal responses of a multistorey structure isolated by a BI system which consists of an "elastic spring" and a velocity-dependent dashpot. In this system, the elastic spring provides the horizontal flexibility and the dashpot supplies a certain amount of viscous damping which may be much greater than the amount of the superstructure's equivalent viscous damping.

Table 5.10 lists the modal and total storey shears of a "shear-beam" structure with $T_{1(UI)}$ = 0.4 secs mounted on two series of this type of BI system. The stiffness of the "elastic spring" in the first series is 5.0W/m whereas in the second series is 1.5 W/m. The amount of viscous damping supplied by the dash-pot in each series is varied from 5% to 40% of the critical damping.

It can be seen in Table 5.10, that the base shear of a structure mounted on a BI system with an elastic stiffness of 5.0W/m and a viscous damping of 5% critical is almost as large as the base shear of the corresponding fixed-base structure. Its upper storey shears, however, are smaller than the upper storey shears of the fixed-base structure which means that it has a less bulged storey shear envelope compared to the shear envelope of the fixed-base structure. It is also found that the increase of the viscous damping reduces the storey shears almost equally. Further reduction can be obtained by using a more flexible "elastic spring".

In Chapter 4, it has been demonstrated that the deformation and the shear force of a displacement-dependent BI system which behaves inelastically can be approximated based on its effective secant stiffness and its additional hysteretic damping. It is therefore worthwhile to

Table 5.9 The Effect of Varying F_y on the Modal Contributions to Storey Shears

F_y/W (%)	R	Storey	Max. Storey Shears (kN) obtained from ISODYN				RUAUMOKO
			Mode 1	Mode 2	Mode 3	Total	Total
3.0	0.20	4	125.6	51.7	22.9	129.9	138.2
		3	236.1	51.7	7.9	217.9	247.6
		2	318.1	0.0	20.1	310.0	329.2
		1	361.7	51.7	14.9	389.1	384.3
		BI	-	-	-	471.9	471.8
5.0	0.31	4	132.1	70.2	28.1	188.7	190.9
		3	248.4	70.2	9.7	304.2	308.1
		2	334.6	0.0	24.7	324.8	348.7
		1	380.5	70.2	18.3	423.0	410.3
		BI	-	-	-	495.1	494.4
7.0	0.37	4	168.3	92.3	39.1	250.0	251.7
		3	316.2	92.3	13.6	403.3	401.9
		2	422.2	0.0	34.3	433.9	428.8
		1	484.5	92.3	25.5	471.9	457.4
		BI	-	-	-	551.0	552.2
10.0	0.42	4	217.3	112.3	47.1	306.1	325.1
		3	408.3	112.3	16.4	512.7	534.6
		2	550.2	0.0	41.4	561.1	556.4
		1	625.6	112.3	30.7	558.5	561.0
		BI	-	-	-	640.6	637.2

Note: $T_{1(UI)}$ = 0.4 secs.

ρ = ∞

αk_o = 1.5 W/m

W = 4000 kN

Fy = 5%W

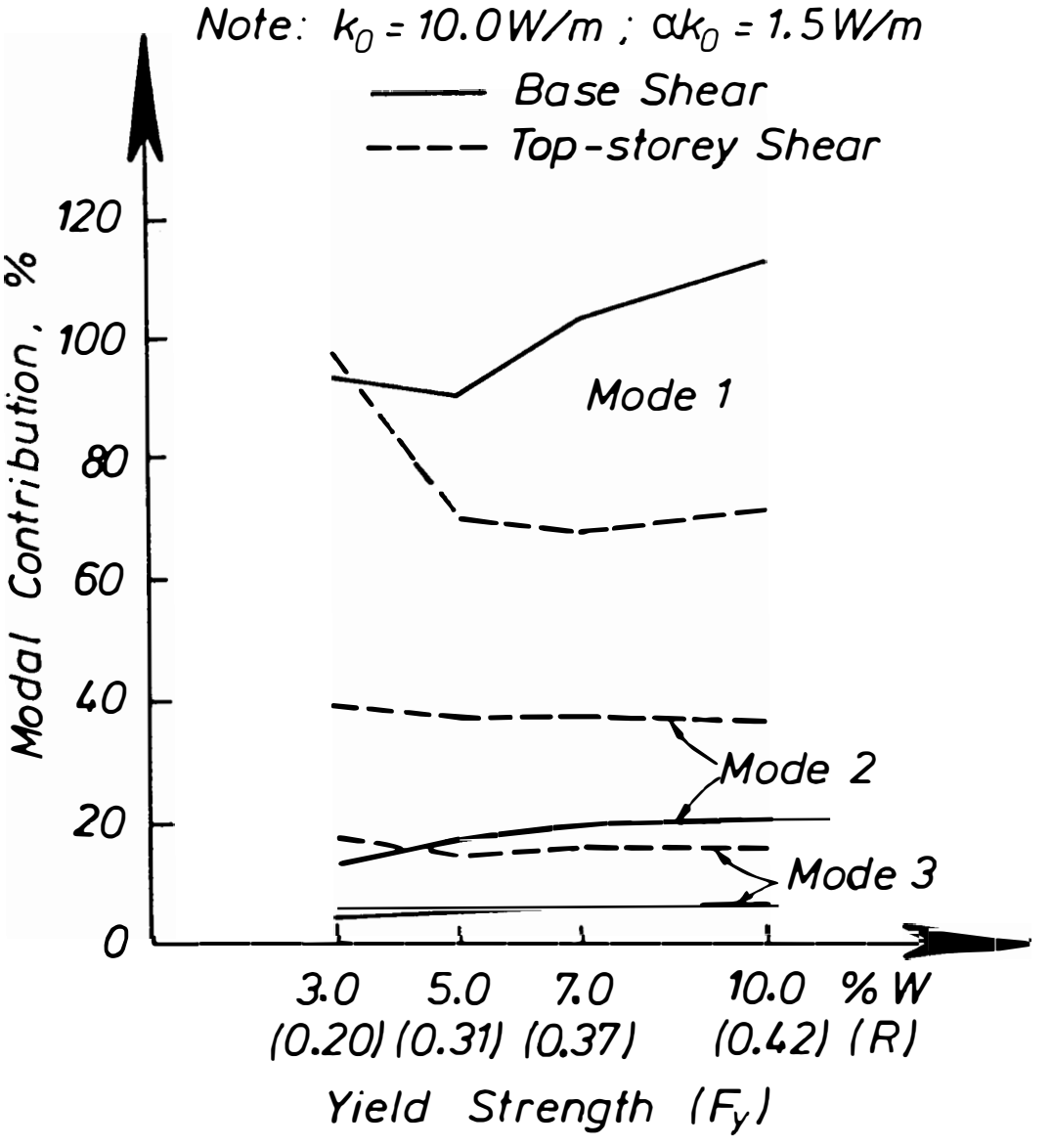

Fig. 5.11 The Effect of Varying F_y on the Modal Contributions to Base and Top-Storey Shears

Table 5.10 The Effect of Viscous Damping of BI System on the Storey Shears

k (W/m)	λ (% crit.)	Storey	Mode 1 (kN)	Mode 2 (kN)	Mode 3 (kN)	Total (kN)
		4	585.7	145.5	49.9	478.7
		3	1100.9	145.5	17.3	955.4
	5.0	2	1483.2	0.0	43.9	1427.0
		1	1686.6	145.5	32.6	1868.9
		BI	-	-	-	2257.2
		4	404.6	104.7	36.3	351.5
		3	760.3	104.7	12.6	682.7
	10.0	2	1024.4	0.0	31.9	986.6
		1	1164.9	104.7	23.7	1290.2
5.0		BI	-	-	-	1564.1
		4	293.5	91.7	29.3	283.3
		3	551.5	91.7	10.2	526.8
	25.0	2	743.1	0.0	25.8	722.2
		1	845.0	91.7	19.1	913.9
		BI	-	-	-	966.7
		4	313.6	94.4	27.4	311.6
		3	589.5	94.4	9.5	586.9
	40.0	2	794.2	0.0	24.1	796.2
		1	903.1	94.4	16.9	923.5
		BI	-	-	-	687.0
		4	192.9	49.7	18.0	158.1
		3	362.5	49.7	6.2	315.1
	5.0	2	488.4	0.0	15.8	468.3
		1	555.3	49.7	11.7	616.2
		BI	-	-	-	754.7
		4	161.3	42.6	15.4	132.9
		3	303.2	42.6	5.3	262.2
	10.0	2	408.5	0.0	13.6	391.1
		1	464.5	42.6	10.1	517.9
1.50		BI	-	-	-	628.5
		4	133.1	42.4	14.3	115.8
		3	250.1	42.4	5.0	221.1
	25.0	2	337.0	0.0	12.6	322.7
		1	383.2	42.4	9.3	432.4
		BI	-	-	-	469.0
		4	126.4	48.7	14.9	114.6
		3	237.6	48.7	5.2	221.5
	40.0	2	320.2	0.0	13.1	314.9
		1	364.1	48.7	9.7	413.8
		BI	-	-	-	385.5
		4	611.4	179.8	48.7	678.1
		3	1149.1	179.8	16.9	1173.8
Fixed-Base		2	1548.2	0.0	42.8	1550.5
		1	1760.5	179.8	31.8	1863.0

Note: $T_{1(UI)} = 0.4$ secs

$\rho = \infty$

compare the responses of a structure, first, mounted on a displacement-dependent BI system and second, on a velocity-dependent BI system which has similar properties as the first-system's equivalent linear properties. Table 5.11 shows this comparison. With fat hysteresis loops, the first BI system has an effective secant stiffness of 1.24W/m and additional hysteretic damping of 35% critical, meaning a total damping of 40% critical since the initial equivalent viscous damping is assumed to be 5% critical. The second system has an elastic stiffness and a viscous damping value of 1.25W/m and 40% critical, respectively.

From Table 5.11, it can be seen that the differences of the base displacements and the BI system shear forces between the two systems are only around 14%. In the top storey, however, the shears differ much by a much larger, i.e. 93%. With the same (effective) stiffness and amount of damping the first system tends to have a more significant second mode contribution and thus a more bulged storey-shear envelope when compared with a structure on the second elastic BI system.

Figs. 5.12.a and 5.12.b show the trends of changes of the modal contributions in the base and top-storey shears due to the inclusion of the velocity-dependent BI system, with elastic stiffness of 5.0W/m and 1.5W/m, respectively. It is obvious that the structural responses are always strongly dominated by their first modes.

5.3.5 THE EFFECT OF SUPERSTRUCTURE'S FRAME ACTION

It has been shown in Section 4.6 that BI structures with different beam-to-column stiffness ratios may have different storey shear envelopes especially when the BI system has fat hysteresis loops. It is informative, therefore, to evaluate the modal storey shears of these structures.

In this evaluation the modal storey shears of four-storey fixed-base and BI structures with "cantilever-beam" and "shear-beam" superstructure models are compared. The "cantilever-beam" model has a beam-to-column stiffness ratio, $\rho = 0.0$ whereas the "shear-beam" model has a $\rho = \infty$. The fundamental period of these structures on a fixed-base is varied from 0.2 to 1.2 seconds. The other modal properties have been described earlier in Section 4.6. The considered BI system has fat hysteresis loops (R = 0.55), i.e.: with an initial stiffness, k_o of 10.0W/m, a post-yield stiffness, αk_o of 0.5W/m and a yield strength, F_y of 5%W.

The normalized modal and total storey shears of the fixed-base and BI structures are listed in Tables 5.12 and 5.13, respectively. Note, structures with different beam-to-column stiffness ratios have different mode shapes. Because of these mode shapes, each type of structure has its unique modal storey shears and structures with $\rho = 0.0$ tend to have more bulged storey shear envelopes than structures with $\rho = \infty$. In BI structures, however, the "shear-beam" type structure may have more bulged storey shear envelopes than the "cantilever-beam" type structures, as can be seen for

Table 5.11 Comparisons Between the Effects of "Displacement-Dependent" and "Velocity-Dependent" BI systems on the Storey Shears and Displacements

(1) $k_o = 10.0\,W/m$ $\alpha = 0.05$ $F_y = 5\%W$

Storey	Storey Shears (kN)				
	Mode 1	Mode 2	Mode 3	Base	Total
4	142.3	77.9	29.8	-	209.9
3	267.5	77.9	10.3	-	345.8
2	360.4	0.0	26.2	-	373.2
1	409.8	77.9	19.4	-	342.3
BI	-	-	-	318.1	318.1
Storey	**Storey Displacements (mm)**				
	Mode 1	Mode 2	Mode 3	Base	Total
4	5.76	0.46	0.07	64.04	68.40
3	6.18	0.00	0.10	64.04	67.95
2	4.59	0.46	0.04	64.04	67.03
1	2.44	0.46	0.11	64.04	65.69
BI	-	-	-	64.04	64.04

(2) $k_o = 10.0\,W/m$ $\alpha = 0.05$ $F_y = 5\%W$

Storey	Storey Shears (kN)				
	Mode 1	Mode 2	Mode 3	Base	Total
4	122.5	43.9	13.9	-	109.0
3	230.2	43.9	4.8	-	211.2
2	310.2	0.0	12.3	-	301.1
1	352.7	43.9	9.1	-	403.8
BI	-	-	-	363.0	363.0
Storey	**Storey Displacements (mm)**				
	Mode 1	Mode 2	Mode 3	Base	Total
4	6.05	0.26	0.03	72.60	77.59
3	5.32	0.00	0.05	72.60	77.02
2	3.95	0.26	0.02	72.60	75.93
1	2.10	0.26	0.05	72.60	74.43
BI	-	-	-	72.60	72.60

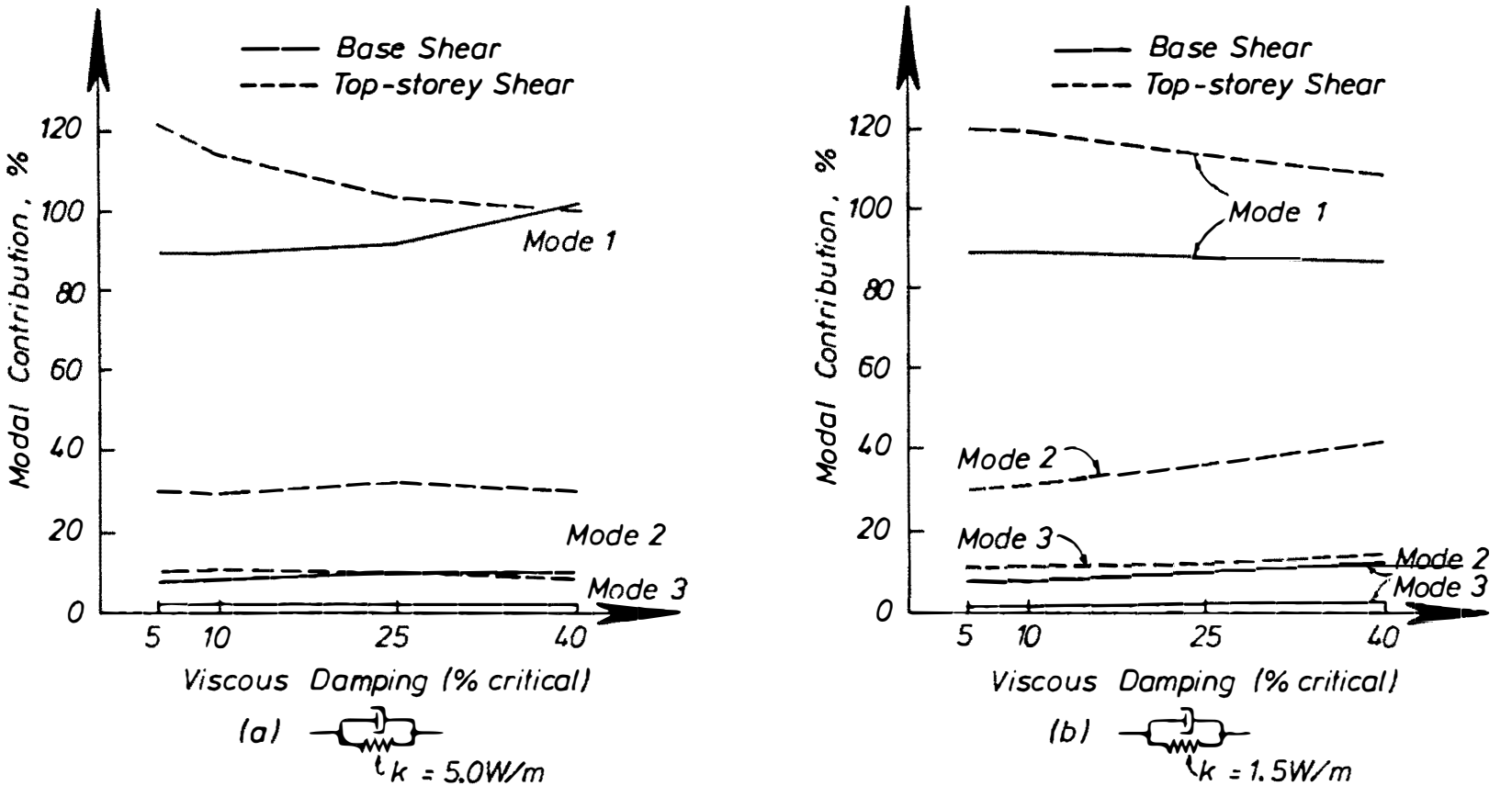

Fig. 5.12 The Effect of Varying the Viscous Damping of the BI System on the Modal Contributions to Base and Top-Storey Shears

Table 5.12 Normalized Modal and Total Storey Shears of Fixed-Base Structures with Different ρ

(a) "Cantilever-Beam" Structures, ρ = 0.0

$T_{1(UI)}$ secs	Storey	Max. Normalized Storey Shears (in W)			
		Mode 1	Mode 2	Mode 3	Total
0.2	4	0.1804	0.0325	0.0106	0.1870
	3	0.2971	0.0081	0.0136	0.2971
	2	0.3563	0.0365	0.0052	0.3591
	1	0.3730	0.0591	0.0196	0.3939
0.4	4	0.1633	0.0433	0.0106	0.1641
	3	0.2689	0.0109	0.0136	0.2627
	2	0.3225	0.0487	0.0052	0.3317
	1	0.3376	0.0788	0.0196	0.3690
0.8	4	0.1497	0.0638	0.0137	0.1743
	3	0.2465	0.0160	0.0175	0.2418
	2	0.2956	0.0717	0.0068	0.3369
	1	0.3095	0.1161	0.0254	0.3839
1.2	4	0.0906	0.0625	0.0130	0.1119
	3	0.1492	0.0157	0.0166	0.1541
	2	0.1789	0.0702	0.0064	0.1878
	1	0.1873	0.1137	0.0024	0.2099

Note : $T_{1(UI)}$ = 0.2 secs W = 2000 kN
0.4 secs 4000 kN
0.8 secs 4500 kN
1.2 secs 6000 kN

(b) "Shear-Beam" Structures, ρ = ∞

$T_{1(UI)}$ secs	Storey	Max. Normalized Storey Shears (in W)			
		Mode 1	Mode 2	Mode 3	Total
0.2	4	0.1619	0.0293	0.0101	0.1720
	3	0.3044	0.0293	0.0353	0.3046
	2	0.4101	0.0000	0.0089	0.4037
	1	0.4663	0.0293	0.0066	0.4703
0.4	4	0.1528	0.0449	0.0122	0.1695
	3	0.2873	0.0449	0.0042	0.2934
	2	0.3870	0.0000	0.0107	0.3876
	1	0.4401	0.0449	0.0079	0.4657
0.8	4	0.1361	0.0511	0.0170	0.1605
	3	0.2558	0.0511	0.0059	0.2828
	2	0.3446	0.0000	0.0149	0.3509
	1	0.3919	0.0511	0.0111	0.3791
1.2	4	0.0840	0.0392	0.0202	0.1084
	3	0.1580	0.0392	0.0062	0.1824
	2	0.2140	0.0000	0.0178	0.2168
	1	0.2434	0.0392	0.0132	0.2276

Note : $T_{1(UI)}$ = 0.2 secs W = 2000 kN
0.4 secs 4000 kN
0.8 secs 8000 kN
1.2 secs 17500 kN

Table 5.13 Normalized Modal and Total Storey Shears of BI Structures with Different ρ

(a) "Cantilever-Beam" Structures, ρ = 0.0

$T_{1(UI)}$ secs	Storey	Max. Normalized Storey Shears (in W)			
		Mode 1	Mode 2	Mode 3	Total
0.2	4	0.0376	0.0126	0.0041	0.0374
	3	0.0619	0.0031	0.0053	0.0619
	2	0.0743	0.0142	0.0020	0.0750
	1	0.0777	0.0230	0.0077	0.0786
	BI	-	-	-	0.0768
0.4	4	0.0411	0.0163	0.0049	0.0459
	3	0.0677	0.0041	0.0063	0.0700
	2	0.0811	0.0184	0.0024	0.0798
	1	0.0849	0.0297	0.0091	0.0844
	BI	-	-	-	0.0784
0.8	4	0.0524	0.0225	0.0064	0.0627
	3	0.0864	0.0056	0.0082	0.0916
	2	0.1036	0.0253	0.0031	0.0981
	1	0.1084	0.0410	0.0118	0.0932
	BI	-	-	-	0.0774
1.2	4	0.0420	0.0366	0.0089	0.0624
	3	0.0693	0.0092	0.0115	0.0755
	2	0.0831	0.0413	0.0044	0.0814
	1	0.0869	0.0668	0.0166	0.0809
	BI	-	-	-	0.0771

Note : $T_{1(UI)}$ = 0.2 secs W = 2000 kN
0.4 secs 4000 kN
0.8 secs 4500 kN
1.2 secs 6000 kN

BI System: k_o = 10.0 W/m, αk_o = 0.5 W/m, F_y = 5%W

(b) "Shear-Beam" Structures, ρ = ∞

$T_{1(UI)}$ secs	Storey	Max. Normalized Storey Shears (in W)			
		Mode 1	Mode 2	Mode 3	Total
0.2	4	0.0280	0.0150	0.0057	0.0333
	3	0.0526	0.0150	0.0020	0.0495
	2	0.0708	0.0000	0.0050	0.0654
	1	0.0805	0.0150	0.0037	0.0729
	BI	-	-	-	0.0787
0.4	4	0.0356	0.0195	0.0074	0.0525
	3	0.0669	0.0195	0.0026	0.0864
	2	0.0901	0.0000	0.0065	0.0933
	1	0.1024	0.0195	0.0048	0.0856
	BI	-	-	-	0.0795
0.8	4	0.0378	0.0273	0.0144	0.0576
	3	0.0711	0.0273	0.0050	0.0889
	2	0.0958	0.0000	0.0126	0.0954
	1	0.1089	0.0273	0.0094	0.0926
	BI	-	-	-	0.0778
1.2	4	0.0331	0.0371	0.0258	0.0608
	3	0.0623	0.0371	0.0089	0.0809
	2	0.0839	0.0000	0.0228	0.0886
	1	0.0954	0.0371	0.0168	0.0980
	BI	-	-	-	0.0830

Note : $T_{1(UI)}$ = 0.2 secs W = 2000 kN
0.4 secs 4000 kN
0.8 secs 8000 kN
1.2 secs 17500 kN

BI System: k_o = 10.0 W/m, αk_o = 0.5 W/m, F_y = 5%W

example in Table 5.13. (or more clearly in Fig. 4.51.b of Section 4.6) for structures with $T_{1(UI)}$ = 0.4 secs.

The above phenomenon can be explained in part by the fact that the inclusion of a BI system does not reduce the higher mode storey shears of structures with $\rho = \infty$ as much as the higher mode storey shears of structures with ρ = 0.0. Because of this fact, the ratios of these higher mode storey shears to the first mode storey shears of structures with $\rho = \infty$ are much higher when compared with the same ratios for structures with ρ = 0.0, especially in the top storey as shown in dashed lines in Fig. 5.13. This increased influence of the higher mode responses in the upper storey levels of structures with $\rho = \infty$ causes their storey shear envelopes to be more bulged. Another aspect which is much more difficult to visualize is how these modal contributions are combined. The individual modal responses during the ground motion may neither be perfectly in phase nor out of phase to each other.

5.3.6 THE EFFECT OF BASE MASS

In Section 4.7.2, it has been pointed out that the base mass of a BI structure has an influence on the degree of buldge of the storey shear envelope. It is worthwhile therefore to evaluate the likely modal contributions to the base and top-storey shears as the base mass is varied from 0.1 to 0.4 of total mass of the structure. For this purpose, a four storey "shear-beam" structure with $T_{1(UI)}$ of 0.4 seconds and mounted on a BI system with k_0 = 10.0W/m, αk_0 = 1.5W/m and F_y = 5%W is selected as the structure model. Note, in this model a base mass equal to 0.2 of total mass represents a structure with a uniformly distributed mass throughout its height.

Fig. 5.14 shows the trends of change of the modal contributions to the base and top-storey shears of BI structures with different base masses. It is found, in general, that the first mode contributions tend to increase, whereas the higher mode contributions tend to decrease as the base mass becomes larger. This indicates that the first mode contributions become more dominant and therefore the storey shear envelope is less bulge in structures with larger base masses (see also Fig.4.56.b). The first mode contribution to the top-storey shear, however, is found to decrease as the base mass increases from 0.1 to 0.2 of total mass. This is because the uniform structure with a base mass of 0.2 of total mass has a more bulged storey shear envelope than the one with a base mass of 0.1 of total mass.

Table 5.14 shows the modal storey shears of the above structures. The total responses are shown to be in good agreement with the inelatic time history analysis results obtained from the computer program RUAUMOKO.

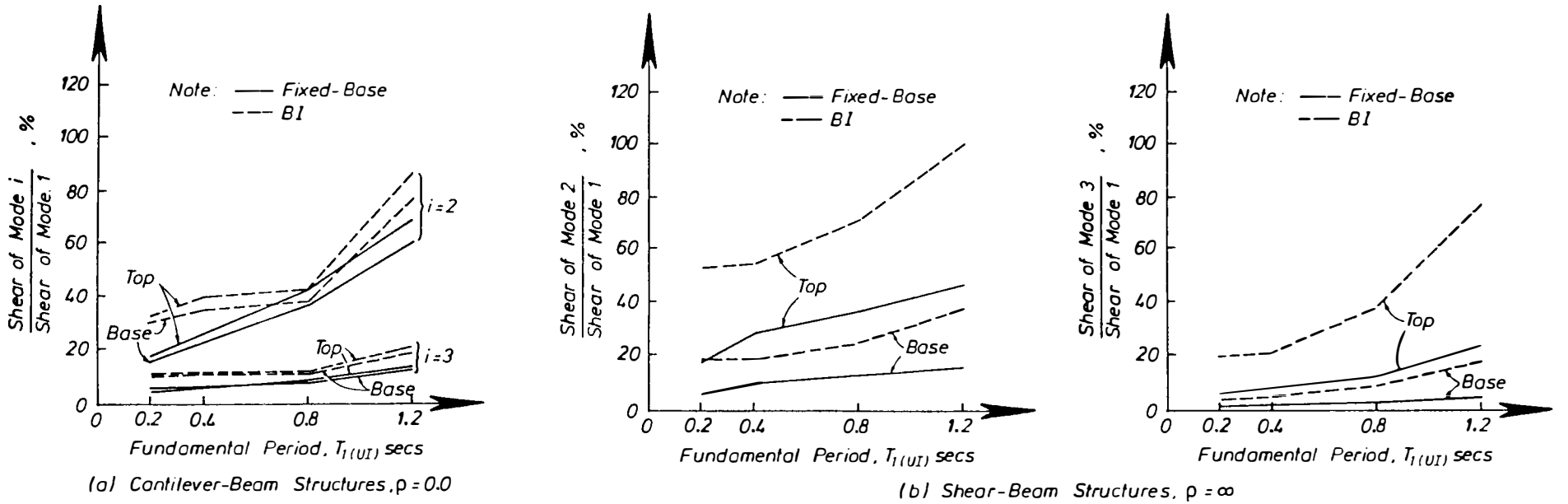

Fig. 5.13 The Effect of BI System in Altering the Ratios of the Higher Mode Shears to the First Mode Shears

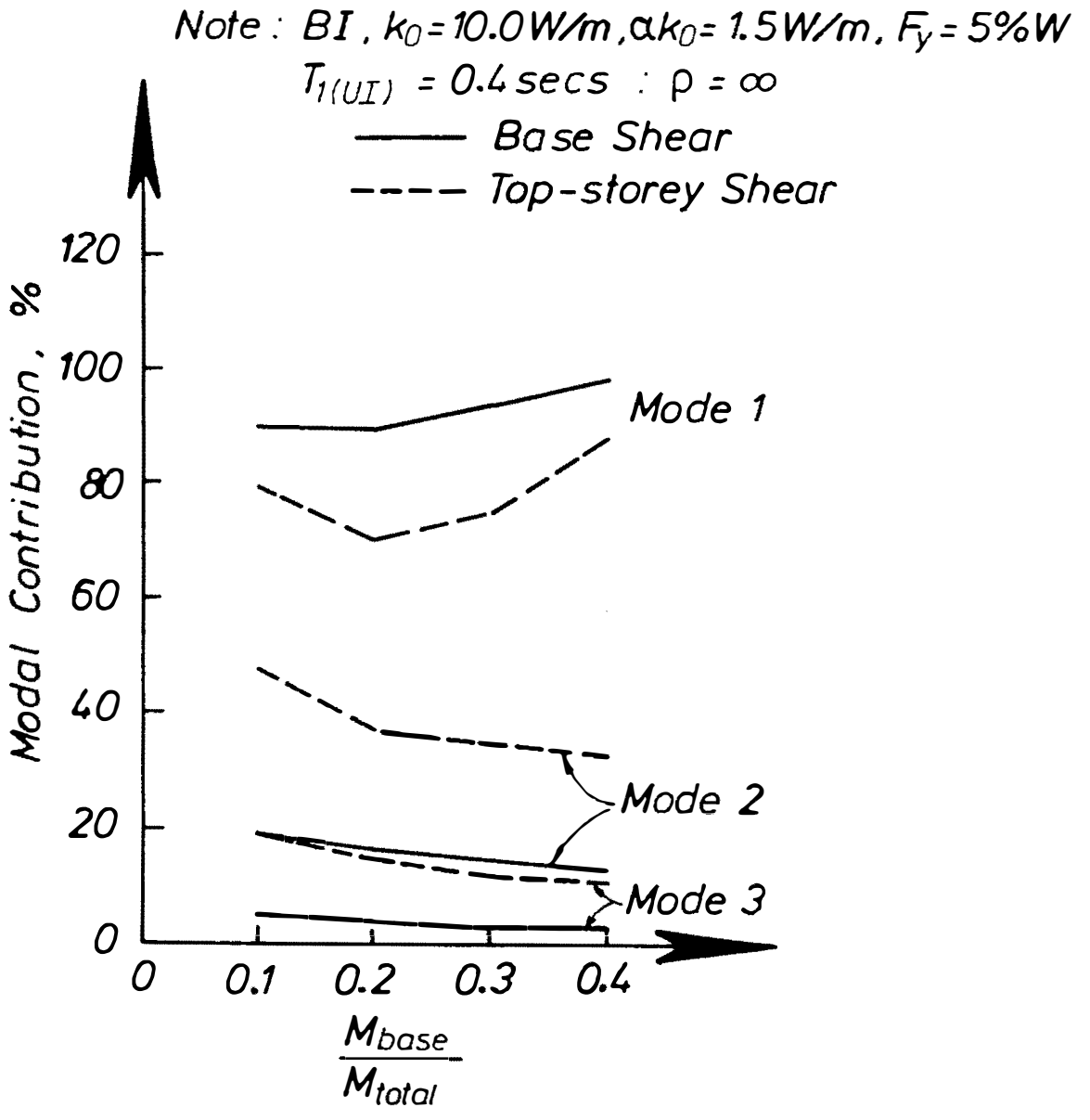

Fig. 5.14 Trends of Changes of the Modal Contributions to Base and Top-Storey Shears of BI "Shear-Beam" Structures with Different Base Masses

Table 5.14 Modal Contributions to the Storey Shears of BI "Shear-Beam" Structures with Different Base Masses and $T_{1(UI)}$ = 0.4 secs

M_{base} / M_{total}	Storey	Max. Storey Shears (kN) obtained from ISODYN				RUAUMOKO
		Mode 1	Mode 2	Mode 3	Total	Total
0.1	4	127.4	76.8	31.2	161.0	172.1
	3	239.5	76.8	10.8	254.5	279.9
	2	322.6	0.0	27.5	325.8	329.0
	1	366.9	76.8	20.4	409.3	401.1
	BI	-	-	-	434.3	409.9
0.2	4	132.1	70.2	28.1	188.7	190.9
	3	248.4	70.2	9.7	304.2	308.1
	2	334.6	0.0	24.7	324.8	348.7
	1	380.5	70.2	18.3	423.0	410.3
	BI	-	-	-	495.1	494.4
0.3	4	156.0	71.8	24.6	207.3	177.5
	3	293.2	71.8	8.5	331.4	311.6
	2	395.0	0.0	21.6	385.9	420.8
	1	449.2	71.8	16.0	477.0	479.8
	BI	-	-	-	567.7	564.6
0.4	4	173.4	65.3	21.4	197.9	187.5
	3	325.8	65.3	7.4	344.2	335.5
	2	439.0	0.0	18.8	432.0	446.5
	1	499.2	65.3	13.9	509.3	515.1
	BI	-	-	-	644.8	635.9

Note : M_{base}/M_{total} = 0.1 W = 3555.5 kN

0.2 4000.0

0.3 4571.0

0.4 5333.0

BI system : k_o = 10.0 W/m αk_o = 1.5 W/m F_y = 5%W

5.3.7 THE EFFECT OF NUMBER OF STOREYS

The modal contributions to the storey shears of a BI eight storey and twelve storey "shear-beam" structures with $T_{1(UI)}$ of 0.8 and 1.2 seconds, respectively, are compared with the modal contributions to the storey shears of their corresponding four storey structures. In these comparisons the first three modal storey shears are given in Tables 5.15 and 5.16 for structures with $T_{1(UI)}$ = 0.8 and 1.2 secs, respectively. The superstructures are mounted on a BI system with k_0 = 10.0W/m, αk_0=1.5W/m and F_y = 5%W. The total responses are also shown to be in good agreement with the results obtained from the inelastic time history analyses.

Figs. 5.15 and 5.16 demontrate that the modal contributions to the base and top storey shears have very similar patterns irrespective the number of storeys. Therefore as obtained earlier in Section 4.6, that regardless of the number of storeys BI structures with the same $T_{1(UI)}$ and BI system parameters have very similar lateral storey shear envelopes. This phenomenon should be expected since adding the number of storeys while keeping $T_{1(UI)}$ constant simply means distributing the mass of the structure more evenly up its height[5.6].

5.4 SUMMARY AND CONCLUDING REMARKS

The concept of the Component Mode Synthesis method is adapted for use as a tool for analysing the seismic response of BI multistorey structures with elastic superstructures. The BI multistorey structure is considered to be formed by two subsystems, i.e. the superstructure on an imaginary fixed-interface and the BI device which may undergo large plastic deformations. The superstructure can now be treated as a linear MDOF system and the structural response can be analyzed more clearly by studying the modal contributions. In general the mode superposition can be employed by only incorporating the first few significant modes of free vibration thus reducing the computational effort.

Some analyses carried out in Chapter 4 are rerun using the Component Mode Synthesis method by incorporating the first three modes of the superstructure. The total responses are then compared with the inelastic time history analysis results obtained earlier and are found to be consistently in good agreement.

The evaluation is concentrated on two aspects, i.e. the trends of change of the modal storey shears of BI structures due to the effect of various structural parameters and the contributions of these modal responses to the total storey shears. To measure these modal contributions the modal responses are expressed in terms of percentages of the total responses. It should be noted, however, that the maximum modal responses do not necessarily occur at the same time thus their total combinations are not simple summations of these maxima. Some important results of this evaluation can be summarized as follows:

Table 5.15 Modal Contributions to the Storey Shears of BI Eight and Four-Storey "Shear-Beam" Structures with $T_{1(UI)}$ = 0.8 secs

$T_{1(UI)}$ secs	Storey	Max. Storey Shears (in W) - from ISODYN				RUAUMOKO
		Mode 1	Mode 2	Mode 3	Total	Total
0.8 8 storeys	8	0.0222	0.0164	0.0113	0.0355	0.0351
	7	0.0436	0.0279	0.0136	0.0615	0.0638
	6	0.0635	0.0310	0.0051	0.0815	0.0842
	5	0.0812	0.0248	0.0074	0.0931	0.0944
	4	0.0962	0.0112	0.0141	0.0991	0.0950
	3	0.1079	0.0057	0.0095	0.1053	0.0952
	2	0.1160	0.0210	0.0026	0.1108	0.0973
	1	0.1201	0.0300	0.0127	0.1136	0.1008
	BI	-	-	-	0.1132	0.1135
0.8 4 storeys	4	0.0419	0.0289	0.0127	0.0596	0.0630
	3	0.0788	0.0289	0.0044	0.0931	0.0959
	2	0.1062	0.0000	0.0111	0.1040	0.0992
	1	0.1207	0.0289	0.0083	0.1122	0.0990
	BI	-	-	-	0.1166	0.1161

Note : BI system's Properties : k_o = 10.0 W/m, αk_o = 1.5 W/m, F_y = 5%W

W = total weight of the structure

Table 5.16 Modal Contributions to the Storey Shears of BI Twelve and Four-Storey "Shear-Beam" Structures with $T_{1(UI)}$ = 1.2 secs

$T_{1(UI)}$ secs	Storeys	Max. Storey Shears (in W) - from ISODYN				RUAUMOKO
		Mode 1	Mode 2	Mode 3	Total	Total
1.2 12 storeys	12	0.0134	0.0152	0.0148	0.0292	0.0310
	11	0.0267	0.0282	0.0239	0.0525	0.0554
	10	0.0395	0.0373	0.0239	0.0658	0.0711
	9	0.0517	0.0411	0.0148	0.0793	0.0788
	8	0.0631	0.0392	0.0000	0.0897	0.0879
	7	0.0786	0.0317	0.0148	0.0976	0.0957
	6	0.0827	0.0198	0.0239	0.1015	0.0980
	5	0.0906	0.0052	0.0239	0.0994	0.1000
	4	0.0971	0.0102	0.0148	0.0965	0.0986
	3	0.1021	0.0242	0.0000	0.1021	0.0998
	2	0.1054	0.0348	0.0148	0.1069	0.1032
	1	0.1071	0.0405	0.0239	0.1096	0.1044
	BI	-	-	-	0.1095	0.1097
1.2 4 storeys	4	0.0380	0.0389	0.0264	0.0637	0.0679
	3	0.0714	0.0389	0.0092	0.0887	0.0872
	2	0.0963	0.0000	0.0232	0.0998	0.1085
	1	0.1094	0.0389	0.0340	0.1109	0.1120
	BI	-	-	-	0.1118	0.1122

Note : BI system's Properties : k_o = 10.0 W/m, αk_o = 1.5 W/m, F_y = 5%W

W = total weight of the structure

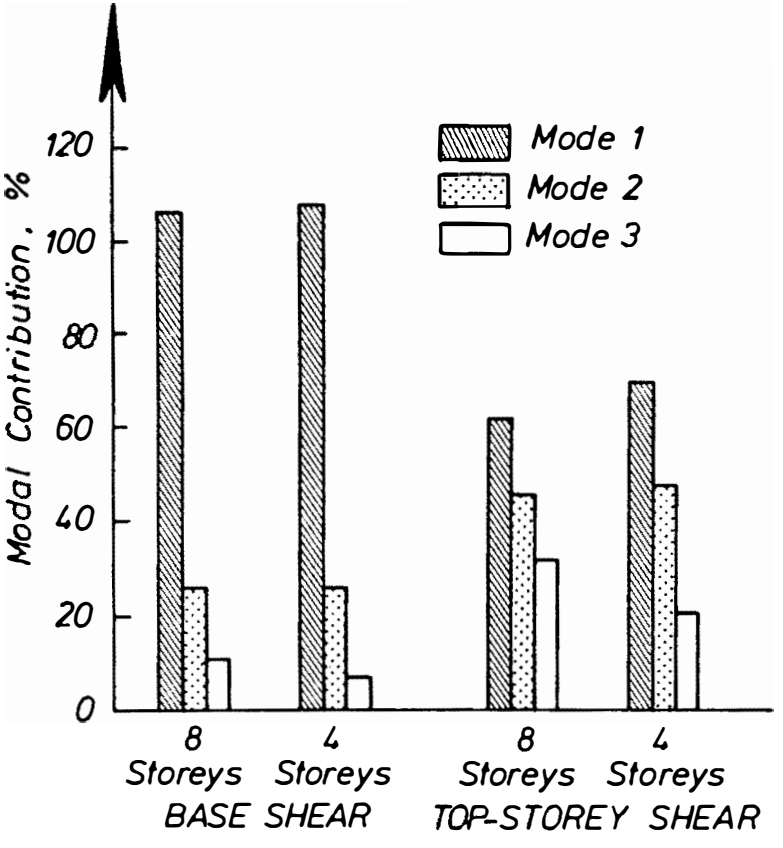

Fig. 5.15 The Effect of Number of Storeys on the Modal Contributions to Base and Top-Storey Shears of BI Structures with $T_{1(UI)} = 0.8$ secs

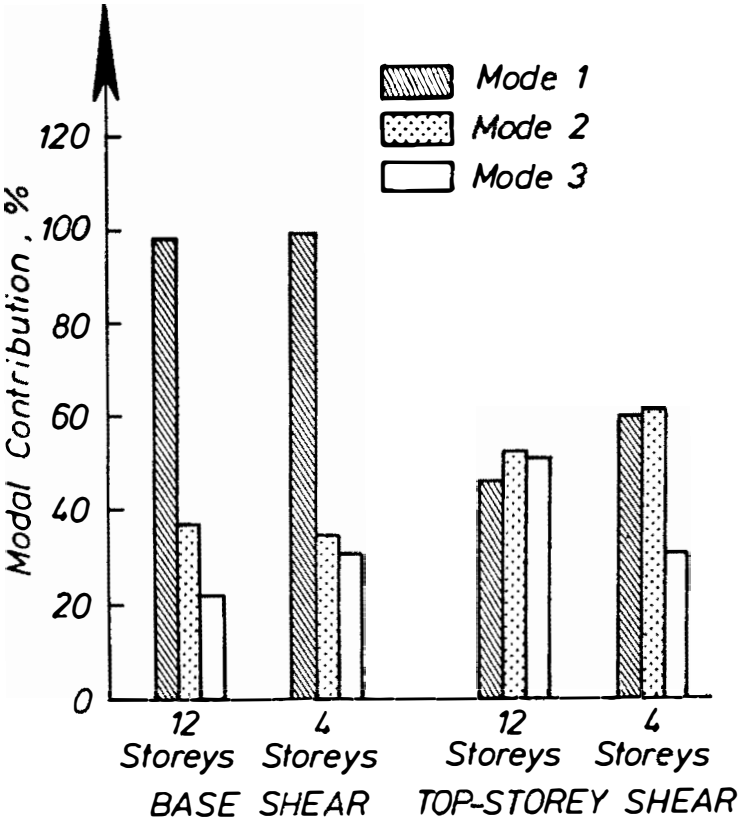

Fig. 5.16 The Effect of Number of Storeys on the Modal Contributions to Base and Top-Storey Shears of BI Structures with $T_{1(UI)} = 1.2$ secs

1. A displacement-dependent BI system may reduce the first mode storey shears significantly but generally do not reduce the higher mode storey shears to the same degree. This causes the higher mode storey shears to become more significant especially in the upper storeys.

2. For short period structures the storey shears are strongly dominated by the first mode. As $T_{1(UI)}$ increases, however, the first mode contributions to the top storey shears tend to decrease while the higher mode contributions tend to increase.

3. As the hysteresis loops of the BI system become fatter, the higher mode effects on the storey shears become more significant. This is caused more by the decrease of the first mode contributions to the top storey shears rather than by increases in the higher mode contributions which tend to remain constant.

4. BI systems with an elastic spring and a velocity-dependent damper tend to suppress the higher mode effects. The storey shear envelope of multistorey structures using this kind of BI system with high viscous damping tends to be much less bulged than the shear envelope of structures mounted on an displacement-dependent BI system with fat hysteresis loops eventhough both systems have the same effective siffness and amount of damping.

5. Due to their modal properties "cantilever-beam" structures tend to have more bulged storey shear envelopes than the "shear-beam" structures. For BI structures, however, the reverse phenomenon may be found since the reduction of the higher mode storey shears in "shear-beam" structures is not as much as in "cantilever-beam" structures, causing the higher mode effects to become increasingly more significant.

6. It is observed that BI structures with a large base mass tend to have less higher mode contributions and thus have a less bulged storey shear envelope.

7. The effect of the number of storeys on the modal contributions to the storey shears is found to be insignificant.

In the future, it is very desirable to be able to develop this Component Mode Synthesis method based on the response spectrum analysis instead of the step-by-step integration used at present. Further research is, however, required to derive an appropriate mode superposition technique for combining the maximum modal responses.

5.5 REFERENCES

5.1 HURTY, W.C., COLLINS, J.D., and HART, G.C. , Dynamic Analysis of Large Structures by Modal Synthesis Techniques, Computer & Structures, Vol.1, 1971, pp. 535-563.

5.2 CRAIG, R.R., Jr., Structural Dynamics - An Introduction to Computer Methods, John Wiley & Sons, 1981, p.567.

5.3 BAYO, E. and WILSON, E.L., Numerical Techniques for the Evaluation of Soil-Structure Interaction Effects in the Time Domain, Report No. UCB/EERC-83/04, University of California, Berkeley, 1983.

5.4 LEVY, S. and WILKINSON, J.P.D., The Component Element Method in Dynamics, McGraw-Hill, 1976, p.300.

5.5 BELL, K., DYNOGS - A Computer Program for Dynamic Analysis of Off-Shore Gravity Platforms, Theoritical Manual, SINTEF, Trondheim, Norway, 1978, 59 pp. plus appendices.

5.6 CLOUGH, R.W and PENZIEN, J., Dynamics of Structures, McGraw-Hill, 1975, pp.191-192.

5.7 PENZIEN, J., Structural Dynamics of Fixed Offshore Structures, The First International Conference on the Behaviour of Offshore Structures, BOSS-76, Trondheim, Norway, 1976.

5.8 NEWMARK, N.M , A Method of Computation of Structural Dynamics, Journal Eng. Mech. Div. , Vol.85, 1959, pp 67-94.

5.9 BATHE, K.J., and WILSON, E.L., Numerical Methods in Finite Element Analysis, Prentice-Hall Inc. , 1976.

5.10 LEE, D.M., The Effect of Base Isolation on Multistorey Shear Structures, Ph.D Thesis, Dept. of Theoritical and Applied Mechanics, Univ of Auckland, New Zealand, 1978.

5.11 KELLY, J.M., EIDINGER, J.M., and DERHAM, C.J., A Practical Soft Storey Earthquake Isolation System, Report No. UCB/EERC-77/27, Earthquake Enginerring Research Centre, Univ. of California, Berkeley, 1977.

CHAPTER 6

EFFECTS OF DIFFERENT EARTHQUAKES ON THE RESPONSE OF BI MULTISTOREY STRUCTURES WITH ELASTIC SUPERSTRUCTURES

6.1 INTRODUCTION

As reported in Chapter 4, an extensive investigation has been carried out to study the response of BI multistorey structures with elastic superstructures subjected to one ground motion, namely the North-South component of El Centro 1940 earthquake. Based on the results of this study a simple code-type design approach is proposed to estimate the base displacements and the lateral storey shears.

It is certainly important to extend the above investigation to cover different earthquakes and New Zealand design-level seismicity. The results may then be used to examine the validity and reliability of the proposed code-type approach. For this purpose, first, some seismological and geological aspects are briefly discussed as presented in Section 6.2. It is then followed, in Section 6.3, by an evaluation of the major structural response quantities, such as base and top displacements, base shears and the lateral storey shear envelopes under the effect of different ground motions. A discussion of design aspects is presented at the end of this section.

There are some concerns on the likely permanent plastic offsets which might be experienced by BI multistorey structures after a severe earthquake. Section 6.4 presents some discussions on this aspect.

6.2 SEISMOLOGICAL AND GEOLOGICAL ASPECTS

6.2.1 GENERAL

For many centuries people have been trying to understand earthquakes and their physical effects on man and manmade works. Only over the last few decades, however, have seismologists and goelogists started to make significant advances in providing data and insight into the seismic phenomena and their regional characteristics. These advances were made possible by the availability of high-sensitivity recordings and the results of the other intensive investigations, such as studies on fault rupture process, recurrence interval of earthquakes, tectonic deformation, and so on.

In spite of the incompleteness of this seismic information it is still very useful in assisting the engineers to choose an acceptable level of seismic risk and appropriate dynamic design criteria. As has been discussed in Chapter 2, the seismic response of a structure can be predicted by conducting an equivalent static force analysis and/or more rigorous dynamic analyses. For this purpose the effects of the ground motion on a given site may be derived from:

1. smoothed design spectra which are based on either an ensemble of earthquakes with magnitude and epicentral distances appropriate for the site and having soil conditions similar to the site or based on a more reasonable seismic hazard analysis.

2. some accelerograms of similar real earthquakes or artificially simulated ground motions to match the design earthquake.

Some attempts have also been made to correlate the structural response with some ground motion characteristics. Zhu, Tso, and Heidebrecht[6.1], for instance, studied the effect of peak ground acceleration to velocity ratio on the ductility demand of inelastic systems in order to incorporate this parameter in the specification of seismic design base shear of conventionally designed unisolated structures. Likewise, as alluded to earlier in Chapter 3, for design purposes Lee[6.2] tried to correlate some earthquake parameters with the seismic response of BI multistorey "shear-beam" structures. It should be realized, however, that many lessons must still be learned from the occurence of recent and future ground motions before the importance of ground shaking parameters used in predicting the structural behaviour can be fully understood[6.3].

6.2.2 RECENT LARGE EARTHQUAKES CONSIDERED IN THIS STUDY

Six real earthquake records and one artificially generated earthquake record were used in this study to investigate the behaviour of BI multistorey structures under different ground motions by conducting a series of inelastic time history analyses and to test the reliability of the proposed Code-Type design approach under various earthquakes. A brief description of these earthquakes and generated accelerogram is given in the following.

1. Imperial Valley, California, 18 May 1940 Earthquake[6.4].

This earthquake was centred along a well defined fault of the San Andreas fault system in southern California and had an average local Richter magnitude, M = 6.4. Its record from the El Centro site has a special significance for earthquake engineering since it was the first strong motion ever recorded in the epicentral region of a moderate sized earthquake. Until the Parkfield earthquake of the mid-1960s the El Centro 1940 accelerogram remained the strongest record of ground shaking both in term of amplitude and duration. As a result many seismic codes worldwide have used this record as a basis for seismic resistant design criteria.

It has also been indicated that this earthquake has a complex pattern of energy release with a series of multiple ruptures moving generally south-eastwards over a distance of 25 km away from the epicentre as well as from the recording site which was located around 10 km north of the epicentre. Four distinct rupture events can be identified in the first 15 seconds of the records. The direction of propagation resulted in less intense levels of shaking and a lower peak ground acceleration (0.34 g) than might have been expected for an earthquake of this magnitude measured in the epicentral region.

In this study a 14-second duration of the North-South component of the El Centro record is used for analyses. Its acceleration and displacement spectra are shown in Fig. 6.1.

2. Imperial Valley, California, 15 October 1979 Earthquake[6.5].

Almost forty years later a similar destructive earthquake again shook the Imperial Valley of sourthern California. The quake had a local magnitude of 6.6 and many after-shocks, the largest of which was of magnitude 5.2. During this earthquake a comprehensive set of strong motion records was obtained from an array of instruments favourably sited at 6 to 196 km from the epicentre, across the active fault line. The rupture propagated towards the instrument array and therefore the recordings were expected to detect a large directivity effect. The peak accelerations of the records varied from 0.11 to 0.72 g.

In this study the North-South component of the acceleration recorded at the free-field site near the Imperial County Services Building in El Centro is considered. The peak acceleration (0.24g) was not as high as that for the El Centro 1940 record. However when compared with the spectra of the 1940 earthquake, the calculated spectra of this record indicate larger response of accelerations and displacements for structures with natural periods between 1.1 to 2.0 seconds as shown in Fig. 6.1.

3. Parkfield, California, 27 June 1966 Earthquake[6.6].

The ground motion was recorded by an array of instruments located across the San Andreas fault at Cholame-Shandon which is about 30 km away from the epicentre near Parkfield, central California. In an engineering sense this 5.6 magnitude earthquake has a special significance, particularly for design considerations of important structures which are to be located close to a fault.

The earthquake was recorded at the nearest station to the fault as an implusive ground motion with a large single displacement pulse of about 260 mm in 1.5 seconds duration. The maximum ground acceleration of the fault was 0.5 g; the strongest ever recorded at that time. The ground motion, however, attenuated very rapidly with distance, losing its pulse-like directional characteristics.

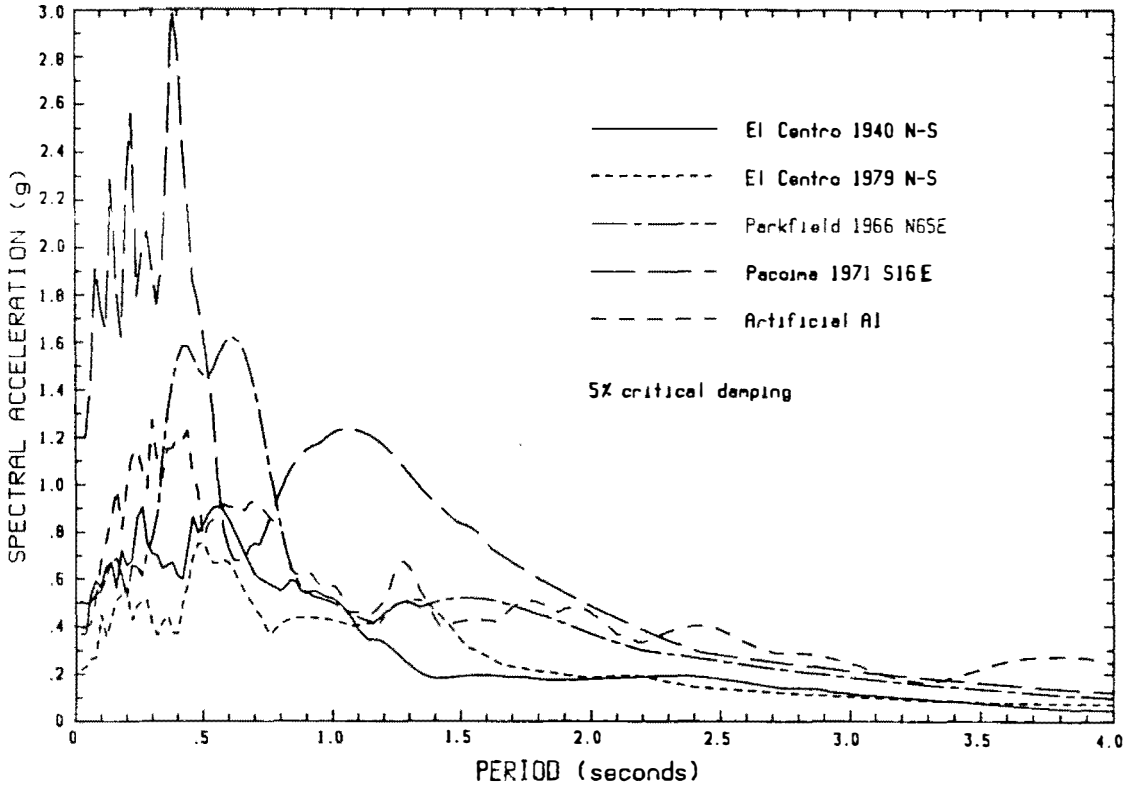

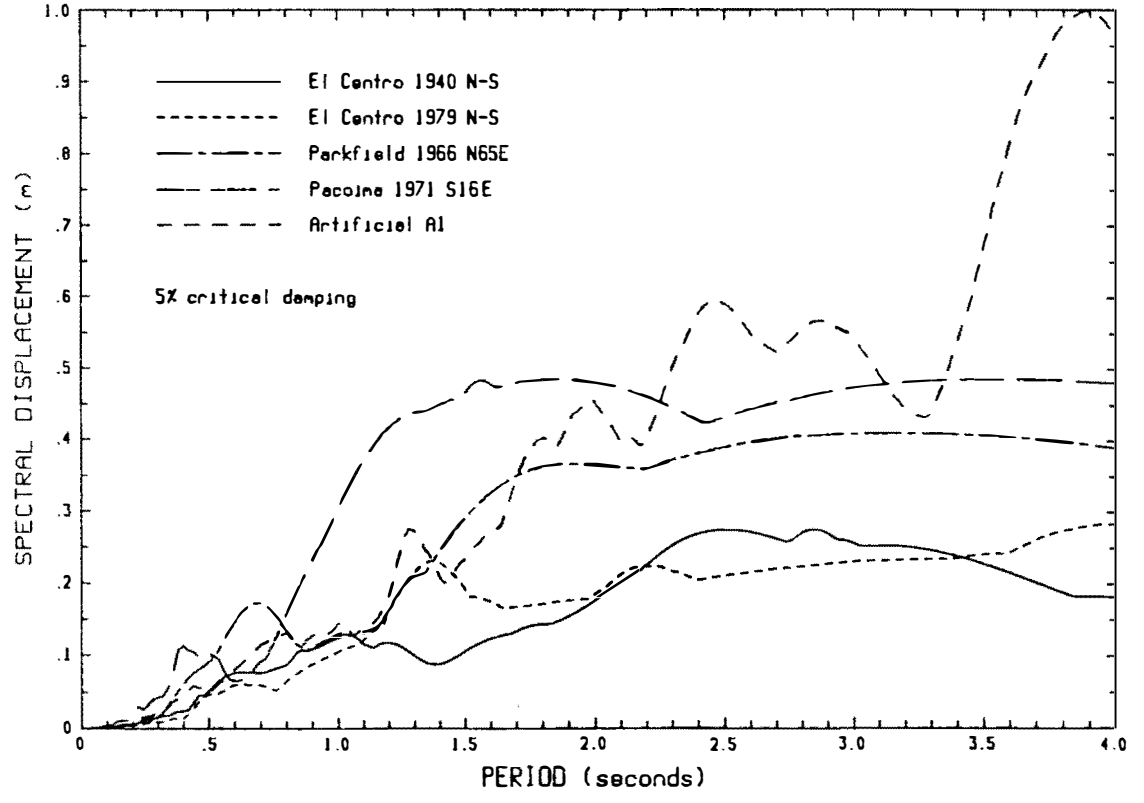

Fig. 6.1 Spectral Accelerations and Spectral Displacements of Earthquakes which have Peak Spectral Accelerations at Short Period Region

In this study the N65E component of the accelerogram recorded at the nearest station of the fault is considered. Its acceleration and displacement spectra are shown in Fig. 6.1.

4. San Fernando, California, 9 February 1971 Earthquake[6.7].

The epicentre of this earthquake was located in a sparsely populated area of the San Gabriel mountains 14 km north of San Fernando, California. During the shock a large number of accelerograms were recorded by a dense network of strong-motion accelerographs sited in central and southern California. More than half of the instruments were located in the Los Angeles area where many of them were installed at various levels of multistorey buildings of distances of 21 to 50 km from the epicentre.

In this study the S16E component of the accelerogram recorded at the Pacoima Dam site in the epicentral region is considered. Its spectral acceleration and spectral displacement can be seen in Fig. 6.1.

Although this earthquake had only a moderate magnitude of 6.6, its peak ground acceleration which reached 1.25 g made one of the most severe ground motions ever recorded. Numerous studies have suggested that the Pacoima Dam record was anomalously high because of topographic amplification since the accelerograph was located on a small rocky ridge near the bottom of large canyon. A recent study using some model tests conducted by Brune[6.8], however, shows that the previous assumptions cannot be justified. It was found that the de-amplification due to the effect of the canyon bottoms dominates any amplification effects due to the small ridge. There is no doubt that technical debate on this matter will continue until more similar records are obtained.

5. Bucharest, Romania, 4 March 1977 Earthquake[6.9].

The source location of this major destructive earthquake (M = 7.1) was at a depth of about 100 km beneath the Vrancea region of the Carpathian mountain arc. During this event a three-component accelerogram (NS,EW,Vertical) was considered as the most useful close-in recording. The records showed the earthquake as a long period ground motion with a peak acceleration of 0.22 g and a peak displacement of 270 mm. It was found that the relatively "simple" form and high amplitudes of this accelerogram were attributed to the small epicentral distance to source depth ratio and the relatively deep soft sediment in the Bucharest area.

This type of ground motion has often been used to discredit the benefits of a displacement-dependent BI system. However, it is informative to include this record for evaluating the behaviour of BI multistorey structures and if possible to suggest an alternative BI system which is more suitable for this type of ground motion. For this purpose, the North-South component of this recorded ground motion was selected to be used in this study. Fig. 6.2 shows its acceleration spectrum in which the peak occurs in the period range at about 1.4 seconds.

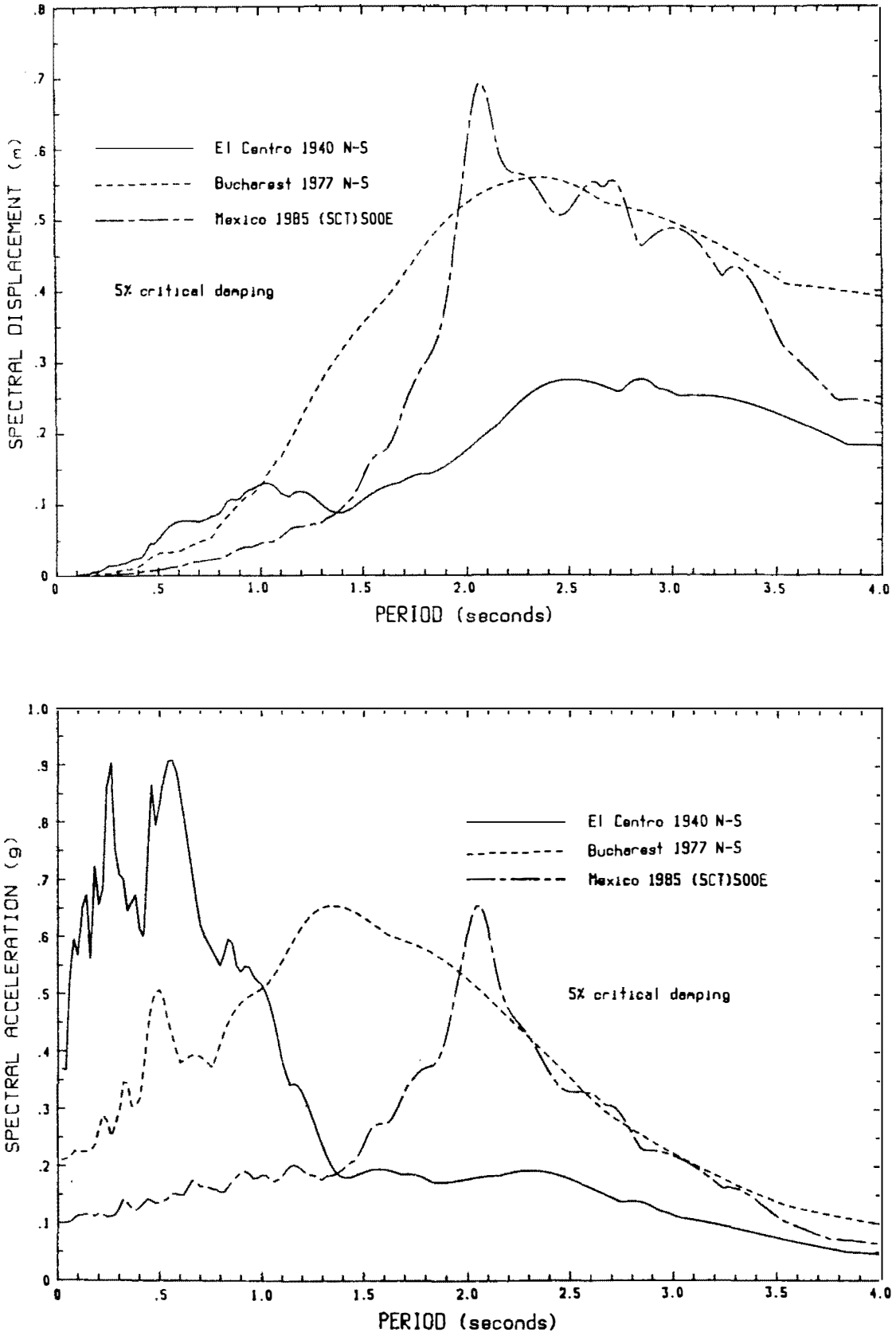

Fig. 6.2 Spectral Accelerations and Spectral Displacements of El Centro 1940 N-S, Bucharest 1977 N-S, and Mexico 1985 (SCT) S00E Earthquakes

6. Mexico, 19 September 1985 Earthquake[6.10].

This damaging earthquake occured on the subduction zone between the North American and Pacific plates, approximately 10 km off the Pacific coast of Mexico, north of Zihuatanejo. The coastal region was, however, not devastated so severely as the Mexico City area, some 350 km away.

Strong motion records of this earthquake (M = 8.1) are obtained at a number of sites in and around Mexico City with various geological conditions, namely the hilly zones with hard and compact soil conditions, the transition zone, and the old lake bed zones with deep clay deposits. The characteristics of the ground motion at the most heavily damaged area which attracted a lot of interest can be represented by the SCT site record. Sufficient studies have been made to indicate that the clay deposits of this area are generally very similar to those at the SCT site although they vary considerably in depth to the hard layer, ranging from about 24 to 44 m.

The longitudinal component of the SCT record is included in this study for the same purpose as the inclusion of the Bucharest record. Fig. 6.2 displays and compares the spectra of this record with the spectra of El Centro 1940 N-S and Bucharest 1977 N-S earthquakes.

7. Simulated Artificial A1 Earthquake[6.11].

This artificial accelerogram is one of a series of simulated records generated by Jennings et al. It is intended to model the shaking of a great earthquake with a local magnitude of 8.0 or greater on a firm ground in the vicinity of a fault. The total duration of the accelerogram is relatively long, i.e. 120 seconds with a 29 seconds portion of constant intense motion. Details of the generation process and description of other artificial earthquakes of this series can be found in Ref. 6.11. The spectra of this simulated artificial A1 earthquake are shown in Fig. 6.1 together with the spectra of other earthquakes which have peak apectral accelerations in short period regions.

6.2.3 NEW ZEALAND DESIGN SEISMIC LOADS

Code-specified earthquake spectra are normally considered as a useful measure of the seismicity of a certain area in which the design seismic loads are based. As has been discussed elsewhere[6.12] in great detail, the elastic response spectra prescribed in the current NZ loadings code for buildings NZS4203:1984[6.13] are mainly based on a smoothed compound spectrum obtained from the El Centro 1940 N-S ground motion. This unrealistic seismic load assessment was caused by the lack of available data of seismicity in New Zealand at the time when the current code and its predecessors published in 1965 and 1976 were prepared. Since 1978, however, a

considerable effort has been directed to revise and rationalize the NZ seismic design loadings code based on the results of seismic hazard analyses conducted in New Zealand.

The assessment of seismic hazard at any site basically involves a probabilistic approach which relies upon a seismicity model and an attenuation relationship. The seismicity model describes the spatial distribution of earthquakes and the frequency of occurence of different earthquake magnitude, epicentral distance, and ground conditions. More detail description of the NZ seismic hazard analyses can be found in References 6.14, 6.15, 6.16, and 6.17.

As a result of conducting the seismic hazard analyses, a revised method of determining seismic design loadings has been suggested and the draft[6.18] has been proposed to replace the current NZ loadings code, NZS4203:1984. If this draft code is adopted in its present form, it will be the first NZ general building code to offer a set of uniform risk horizontal acceleration spectra for use to establish the level of inertia forces for which structures should be designed.

In this new draft[6.18] the total horizontal seismic force in each direction under consideration is given as follows:

$$V = C_{\mu} R Z W \tag{6.1}$$

where : C_{μ} = a basic seismic coefficient as can be found from Fig. 6.3. This coefficient depends on the structure's fundamental period, the soil condition, and the available structure dispalcement ductility factor as specified by the code.

R = a risk factor which modifies the design load to take into account the annual probability of exceedance f_E. As shown in Fig. 6.14, R = 1.0 for a return period of approximately 150 years which is suggested as a basis for the design level seismic load.

Z = a zone factor as specified in Fig. 6.5 which allows for variations in seismic hazard over New Zealand.

W = the gravity load (dead+live) of structure considered to be present during earthquake.

It has been realized that to conduct inelastic time history analyses digitized accelerograms are required. Therefore, for the purpose of this study it is desirable to be able to use generated artificial earthquake records having response spectra which closely match the elastic design spectra proposed in the new draft code[6.18]. A series of artificial earthquake records based on the above design spectra have been generated for research purposes at the University of Canterbury using the existing computer program SIMQKE[6.19]. Two records of this series are selected and used in this study. Each record represents the likely ground shaking on different ground

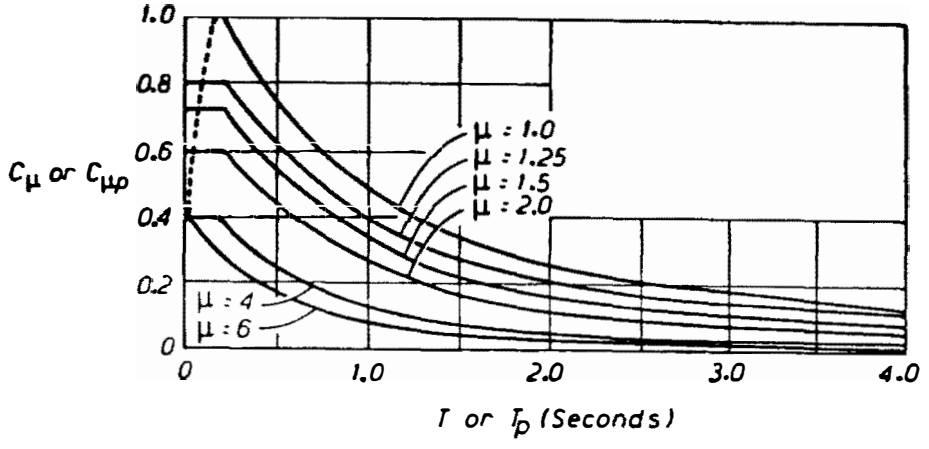

(a) NORMAL SOILS

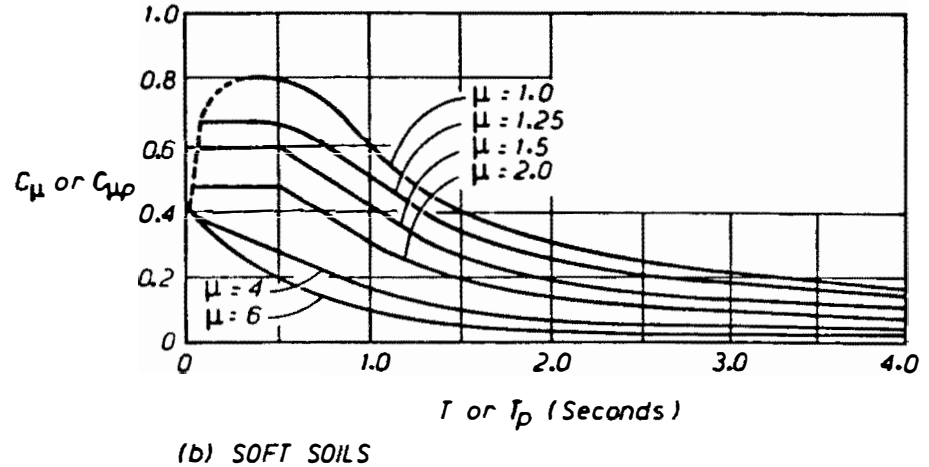

(b) SOFT SOILS

Notes:

1. For structures (or parts) with R = 0.4 to 1.3 values of C_μ (or $C_{\mu p}$) need not exceed 0.8
2. The dotted portion of the curves shall be used instead of the plateaus to obtain ordinates for elastically responding structures and the ordinates for higher modes of other structures when the dominant response is in the first mode.

Fig. 6.3 Basic Seismic Acceleration Coefficients Proposed in the Draft of NZS 4203[6.18]

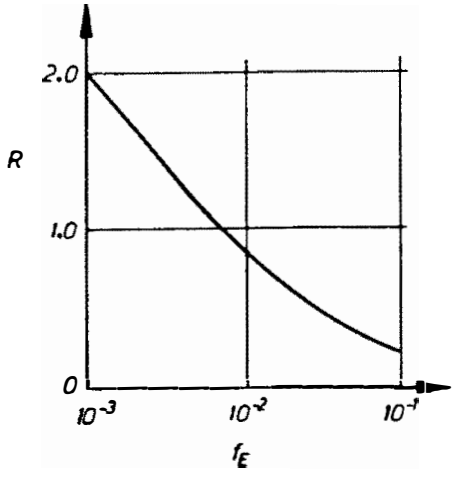

Fig. 6.4 Relationship Between Risk Factor R and Annual Probability of Exceedence f_E proposed in the Draft of NZS4203[6.18]

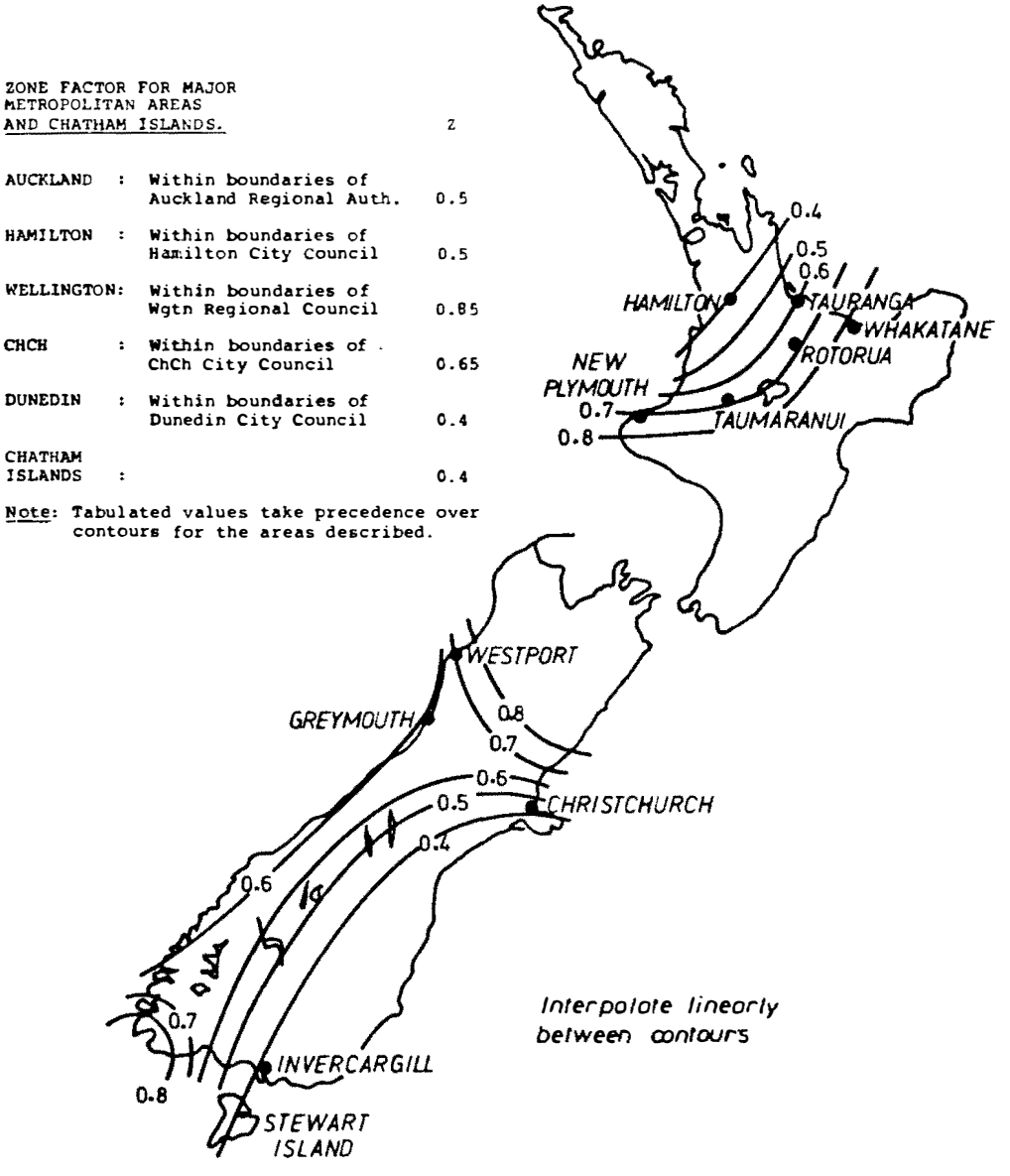

Fig. 6.5 Zone Factor Z Proposed in the Draft of NZS4203[6.18]

conditions, i.e. normal and soft soils of the highest seismicity zones in New Zealand. More detailed information about these two artificial recods are given in Appendix B.

6.3 EVALUATION OF MAJOR STRUCTURAL RESPONSE QUANTITIES

6.3.1 GENERAL

During a strong earthquake, it is expected that displacement-dependent BI devices will provide sufficient horizontal flexibility to lengthen the fundamental period of the structures and will supply some extra damping due to their hysteretic damping. For some earthquakes with spectral accelerations which reach their peaks in the short period region and diminish in longer periods, the fundamental period shift by these BI systems will definitely reduce the earthquake energy transmitted to the structure. However, for other earthquakes which have peak spectral accelerations in long period regions, shifting the fundamental period of the structure is not beneficial as it may place the structure in a more dominant earthquake energy region.

Figs. 6.1 and 6.2 show the acceleration spectra of both groups of ground motions considered in this study. Five earthquake records can be categorized in the first group for which the displacement-dependent BI systems are obviously beneficial. They are El Centro 1940 N-S, El Centro 1979 N-S, Parkfield 1966 N65E, Pacoima Dam 1971 S16E, and Artificial A1. Two other earthquake records, i.e. Bucharest 1977 N-S and Mexico 1985 at the SCT site, belong to the second group, and which are often used in attempts to discredit the benefits of displacement-dependent BI systems.

In this section the above phenomenon is discussed. For this purpose, extensive analyses are carried out to evaluate the structural response under these ground motions and the NZ design-level earthquakes for normal and soft soils in Zone-A.

A discussion of design aspects is presented at the end of this section in order to examine the validity and reliability of the proposed Code-Type design approach for various BI multistorey structures and to discuss the suitability of various BI systems under these different earthquakes.

6.3.2 BASE SHEAR

The maximum normalized base shear of fixed-base and BI structures subjected to five different earthquakes are shown in Figs. 6.6.a and 6.6.b. The superstructure model used in this evaluation is a series of four storey "shear-beam" structures, with $T_{1(UI)}$ of 0.1 to 2.0 seconds. The BI system has a bilinear hysteresis loop model with an initial stiffness, k_o of 10.0 W/m, a post-yield stiffness, αk_o of 1.5 W/m, and a yield strength, F_y of 5%W, where W is the total weight of the structure.

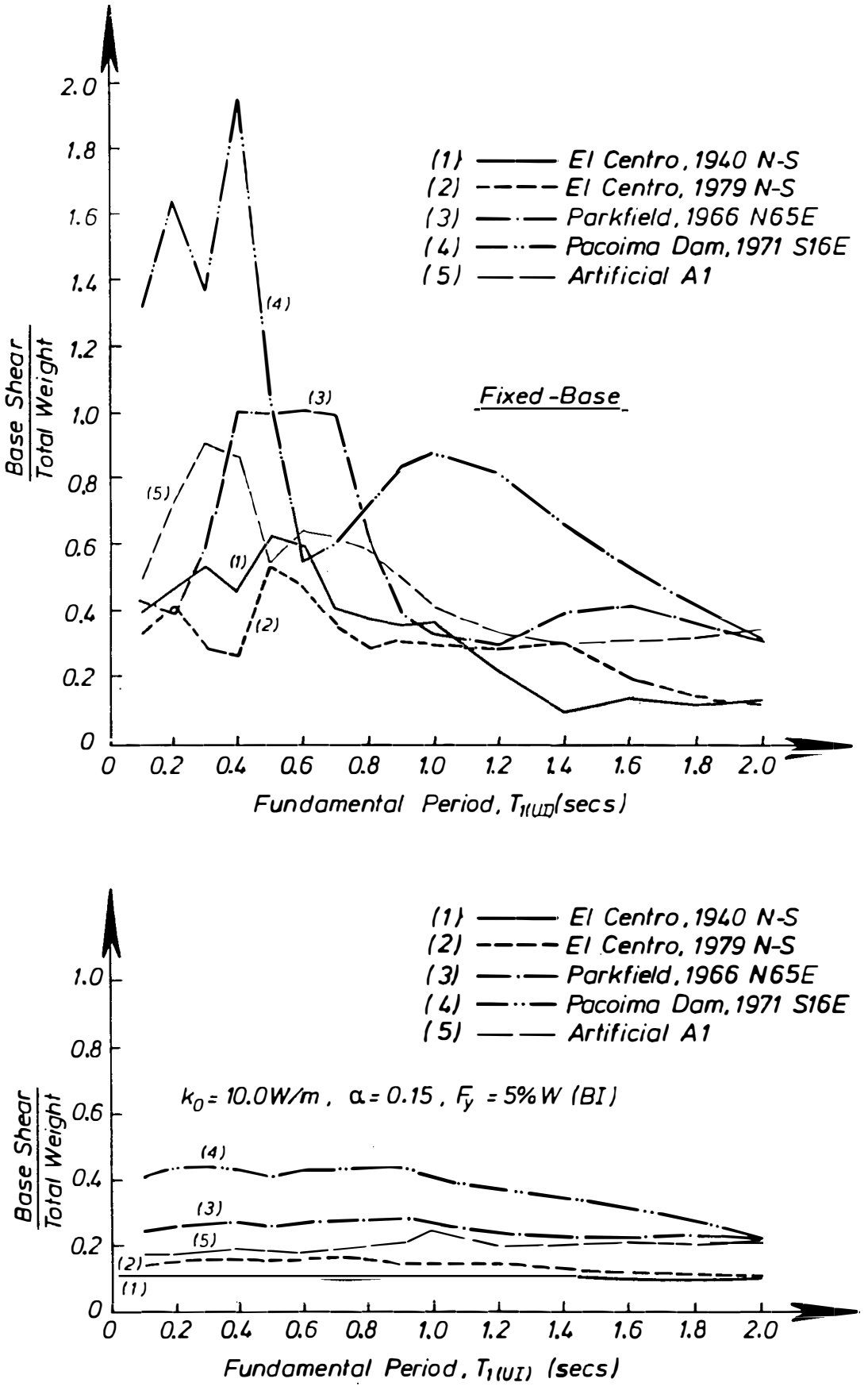

Fig. 6.6 Normalized Base Shears of Fixed-Base and BI Structures of Different $T_{1(UI)}$ Subjected to Earthquakes with Peak Spectral Accelerations at Short Period Region

It can be seen from these figures that the maximum base shears of fixed-base structures with different $T_{1(UI)}$ follow closely the shape of the corresponding earthquake acceleration spectra as has been indicated earlier in Chapter 4 with the El Centro 1940 N-S earthquake. With the inclusion of the BI system, the base shears become significantly lower especially for short period structures and they are almost in the same magnitudes throughout the range of the considered fundamental periods, $T_{1(UI)}$. As explained earlier in Chapter 4, this phenomenon is caused by the combination effects of the fundamental period shift, the additional hysteretic damping, and the shape of the acceleration spectra which have lower magnitudes and much less dramatic changes in the long period regions.

When the BI system is applied for the second group of ground motions, i.e. Bucharest 1977 N-S and Mexico 1985 at the SCT site, the maximum base shears of BI structures are not necessarily lower than the maximum base shears of the fixed-base unisolated structures, as can be seen in Fig. 6.7. The peak spectral accelerations of Bucharest 1977 N-S and Mexico 1985 at the SCT site eartquakes occur at around 1.4 and 2.0 second, respectively. For short period BI structures, the fundamental periods will be shifted into a longer period region in which the spectral accelerations are increasing and greater base shears should be expected. For longer period structures, the fundamental periods may be shifted beyond the region of the peak spectral accelerations into the descending part of the spectrum. Hence, lower base shears can be obtained for these BI structures as also shown in Fig. 6.7. However, the reduction is not so significant as obtained for the first group ground motions.

It is also informative to evaluate the likely base shears of fixed-base and BI structures subjected to NZ design level earthquakes for Zone A. Fig. 6.8 shows that the base shears of BI structures at normal and soft soil conditions are significantly lower than the base shears of their counterparts, the fixed-base unisolated structures.

So far only one type of BI system is considered. To evaluate the effects of varying the BI parameters under different eartquakes, similar analyses as conducted earlier in Section 4.5 for El Centro 1940 N-S earthquake are carried out. For this purpose, a four storey "shear-beam" structure model with $T_{1(UI)}$ of 0.4 secs is used and the BI parameters are varied as follows. First, the post-yield stiffness, αk_o is kept constant at 1.25 W/m while the initial stiffness, k_o and the yield strength, F_y are varied from 2.5 to 25.0 W/m and from 1.0 to 25.0%W, respectively. Second, k_o is kept constant at 10.0 W/m while αk_o and F_y are varied from 0.5 to 2.5 W/m and from 1.0 to 25.0 %W, respectively.

Fig. 6.9 shows the results of the analyses for El Centro 1979 N-S, Parkfield 1966 N65E, Pacoima Dam 1971 S16E, Artificial A1, and NZ design-level earthquakes in Zone A. Similar trends as found earlier for El Centro 1940 N-S earthquake are also observed in these analyses. At low yield strength levels the post-yield stiffness governs the structural response. Hence, at a constant post-yield stiffness, a BI system with a large initial stiffness tends to induce a smaller maximum base

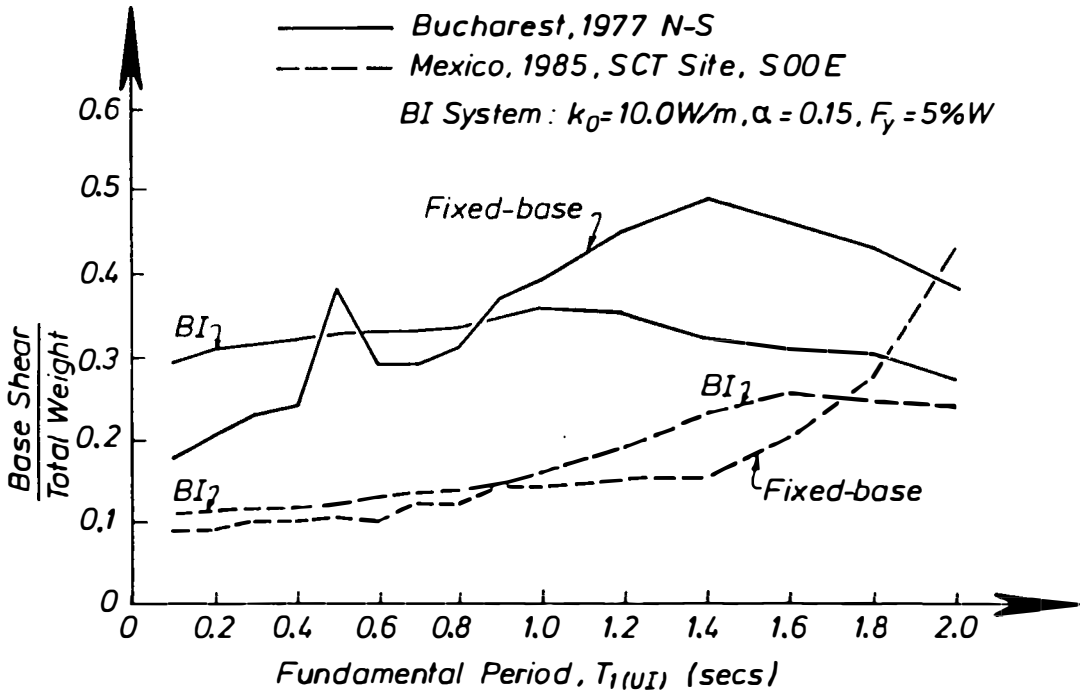

Fig. 6.7 Normalized Base Shears of Fixed-Base and BI Structures of Different $T_{1(UI)}$ Subjected to Earthquakes with Peak Spectral Accelerations at Long Period Region

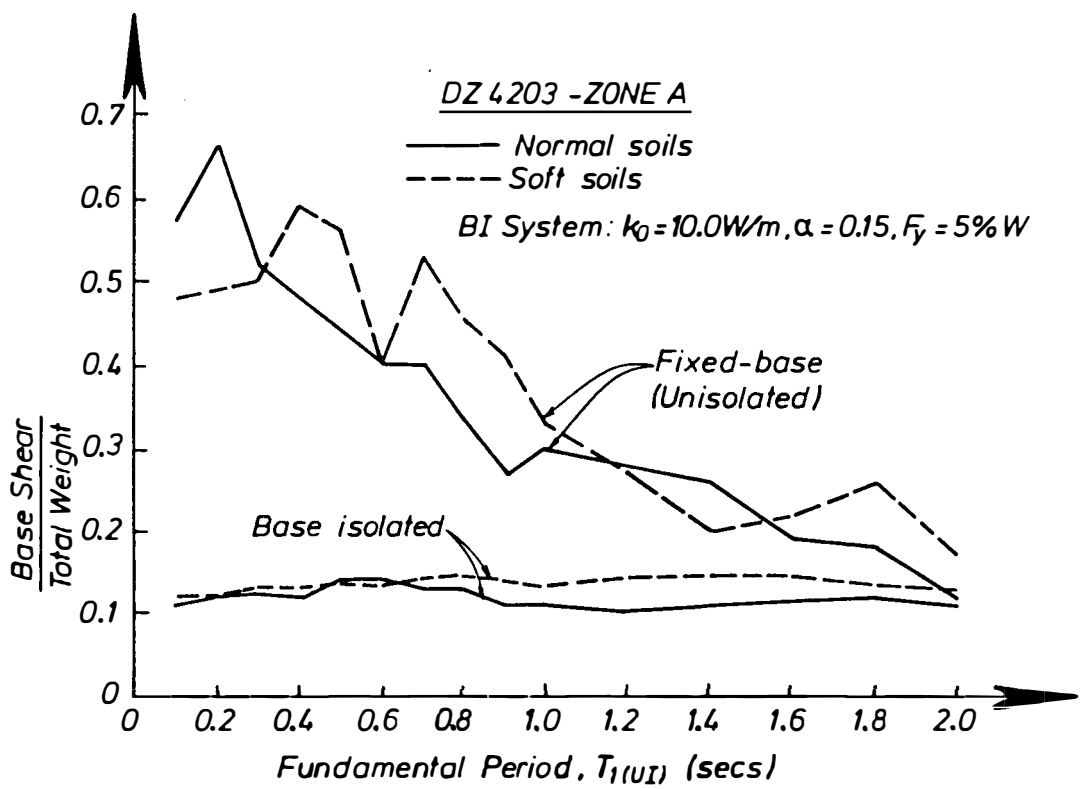

Fig. 6.8 Normalized Base Shears of Fixed-Base and BI Structures of Different $T_{1(UI)}$ Subjected to NZ Design-Level Earthquakes for Zone A

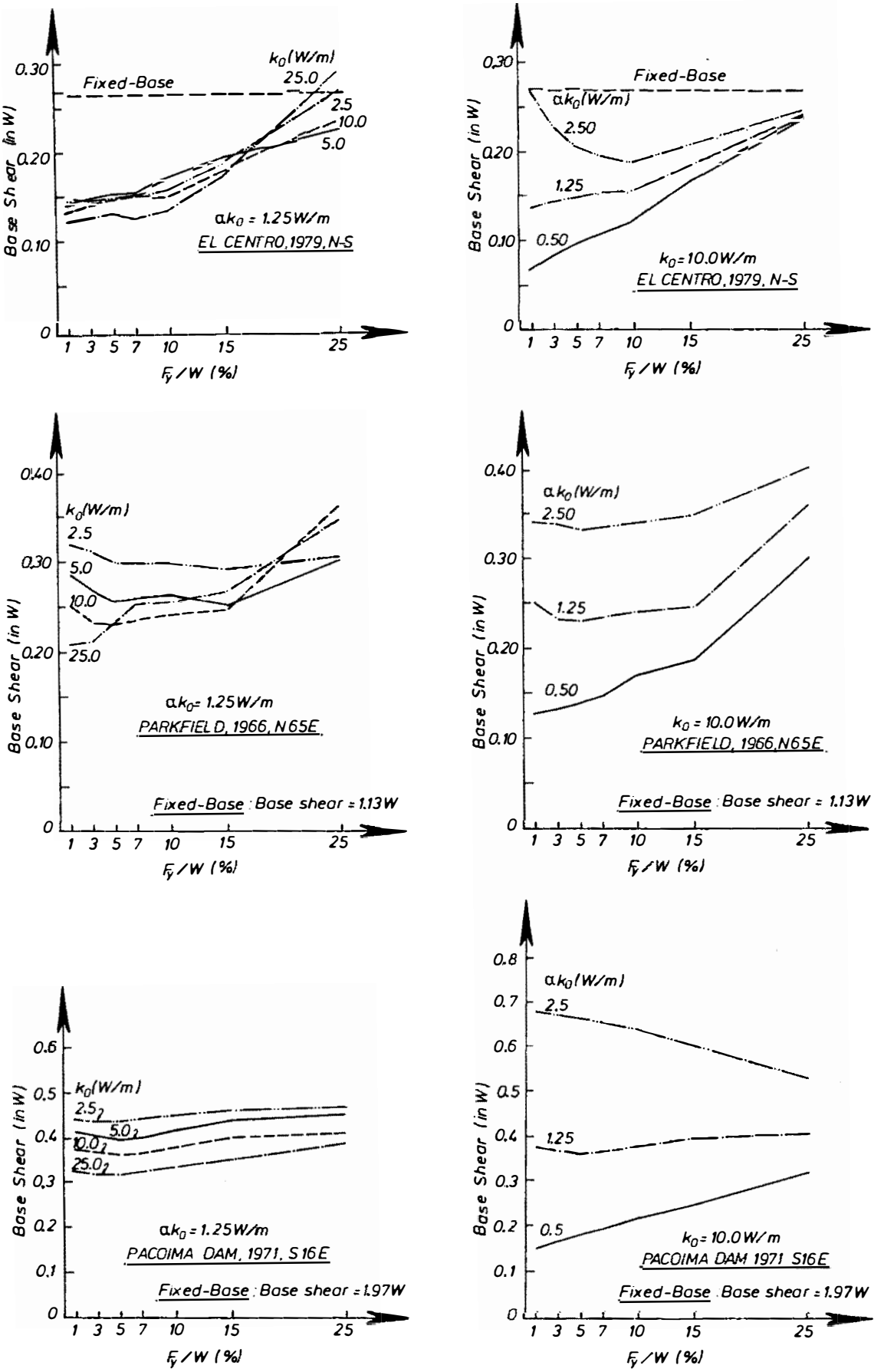

Fig. 6.9 The Effects of Varying BI Parameters on Base Shears Under Different Earthquakes

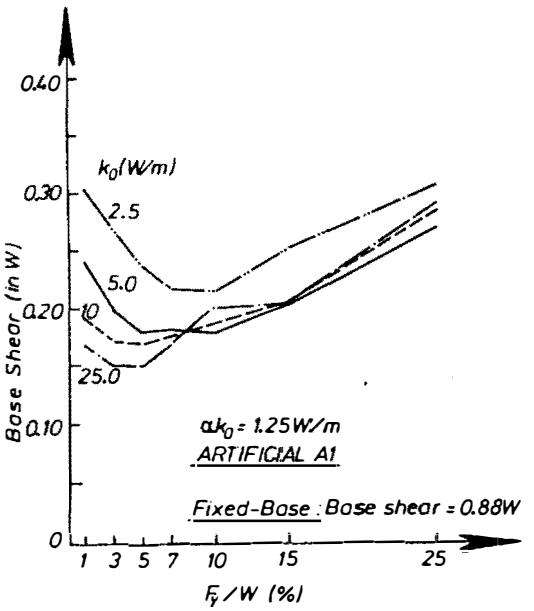

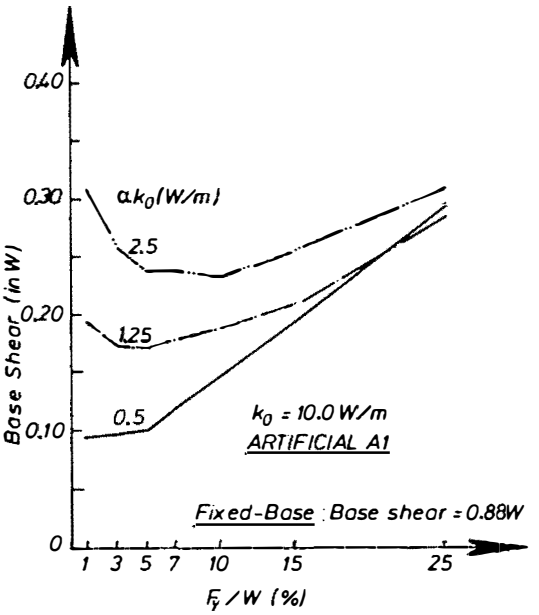

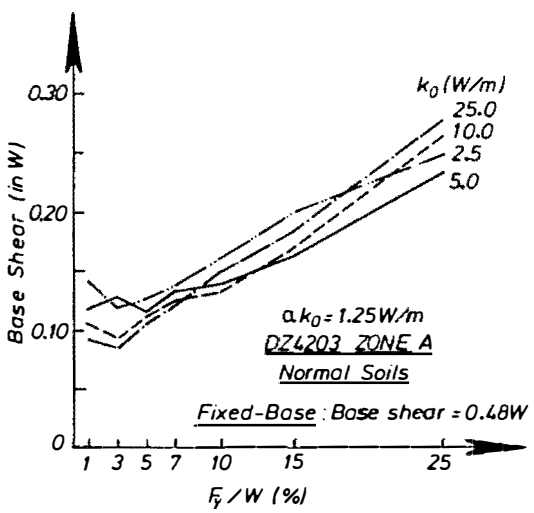

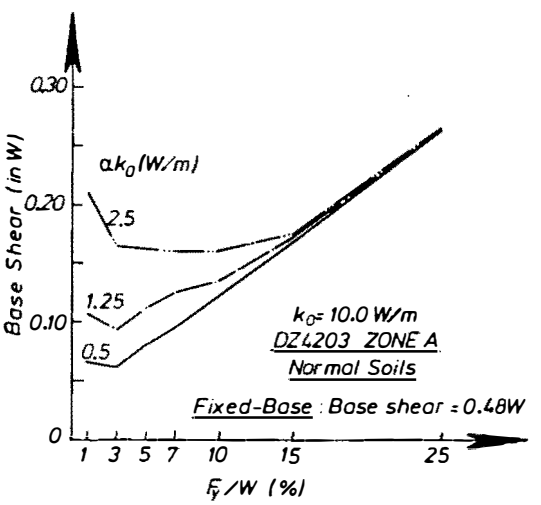

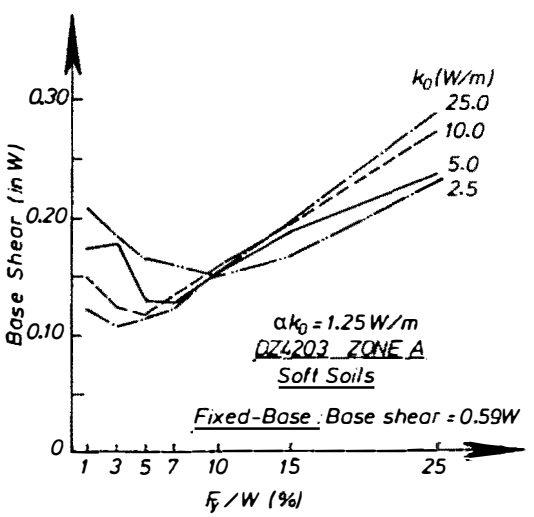

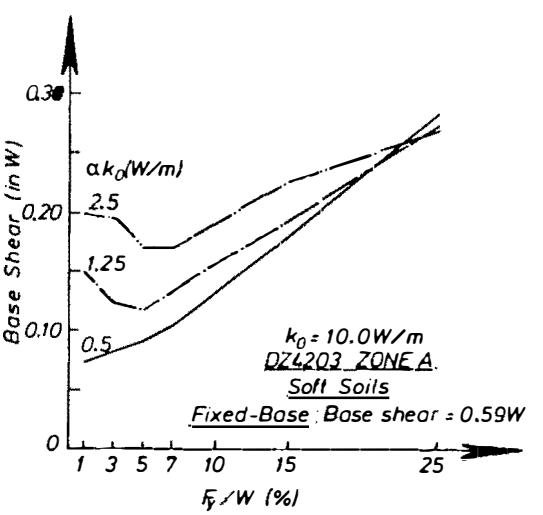

Fig. 6.9 ... (continued)

shear than a BI system with a small initial stiffness, since the former has a wider hysteresis loop area or a greater energy dissipation capacity. This phenomenon becomes more apparent when the initial stiffness is kept constant. In this case a BI system with a small post-yield stiffness has a longer effective fundamental period as well as a greater amount of hysteretic damping, thus causing a smaller base shear when compared with the one which has a large post-yield stiffness.

As a contrast, at high levels of yield strength the initial stiffness governs the structural response and generally the amount of extra damping becomes insignificant in reducing the transmitted earthquake energy. The decreasing influence of the post-yield stiffness can be seen clearly when the initial stiffness is kept constant as the increasing base shear tends to converge. When the post-yield stiffness is kept constant, a BI system with a large initial stiffness tends to induce a greater base shear except for the case of the Pacoima Dam 1971 earthquake. In this case the earthquake has extraordinarily large displacement spectra that cause the BI structure to be in the post-yield condition most of the time in spite of the high level of yield strength.

In almost all cases there are so called optimum yield strength levels in which the base shear reaches its minimum. As has been described earlier in Chapter 4, at these levels of yield strength the extra hysteretic damping increases to its maximum.

6.3.3 BASE AND TOP DISPLACEMENTS

The maximum base and top displacements of the same structural models as mentioned above are also evaluated. Since these displacements are the structural deformations measured relative to the ground, the fixed-base structures have zero base displacements. Fig. 6.10, therfore, shows only the top displacements of the fixed-base structures whereas Fig. 6.11 shows the base and top displacements of BI structures with different T1(UI) subjected to five different ground motions, namely El Centro 1940 N-S, El Centro 1979 N-S, Parkfield 1966 N65E, Pacoima Dam 1971 S16E, and Artificial A1 earthquakes.

It is recognized that the inclusion of a BI system may reduce significantly the interstorey drifts of the superstructure. As can be observed from Fig. 6.11 the top displacements of the BI structures relative to their base displacements are much less than the top displacements of the fixed-base structure as shown in Fig. 6.10, especially at short $T_{1(UI)}$. However, when the BI system is implemented for the second group of ground motions, i.e. Bucharest 1977 N-S and Mexico 1985 at the SCT site earthquakes, the relative top displacements of the BI structures are no longer significantly less than the top displacements of their unisolated counterparts. For some cases they may even exceed the top displacements of fixed-base structures as displayed in Figs 6.12.a and 6.12.b.

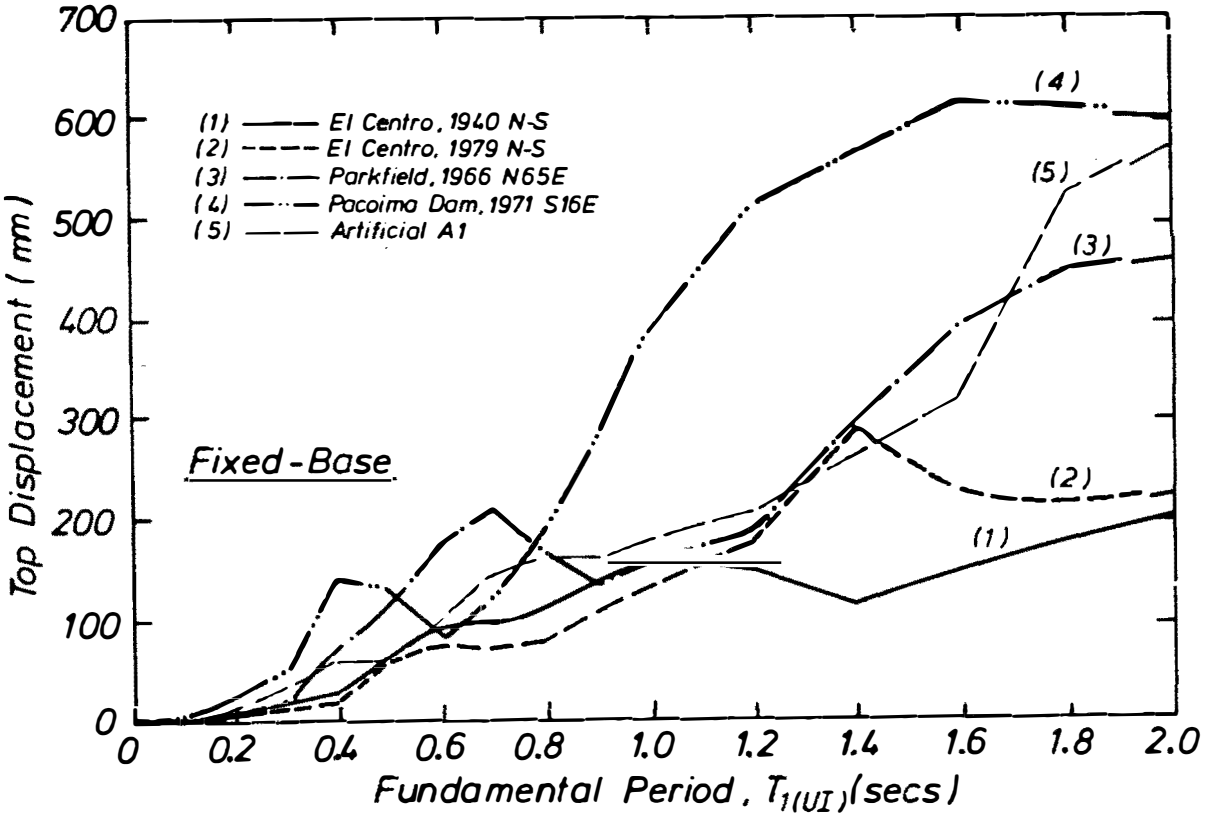

Fig. 6.10 Top-Floor Displacements of Fixed-Base Structures of Different $T_{1(UI)}$ Subjected to Earthquakes with Peak Spectral Accelerations at Short Period Region

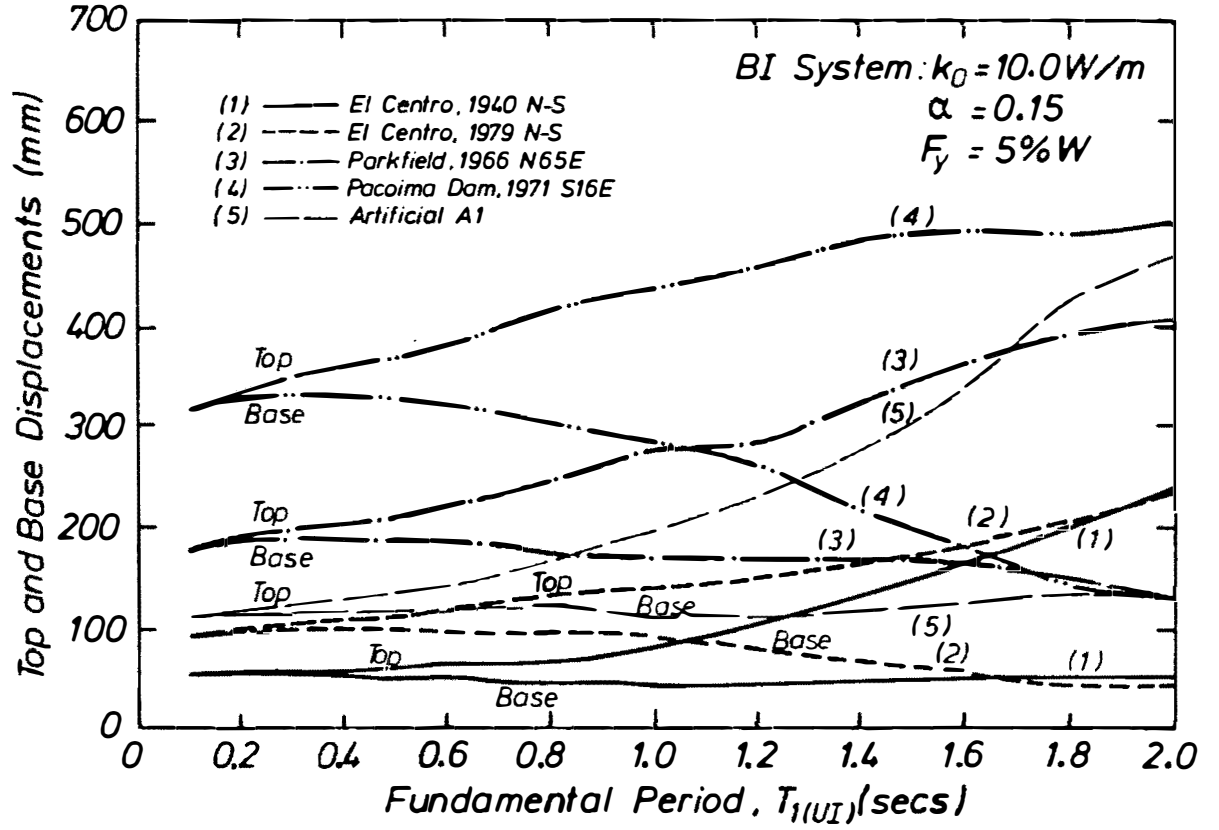

Fig. 6.11 Top and Base Displacements of BI Structures of Different $T_{1(UI)}$ Subjected to Earthquakes with Peak Spectral Accelerations at Short Period Region

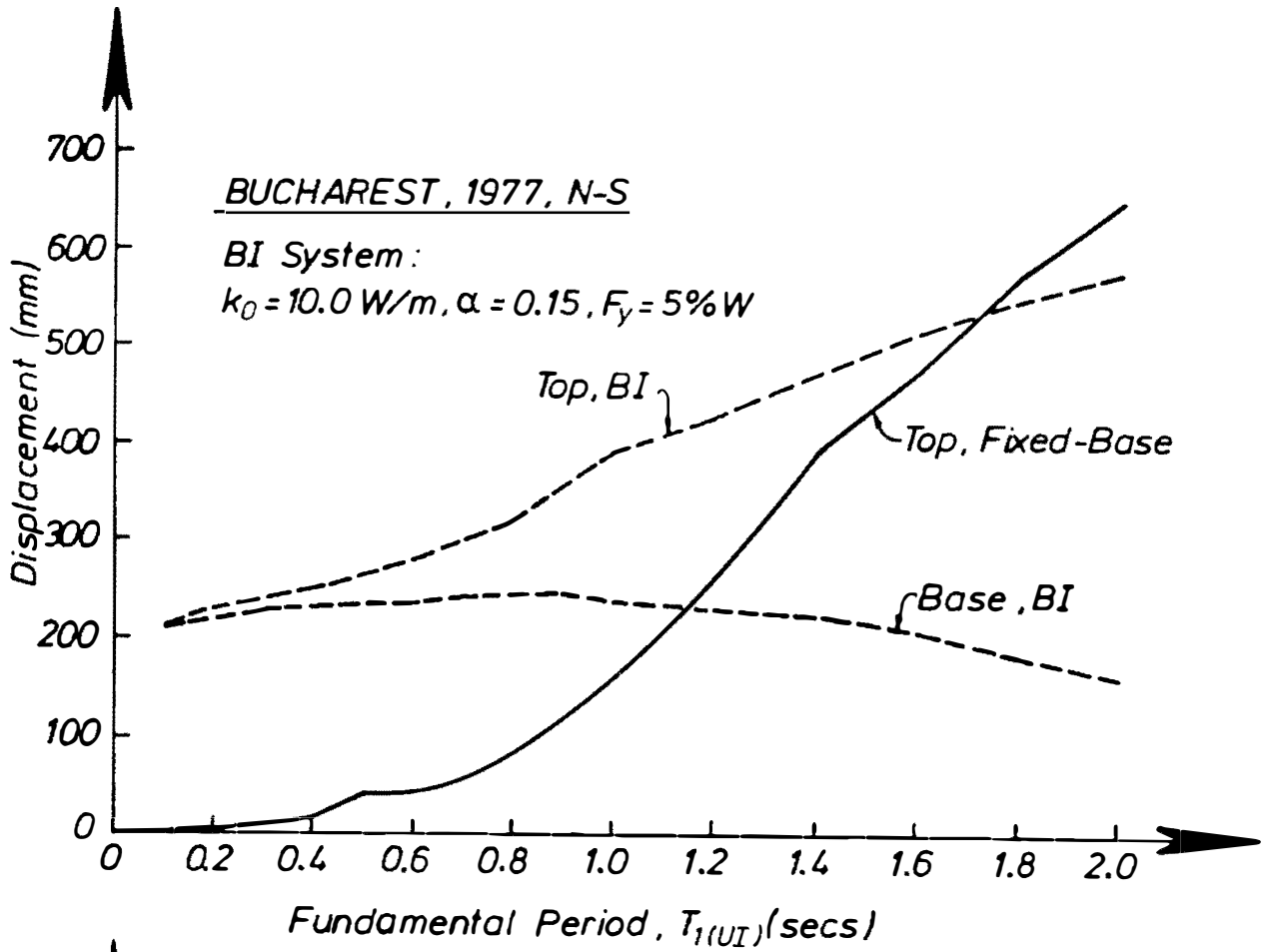

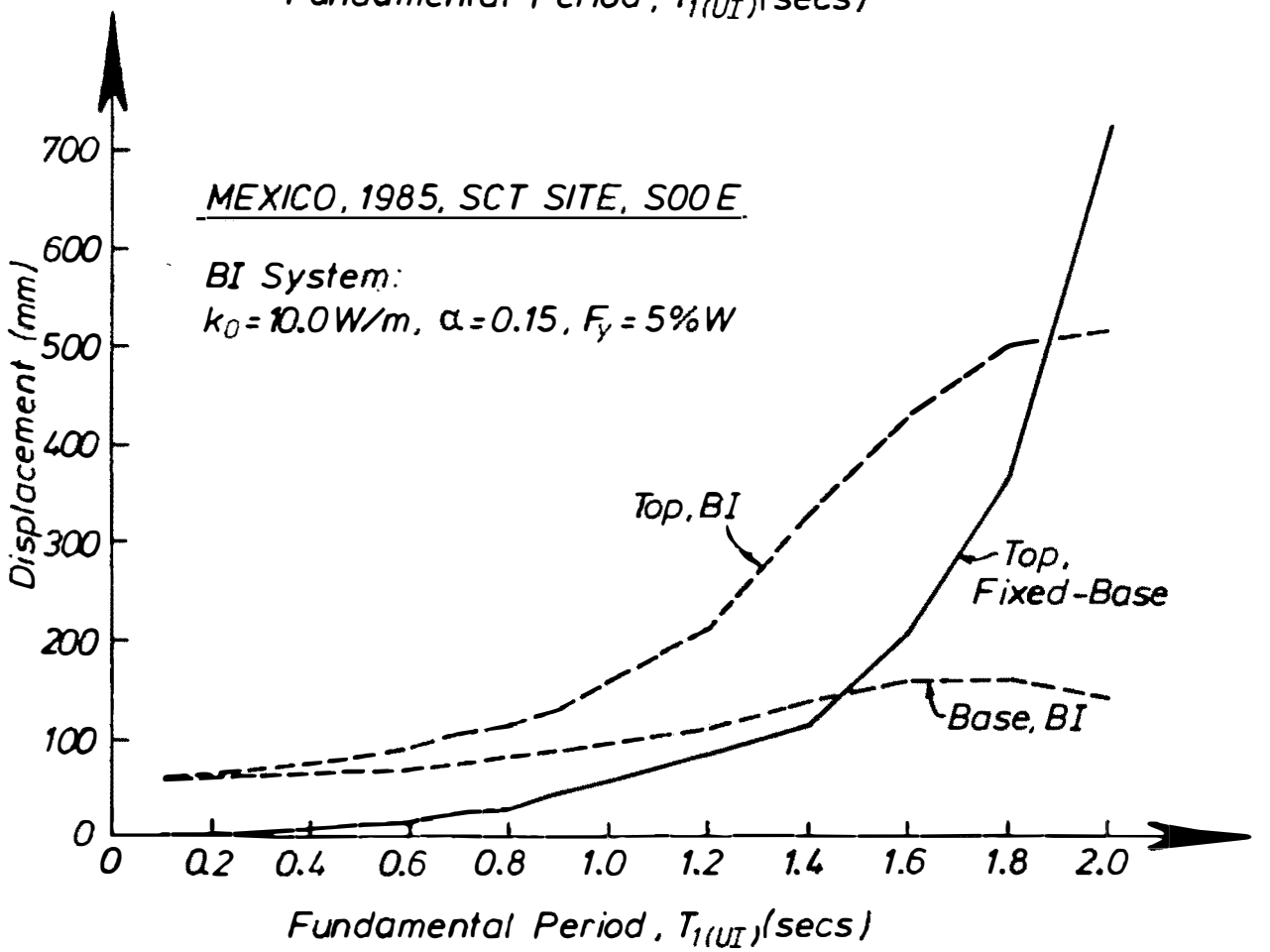

Fig. 6.12 Top and Base Displacements of Fixed-Base and BI Structures of Different $T_{1(UI)}$ Subjected to Earthquakes with Peak Spectral Accelerations at Long Period Regions

The likely maximum base and top displacements under the NZ design-level earthquakes for Zone A are also evaluated as shown in Fig. 6.13. For both normal and soft soil conditions, the top floor displacements of the BI structures relative to the base displacements are generally much less when compared with the top displacements of the fixed-base structures, especially in short periods.

It is also informative to evaluate the effect of varying the BI parameters on base displacements of BI structures subjected to different earthquakes. The evaluation is based on the results of the same series of analyses conducted to investigate the effects of varying the BI paramters on the base shear as described in the previous section.

The effect of these parameter variations is shown in Fig. 6.14. Similar trends of behaviour as found earlier in Section 4.5.4 for El Centro 1940 N-S earthquake are observed. When the initial stiffness, k_o and the yield strength, F_y are varied while the post-yield stiffness, αk_o is kept constant, it can be seen that a BI system with a large k_o induces smaller base displacements than the one with a small k_o. This is caused by a shorter effective period as well as a greater amount of hysteretic damping inherited by a BI system with a large ko. When k_o is kept constant while αk_o and F_y are varied, a BI system with a small αk_o tends to induce larger base displacements when compared with the one having a large αk_o. Smaller effective secant stiffness of the former BI system seems to be the main cause of the above phenomenon.

It can also be seen in Fig. 6.14 that low yield strengths cause large base displacements since the BI system has only a small amount of additional hysteretic damping. As the yield strength increases so does the amount of damping and the base displacements become smaller. The optimum level of yield strength is normally reached when both the base displacement and the BI system shear force are found to be the smallest. Based on this evaluation it can be confirmed that BI systems which have yield strengths in the range of 3 to 7%W will show the most optimal performance.

6.3.4 LATERAL STOREY SHEAR ENVELOPE

As described earlier in Chapter 4 based on the characteristics of the El Centro 1940 N-S earthquake, it is found that there is a strong correlation between the hysteresis loop ratio, R and the exponent p used in Eq. 6.2 for predicting the equivalent static lateral force distribution of a BI multistorey structure.

$$F_i = V \frac{W_i \, h_i^p}{\Sigma \, W_i \, h_i^p} \qquad (6.2)$$

where V is the base shear, W_i and h_i are the weight and height of floor i, respectively.

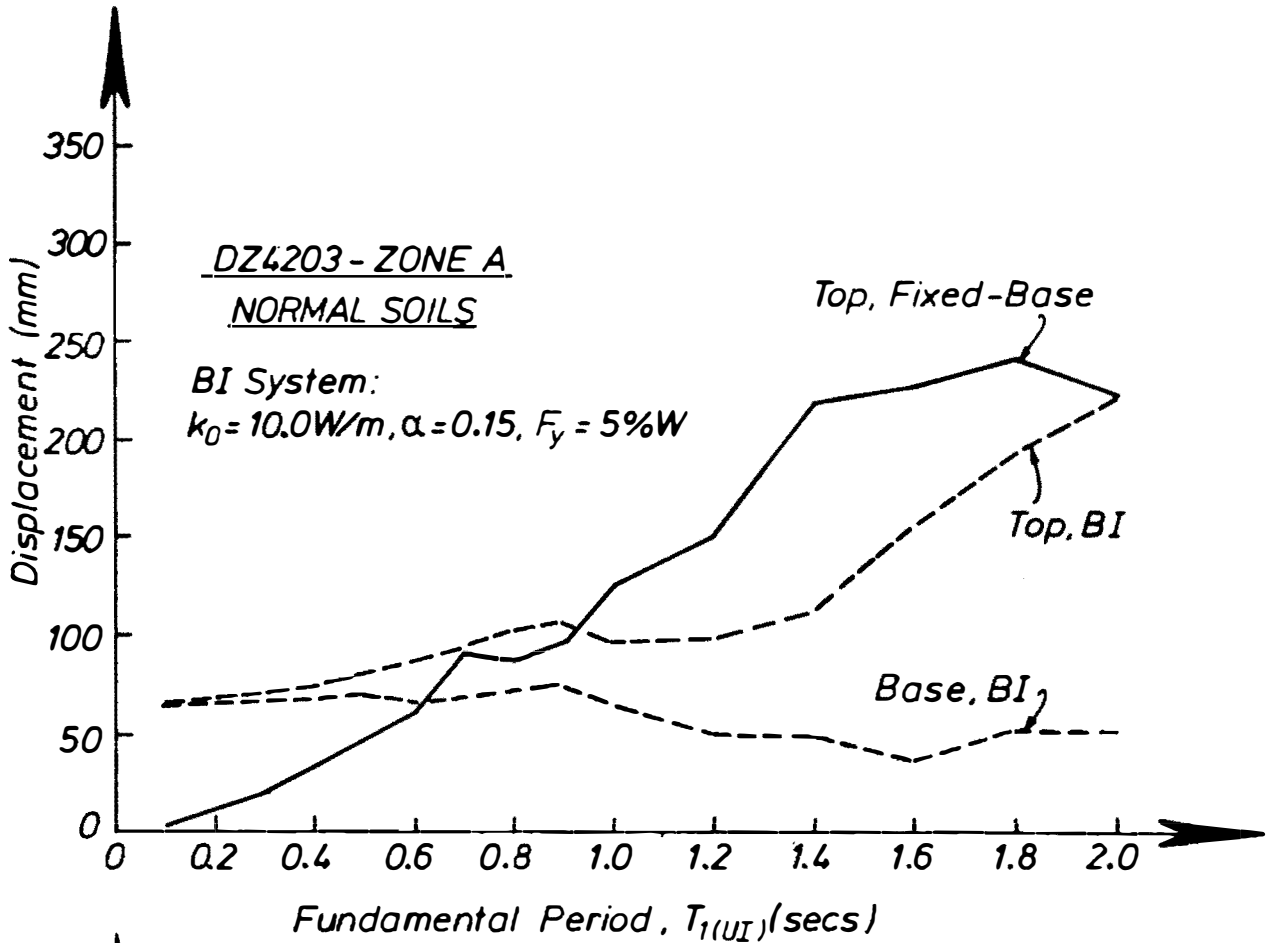

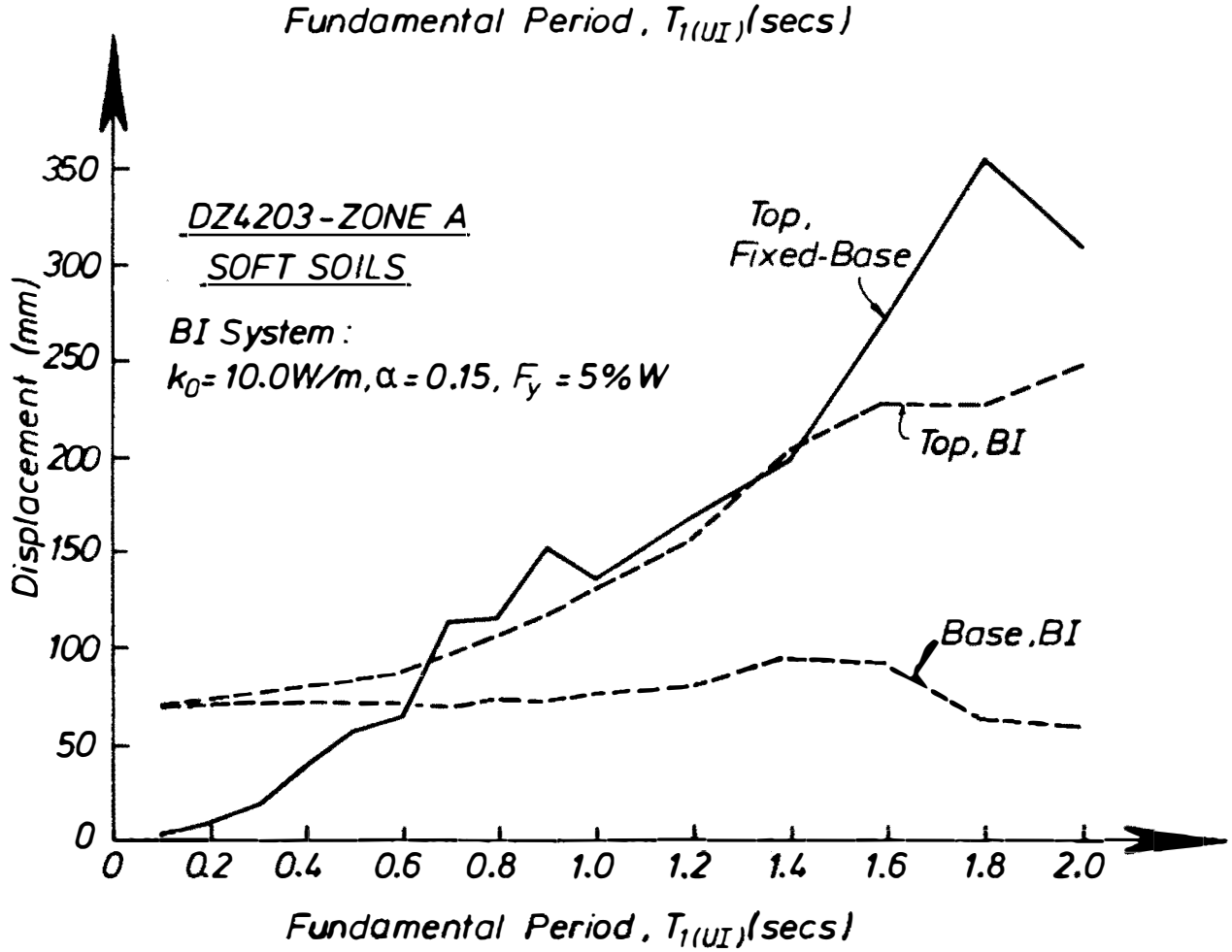

Fig. 6.13 Top and Base Displacements of Fixed-Base and BI Structures of Different $T_{1(UI)}$ Subjected to NZ Design-Level Earthquakes for Zone A

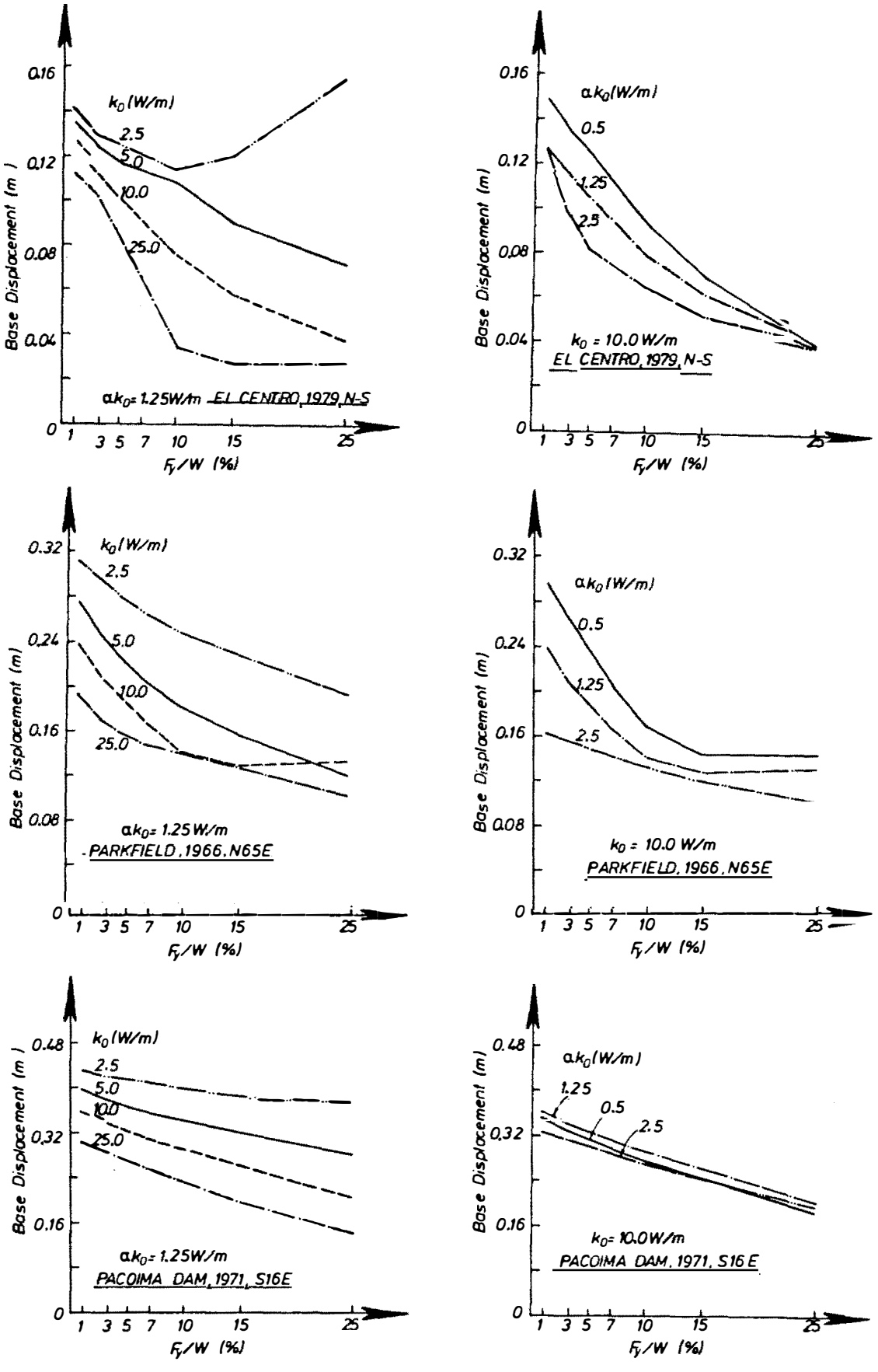

Fig. 6.14 The Effects of Varying BI Parameters on Base Displacements Under Different Earthquakes

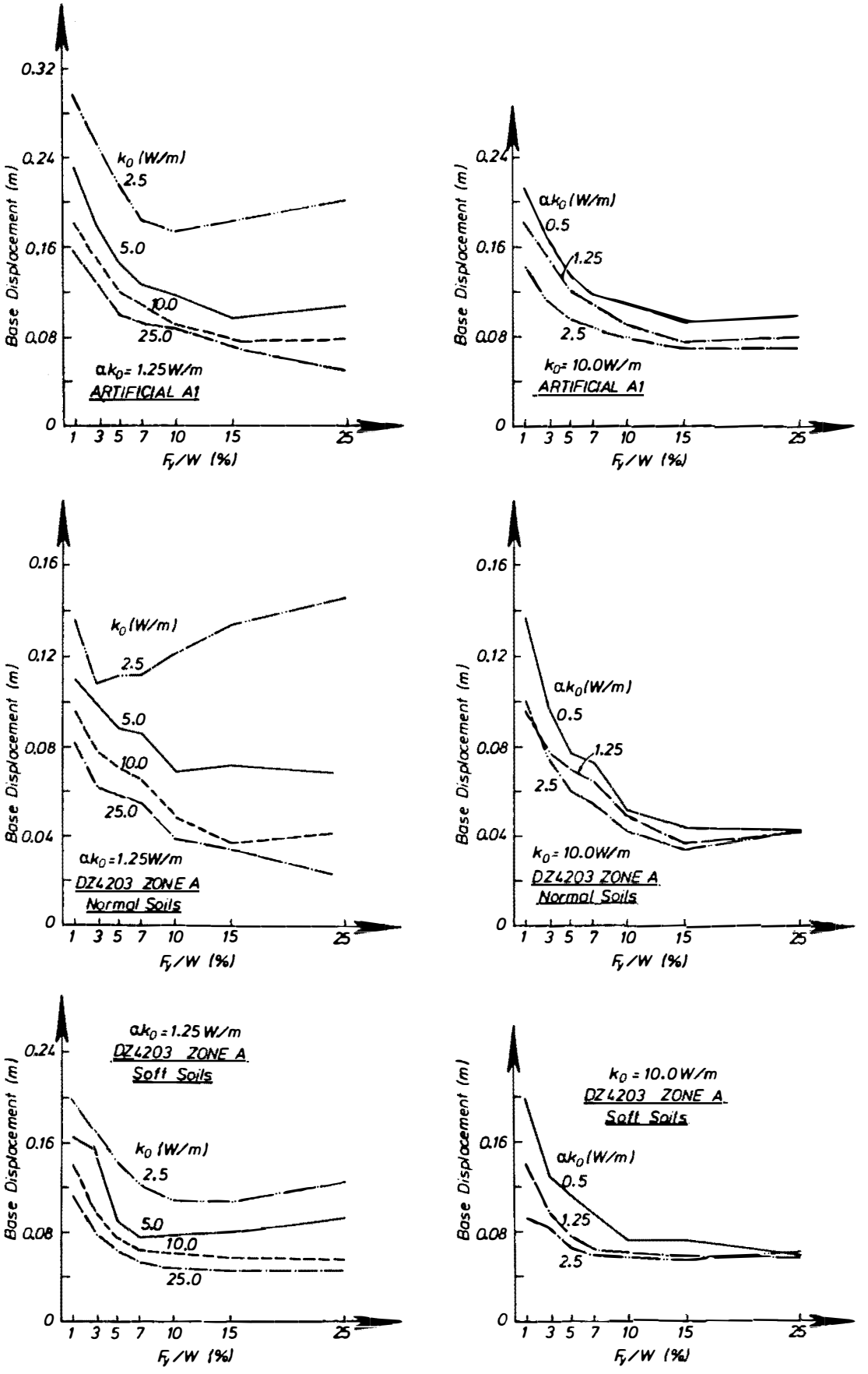

Fig. 6.14 ... (continued)

It is important, therefore, to evaluate the likely correlations between R and p mentioned above for different types of earthquake. For this purpose, a series of four storey "shear-beam" superstructure with $T_{1(UI)}$ of 0.2, 0.4, and 0.8 secs are used. These superstructures are mounted on a wide range of BI systems which have yield strengths between 3 to 7%W. As has been shown in the previous sections, at these levels of yield strength the BI system normally reaches its optimum performance.

Fig. 6.15 shows the correlations which are obtained based on the characteristics of five different ground motions, namely El Centro 1940 N-S, El Centro 1979 N-S, Parkfield 1966 N65E, Pacoima Dam 1971 S16E, and Artificial A1 earthquakes. In general strong linear correlations are encountered as indicated by high values of the coefficients of correlation, r. Note, that r = 1.0 implies to a perfectly linear correlation and that r = 0.0 shows there is no correlation.

It can be seen from Fig. 6.15 that the correlations between R and p are earthquake dependent. BI multistorey structures subjected to Pacoima Dam 1971 S16E earthquake consistently show more buldged lateral shear envelopes, thus more significant higher mode effects than BI structures subjected to the other ground motions. The Parkfield 1966 N65E and the El Centro 1979 N-S earthquake seem to cause the least significant higher mode effects. It should be noted, however, that the El Centro 1979 earthquake reveals consistently low coefficient of correlations which means there are some possibility of having much greater as well as lower values of exponent p than predicted from the correlations.

The maximum values of R observed in these analyses are also earthquake dependent. The same BI system may undergo smaller or larger maximum displacements depending on the amplitude of the ground motion. As can be seen in Fig. 6.16 a BI system which undergoes larger displacements tend to have a smaller hysteresis loop area, thus a lower value of R.

The likely lateral shear envelopes of BI structures subjected to NZ design-level earthquakes for Zone A are also studied. The results are listed in Table 6.1 and shown in Fig. 6.17. In this case two models of superstructure are considered, i.e. "shear-beam" type structures with beam-to-column stifness ratio, $\rho = \infty$ and "cantilever" type structures with $\rho = 0.0$. Consistently strong correlations between R and p are found for both normal and soft soil conditions.

The correlations between the hysteresis loop ratio, R and the exponent p of BI structures subjected to Bucharest 1977 N-S and Mexico 1985 at the SCT site earthquakes are not eveluated since the implementation of displacement-dependent BI systems for this second group ground motion may not reduce the lateral storey shears. Fig. 6.18 demonstrates this phenomenon and contrasts the effects of a BI system on the lateral storey shear envelopes of structures subjected to El Centro 1940 N-S, Bucharest 1977 N-S, and Mexico 1985 earthquakes. Three types of BI system with thin (k_o = 2.5 W/m, α = 0.5, F_y = 5%W), moderate (k_o = 10.0 W/m, α = 0.15, F_y = 5%W), and fat (k_o = 10.0 W/m, α = 0.05, F_y = 5%W) hysteresis loops are considered. It can be seen in Fig. 6.18 that for ground motions which has peak spectral accelerations in the short period region, such as El

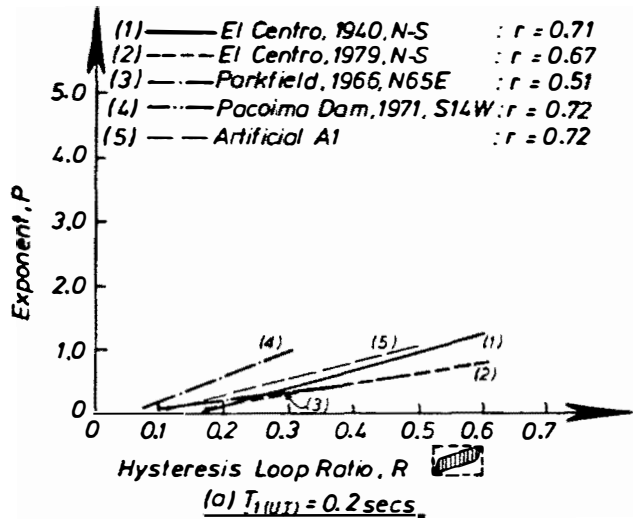

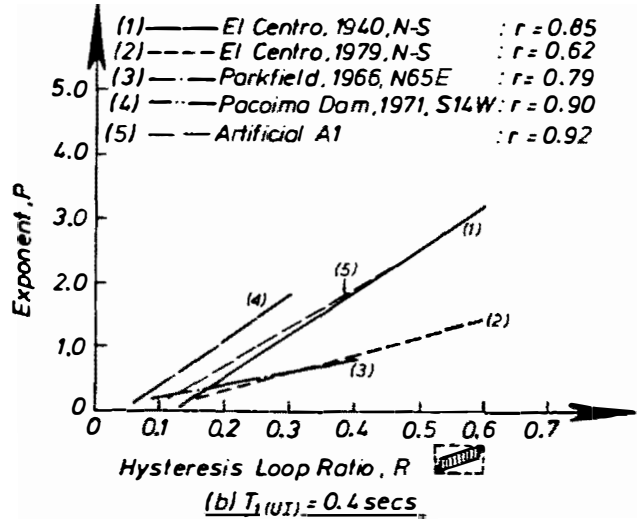

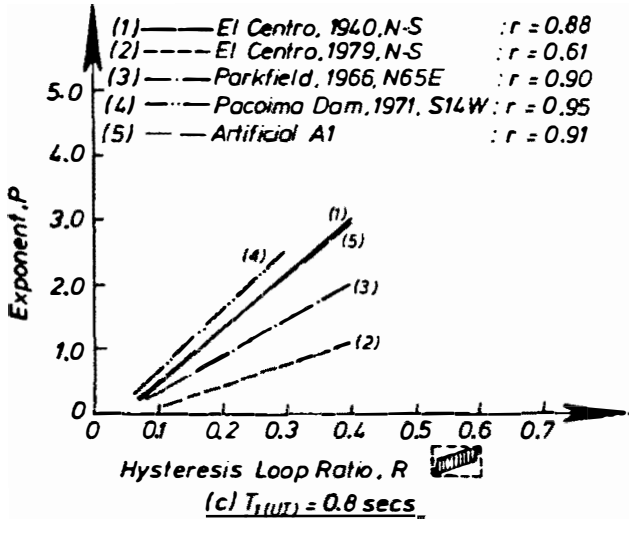

Fig. 6.15 Relationships Between R and p for Different $T_{1(UI)}$ under Various Earthquakes

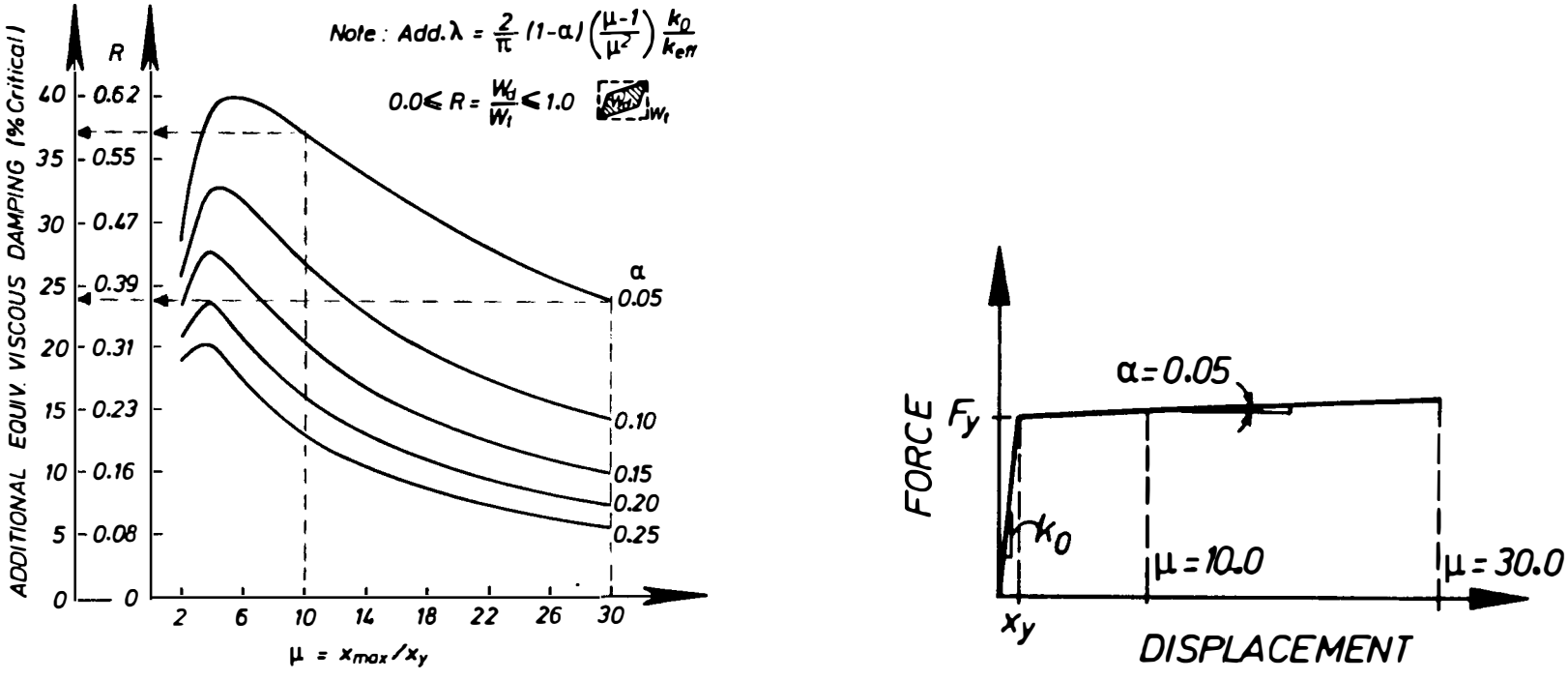

Fig. 6.16 The Effect of Maximum Base Displacement on the Value of R of a BI System

Table 6.1 Correlations Between the Hysteresis Loop Ratio, R and the Exponent p for NZ Design-Level Earthquake in Zone A

Soil Condition	$T_{1(UI)}$ secs	ρ	Linear Regression		
			A	B	r
Normal	0.2	0.0	-0.55	3.88	0.81
		∞	-0.31	2.57	0.66
	0.4	0.0	-0.40	6.45	0.83
		∞	-0.66	6.12	0.83
	0.8	0.0	0.16	5.90	0.79
		∞	-0.45	7.41	0.88
Soft	0.2	0.0	-0.32	3.05	0.77
		∞	-0.26	2.14	0.74
	0.4	0.0	-0.18	4.34	0.87
		∞	-0.64	6.20	0.89
	0.8	0.0	0.10	7.28	0.78
		∞	0.20	5.18	0.80

Note : Exponent p = A + BR

R = Hysteresis Loop Ratio

r = correlation coefficient

(≈ 1.00 implies a perfectly linear correlation)

ρ = beam-to-column stiffness ratio

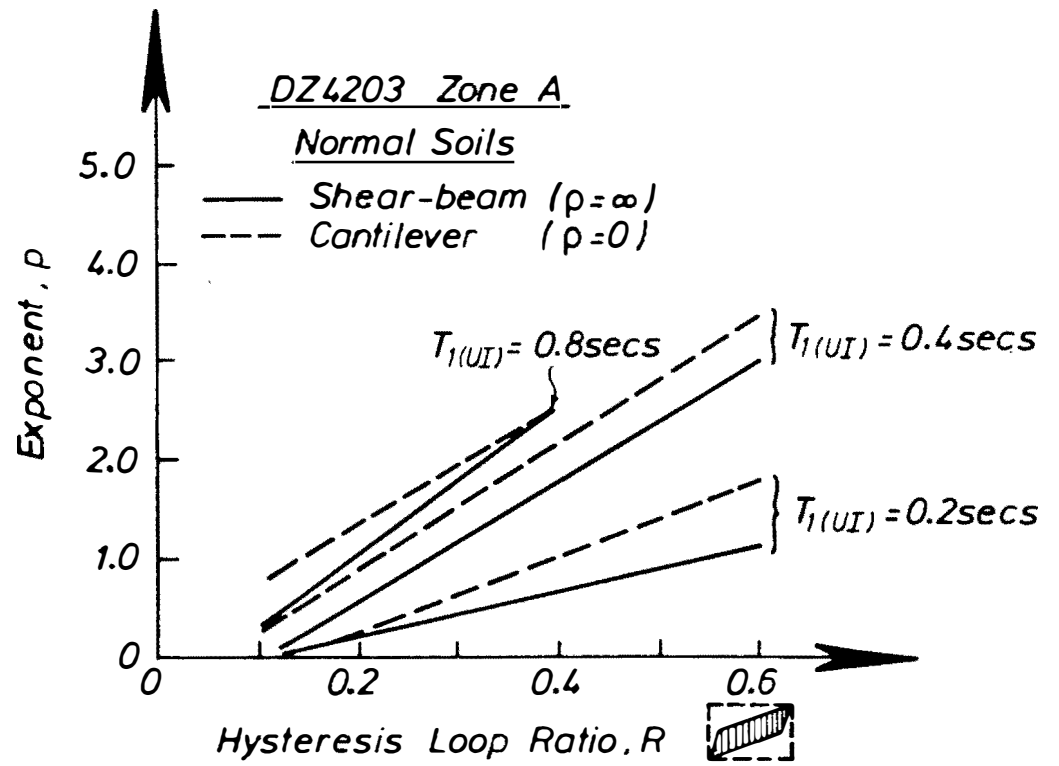

(a)

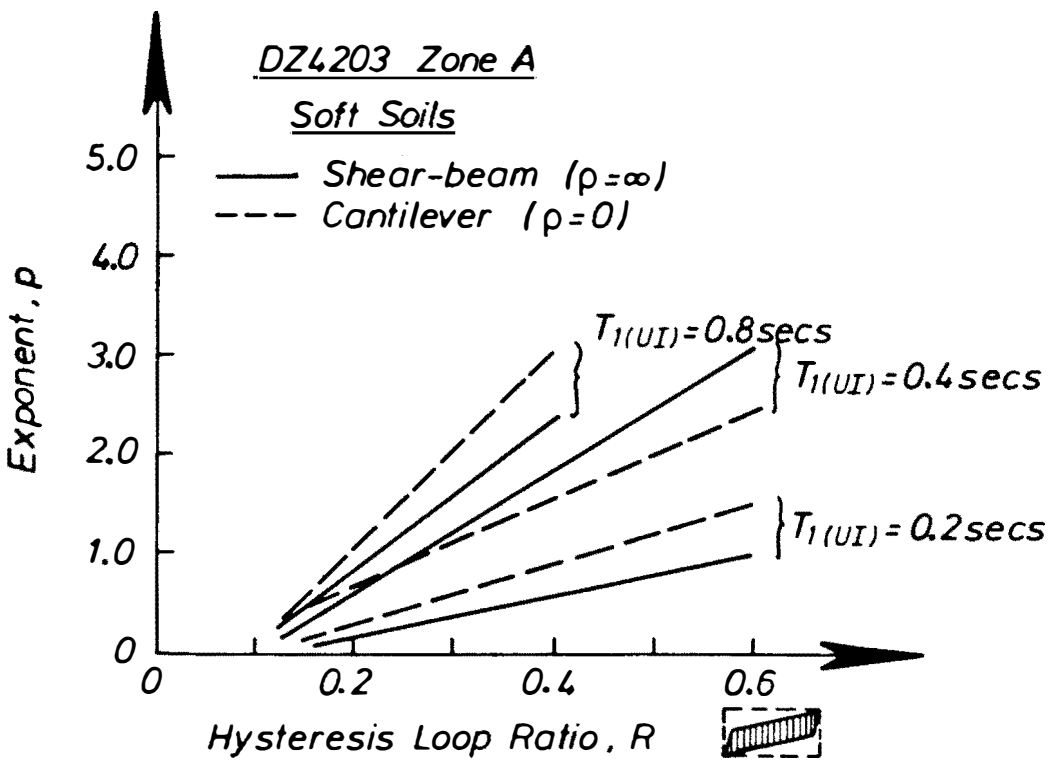

(b)

Fig. 6.17 Relationships Between R and p for Different $T_{1(UI)}$ under NZ Design-Level Earthquakes for Zone A

Centro 1940 N-S earthquake, the inclusion of any type of BI system can cause significant reduction of the lateral storey shears. As a contrast, under Bucharest 1977 N-S and Mexico 1985 (SCT sites) earthquakes, which have peak spectral accelerations at about 1.4 and 2.0 seconds respectively, the inclusion of a displecement-dependent BI system may even increase the lateral storey shears. As shown in Fig. 6.18, structures mounted on thin and moderately fat hysteresis loops have larger storey shears than their fixed-base counterparts. Some reductions can only be achieved by using BI systems with large energy dissipation capacities. However these reductions are still not so dramatic as in the El Centro 1940 N-S earthquake.

6.3.5 DISCUSSION OF THE DESIGN ASPECTS

In Chapter 4, a Code-Type design approach has been shown to be able to satisfactorily estimate the lateral storey shears of BI multistorey structures subjected to El Centro 1940 N-S earthquake. To further examine its reliability, this Code-Type approach is applied in this section to predict the lateral storey shears of BI multistorey structures subjected to a series of different earthquakes. A similar procedure to that described in Chapter 4 is followed. An example of the detailed calculations can be found in Chapter 7.

Table 6.2 shows that the predicted lateral storey shears of four different earthquakes are satisfactorily close to the time history analysis results. In this case, the fundamental periods of the structures on an equivalent fixed-base, $T_{1(UI)}$ are 0.4 and 0.8 secs and the BI system has an initial stiffness, k_o of 10.0 W/m, a post-yield stiffness, αk_o of 1.5 W/m, and a yield strength, F_y of 5%W.

It is also important to evaluate the use of this Code-Type design approach for estimating the lateral storey shears of BI multistorey structures under the NZ design-level earthquakes for Zone A. For this purpose, a series of four storey BI structures with $T_{1(UI)}$ of 0.4 and 0.8 seconds are considered. Two superstructure models are included, i.e. "shear-beam" and "cantilever" type structures which have beam-to-column stiffness ratios, $\rho = \infty$ and 0.0 respectively. These supertructures are mounted on two types of BI system. The first system (Case A) has moderately fat hysteresis loops with k_o = 10.0 W/m, αk_o = 1.5 W/m, and F_y = 5% W and the second one (Case B) has fat hysteresis loops with k_o = 10.0 W/m, αk_o = 0.5 W/m, and F_y = 5%W. The predicted lateral storey shears are compared with the time history analysis results as shown in Tables 6.3 and 6.4 for normal and soft soil conditions respectively.

It is found in Case A, for both normal and soft soil conditions, that the Code-Type approach satisfactorily estimates the lateral storey shears with reasonably higher values when compared with the inelastic time history analysis results. In Case B, however, the safety margins are found to be slightly excessive. It seems that the main cause of these discrepancies lies on the "over" prediction of the maximum base shear from the BI system's maximum shear force using the modification factors shown in Fig. 6.19. As also shown earlier in Fig. 4.43 of

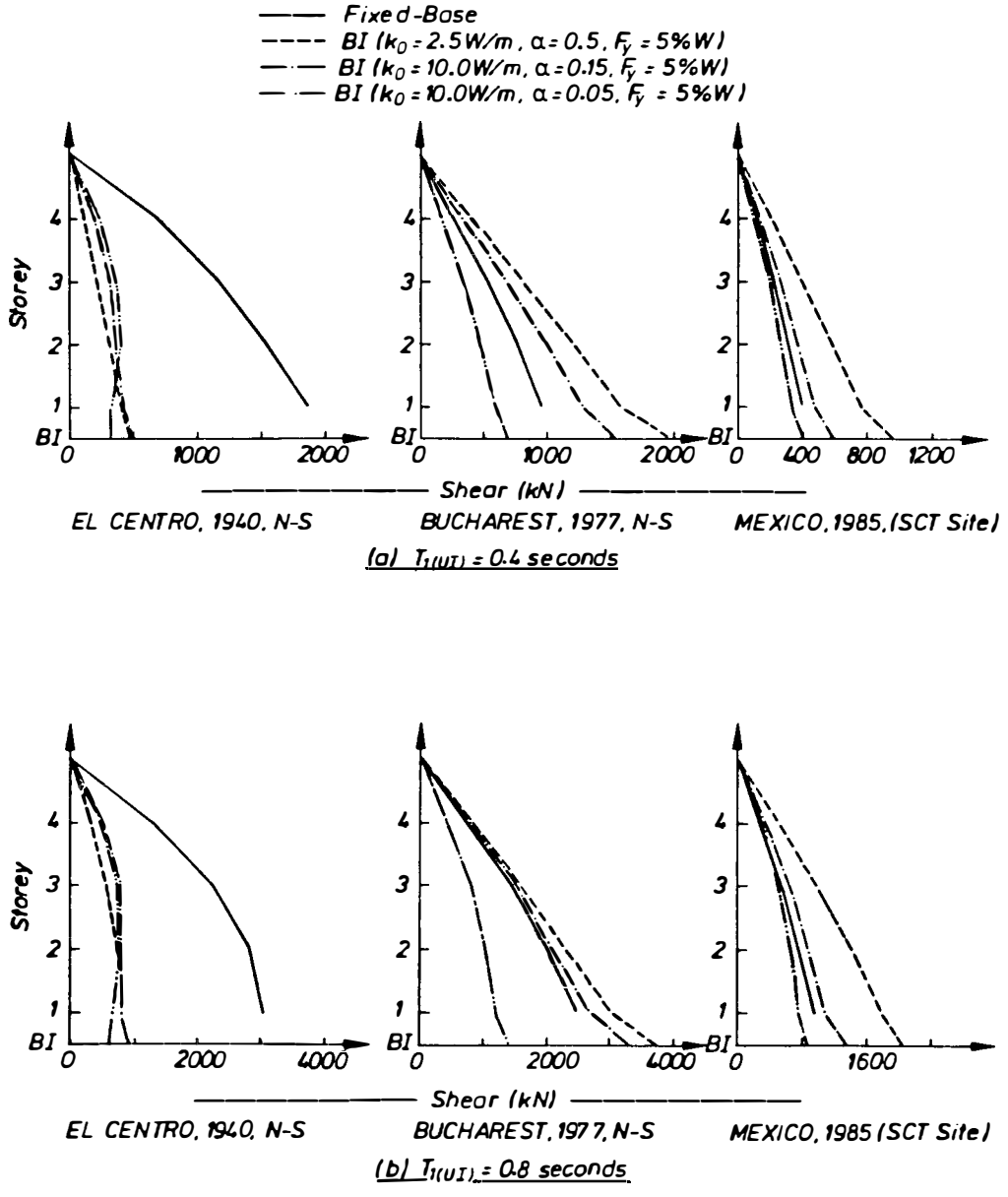

Fig. 6.18 The Effects of Various BI Systems on the Lateral Storey Shears of Structures Subjected to Different Types of Earthquake

Table 6.2 Lateral Storey Shears of BI Structures Subjected to Various Earthquakes As Predicted By the Code-Type Approach

Earth-quake	$T_{1(UI)}$ secs	μ	k_{eff} (W/m)	T_{1eff} secs	λ % crit.	R	p	Sto. Shear (kN) App.	Sto. Shear (kN) THA	Diff. %
El Centro 1979 N-S	0.4	19.7	1.93	1.48	18.5	0.21	0.31	191.8	185.4	3.4
								364.4	352.4	3.4
								517.8	507.8	2.0
								639.3	642.7	-0.5
								752.1*	761.1*	-1.2
	0.8	17.5	1.99	1.59	19.7	0.23	0.56	410.0	472.6	-13.2
								770.0	847.5	-9.1
								1055.7	1047.0	0.8
								1242.0	1252.0	-0.8
								1380.0*	1484.0*	-7.0
Parkfield 1966 N65E	0.4	45.8	1.68	1.58	11.9	0.11	0.21	346.0	326.1	6.1
								679.7	615.9	10.3
								976.3	877.4	11.3
								1235.8	1089.0	13.5
								1544.7*	1289.0*	19.8
	0.8	42.3	1.70	1.69	12.3	0.1	0.38	738.2	651.6	13.3
								1381.2	1229.0	12.4
								1952.7	1770.0	10.3
								2381.4	2199.0	8.3
								2976.7*	2430.0*	22.5
Pacoima 1971 S16E	0.4	79.8	1.61	1.61	9.2	0.06	0.09	535.6	460.8	16.2
								1071.2	916.3	16.9
								1586.2	1352.0	17.3
								2060.0	1741.0	18.3
								2575.0*	2165.0*	18.9
	0.8	70.1	1.62	1.72	9.7	0.07	0.38	1131.1	1090.0	3.8
								2116.2	2046.0	3.4
								2991.9	2813.0	6.3
								3638.7	3542.0	2.7
								4548.4*	3990.0*	14.0
Artificia A1	0.4	23.6	1.86	1.51	16.8	0.18	0.58	275.9	222.7	23.9
								503.1	434.4	15.8
								689.8	618.8	11.5
								811.5	755.8	7.4
								1014.4*	878.4*	15.5
	0.8	27.6	1.81	1.65	15.4	0.16	1.00	655.4	594.2	10.3
								1146.9	982.9	16.7
								1474.6	1302.0	13.2
								1638.4	1575.0	4.0
								2048.0*	1816.0*	12.8

Note : * denotes the BI system shear force

Table 6.3 Lateral Storey Shears of BI Structures on Normal Soils Subjected to a NZ Design-Level Earthquake for Zone A As Predicted by the Code-Type Approach

(a) Case A : $k_o = 10.0$ W/m $\alpha = 0.15$ $F_y = 5\%W$

T_1(UI) secs	ρ	μ	k_{eff} (W/m)	T_{1eff} secs	λ %crit.	R	p	Storey Shears (kN) App.	Storey Shears (kN) THA	Diff. %
0.4	0.0	17.4	1.99	1.46	19.7	0.23	1.08	241.0	220.4	9.3
								417.4	347.2	20.2
								535.0	424.8	25.9
								587.9	496.6	18.4
								(691.6)	(566.5)	(22.1)
	∞	17.2	2.00	1.46	19.8	0.23	0.75	211.6	180.3	17.3
								388.0	315.3	23.1
								511.5	418.1	22.3
								587.9	485.3	21.1
								(691.6)	(579.4)	(19.4)
0.8	0.0	14.8	2.07	1.53	21.4	0.26	1.69	303.2	236.8	28.0
								495.0	365.7	35.3
								587.8	406.1	44.7
								618.7	502.5	23.1
								(687.5)	(682.7)	(0.70)
	∞	13.9	2.11	1.55	22.1	0.27	1.55	485.2	464.4	4.5
								788.4	717.9	9.8
								950.1	914.6	3.9
								1010.7	1048.0	3.7
								(1175.3)	(1206.0)	(-2.5)

(b) Case B : $k_o = 10.0$ W/m $\alpha = 0.05$ $F_y = 5\%W$

T_1(UI) secs	ρ	μ	k_{eff} (W/m)	T_{1eff} secs	λ %crit.	R	p	Storey Shears (kN) App.	Storey Shears (kN) THA	Diff. %
0.4	0.0	13.8	1.19	1.87	39.2	0.54	3.21	257.4	192.8	33.5
								358.8	298.0	20.4
								386.1	329.7	17.1
								390.0	327.8	19.0
								(325.0)	(345.5)	(-5.93)
	∞	12.4	1.27	1.81	40.4	0.56	2.77	244.3	180.9	35.0
								354.6	293.0	21.0
								390.1	323.8	20.5
								394.0	319.0	23.5
								(328.3)	(344.8)	(-4.8)
0.8	0.0	12.4	1.27	1.88	40.4	0.56	3.46	292.8	233.3	25.5
								400.4	352.8	13.5
								426.3	378.0	12.8
								430.6	353.1	21.9
								(358.8)	(368.0)	(-2.5)
	∞	12.3	1.27	1.88	40.5	0.56	3.70	529.2	448.0	18.1
								710.6	703.2	1.0
								756.0	743.9	1.6
								756.0	696.5	8.7
								(630.0)	(683.6)	(-7.8)

Note : THA = Time History Analysis

( ) denotes the BI system shear force

Table 6.4 Lateral Storey Shears of BI Structures on Soft Soils Subjected to a NZ Design-Level Earthquake for Zone A As Predicted by the Code-Type Approach

(a) Case A : $k_o = 10.0$ W/m $\alpha = 0.15$ $F_y = 5\%W$

T_1(UI) secs	ρ	μ	k_{eff} (W/m)	T_{1eff} secs	λ %crit.	R	p	Storey Shears (kN) App.	Storey Shears (kN) THA	Diff. %
0.4	0.0	17.4	1.99	1.46	19.7	0.23	0.82	218.0	212.1	2.8
								394.8	358.8	10.0
								518.6	448.2	15.7
								589.3	497.0	18.6
								(693.3)	(581.2)	(19.3)
	∞	17.2	1.99	1.46	19.7	0.23	0.79	218.0	203.9	6.9
								388.9	328.0	18.6
								518.6	432.2	20.0
								589.3	518.9	13.6
								(693.3)	(597.2)	(16.1)
0.8	0.0	17.2	1.99	1.55	19.8	0.23	1.77	334.8	299.0	12.0
								531.7	471.4	12.8
								630.1	522.2	20.7
								656.4	520.5	26.1
								(772.3)	(659.0)	(17.2)
	∞	17.3	1.99	1.59	19.8	0.23	1.39	538.9	509.9	5.7
								890.3	856.9	3.9
								1089.5	1020.0	6.8
								1171.5	1159.0	1.0
								(1378.2)	(1199.0)	(14.9)

(b) Case B : $k_o = 10.0$ W/m $\alpha = 0.05$ $F_y = 5\%W$

T_1(UI) secs	ρ	μ	k_{eff} (W/m)	T_{1eff} secs	λ %crit.	R	p	Storey Shears (kN) App.	Storey Shears (kN) THA	Diff. %
0.4	0.0	23.5	0.90	2.14	32.2	0.43	1.69	251.1	173.2	45.0
								409.9	263.4	55.6
								486.8	303.8	60.2
								512.4	347.5	47.4
								(427.0)	(405.1)	(5.4)
	∞	23.7	0.90	2.11	32.1	0.43	2.03	279.8	215.9	29.6
								435.3	323.2	34.7
								502.6	318.3	57.9
								518.2	367.4	41.0
								(432.8)	(412.7)	(4.6)
0.8	0.0	22.3	0.93	2.17	33.0	0.44	3.30	376.8	303.4	24.2
								523.0	442.8	18.1
								556.8	447.2	24.5
								562.4	376.3	49.4
								(468.7)	(402.1)	(16.6)
	∞	22.3	0.93	2.19	33.0	0.44	2.48	590.5	468.7	26.0
								880.8	809.9	8.7
								980.9	778.5	26.0
								1000.9	733.9	36.4
								(834.1)	(706.0)	(18.1)

Note : THA = Time History Analysis

( ) denotes the BI system shear force

Chapter 4 these modification factors are actually derived from extensive observations of time history analysis results carried out under El Centro 1940 N-S earthquake which may have a different nature from the simulated NZ earthquakes. Further investigation is required to be able to adjust the above modification factors for BI systems with fat hysteresis loops, and which are to be installed in New Zealand.

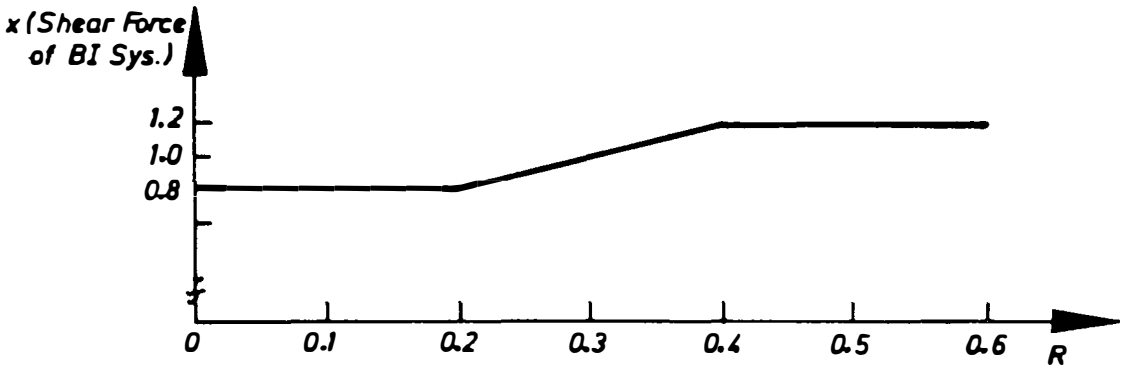

Fig. 6.19 Modification Factors Used for Predicting the Maximum Base Shear from the BI system's Maximum Shear Force.

Although Bucharest-type ground motion is not a typical NZ earthquake it is informative to evaluate briefly the possibility of implementing a suitable BI system in areas with this type of ground motion. Fig. 6.20 shows the lateral storey shear envelopes and storey displacements of a typical four storey structure ($T_{1(UI)}$ = 0.4 secs) on a fixed-base and on a BI system subjected to Bucharest 1977 N-S earthquake.

Five different types of BI system are considered. Two of them are displacement-dependent BI systems with moderately and extremely fat hysteresis loops (Cases 2 and 3). Both systems have the same initial stiffness, i.e. k_0 = 10.0 W/m, but different post-yield stiffnesses, i.e 1.5 and 0.0 W/m, and different yield strengths, i.e. 5.0 and 3.0%W for the former and the latter systems respectively. Two other types (Case 4 and 5) are combinations between the bilinear BI systems with extremely fat hysteresis loops and velocity-dependent dampers. The last system (Case 6) consists of elastomeric bearings, with a total elastic stiffness of 0.5 W/m, and a viscous damper of 725 kN/ms^{-1} or equivalent to 40% critical damping.

It can be readily seen from Fig. 6.20 that the displacement-dependent BI system with moderately fat hysteresis loops causes greater storey shears than the shears of the fixed-base structure. In

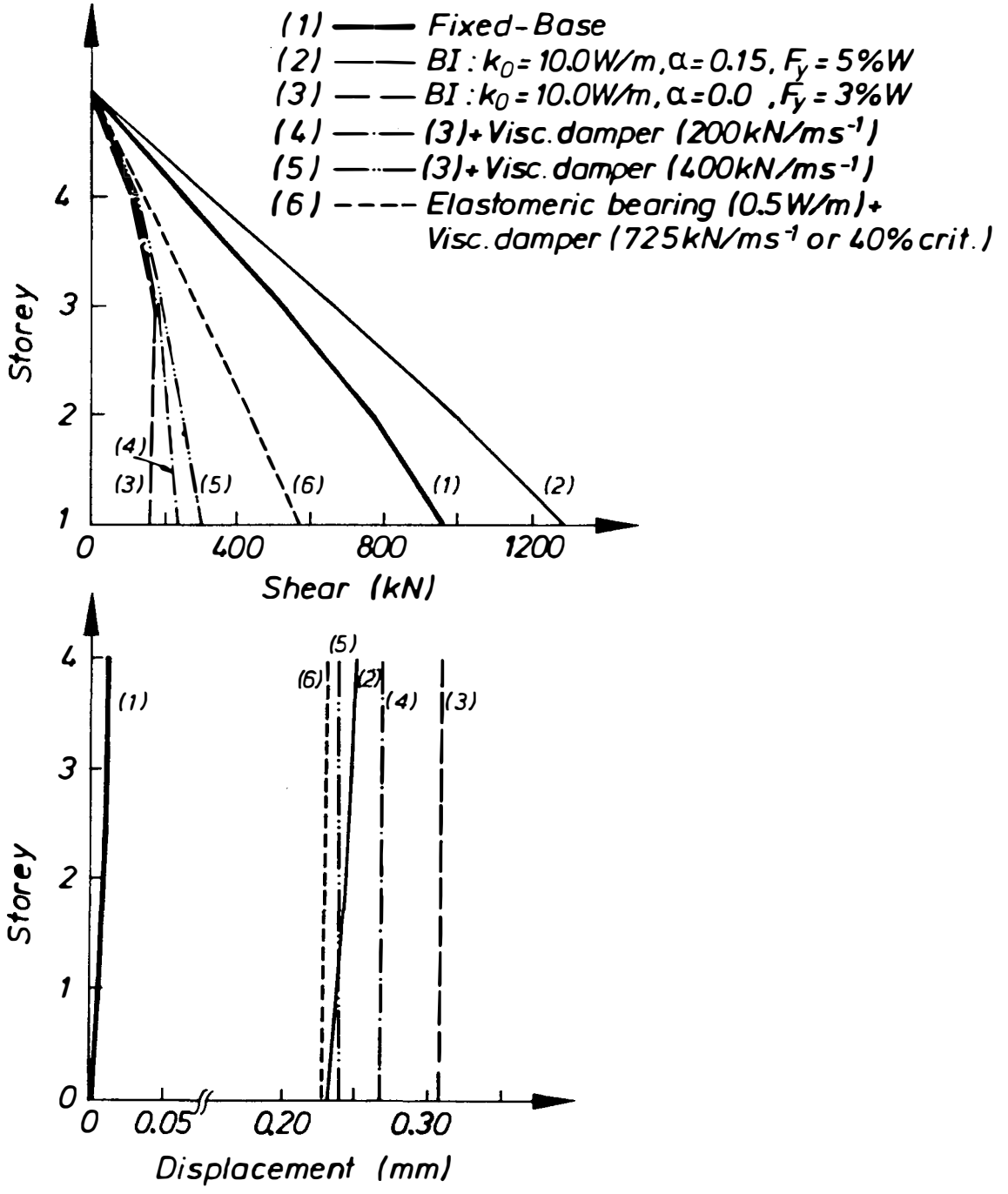

Fig. 6.20 Lateral Storey Shear Envelopes and Storey Displacements of a Four-Storey Structure on a Fixed-Base and Various BI Systems Subjected to Bucharest 1977 N-S Earthquake

this case the BI system shifts the fundamental period of the structure into a more dominant earthquake energy region and it does not have sufficiently large hysteretic damping to counteract it. When this BI system is replaced by the other displacement-dependent BI system which has extremely fat hysteresis loops, significantly lower inertia forces can be obtained. This system is flexible enough to shift the fundamental period of the structure ($T_{1\ eff}$ > 2.0 secs) well beyond the peak spectral acceleration region (1.4 secs). The amount of its hysteretic damping has also a major contribution in lowering these forces as well as avoiding excessive base displacements. These displacements can still be reduced by introducing some more damping as shown in Cases 4 and 5. As the damping value is increased, however, a slightly greater base shear is observed.

As mentioned earlier in Chapter 2, the BI system designated as Case 6 is normally used in Japan[6.20] and is probably recognized to date as the most suitable device for Bucharest-type ground motion. It shows definitely much lower displacements when compared with the displacement caused by the displacement-dependent BI system in Case 3. However, it may induce larger storey shears as shown in Fig. 6.20. Based on these analysis results, BI systems with large damping are recommended for sites with peak spectral accelerations of their ground motions occur in the longer periods. Using this type of BI system, significant reductions of lateral inertia forces can be achieved. The combination of hysteretic and viscous dampers seems to show better performance than the combination of elastomeric bearings and viscous dampers.

6.4 EVALUATION OF PERMANENT PLASTIC OFFSET

It should be realized that any hysteretic inelastic system has the possibility of undergoing a permanent plastic offset. Systems with a large non-linearity are normally more prone to a permanent plastic offset than systems with a small non-linearity.

As mentioned earlier in Chapter 2, a desirable BI system should have a sufficient restoring force to relocate the structure as close as possible to its original position after an earthquake attack. It is therefore important to conduct a sensitivity study to evaluate the effects of the BI system parameters as well as the ground motion characteristics on plastic offsets. For this purpose, a four storey "shear-beam" with $T_{1(UI)}$ of 0.4 secs is used. The superstructure is mounted on five different types of BI system and subjected to two different ground motions, i.e. El Centro 1940 N-S and Parkfield 1966 N65E earthquakes. As shown in Fig. 6.21, the former ground motion is a vibratory-type earthquake with a maximum displacement of 109 mm occuring at around 8.5 secs during its duration. The latter ground motion has a pronounced displacement of 265 mm at about 4.0 seconds during its duration[6.21].

Figs 6.22.a and 6.22.b show the response history of base displacements under El Centro 1940 N-S and Parkfield 1966 N65E, respectively. To obtain these results, the time history analyses are run using a 20-second duration of the earthquake records and another 20 seconds of free vibration.

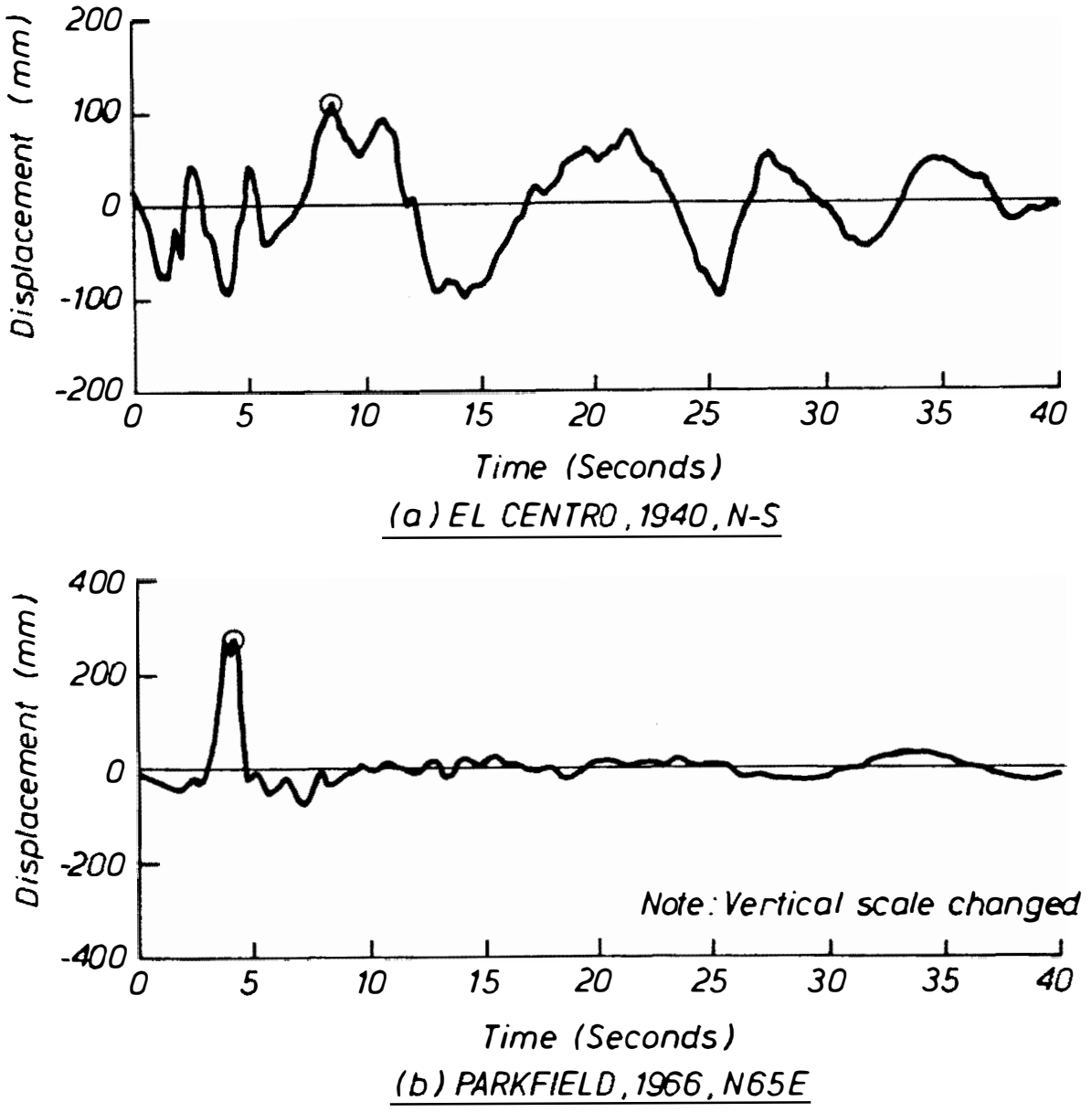

Fig. 6.21 Integrated Displacements for El Centro 1940 N-S and Parkfield 1966 N65E Earthquake Records[6.21]

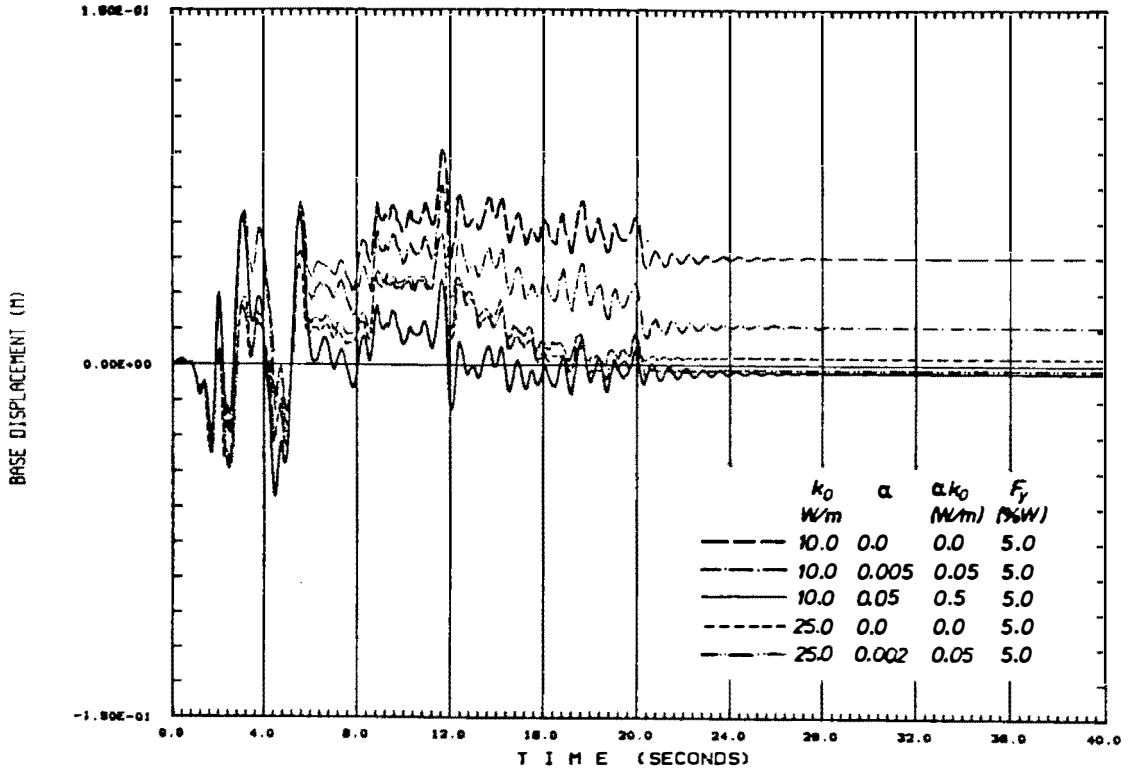

(a) EL CENTRO, 1940, N-S

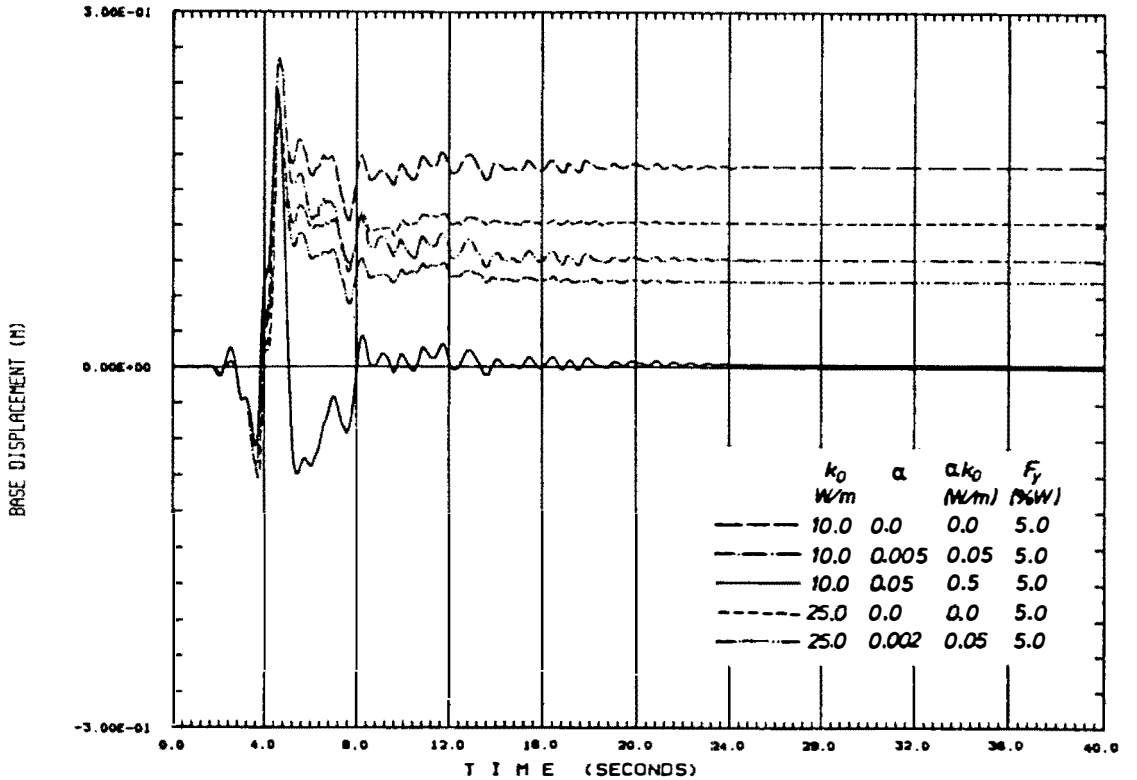

(b) PARKFIELD, 1966, N65E

Fig. 6.22 Response History of Base Displacements and Permanent Plastic Offset of a Four-Storey Structure on Various BI Systems

Irrespective of the earthquake type an elasto-plastic BI system with an initial stiffness, k_o of 10.0 W/m (Case 1) tends to induce relatively large permanent plastic offsets. By increasing the post-yield stiffness, αk_o, these plastic offsets can be reduced, as demontrated in Cases 2 and 3. Under the vibratory El Centro 1940 N-S earthquake, the permanent plastic offset becomes insignificant when k_o is increased to 25.0 W/m (Case 4). However, under the impulsive Parkfield 1966 N65E earthquake the permanent offset is still large although some reductions are observed. A similar phenomenon is also encountered by comparing Case 5 for both ground motions. It seems that regardless of the earthquake type, excessive permanent plastic offsets can be avoided by providing the BI system with a sufficient post-yield stiffness as demonstrated in Case 3.

6.5 SUMMARY AND CONCLUDING REMARKS

A series of inelastic time history analyses have been carried out to investigate the response of BI multistorey structures under several ground motions and NZ design-level earthquakes for areas with the highest seismic risk. Basically the considered earthquakes can be categorized into two groups. The first group consists of earthquakes which have peak spectral accelerations in the short period region whereas the second group comprises of ground motions with peak spectral accelerations at longer periods.

It has been shown that under the first group ground motions there are significant reductions of base shear and interstorey drifts, especially for short period structures. Under the second group earthquakes the inclusion of a BI system may even increase the inertia forces of the structure. With the addition of a large amount of damping it is possible to reduce the transmitted energy into the superstructure. However, it should be noted that Base Isolation is not a sensible option for this type of ground motion and would not be normally considered for design.

The effect of varying the BI parameters on the response of structures subjected to different earthquakes was evaluated. Similar trends as found previously under El Centro 1940 N-S earthquake are also encountered for the other first group ground motions and the NZ design-level earthquakes in Zone A.

Based on linear regression analyses, it was found that there are strong correlations between the hysteresis loop ratio, R and the exponent p used in the Code-Type approach formula to predict the lateral storey shear envelope of a BI multistorey structure. The correlations are dependent on the characteristics of the ground motion as well as the superstructure's fundamental period, $T_{1(UI)}$ and the beam-to-column stiffness ratio, ρ.

The Code-Type approach seems to be reasonably reliable for use in predicting the lateral storey shear envelopes of BI multistorey structures. Slight overestimates in predicting the lateral storey shears of structures mounted on BI systems with fat hysteresis loops are found in the case of

NZ design-level earthquakes. It should be easily corrected by using more appropriate modification factors to determine the maximum base shear from the BI system's shear force.

Permanent plastic offset can be suppressed by increasing the stiffness of the system, either at the initial or at the post-yield conditions. By using a sufficient post-yield stiffness, say 5% of the initial stiffness, the permanent plastic offset can be minimized irrespective of the type of earthquake, either vibratory ones or those with a large acceleration impulse.

6.6 REFERENCES

6.1 ZHU, T.J., TSO, W.K., and HEIDEBRECHT, A.C. , Effect of Peak Ground a/v Ratio on Structural Damage, Journal of Struct. Eng. , Vol. 114, No.5 , May 1988, pp. 1019-1037.

6.2 LEE, D.M., The Effect of Base Isolation on Multistorey Shear Structures, Ph.D. Thesis, Dept. of Theoritical and Applied Mechanics, University of Auckland, 1978.

6.3 Earthquake Engineering Research Institute (EERI), Reducing Earthquake Hazards : Lessons Learned from Earthquakes, Publication No. 86-02, Nov.1986, 208pp.

6.4 TRIFUNAC, M.D. and BRUNE, J.N. , Complexity of Energy Release During the Imperial Valley, California Earthquake of 1940, Bull. of the Seism. Soc. of America, Vol.60, No.1, February 1970, pp. 137-160.

6.5 BRANDON, G.E. (Coord.) and LEEDS, D.J. (Ed.), Reconnaissance Report : Imperial County, California, Earthquake, Oct.15, 1979, Earthquake Engineering Research Institute (EERI), 1980.

6.6 HOUSNER, G.W. and TRIFUNAC, M.D., Analysis of Accelerograms - Parkfield Earthquake, Bull. of the Seism. Soc. of America, Vol.57, No.6, Dec.1967, pp.1193-1220.

6.7 OAKESHOTT, G.B. (Ed.), San Fernando, California, Earthquake of 9 February 1971, California Division of Mines and Geology, Bulletin 196, 1975, 463pp.

6.8 BRUNE, J. N. , Preliminary Results on Topographic Seismic Amplification Effect on a Foam Rubber Model of the topography Near Pacoima Dam, Proc. of the 8th. WCEE, 1984, pp.663-669.

6.9 HARTZELL, S., Analysis of the Bucharest Strong Ground Motion Record for the March 4, 1977 Romanian Earthquake, Bull. of the Seism. Soc. of America, Vol.69, No.2, April 1979, pp. 513-530.

6.10 SEED, H. B., et al., The Mexico Earthquake of September 19, 1985 - Relationship between Soil Conditions and Earthquake Ground Motions, Earthquake Spectra, Vol. 4, No. 4 , 1988.

6.11 JENNINGS, P.C., et al., Simulated Earthquake Motions, Earthquake Engineering Research Laboratory, California Institute of Technology, 1968, 21pp. + app.

6.12 PARK, R. and ANDREWS, A. L ., Philosophy of Design Approach, Study Group Report on Structures of Limited Ductility, Bull. of the NZNSEE, Vol.19, No.4, Dec. 1986, pp. 826-298.

6.13 Code of Practice for general Structural Design and Design Loadings for Buildings, NZS4203:1984, Standard Association of New Zealand, 1984.

6.14 BERILL, J.B., Seismic Hazard Analysis and Design Loads, Bull. of the NZNSEE, Vol.18, No.2, June 1985, pp.139-151.

6.15 BERILL, J.B., Distribution of Scatter in NZ Accelerograph Data, Bull. of the NZNSEE, Vol.18, No. 2, June 1985, pp.151-164.

6.16 MATUSCHKA, G.H., et al, New Zealand Seismic Hazard Analysis, Bull. of the NZNSEE, Vol.18, No.4, Dec. 1985, pp.313-322.

6.17 McVERRY, G.H., Uncertainties in Attenuation Relations for New Zealand Seismic Hazard Analysis, Bull. of the NZNSEE, Vol.19, No.1, March 1986, pp.28-39.

6.18 Draft Replacement for Code of Practice for general Structural Design and Design Loadings for Buildings, DZ4203, Standard Association of New Zealand , 1986.

6.19 GASPARINI, D. and VANMARCKE, E. H., Simulated Earthquake Motions Compatible with Prescribed Response Spectra, M.I.T. Departement of Civil Engineering, Research Report R76-4, Order No.527, January 1976.

6.20 MAKIGUCHI, Y., Present Status of Base Isolated Building in Japan, Japan-NZ Workshop on Base Isolation of Higway Bridges, Wellington, Nov.1987.

6.21 LEE, D.M., et al, A Selection of important Strong Motion Earthquake Records, Report No. EERL 80-01, California Institute of technology, January 1980.

CHAPTER 7

THE PROPOSED DESIGN PROCEDURES FOR BASE ISOLATED MULTISTOREY STRUCTURES

7.1 INTRODUCTION

As has been reported in the previous chapters, a large number of inelastic time history analyses have been carried out to investigate the seismic response of a wide variety of BI multistorey structures subjected to different types of ground motion. In addition, some analyses were conducted using the adapted Component Mode Synthesis method to investigate the effects of various structural parameters on the modal contributions to the storey shears of multistorey structures mounted on different types of BI system. The inadequacies of some currently available design procedures have also been reviewed. As a result, two simplified analysis methods are proposed for use in design of BI multistorey structures.

The first proposed method is called the Code-Type approach. This design procedure is suitable for a preliminary design or even a final design of uniform BI multistorey structures with $T_{1(UI)}$ less than approximately 0.8 seconds. Its reliability has been satisfactorily verified for various cases as presented in Chapters 4 and 6. The step-by-step procedure of this Code-Type approach will be discussed in more detail in Section 7.2. An illustrative design example using this simple approach is given in Section 7.3.

The second method is based on the Component Mode Synthesis concept and is proposed for use in design of BI multistorey structures with more irregular and/or more flexible superstructures. A brief summary of this Component Mode Synthesis method is presented in Section 7.2.

With the availability of these simple approximation methods inelastic time history analyses will no longer be necessary for practical design purposes. However, inelatic time history analyses may still be required to evaluate the inelastic behaviour of the superstructure under a very severe earthquake in order to ensure that the superstructure will have a satisfactory failure mechanism. This aspect is discussed in Section 7.4.

7.2 DESCRIPTION OF THE SIMPLIFIED ANALYSIS METHODS PROPOSED FOR DESIGN PURPOSES

7.2.1 GENERAL

In this era of modern computers one might argue against the necessity of developing simple analysis methods for practical design purposes of BI multistorey structures. However, there are at least three main reasons why simple seismic analysis methods are in fact very desirable.

First, it is definitely impractical to use mathematically precise analyses, such as deterministic inelastic time history analyses, at a preliminary design stage where the complete physical properties of the structure are still to be determined. It has been realized that the results of such analyses are highly dependent on the assumptions made in the formulation of the mathematical model. Unless a large number of analyses are carried out during the refined design process the results are generally no better than, and may in fact be inferior to, what could be achieved at far lower cost by simpler though less precise approaches[7.1]. In design practice normally only a limited number of inelastic time history analyses are conducted due to limitation of funds and time.

Second, simple design procedures enable the structural response to be readily estimated and visualized without the need of elaborate calculations. Simple approaches normally give the designer a clearer insight or a better feel towards the effects of varying the design parameters on the overall structural behaviour. This encourages the exercise of "engineering judgement" which is essential to a successful design as indicated by Veletsos[7.1].

Third, in order to promote the use of a new technique, such as Base Isolation, a reasonably simple yet reliable approach is required. Practitioners need to be ensured that it is possible to design a BI multistorey structure using a simple and familiar approach. It is also hoped that due to its simplicity and reliability the approach will be incorporated in the general design code which in turn will enhance the confidence of structural engineers in adopting Base Isolation techniques.

The detail description of the proposed Code-Type approach is presented in the following subsection. This is then followed by a brief description of the Component Mode Synthesis method suggested for the design of more complex BI multistorey structures.

7.2.2 CODE-TYPE APPROACH

The proposed Code-Type approach is developed by adapting the well-known equivalent static lateral force analysis procedure to suit the seismic behaviour of BI multistorey structures. It is hoped that this similarity will help the designer to become familiar with this proposed

approach. A flow chart shown in Fig. 7.1 illustrates the step-by-step procedure of this simple design method.

STEP 1 : Determine the fundamental period of the unisolated superstructure ($T_{1(UI)}$).

This first step can be carried out as usual by assuming that the superstructure is not mounted on a BI system. At a preliminary design stage approximate formulas as recommended by some codes[7.2,7.3,7.4,7.5] can be used to estimate the fundamental period of this fixed-base superstructure.

STEP 2 : Make a trial selection of the BI system.

The required reduction of lateral inertia forces is normally the main consideration for selecting or predicting the idealized bilinear hysteresis loop parameters of a BI system, i.e. its initial stiffness, k_0, its post-yield stiffness, αk_0, and its yield strength, F_y. Other requirements such as the maximum allowable horizontal displacements at working loads (due to wind and small earthquakes) and ultimate load levels (stability of the BI system) should also be considered.

For this purpose a designer must know the design-level seismic load specified by the code for the particular site where the structure will be built, as well as the essential characteristics of a desirable BI system as discussed earlier in Chapter 2. The results obtained in Chapters 4, 5, and 6 are useful in guiding the designer to select the most suitable BI system for his structure and to conduct Step 3.

STEP 3 : Assume the maximum base displacement under the design-level earthquake and calculate the so-called maximum displacement ductility ratio, $\mu_{assumed}$.

STEP 4 : Obtain the effective (secant) stiffness of the BI system at the maximum base displacement by using Eq. 7.1 or from the chart shown in Fig. 7.2.

$$k_{eff} = k_0 \left(\frac{1 - \alpha}{\mu} + \alpha \right) \qquad (7.1)$$

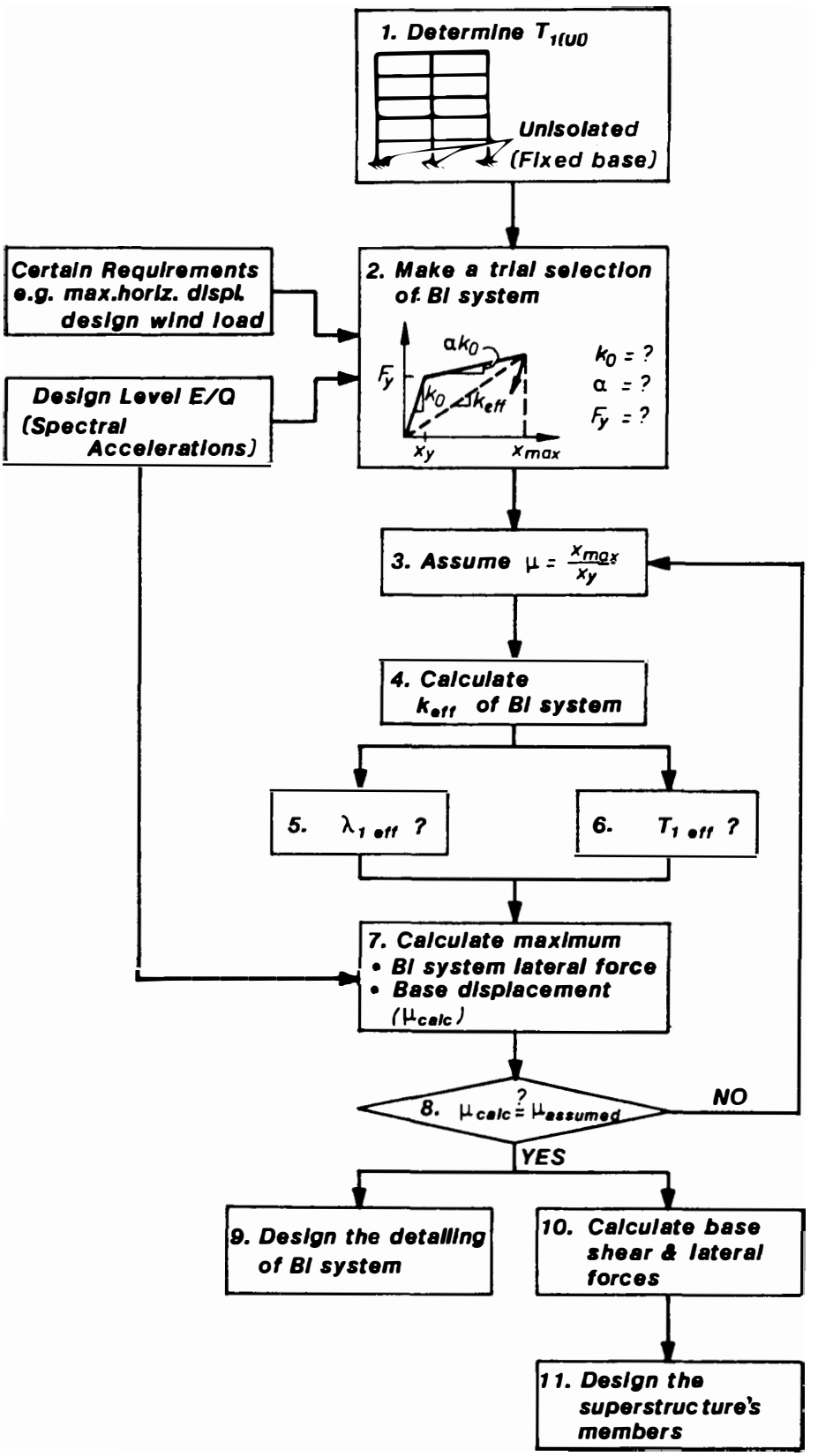

Fig. 7.1 Step-by-Step Design Procedure of the Proposed Code-Type Approach for BI Multistorey Structure

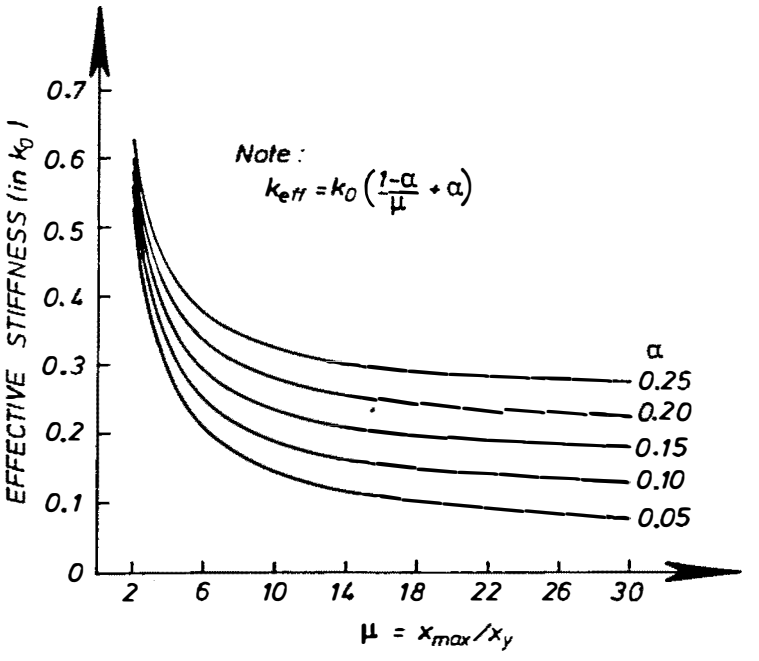

Fig. 7.2 Effective Stiffness of BI Systems with Bilinear Hysteresis Loop Model

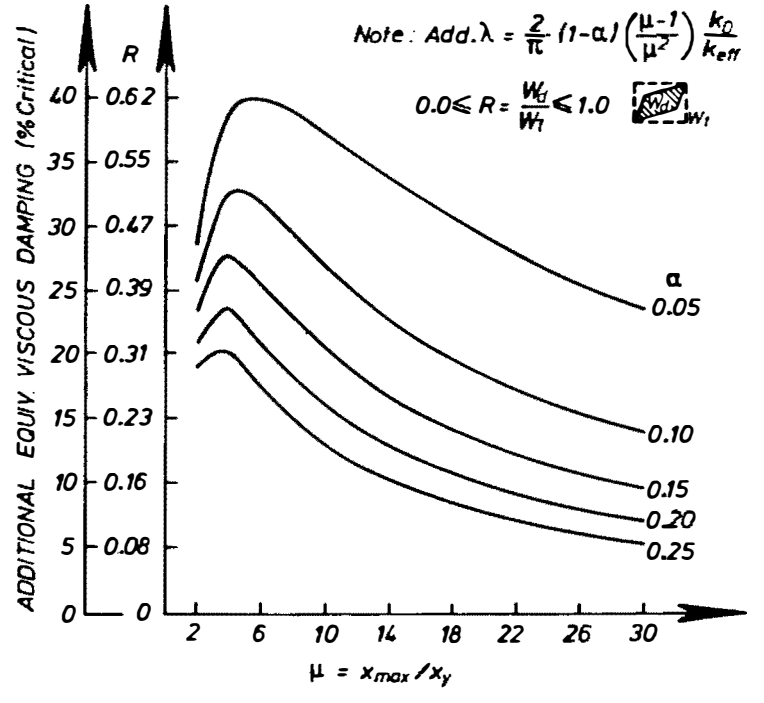

Fig. 7.3 Additional Damping of BI Systems with Bilinear Hysteresis Loop Model

STEP 5 : Determine the increase in damping due to the hysteretic behaviour of the BI system using Eq. 7.2 or the chart shown in Fig. 7.3. Then calculate the effective damping of the structure as the sum of the inherent damping of the structure and this additional hysteretic damping.

$$\text{Add. } \lambda = E_h = \frac{2}{\pi} R \qquad (7.2.a)$$

$$R = (1 - \alpha)\left(\frac{\mu - 1}{\mu^2}\right)\frac{k_0}{k_{eff}} \qquad (7.2.b)$$

In this study R is called the hysteresis loop ratio, i.e. the ratio of the hysteresis loop area to the area of the circumscribing rectangle. This value will be used further in Step 10.

STEP 6 : Determine the effective fundamental period of the BI multistorey structure from the chart shown in Fig. 7.4. Note that this chart is developed for BI multistorey structures with uniform floor mass and storey stiffness. Charts for other variations of floor mass and storey stiffness may be developed later. In the absence of such charts a proper modal analysis should be conducted to calculate the effective fundamental period of the BI multistorey structure.

STEP 7 : Based on the effective fundamental period and effective damping of the structure determine the maximum BI system shear force from the appropriate acceleration spectra specified by the loadings code (see examples listed in Appendix B). Then calculate the maximum base displacement and the maximum displacement ductility ratio, μ_{calc}.

STEP 8 : Compare the calculated maximum displacement ductility ratio, μ_{calc} with the maximum displacement ductility ratio assumed in Step 3, $\mu_{assumed}$.

If the difference between these two values are relatively great, say above 5% or so, Steps 3 to 8 should be repeated. The calculated maximum displacement ductility ratio may be used as a new assumed value until the two values converge. As demonstrated in Chapters 4 and 6 the convergence in this trial and error process is normally achieved very rapidly. Otherwise the design process can be continued to Step 9.

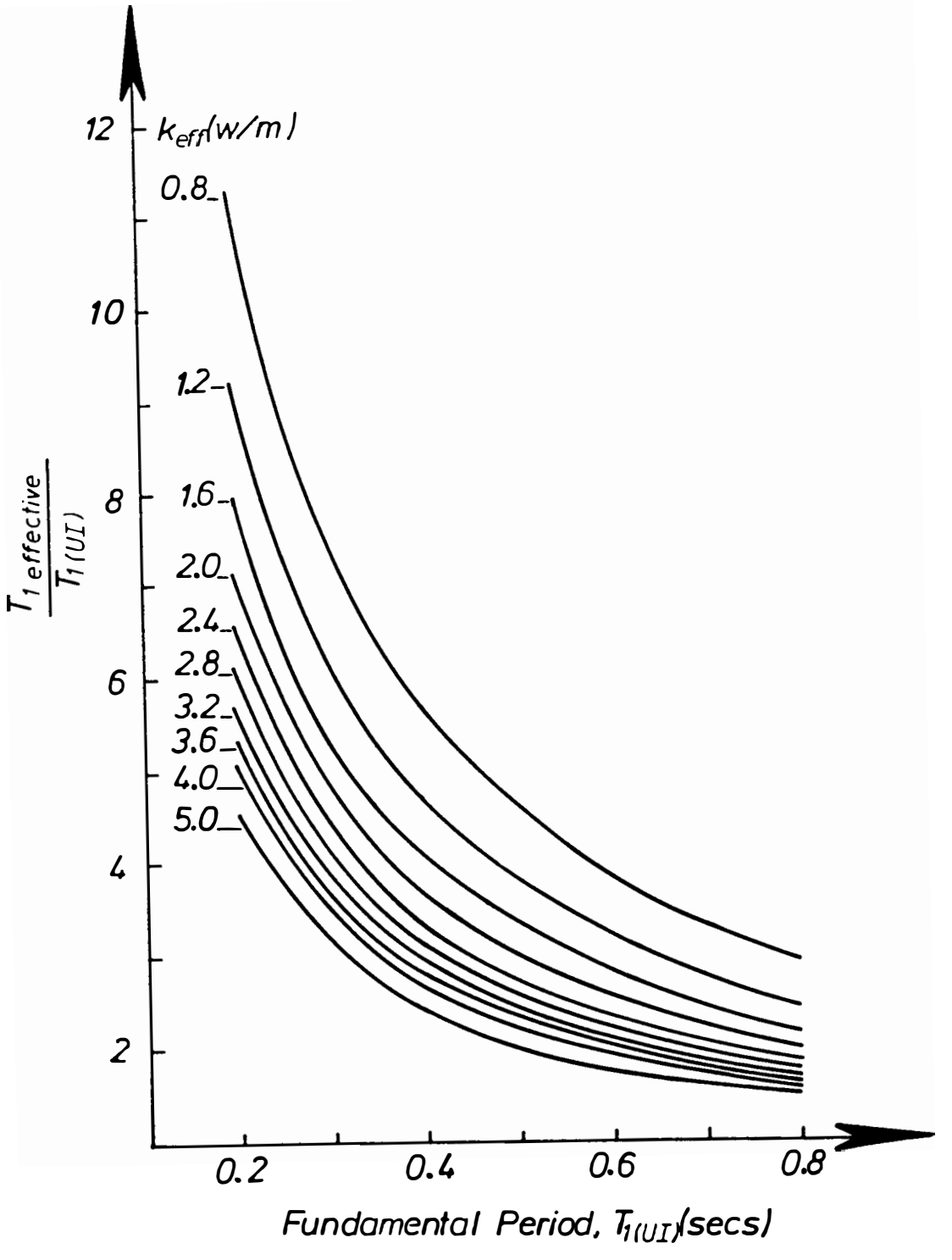

Fig. 7.4 Effective Fundamental Period of Uniform BI Multistorey Structures

STEP 9 : Design the detailing of the BI system.

Some manuals and/or experimental test results of BI devices discussed earlier in Chapters 2 and 3 can be used as a guidance to design the selected BI system in detail. It is beyond the scope of this study to discuss this step further.

STEP 10 : Determine the equivalent static lateral force distribution over the entire height of the multistorey structure.

As demonstrated in Chapters 4 and 6, the equivalent static lateral force, F_i at floor i can be accurately predicted by the following formula:

$$F_i = V \frac{W_i \, h_i^p}{\Sigma \, W_i \, h_i^p} \qquad (7.3)$$

where V is the base shear, W_i and h_i are the weight and height of floor i respectively. The exponent p can be determined from the strong linear correlation with the BI system's hysteresis loop ratio as demontrated earlier in Figs. 6.15 and 6.17. A modification factor as shown in Fig. 6.19 should also be used to obtain the maximum value of the base shear of the superstructure from the BI system's shear force.

STEP 11 : Design the superstructure's members.

Once the lateral forces are satisfactorily determined the member forces can be computed and the members of the superstructure can be designed in more detail.

As in the use of the equivalent static lateral force procedure for non-isolated buildings, this Code-Type approach would, in general, be adequate for BI multistorey structures which have a uniform property configuration in all storeys or floors. The results of the investigation presented in the previous chapters show that this simple approach can reliably predict the response of short to medium-rise BI structures ($T_{1(UI)} \leq 0.8$ secs) with floor masses which do not differ by more than, say 25% in adjacent floors and similarly the lateral storey stiffnesses do not differ by more than 25% in adjacent storeys.

7.2.3 COMPONENT MODE SYNTHESIS METHOD

In the design of non-isolated structures, analysis methods using a mode-superposition technique are normally employed if the equivalent static lateral force procedure is no longer able to satisfactorily predict the structural response. In a similar way the Component Mode Synthesis method is suggested as a means of analysis for more complex BI multistorey structures.

The basic principles of the Component Mode Synthesis method has been described earlier in Chapter 5. In brief, this method treats a BI multistorey structure as two seperate components, i.e. the superstructure and the BI system. The superstructure, which is expected to remain elastic under the design-level earthquake, can now be considered as a linear MDOF system and hence the ordinary modal analysis procedure can employed independent of the inelastic behaviour of the BI system.

This scheme is still based on a step-by-step integration. However, since it is normally appropriate to approximate the structural response by only incorporating the first few significant modes this method requires less computational effort when compared with the inelastic time history analysis. Furthermore the Component Mode Synthesis method gives the designer clearer insight into the structural response by showing the modal contributions. Examples of its application have been demonstrated in Chapter 5. A computer program named ISODYN based on this concept was developed and can be used for design purposes.

However, it is desirable that this method should operate on the response spectrum analysis approach rather than the step-by-step integration. More research work is required however, especially in deriving a scheme to combine the modal contributions, before this goal is achieved. It is obvious from the evaluation presented in Chapter 5 that the well-known SRSS procedure is no longer applicable.

7.3 A DESIGN EXAMPLE USING THE CODE-TYPE APPROACH

To illustrate the step-by-step procedure of the proposed Code-Type approach a design example is presented in this section. The superstructure is a six-storey reinforced concrete moment-resistant frame shown in Fig. 7.5. The dimensions of the frame structure are listed in Table 7.1. Originally this non-isolated six-storey structure was one of the models used by Jury[7.6] in his analytical study. To suit it to the implementation of BI system a stiff horizontal diaphragm is added across the columns at the base of the superstructure. It was assumed that the frames would be required to resist the component of earthquake motion in the plane of the frame only. The component in the perpendicular direction was assumed to be taken by some other resisting system, for example shear walls. No torsional effects for the building as a whole were take into account.

The floor masses as listed in Appendix C were calculated based on the New Zealand Code of Practice for General Structural Design and Design Loadings for Buildings, NZS4203:1976[7.7]. Including the base mass, the total weight of the structure, W is 3322 kN. The building will be located on a normal soil in NZ seismic Zone A.

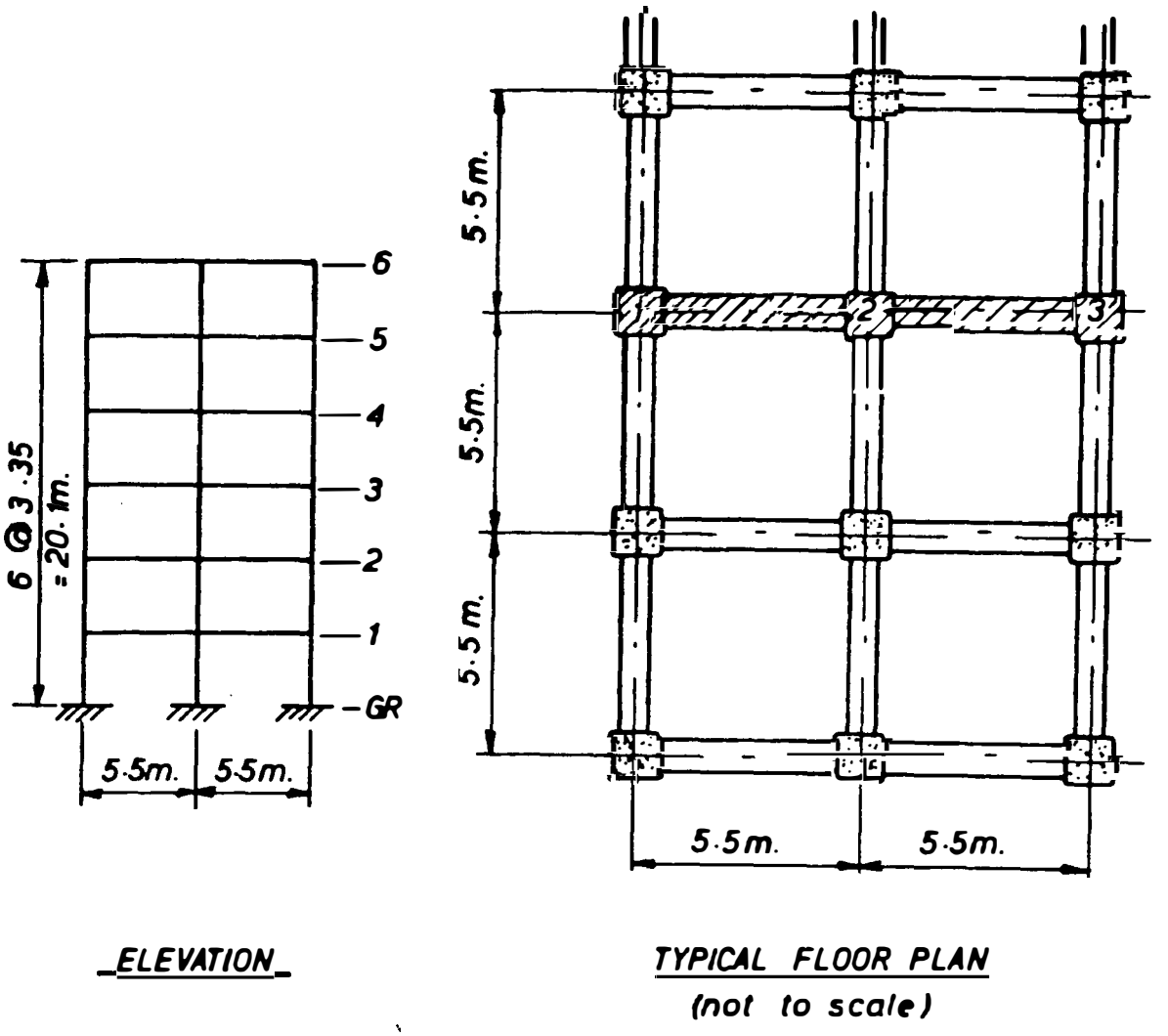

Fig. 7.5 Building Dimensions for the Six-Storey Superstructure (after Jury[7.6])

Table 7.1 Member Dimensions for the Six-Storey Superstructure (after Jury[7.6])

		FLOOR	
		1 - 3	4 - 6
Main Beams	(mm)	600 x 350	550 x 350
Columns 1 & 3	(mm)	500 x 450	450 x 450
Column 2	(mm)	550 x 550	500 x 500

Note : (i) Slab thickness is 120 mm throughout

(ii) Concrete compression strength = 28 MPa

STEP 1 : The fundamental period of the non-isolated frame superstructure, $T_{1(UI)}$ is 0.8 secs as calculated by Jury[7.6] based on the cracked section properties listed in Appendix C.

STEP 2 : Suppose it is desired to have a BI system with an initial stiffness, k_0 = 10.0 W/m (33220 kN/m) and a yield strength, F_y = 0.05 W (166.1 kN). Lead-Rubber Bearings (LRB) are considered to be the BI systems in this first trial. The ratio between the post-yield stiffness and the initial stiffness of these LRB is approximately 0.15[7.8].

STEP 3 : Assume μ = 14.0 (x_{max} = 70.0 mm; $x_y = F_y/k_0$ = 5 mm).

STEP 4 : Using Eq. 7.1 or the chart shown in Fig. 7.2, the effective stiffness of the BI system at the maximum base displacement can be determined.

$$k_{eff} = k_0 \left(\frac{1 - \alpha}{\mu} + \alpha \right)$$

$$= 10.0 \left(\frac{1 - 0.15}{14.0} + 0.15 \right) = 2.11 \text{ W/m } (7009.4 \text{ kN/m})$$

STEP 5 : Using Eq. 7.2 or the chart shown in Fig. 7.3 the hysteresis loop ratio, R and the additional damping due to the hysteretic behaviour of the BI system can be found as follows :

$$R = (1 - \alpha) \left(\frac{\mu - 1}{\mu^2} \right) \frac{k_0}{k_{eff}}$$

$$= (1 - 0.15) \left(\frac{14.0 - 1.0}{14.0^2} \right) \frac{10.0}{2.11}$$

$$= 0.27$$

$$\text{Add. } \lambda = E_h = \frac{2}{\pi} R$$

$$= 0.17 \text{ or } 17\% \text{ critical damping.}$$

Thus, $\lambda_{1\,eff}$ = 17% + 5% = 22% critical damping.
(Note, the inherent damping is assumed to be 5% critical).

STEP 6 : For k_{eff} = 2.11 W/m and $T_{1(UI)}$ = 0.8 secs, the effective fundamental period of the BI structure can be estimated from the chart shown in Fig. 7.4.

$$\frac{T_{1eff}}{T_{1(UI)}} = 1.9$$

$T_{1\,eff}$ = 1.9 x 0.8 = 1.52 secs.

(compared with a more rigorous modal analysis : $T_{1\,eff}$ = 1.47 secs).

Note that the above superstructure does not have perfectly uniform properties in all floors and storeys as assumed in the chart shown in Fig. 7.4.

STEP 7 : Based on the NZ design-level earthquake for normal soils in seismic zone A the spectral acceleration, S_a is 0.180 g for T_{1eff} = 1.52 secs and λ_{1eff} = 22% critical damping. (see Appendix B for the values of NZ spectral accelerations).

Thus, the maximum BI system shear force = 0.18 W or 598 kN. From the bilinear force-displacement relationship it can be found that the maximum base displacement, x_{max} = 91.7 mm or μ_{calc} = 91.7/5 = 18.3.

STEP 8 : μ_{calc} (= 18.3) > $\mu_{assumed}$ (= 14.0); 30.7% difference.

Steps 3 to 8, therefore, should be repeated using μ_{calc} as the new assumed value until the convergence is achieved. After repeating the procedure for the third time with $\mu_{assumed}$ = 17.2 it is found that :

k_{eff} = 1.99 W/m (6610.8 kN/m)
T_{1eff} = 1.60 secs (c.f. from modal analysis : 1.57 secs)
λ_{1eff} = 14.8% + 5% = 19.8% critical damping
R = 0.23
Maximum BI system shear force = 569.4 kN
Maximum base displacement = 85.9 mm
μ_{calc} = 85.9/5 = 17.18 ≈ $\mu_{assumed}$ (=17.2)

STEP 9 : See Ref. 7.8 for further guidance to select or design LRB in detail. Note, this step could be omitted if LRB with appropriate dimensions have already been selected in Step 2.

STEP 10 : First, the maximum base shear, V should be determined from the maximum BI system shear force using a certain modification factor which corresponds to R = 0.23.

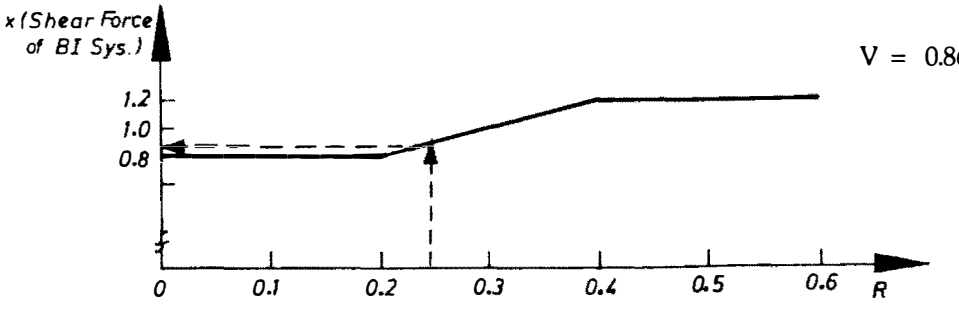

V = 0.86 x 569.4 = 489.7 kN

The exponent p used in Eq. 7.3 can be found from the linear correlations between R and p as listed in Table 6.1 or Figs. 6.17.a as follows :

For $T_{1(UI)}$ = 0.8 secs; $\rho = \infty$, $p = -0.45 + 7.41\,R$

$\rho = 0.0$, $p = 0.16 + 5.90\,R$

As R = 0.23 the values of p are 1.25 and 1.52 for $\rho = \infty$ and 0.0, respectively.

The superstructure's beam-to-column stiffness ratio, ρ is about 0.70. Thus the value of p may be estimated in between 1.25 and 1.52, say 1.40.

Storey i	h_i (m)	W_i (kN)	$W_i h_i^p$ (10^3 kNm)	F_i (kN)	Storey Shear (kN)
6	20.10	440	18.73	146.2	146.2
5	16.75	469	15.89	124.0	270.2
4	13.40	469	12.02	93.8	364.0
3	10.05	483	8.64	67.4	431.4
2	6.70	487	5.25	41.0	472.4
1	3.35	487	2.21	17.2	489.7
GR					(569.4)
		Σ	62.74		

Note : ( ) denotes the BI system shear force.

Fig. 7.6.a shows that the result of this approach shown above are in good agreement with the result obtained from the time history analysis conducted for comparison purposes. It can also be seen from this figure that the storey shears of the non-isolated fixed-base structure are significantly reduced due to the inclusion of the BI system, i.e. by factors 2.7 and 2.3 at the first and top-storey respectively.

If a smaller base shear is prefered a different type of BI system may be used instead of the LRB. In the second trial a BI system with α = 0.05 is considered. The initial stiffness and the yield

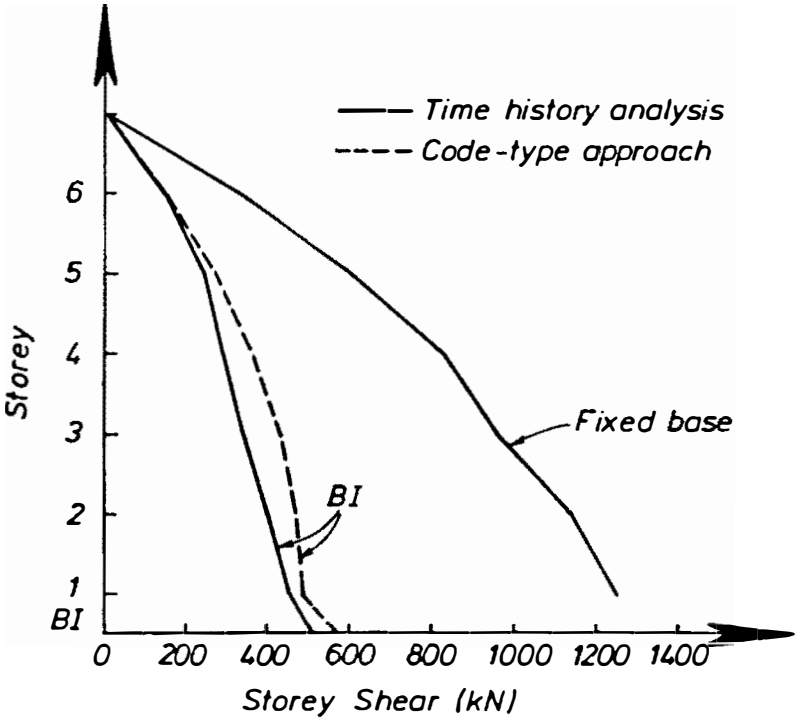

(a) BI System : $k_0 = 10.0 W/m$, $\alpha = 0.15$, $F_y = 5\% W$

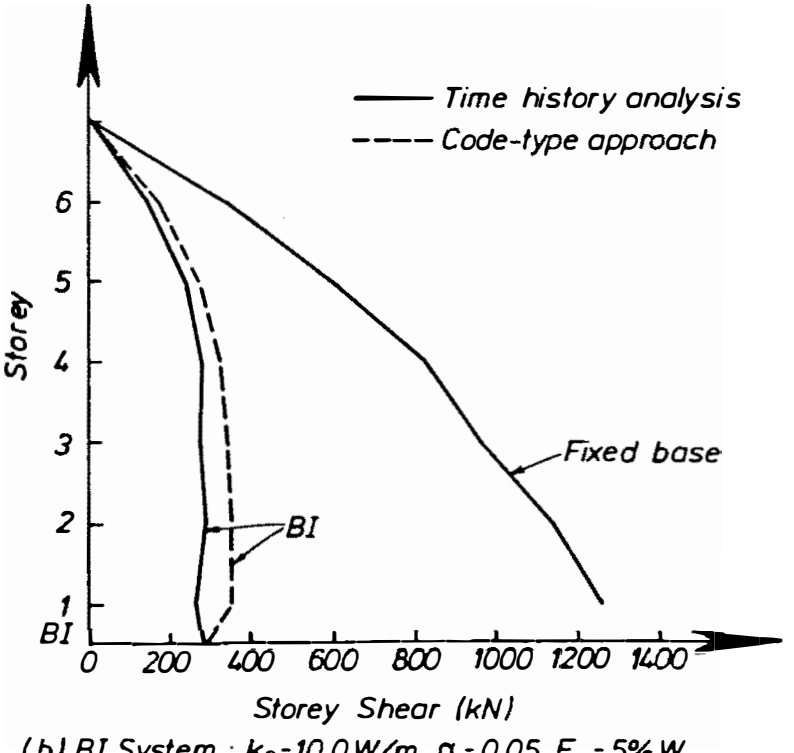

(b) BI System : $k_0 = 10.0 W/m$, $\alpha = 0.05$, $F_y = 5\% W$

Fig. 7.6 The Predicted Lateral Storey Shear Envelopes by the Code-Type Approach and the Time History Analyses

strength remain the same, i.e. k_o = 10.0 W/m and F_y = 0.05 W. The same procedure is carried out. It converges at μ = 16.7.

k_{eff} = 1.07 W/m (3554.5 kN/m)

T_{1eff} = 2.08 secs (c.f. from modal analysis : 2.04 secs)

λ_{1eff} = 32.0% + 5% = 37.0% critical damping

(Note, the inherent damping is assumed to be 5% critical)

R = 0.50

The spectral acceleration, Sa = 0.0892 g

The maximum BI system shear force = 0.0892 x 332 = 296.3 kN

The maximum base shear = 1.2 x 296.3 = 355.6 kN

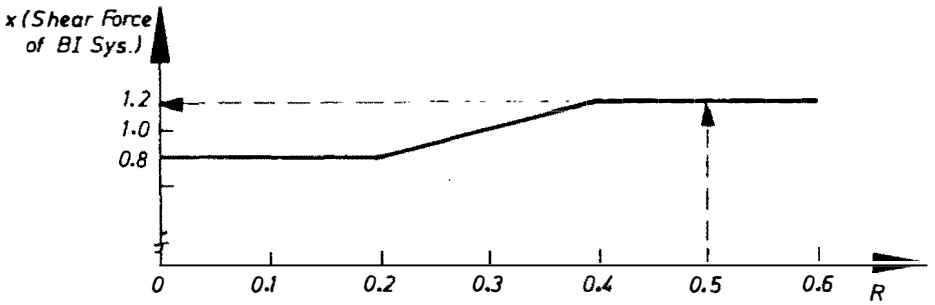

For $T_{1(UI)}$ = 0.8 secs; $\rho = \infty$, p = -0.45 + 7.41 x 0.50 = 3.25

ρ = 0.0, p = 0.16 + 5.90 x 0.50 = 3.11

$\rho \approx 0.7$, $p \approx$ 3.18

Storey i	h_i (m)	W_i (kN)	$W_i h_i^p$ (10^3 kNm)	F_i (kN)	Storey Shear (kN)
6	20.10	440	6132.2	173.5	173.5
5	16.75	469	3660.5	103.6	277.1
4	13.40	469	1800.4	50.9	328.0
3	10.05	483	742.7	21.0	349.0
2	6.70	487	206.3	5.8	354.8
1	3.35	487	22.7	0.6	355.6
GR					(296.3)
		Σ	12564.8		

Note : ( ) denotes the BI system shear force.

Fig. 7.6.b shows that the result of the Code-Type approach shown above are in good agreement with the result obtained from the time history analysis conducted for comparison purposes. The top-storey and base shears of the non-isolated fixed-base structure are now reduced by factors of 2.2 and 4.6, respectively.

7.4 THE INELASTIC BEHAVIOUR OF THE SUPERSTRUCTURE UNDER SEISMIC LOAD CONDITIONS BEYOND THE DESIGN LEVEL.

The ability of a BI system to significantly attenuate the transmitted ground motion energy into the superstructure has been demonstrated in the previous chapters. A reduction of the lateral inertia forces by factors of up to six can be readily achieved due to the implementation of a BI system. Hence, it is possible to expect the superstructure to behave elastically under the design-level earthquakes. It is also important, however, to understand how a BI multistorey structure will behave under seismic load conditions beyond the design level.

In this section the inelastic behaviour of the six-storey reinforced concrete moment-resistant frame as an example was originally designed by Jury[7.6] based on the Capacity Design approach[7.8] and in accordance with the provisions of the NZ loadings code NZS4203:1976[7.7]. The complete properties of the structure are listed in Appendix C.

The inelastic responses of this six-storey structure with and without BI system are compared and the effect of using two different types of BI system as incorporated in the previous example presented in Section 7.3 is also studied. For this purpose the inelastic time history analyses are conducted using the computer program RUAUMOKO[7.9]. The dynamic response is determined by a step-by-step procedure based on Newmark's constant acceleration method[7.10] with an intergration step of 0.01 seconds.

Both the non-isolated and BI structures are subjected to 1.4 El Centro 1940 N-S and Parkfield 1966 N65E earthquakes. The El Centro 1940 N-S record is scaled by a factor of 1.4 to give the same peak ground acceleration as the Parkfield's, i.e. 0.49 g. Some researchers[7.11] have used the 1.4 scaled El Centro 1940 N-S earthquake record to simulate earthquakes with 450 year return period which is beyond the NZ Zone A's seismic design-level. As discussed earlier in Chapter 6, these two ground motions have different characteristics and therfore may cause different effects on the inelastic behaviour of the structure. The Parkfield earthquake is incorporated in this evaluation to take into account the possibility of the structure being located close to a fault.

The results of the inelastic time history analyses can be described as follows :

1. Plastic Hinge Formation, Ductility Demands, and Interstorey Drifts.

Figs. 7.7.a, 7.7.b, and 7.7.c show the storey displacements and the instant plastic hinge formation of the fixed-base and BI six-storey structures subjected to 1.4 El Centro 1940 N-S earthquake. It can be seen in Fig. 7.7.a that during this ground motion plastic hinges occur at all beam-ends and column bases of the conventionally designed fixed-base structure. The inclusion of BI system with k_o = 10.0 W/m, α = 0.15, and F_y = 5% W significantly suppresses the formation of these plastic hinges as demonstrated in Fig. 7.7.b. Further suppression is achieved by using a BI system which has lower post-yield stiffness and greater energy dissipating capacity (k_o = 10.0 W/m, α = 0.05, F_y = 5%W). Fig. 7.7.c shows this phenomenon.

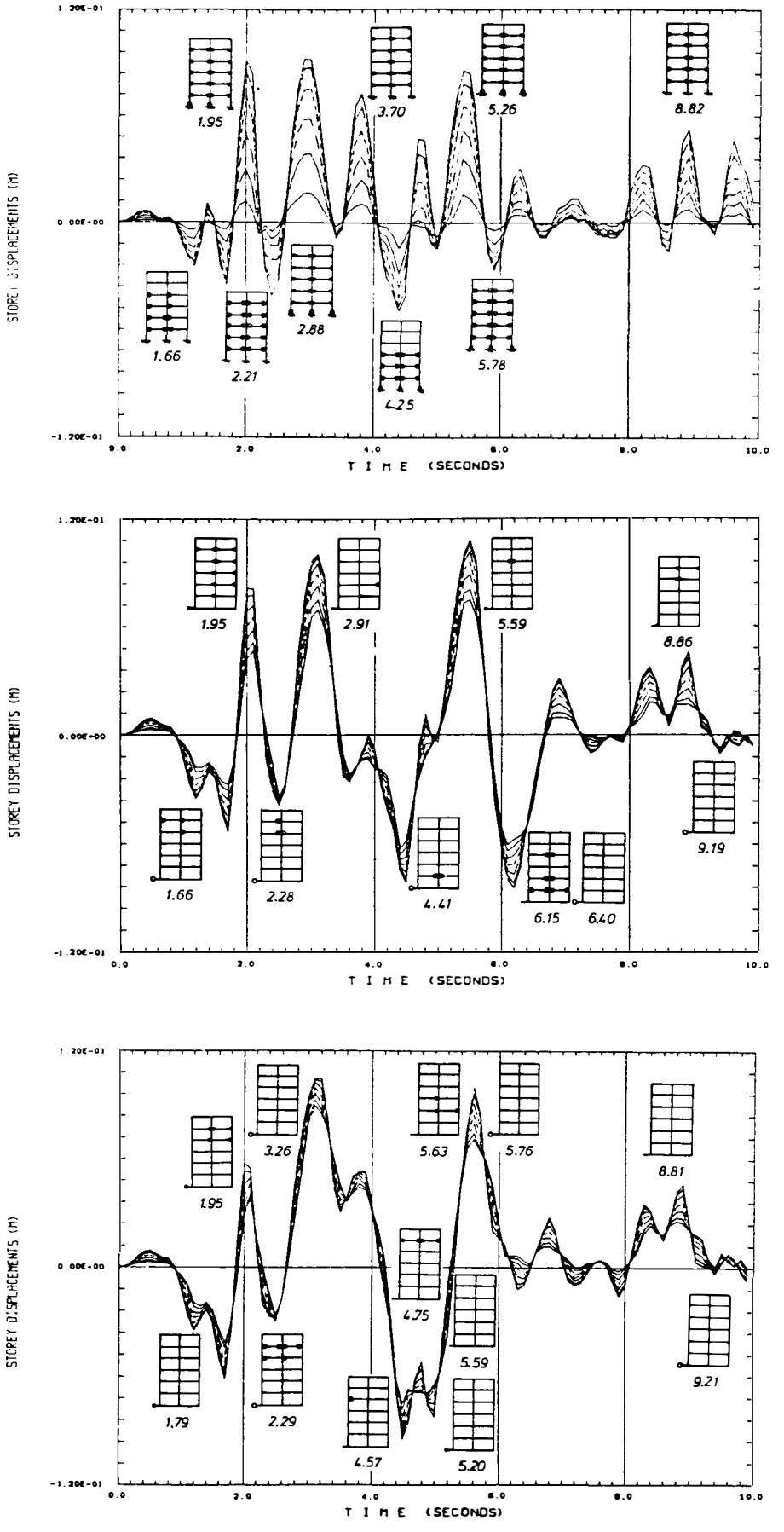

Fig. 7.7 The Storey Displacement History and the Instant Formation of Plastic Hinges Under 1.4 El Centro 1940 N-S Earthquake

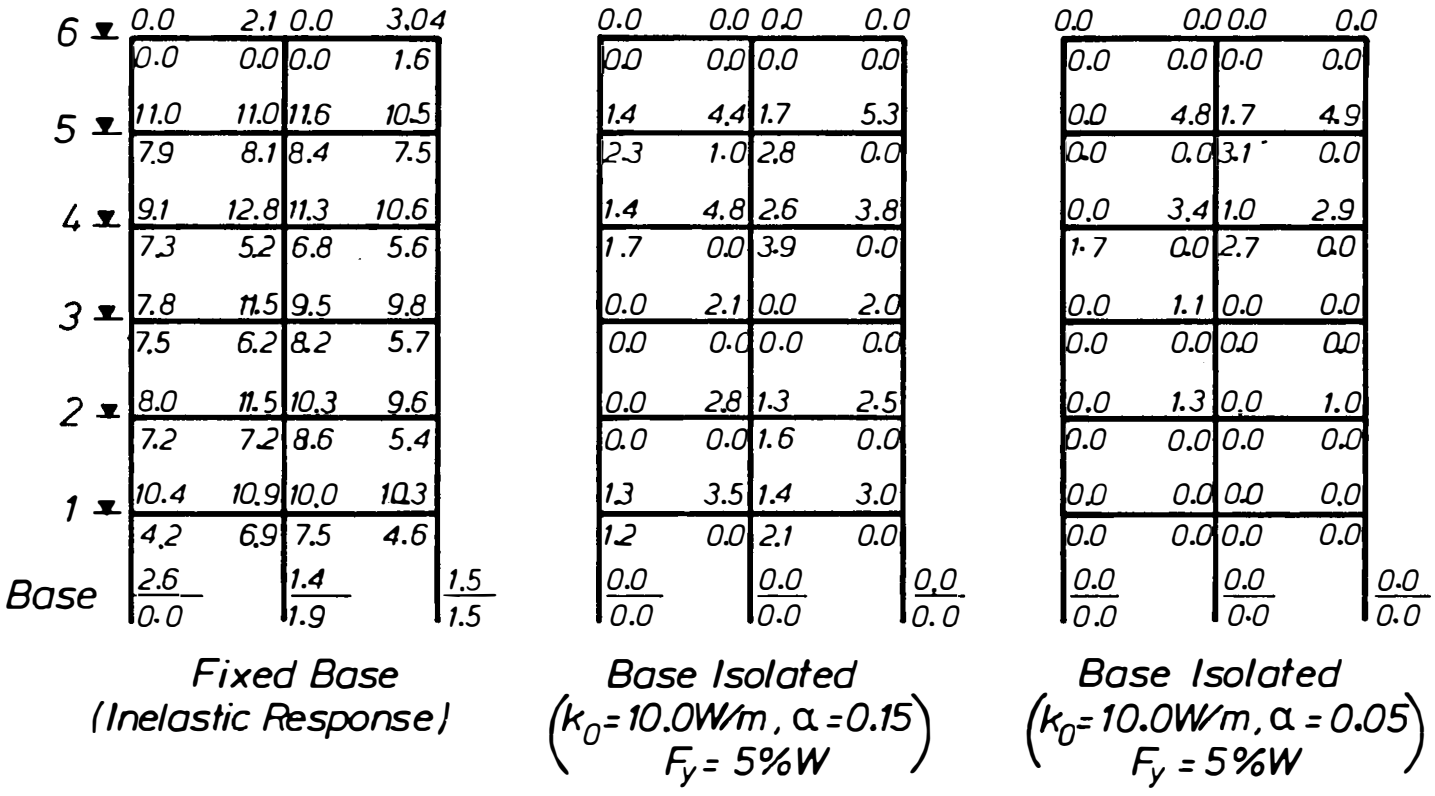

Fig. 7.8 Curvature Ductility Demands at Beam Ends and Column Bases Under 1.4 El Centro 1940 N-S Earthquake

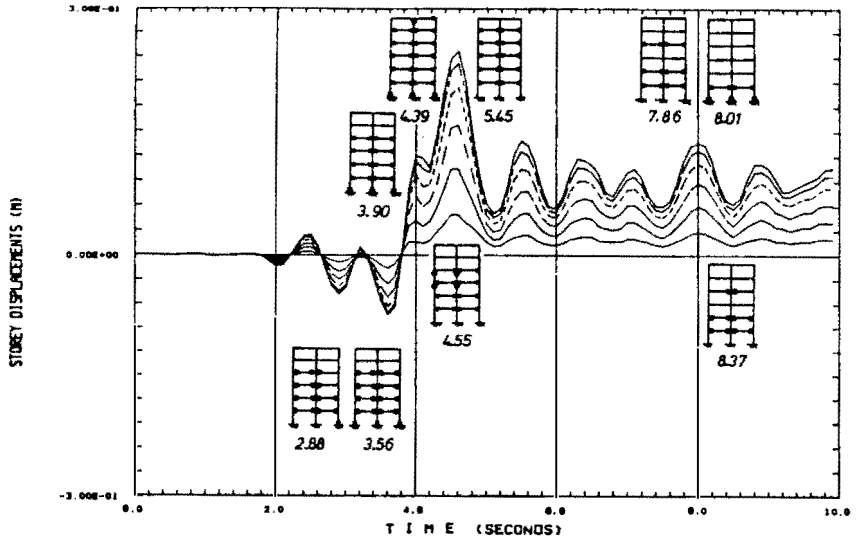

(a) Fixed-Base

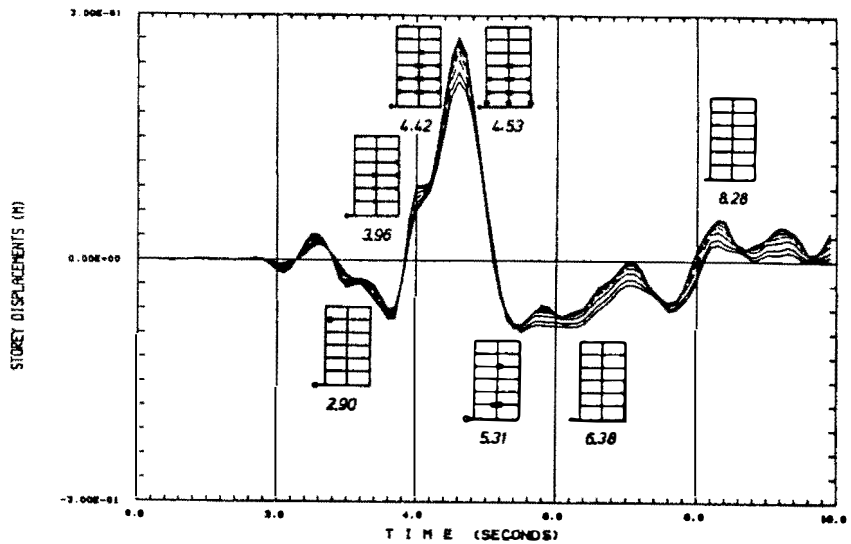

(c) BI System : k_0 = 10.0 W/m, α = 0.05, F_y = 5 %W

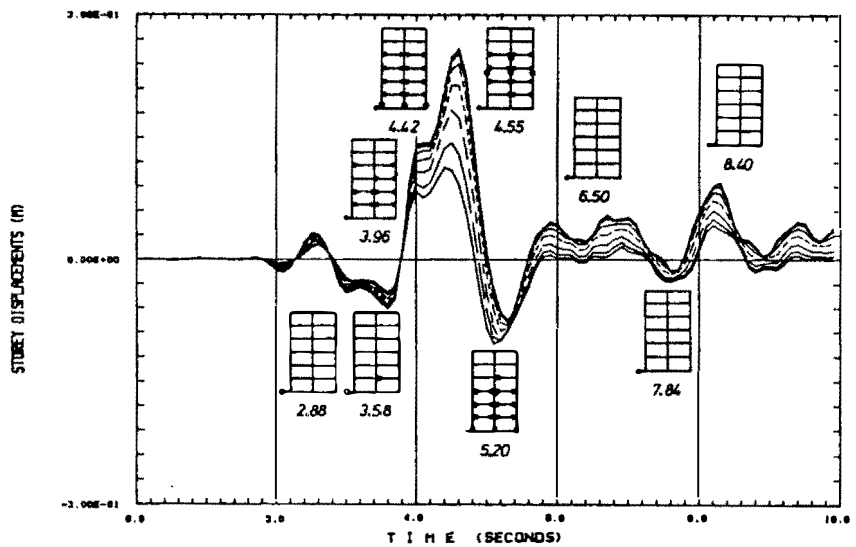

(b) BI System : k_0 = 10.0 W/m, α = 0.15, F_y = 5 %W

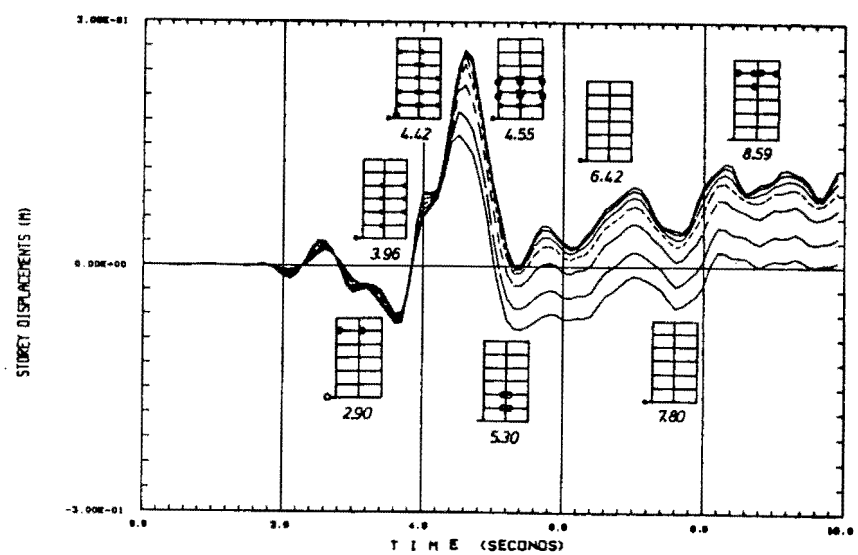

(d) BI System : k_0 = 10.0 W/m, α = 0.05, F_y = 5 %W + "stop"

Fig. 7.9 The Storey Displacement History and the Instant Formation of Plastic Hinges Under Parkfield 1966 N65E Earthquake

The curvature ductility demands at beam-ends and column bases of the fixed-base and BI structures under the 1.4 El Centro 1940 N-S earthquake are shown in Fig. 7.8. Zero indicates that no plastic hinge occurs. It is obvious that the BI structures have lower ductility demands than the fixed-base counterpart. Moreover, hinge reversals are only found in some beam-ends and column bases of BI structures whereas almost all beam-ends and column bases of the conventionally designed fixed-base structure have reversals of plastic rotations.

The storey displacements and the instant plastic hinge formation of the fixed-base and BI structures under Parkfield 1966 N65E earthquake are shown in Fig. 7.9. As indicated by Jury[7.6], one-end hinging occurs in some columns above the ground floor during this impulsive ground motion. Although the maximum curvature ductility demands at the worst column hinge are not high, i.e. 6.8, the structure should survive but significant damage would be expected. The implementation of a BI system with k_0 = 10.0 W/m, α = 0.15, and F_y = 5% W reduces the ductility demands in the columns above the ground floor to only about 1.5. These undesirable column hinges can be totally avoided by using a BI system which has a post-yield stiffness to initial stiffness ratio, α = 0.05 as demonstrated in Fig. 7.9.c.

The lateral flexibility of BI systems may lead to excessive base displacements. It may be necessary to set a limit to the maximum base horizontal movement. Peripheral basement walls[7.12] or a kind of "stop"[7.13] have been used in designs of some real structures. It is informative to study the effect of this kind of "stop" on the structural behaviour. For this purpose a limit of 150 mm is set in this evaluation. As shown in Fig. 7.9.c the maximum displacement of the BI system with k_0 = 10.0 W/m, α = 0.05, and Fy = 5%W under Parkfield 1966 N65E is 220 mm. This is the only case where the 150 mm limit would be exceeded. In this example the stiffness of the "stop" is assumed to be equal to the initial stiffness of the BI system, k_0. The hysteresis parameters of the BI system, the "stop", and their combined system are shown in Fig. 7.10.

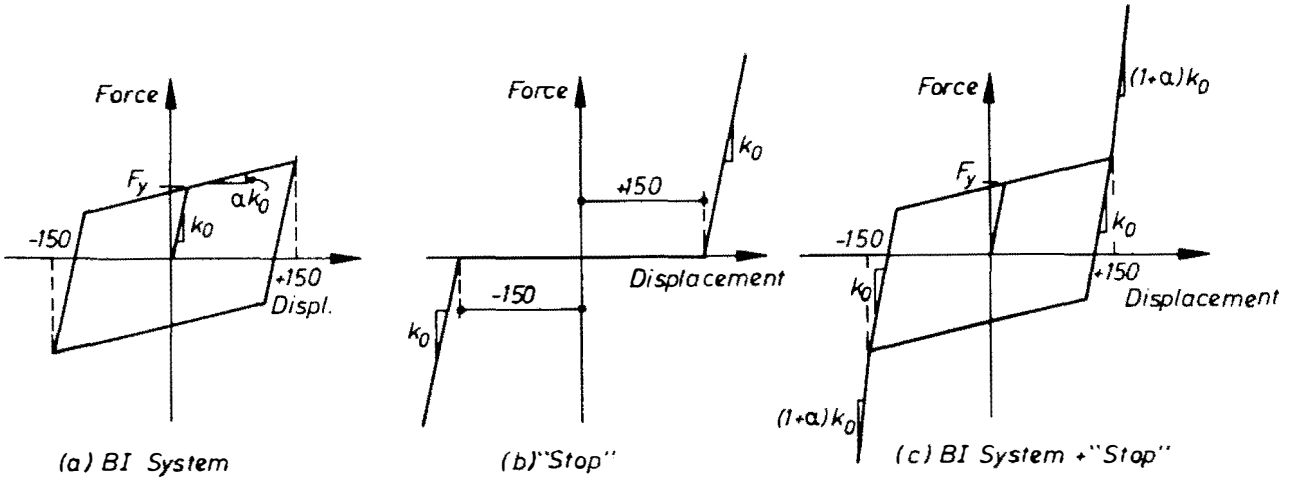

Fig. 7.10 Hysteresis Loop Parameters of A BI System with A "Stop" at 150 mm

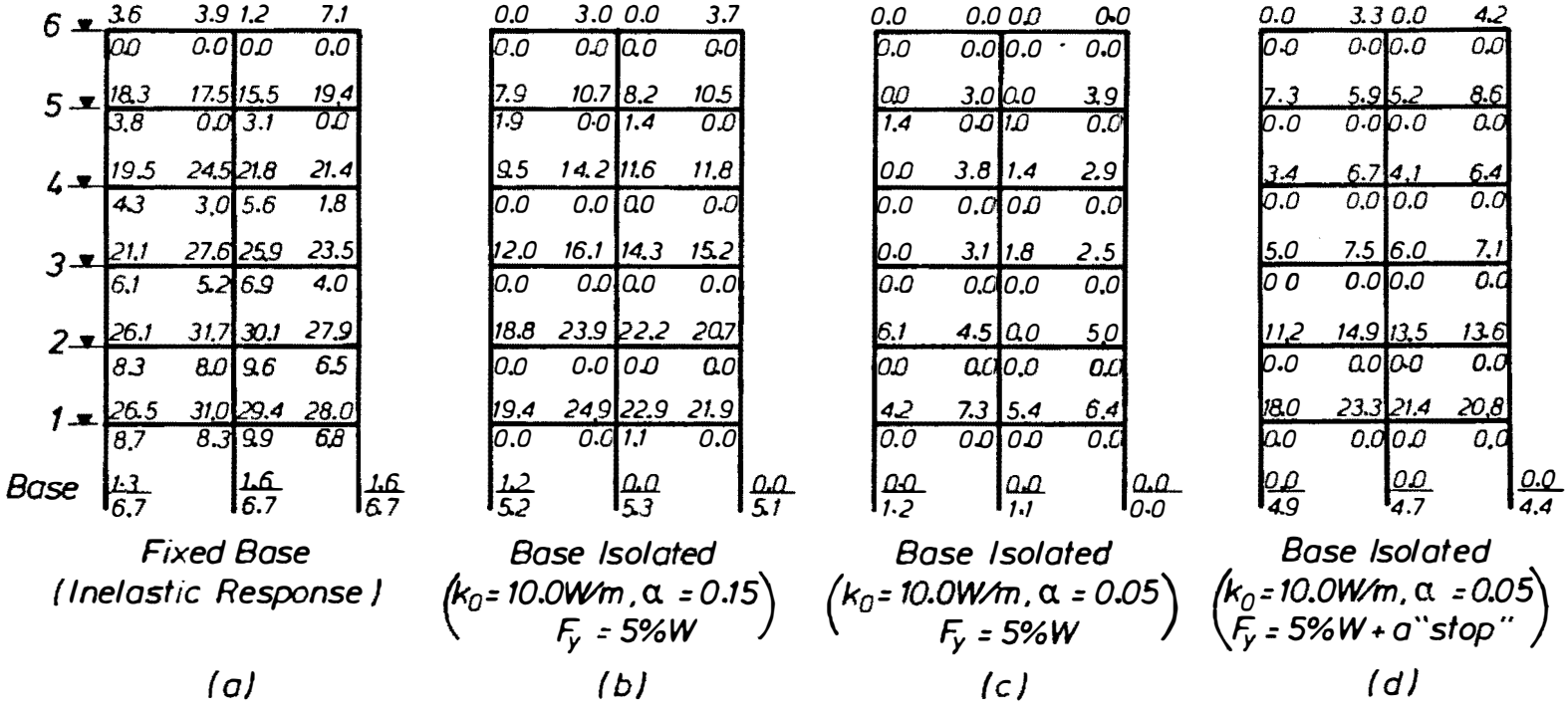

Fig. 7.11 Curvature Ductility Demands at Beam Ends and Column Bases Under Parkfield 1966 N65E Earthquake

Figs. 7.9.d and 7.11.d demonstrate the effects of the "stop" on the instant plastic hinge formation and the curvature ductility demands in the beam-ends and the column bases. More plastic hinges and higher ductility demands are observed due to the inclusion of the "stop" when compared with the plastic hinge formation and the ductility demands in members of the structure mounted on the same BI system but without the "stop" as shown in Figs. 7.9.c and 7.11.c, respectively. However, the ductility demands of the BI structure with the "stop" are still lower than the ductility demands of the conventionally designed non-isolated structure shown in Fig. 7.11.a and the structure mounted on BI system with k_o = 10.0 W/m, α = 0.15, and F_y = 5%W (Fig. 7.11.b).

From the storey displacement history shown in Figs. 7.7 and 7.9 it can be clearly seen that the inclusion of BI systems reduces the interstorey drifts of the superstructure. Figs. 7.12.a and 7.12.b compare the maximum interstorey drifts of fixed-base and BI structures subjected to two different ground motions. Under the 1.4 El Centro 1940 N-S earthquake it is obvious that the interstorey drifts of structures mounted on both types of BI system are much less than the interstorey drifts of the conventionally designed fixed-base structure. Under the Parkfield 1966 N65E ground motion the BI system with k_o = 10.0 W/m, α = 0.05, F_y = 5%W cause more pronounced reduction of interstorey drifts than the BI system with k_o = 10.0 W/m, α = 0.15, and F_y = 5%W. The interstorey drifts of the BI structure with the "stop" lie in between the interstorey drifts of BI structures mounted on these two types of BI system.

In all cases the interstorey drifts are much less than the allowable limit specified by NZ code[7.3], i.e. 0.017h or 57 mm. However, the maximum drift between the first and the second floors of the fixed-base structure under Parkfield 1966 N65E ground motion almost reaches this value as shown in Fig. 7.12.b.

2. Storey Shears.

Figs. 7.13.a and 7.13.b show how much the storey shears of the elastic fixed-base structure can be reduced by the implementation of different types of BI system and by the application of the conventionally ductile design approach. Under the 1.4 El Centro 1940 N-S earthquake the storey shears of structures mounted on both types of BI system are less than the storey shears of its inelastic fixed-base counterpart. The maximum reduction of the base shear due to the conventional ductile design approach is 3.4 whereas the BI systems with k_o = 10.0 W/m, α = 0.15, F_y = 5%W and k_o = 10.0 W/m, α = 0.05, F_y = 5%W can reduce the elastic base shear by factors of 3.8 and 6.0, respectively. Under the Parkfield 1966 N65E ground motion the structure mounted on BI system with k_o = 10.0 W/m, α = 0.15, F_y = 5%W has slightly larger storey shears than the conventionally designed ductile structure, but without the significant inelastic deformations. The storey shears of structures mounted on BI system with lower post-yield stiffness are always the smallest regardless of the ground motion.

As displayed in Fig. 7.13.b the "stop" causes only insignificant increase in the storey shears. Further investigation is, however, required to study this case more extensively before final

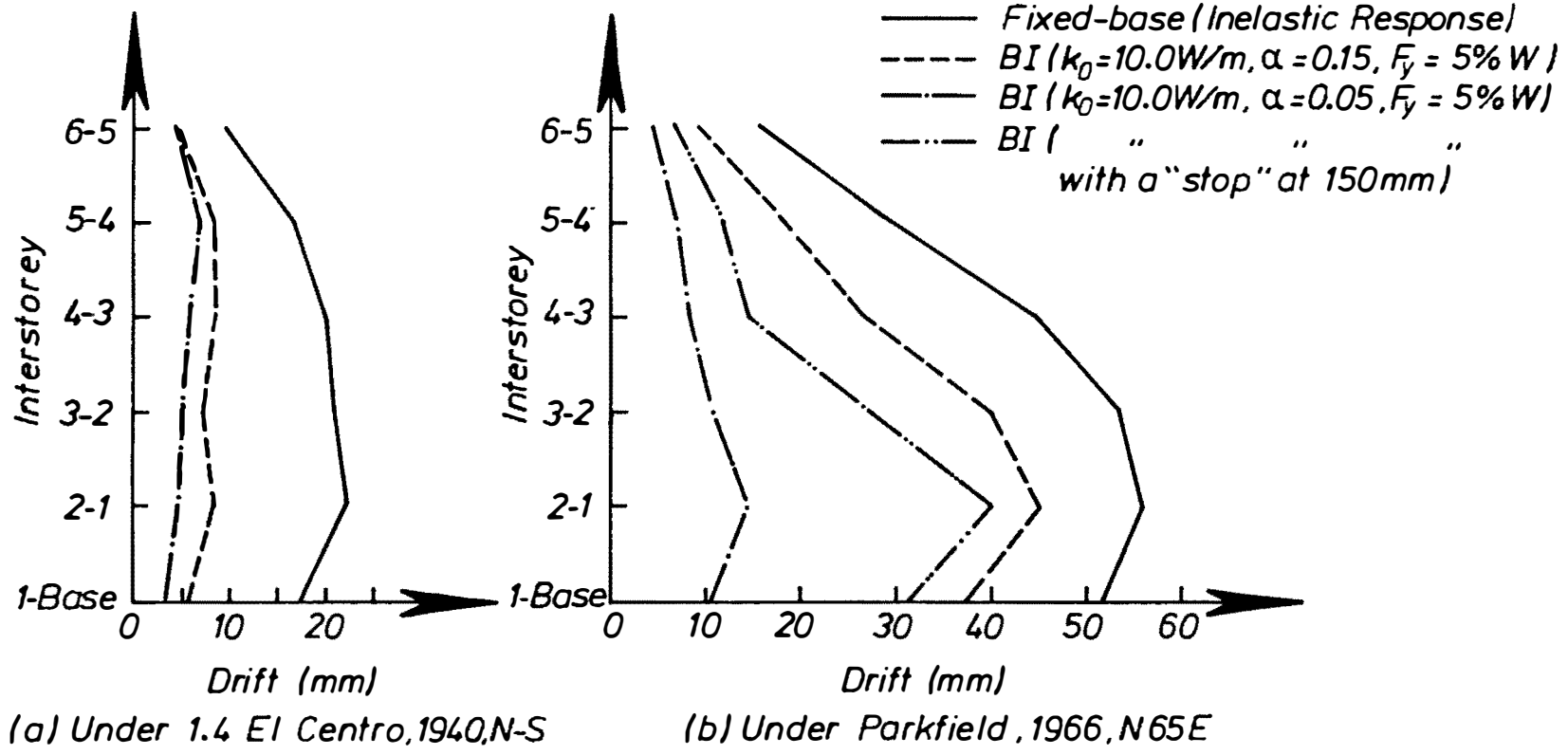

Fig. 7.12 Maximum Interstorey Drifts of Fixed-Base and BI Structures Subjected to 1.4 El Centro 1940 N-S and Parkfield 1966 N65E Earthquakes

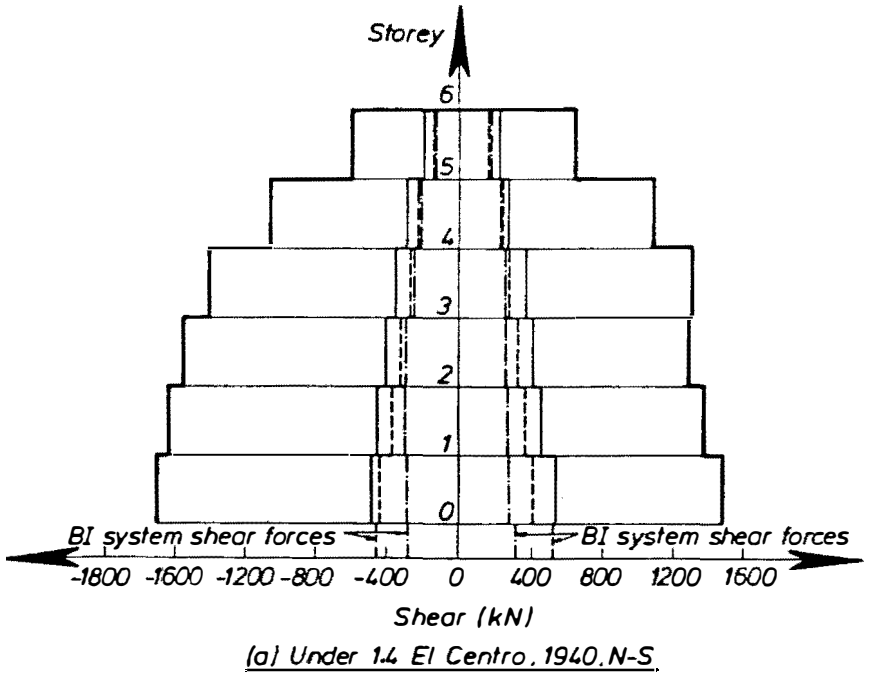

(a) Under 1.4 El Centro, 1940, N-S

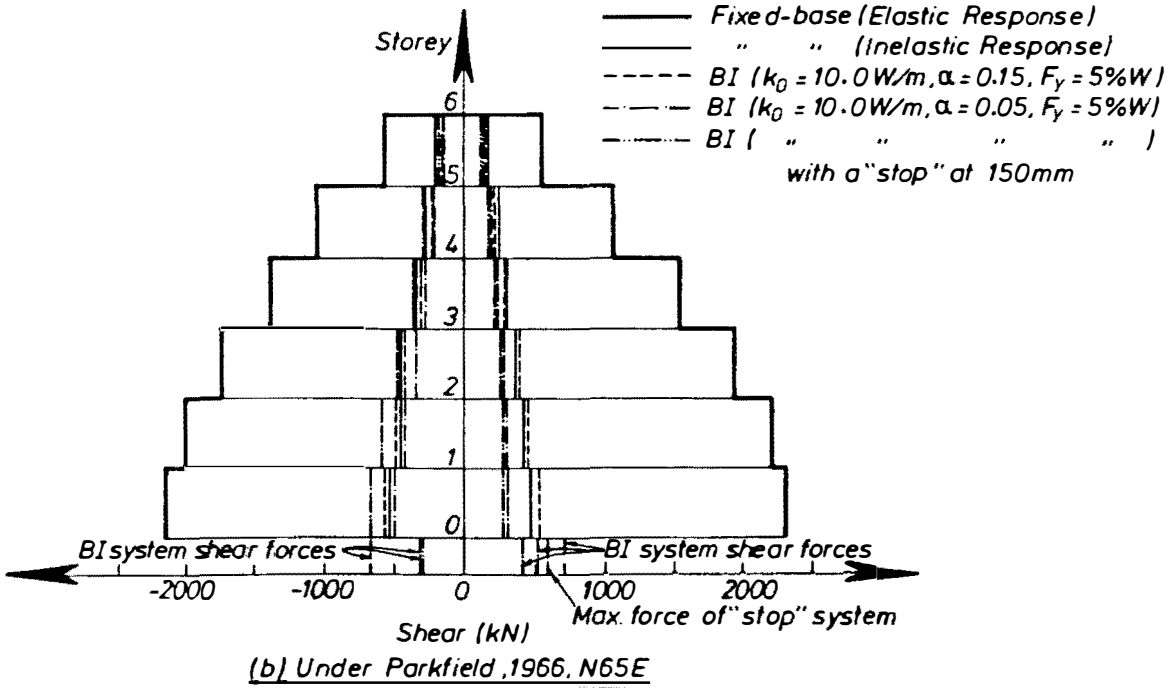

(b) Under Parkfield, 1966, N65E

Fig. 7.13 Lateral Storey Shear Envelopes of Fixed-Base and BI Structures Subjected to 1.4 El Centro 1940 N-S and Parkfield 1966 N65E Earthquakes

conclusions can be drawn. The distance of the "clearance" to activate the "stop" and its stiffness would seem to be important factors for further investigation.

In regard to this "stop" it is worthwhile noting that Kelly et al[7.13] have carried out an experimental study in an attempt to find a satisfactory way for reducing excessive base displacements. In their study the BI system utilized elastomeric bearings and a skid system which comes into operation at preset levels of relative horizontal displacement between the structure and the foundations. The "fail-safe" skid system provides hysteretic damping as it is "touched" by the base of the superstructure and prevents failure of the isolation system in the event of an earthquake beyond the design level. The results show that the hysteretic effect of this "fail-safe" system does not greatly increase the accelerations and thus the storey shears of the structure.

7.5 SUMMARY AND CONCLUDING REMARKS

Two simplified analysis methods are proposed for design purposes of BI multistorey structures. The first method called the Code-Type approach is suitable for use in the preliminary design stage. It is, however, also believed to be adequate for the final design of uniform structures. An illustrative example was presented to demonstrate the step-by-step design procedure of this Code-Type approach. The storey shears predicted by this simple approach are in good agreement with the results obtained from the inelastic time history analyses.

The second proposed design procedure is the Component Mode Synthesis method which is suggested for the design of more complex structures. A computer program named ISODYN was developed using this method with a step-by-step integration scheme. Some example of its application can be found in Chapter 5. It is hoped that in the future this method can be adapted to use the response spectrum analysis procedure.

Inelastic behaviour of a six-storey reinforced concrete frame superstructure with and without BI system was compared when it was subjected to above design-level excitation. It was found that a superstructure mounted on a BI system has fewer plastic hinges than a conventionally designed ductile superstructure. Significant reductions in curvature ductility demands, interstorey drifts, and storey shears are more easily obtained in BI structures than in their inelastic fixed-base counterpart. Due to the reduced ductility demands the structural members of BI structures may not need to be designed with fully ductile design requirements. Consequently, this may allow wider choice of architectural form and structural materials.

A preliminary study on the use of a "stop" to limit excessive base displacements showed that the increase in storey shears and interstorey drifts was insignificant. Further study is, however, required to investigate this matter more thoroughly.

7.6 REFERENCES

7.1 VELETSOS, A.S., Need For Simple Approaches in Structural Dynamics, State-of-the-art in Earthquake Engineering 1981, Panel Reports Prepared for the Occasion of the 7th WCEE in Istanbul, Turkey, September 1980, pp.258-259.

7.2 Code of Practice for General Structural Design and Design Loadings for Buildings, NZS4203:1984, Standards Association of New Zealand, 1984.

7.3 Draft Replacement for Code of Practice for General Structural Design and Design Loadings for Buildings, NZS4203:1984, Standards Association of New Zealand, 1986.

7.4 Tentative Provisions for the Development of Seismic Regulations for Buildings, prepared by Applied Technology of Council, NBS Special Publication 510, Washington, D.C., 1978.

7.5 Recommended Lateral Force Requirements and Commentary, Seismology Committee, Structural Engineers Association of California, 1974.

7.6 JURY, R.D., Seismic Load Demands of Columns of Reinforced Concrete Multistorey Frames, Research Report 78-12, Dept. of Civil Engineering, University of Canterbury, 1978.

7.7 Code of Practice for General Structural Design and Design Loadings for Buildings, NZS4203:1976, Standards Association of New Zealand, 1976.

7.8 PARK, R. and PAULAY, T., Reinforced Concrete Structures, John Wiley and Sons, Inc., 1975, pp.545-607.

7.9 CARR, A.J., Ruaumoko, Computer Program Library, Dept. of Civil Engineering, University of Canterbury, 1986.

7.10 BATHE, K.J. and WILSON, E.L., Numerical Methods in Finite Element Analysis, Prentice-Hall, Inc., 1976.

7.11 CHARLESON, A.W., WRIGHT, P.D., and SKINNER, R.I., Wellington Police Station - Base Isolation of An Essential Facility, Proc. of Pacific Conference on Earthquake Engineering, New Zealand, 5-8 August 1987, pp.377-388.

7.12 MEGGET, L.M., Analysis and Design of A Base Isolated Reinforced Concrete Frame Building, Bull. of the NZNSEE, Vol.11, No.4, Dec.1978, pp.245-254.

7.13 KELLY, J.M., BEUCKE, K.E., and SKINNER, M.S., Experimental Testing of A Friction Damped Aseismic Base Isolation System with Fail-Safe Characteristics, Report No. UCB/EERC-80/18, Univ. of California, Berkeley, July 1980, 58pp.

CHAPTER 8

CONCLUSIONS AND RECOMMENDATIONS

8.1 CONCLUSIONS

In this research the seismic response of a wide variety of BI multistorey structures subjected to different types of ground motion was investigated with a fresh viewpoint. The shortcomings of the current design methods were reviewed. Based on the results obtained from the above investigation and review, two simplified analysis methods have been developed and proposed for practical design purposes. The first method is called the Code-Type approach due to its simplicity and similarity with the well-known equivalent lateral static force analysis procedure which has been adopted by many loadings codes for use in design of non-isolated structures. The second proposed method is based on the Component Mode Synthesis concept and is suggested for final design purposes of more complex BI multistorey structures.

The conclusions for each section of the work undertaken were generally stated at the end of each chapter. Thus only a summary of the most important findings is presented below:

1. The benefits of implementing a BI system were demonstated by contrasting the performance of isolated and non-isolated multistorey structures. With the inclusion of the BI system, the inertia forces and the interstorey drifts can be significantly reduced. As a result, the superstructure can be designed to behave elastically under design-level earthquakes. The much smaller interstorey drifts avoid the early occurence of non-structural damage during moderate ground motions.

2. Under earthquakes beyond the design-level excitations, a superstructure mounted on a BI system shows many fewer plastic hinges and has much lower ductility demands when compared with a conventionally designed ductile structure. Due to these significantly reduced ductility demands, the structural members of BI multistorey structures may not necessarily be designed to full ductility requirements. Consequently, this isolation technique widens the choice of architectural forms and structural materials.

3. It was verified that the base displacement and the base shear of a BI multistorey structure are strongly influenced by the characteristics of the BI system and their maximum values can therefore be predicted from the effective stiffness and the additional hysteretic damping of the BI system.

4. BI systems with low effective stiffness may cause significant lengthening of the fundamental period, especially for very stiff superstructures. Under earthquakes with spectral accelerations that diminish at longer periods this fundamental period shift causes a

considerable reduction in inertia forces. However, without sufficient additional hysteretic damping, an excessive base displacement may occur.

5. Multistorey structures mounted on a BI system with a small energy dissipation capacity or thin hysteresis loops are strongly first mode dominated. In this case the equivalent lateral forces are almost equally distributed over the entire height of the superstructure. In contrast if the BI system has a great energy dissipation capacity, which can be indicated by the high ratio of its hysteresis loop area to the area of the enclosing force-displacement rectangle (R), the contribution of the higher modes becomes more significant and causes the lateral shear envelope to be more bulged. A strong correlation was found between the hysteresis loop ratio, R and the shape of the lateral shear envelope. By utilising the strong correlation, the distribution of the equivalent lateral inertia forces of BI structures can be predicted with satisfactory accuracy. This correlation is dependent upon $T_{1(UI)}$, the beam-to-column stiffness ratio of the superstructure, and the ground motion.

6. The concept of the Component Mode Synthesis method has been adapted for use as a tool to evaluate the trends of changes of the modal storey shears due to the effects of various structural parameters and the contributions of these modal responses to the total storey shears. Among the observed results, it was found that as the hysteresis loops of the BI system become fatter, the higher mode effects on the storey shears of the same superstructure become more significant. This is caused more by the decrease of the first mode contributions to the upper storey shears rather than by the contributions of the higher modes which tend to remain constant.

7. Any hysteretic inelastic system has the possibility of undergoing a permanent plastic offset. Systems with a large non-linearity are more prone to a permanent plastic offset than systems with a small non-lineartity. It was found, however, that by using a sufficient post-yield stiffness, say 5% of the initial stiffness, the permanent plastic offset can be minimized irrespective of the type of earthquake, whether vibratory ones or those with a large acceleration impulse.

8. For sites with ground motions which have peak spectral accelerations in longer periods the inclusion of a BI system may shift the fundamental period of the structure into a more dominant earthquake forces of the structure. However, it seems possible to reduce the transmitted energy of this type of earthquake into the supertructure by using systems that provide large amounts of additional damping.

8.2 RECOMMENDATIONS FOR FURTHER RESEARCH

Some impotant aspects of the seismic performance and the design of BI multistorey structures have been highlighted. However, further research of the following issues is thought necessary in order to be able to establish a complete design philosophy for this type of structure.

1. It is very desirable that the application of the Component Mode Synthesis method can be enhanced, so that it can use a response spectrum analysis approach rather than step-by-step integration used at present. This will require a suitable mode-superposition technique for combining the maximum modal responses of the superstructure.

2. Further analyses with 3D-models are required to investigate the effects of various BI systems on the torsional response. A simple method which takes into account the torsional effects of unsymmetrical BI multistorey structures is required to be part of the Code-Type approach.

3. Slight overestimates in predicting the maximum base shears of structures mounted on BI systems with fat hysteresis loops were found in the case of NZ design-level earthquakes. Further investigation is needed to refine the modification factor used in the proposed Code-Type approach for determining the maximum base shear from the maximum BI system shear force. It is probably necessary to take into account the effect of $T_{1(UI)}$ on these modification factors.

4. Further research is required to investigate the effects of BI systems on the seismic response of multistorey structures with non-uniform inelastic superstructure models. The results are expected to clarify the effectiveness of BI systems in protecting buildings with soft-storeys, set-backs, etc and to give more guidance in designing the superstructure's members and their detailings without the full ductility requirements.

5. The effects of rocking in a BI multistorey structure are not investigated in this study by assuming that the Bl system and the ground underneath have infinite vertical stiffness and the effect of the vertical component of the earthquakes is negligable. For certain situations, however, the rocking effects may be significant. It is important, therefore, to account for the rocking effect in the Code-Type approach.

6. Further sensitivity study is required to compare more extensively the difference between the effects of BI systems with bilinear hysteresis loop models and the effects of BI systems with more complicated hysteresis loop models, such as the Ramberg-Osgood model, on the seismic performance of multistorey structures.

7. A simple analysis method for predicting the seismic response of appendages mounted on the floors of a BI multistorey structure is required to be developed in conjunction with the Code-Type approach.

APPENDIX A

An Illustrative Example of Kelly et al's Design Procedure.

As reported in Chapter 4 the design method proposed by Kelly et al[1] has been evaluated. The example presented in the following is meant to illustrate the steps of the calculations undertaken for the evaluation purposes.

Suppose the superstructure is a cantilever-wall which can be modelled as shown in Fig. A-1.

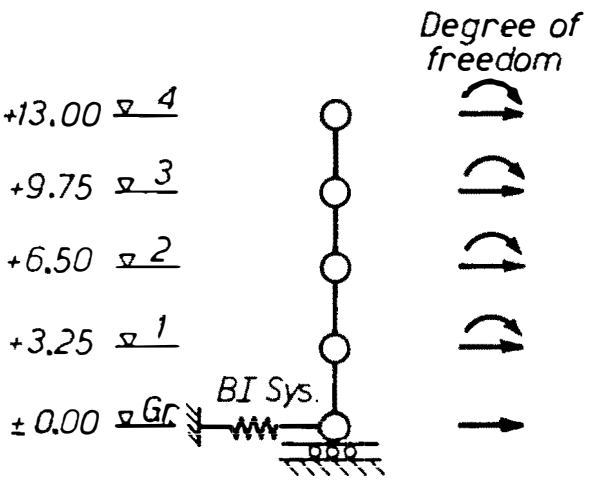

Weight of each floor mass = 900 kN
Total Weight, W = 4500 kN
Moment of Inertia, I = 0.26 m^4
Inherent Damping (for all modes) = 5% crit.
Beam-to-Column Stiff. ratio, ρ = 0.0

Fig. A-1 The Superstructure Model

The superstructure is mounted on a BI system which has a hysteresis loop model as displayed in Fig. A-2 and is subjected to El Centro 1940 N-S earthquake.

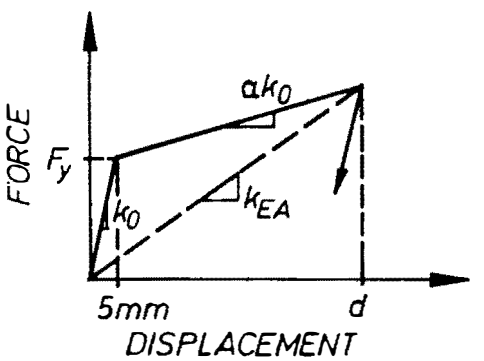

k_o = 10.0 W/m
α = 0.15
F_y = 5%W
k_{EA} = effective secant stiffness
d = peak displacement

Fig. A-2 The Parameters of the BI system's Bilinear Hysteresis Loop Model.

---

[1]KELLY, J.M., EIDINGER, J.M., and DERHAM, C.J., A Practical Soft Storey Earthquake Isolation System, Report No. UBC/EERC-77/27, Univ. of California, Berkeley, 1977.

Conduct modal analyses to calculate the natural periods and the mode shapes at the initial and post-yielded base conditions.

Initial or elastic condition (k_o)

T_{1e} = 0.95 secs $\quad$ T_{2e} = 0.36 secs

PF_{1e} = 1.433 $\quad$ PF_{2e} = 0.604

$$\{\phi_{1e}\} = \begin{Bmatrix} 1.0000 \\ 0.7383 \\ 0.5004 \\ 0.3225 \\ 0.2515 \end{Bmatrix} \qquad \{\phi_{2e}\} = \begin{Bmatrix} -0.7587 \\ -0.0590 \\ 0.5266 \\ 0.8910 \\ 1.0000 \end{Bmatrix}$$

Yielded condition (αk_o)

T_{1y} = 1.75 $\quad$ T_{2y} = 0.49 secs

PF_{1e} = 1.159 $\quad$ PF_{2y} = 0.163

$$\{\phi_{1y}\} = \begin{Bmatrix} 1.0000 \\ 0.9127 \\ 0.8327 \\ 0.7714 \\ 0.7465 \end{Bmatrix} \qquad \{\phi_{2y}\} = \begin{Bmatrix} -1.0000 \\ -0.3345 \\ 0.2485 \\ 0.6523 \\ 0.7973 \end{Bmatrix}$$

Assume a peak displacement of the BI system. In this example the value obtained from the time history analysis under El Centro 1940 N-S earthquake is used, i.e. d = 49.7 mm or μ= 49.7/5 = 9.94.

Calculate the effective fundamental period, T_{1eff}. Note, as discussed in Chapter 3 of this thesis, the formula suggested by Kelly et al to find T_{1eff} (as a linear function of d) was derived from the experimental results for a specific superstructure model and specific BI systems. Therefore, it would not be appropriate for use in the general design case. In this evaluation T_{1eff} was calculated using a modal analysis based on the effective secant stiffness of the BI system, k_{EA} and the properties of the superstructure.

$$k_{EA} = k_0 \left(\frac{1 - \alpha}{\mu} \right) = 10 \left(\frac{1 - 0.15}{9.94} + 0.15 \right) = 2.35 \text{ W/m}$$

First mode :

T_{1eff} = 1.46 secs

$$C = \frac{T_{1eff} - T_{1e}}{T_{1y} - T_{1e}} = \frac{1.46 - 0.95}{1.75 - 0.95} = 0.64$$

$$PF_{1eff} = PF_{1e} + C\,(PF_{1y} - PF_{1e})$$
$$= 1.433 + 0.64\,(1.159 - 1.433)$$
$$= 1.258$$

$$\{\phi_{1eff}\} = \{\phi_{1e}\} + C\,(\{\phi_{1y}\} - \{\phi_{1e}\})$$

$$= \begin{Bmatrix} 1.0000 \\ 0.8499 \\ 0.7129 \\ 0.6098 \\ 0.5683 \end{Bmatrix}$$

$$\text{Add. } \lambda = E_h = \frac{2}{\pi}(1-\alpha)\frac{\mu - 1}{\mu}\frac{k_0}{k_{EA}}$$
$$= \frac{2}{\pi}(1-0.15)\frac{9.94 - 1}{9.94^2}\frac{10}{2.35} = 0.208$$

λ_{1eff} = 20.8 + 5 (inherent) = 25.8% critical.

From the spectral displacements and spectral accelerations of El Centro 1940 N-S earthquake :

S_{d1} = 63 mm

S_{a1} = 0.1189 g

Second mode :

$$T_{2eff} = T_{2e} + C\,(T_{2y} - T_{2e})$$
$$= 0.36 + 0.64\,(0.49 - 0.36)$$
$$= 0.44 \text{ secs}$$

$PF_{2eff} = PF_{2e} = 0.604$ (as suggested by Kelly et al)

$$\{\phi_{2eff}\} = \{\phi_{2e}\} + C\,(\{\phi_{2y}\} - \{\phi_{2e}\})$$

$$= \begin{Bmatrix} -0.9131 \\ -0.2353 \\ 0.3486 \\ 0.7382 \\ 0.8733 \end{Bmatrix}$$

λ_{2eff} = 5% critical.

From the spectral displacements and spectral accelerations of El Centro 1940 N-S earthquake :

S_{d2} = 35 mm

S_{a2} = 0.7280 g

Structural response :

(a). Maximum Storey Displacements (mm)

First mode : $\{\phi_{1eff}\}\ PF_{1eff}\ S_{d1}$

$$\begin{Bmatrix}1.0000\\0.8499\\0.7129\\0.6098\\0.5683\end{Bmatrix} 1.258 \quad 63.0 = \begin{Bmatrix}79.3\\67.3\\56.5\\48.3\\45.0\end{Bmatrix} \text{mm}$$

Second mode : $\{\phi_{2eff}\}\ PF_{2eff}\ S_{d2}$

$$\begin{Bmatrix}-0.9131\\-0.2353\\0.3486\\0.7382\\0.8733\end{Bmatrix} 0.604 \quad 35.0 = \begin{Bmatrix}-19.3\\-5.0\\7.4\\15.6\\18.5\end{Bmatrix} \text{mm}$$

Total (with SRSS combination) :

$$\begin{Bmatrix}81.6\\67.5\\57.0\\50.7\\48.6\end{Bmatrix} \text{mm}$$

Peak Base Displacements :

Calculated 48.6 mm

Assumed 49.7 mm

% difference 2.2 % (close enough)

(b). Maximum Lateral Inertia Forces (kN)

First mode : $\{\phi_{1eff}\}\ PF_{1eff}\ S_{a1}$ { floor mass }

$$\begin{Bmatrix}1.0000\\0.8499\\0.7129\\0.6098\\0.5683\end{Bmatrix} \cdot 1.258 \;\; 0.1189 \;\; 900 = \begin{Bmatrix}134.6\\114.4\\96.0\\82.1\\76.5\end{Bmatrix} \cdot \text{kN}$$

Second mode: $\{\phi_{2eff}\}\ PF_{2eff}\ S_{a2}$ { floor mass }

$$\begin{Bmatrix}-0.9131\\-0.2353\\0.3486\\0.7382\\0.8733\end{Bmatrix} \cdot 0.604 \;\; 0.7280 \;\; 900 = \begin{Bmatrix}-361.3\\-\ 93.1\\137.9\\292.1\\345.6\end{Bmatrix} \cdot \text{kN}$$

Maximum Total Storey Shears (with SRSS combination) :

$$\begin{Bmatrix}385.5\\518.0\\468.0\\427.8\\597.4\end{Bmatrix} \cdot \text{kN}$$

Note, these values are listed in Table 4.14.c of Chapter 4.

APPENDIX B

B.1 GENERATION OF ARTIFICIAL EARTHQUAKES

As discussed in Chapter 6, a series of artificial earthquake records were generated for research purposes in the University of Canterbury using the computer program SIMQKE to match the normal and soft ground elastic spectral accelerations given in the draft of NZ Loadings Code (DZ4203:1986). These records may be used for any site in New Zealand or for any return period simply by scaling the records with appropriate zone and return period factors.

Typical input information to the computer program SIMQKE used to obtain the artificial records is given in the following :

(a) NORMAL SOILS : (after MacRae[1])

Smallest period in range of frequencies contributing to simulation		= 0.2 secs
Largest period in range of frequencies contributing to simulation		= 4.0 secs
Trapezoidal intensity function used	- Build-up time	= 2.0 secs
	- Level time	= 15.0 secs
Duration of generated accelerogram		= 20.0 secs
Discretization interval for generated accelerogram		= 0.02 secs
Desired maximum ground acceleration		= 0.4 g
Seed number provided for selection of random phase angles		= arbitrary
Number of iteration cycles of matching to target spectrum		= 3
Number of points used to describe the target spectrum		= 18
Percentage of critical damping appropriate to target spectrum		= 5 %

(b) SOFT SOILS : (after Whittaker et al[2])

Smallest period in range of frequencies contributing to simulation		= 0.2 secs
Largest period in range of frequencies contributing to simulation		= 8.0 secs
Trapezoidal intensity function used	- Build-up time	= 1.0 secs
	- Level time	= 15.0 secs
Duration of generated accelerogram		= 20.0 secs
Discretization interval for generated accelerogram		= 0.02 secs
Desired maximum ground acceleration		= 0.4 g
Seed number provided for selection of random phase angles		= arbitrary
Number of iteration cycles of matching to target spectrum		= 3

[1] MacRAE, G.A., The Seismic Response of Steel Frames, Ph.D. Thesis, Dept. of Civil Eng. Univ. of Canterbury, 1989.

[2] WHITTAKER, D., PARK, R., and CARR, A.J., Seismic Performance of Offshore Concrete Gravity Platforms, Research Report 88-1, Dept. of Civil Eng., Univ. of Canterbury, 1988.

Number of points used to describe the target spectrum	= 25
Percentage of critical damping appropriate to target spectrum	= 5 %

Figs. B-1 and B-2 show two generated acceleration records used in some of the time history analyses reported in Chapter 6. The acceleration response spectra of these two accelerograms and their target spectrum for SDOF oscillators with 5% of critical damping are shown in Figs. B-3 and B-4.

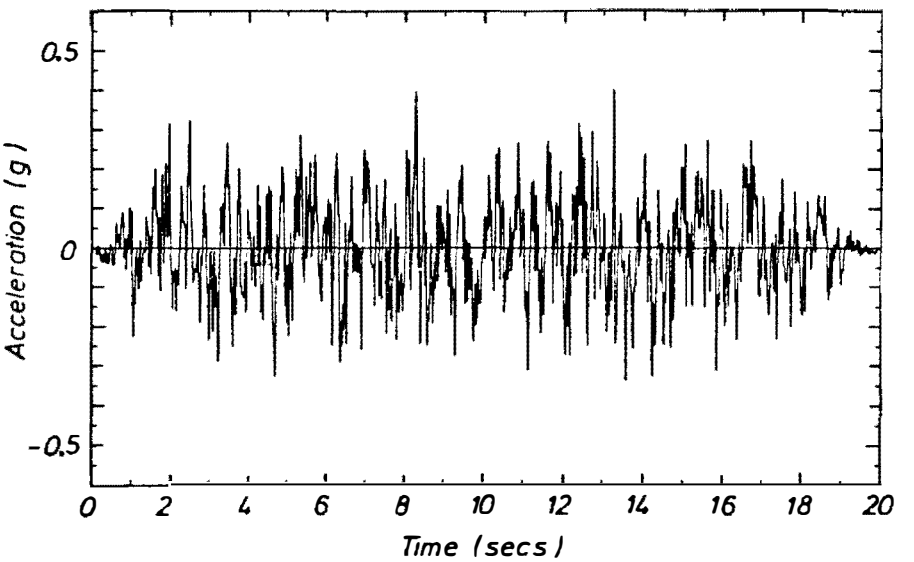

Fig. B-1 Artificial Accelerogram Generated by SIMQKE to Match DZ4203:1986-Normal Soils Design Acceleration Response Spectrum

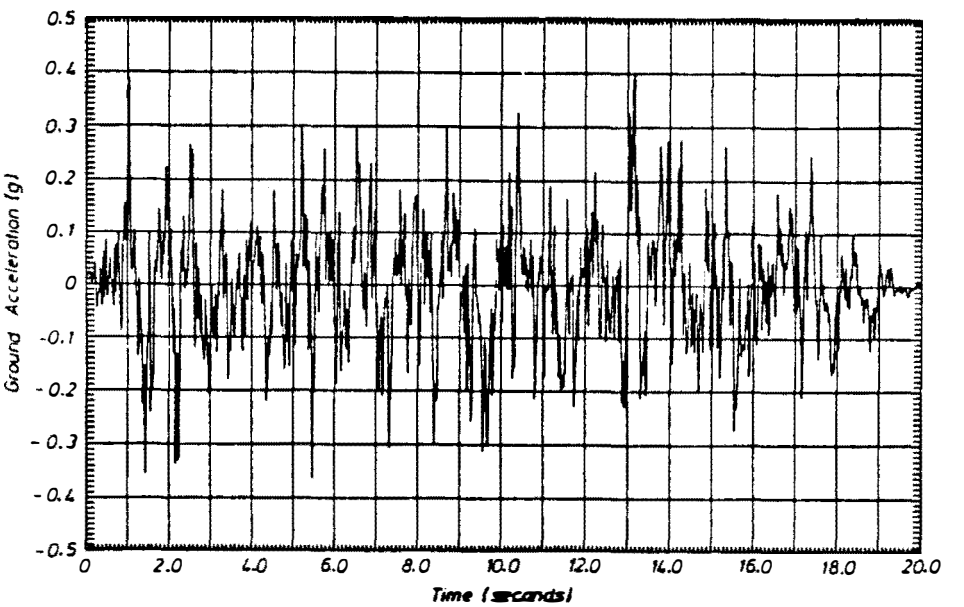

Fig. B-2 Artificial Accelerogram Generated by SIMQKE to Match DZ4203:1986-Soft Soils Design Acceleration Response Spectrum

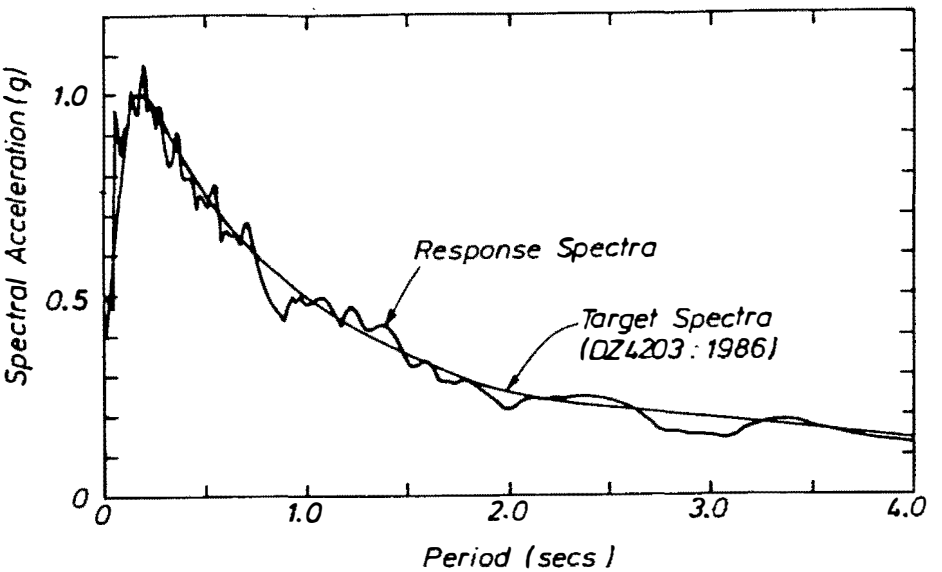

Fig. B-3 Match of Acceleration Response Spectrum and Target Spectrum (DZ4203:1986-Normal Soils-Artificial Motion 1)

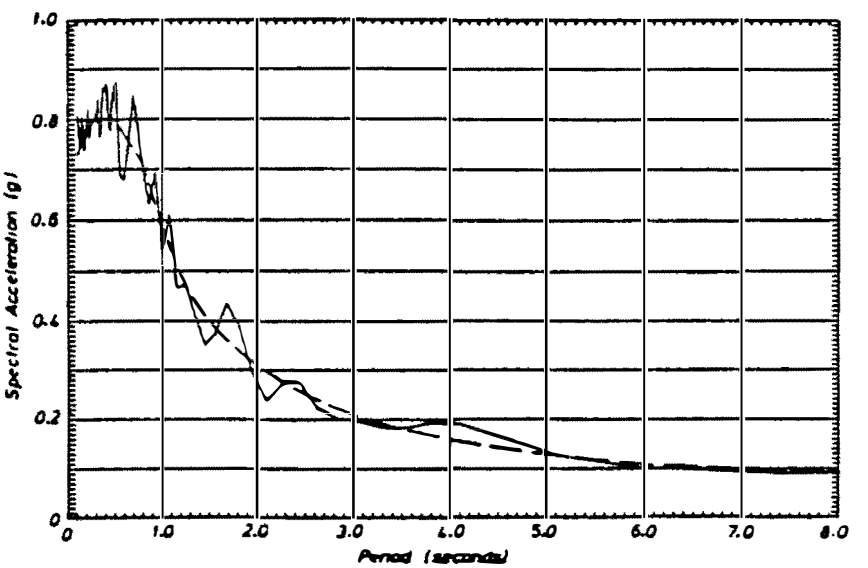

Fig. B-4 Match of Acceleration Response Spectrum and Target Spectrum (DZ4203:1986-Soft Soils-Artificial Motion 1)

B.2 VALUES OF THE ELASTIC SPECTRAL ACCELERATIONS - DZ4203:1986

(a). NORMAL SOILS

PERIOD (secs)	2.0 %	5.0 %	10.0 %	15.0 %	20.0 %	25.0 %	30.0 %	35.0 %	40.0 %	45.0 %
	(critical damping)									
0.0500	1.4468	0.9310	0.6846	0.6107	0.5574	0.5170	0.4849	0.4582	0.4354	0.4246
0.1000	1.2352	0.9141	0.7394	0.6430	0.5675	0.5042	0.4518	0.4274	0.4054	0.3856
0.1500	1.4961	0.9650	0.6411	0.5377	0.4878	0.4563	0.4374	0.4188	0.4011	0.3859
0.2000	1.5806	1.0774	0.7426	0.6335	0.5585	0.5018	0.4574	0.4219	0.3931	0.3694
0.2500	1.6867	0.9685	0.7384	0.6100	0.5182	0.4493	0.3961	0.3539	0.3297	0.3131
0.3000	1.2838	0.8464	0.5986	0.5073	0.4402	0.3883	0.3476	0.3147	0.2877	0.2650
0.3500	1.3843	0.8810	0.5959	0.4759	0.3984	0.3454	0.3113	0.2886	0.2736	0.2593
0.4000	0.9973	0.7818	0.5908	0.4537	0.3854	0.3339	0.3072	0.2865	0.2676	0.2503
0.4500	1.0887	0.7621	0.5056	0.3955	0.3542	0.3274	0.3011	0.2769	0.2551	0.2358
0.5000	1.0469	0.7283	0.5166	0.4076	0.3600	0.3217	0.2887	0.2607	0.2369	0.2165
0.5500	1.1069	0.7804	0.5382	0.4224	0.3526	0.3039	0.2670	0.2377	0.2139	0.1976
0.6000	0.8979	0.6592	0.4689	0.3702	0.3147	0.2710	0.2411	0.2179	0.2032	0.1926
0.6500	0.9636	0.6379	0.4382	0.3382	0.2992	0.2641	0.2345	0.2137	0.2014	0.1904
0.7000	1.0702	0.6822	0.4514	0.3562	0.2985	0.2570	0.2254	0.2114	0.1997	0.1889
0.7500	0.8576	0.5943	0.4377	0.3428	0.2824	0.2408	0.2218	0.2094	0.1978	0.1870
0.8000	0.7233	0.5154	0.3633	0.2948	0.2491	0.2349	0.2210	0.2079	0.1958	0.1845
0.8500	0.7114	0.4684	0.3338	0.2835	0.2559	0.2361	0.2200	0.2058	0.1930	0.1814
0.9000	0.6166	0.4315	0.3268	0.2842	0.2556	0.2346	0.2175	0.2027	0.1895	0.1776
0.9500	0.7560	0.4888	0.3373	0.2727	0.2493	0.2301	0.2135	0.1986	0.1853	0.1731
1.0000	0.5980	0.4853	0.3509	0.2722	0.2407	0.2242	0.2085	0.1939	0.1803	0.1681
1.0500	0.5585	0.4781	0.3509	0.2664	0.2333	0.2188	0.2034	0.1886	0.1749	0.1625
1.1000	0.6779	0.4905	0.3299	0.2455	0.2298	0.2148	0.1987	0.1834	0.1693	0.1568
1.1500	0.7672	0.4433	0.2907	0.2459	0.2303	0.2119	0.1940	0.1777	0.1633	0.1506
1.2000	0.7498	0.4500	0.3033	0.2603	0.2324	0.2090	0.1889	0.1717	0.1569	0.1442
1.2500	0.6305	0.4559	0.3268	0.2695	0.2326	0.2050	0.1831	0.1651	0.1502	0.1376
1.3000	0.4373	0.4119	0.3298	0.2703	0.2292	0.1993	0.1764	0.1581	0.1432	0.1309
1.3500	0.5507	0.4209	0.3253	0.2643	0.2221	0.1917	0.1686	0.1506	0.1360	0.1242
1.4000	0.5821	0.4231	0.3164	0.2557	0.2140	0.1835	0.1605	0.1427	0.1287	0.1174
1.4500	0.4866	0.3815	0.3000	0.2448	0.2053	0.1760	0.1537	0.1362	0.1221	0.1108
1.5000	0.3560	0.3286	0.2803	0.2314	0.1949	0.1676	0.1466	0.1300	0.1167	0.1058
1.5500	0.3813	0.3232	0.2630	0.2165	0.1833	0.1584	0.1390	0.1236	0.1111	0.1010
1.6000	0.5245	0.3352	0.2431	0.2004	0.1713	0.1489	0.1311	0.1169	0.1055	0.0966
1.6500	0.5028	0.2965	0.2154	0.1833	0.1591	0.1394	0.1233	0.1103	0.1014	0.0947
1.7000	0.3954	0.2817	0.1941	0.1667	0.1474	0.1301	0.1169	0.1080	0.1001	0.0932
1.7500	0.4260	0.2729	0.1940	0.1581	0.1408	0.1274	0.1163	0.1068	0.0986	0.0915
1.8000	0.4205	0.2855	0.1987	0.1634	0.1426	0.1275	0.1154	0.1054	0.0970	0.0897
1.8500	0.3456	0.2639	0.1998	0.1654	0.1431	0.1267	0.1140	0.1036	0.0950	0.0878
1.9000	0.3066	0.2468	0.1953	0.1649	0.1422	0.1252	0.1121	0.1016	0.0930	0.0857
1.9500	0.2771	0.2256	0.1905	0.1629	0.1403	0.1231	0.1099	0.0994	0.0908	0.0836
2.0000	0.2410	0.2087	0.1879	0.1600	0.1375	0.1203	0.1072	0.0968	0.0884	0.0813
2.0500	0.2575	0.2251	0.1867	0.1564	0.1338	0.1170	0.1042	0.0941	0.0859	0.0790
2.1000	0.3044	0.2393	0.1842	0.1516	0.1293	0.1131	0.1009	0.0912	0.0833	0.0767
2.1500	0.3222	0.2406	0.1785	0.1455	0.1240	0.1088	0.0973	0.0885	0.0814	0.0749
2.2000	0.3311	0.2357	0.1694	0.1379	0.1181	0.1062	0.0966	0.0882	0.0807	0.0740
2.2500	0.3378	0.2403	0.1687	0.1388	0.1205	0.1073	0.0967	0.0877	0.0798	0.0730
2.3000	0.3176	0.2406	0.1768	0.1434	0.1227	0.1079	0.0965	0.0870	0.0789	0.0718
2.3500	0.3035	0.2444	0.1818	0.1462	0.1239	0.1080	0.0959	0.0860	0.0777	0.0705
2.4000	0.2950	0.2444	0.1837	0.1473	0.1239	0.1075	0.0950	0.0849	0.0764	0.0692
2.4500	0.2900	0.2416	0.1825	0.1463	0.1230	0.1065	0.0938	0.0836	0.0750	0.0677
2.5000	0.2883	0.2362	0.1783	0.1438	0.1212	0.1049	0.0923	0.0820	0.0735	0.0662

(a). NORMAL SOILS (continued)

PERIOD (secs)	2.0 %	5.0 %	10.0 %	15.0 %	20.0 %	25.0 %	30.0 %	35.0 %	40.0 %	45.0 %
	(critical damping)									
2.5500	0.2859	0.2278	0.1719	0.1400	0.1187	0.1030	0.0905	0.0803	0.0718	0.0651
2.6000	0.2789	0.2176	0.1639	0.1353	0.1158	0.1007	0.0886	0.0785	0.0701	0.0654
2.6500	0.2604	0.2023	0.1558	0.1302	0.1125	0.0983	0.0865	0.0766	0.0684	0.0656
2.7000	0.2300	0.1812	0.1467	0.1258	0.1092	0.0958	0.0843	0.0746	0.0687	0.0657
2.7500	0.2006	0.1574	0.1374	0.1216	0.1067	0.0934	0.0821	0.0726	0.0689	0.0658
2.8000	0.2066	0.1572	0.1289	0.1177	0.1043	0.0916	0.0803	0.0726	0.0690	0.0658
2.8500	0.2067	0.1540	0.1219	0.1144	0.1021	0.0898	0.0787	0.0727	0.0690	0.0657
2.9000	0.2006	0.1472	0.1175	0.1118	0.1000	0.0880	0.0771	0.0727	0.0690	0.0656
2.9500	0.1958	0.1475	0.1159	0.1099	0.0981	0.0862	0.0767	0.0728	0.0690	0.0655
3.0000	0.1924	0.1447	0.1166	0.1086	0.0964	0.0843	0.0767	0.0727	0.0689	0.0653
3.0500	0.1902	0.1387	0.1194	0.1078	0.0946	0.0825	0.0767	0.0726	0.0688	0.0651
3.1000	0.1853	0.1414	0.1226	0.1072	0.0929	0.0815	0.0767	0.0725	0.0686	0.0648
3.1500	0.1975	0.1563	0.1262	0.1065	0.0912	0.0819	0.0767	0.0724	0.0684	0.0646
3.2000	0.2245	0.1710	0.1290	0.1059	0.0920	0.0821	0.0766	0.0722	0.0681	0.0644
3.2500	0.2435	0.1806	0.1306	0.1056	0.0924	0.0822	0.0766	0.0721	0.0679	0.0640
3.3000	0.2533	0.1858	0.1308	0.1065	0.0928	0.0821	0.0765	0.0719	0.0676	0.0637
3.3500	0.2549	0.1858	0.1293	0.1069	0.0927	0.0817	0.0763	0.0716	0.0673	0.0633
3.4000	0.2497	0.1820	0.1264	0.1071	0.0925	0.0816	0.0763	0.0714	0.0670	0.0630
3.4500	0.2419	0.1748	0.1264	0.1068	0.0921	0.0816	0.0760	0.0711	0.0667	0.0626
3.5000	0.2406	0.1669	0.1259	0.1062	0.0913	0.0814	0.0758	0.0708	0.0663	0.0622
3.5500	0.2315	0.1633	0.1249	0.1052	0.0904	0.0811	0.0755	0.0704	0.0659	0.0618
3.6000	0.2154	0.1560	0.1236	0.1041	0.0893	0.0808	0.0751	0.0701	0.0655	0.0614
3.6500	0.1949	0.1479	0.1219	0.1026	0.0880	0.0804	0.0748	0.0697	0.0651	0.0609
3.7000	0.1733	0.1454	0.1199	0.1009	0.0865	0.0800	0.0745	0.0694	0.0647	0.0605
3.7500	0.1616	0.1425	0.1176	0.0990	0.0855	0.0796	0.0741	0.0689	0.0643	0.0600
3.8000	0.1579	0.1392	0.1150	0.0970	0.0849	0.0791	0.0736	0.0686	0.0638	0.0595
3.8500	0.1539	0.1358	0.1123	0.0948	0.0842	0.0787	0.0732	0.0681	0.0633	0.0590
3.9000	0.1496	0.1322	0.1094	0.0924	0.0836	0.0784	0.0729	0.0677	0.0629	0.0585
3.9500	0.1452	0.1284	0.1065	0.0900	0.0831	0.0779	0.0724	0.0672	0.0624	0.0580
4.0000	0.1408	0.1245	0.1035	0.0875	0.0826	0.0775	0.0720	0.0667	0.0618	0.0574

(b). SOFT SOILS

PERIOD (secs)	2.0 %	5.0 %	10.0 %	15.0 %	20.0 %	25.0 %	30.0 %	35.0 %	40.0 %	45.0 %
	(critical damping)									
0.0500	0.9359	0.7477	0.5721	0.5085	0.4808	0.4607	0.4447	0.4312	0.4192	0.4083
0.1000	1.0310	0.7657	0.6404	0.5775	0.5283	0.4891	0.4576	0.4318	0.4102	0.3919
0.1500	1.0758	0.7759	0.5927	0.5053	0.4499	0.4109	0.3823	0.3607	0.3506	0.3419
0.2000	1.2685	0.8071	0.5922	0.5034	0.4485	0.4026	0.3638	0.3429	0.3357	0.3281
0.2500	1.2485	0.8698	0.6468	0.5254	0.4420	0.3804	0.3468	0.3400	0.3319	0.3228
0.3000	1.2804	0.7958	0.5658	0.4702	0.4173	0.3797	0.3646	0.3514	0.3376	0.3235
0.3500	1.2802	0.8091	0.5730	0.4735	0.4316	0.4069	0.3834	0.3620	0.3413	0.3217
0.4000	1.3799	0.9362	0.6283	0.5218	0.4731	0.4325	0.3971	0.3659	0.3411	0.3242
0.4500	1.4989	0.8452	0.6103	0.5441	0.4857	0.4360	0.3943	0.3652	0.3430	0.3230
0.5000	1.2780	0.8743	0.6556	0.5531	0.4802	0.4237	0.3910	0.3637	0.3388	0.3162
0.5500	1.0000	0.7030	0.5986	0.5182	0.4649	0.4245	0.3891	0.3578	0.3307	0.3067
0.6000	0.8700	0.6651	0.5671	0.5146	0.4659	0.4218	0.3829	0.3491	0.3199	0.2945
0.6500	1.2431	0.7698	0.5734	0.5207	0.4638	0.4133	0.3709	0.3352	0.3050	0.2794
0.7000	1.1016	0.8691	0.6472	0.5315	0.4551	0.3979	0.3529	0.3165	0.2866	0.2617
0.7500	1.1319	0.7441	0.6094	0.5069	0.4309	0.3734	0.3292	0.2941	0.2657	0.2425
0.8000	1.0077	0.7024	0.5551	0.4663	0.3973	0.3441	0.3031	0.2710	0.2450	0.2239
0.8500	1.0323	0.6630	0.5077	0.4208	0.3571	0.3100	0.2746	0.2467	0.2245	0.2060
0.9000	0.9882	0.6878	0.4855	0.3820	0.3149	0.2742	0.2449	0.2222	0.2040	0.1886
0.9500	1.0484	0.6540	0.4534	0.3535	0.2913	0.2576	0.2321	0.2124	0.1960	0.1821
1.0000	0.7578	0.5414	0.3807	0.3313	0.2885	0.2521	0.2238	0.2049	0.1890	0.1754
1.0500	0.7814	0.5692	0.4145	0.3353	0.2828	0.2436	0.2139	0.1961	0.1811	0.1683
1.1000	0.9263	0.5948	0.4116	0.3263	0.2713	0.2317	0.2031	0.1866	0.1727	0.1608
1.1500	0.7275	0.4792	0.3750	0.3060	0.2549	0.2218	0.1970	0.1769	0.1641	0.1529
1.2000	0.5586	0.4614	0.3432	0.2812	0.2439	0.2152	0.1905	0.1696	0.1552	0.1452
1.2500	0.6438	0.4729	0.3143	0.2633	0.2351	0.2075	0.1831	0.1621	0.1467	0.1374
1.3000	0.6955	0.4468	0.2957	0.2571	0.2277	0.1997	0.1750	0.1540	0.1412	0.1301
1.3500	0.6640	0.4089	0.2931	0.2543	0.2208	0.1915	0.1665	0.1520	0.1393	0.1278
1.4000	0.4781	0.3704	0.2977	0.2508	0.2135	0.1827	0.1648	0.1503	0.1372	0.1253
1.4500	0.4099	0.3516	0.2953	0.2456	0.2053	0.1808	0.1637	0.1484	0.1347	0.1226
1.5000	0.4278	0.3458	0.2950	0.2419	0.2024	0.1809	0.1622	0.1460	0.1319	0.1205
1.5500	0.4364	0.3688	0.2980	0.2379	0.2040	0.1800	0.1600	0.1431	0.1287	0.1204
1.6000	0.5224	0.4060	0.3010	0.2376	0.2040	0.1779	0.1570	0.1397	0.1251	0.1202
1.6500	0.5949	0.4299	0.3019	0.2388	0.2018	0.1745	0.1531	0.1356	0.1250	0.1199
1.7000	0.6080	0.4361	0.2969	0.2357	0.1975	0.1699	0.1488	0.1319	0.1249	0.1194
1.7500	0.5797	0.4267	0.2925	0.2337	0.1960	0.1689	0.1480	0.1311	0.1244	0.1187
1.8000	0.5322	0.3985	0.2849	0.2299	0.1938	0.1674	0.1466	0.1306	0.1238	0.1178
1.8500	0.5187	0.3554	0.2701	0.2231	0.1902	0.1648	0.1445	0.1298	0.1228	0.1168
1.9000	0.4703	0.3245	0.2512	0.2144	0.1852	0.1613	0.1417	0.1287	0.1217	0.1156
1.9500	0.3761	0.2939	0.2323	0.2052	0.1796	0.1573	0.1383	0.1274	0.1205	0.1143
2.0000	0.3170	0.2622	0.2165	0.1968	0.1741	0.1530	0.1347	0.1259	0.1190	0.1129
2.0500	0.3032	0.2371	0.2059	0.1897	0.1687	0.1485	0.1318	0.1243	0.1176	0.1115
2.1000	0.3134	0.2364	0.2007	0.1843	0.1637	0.1440	0.1300	0.1227	0.1159	0.1099
2.1500	0.3376	0.2406	0.1997	0.1802	0.1589	0.1394	0.1284	0.1210	0.1143	0.1082
2.2000	0.3433	0.2539	0.2011	0.1768	0.1542	0.1346	0.1267	0.1193	0.1126	0.1066
2.2500	0.3441	0.2688	0.2030	0.1736	0.1495	0.1332	0.1250	0.1175	0.1108	0.1048
2.3000	0.3655	0.2770	0.2036	0.1699	0.1446	0.1320	0.1234	0.1157	0.1089	0.1030
2.3500	0.3741	0.2796	0.2022	0.1653	0.1411	0.1306	0.1216	0.1138	0.1070	0.1012
2.4000	0.3782	0.2810	0.1983	0.1597	0.1405	0.1290	0.1196	0.1118	0.1051	0.0993
2.4500	0.3687	0.2732	0.1914	0.1559	0.1395	0.1272	0.1176	0.1097	0.1030	0.0974
2.5000	0.3471	0.2581	0.1821	0.1556	0.1379	0.1252	0.1154	0.1075	0.1010	0.0955

(b). SOFT SOILS (continued)

PERIOD (secs)	2.0 %	5.0 %	10.0 %	15.0 %	20.0 %	25.0 %	30.0 %	35.0 %	40.0 %	45.0 %
	(critical damping)									
2.5500	0.3160	0.2365	0.1818	0.1540	0.1357	0.1228	0.1130	0.1053	0.0989	0.0936
2.6000	0.2828	0.2251	0.1793	0.1513	0.1330	0.1201	0.1105	0.1029	0.0968	0.0916
2.6500	0.2603	0.2196	0.1752	0.1477	0.1298	0.1172	0.1078	0.1005	0.0946	0.0897
2.7000	0.2589	0.2121	0.1698	0.1435	0.1261	0.1140	0.1051	0.0981	0.0924	0.0877
2.7500	0.2654	0.2031	0.1635	0.1387	0.1222	0.1107	0.1022	0.0956	0.0903	0.0858
2.8000	0.2720	0.1982	0.1567	0.1335	0.1182	0.1073	0.0993	0.0931	0.0881	0.0839
2.8500	0.2727	0.2056	0.1523	0.1281	0.1139	0.1039	0.0964	0.0906	0.0859	0.0820
2.9000	0.2691	0.2090	0.1565	0.1294	0.1119	0.1005	0.0935	0.0882	0.0838	0.0801
2.9500	0.2590	0.2078	0.1586	0.1309	0.1126	0.0987	0.0907	0.0857	0.0817	0.0782
3.0000	0.2442	0.2031	0.1589	0.1316	0.1128	0.0985	0.0879	0.0834	0.0797	0.0765
3.0500	0.2346	0.1966	0.1582	0.1317	0.1127	0.0980	0.0863	0.0811	0.0777	0.0747
3.1000	0.2286	0.1893	0.1564	0.1312	0.1121	0.0973	0.0854	0.0789	0.0758	0.0730
3.1500	0.2214	0.1882	0.1542	0.1302	0.1113	0.0964	0.0843	0.0768	0.0739	0.0714
3.2000	0.2146	0.1870	0.1518	0.1288	0.1101	0.0952	0.0831	0.0747	0.0721	0.0698
3.2500	0.2100	0.1856	0.1492	0.1271	0.1087	0.0938	0.0818	0.0728	0.0705	0.0683
3.3000	0.2081	0.1847	0.1468	0.1251	0.1070	0.0922	0.0803	0.0709	0.0688	0.0669
3.3500	0.2084	0.1840	0.1457	0.1230	0.1050	0.0905	0.0787	0.0692	0.0673	0.0655
3.4000	0.2107	0.1840	0.1446	0.1207	0.1030	0.0886	0.0769	0.0675	0.0658	0.0642
3.4500	0.2132	0.1837	0.1430	0.1183	0.1007	0.0865	0.0750	0.0663	0.0644	0.0630
3.5000	0.2156	0.1837	0.1412	0.1157	0.0984	0.0844	0.0731	0.0663	0.0631	0.0618
3.5500	0.2183	0.1836	0.1395	0.1130	0.0958	0.0821	0.0728	0.0671	0.0626	0.0606
3.6000	0.2208	0.1842	0.1402	0.1102	0.0932	0.0817	0.0738	0.0678	0.0630	0.0596
3.6500	0.2247	0.1867	0.1417	0.1106	0.0938	0.0830	0.0748	0.0685	0.0634	0.0590
3.7000	0.2286	0.1894	0.1433	0.1122	0.0957	0.0843	0.0759	0.0691	0.0637	0.0591
3.7500	0.2317	0.1916	0.1450	0.1135	0.0969	0.0854	0.0765	0.0695	0.0639	0.0591
3.8000	0.2345	0.1940	0.1465	0.1145	0.0982	0.0863	0.0771	0.0700	0.0640	0.0590
3.8500	0.2368	0.1957	0.1475	0.1154	0.0993	0.0871	0.0777	0.0702	0.0640	0.0589
3.9000	0.2379	0.1965	0.1478	0.1167	0.1002	0.0879	0.0781	0.0704	0.0640	0.0588
3.9500	0.2367	0.1959	0.1472	0.1173	0.1008	0.0883	0.0783	0.0703	0.0639	0.0586
4.0000	0.2351	0.1946	0.1462	0.1181	0.1013	0.0886	0.0784	0.0703	0.0637	0.0583

APPENDIX C

INPUT DATA FOR COMPUTER ANALYSES : The Superstructure Model of Six-Storey Frame
(Section 7.4)

Table C.1 - PROPERTIES

	Axial and Shear Areas (m^2)			Moment of Inertia (10^3 m^4)			Plastic Hinge Length (m)			Rigid End Blocks at (m)			E (10^7 kPa)	G (10^7 kPa)	Initial End Cond. for Beams (kNm)		(kN)	
Level	Col. 1-3	Col. 2	Beams	Col. 1-3	Col. 2	Beams	Col. 1-3	Col. 2	Beams	Col. 1-3	Col. 2	Beams			M1	M2	V1	V2
0-3	0.1125	0.1513	0.1050	3.518	5.723	6.758	0.350	0.385	0.410	0.250	0.275	0.300	2.50	1.04	-41.25	40.04	48.33	48.33
3-6	0.1013	0.1250	0.0963	2.565	3.908	5.280	0.315	0.350	0.375	0.225	0.250	0.290	2.50	1.04	-41.68	40.05	47.33	47.33

Note :

Initial Conditions are derived so that moments at centre lines = M + V x (rigid end bl. length)

Table C.2 Ultimate Strengths

	END 1					END 2					
Level	M_1 (10^3 kNm)	M_{bal} (10^3 kNm)	P_{bal} (10^3 kN)	P_{yc} (10^3 kN)	P_{yt} (10^3 kN)	M_1 (10^3 kNm)	M_{bal} (10^3 kNm)	P_{bal} (10^3 kN)	P_{yc} (10^3 kN)	P_{yt} (10^3 kN)	
0 - 3	0.177	0.501	-2.483	-5.942	0.900	0.177	0.501	-2.483	-5.942	0.900	)
3 - 4	0.158	0.406	-2.155	-5.427	0.891	0.144	0.406	-2.235	-5.348	0.801	) Cols. 1-3
4 - 6	0.144	0.406	-2.235	-5.348	0.801	0.144	0.406	-2.235	-5.348	0.801	)
0 - 3	0.262	0.741	-3.338	-7.988	1.210	0.262	0.741	-3.338	-7.988	1.210	)
3 - 4	0.246	0.557	-2.660	-6.799	1.200	0.197	0.557	-2.759	-6.602	1.000	) Col. 2
4 - 6	0.197	0.557	-2.759	-6.602	1.000	0.197	0.557	-2.759	-6.602	1.000	)

	M_1 (10^3 kNm)	M_2 (10^3 kNm)		M_3 (10^3 kNm)	M_4 (10^3 kNm)	
1 - 3	0.262	-0.262		0.232	-0.232	)
4	0.173	-0.184		0.155	-0.155	) Beam Capacities
5	0.115	-0.131	• indicates the side of yielding steel.	0.119	-0.115	)
6	0.115	-0.115		0.115	-0.115	)

Table C.3 External Loading and Weight (based on D + L/3)

Level		Weight of Mass (kN)		External Vert. Loading (kN)	
		External Node	Internal Node	External Node	Internal Node
Ground	Base Isolated	134.00	219.00	-85.34	-122.50
	Fixed-Base	10.00	13.00	-20.00	-26.00
1		134.00	219.00	-85.34	-122.50
2		134.00	219.00	-85.34	-122.50
3		133.00	217.00	-83.34	-118.50
4		129.00	211.00	-81.33	-116.50
5		129.00	211.00	-81.33	-116.50
6		120.00	200.00	-63.30	-94.50

Note :

(1) The sum of external vertical loads and beam shears at each node gives the total axial load due to D + L/3 to be applied at that node.

(2) Percentages of critical damping for first and sixth modes = 5% critical (Rayleigh's Damping model)

(3) Definition of LEVELS can be seen in Fig. 7.1

Classn :

SEISMIC RESISTANT DESIGN OF BASE ISOLATED MULTISTOREY STRUCTURES

T. Andriono

ABSTRACT : Extensive time history analyses are conducted to investigate in detail the effects of various structural parameters and ground motion characteristics on the seismic behaviour of Base Isolated multistorey structures. The shortcomings of the current design methods are reviewed. The results of this study are then used to develop two simplified analysis methods for practical design purposes.

Department of Civil Engineering, University of Canterbury
Doctor of Philosophy Thesis, 1989.